

Dissertation zur Erlangung des Doktorgrades  
der Fakultät für Chemie und Pharmazie  
der Ludwig-Maximilians-Universität München

# **Total Synthesis of Wickerol A**

–

## **Development of a Photoswitchable AMPA Receptor Antagonist**

von

Shu-An Liu

aus

Villach, Österreich

2017

**Erklärung**

Diese Dissertation wurde im Sinne von § 7 der Promotionsordnung vom 28.November 2011 von Herrn Prof. Dr. Dirk Trauner betreut.

**Eidesstattliche Versicherung**

Diese Dissertation wurde eigenständig und ohne unerlaubte Hilfe erarbeitet.

München, .....

.....

Shu-An Liu

Dissertation eingereicht am	08. Juni 2017
1. Gutachter:	Prof. Dr. Dirk Trauner
2. Gutachter:	Dr. Dorian Didier
Mündliche Prüfung am	17.07.2017

**For my family.**

謹以此文獻給我的家庭.

**Parts of this thesis have been published in peer-reviewed journals:**

“Synthesis of the Antiviral Diterpene Wickerol A”, S.-A. Liu, D. Trauner, *J. Am. Chem. Soc.*, **2017**, ASAP.

“Optical control of AMPA receptors using a photoswitchable quinoxaline-2,3-dione antagonist”, D. M. Barber, <sup>†</sup> S.-A. Liu, <sup>†</sup> K. Gottschling, M. Sumser, M. Hollmann, D. Trauner, *Chem. Sci.* **2017**, 8, 611-615.

<sup>†</sup> These authors contributed equally to this work.

**Parts of this thesis have been presented at a scientific conference:**

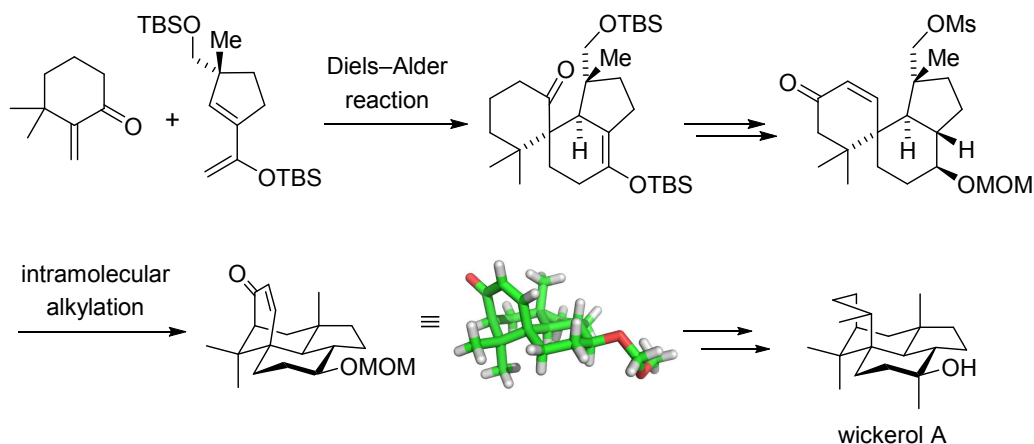
**16th Tetrahedron Symposium: Challenges in Bioorganic & Organic Chemistry**

Poster presentation: “Light Controlled Antagonists of AMPA Receptors”.

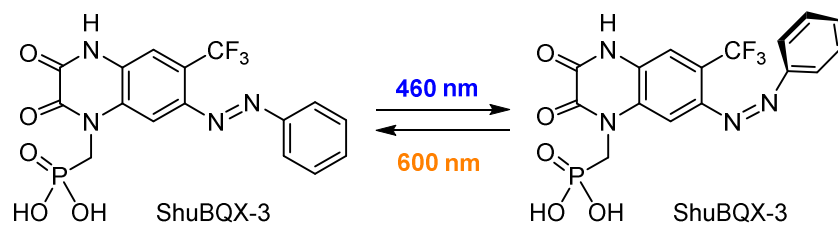
Berlin, Germany, June 2015

## Abstract

**Part I:** Terpenes represent the largest family of natural products and comprise compounds with extremely diverse biological and physical properties. One unique member of this class is wickerol A, an antiviral diterpene isolated from the fungus *Trichoderma atroviride* FKI-3849. It features an unprecedented and highly congested carbon framework with seven stereocenters, of which two are quaternary carbons. Out of several failed approaches to wickerol A evolved a route which ultimately led to its first total synthesis. The highly convergent strategy is based on a Diels–Alder reaction and an intramolecular alkylation to complete the 6-5-6-6 ring system.



**Part II:** AMPA receptors are a subclass of ionotropic glutamate receptors which play a crucial role in excitatory neurotransmission. They are also involved in processes such as memory and learning as well as several psychiatric disorders. In the second part of this thesis, we present the development of the first photoswitchable antagonist that is selective for AMPA receptors. Our light-responsive ligand, ShuBQX-3, blocks the receptor in its dark-adapted *trans*-isomer and can be switched to its significantly less active *cis*-isomer using blue light. Control of action potential firing in hippocampal CA1 neurons could be demonstrated with ShuBQX-3. In addition, it exhibits a remarkable red-shifting of its photoswitching properties through interactions with the AMPA receptor ligand binding site.



---

## Acknowledgement

This PhD has certainly been the most challenging endeavor of my life so far. When I embarked on it four years ago, I had no idea how difficult it would be but I'd like to think that all the hardship was worth it, that I learned a lot and that I have become a better person through it. This journey was shaped by many people, some of which I'd like to thank here:

I want to express my gratitude to Prof. Dr. Dirk Trauner for giving me the opportunity to work in his group and to the permanent staff: Heike Traub, Alexandra Grilic, Dr. Martin Sumser, Carrie Louis, Luis de la Osa de la Rosa and Mariia Palchyk.

I would also like to thank Dr. Dorian Didier, Dr. Thomas Magauer, Prof. Dr. Franz Bracher and Prof. Dr. Manfred Heuschmann for being part of my defense committee and the Studienstiftung des deutschen Volkes for financial support.

My gratitude also goes to Dr. David Barber and Dr. Martin Sumser, who worked with me on the ShuBQX-3 project, as well as Dr. Guillaume Journot and Dr. Bryan Matsuura, who helped me with the total synthesis of wickerol A. I also want to thank all my interns: Alexander Harjung, Jens Popp, Julius Hillenbrand, Peter Gänsheimer and Simon Graßl.

Furthermore, I am grateful to the analytical department of the LMU Munich: Claudia Dubler, Dr. David Stephenson, Dr. Werner Spahl, Sonja Kosak and particularly Dr. Peter Mayer.

I am very thankful to all the past and present members of the Trauner and Magauer group who have generated a great working environment, especially to Dr. Martin Olbrich (for his humor), Dr. David Barber (for all the great coffee breaks and proofreading so many documents), Dr. Cedric Hugelshofer (for his early morning visits), Dr. Robin Meier (for always having encouraging words), Matthias Schmid (for his cheerfulness) and Dr. Hong-Dong Hao (for his calmness and helpful discussions). In addition, I want to thank Dr. Guillaume Journot, Dr. Nicolas Armanino and Dr. Bryan Matsuura for having been awesome hood mates who patiently dealt with all my craziness.

I am especially grateful to Dr. Giulio Volpin, Antonio Rizzo and Dr. Julius Reyes for their friendship and support: without you I would have been lost.

I can also call myself lucky to have enjoyed the friendship of Edris Parsa, Jürgen Vorndran and especially Julia Kress, who always tried to get me out of the lab and show me new things.

Last but not least, I want to thank my parents and my sister for all their support and their sacrifices. Without them, this journey would not have been possible.

## List of Abbreviations

Å	angstrom	DMAP	4-(dimethylamino)pyridine
Ac	acetyl	DMAPP	dimethylallyl pyrophosphate
acac	acetylacetone	DMDO	dimethyldioxirane
AIBN	azobisisobutyronitrile	DME	1,2-dimethoxyethane
AMPA	2-amino-3-(5-methyl-3-hydroxyisoxazol-4-yl)propanoic acid	DMF	dimethylformamide
		DMP	Dess–Martin periodinane
aqu	aqueous	DMSO	dimethylsulfoxide
ATP	adenosine triphosphate	DNA	deoxyribonucleic acid
ATR	attenuated total reflection	d.r.	diastereomeric ratio
Bn	benzyl	<i>E</i>	opposite, <i>trans</i>
br	broad (NMR spectroscopy, IR spectroscopy)	EDG	electron donating group
Bu	butyl	<i>ee</i>	enantiomeric excess
°C	degree Celsius	EI	electron impact ionization
cal	calorie(s)	<i>ent</i>	enantiomer
CAN	ceric ammonium nitrate	enz	enzyme
CCDC	Cambridge Crystallographic Data Centre	<i>epi</i>	epimer
CNS	central nervous system	eq	equivalent(s)
CoA	coenzyme A	ESI	electron spray ionization (mass spectrometry)
COSY	homonuclear correlation spectroscopy	Et	ethyl
Cp	cyclopentadienyl	EWG	electron withdrawing group
CTP	cytidine triphosphate	FDA	Food and Drug Administration
δ	chemical shift (NMR)	FPP	farnesyl diphosphate
d	doublet (NMR spectroscopy)	g	gram(s)
D	dexter (“right”)	GABA	γ-aminobutyric acid
D	Debye	gem	germinal
d	day(s)	GG	geranylgeranyl
DBU	1,8-diazabicyclo[5.4.0]undec-7-ene	GluR	glutamate receptor
DCE	1,2-dichloroethane	GPP	geranyl diphosphate
DCM	dichloromethane	h	hour(s)
DIBAL-H	diisobutylaluminium hydride	HG II	Hoveyda-Grubbs II catalyst
DIPA	diisopropylamine	HMDS	hexamethyldisilazide
DIPEA	diisopropylethylamine	HMPA	hexamethylphosphoramide
DIPT	diisopropyl d-tartrate	h-ν	irradiation
		HSQC	heteronuclear single quantum coherence
		Hz	Hertz (frequency)

<i>i</i>	<i>iso</i> (mer)	NMDA	<i>N</i> -methyl-d-aspartate
IC <sub>50</sub>	half maximal inhibitory concentration	NMO	<i>N</i> -methylnmorpholine- <i>N</i> -oxide
imid	imidazole	NMP	1-methyl-2-pyrrolidinone
IPP	isopentenyl pyrophosphate	NMR	nuclear magnetic resonance
IR	infrared	NOESY	nuclear Overhauser effect correlation spectroscopy
IUPAC	International Union of Pure and Applied Chemistry	Nu	nucleophile
<i>J</i>	coupling constant (NMR)	<i>p</i>	<i>para</i> (isomer)
k	kilo	PG	protecting group
L	liter(s)	PIDA	phenyliodonium diacetate
L	laevus ("left")	Piv	pivaloyl
LBD	ligand binding domain	Ph	phenyl
LDA	lithium diisopropylamide	PMB	<i>para</i> -methoxybenzyl ether
LG	leaving group	PP	pyrophosphate
LHMDS	lithium hexamethyldisilazide	ppm	parts per million
M	molar	PPTS	pyridinium <i>para</i> -toluene-sulfonate
m	meter(s)	<i>p</i> -TsOH	<i>para</i> -toluenesulfonic acid
m	medium (IR spectroscopy)	pyr	pyridine
m	multiplet (NMR spectroscopy)	q	quartet (NMR spectroscopy)
<i>m</i>	<i>meta</i>	R	undefined substituent
MABR	methylaluminum bis(4-bromo -2,6-di- <i>t</i> -butylphenoxide)	<i>rac</i>	racemic
<i>m</i> -CPBA	<i>meta</i> -chloroperbenzoic acid	RCM	ring closing metathesis
Me	methyl	R <sub>f</sub>	retardation factor
MEP	methylerythritol phosphate	r.t.	room temperature
min	minute(s)	s	strong (IR spectroscopy)
mL	milliliter(s)	s	singlet (NMR spectroscopy)
mmol	millimole(s)	SAR	structure activity relationship
MOM	methoxymethyl	sat	saturated
MS	mass spectrometry	S <sub>N</sub>	nucleophilic substitution
MS	molecular sieves	T	temperature
Ms	methanesulfonyl	t	time
MVA	mevalonate	<i>t</i>	tertiary
NADPH	nicotinamide adenine dinucleotide phosphate hydrogen	t	triplet (NMR spectroscopy)
NBS	<i>N</i> -iodosuccinimide	TBAF	tetrabutylammonium fluoride
NHC	<i>N</i> -heterocyclic carbene	TBAI	tetrabutylammonium iodide
NIS	<i>N</i> -iodosuccinimide	TBDPS	<i>tert</i> -butyldiphenylsilyl
		TBHP	<i>tert</i> -butyl hydrogenperoxide
		TBS	<i>tert</i> -butyldimethylsilyl
		TES	triethylsilyl

---

Tf	trifluoromethanesulfonyl
TFA	trifluoroacetic acid
THF	tetrahydrofurane
TIPS	triisopropyl
TLC	thin layer chromatography
TMS	trimethylsilyl
TPP	thiamine pyrophosphate
TRPV	transient receptor potential channels vanilloid
Ts	tosyl
TTMSS	tris(trimethylsilyl)silane
tol	toluene
UV	ultraviolet (irradiation)
w	weak (IR spectroscopy)
wt%	weight percent
Z	zusammen, "together"

# Table of Content

<b>Abstract</b> .....	<b>I</b>
<b>Acknowledgement</b> .....	<b>III</b>
<b>List of Abbreviations</b> .....	<b>V</b>
<b>1. General Introduction</b> .....	<b>2</b>
1.1. Biosynthesis of Terpenes .....	2
1.1.1. Diterpenes.....	7
1.2. Synthesis of Complex Diterpenes .....	11
<b>2. Project Background and Aims</b> .....	<b>26</b>
2.1. Isolation and Structure of Wickerol A and B.....	26
2.2. Biological Activity.....	27
2.3. Biosynthesis of Wickerol A and B .....	27
2.4. Previous Work .....	28
2.5. Project Outline.....	29
<b>3. Results and Discussion</b> .....	<b>31</b>
3.1. First Generation Approach.....	31
3.2. Second Generation Approach .....	40
3.3. Synthesis of the Antiviral Diterpene Wickerol A .....	45
<b>4. Conclusion and Outlook</b> .....	<b>50</b>
<b>5. Photopharmacology</b> .....	<b>52</b>
5.1. Introduction.....	52
5.2. Photoswitches .....	53
5.3. Design Principles.....	58
<b>6. AMPA Receptors</b> .....	<b>65</b>
6.1. Ionotropic Glutamate Receptors.....	65
6.2. AMPA Agonists and Antagonists .....	67
6.3. Photochromic AMPA Receptor Agonist.....	70
6.4. Project Outline.....	72

---

<b>7. Results and Discussion.....</b>	<b>74</b>
7.1. Optical control of AMPA receptors using a photoswitchable quinoxaline-2,3-dione antagonist.....	74
<b>8. Conclusion and Outlook.....</b>	<b>80</b>
<b>9. Summary.....</b>	<b>81</b>
<b>10. Experimental Section.....</b>	<b>86</b>
10.1. General Experimental Details.....	86
10.2. Supporting Information for Chapter 3.1.....	89
10.2.1. Experimental Procedures .....	89
10.2.2. NMR Spectra for Chapter 3.1.....	101
10.2.3. X-ray Crystallographic Data for Chapter 3.1.....	109
10.3. Supporting Information for Chapter 3.2.....	113
10.3.1. Experimental Procedures .....	113
10.3.2. NMR Spectra for Chapter 3.3.....	117
10.4. Supporting Information for Chapter 3.3.....	119
10.4.1. Experimental Procedures .....	119
10.4.2. Screening Tables.....	150
10.4.3. NMR Spectra for Chapter 3.3.....	152
10.4.4. X-ray Crystallographic Data for Chapter 3.3.....	191
10.5. Supporting Information for Chapter 7.1.....	197
10.5.1. Experimental Procedures 7.1.....	197
10.5.2. NMR Spectra for Chapter 7.1.....	212
10.5.3. Supplementary Figures.....	227
10.5.4. Electrophysiology .....	232
<b>11. References .....</b>	<b>235</b>

**Part I:**

**Total Synthesis**

**of**

**Wickerol A**

## 1. General Introduction

### 1.1. Biosynthesis of Terpenes

Terpenoids, with over 55 000 members, represent the largest family of natural products and comprise compounds with extremely diverse biological and physical properties. Consequently, their applications range from flavors<sup>[1]</sup> and fragrances<sup>[2]</sup> to hormones, therapeutic agents<sup>[3]</sup> and materials. The name “terpene” is derived from turpentine, an oil distilled from pine tree resin. Nowadays, the terms terpenoid and terpene are used interchangeably in the literature, though according to IUPAC the latter only comprises pure hydrocarbons. Terpenoids are defined through their biosynthetic origin that is the two C<sub>5</sub>-monomers isopentenyl pyrophosphate (**1.2**, IPP) and dimethylallyl pyrophosphate (**1.3**, DMAPP) (Figure 1.1).<sup>[4]</sup> Both units are joined in a head to tail fashion which results in carbon structures that consists of (C<sub>5</sub>)<sub>n</sub> members. This pattern had been recognized by Otto Wallach<sup>[5]</sup> by the end of the 19<sup>th</sup> century and was later formalized by Leopold Ruzicka<sup>[6]</sup> though they wrongly assumed that all terpenoids arose from a varying number of isoprene (**1.1**) units (the ‘isoprene rule’). Only later, through studies of Konrad E. Bloch and Feodor Lynen, were the true building blocks of nature identified as IPP (**1.2**) and DMAPP (**1.3**).<sup>[7]</sup> They in turn arise from either the mevalonate (MVA) or the methylerythritol phosphate (MEP) pathway (Scheme 1.1 and Scheme 1.2).

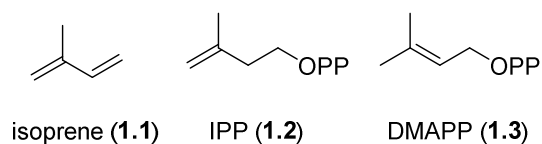
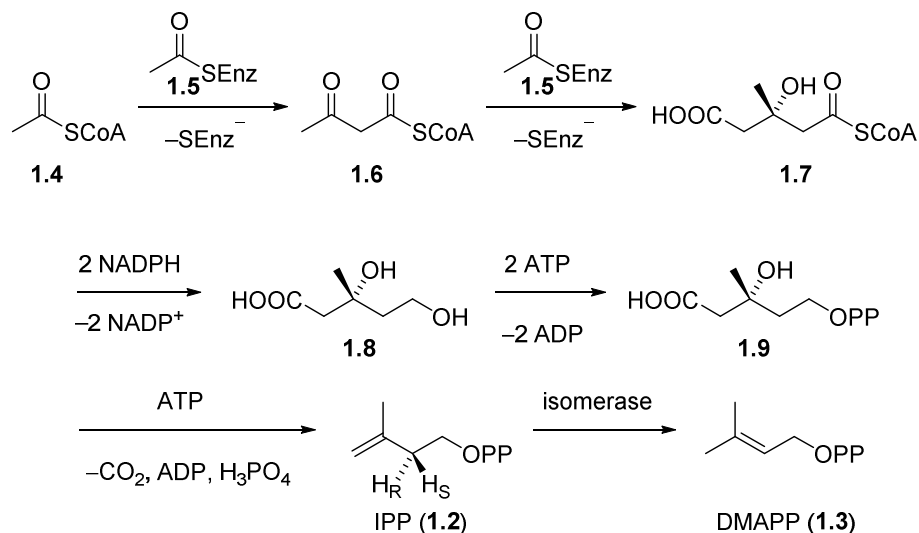


**Figure 1.1.** Structure of isoprene (**1.1**), IPP (**1.2**) and DMAPP (**1.3**).

The mevalonate pathway begins with Claisen condensation of two acetyl-CoA (**1.4**) units to give acetoacetyl-CoA (**1.6**) which undergoes a regiochemically unusual Aldol reaction with another enzyme bound acetyl-CoA moiety (**1.5**) (Scheme 1.1). The product is then hydrolyzed to afford 3-hydroxy-3-methylglutaryl-CoA (**1.7**, HMG-CoA) which is then reduced with 2 equivalents of NADPH to mevalonic acid (**1.8**, MVA). IPP (**1.2**) is then formed through phosphorylation of the primary hydroxyl group of **1.8**, decarboxylation and elimination of the tertiary alcohol. Isomerization to

DMAPP (**1.3**) is catalyzed by an isomerase enzyme and proceeds *via* protonation and elimination of the H<sub>R</sub>-proton.<sup>[4]</sup>

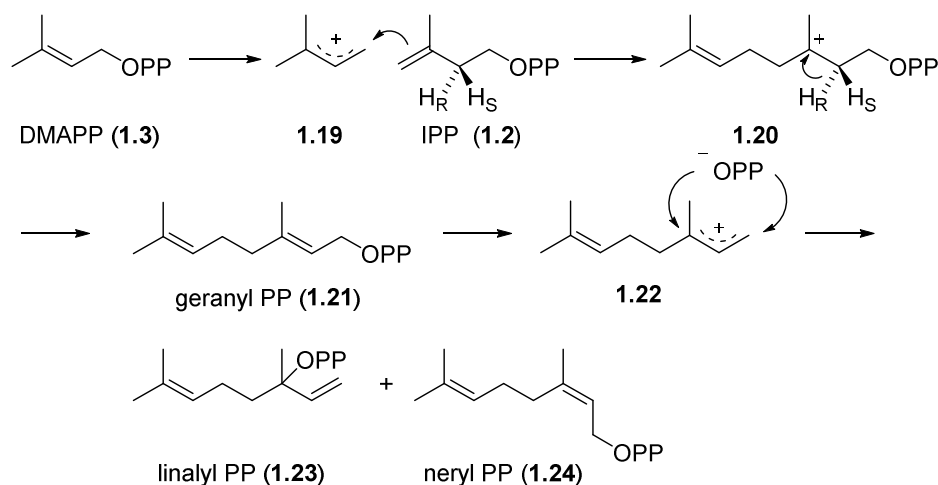


**Scheme 1.1.** The mevalonate pathway.

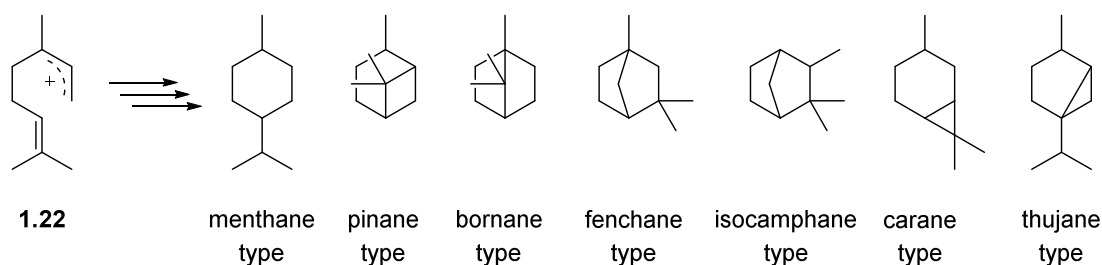
The mevalonate-independent pathway or the methylerythritol phosphate (**1.14**, MEP) pathway represents an alternative way to produce IPP (**1.2**) and can be found in bacteria and plants. It starts from the glycolytic pathway intermediate pyruvic acid (**1.10**) and glyceraldehyde 3-phosphate (**1.11**) which form diol **1.12** in a thiamin pyrophosphate (TPP, structure not shown) dependent process (Scheme 1.2). A retro-Aldol/Aldol cascade affords **1.13** which is reduced to MEP (**1.14**) by NADPH. MEP (**1.14**) is then converted to the cyclic intermediate **1.17** through cytidylation (CTP-dependent), phosphorylation of the tertiary alcohol (ATP-dependent) and intramolecular hydrolysis. The mechanisms of subsequent transformations are the least understood of the pathway and subject to ongoing research. It is clear though that ring opening and reductive dehydration of **1.17** gives primary alcohol **1.18** that in turn is converted into both IPP (**1.2**) and DMAPP (**1.3**) by reductive processes, with a preference for the former. Whether the mevalonate pathway or the MEP pathway is the source of building blocks for a particular terpenoid has to be established experimentally. Animals seem to lack the MEP pathway, whereas many other organisms, including plants, are able to employ both, often concurrently.<sup>[8]</sup>



a)



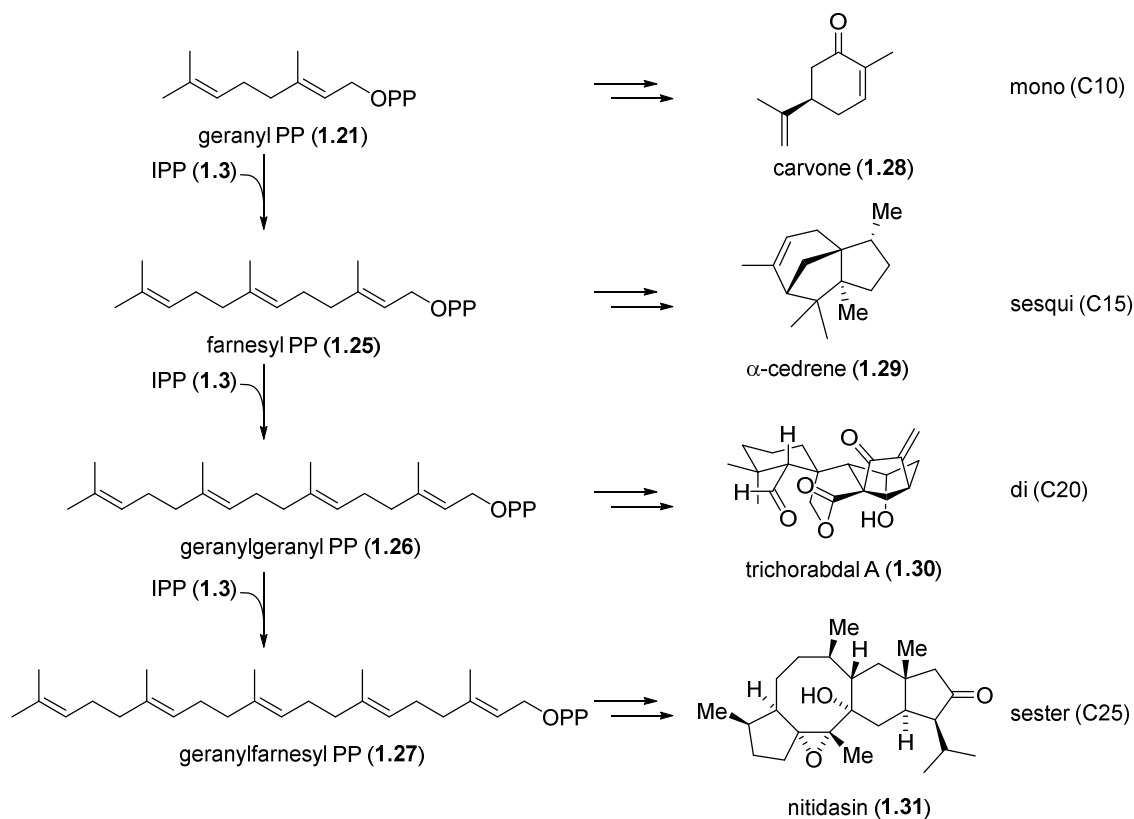
b)



**Scheme 1.3.** a) Biosynthesis of geranyl pyrophosphate (**1.21**, GPP). b) Different types of monoterpene carbon skeletons.

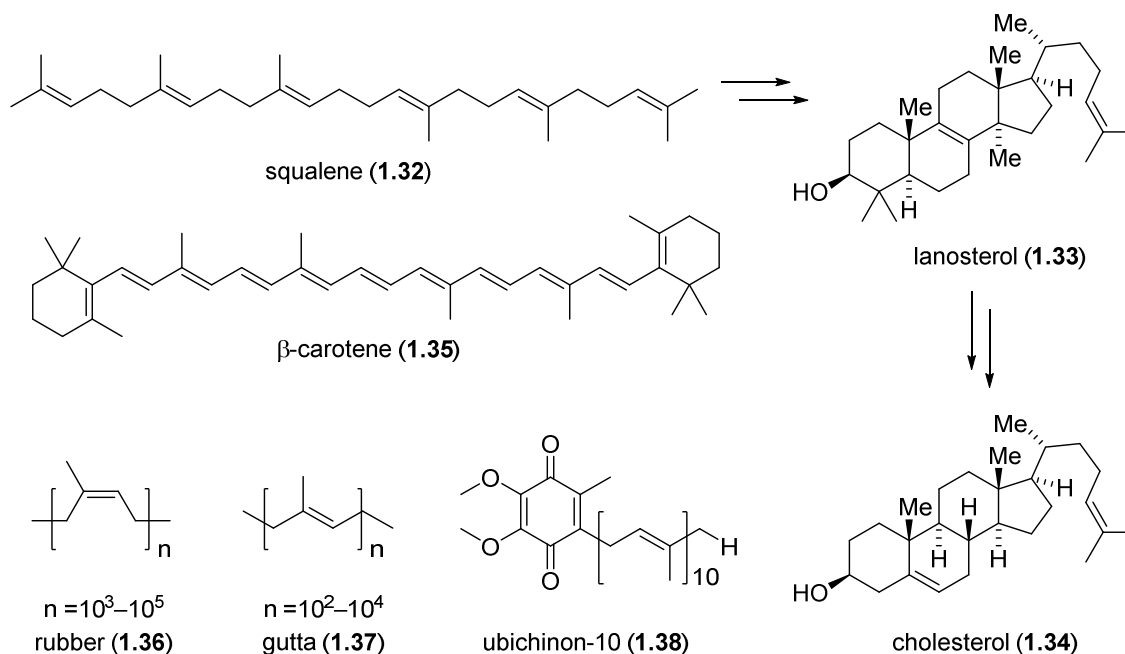
Sequential elongation of GPP (**1.21**) with IPP (**1.2**) units following the same mechanism as described above affords farnesyl pyrophosphate (**1.25**, FPP, C<sub>15</sub>), geranylgeranyl pyrophosphate (**1.26**, C<sub>20</sub>) or geranylgeranyl pyrophosphate (**1.27**, C<sub>25</sub>) (Scheme 1.4). Analogously to monoterpenes, these linear precursors give rise to a plethora of structurally diverse natural products through cyclization reactions, rearrangements and oxidation processes. According to the number of C<sub>5</sub>-units, they are classified as mono- (C<sub>10</sub>), sesqui- (C<sub>15</sub>), di- (C<sub>20</sub>) and sesterterpenes (C<sub>25</sub>). An example of each class is depicted in Scheme 1.4.

However, squalene (**1.32**, C<sub>30</sub>), from which triterpenes (C<sub>30</sub>) are derived, is not formed by homology of geranylgeranyl pyrophosphate (**1.27**) but from the tail-to-tail fusion of two farnesyl subunits. Polyene cyclization of **1.32** gives penta- and tetracyclic triterpenoids such as lanosterol (**1.33**). Through the loss of three carbon atoms, **1.33** is transformed into cholesterol **1.34**, the principal animal sterol (Scheme 1.5).



**Scheme 1.4.** Biosynthetic precursors for mono-, sesqui-, di- and sesterterpenes with a representative member of each class.

Analogously to triterpenes, tetraterpenes arise from the tail-to-tail coupling of two molecules of geranylgeranyl diphosphate (1.26, GGPP). They comprise only carotenoids, organic pigments that play an important role in photosynthesis and as protectants against photo-oxidative damage. A famous example is  $\beta$ -carotene (1.35), which is bright red-orange and serves as precursor for vitamin A (Scheme 1.5).



**Scheme 1.5.** Examples for tri- and tetraterpenes as well as higher terpenes.

Nature also produces higher terpenoids such as rubber (1.36) and gutta percha (1.37), which contain polyisoprene chains. Furthermore,  $C_{40}$ - $C_{50}$  terpenoid side chains can be found in ubiquinones, a family of natural products that arise from the shikimate pathway, e.g. ubiquinone-10 (1.38, Coenzyme  $Q_{10}$ ) (Scheme 1.5).<sup>[10]</sup>

### 1.1.1. Diterpenes

Diterpenes represent a large and structurally diverse subgroup of terpenoids that are derived from GGPP (1.26). One of the simplest and most important one is phytol (1.45) (Figure 1.2) which forms the lipophilic side-chain of the chlorophylls. Cyclization of the linear precursor 1.26 through diterpene synthases gives rise to a multitude of molecular scaffolds of varying ring sizes, some examples being given in Figure 1.2. After construction of the carbon skeleton follows the chemo-, regio-, and stereoselective oxidation by P450-dependent mono-oxygenases.<sup>[4]</sup>

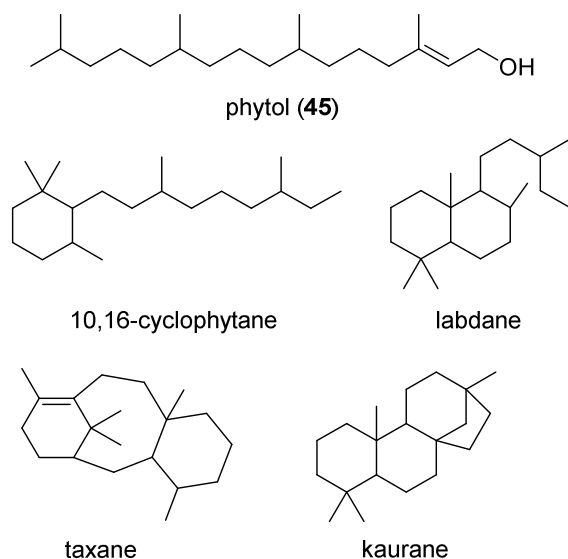
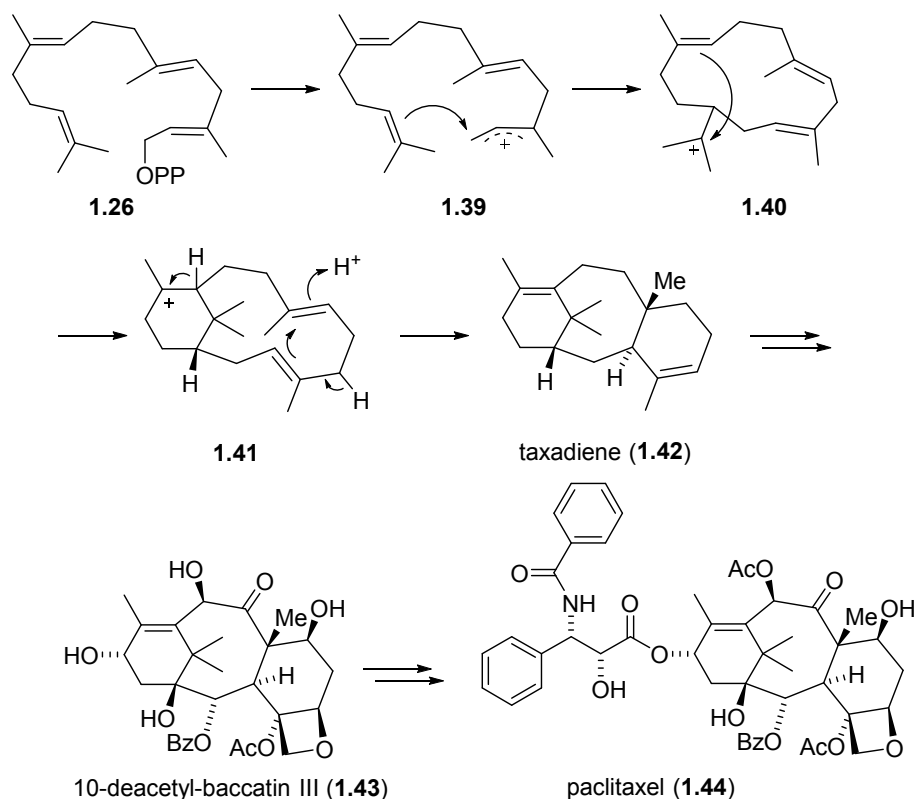


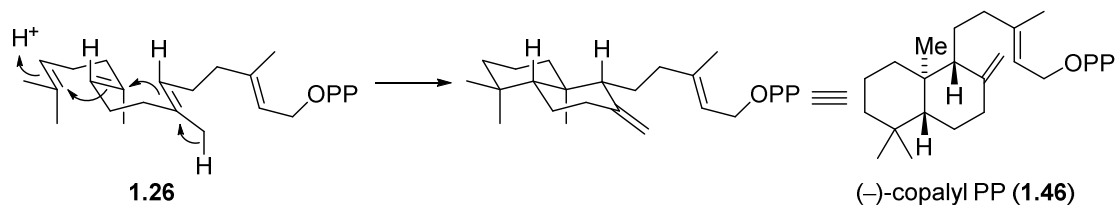
**Figure 1.2.** Structure of phytol (**1.45**) and some representative examples of diterpene carbon scaffolds.

A very prominent diterpenoid is the best-selling drug paclitaxel (**1.44**) (more commonly known as Taxol). The cyclization leading to taxadiene (**1.42**), the first committed intermediate in the biosynthesis of **1.44** is depicted in Scheme 1.6. Loss of diphosphate induces a cyclization cascade resulting in the bicyclic vorticallyl cation (**1.41**) that eliminates a proton and forms taxadiene (**1.42**) *via* a sequence of protonation, electrophilic cyclization and elimination. Intermediate **1.42** is then transformed to 10-deacetyl-baccatin III (**1.43**) and then paclitaxel (**1.44**), in which the side chains containing aromatic rings are derived from the shikimate pathway. Natural product **1.44** was isolated from the bark of the Pacific yew (*Taxus brevifolia*) in 1971 and was approved by the FDA in 1992.<sup>[11]</sup> Ever since then it has become one of the most important anticancer drugs on the market. In the beginning, accessing enough material for therapeutic use presented a significant challenge since three 100-year-old trees gave about one gram of paclitaxel (**1.44**), whereas treatment of a single patient may need double that amount. To meet this challenge, tremendous efforts throughout the 1980's and 1990's were made to access **1.44** through total synthesis. Though several endeavors were successful, the routes proved to be too costly for industrial production. Ultimately, paclitaxel (**1.44**) was made through semi-synthesis from more easily isolated 10-deacetyl-baccatin III (**1.43**) and nowadays it can be produced through plant cell cultures.<sup>[12]</sup>



**Scheme 1.6.** Biosynthesis of taxadiene (**1.42**), the precursor of 10-deacetyl-baccatin III (**1.43**) and then paclitaxel (**1.44**).

In contrast to the cyclization sequence shown in Scheme 1.6, where loss of pyrophosphate generates the initial carbocation, many diterpenes arise by a different mechanism. Carbocation formation can also be initiated by protonation of the double bond at the head of the GGPP (**1.26**) chain leading to a polyene cyclization (Scheme 1.7). The stereochemistry in the product is controlled by the folding of the substrate on the enzyme surface, which either leads to (+)- or (–)-copalyl PP (**1.46**). Subsequent loss of diphosphate produces another carbocation that can undergo a multitude of transformations, resulting in the broad spectrum of scaffolds and oxidation patterns found in nature.<sup>[4]</sup>



**Scheme 1.7.** Formation of (–)-copalyl PP (**1.46**).

The structural diversity of terpenoids combined with their broad range of biological activities have made them the focus of extensive research and inspired organic chemists to access these natural products through total synthesis. Some recent examples thereof will be discussed in the following chapter.

## 1.2. Synthesis of Complex Diterpenes

Terpenoids, with their interesting structural, physical and biological properties, have prompted extensive studies of their biosynthesis (see Chapter 1.1.) and function in nature. For organic chemists, terpenoids have been a source of intriguing targets since the dawn of natural product synthesis.<sup>[13]</sup> One of the earliest examples is the preparation of camphor (**1.47**) on an industrial scale at the beginning of the 1900's.<sup>[14]</sup> By mid-century, pioneering work by Robert B. Woodward resulted in the synthesis of complex steroids such as cholesterol (**1.34**).<sup>[15]</sup> The following decades saw the rise of crucial technological advances, including chromatography techniques and NMR spectroscopy, which enabled the synthesis of terpenoids with increasing complexity.<sup>[13a]</sup> Some interesting examples from the 1970's and 80's are gibberellic acid (**1.48**),<sup>[16]</sup> ginkgolide B (**1.49**)<sup>[17]</sup> and retigeranic acid (**1.50**)<sup>[18]</sup> (Figure 1.3.a). In addition to being interesting targets, terpenes serve also as useful building blocks („chiral pool“) to access a wide variety of other molecular scaffolds.<sup>[19]</sup> Some recent examples of natural products syntheses based on this strategy are jiadifenolide (**1.52**)<sup>[20]</sup> and ryanodol (**1.54**) (Figure 1.3.b).<sup>[21]</sup> In both cases, the complex targets could be synthesized in a concise way starting from simple monoterpenes.

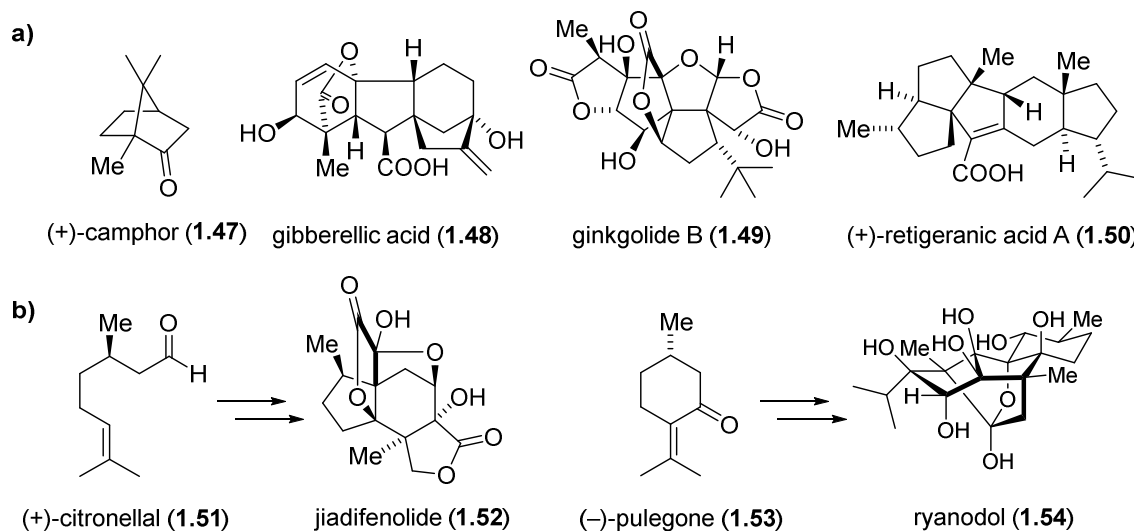


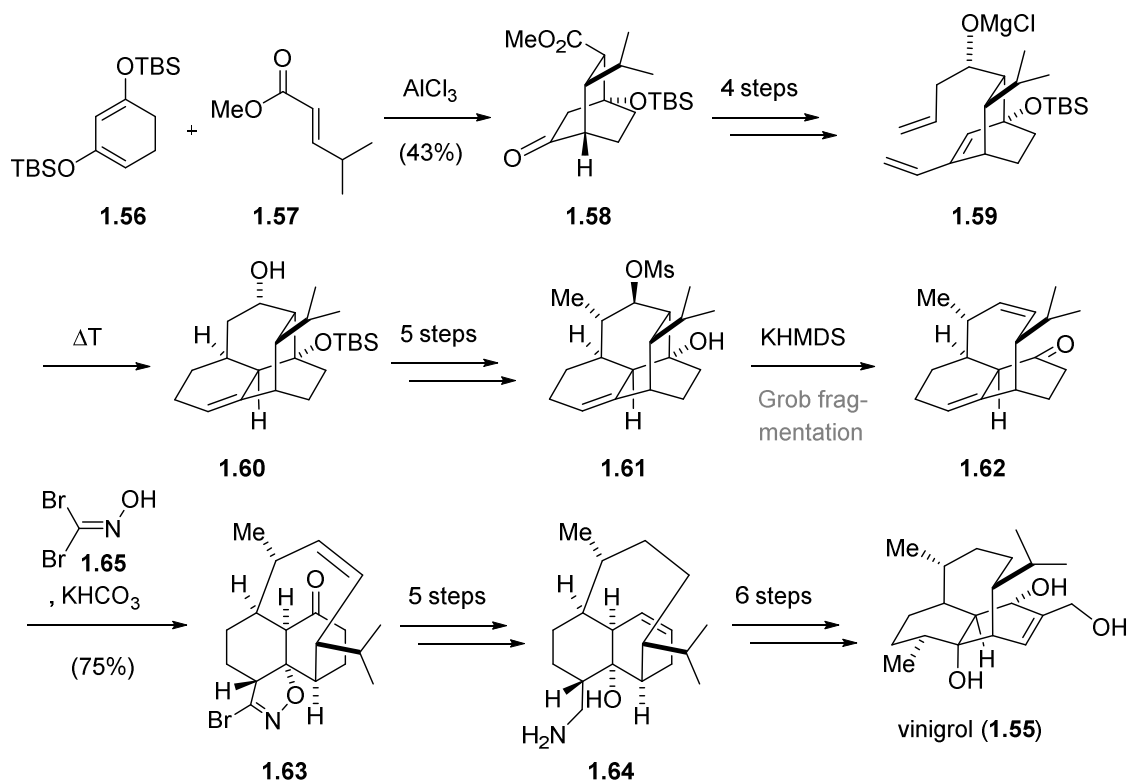
**Figure 1.3.** a) Some historic examples of terpenes made by total synthesis. b) Recent examples of natural products syntheses using terpenes as building blocks.

Despite the successful preparation of many complex molecular scaffolds through total synthesis, and the guidelines that can be followed when subjecting a new target to retrosynthetic analysis, it

is impossible to predict the outcome when embarking on such a project. Success is often based on a combination of ingenious disconnections, problem solving, extensive experimentation and perseverance, thus making total synthesis such a challenging endeavor.

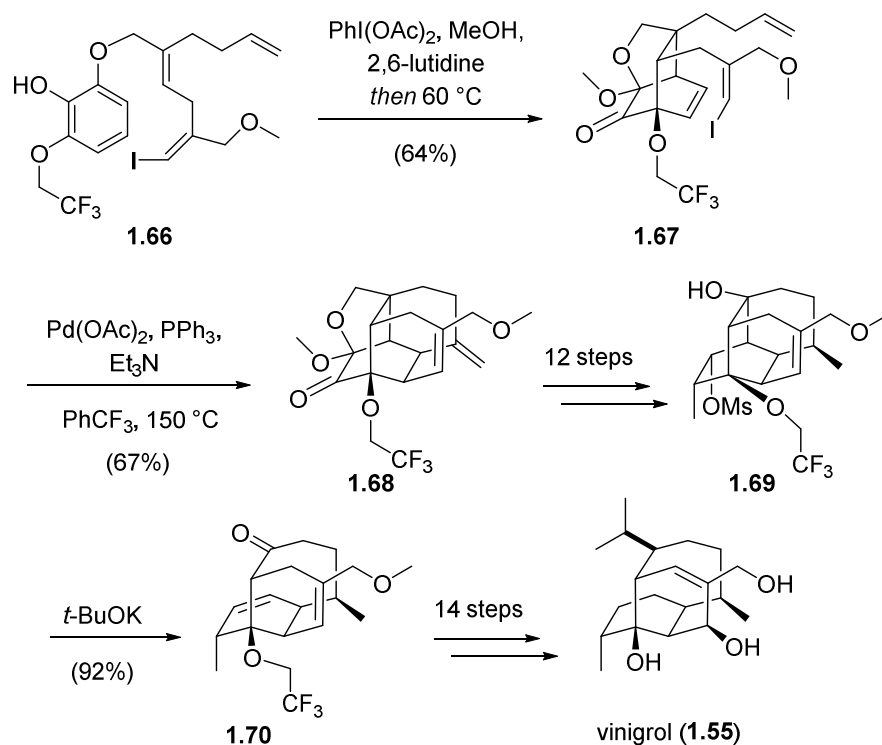
In the following chapter the key transformations in selected total syntheses of complex diterpenes will be discussed. The chosen examples were published in the past decade and are ordered according to the number of carbocycles. Far from being comprehensive, they should give the reader an overview of recent methods employed for the construction of challenging molecular structures.<sup>[22]</sup>

Isolated in 1987, vinigrol (**1.55**),<sup>[23]</sup> through its unique decahydro-1,5-butanonaphthalene ring system containing eight contiguous stereocenters, had prompted numerous attempts at its synthesis<sup>[24]</sup> but it took over two decades until the first total synthesis was disclosed by the Baran group (Scheme 1.8).<sup>[25]</sup> Their strategy was based on first an inter- followed by an intramolecular Diels–Alder reaction to forge the carbon scaffold. Thus,  $\text{AlCl}_3$  mediated [4+2]-cycloaddition of silyl enol ether **1.56** and ester **1.57** afforded intermediate **1.58** which was further elaborated to triene **1.59**. Even though the olefinic moieties in **1.59** were electronically not favorable for a Diels–Alder reaction, **1.59** still underwent the thermally induced cycloaddition to give tetracycle **1.60**, presumably due to a strong proximity effect. The decahydro-1,5-butanonaphthalene motif was then established through Grob fragmentation of alcohol **1.61**. To functionalize the decalin system an ingenious dipolar cycloaddition using dibromoformaldoxime (**1.65**) was used. The formed bromoisoxazole gave later rise to the vicinal methyl and tertiary hydroxyl group in **1.55**. This required first LAH reduction to amine **1.64** followed by primary isonitrile formation and radical deamination. Further six-step-modifications of the carbon framework lead to vinigrol (**1.55**).



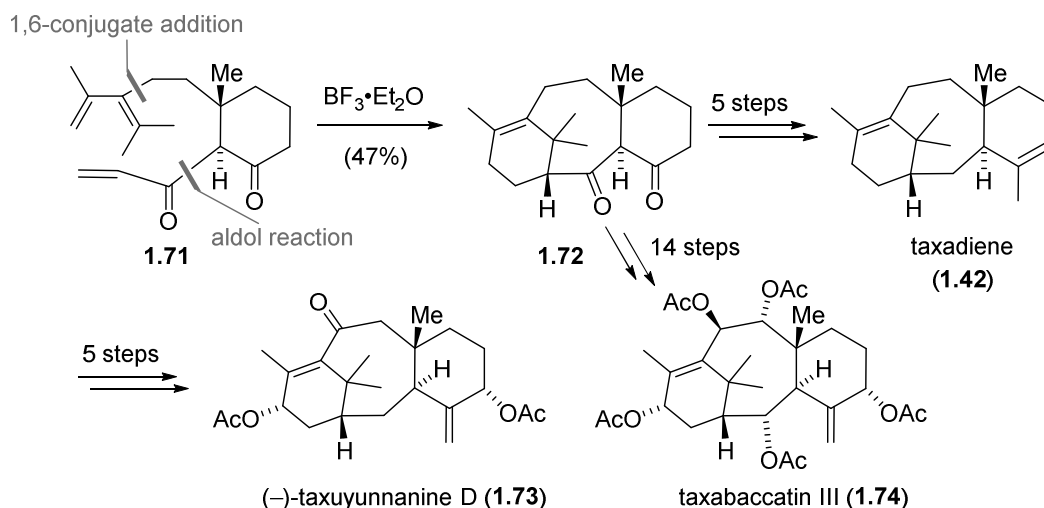
**Scheme 1.8.** Baran's synthesis of vinigrol (**1.55**).

In 2013 the Njardason group disclosed a different approach to (**1.55**) (Scheme 1.9), which built up the carbocyclic core in only two steps *via* a one-pot oxidative dearomatization/Diels–Alder sequence of **1.66** followed by a Heck cyclization cascade of product **1.67** to afford intermediate **1.68**.<sup>[26]</sup> Further functional group transformations resulted in alcohol **1.69** which upon treatment with base fragmented to unravel the bridged bicyclic framework of **1.55**, similar to the Baran synthesis. In the following 14 steps the isopropyl and the secondary, allylic hydroxyl groups were installed and the tertiary alcohol deprotected to give vinigrol (**1.55**).



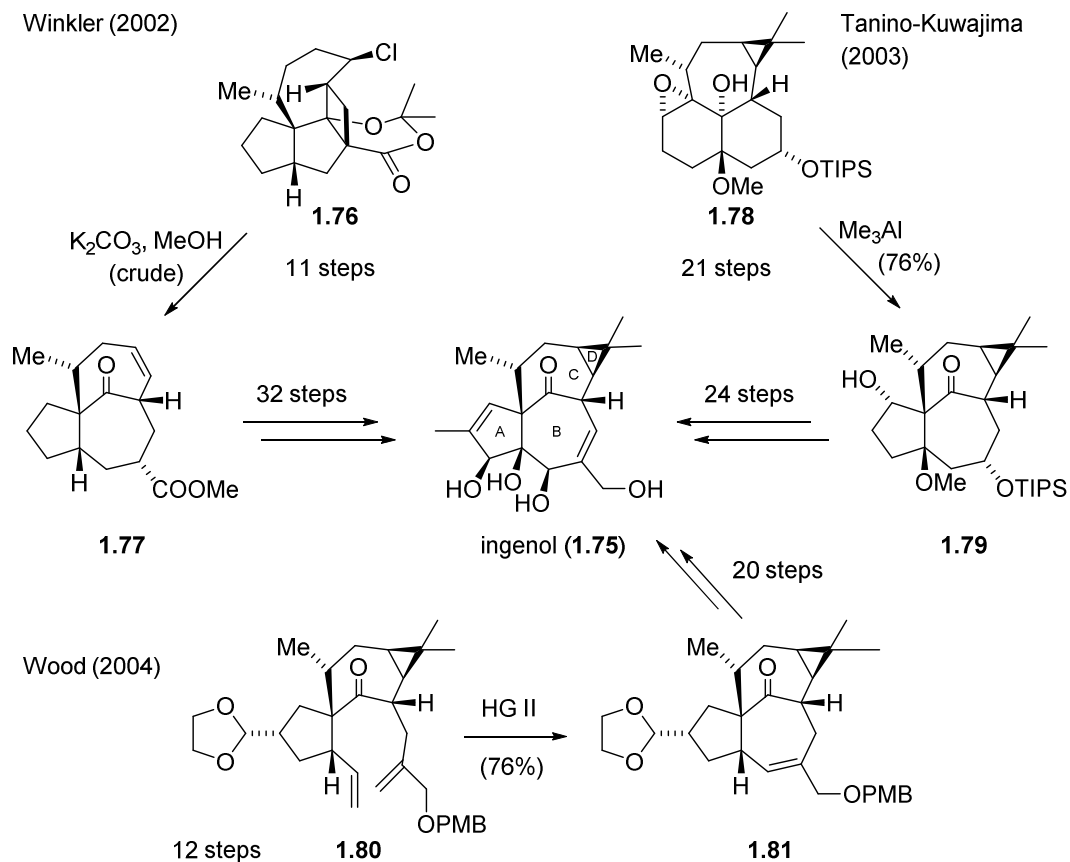
**Scheme 1.9.** Njardason's approach to vinigrol (**1.55**).

Taxadiene **1.42** is the least oxidized member of the taxanes, a family of terpenes comprising over 350 members. Its carbon skeleton has been a highly popular target as it is found in the famous cancer drug paclitaxel (**1.44**, see Chapter 1.1.1). In 2012, the Baran group disclosed a concise synthesis of **1.42** performed on gram-scale (Scheme 1.10).<sup>[27]</sup> To construct the tricyclic core they used triene **1.71**, assembled in four steps, in a Lewis acid mediated intramolecular Diels–Alder reaction which afforded diketone **1.72**. Subsequent removal of the carbonyl groups and introduction of a methyl moiety gave taxadiene (**1.42**). Based on this strategy to assemble the carbon framework, Baran and co-workers also developed syntheses for (–)-taxuyunnanin D (**1.73**)<sup>[28]</sup> and taxabaccatin III (**1.74**).<sup>[29]</sup>



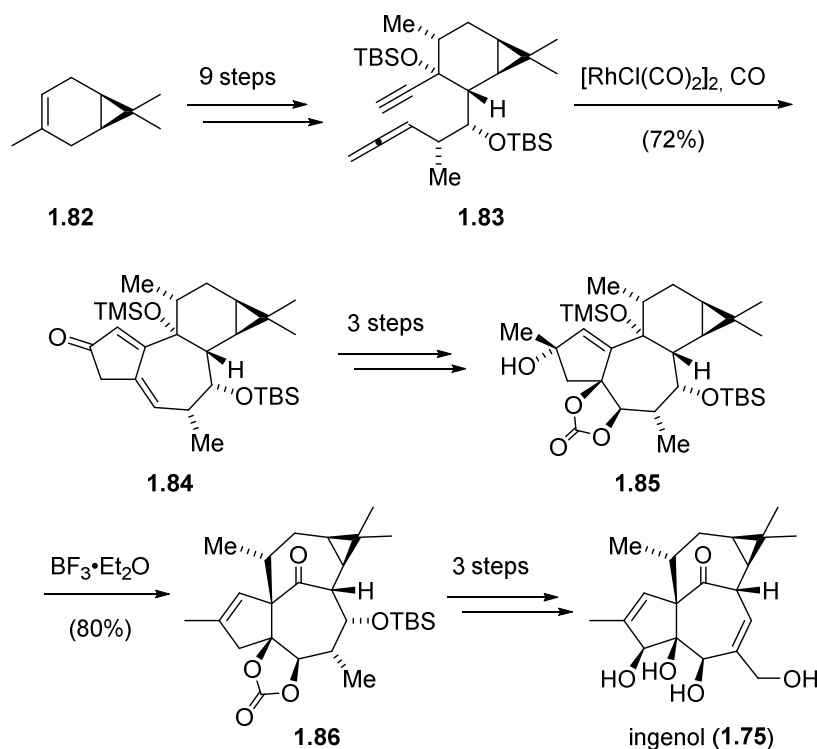
**Scheme 1.10.** Synthesis of taxadiene (**1.42**) and higher oxidized members of the taxane family.

Another unique diterpene is tetracyclic ingenol (**1.75**), a member of the phorboid family isolated from the genus *Euphorbia* in 1968 (Scheme 1.11).<sup>[30]</sup> Various esters of ingenol (**1.75**) have shown remarkable anticancer and anti-HIV activity.<sup>[31]</sup> Ingenol mebutate (structure not shown), the angelic acid ester of ingenol (**1.75**), has already become a FDA approved drug as topical treatment of actinic keratosis, a precancerous skin condition.<sup>[32]</sup> Structurally, ingenol (**1.75**) contains an unusual *trans*-fused (“in,out”)-bicyclo[4.4.1]undecane ring system, which makes the molecule considerably more strained than the *cis*-fused (“out,out”) analogue and represents a significant synthetic challenge. Ingenol’s (**1.75**) biological and structural characteristics have made it a very popular target in the organic community<sup>[33]</sup> with four total syntheses disclosed to date. The first one was published by the Winkler group in 2002 and was based on a DeMayo reaction to construct the ingenol core (Scheme 1.11). From ketone **1.77** a lengthy sequence of 32 steps led ultimately to ingenol (**1.75**).<sup>[34]</sup> In contrast to Winkler’s approach, Tanino-Kuwajima’s 43 step synthesis used a Pinacol-type rearrangement of epoxide **1.78** to establish the *trans*-fused BC-ring system.<sup>[35]</sup> The Wood group addressed the problem of constructing the ingenane skeleton by first building up spirocycle **1.80** and then closing the B-ring through a RCM.<sup>[36]</sup>



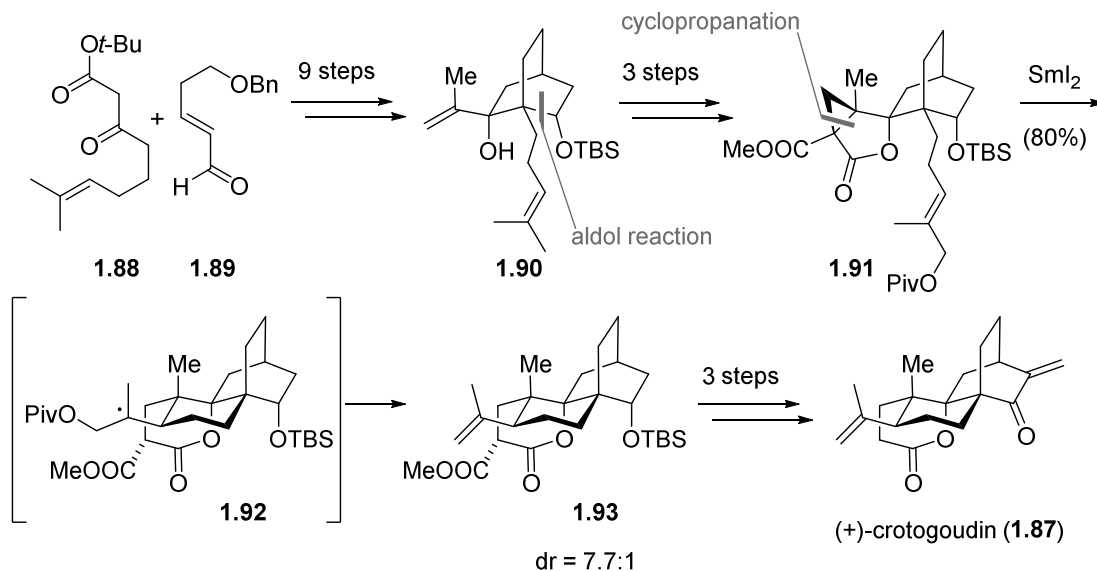
**Scheme 1.11.** Previous syntheses of ingenol (**1.75**).

In 2013, the Baran group disclosed a novel strategy to access ingenol (**1.75**) (Scheme 1.12) that represented a tremendous improvement in comparison to the previous routes, as it cut the necessary steps by more than half.<sup>[32]</sup> Starting from (+)-carene (**1.82**), alkyne **1.83** was quickly assembled in four steps and then used in a Pauson-Khand cyclization to form the fused 5-7-ring system of **1.75**. Subsequent 1,2-addition, dihydroxylation and carbonate formation gave **1.85** which upon exposure to  $BF_3 \cdot Et_2O$  underwent the crucial vinylogous Pinacol rearrangement, forming ketone **1.86**. The synthesis was then completed with a short series of standard transformations.



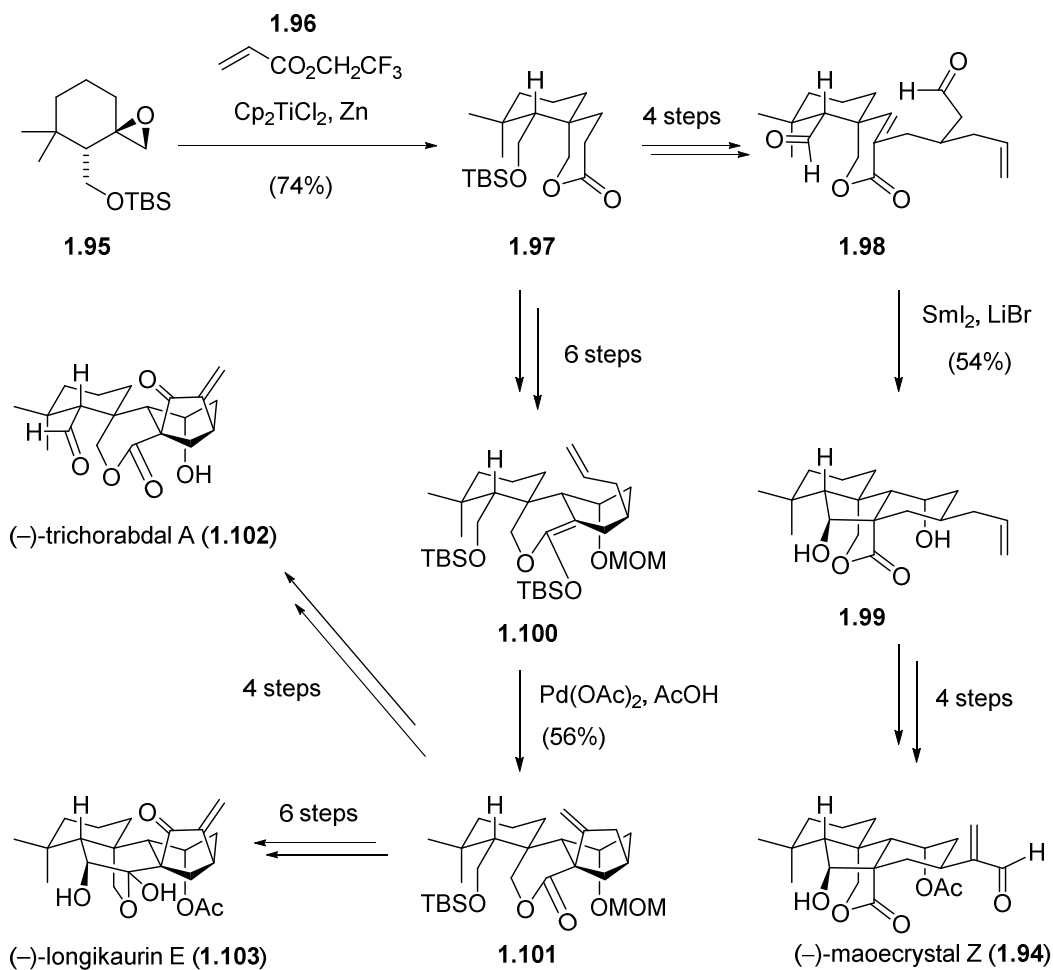
**Scheme 1.12.** Baran's synthesis of ingenol (**1.75**).

Another diterpene with a congested carbon framework is crotogoudin (**1.87**), isolated in 2010 from *Croton* plants.<sup>[37]</sup> Natural product **1.87** belongs to the rare 3,4-*seco* atisane family and its tetracyclic skeleton contains four contiguous stereocenters, two of which are quaternary carbons (Scheme 1.13). The first and so far only total synthesis was published by the Carreira group and relied on an elegant radical cyclopropane-opening/annulation/elimination cascade.<sup>[38]</sup> Starting from diketone **1.88** and enone **1.89**, bicycle **1.90** was prepared in nine steps, including an intramolecular aldol addition to build up the bicyclo[2.2.2]octane fragment of **1.87** and desymmetrization by baker's yeast reduction. Subsequent rhodium-catalyzed cyclopropanation, allylic oxidation and ester formation gave the key precursor **1.91**. Subjecting **1.91** to  $\text{SmI}_2$  initiated a sequence of cyclopropane ring opening, 6-*exo* trig cyclization to intermediate **1.92**, reduction and subsequent anionic  $\beta$ -elimination to afford alkene **1.93**. Having established the tetracyclic framework, (+)-crotogoudin (**1.87**) was synthesized in three additional steps, thereby establishing the absolute configuration of the natural product.



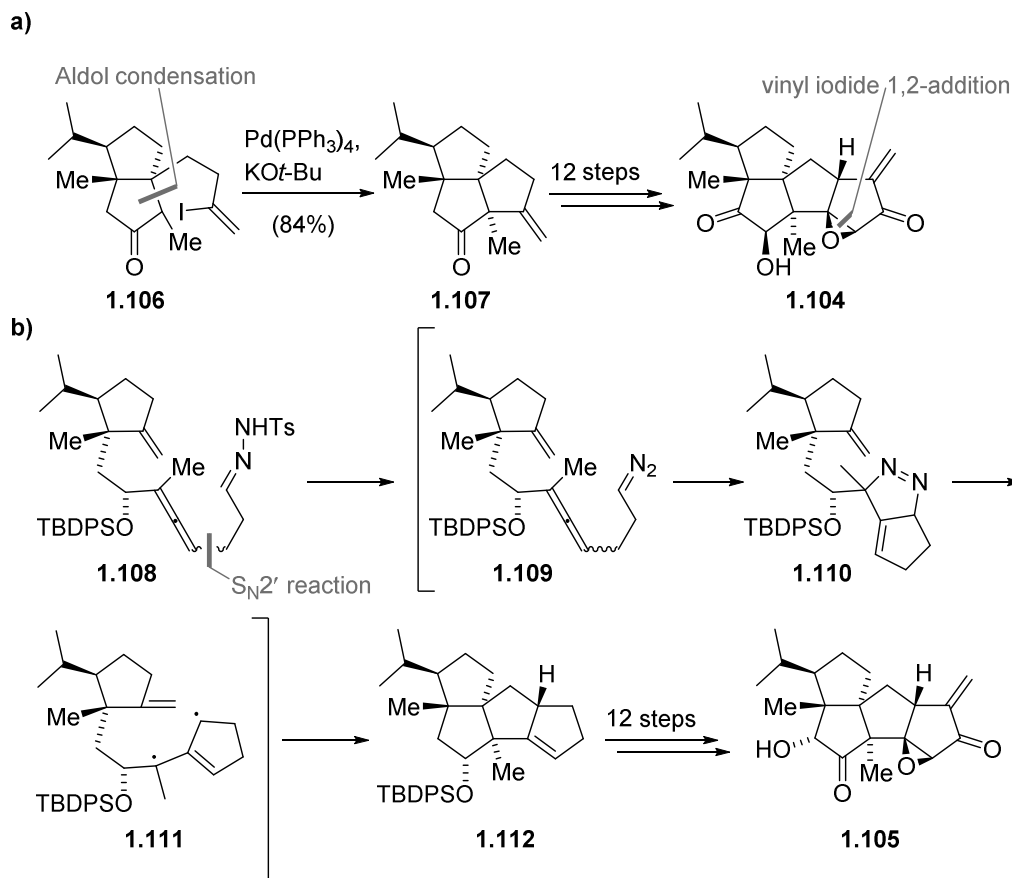
**Scheme 1.13.** Carreira's synthesis of (+)-crotogoudin (**1.87**).

A radical cascade was also employed as the key step in the Reisman synthesis of maeocrystal Z (**1.94**) (Scheme 1.14), a 6,7-*seco-ent*-kauranoid natural product that has a compact tetracyclic ring system with six vicinal stereocenters, two of which are all-carbon quaternary centers.<sup>[39]</sup> The first of them was set through a diastereoselective Ti(III)-mediated reductive coupling of epoxide **1.95** and trifluoroethyl acrylate (**1.96**) that gave spiro lactone **1.97** as a single diastereomer. Intermediate Compound **1.97** was then elaborated to dialdehyde **1.98** which underwent a radical cyclization cascade upon exposure to a mixture of SmI<sub>2</sub> and LiBr, which closed two rings and generated four stereocenters. Having constructed the tetracyclic carbon framework, a sequence of acetylation, ozonolysis, methylenation and saponification of alkene **1.99** delivered maeocrystal Z (**1.94**). Using spirocycle **1.97**, Reisman and co-workers could also access (–)-trichorabdal A (**1.102**) and (–)-lanogikaurin E (**1.103**) (Scheme 1.14),<sup>[40]</sup> two diterpenes closely related to **1.94**. Key step in both syntheses was the Pd-mediated oxidative cyclization of silyl ketene acetal **1.100**, derived from **1.97**, to construct the bicyclo[3.2.1]-octane motif. From tetracycle **1.101**, a series of standard transformations afforded (–)-trichorabdal A (**1.102**), whereas **1.103** was accessed in a six-step sequence comprising a Sm(II)-mediated Pinacol-type coupling between an aldehyde and lactone moiety (not shown).



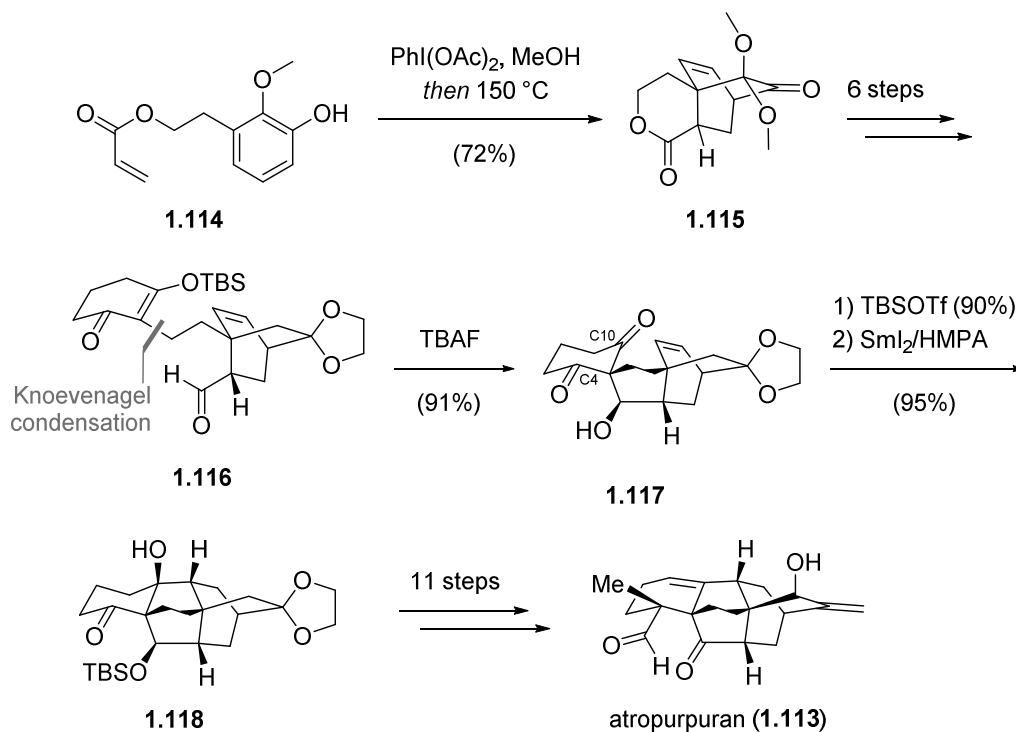
**Scheme 1.14.** Total syntheses of maoecrystal Z (**1.94**), (-)-trichorabdal A (**1.102**) and (-)-lanogikaurin E (**1.103**).

Crinipellins are a family of diterpenes that feature a unique tetraquinane scaffold, previously accessed by the Piers group in their total synthesis of crinipellin B (**1.104**) (Scheme 1.15.a).<sup>[41]</sup> They built the congested carbon skeleton in a sequential fashion, first by an Aldol condensation, followed by a Pd-mediated vinyl iodide coupling of **1.106**. The last 5-membered ring was then constructed by an intramolecular 1,2-addition. In 2014, Lee and co-workers disclosed a total synthesis of crinipellin A (**1.105**) (Scheme 1.15.b) based on a tandem [2+3] cycloaddition reaction of allenyl diazo **1.109**, generated from tosyl hydrazone **1.108**.<sup>[42]</sup> Nitrogen extrusion of **1.110** gave the diradical **1.111** which underwent another intramolecular cyclization to afford tetraquinane **1.112**. A series of 12 additional steps was needed to reach crinipellin A (**1.105**).



**Scheme 1.15.** a) Total synthesis of crinipellin B (**1.104**). b) Total synthesis of crinipellin A (**1.105**).

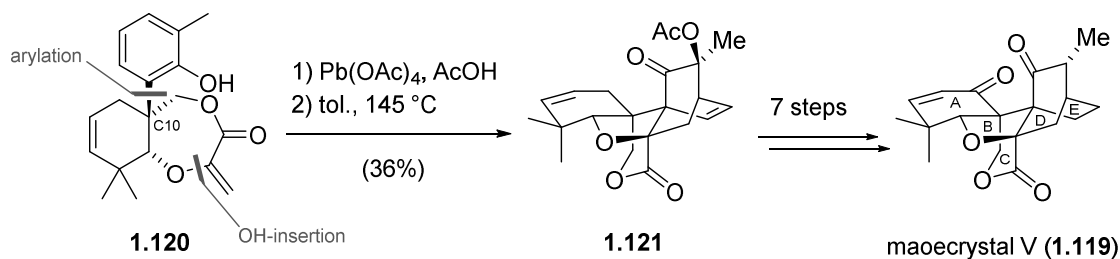
A complex pentacyclic diterpene is atropurpuran (**1.113**), isolated from *Aconitum hemisleyanum* var. *atropurpureum* in 2009.<sup>[43]</sup> To access its caged framework, the Qin group devised a strategy starting with an oxidative dearomatization/Diels–Alder cycloaddition cascade of phenol **1.114** which forged the bicyclo[2.2.2]octane part of **1.113** (Scheme 1.16).<sup>[44]</sup> Intermediate **1.115** was then elaborated to silyl enol ether **1.116** in six steps, including a reductive Knoevenagel condensation. This set the stage for an intramolecular aldol reaction followed by a  $\text{SmI}_2$  mediated ketyl-olefin cyclization which provided the congested framework of **1.113**. Interestingly, it was found that TBS protection of the secondary alcohol of **1.117** was crucial for the radical cyclization, presumably due to repulsion of the silyl group and the C4-ketone which brings the C10-carbonyl group into close proximity to the olefin. Further elaborations of **1.118** gave the natural product in additional 11 steps.



**Scheme 1.16.** Total synthesis of atropurpuran (**1.113**).

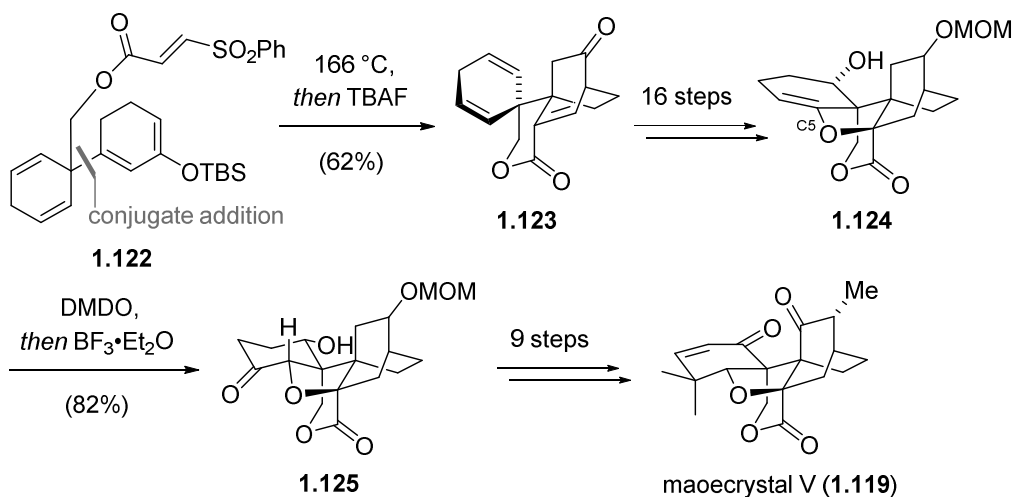
Another pentacyclic diterpenoid, maoecrystal V (**1.119**), was isolated in 1994 from the Chinese medicinal herb *Isodon eriocalyx* but uncertainty about the structural assignment prevented its disclosure. Eventually, in 2004 X-ray structure analysis unambiguously revealed the unique architecture of maoecrystal V (**1.119**),<sup>[45]</sup> which features a highly congested pentacyclic carbon skeleton adorned with six stereocenters, of which two are vicinal quaternary carbons (Scheme 1.17). In addition, **1.119** was found to display selective and potent activity against HeLa cells, with an  $\text{IC}_{50}$  value of 20 ng/mL. Its interesting biological properties in combination with its fascinating structure prompted many towards studies<sup>[46]</sup> resulting in several syntheses of **1.119**.<sup>[47]</sup> The first was published in 2011 by the Yang group, who used an elegant two-step sequence for the rapid construction of the complex core of the natural product (Scheme 1.17).<sup>[48]</sup> Enone **1.120** was prepared in 9 steps including an oxidative arylation to install the C10 quaternary carbon and a Rh-catalyzed O-H bond insertion. Treating **1.120** with  $\text{Pb}(\text{OAc})_4$ , AcOH lead to a Wessely oxidative dearomatization, leading to a diene that was then used in a thermally induced intramolecular Diels–Alder reaction, giving rise to the pentacycle **1.121**. In the remaining seven steps the allylic position was oxidized and the acetoxy group removed to afford maoecrystal V (**1.119**). Five years

later, the same group published an asymmetric synthesis based on a semipinacol rearrangement to obtain enantiopure **1.120**.<sup>[49]</sup>



**Scheme 1.17.** Yang's approach to maoecrystal V (**1.119**).

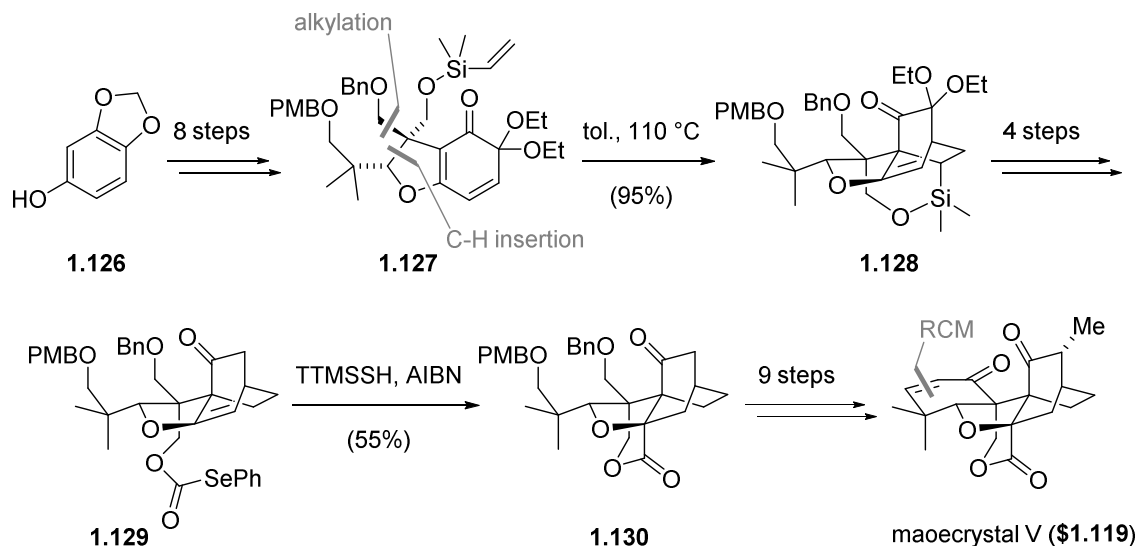
Danishefsky's approach to maoecrystal V (**1.119**) also hinges on an intramolecular Diels–Alder reaction to forge the [2.2.2] bicyclooctane motif of the molecule (Scheme 1.18), but uses silyl enol ether **1.122** as the substrate.<sup>[50]</sup> In order to establish the desired stereochemistry at the C5 position, they had to elaborate tetracycle **1.123** in a lengthy sequence to intermediate **1.124** which after epoxidation underwent a Meinwald rearrangement, setting the correct ring junction. Ketone **1.125** was then modified further to maoecrystal V (**1.119**) in nine steps.



**Scheme 1.18.** Danishefsky's approach to maoecrystal V (**1.119**).

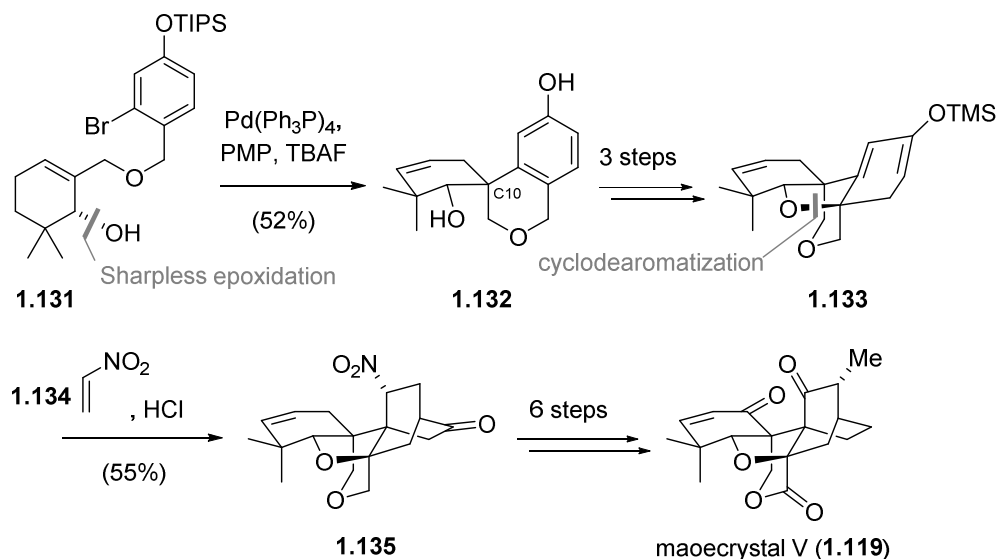
In another total synthesis of maoecrystal V (**1.119**) published by Zakarian and co-workers, the [2.2.2] bicyclooctane part was also constructed through an intramolecular Diels–Alder reaction but

in their case a silicon tethered dienophile was used (Scheme 1.19).<sup>[51]</sup> Compound **1.127** prepared in eight steps from sesamol (**1.126**), including a Rh-catalyzed C-H insertion to close the tetrahydrofuran ring. In contrast to Danishefsky's synthesis, the [4+2] cycloaddition product **1.128** already featured the central B-ring, whereas the lactone and A-ring were missing. The former was accessed employing a radical cyclization of selenocarbonate **1.129**, whilst the latter was built through RCM.



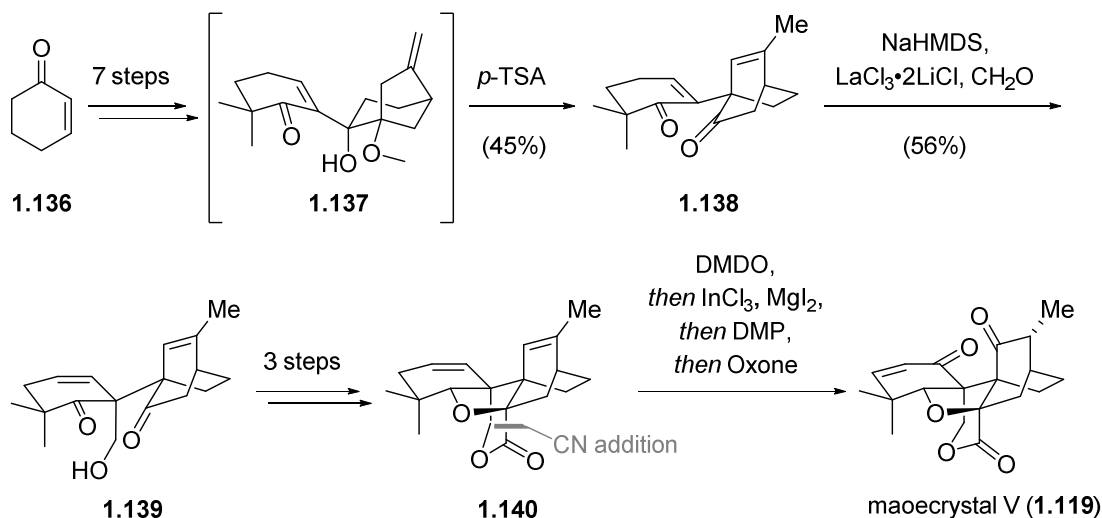
**Scheme 1.19.** Zakarian's approach to maoecrystal V (**1.119**).

A year later the Thomson laboratory published an enantioselective synthesis of **1.119**, where the quaternary C10-carbon was forged *via* a Heck spirocyclization of alkene **1.131**, whose one stereocenter was set using a Sharpless epoxidation (Scheme 1.20).<sup>[52]</sup> Intermediate **1.132** gave rise to silyl enol ether **1.133** in three steps, including an oxidative cyclodearomatization using  $\text{PhI}(\text{OAc})_2$  to close the tetrahydrofuran ring. Diene **1.133** then underwent an intermolecular Diels-Alder reaction with nitroethylene (**1.134**) through which the eastern bicyclic fragment of **1.119** was generated. Ketone **1.135** was then transformed to maoecrystal V (**1.119**) in six additional steps, the final one being a C-H oxidation to introduce the lactone-carbonyl group.



**Scheme 1.20.** Thomson's approach to maoecrystal V (**1.119**).

In contrast to the previous routes, Baran's strategy, published in 2016,<sup>[53]</sup> did not trace the [2.2.2] bicyclooctane motif back to a Diels–Alder reaction (Scheme 1.21). Instead, they prepared tertiary alcohol **1.137** starting from enone **1.136**. Upon treatment with *p*-TSA **1.137** underwent a Pinacol shift and double bond isomerization to afford tricycle **1.138**. Subsequent aldol reaction to install the C10 quaternary carbon represented a daunting challenge due to steric hindrance of that position, as well as chemo- and regioselectivity issues that needed to be overcome. After extensive experimentation it was found that the desired alcohol **1.139** could be obtained using NaHMDS with  $\text{LaCl}_3 \cdot 2\text{LiCl}$ . The missing B- and C-rings were then closed *via* ketal formation, cyanide addition followed by saponification. Additional transformations of intermediate **1.140** without work up afforded maoecrystal V (**1.119**) whose bioactivity was tested in different laboratories but contrary to previous reports, was not found to be active against various cancer cell lines (including HeLa).



**Scheme 1.21.** Baran's approach to maoecrystal V (**1.119**).

Terpenes such as maoecrystal V (**1.119**) or ingenol (**1.75**) are beautiful examples of how a single molecule can inspire a variety of approaches and how ingenious disconnections can lead to more concise and efficient syntheses. Despite the broad array of natural products that has been synthesized in the past decades, the construction of complex structures through synthetic means still remains a huge challenge, revealing the shortcomings of the tools available to organic chemists. Thus, intriguing molecules isolated from nature will continue to motivate chemists to push the possibilities of synthetic methods to their limits.

## 2. Project Background and Aims

### 2.1. Isolation and Structure of Wickerol A and B

In 2012, over the course of screening for novel antiviral compounds from microbial metabolites, the groups of Omura and Shiomi isolated wickerol A (**2.1**) and B (**2.2**) from the culture broth of the fungus *Trichoderma atroviride* FKI-3849.<sup>[54]</sup> They also isolated wickerol A (**2.1**) from a different fungus, *T. atroviride* FKI-3737, whereas B (**2.2**) was isolated by another group from *T. atroviride* S361, thus named trichodermanin A.<sup>[55]</sup> Elucidation of the relative configuration revealed the two natural products to be diterpenes with a caged tetracyclic carbon framework, with wickerol B (**2.2**) differing from A (**2.1**) only through the presence of a single hydroxyl group at the C8 position (Figure 2.1). While a 6-5-6 fused ring motif can be found in sesquiterpenes such as stereumins H-J (structure not shown),<sup>[56]</sup> the 6-5-6-6 carbon framework of the wickerols is unprecedented. The remarkable steric congestion of these molecules is reflected in the presence of numerous 1,3-diaxial interactions and the *syn*-pentane interactions resulting from the boat-type conformation adopted by ring D. Wickerol A (**2.1**) and B (**2.2**) possess seven and eight stereocenters respectively, of which two are quaternary carbons. An additional interesting structural feature is the C10a-C10b-C2a triad, which forms the BC- and BA-ring junction, both in a *trans*-fashion.

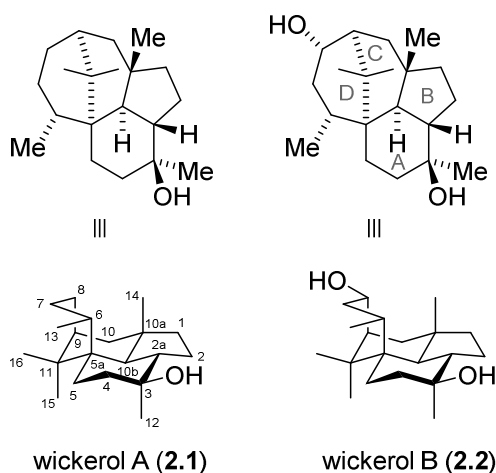


**Figure 2.1.** Structure of wickerol A (**2.1**) and B (**2.2**).

## 2.2. Biological Activity

*In vitro* evaluation of the biological activity of wickerol A (**2.1**) revealed that **2.1** was highly active against two type A/H1N1 viruses (A/PR/8/34 and A/WSN/33) with an  $IC_{50}$  of 0.07  $\mu\text{g}/\text{mL}$ , but not active against two A/H3N2 viruses (A/Guizhou/54/89 and A/Aichi/2/68) nor a B-type virus (B/Ibaraki/2/85). *In vitro* cytotoxicity was tested using MDCK cells and gave an  $IC_{50}$  value of 7.0 mg/mL. Interestingly, wickerol B (**2.2**), despite its only small structural difference from A (**2.1**), exhibited a very different biological profile. While **2.2** showed an antiviral effect against type A/H1N1 virus A/PR/8/34 ( $IC_{50}$  of 5.0  $\mu\text{g}/\text{mL}$ ), it did not inhibit the proliferation of other flu viruses at 100 mg/mL, nor of MDCK cells. The standard antiviral therapeutics amantadine hydrochloride (**2.3**), an M2 ion channel blocker, oseltamivir phosphate (**2.4**, Tamiflu) and zanamivir (**2.5**, Relenza) (Figure 2.2), two neuraminidase inhibitors, demonstrated a different antiviral spectrum than the wickerols, indicating that their mode of action might differ from **2.1** and **2.2**.<sup>[54]</sup>

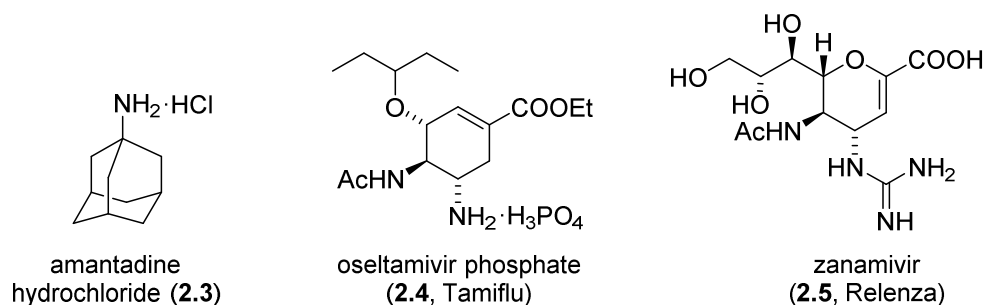
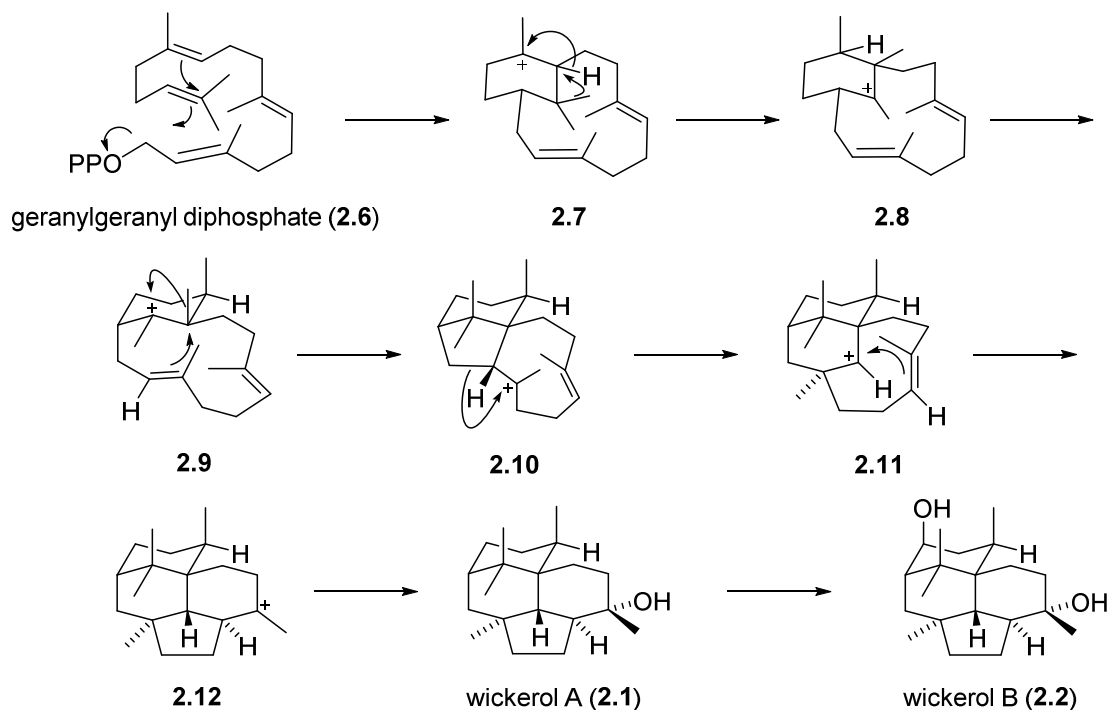


**Figure 2.2.** Structure of standard influenza therapeutics.

## 2.3. Biosynthesis of Wickerol A and B

Based on feeding experiments with  $^{13}\text{C}$ -labeled sodium acetate the groups of Omura and Shiomi proposed the biosynthesis depicted in Scheme 2.1.<sup>[54]</sup> The novel skeleton of **2.1** and **2.2** was suggested to be derived from geranylgeranyl diphosphate (**2.6**, GGPP), from which pyrophosphate is ejected in the first step. The resulting cation cyclizes to form a verticillen-12-yl cation intermediate **2.7** that is also proposed in the first step of the phomactatriene and taxadiene biosynthesis (see chapter 1.1.1). Next, a 1,2-shift of a  $\beta$ -methyl group, followed by an  $\alpha$ -hydride shift gives cation **2.8**, which undergoes a ring inversion and cyclization to form the 6-5-9 fused intermediate **2.10**. Subsequent ring expansion of **2.10** and attack of the remaining double bond

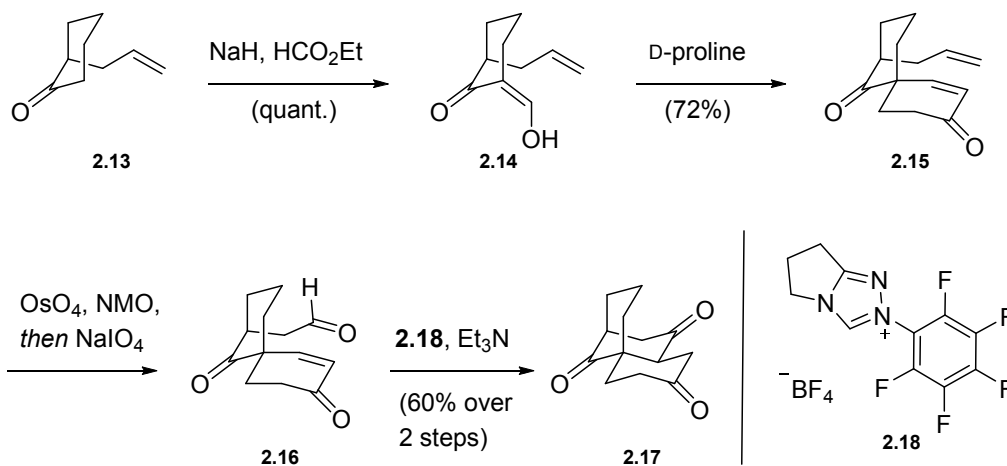
results in the formation of the fused 6-5-6-6 ring skeleton of the wickerols. In the final step, the C8-position of **2.1** is oxidized by a cytochrome P450 to form **2.2**.



**Scheme 2.1.** Proposed biosynthesis of wickerol A (**2.1**) and B (**2.2**).

## 2.4. Previous Work

To the best of our knowledge, only one study towards wickerol A (**2.1**) has been published. In 2014, Richard and co-workers disclosed a five step synthesis of the 6-6-6 tricyclic carbon motif of **2.1** (Scheme 2.2).<sup>[57]</sup> Starting from commercially available allylcyclohexanone (**2.13**), formylation and D-proline mediated Robinson annulation gave spirocycle **2.15**. Subsequent Lemieux–Johnson cleavage and NHC-catalyzed Stetter reaction delivered tricycle **2.17**. Since attempts at differentiating the keto groups were unsuccessful, the route was not pursued further.

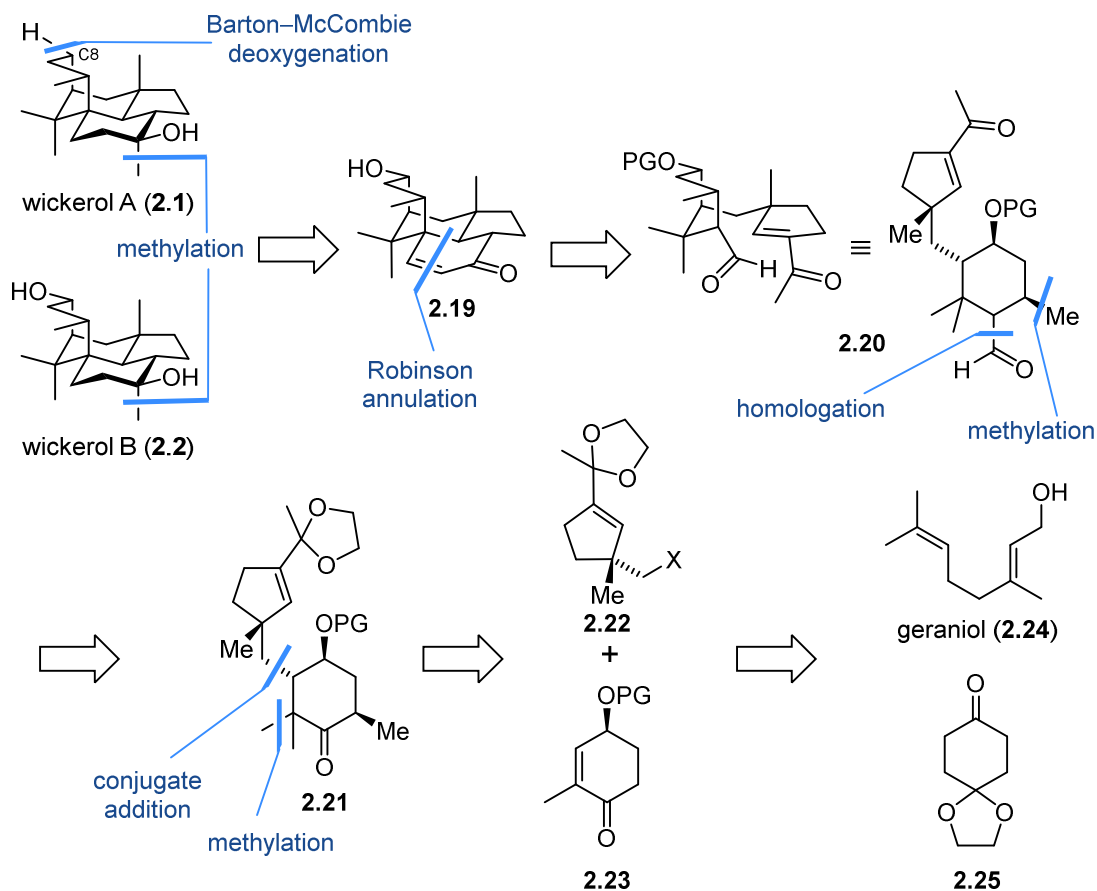


**Scheme 2.2.** Synthesis of the 6-6-6 tricyclic carbon framework of wickerol A (**2.1**).

## 2.5. Project Outline

Influenza viruses have a huge socioeconomic impact worldwide since they are responsible for the seasonal flu and pandemics. According to the WHO, seasonal flu is estimated to result in 250,000 to 500,000 deaths worldwide every year, whereas the occurrence and severity of a pandemic are unpredictable.<sup>[58]</sup> In the last 100 years, four outbreaks of influenza have developed into pandemics,<sup>[59]</sup> the last time in 2009, when a novel strain of the H1N1 virus, termed “swine flu”, spread globally and caused the deaths of over 18 000 people.<sup>[60]</sup> Despite the threat influenza poses, only a handful of antiviral drugs are available and there is growing concern over drug resistant influenza viruses rendering these treatments obsolete. As a consequence, there is a pressing need for the development of new antiviral therapeutics.

Such drugs might be found in nature, for example through screening microbial metabolites. During the course of such an endeavor, the groups of Omura and Shiomi isolated wickerol A (**2.1**) and B (**2.2**) from the culture broth of the fungus *Trichoderma atroviride* FKI-3849. Wickerol A (**2.1**) was found to be highly active against two type A/H1N1 viruses, whereas **2.2** possessed much weaker potency.<sup>[54]</sup> With their interesting biological activity and remarkable structure (see Chapter 2.1.) wickerol A (**2.1**) and B (**2.2**) represent formidable targets for total synthesis for which our original retrosynthetic plan is depicted in Scheme 2.3.



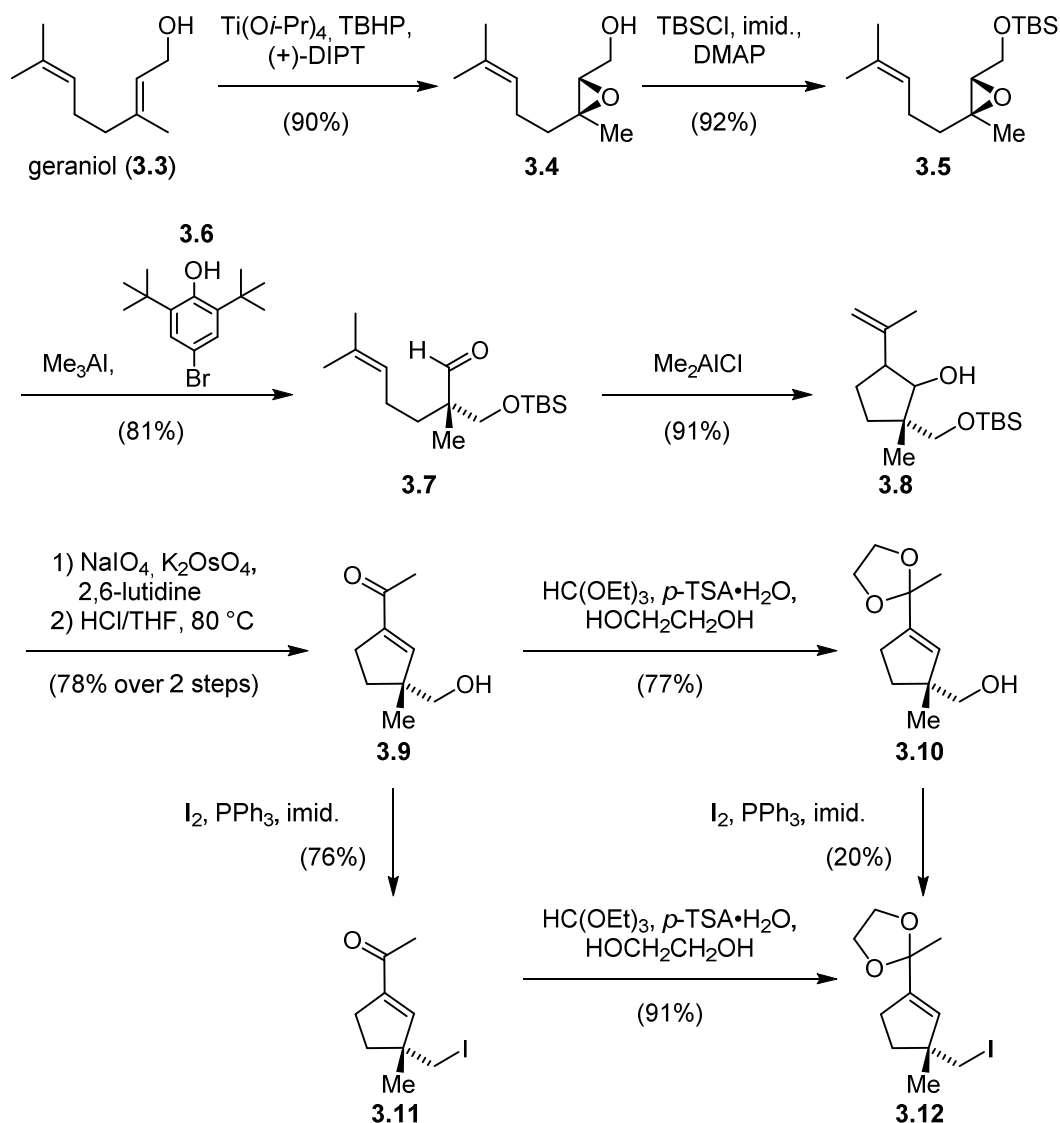
**Scheme 2.3** Retrosynthetic analysis of wickerol A (**2.1**) and B (**2.2**).

We envisioned that both natural products could be prepared from the common precursor **2.19** via hydrogenation and subsequent methyl addition with additional deoxygenation of the C8-position in the case of wickerol A (**2.1**). Formation of tetracyclic enone **2.19** represented the key step of our synthetic plan and could be achieved through an organocatalytic, diastereoselective intramolecular Robinson annulation of aldehyde **2.20**. Intermediate **2.20** could be accessed through epoxidation and Meinwald rearrangement of ketone **2.21** which in turn would arise from conjugate addition of the two building blocks **2.22** and **2.23**. Ketal **2.22** could be traced back to geraniol (**2.24**), whereas compound **2.23** would be prepared from ketone **2.25**. This strategy would lead to a highly convergent synthesis of wickerol A (**2.1**) and B (**2.2**) using of relative simple building blocks to quickly build up molecular complexity.

### 3. Results and Discussion

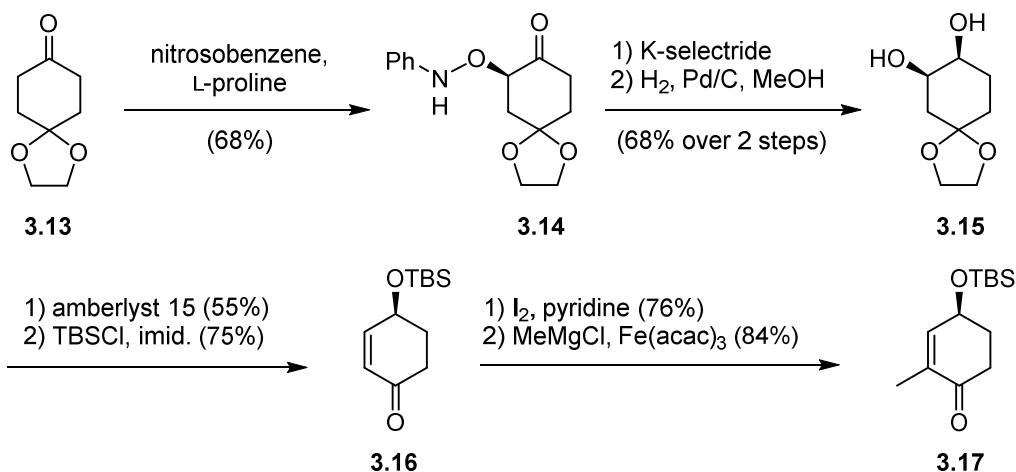
#### 3.1. First Generation Approach

Our endeavor towards the synthesis of wickerol A (**3.1**) and B (**3.2**) began with the preparation of building block **3.12** which we envisaged to be accessible through halogenation of geraniol (**3.3**) derived alcohol **3.9**. Following a route described by Yao and co-workers,<sup>[61]</sup> the sequence started with Sharpless asymmetric epoxidation<sup>[62]</sup> of geraniol (**3.3**), giving the product **3.4** in 80% *ee* as determined by Mosher ester analysis<sup>[63]</sup> (Scheme 3.1). After TBS-protection of the primary alcohol, **3.5** was subjected to a Yamamoto rearrangement using the *in situ* generated bulky Lewis acid MABR (methylaluminum bis(4-bromo-2,6-di-*t*-butylphenoxy))<sup>[64]</sup> which established the first quaternary stereocenter of wickerol A (**3.1**) and B (**3.2**). The next step comprised a [SmI<sub>3</sub>(THF)<sub>3.5</sub>]-complex mediated carbonyl ene-reaction of aldehyde **3.7** but in our hands product **3.8** could only be isolated in low yields. We therefore tested different Lewis acids and found that treating **3.7** with Me<sub>2</sub>AlCl afforded desired alcohol **3.8** as an inconsequential mixture of diastereomers (d.r.1:1.8:0.6:1.8) in excellent yields.<sup>[65]</sup> Subsequent Lemieux–Johnson cleavage<sup>[66]</sup> and elimination of the hydroxyl group with concomitant deprotection of the primary alcohol under acidic conditions furnished enone **3.9**. The following ketal formation could not be accomplished using the disclosed conditions (BF<sub>3</sub>·Et<sub>2</sub>O, ethylene glycol, HC(OEt)<sub>3</sub> at -78 °C) but we found that *p*-TSA·H<sub>2</sub>O in combination with a large excess of ethylene glycol and HC(OEt)<sub>3</sub> worked. We then focused our attention on iodination of alcohol **3.10**. Under Garegg–Samuelsson conditions,<sup>[67]</sup> iodide **3.12** could be isolated but only in low yields, due to incomplete conversion and ketone deprotection. This issue could not be alleviated by neither modifying the reaction parameters nor a two-step sequence including mesylation or tosylation of alcohol **3.10** followed by Finkelstein reaction.<sup>[68]</sup> Finally, we discovered that iodide **3.12** could be accessed by changing the order of events: halogenation of enone **3.9** first and then ketal formation gave the desired product **3.12** in excellent yields.



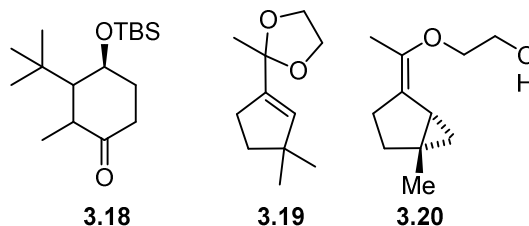
**Scheme 3.1.** Synthesis of iodide **3.12**.

The second building block, enone **3.17**, was prepared starting from commercially available ketone **3.13** (Scheme 3.2). In the first step, an enantioselective L-proline-catalyzed  $\alpha$ -aminoxylation<sup>[69]</sup> gave **3.14** which was diastereoselectively reduced using K-selectride. Subsequent reductive cleavage of the N–O bond, removal of the ketal with concomitant elimination of one secondary alcohol, followed by TBS-protection of the remaining hydroxyl group gave rise to enone **3.16**.<sup>[70]</sup> From **3.16**, iodination and iron-catalyzed cross coupling<sup>[71]</sup> afforded enone **3.17**.

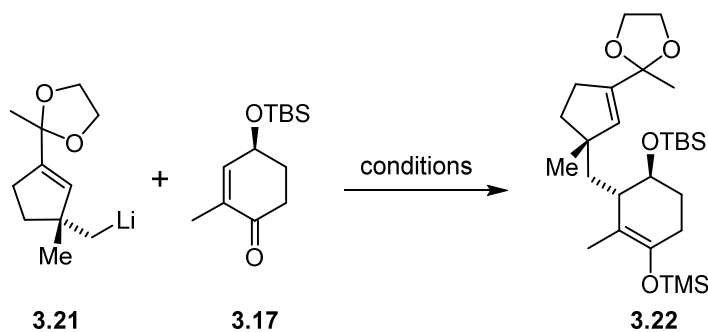


**Scheme 3.2.** Synthesis of enone **3.17**.

With both building blocks **3.12** and **3.17** in hand, we began investigating the conjugate addition (Table 3.1). Initial attempts using organolithium species **3.21**, generated from **3.12** with *t*-BuLi,<sup>[72]</sup> in combination a variety of copper sources were met with failure. Only starting material **3.17** and side products such as **3.18**, **3.19** and cyclopropane **3.20** were isolated (Figure 3.1). Vinyl ether **3.20** presumably arose from the intramolecular, nucleophilic attack of the organolithium species **3.21** onto the double bond, which could be prevented by keeping the mixture at  $-78\text{ }^\circ\text{C}$ . We then tried the conjugate addition in the presence of  $\text{BF}_3\cdot\text{Et}_2\text{O}$  or  $\text{TMSCl}$ , alone or in combination with  $\text{HMPA}$ ,<sup>[73]</sup> and could isolate some desired product using Li-thienylcyanocuprate<sup>[74]</sup> together with  $\text{TMSCl}/\text{HMPA}$  (Table 3.1, entry 10). After this positive result extensive screening of reaction conditions, changing equivalents, solvent and time was necessary (Table 3.2) but ultimately, robust conditions could be established that enabled performing the reaction on 2.34 mmol scale.



**Figure 3.1.** Identified side products of conjugate addition.

**Table 3.1.** Initial screening of conditions for conjugate addition.<sup>a</sup>

Entry	Copper source (eq.)	Eq. of <i>t</i> -BuLi	Lewis acid	Observation
1	CuI (0.5)	2	-	<b>3.17</b> + side products
2	CuBr·DMS (0.5)	2	-	<b>3.17</b> + side products
3	CuCN (0.5)	2	-	<b>3.17</b> + side products
4	CuI (0.5)	2	TMSCl	<b>3.17</b> + side products
5	CuBr·DMS (0.5)	2	TMSCl	<b>3.17</b> + side products
6	CuCN (0.5)	2	TMSCl	<b>3.17</b> + side products
7	Li-thienyl-cyanocuprate (1)	2	TMSCl	<b>3.17</b> + side products
8	CuBr·DMS (0.5)	2	TMSCl/HMPA	<b>3.17</b> + side products
9	CuCN (0.5)	2	TMSCl/HMPA	<b>3.17</b> + side products
10	Li-thienyl-cyanocuprate (1)	2	TMSCl/HMPA	<b>3.17</b> + side products + <b>3.22</b>

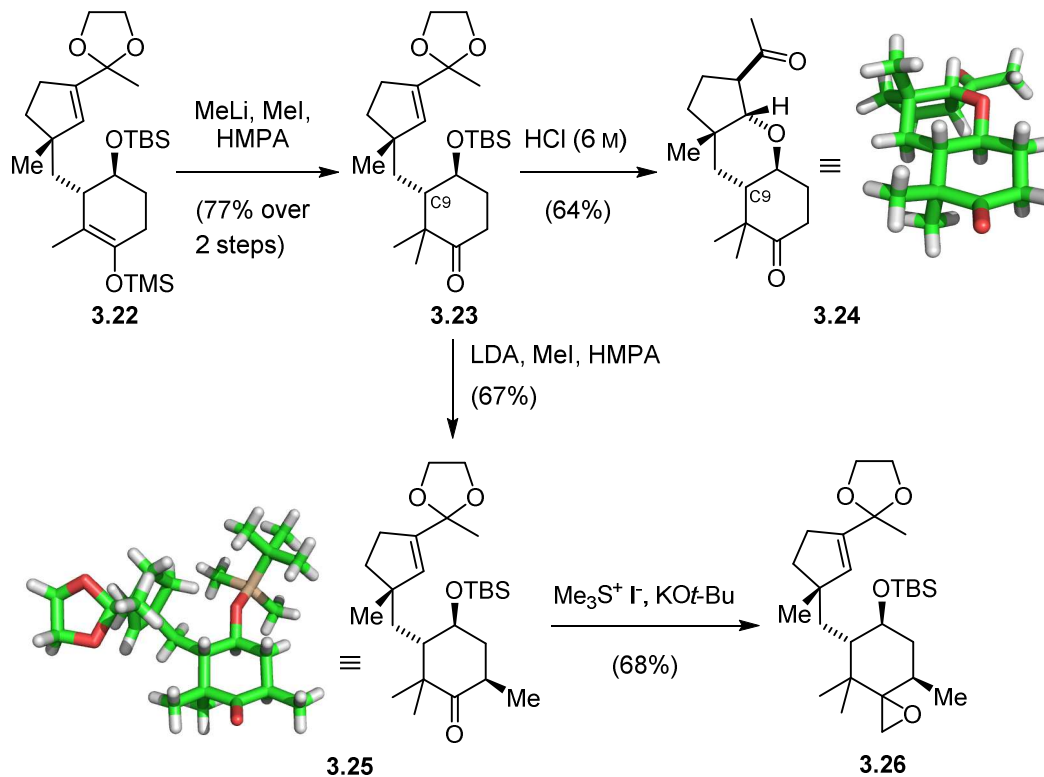
a) Reactions were carried out on a 0.025 mmol scale.

**Table 3.2.** Optimization of conjugate addition.<sup>a</sup>

Entry	Solvent	Eq. of <i>t</i> -BuLi	Lewis acid	Observation
1	Et <sub>2</sub> O/THF	2.0	TMSCl/HMPA	<b>3.22</b> + side products
2	Et <sub>2</sub> O/THF	1.5	TMSCl/HMPA	<b>3.22</b> + side products
3	Et <sub>2</sub> O/THF	1.5	TMSBr/HMPA	<b>3.22</b> + <b>3.17</b> + side products
4	Et <sub>2</sub> O/hexane	1.5	TMSCl/HMPA	<b>3.22</b> + <b>3.17</b> + side products
5	Et <sub>2</sub> O/THF	1.0	TMSCl/HMPA	<b>3.22</b> + <b>3.17</b> + side products

6	THF	1.5	TMSCI/HMPA	only side products
7 <sup>b</sup>	Et <sub>2</sub> O/THF	1.5	TMSCI/HMPA	<b>3.22</b> + <b>3.17</b> + side products
8	Et <sub>2</sub> O	2.0	BF <sub>3</sub> ·Et <sub>2</sub> O	only side products

a) Reactions were carried out on a 0.025 mmol scale. b) TMSCI/HMPA added before enone **3.17**.



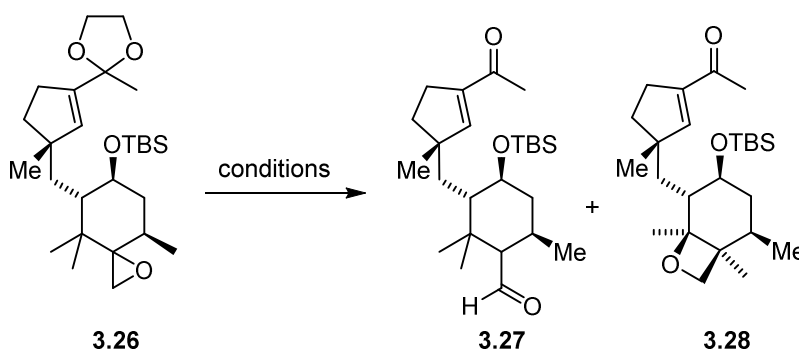
**Scheme 3.3.** Synthesis of epoxide **3.26**.

Silyl enol ether **3.22** was then methylated to afford ketone **3.23** which upon treatment with HCl underwent global deprotection and oxa-Michael reaction to give tetrahydropyran **3.24** of which was verified by X-ray crystallography, confirming the correct configuration at C9 (Scheme 3.3).

The synthesis proceeded with diastereoselective alkylation of ketone **3.23** resulting in **3.25** of which a X-ray crystal structure could be obtained. Subsequent Corey–Chaykovsky epoxidation<sup>[75]</sup> gave the product **3.26** with a d.r. of 1:0.6. Treating epoxide **3.26** with BF<sub>3</sub>·Et<sub>2</sub>O promoted ketal removal and the desired Meinwald rearrangement<sup>[68, 76]</sup> to aldehyde **3.27** in low yields with oxetane **3.28** formed as the major product (Table 3.3). This side product presumably arose from epoxide opening, followed by a Wagner–Meerwein shift and attack of the tertiary cation by the

oxygen atom. A number of different Lewis and Brønsted acids were tested (Table 3.3), but rearrangement to the undesired oxetane **3.28** could not be prevented. The best result was obtained using  $\text{InCl}_3$ <sup>[77]</sup> with a 1:0.6 ratio of product **3.27** to side product **3.28** which corresponded to the d.r. of epoxide **3.26**. These results indicated that only one of the diastereomers of **3.26** was able to undergo the Meinwald rearrangement whereas the other one gave oxetane **3.28**. Since it seemed that formation of significant amounts of **3.28** was unavoidable and its separation from product **3.27** was very difficult, we decided to investigate an alternative approach to access intermediate **3.27**.

**Table 3.3.** Conditions for rearrangement of epoxide **3.26**.<sup>a</sup>

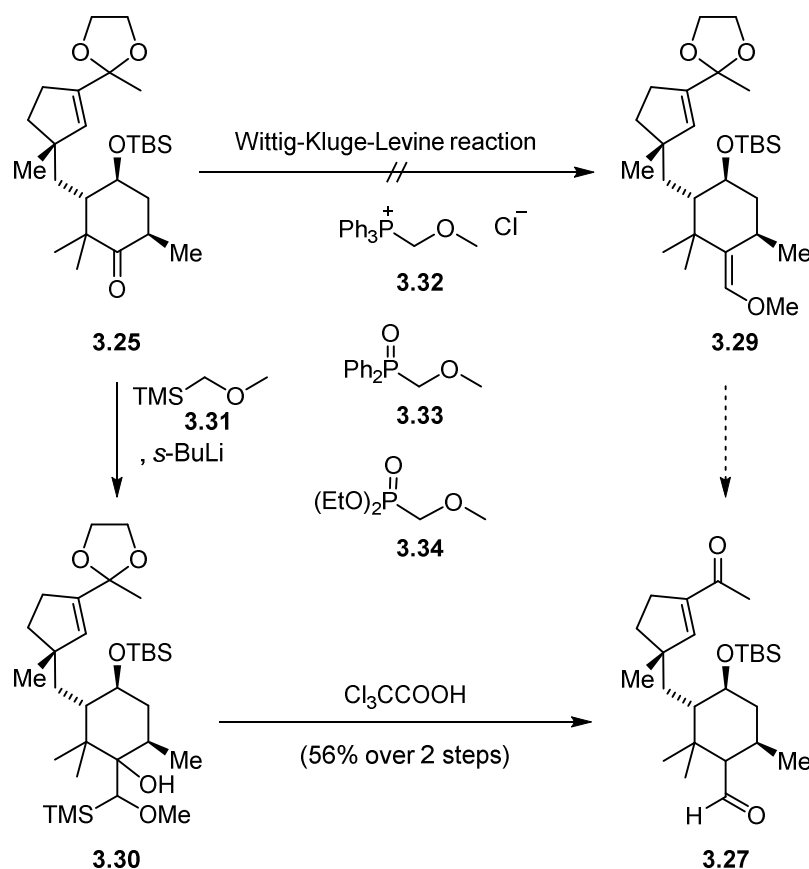


Entry	Lewis/ Brønstedt acid	Solvent	Ratio of <b>3.27</b> : <b>3.28</b>
1	$\text{BF}_3 \cdot \text{Et}_2\text{O}$	DCM	0.2:1
2	$\text{BiCl}_3$	benzene	1:0.6
3	$\text{InCl}_3$	benzene	1:0.6
4	$p\text{-TSA} \cdot \text{H}_2\text{O}$	benzene	0.2:1
5	$\text{MgBr}_2$	benzene	complex mixture
6	$\text{ZnBr}_2$	benzene	only ketal removal
7	$\text{SnCl}_4$	benzene	only ketal removal
8	$\text{TiCl}_4$	DCM	complex mixture
9	MABR	DCM	complex mixture
10	$\text{Bi}(\text{OTf})_3$	benzene	0.6:1
11	$\text{In}(\text{OTf})_3$	benzene	0.6:1

12	Sc(OTf) <sub>3</sub>	benzene	0.4:1
13	Yb(OTf) <sub>3</sub>	benzene	0.3:1
14	PPTS	benzene	complex mixture
15	NbCl <sub>5</sub>	toluene	complex mixture
16	(C <sub>6</sub> F <sub>5</sub> ) <sub>3</sub> B	toluene	only ketal removal
17	Et <sub>2</sub> AlCl	DCM	complex mixture
18	InCl <sub>3</sub>	toluene	1:0.6
19 <sup>b</sup>	InCl <sub>3</sub>	DCM	complex mixture
20 <sup>b</sup>	InCl <sub>3</sub>	MeCN	complex mixture

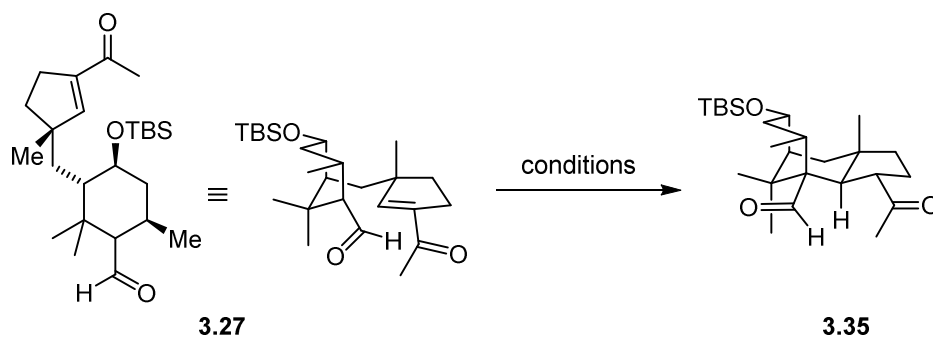
a) Reactions were carried out on a 3.2 μmol scale. b) 40 °C over night.

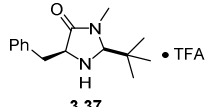
Next, we resorted to the Wittig–Kluge–Levine reaction followed by hydrolysis as an alternative homologation strategy. Unfortunately, neither phosphonium salt **3.32**<sup>[78]</sup> nor the less bulky phosphine oxide **3.33**,<sup>[79]</sup> nor phosphonate **3.34**<sup>[80]</sup> gave any product. We therefore opted for a Peterson olefination using methoxymethyltrimethylsilane (**3.31**).<sup>[81]</sup> Deprotonation of **3.31** using *s*-BuLi, followed by addition of ketone **3.25** led to the 1,2-addition product **3.30** which was then treated with KO<sup>t</sup>-Bu to elicit the elimination to vinyl ether **3.29**. This gave a complex and difficult to purify mixture and we therefore decided to isolate adduct **3.30** and treat it with acid, hoping for a one-pot elimination followed by hydrolysis. Indeed, the desired aldehyde **3.27** could be isolated as a 1:1 mixture of diastereomers in moderate yields.



**Scheme 3.4.** Synthesis of aldehyde **3.27**.

With the key intermediate **3.27** in hand, we began screening reagents for the Robinson annulation (Table 3.4). Inspired by work of the Yamamoto group, who used L-proline to mediate the diastereoselective, intramolecular Michael addition of an aldehyde onto an enone,<sup>[82]</sup> we subjected **3.27** to the same conditions (Table 3.4, entry 1) but observed no reaction, neither at elevated temperature nor in the presence of benzylamine<sup>[83]</sup> (Table 3.4, entry 2 and 3). Attempts to engage substrate **3.27** in a productive fashion with other cyclic amines<sup>[84]</sup> (Table 3.4, entry 4-7) were also met with failure. Trying to elicit the intramolecular ring closure with different bases mainly led to decomposition (Table 3.4, entry 8-13). We attributed these results to the steric hindrance of the substrate and the unfavorable conformation (both large substituents in axial positions) necessary to bring the nucleophilic and electrophilic site into close proximity. In light of these issues, we decided to focus our attention on a different strategy which is outlined in the next section.

**Table 3.4.** Conditions for intramolecular ring closure of **3.27**.

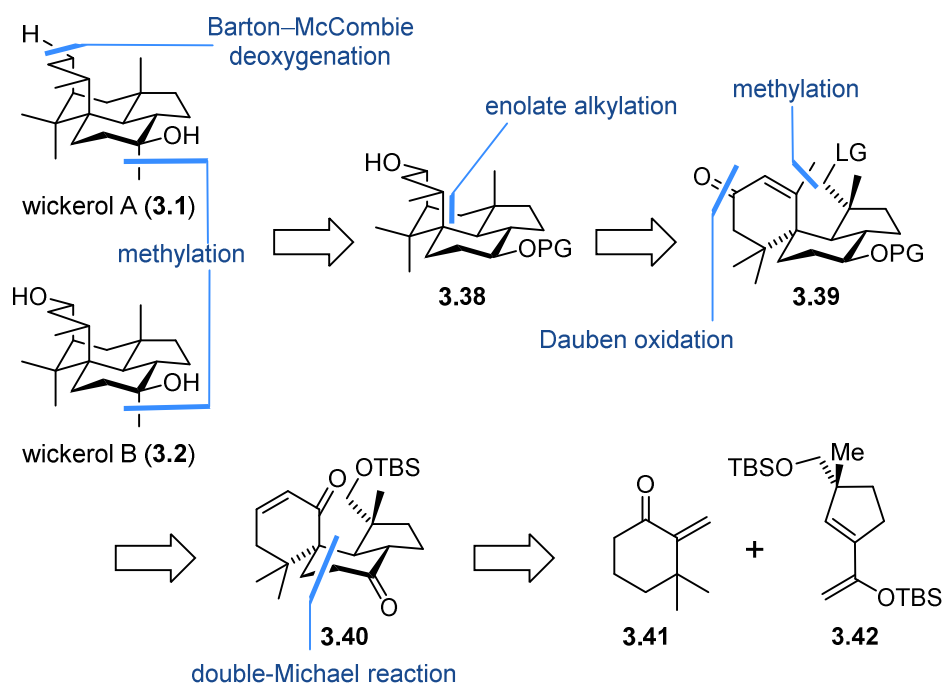
Entry	Reagents	Solvent	T [°C]	Observation
1	L-proline	DMF	r.t.	no reaction
2	L-proline	DMF	150	no reaction
3	L-proline. benzylamine	DCE	90	no reaction
4	pyrrolidine	DMF	150	decomposition
5	 3.36, benzylamine	DCE	90	complex mixture
6	morpholine	DMF	150	no reaction
7	 3.37 • TFA	THF	80	complex mixture
8	NaOMe	MeOH	r.t.	decomposition
9	NaOMe	THF	75	complex mixture
10	KOt-Bu/TBAB	toluene	130	decomposition
11	KOt-Bu	THF	r.t.	decomposition
12	DBU	toluene	130	decomposition
13	Et <sub>3</sub> N	toluene	130	decomposition

a) Reactions were carried out on a 7.1 μmol scale.

## 3.2. Second Generation Approach

### 3.2.1. Retrosynthetic Analysis

In our 2<sup>nd</sup> generation strategy (Scheme 3.5), the endgame for wickerol A (**3.1**) and B (**3.2**) would basically stay the same but we envisioned the common precursor **3.38** to be formed *via* an intramolecular alkylation of **3.29**, followed by reduction. Enone **3.29** could be accessed through a 1,2-methyl addition and Dauben oxidation<sup>[85]</sup> of spirocycle **3.40** which in turn would arise from a double-Michael-reaction<sup>[86]</sup> of enone **3.41** and diene **3.42**. Enone **3.41** is literature known<sup>[87]</sup> and can be prepared from commercially available 3-methyl cyclohexenone (**3.43**) in three steps whereas silyl enol ether **3.42** could be derived from alcohol **3.9**, an intermediate from our previous approach. This route would allow for rapid assembly of the congested central stereocenters with an early stage key step that can be tested with readily available building blocks.

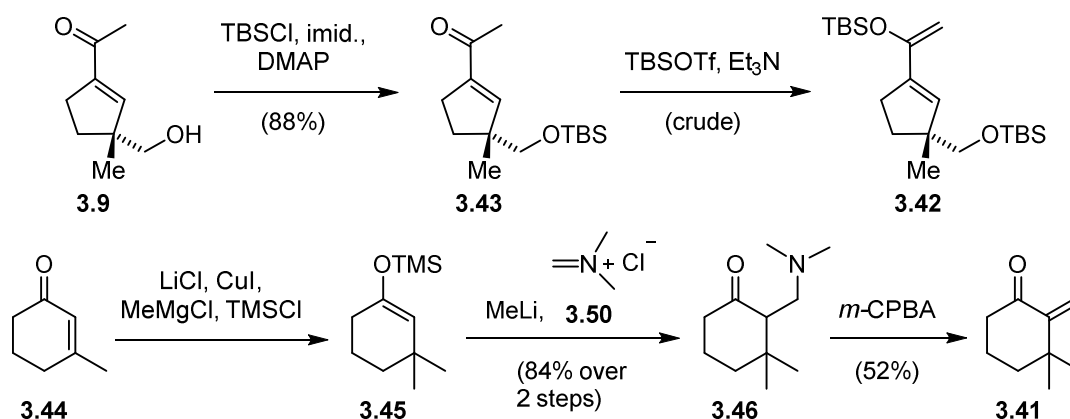


**Scheme 3.5.** 2<sup>nd</sup> generation retrosynthetic analysis of wickerol A (**3.1**) and B (**3.2**).

### 3.2.2. Results and Discussion

Building block **3.42** was prepared from **3.9** through TBS-protection of the hydroxyl group followed by silyl enol ether formation using TBSOTf and Et<sub>3</sub>N (Scheme 3.6). We could also access **3.43** *via* elimination of the secondary alcohol of compound **3.8** after Lemieux–Johnson cleavage, thereby avoiding a deprotection-reprotection sequence, but the overall yield was significantly lower.

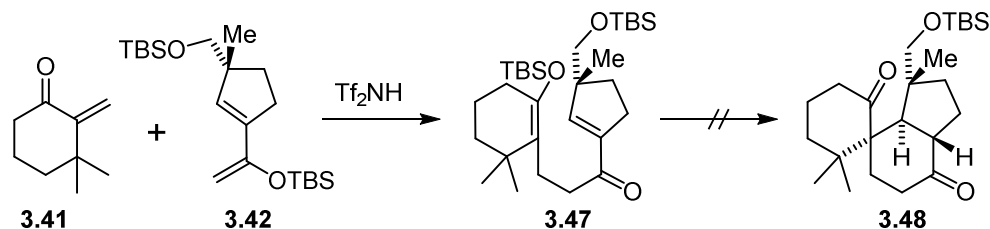
Next, we focused our attention on the synthesis of enone **3.41** (Scheme 3.6). In the first step, 3-methyl cyclohexenone (**3.44**) was subjected to conjugate addition with trapping of the enolate as TMS-silyl ether **3.45**,<sup>[88]</sup> followed by alkylation to give amine **3.46**. This in turn was oxidized with *m*-CPBA and underwent a Cope elimination<sup>[89]</sup> to form volatile enone **3.41** which was kept as a solution in toluene at –26 °C to avoid hetero-Diels–Alder reaction.



**Scheme 3.6.** Synthesis of silyl enol ether **3.42** and enone **3.41**.

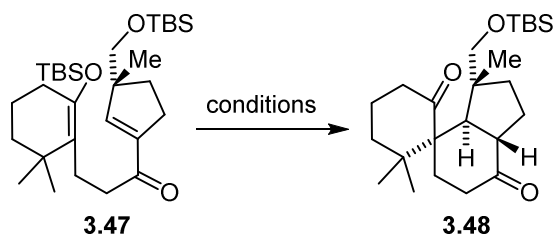
With both building blocks in hand, we began investigation the envisioned double-Michael reaction (Scheme 3.7). Intrigued by the work of the Jung group, who reported the double-Michael reaction of hindered silyloxydiene-dienophile pairs,<sup>[90]</sup> we treated **3.42** with Tf<sub>2</sub>NH in the presence of enone **3.41** in DCM at –78 °C. In addition to desilylation of **3.42**, we did observe the product of the Mukaiyama–Michael addition but neither addition of more Tf<sub>2</sub>NH nor letting the reaction mixture warm up to 0 °C led to spirocycle formation, contrary to the examples disclosed by Jung. Changing the reaction parameters such as concentration, equivalents, temperature and solvent did not change the outcome. We therefore tried to close the 6-membered ring in a separate step and subjected silyl enol ether **3.47** to a variety of Lewis acids (Table 3.5). Unfortunately, no product

**3.48** was isolated and mainly desilylation was observed, presumably due to steric hindrance of the substrate.



**Scheme 3.7.** Attempted double-Michael reaction.

**Table 3.5.** Conditions for intramolecular Mukaiyama–Michael reaction of **3.47**.<sup>a</sup>



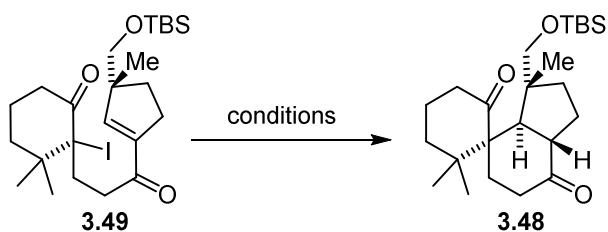
Entry	Lewis Acid	T [°C]	Observation
1	TBSOTf	-78	desilylation
2	$\text{Me}_3\text{Al}$	-78 to r.t.	desilylation
3	$\text{Me}_2\text{AlCl}$	-78 to -20	desilylation
4	$\text{Et}_2\text{AlCl}$	-78 to -50	complex mixture
5	$\text{Sc}(\text{OTf})_3$	0 to r.t.	complex mixture
6	$\text{Zn}(\text{OTf})_2$	0 to r.t.	complex mixture
7	$\text{Bi}(\text{OTf})_3$	r.t.	desilylation
8	$\text{Yb}(\text{OTf})_3$	r.t.	desilylation
9	$\text{Me}_3\text{Al}/\text{AlBr}_3$	-5	complex mixture
10	$\text{MeAl}(\text{NTf}_2)_2$	0 to r.t.	decomposition
11	$\text{TiCl}_4$	-78	desilylation
12	$\text{SnCl}_4$	-78	desilylation

13	BF <sub>3</sub> ·Et <sub>2</sub> O	-78	desilylation
----	------------------------------------	-----	--------------

a) Reactions were carried out on a 7.7 μmol scale.

Since ring closure *via* an intramolecular Mukaiyama–Michael reaction was unfruitful, we turned our attention to a radical cyclization. Radicals offer the advantage that they can be generated under mild conditions and are highly reactive which makes them very useful for the formation of congested bonds.<sup>[91]</sup> To that end, we prepared α-iodoketone **3.49** from **3.47** with I<sub>2</sub> in the presence of Cu(NO<sub>3</sub>)<sub>2</sub>·3H<sub>2</sub>O<sup>[92]</sup> and subjected it to a variety of conditions (Table 3.6). Using AIBN with different hydride sources such as Bu<sub>3</sub>SnH,<sup>[93]</sup> TTMSS<sup>[94]</sup> or Et<sub>3</sub>SiH<sup>[95]</sup> mainly resulted in dehalogenation. That was also the case when substoichiometric Bu<sub>3</sub>SnCl with NaBH<sub>4</sub>, a combination developed by Corey that keeps the Bu<sub>3</sub>SnH concentration low,<sup>[96]</sup> was employed. Trying to elicit ring closure using Sml<sub>2</sub><sup>[97]</sup> was also met with failure so we shifted focus to a Diels–Alder based strategy to construct spirocycle **3.48**, which will be described in the next section.

**Table 3.6.** Conditions for intramolecular, radical cyclization of **3.49**.<sup>a</sup>



Entry	Reagents	Solvent	Conc.[M]	Observation
1	AIBN, Bu <sub>3</sub> SnH (ΔT)	benzene	0.014	dehalogenation
2	AIBN, Bu <sub>3</sub> SnH (ΔT)	benzene	0.002	dehalogenation
3	AIBN, TTMSS (h·v)	benzene	0.009	dehalogenation
4	AIBN, TTMSS (ΔT)	benzene	0.002	dehalogenation
5	AIBN, Et <sub>3</sub> SiH (h·v)	benzene	0.009	dehalogenation
6	AIBN, Bu <sub>3</sub> SnCl, NaCNBH <sub>3</sub> (ΔT)	<i>t</i> -BuOH	0.008	dehalogenation
7	AIBN, Bu <sub>3</sub> SnCl, NaCNBH <sub>3</sub> (ΔT)	EtOH	0.008	complex mixture
8	AIBN, Bu <sub>3</sub> SnCl, NaCNBH <sub>3</sub> (h·v)	<i>t</i> -BuOH	0.009	dehalogenation
9	Bu <sub>6</sub> Sn <sub>2</sub> (h·v)	benzene	0.009	dehalogenation

---

10	Sml <sub>2</sub>	THF	0.015	dehalogenation
11	Sml <sub>2</sub>	THF	0.008	dehalogenation
12	Sml <sub>2</sub> , HMPA	THF	0.008	dehalogenation
13	Sml <sub>2</sub> , HMPA, <i>t</i> -BuOH	THF	0.008	dehalogenation
14	Sml <sub>2</sub> , HMPA, MeOH	THF	0.008	decomposition

---

a) Reactions were carried out on a 7.5–9.4 μmol scale.

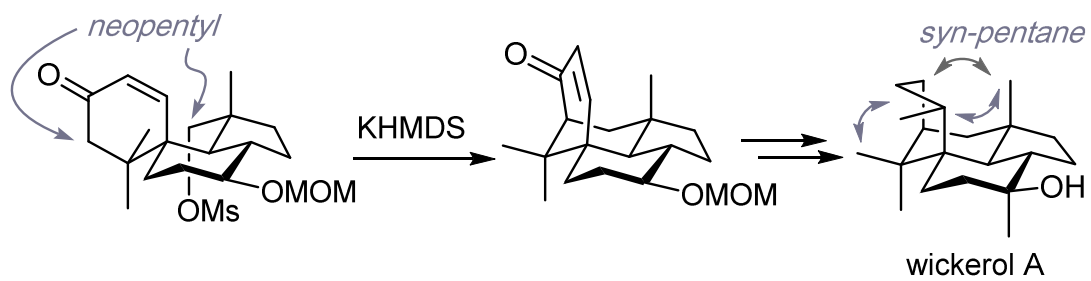
### 3.3. Asymmetric Synthesis of the Antiviral Diterpene Wickerol A

Reprinted with permission from:

S.-A. Liu and D. Trauner,

*J. Am. Chem. Soc.*, **2017**, ASAP.

Copyright © 2017 The American Chemical Society



## Asymmetric Synthesis of the Antiviral Diterpene Wickerol A

Shu-An Liu<sup>†</sup> and Dirk Trauner<sup>\*,†,‡,§</sup>

<sup>†</sup>Department of Chemistry and Center for Integrated Protein Science, Ludwig-Maximilian University Munich, Butenandtstraße 5-13, 81377 Munich, Germany

<sup>‡</sup>Department of Chemistry, New York University, 100 Washington Square East, New York, New York 10003, United States

**S** Supporting Information

**ABSTRACT:** Wickerol A (1) is an unusual diterpene with remarkable activity against the H1N1 influenza virus. Its tetracyclic skeleton contains three quaternary carbons and is marked by several *syn*-pentane interactions which force a six-membered ring into a twist-boat conformation. We present an asymmetric synthesis of wickerol A (1) that is based on a Jung Diels–Alder reaction, an intramolecular alkylation to complete the 6–5–6–6 ring system, and a conjugate addition, all of which overcome considerable steric strain. During the synthesis, we isolated an unexpected cyclopropane that presumably stems from a carbonium ion intermediate.

Terpenes continue to challenge synthetic chemists with the complexity of their hydrocarbon scaffolds,<sup>1</sup> which are often highly strained. This strain can be photochemical in origin but usually stems from the ability of terpene cyclases to bend linear cyclization precursors into high-energy conformations and promote hydride and carbon–carbon bond shifts that are otherwise unlikely to proceed.<sup>2</sup> A case in point are the wickerols, two bioactive diterpenes isolated from the fungus *Trichoderma atroviride* FKI-3849 by Ōmura and Shioimi (Figure 1).<sup>3</sup> Wickerol A (1) proved to be highly active

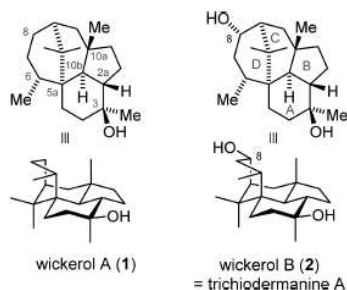


Figure 1. Structure of wickerol A (1) and B (2).

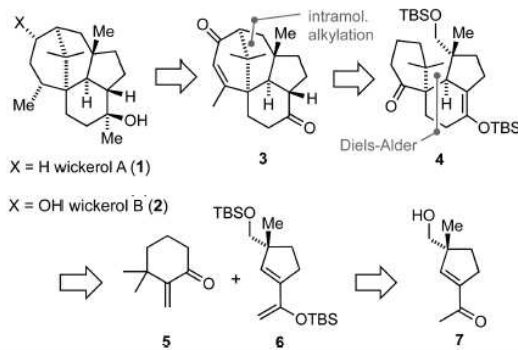
against the type A/H1N1 influenza virus with an  $IC_{50}$  of 0.07  $\mu\text{g}/\text{mL}$ , whereas wickerol B (2), which differs from its congener only by hydroxylation at C8, was significantly less potent ( $IC_{50}$  of 5.0  $\mu\text{g}/\text{mL}$ ). Wickerol B (2) turned out to be identical with the previously reported natural product trichodermanine A (2).<sup>4</sup> Both natural products feature a unique tetracyclic carbon skeleton that comprises two adjacent quaternary carbons and seven or eight stereocenters, respectively, two of which are

quaternary as well. Although the 6–5–6–6 skeleton of the wickerols contains only five and six-membered primary rings, the molecules are remarkably strained due to numerous *syn*-pentane interactions. These primarily involve the angular methyl group at C10a that force the D-ring into a boat conformation, as confirmed by X-ray analysis.<sup>3</sup> The corresponding strain was estimated to be in the range of 60–70 kJ/mol (see Supporting Information for DFT calculations on isomers of wickerol A (1)).

Despite the formidable challenge posed by the wickerols, only a single synthetic study has been disclosed to date.<sup>5</sup> We now report an asymmetric synthesis of wickerol A (1) that is a testament to the power of catalysis in cycloadditions and the many pleasant and unpleasant surprises that one encounters when working with complex, sterically congested molecules.

Our synthetic strategy toward the wickerols is shown in Scheme 1. We envisioned that both could be derived from a

### Scheme 1. Retrosynthetic Analysis of the Wickerols



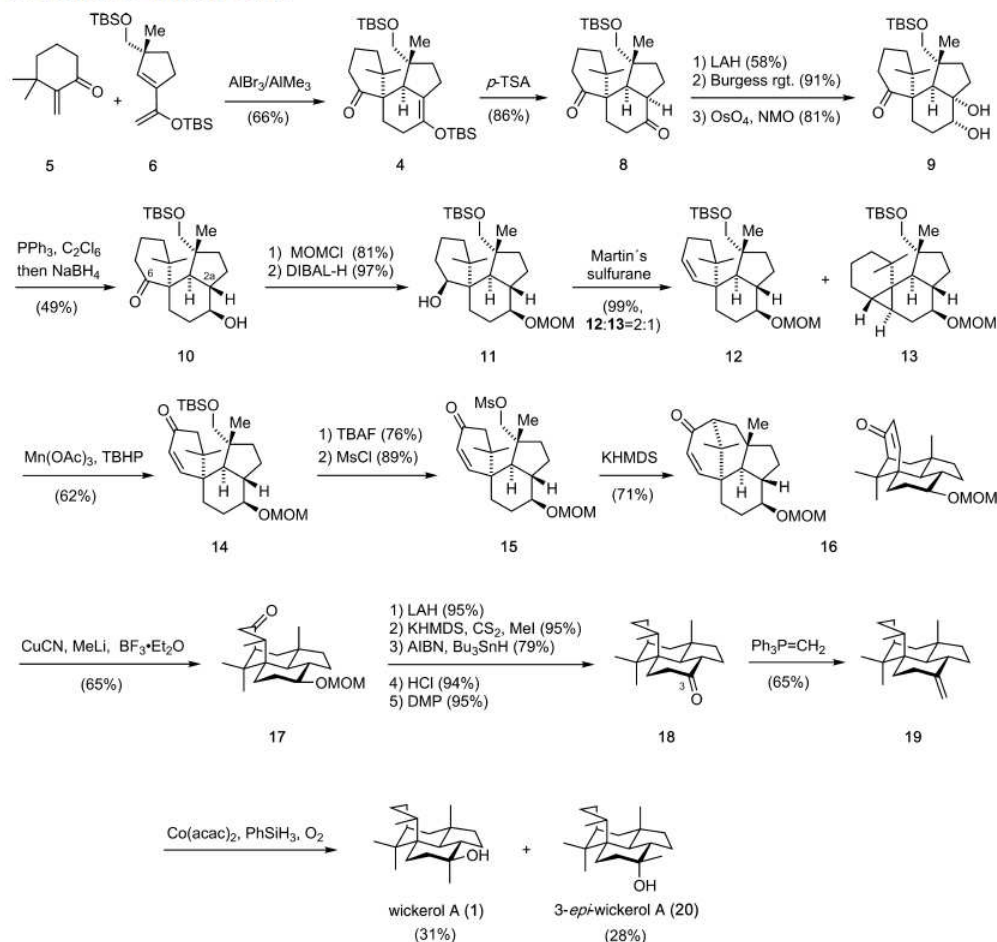
diketone of type 3 via conjugate reduction and addition of a methyl group. Disconnection of the C-ring would lead to a *spiro* tricycle of type 4. In the forward direction, the ring would be closed through an intramolecular alkylation.

Key intermediate 4, which contains all carbons of the wickerols save two, could be accessed with a Diels–Alder addition<sup>6</sup> of known enone 5<sup>7</sup> to diene 6. The latter in turn, would be derived from known ketone 7, which is readily accessible from geraniol via Sharpless-epoxidation, Yamamoto-rearrangement<sup>8</sup> and carbonyl–ene cyclization.<sup>9</sup>

Received: May 19, 2017

Published: June 18, 2017

Scheme 2. Synthesis of Wickerol A (1)



Our actual synthesis commenced with the Diels–Alder addition<sup>10</sup> of the achiral enone 5 to the chiral diene 6 (Scheme 2), which could be procured from 7<sup>9</sup> in two steps (see Supporting Information). The intermolecular cycloaddition represented a major challenge because both partners, though electronically matched, are sterically very hindered. Initially, we explored thermal or high pressure conditions,<sup>11</sup> but all our efforts in this regard proved to be unsuccessful.

We then focused our attention on Lewis and Brønsted acid activation and found that commonly used Lewis acids such as  $\text{BF}_3 \cdot \text{Et}_2\text{O}$ ,  $\text{BCl}_3$ ,  $\text{TiCl}_4$ ,  $\text{SnCl}_4$ ,  $\text{Ti}_2\text{NH}$ ,<sup>12</sup>  $\text{Me}_2\text{AlNTf}_2$ ,<sup>13</sup>  $\text{Me}_2\text{AlCl}$ ,  $\text{Et}_2\text{AlCl}$  or  $\text{AlCl}_3$  resulted in desilylation of 6, dimerization of 5 via hetero-Diels–Alder reaction, or Mukaiyama–Michael addition without ring closure. However, Jung's conditions, which employ a mixture of  $\text{AlBr}_3/\text{AlMe}_3$  as a catalyst, gave the desired *endo*-product 4 as a single diastereomer.<sup>14</sup> Both the quaternary and the neopentyl stereocenters were set with the correct simple and induced diastereoselectivity. Presumably, the enone approaches the diene via an *endo*-transition state and the methyl group provides less steric hindrance than the siloxy methyl moiety.

With three of the four rings of wickerol A (1) established, we set out to prepare the requisite precursor for the intramolecular

alkylation. For that purpose, a 1,3-transposition of the carbonyl group in 4 was necessary, which we envisioned to achieve through 1,2-methyl addition, elimination of the resulting tertiary alcohol and allylic oxidation. Unfortunately, all attempts to add an organometallic reagent<sup>15</sup> to 4 or perform an olefination<sup>16</sup> failed, presumably due to the extreme steric hindrance of the carbonyl group or its competing enolization. We hypothesized that establishing the correct configuration at the A,B-ring junction would lead to a conformational change that would make the ketone more accessible. Upon hydrolysis of Diels–Alder product 4, however, we obtained unwanted *cis*-hydrindanone 8 as the sole product. Notably, the corresponding *cis*-fused isomer of wickerol A (1) is less stable than the *trans*-fused isomer (see Supporting Information for DFT calculations). Epimerization to the desired *trans*-hydrindanone under a variety of conditions proved unsuccessful, reflecting a thermodynamic preference of ca. 14 kJ/mol for the *cis*-fusion (see Supporting Information).<sup>17</sup> To solve this problem, we turned to the Grainger method, which has proven to be very useful in the synthesis of *trans*-hydrindanes.<sup>18</sup> Thus, we selectively reduced one of the carbonyl groups in 8, eliminated the resultant secondary alcohol regioselectively using Burgess reagent,<sup>19</sup> and dihydroxylated<sup>20</sup> the resultant alkene from the

more accessible face, which yielded diol 9. Treatment of 9 under Grainger's<sup>18b</sup> conditions indeed afforded the desired *trans*-fused hydrindanone via stereospecific hydride shift. To prevent epimerization during workup, we reduced the carbonyl group *in situ*, which gave alcohol 10. The desired A,B-ring *trans*-junction was confirmed by X-ray structure analysis of diol 21, obtained through TBS-deprotection of the primary hydroxyl group (Figure 2 and Supporting Information).

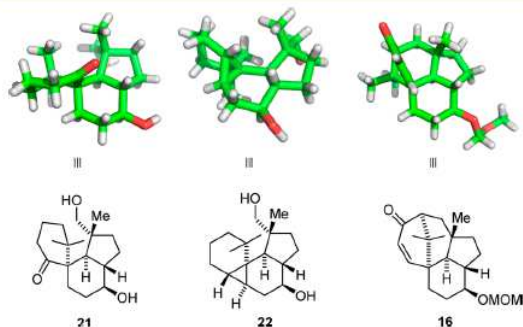


Figure 2. X-ray structures of 21, 22 and 16.

Having set the correct configuration at C2a, we turned to the modification of ring D. Again, the carbonyl group at C6 proved to be unreactive toward methyl addition or methylenation.

Therefore, we protected the secondary alcohol as a MOM ether and reduced the resultant ketone with DIBAL-H, which gave alcohol 11 in excellent yield. Subsequent elimination could only be achieved by exposure to Martin's sulfurane.<sup>21</sup> This gave alkene 12, albeit together with an inseparable side product in a 2:1 ratio. Because all attempts at improving this ratio were unsuccessful, we subjected the mixture to a Mn(OAc)<sub>3</sub>-mediated allylic oxidation,<sup>22</sup> which provided enone 14. The unreacted side product could be separated at this stage. It was identified as cyclopropane 13 through NMR and X-ray structure analysis of a derivative, diol 22 (Figure 2). Presumably, 13 is formed via a carbonium ion, which nicely corresponds to the biosynthesis of terpenoid cyclopropanes.<sup>25</sup>

To set the stage for the crucial intramolecular ring closure, the primary alcohol function in 14 was deprotected and mesylated, giving rise to the key intermediate 15. To our delight, treatment of 15 with KHMDS gave the desired tetracycle 16, of which a X-ray structure could be obtained (Figure 2). The ease with which this intramolecular alkylation proceeded was surprising considering the *syn*-pentane strain built up in its course and the conformational changes that are necessary for the two ends to meet.<sup>24</sup> Interestingly, the reaction showed a strong counterion effect, with the yield significantly decreasing when NaHMDS or LiHMDS were employed.

With the ring system of wickerol A (1) complete, we turned to the introduction of the missing methyl groups. The methyl group on the D-ring could be added with complete diastereoselectivity by exposure of 16 to methyl lithiocyanocuprate in the presence of BF<sub>3</sub>·Et<sub>2</sub>O.<sup>25</sup> Given the steric hindrance at the neopentyl β-position and the introduction of additional *syn*-pentane strain, it is remarkable that this reaction proceeded at all.

Next, we attempted the removal of the carbonyl group in the resultant ketone 17 via Wolff–Kishner<sup>26</sup> or Mozingo reduction.<sup>27</sup> Because these failed, we developed a reliable

three-step sequence involving hydride reduction, xanthate formation and Barton–McCombie deoxygenation.<sup>28</sup> Deprotection of the MOM ether and oxidation with DMP then afforded ketone 18.

The final challenge of the synthesis was provided by the methyl addition to 18 to afford wickerol A (1). Addition of a methyl Grignard or methyllithium species to ketone 18 gave 3-*epi*-wickerol A (20) as the sole product. In the presence of the Lewis acid MAD,<sup>29</sup> which is known to invert the stereoselectivity of nucleophilic attacks to cyclohexanones, we obtained a 1:4 mixture of wickerol A (1) and its C3-epimer. Because we were not able to overcome the strong substrate bias with additives,<sup>30</sup> we subjected ketone 18 to Wittig olefination. A subsequent Mukaiyama hydration<sup>31</sup> gave wickerol A (1) together with 3-*epi*-wickerol A (20) as an almost equimolar mixture, which could be separated by chromatography.

The <sup>1</sup>H and <sup>13</sup>C NMR data of our synthetic wickerol A (1) are identical in all respects to those reported by Shiomi and co-workers. All other data also match with the exception of the optical rotation, which was reported as [α]<sub>D</sub> = −2.8 (c = 0.1, MeOH).<sup>3</sup> We were unable to dissolve wickerol A (1) in methanol, as originally reported, but obtained a positive value in chloroform ([α]<sub>D</sub> = +21.7, c = 0.23, CHCl<sub>3</sub>). This suggests that natural wickerol A (1) has the opposite absolute configuration of our synthetic product. In principle, (−)-wickerol A (1) could be accessed from *ent*-6, which in turn could be prepared from geraniol using a Sharpless epoxidation with (−)-DIPT.<sup>9,32</sup>

In summary, we have developed the first total synthesis of a wickerol. Our convergent strategy allowed for the rapid assembly of the complex carbon framework but encountered problems with steric hindrance and unexpected thermodynamic and kinetic preferences, which could be successfully overcome. Salient features of our synthesis are a powerful Diels–Alder reaction to provide most of the rings and carbons, a stereospecific hydride shift to install the challenging A,B-ring *trans*-junction, and an intramolecular alkylation to close a bond between two neopentyl carbons. Also of note are a stereoselective conjugate addition to a sterically hindered enone and a final Mukaiyama hydration to establish the tertiary alcohol. The isolation of cyclopropane 13 is another example of the unexpected results that make the total synthesis of complex natural products so rewarding.

## ■ ASSOCIATED CONTENT

### Supporting Information

The Supporting Information is available free of charge on the ACS Publications website at DOI: 10.1021/jacs.7b05046.

- Detailed experimental procedures, spectral data and X-ray crystallography (PDF)
- Crystallographic data for 21 (CIF)
- Crystallographic data for 22 (CIF)
- Crystallographic data for 16 (CIF)

## ■ AUTHOR INFORMATION

### Corresponding Author

\*dirktrauner@nyu.edu

### ORCID

Dirk Trauner: 0000-0002-6782-6056

### Notes

The authors declare no competing financial interest.

## ■ ACKNOWLEDGMENTS

We thank the Deutsche Forschungsgemeinschaft (SFB749) and the Studienstiftung des Deutschen Volkes for financial support, Dr. Bryan Matsuura for experimental help with the synthesis, and Dr. Peter Mayer for X-ray analysis. Furthermore, we are grateful to Dr. Julius R. Reyes and Dr. Hong-Dong Hao for helpful discussions and to Dr. Giulio Volpin and Matthias Schmid for assistance with preparing this paper. CCDC 1550221–1550223 contain the supplementary crystallographic data for 21, 22 and 16 and can be obtained free of charge from The Cambridge Crystallographic Data Centre via <https://www.ccdc.cam.ac.uk/structures/>.

## ■ REFERENCES

- (1) For reviews, see: (a) Maimone, T. J.; Baran, P. S. *Nat. Chem. Biol.* **2007**, *3*, 396–407. (b) Büschleb, M.; Dorich, S.; Hanessian, S.; Tao, D.; Schenthal, K. B.; Overman, L. E. *Angew. Chem., Int. Ed.* **2016**, *55*, 4156–4186.
- (2) (a) Dewick, P. M. *Medicinal Natural Products: A Biosynthetic Approach*, 3rd ed.; John Wiley & Sons, Ltd: Chichester, 2009; (b) Christianson, D. W. *Chem. Rev.* **2006**, *106*, 3412–3442.
- (3) Yamamoto, T.; Izumi, N.; Ui, H.; Sueki, A.; Masuma, R.; Nonaka, K.; Hirose, T.; Sunazuka, T.; Nagai, T.; Yamada, H.; Omura, S.; Shiomi, K. *Tetrahedron* **2012**, *68*, 9267–9271.
- (4) Sun, P.-X.; Zheng, C.-J.; Li, W.-C.; Jin, G.-L.; Huang, F.; Qin, L.-P. *J. Nat. Med.* **2011**, *65*, 381–384.
- (5) Ye, D. K. J.; Richard, J.-A. *Tetrahedron Lett.* **2014**, *55*, 2183–2186.
- (6) Quasdorf, K. W.; Overman, L. E. *Nature* **2014**, *516*, 181–191.
- (7) (a) Adams, J.; Lepine-Frenette, C.; Spero, D. M. *J. Org. Chem.* **1991**, *56*, 4494–4498. (b) Inoue, M.; Carson, M. W.; Frontier, A. J.; Danishefsky, S. J. *J. Am. Chem. Soc.* **2001**, *123*, 1878–1889.
- (8) Maruoka, K.; Ooi, T.; Nagahara, S.; Yamamoto, H. *Tetrahedron* **1991**, *47*, 6983–6998.
- (9) Yang, Z.-Y.; Liao, H.-Z.; Sheng, K.; Chen, Y.-F.; Yao, Z.-J. *Angew. Chem., Int. Ed.* **2012**, *51*, 6484–6487.
- (10) For a review, see: (a) Nicolaou, K. C.; Snyder, S. A.; Montagnon, T.; Vassilikogiannakis, G. *Angew. Chem., Int. Ed.* **2002**, *41*, 1668–1698. Selected references on Diels–Alder reactions with cycloalkenones: (b) Fringuelli, F.; Pizzo, F.; Taticchi, A.; Wenkert, E. *J. Org. Chem.* **1983**, *48*, 2802–2808. (c) Ge, M.; Stoltz, B. M.; Corey, E. J. *Org. Lett.* **2000**, *2*, 1927–1929. For intramolecular Diels–Alder reactions, see: (d) Takao, K.-i.; Munakata, R.; Tadano, K.-i. *Chem. Rev.* **2005**, *105*, 4779–4807.
- (11) (a) Ballerini, E.; Minuti, L.; Piematti, O. *J. Org. Chem.* **2010**, *75*, 4251–4260. (b) Hugelshofer, C. L.; Magauer, T. *Synthesis* **2014**, *46*, 1279–1296.
- (12) Jung, M. E.; Ho, D. G. *Org. Lett.* **2007**, *9*, 375–378.
- (13) Jung, M. E.; Guzaev, M. *Org. Lett.* **2012**, *14*, 5169–5171.
- (14) (a) Lee, E.; Song, H. Y.; Kang, J. W.; Kim, D.-S.; Jung, C.-K.; Joo, J. M. *J. Am. Chem. Soc.* **2002**, *124*, 384–385. (b) Jung, M. E.; Ho, D.; Chu, H. V. *Org. Lett.* **2005**, *7*, 1649–1651. (c) Jung, M. E.; Guzaev, M. *J. Org. Chem.* **2013**, *78*, 7518–7526.
- (15) Examples of tried methods include  $\text{Me}_3\text{AlMgCl}$ : (a) Webb, T. R. *Tetrahedron Lett.* **1988**, *29*, 3769–3772. Addition of  $\text{CeCl}_3$ : (b) Imamoto, T.; Takiyama, N.; Nakamura, K.; Hatajima, T.; Kamiya, Y. *J. Am. Chem. Soc.* **1989**, *111*, 4392–4398. Addition of a Lewis acid: (c) Kato, T.; Hirukawa, T.; Ueyehara, T.; Yamamoto, Y. *Tetrahedron Lett.* **1987**, *28*, 1439–1442.  $\text{MeLi}$ : (d) Chu, K.-C.; Liu, H.-J.; Zhu, J.-L. *Synlett* **2010**, *2010*, 3061–3064. Addition of  $\text{LaCl}_3\cdot 2\text{LiCl}$ : (e) Krasovskiy, A.; Kopp, F.; Knochel, P. *Angew. Chem., Int. Ed.* **2006**, *45*, 497–500.
- (16) Examples of tried methods include Wittig olefination: (a) Maryanoff, B. E.; Reitz, A. B. *Chem. Rev.* **1989**, *89*, 863–927. Petasis reagent: (b) Petasis, N. A.; Bzowej, E. I. *J. Am. Chem. Soc.* **1990**, *112*, 6392–6394. Nysted reagent: (c) Matsubara, S.; Sugihara, M.; Utimoto, K. *Synlett* **1998**, *1998*, 313–315. (d) Aïssa, C.; Riveiros, R.; Ragot, J.; Fürstner, A. *J. Am. Chem. Soc.* **2003**, *125*, 15512–15520. Rh-catalyzed methylenation: (e) Lebel, H.; Paquet, V. *J. Am. Chem. Soc.* **2004**, *126*, 320–328.  $\text{Mg/TiCl}_4$ : (f) Yan, T.-H.; Tsai, C.-C.; Chien, C.-T.; Cho, C.-C.; Huang, P.-C. *Org. Lett.* **2004**, *6*, 4961–4963.
- (17) (a) Gordon, H. L.; Freeman, S.; Hudlicky, T. *Synlett* **2005**, *2005*, 2911–2914. (b) Tori, M. *Molecules* **2015**, *20*, 1509–1518.
- (18) (a) DeCamp, A. E.; Mills, S. G.; Kawaguchi, A. T.; Desmond, R.; Reamer, R. A.; DiMichele, L.; Volante, R. P. *J. Org. Chem.* **1991**, *56*, 3564–3571. (b) Defaut, B.; Parsons, T. B.; Spencer, N.; Male, L.; Kariuki, B. M.; Grainger, R. S. *Org. Biomol. Chem.* **2012**, *10*, 4926–4932. (c) Hugelshofer, C. L.; Magauer, T. *J. Am. Chem. Soc.* **2016**, *138*, 6420–6423.
- (19) (a) Atkins, G. M.; Burgess, E. M. *J. Am. Chem. Soc.* **1968**, *90*, 4744–4745. (b) Burgess, E. M.; Penton, H. R.; Taylor, E. A. *J. Org. Chem.* **1973**, *38*, 26–31.
- (20) (a) VanRheenen, V.; Kelly, R. C.; Cha, D. Y. *Tetrahedron Lett.* **1976**, *17*, 1973–1976. (b) Schroeder, M. *Chem. Rev.* **1980**, *80*, 187–213.
- (21) Arhart, R. J.; Martin, J. C. *J. Am. Chem. Soc.* **1972**, *94*, 5003–5010.
- (22) (a) Shing, T. K. M.; Yeung, S. P. L. *Org. Lett.* **2006**, *8*, 3149–3151. (b) Nakamura, A.; Nakada, M. *Synthesis* **2013**, *45*, 1421–1451.
- (23) (a) Maskill, H.; Wilson, A. A. *J. Chem. Soc., Perkin Trans. 2* **1984**, 119–128. (b) Silva, C. J.; Giner, J. L.; Djerassi, C. *J. Am. Chem. Soc.* **1992**, *114*, 295–299. (c) Giner, J.-L.; Buzek, P.; Schleyer, P. v. R. *J. Am. Chem. Soc.* **1995**, *117*, 12871–12872. (d) Thibodeaux, C. J.; Chang, W.-c.; Liu, H.-w. *Chem. Rev.* **2012**, *112*, 1681–1709.
- (24) Some selected examples of intramolecular alkylations to construct a 6-membered ring: (a) Corey, E. J.; Behforouz, M.; Ishiguro, M. *J. Am. Chem. Soc.* **1979**, *101*, 1608–1609. (b) Danishefsky, S.; Vaughan, K.; Gadwood, R.; Tsuzuki, K. *J. Am. Chem. Soc.* **1981**, *103*, 4136–4141. (c) Dodds, D. R.; Jones, J. B. *J. Chem. Soc., Chem. Commun.* **1982**, 1080–1081. (d) Srikrishna, A.; Ravi, G.; Satyanarayana, G. *Tetrahedron Lett.* **2007**, *48*, 73–76. (e) Adams, G. L.; Carroll, P. J.; Smith, A. B., 3rd. *J. Am. Chem. Soc.* **2012**, *134*, 4037–4040. (f) Wang, D.; Crowe, W. E. *Chin. Chem. Lett.* **2015**, *26*, 238–242. (g) Wang, D.; Hou, M.; Ji, Y.; Gao, S. *Org. Lett.* **2017**, *19*, 1922–1925.
- (25) (a) Yamamoto, Y.; Maruyama, K. *J. Am. Chem. Soc.* **1978**, *100*, 3240–3241. (b) Yamamoto, Y.; Yamamoto, S.; Yatagai, H.; Ishihara, Y.; Maruyama, K. *J. Org. Chem.* **1982**, *47*, 119–126. (c) Yamamoto, Y. *Angew. Chem., Int. Ed. Engl.* **1986**, *25*, 947–959.
- (26) (a) Grundon, M. F.; Henbest, H. B.; Scott, M. D. *J. Chem. Soc.* **1963**, *0*, 1855–1858. (b) Caglioti, L.; Magi, M. *Tetrahedron* **1963**, *19*, 1127–1131. (c) Hutchins, R. O.; Milewski, C. A.; Maryanoff, B. E. *J. Am. Chem. Soc.* **1973**, *95*, 3662–3668. (d) Furrow, M. E.; Myers, A. G. *J. Am. Chem. Soc.* **2004**, *126*, 5436–5445. (e) Green, J. C.; Pettus, T. R. *J. Am. Chem. Soc.* **2011**, *133*, 1603–1608.
- (27) (a) Mozingo, R.; Wolf, D. E.; Harris, S. A.; Folkers, K. J. *J. Am. Chem. Soc.* **1943**, *65*, 1013–1016. (b) Wolfrom, M. L.; Karabinos, J. V. *J. Am. Chem. Soc.* **1944**, *66*, 909–911. (c) Bosch, J.; Bonjoch, J. *J. Org. Chem.* **1981**, *46*, 1538–1543. (d) Ihara, M.; Makita, K.; Takasu, K. *J. Org. Chem.* **1999**, *64*, 1259–1264.
- (28) (a) Lopez, R. M.; Hays, D. S.; Fu, G. C. *J. Am. Chem. Soc.* **1997**, *119*, 6949–6950. (b) Trost, B. M.; Cramer, N.; Bernsmann, H. *J. Am. Chem. Soc.* **2007**, *129*, 3086–3087.
- (29) Maruoka, K.; Itoh, T.; Yamamoto, H. *J. Am. Chem. Soc.* **1985**, *107*, 4573–4576.
- (30) Similar substrate bias was also encountered in: Lu, H.-H.; Pronin, S. V.; Antonova-Koch, Y.; Meister, S.; Winzler, E. A.; Shenvi, R. A. *J. Am. Chem. Soc.* **2016**, *138*, 7268–7271. Oxymmercuration gave worse results than Mukaiyama hydration in our case.
- (31) (a) Isayama, S.; Mukaiyama, T. *Chem. Lett.* **1989**, *18*, 1071–1074. (b) Feng, X.; Jiang, G.; Xia, Z.; Hu, J.; Wan, X.; Gao, J.-M.; Lai, Y.; Xie, W. *Org. Lett.* **2015**, *17*, 4428–4431. (c) Crossley, S. W. M.; Obradors, C.; Martinez, R. M.; Shenvi, R. A. *Chem. Rev.* **2016**, *116*, 8912–9000.
- (32) Maruoka, K.; Murase, N.; Bureau, R.; Ooi, T.; Yamamoto, H. *Tetrahedron* **1994**, *50*, 3663–3672.

## 4. Conclusion and Outlook

In conclusion, the first total synthesis of the complex diterpene wickerol A was accomplished in an enantioselective fashion.

The initial approach envisaged an intramolecular Robinson annulation to construct the complex scaffold of the natural product. Preparation of the key precursor **3.27** included a challenging conjugate addition, stereoselective methylation and homologation using a Peterson olefination. Unfortunately, the desired Robinson annulation could not be achieved, presumably due to the steric hindrance of the substrate. In our second generation strategy, we attempted to access wickerol A *via* spirocycle **3.48** which we tried to prepare using a double-Michael reaction of **3.41** and **3.42** or a radical cyclization of **3.49**. But all our efforts in this regard were met with failure, which led us to our third and final approach.

Our successful synthesis was highly convergent through the use of two readily accessible building blocks that underwent an extremely challenging Diels–Alder reaction. This cycloaddition built up two crucial stereocenters of wickerol A, both of which are neopentyl and one a quaternary carbon, demonstrating the remarkable power of the Diels–Alder reaction. Establishing the *trans*-BA-ring junction proved to be problematic but could be achieved through a Pinacol-type rearrangement using Grainger's conditions. The last ring was closed through a remarkable intramolecular alkylation between two neopentyl carbons. Having built the congested carbon framework of the natural product, stereoselective conjugate addition to the sterically hindered enone introduced the C6-methyl group which was followed by a Barton–McCombie deoxygenation. Installation of the tertiary alcohol was challenging due to a strong, unfavorable substrate bias but could be accomplished using a sequence of olefination followed by Mukaiyama hydration.

The developed strategy could be used to access wickerol B in the future.

## **Part II:**

# **Development of a Photoswitchable AMPA Receptor Antagonist**

## 5. Photopharmacology

### 5.1. Introduction

Pharmacotherapy is a form of therapy that treats a disease through the administration of drugs.<sup>[98]</sup> In a broader sense, this dates back to prehistoric times when herbs were used as medicine. Later on, ancient cultures such as the Egyptians or the Babylonians developed treatments for a broad variety of ailments. In India and China a large body of pharmacotherapy evolved over centuries and has become the basis of ayurveda and traditional Chinese medicine, which are still employed today.<sup>[99]</sup>

Modern pharmacotherapy is based on pharmacology, the scientific study of the biological effect of drugs. The broad range of therapeutics that is available to us nowadays has drastically improved the quality and length of life.<sup>[100]</sup> Nevertheless there are still issues that need to be addressed such as drug-selectivity and resistance.<sup>[101]</sup> Poor drug selectivity is caused by the undesired interaction of a drug with targets other than that intended. This is not easily prevented since a drug acts by interfering with processes that belong to complex signaling and metabolic pathways.<sup>[102]</sup> Good examples are anti-cancer drugs that impair mitosis of malignant cells but can also affect healthy, fast-dividing cells, causing severe side effects such as hair loss, mucositis, and anemia. To alleviate this problems, substantial research is aimed at targeted therapy<sup>[103]</sup> but a universal solution is still lacking.<sup>[104]</sup> Poor selectivity also leads to a lower threshold level of toxicity and consequently a smaller therapeutic window. This means that even if a compound is discovered that causes the desired effect, its insufficient selectivity precludes it from being used as a treatment.<sup>[105]</sup>

To improve drug selectivity, it would be necessary to have better control over its activity in time and space; i.e. when and where the drug is active. To achieve this by employing light is the fundamental principal underlying photopharmacology.<sup>[106]</sup> Light as a regulatory element has a lot of potential since it can be delivered with very high spatial and temporal precision and regulated in a qualitative and quantitative manner by adjusting wavelength and intensity, respectively.<sup>[107]</sup> In previous approaches, ligands with a photolyzable moiety were used, so called “caged ligands”.<sup>[108]</sup> The major limitation of this method is its irreversibility: once photodeprotected, control over the drug’s activity is lost. Reversible optical control over biological functions can be achieved using optogenetics, which relies on the expression of photoresponsive proteins.<sup>[109]</sup> Though an extremely useful research tool, the necessity for genetic manipulation limits its application.

In order to control the function of a bioactive compound with light, photopharmacology uses photoswitchable substructures that are introduced into the pharmacophore of a known drug, or as an appendage to it. These photo-responsive moieties change the structure of bioactive agents upon irradiation with light and consequently their pharmacodynamic and pharmacokinetic properties, which are directly related to their molecular structure. In the following section, some photoswitchable structures that have been successfully employed are discussed.

## 5.2. Photoswitches

Being able to control the conformation and activity of biomolecules in a reversible manner is important for studying and interfering with complex processes in living cells. To do this, photopharmacology renders small, freely diffusible and bioactive molecules light-sensitive through the introduction of molecular photoswitches that undergo a reversible change in their structure upon irradiation with light.<sup>[110]</sup>

The most common chromophores employed in the field of photopharmacology can be divided into two groups: compounds that interconvert between closed and open forms (spiropyrans, diarylethenes, and fulgides) (Figure 5.1) or switch between *cis*- and *trans*- isomers (azobenzenes, stilbenes, and hemithioindigos) (Figure 5.2).<sup>[107e]</sup> Apart from the geometry, photoisomerization may also change the polarity and charge distribution of the compound. Important characteristics of photoswitches are the absorption maxima of their isomeric forms which shouldn't be too similar and the photostationary state, defined as the equilibrium composition during irradiation. Ideally, photoswitches possess a highly fatigue resistant switching process that is also fast in order to prevent competing side-reactions that lead to deexcitation (fluorescence, phosphorescence, and unproductive relaxations to the ground state). Furthermore, they should have slow thermal relaxation rates and a large extinction coefficient with high quantum yield at wavelengths that are nondestructive for a living cell.<sup>[107e]</sup>

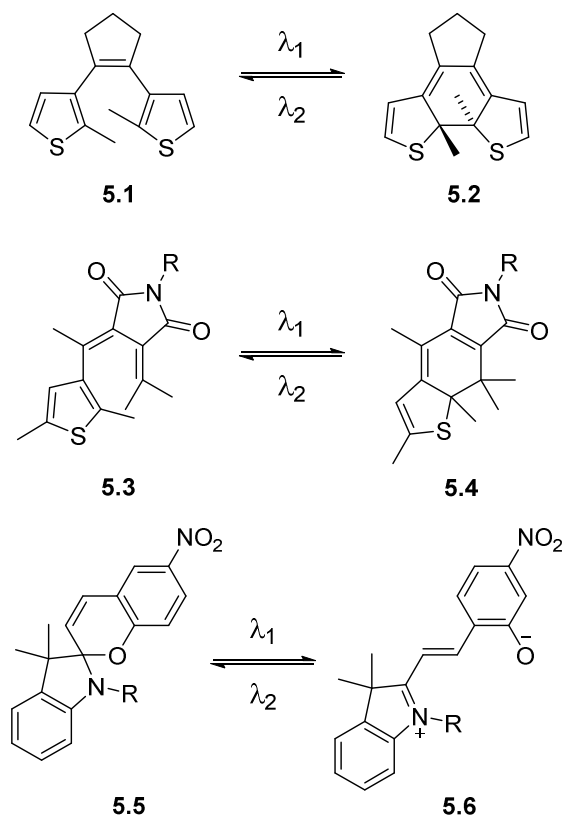


**Figure 5.1.** Photochromic switches that interconvert between closed and open forms.

Diarylethenes possess a hexatriene motif that is incorporated in a tricyclic structure normally containing two (hetero)aromatic moieties (Figure 5.1).<sup>[111]</sup> The triene can undergo a reversible conrotatory  $6\pi$ -electrocyclization to a cyclohexadiene ring upon irradiation. The first diarylethenes were established in the mid-1960's from detailed investigations of the photochemistry of stilbenes and heteroarylstilbenes.<sup>[112]</sup> Later on, the potential of 1,2-diheteroarylethenes as thermally stable photochromic switches was recognized and investigated.<sup>[113]</sup> It was found that their absorption spectrum can be modified through the substitution pattern on the rings and that they exhibit very high fatigue resistance, meaning that switching cycles can be repeated over several thousand times. Diarylethenes with thiophene rings (simplest example being **5.1**) have been used to photocontrol the inhibition of human carbonic anhydrase I<sup>[114]</sup> and to regulate the helicity of a DNA-binding peptide incorporated into nucleobases.<sup>[115]</sup>

As in the case of diarylethenes, the photochromism of fulgides is based on the reversible photochemical cyclization of a hexatriene system (Figure 5.1). They were discovered at the beginning of the 20<sup>th</sup> century but it took several decades until the first thermally stable member

was synthesized.<sup>[116]</sup> For the electrocyclicization to occur the three conjugated double bonds need to be in a *s-cis*-conformation which is dependent on the steric bulk of the substituents. This means that the conformation of fulgides at their ground state influences the quantum yield of photocyclization. Thiophenefulgide based switches (for example **5.3**) were shown to be able to regulate activity of the protease  $\alpha$ -chymotrypsin.<sup>[117]</sup>

Spiropyrans (simplest example being **5.5**, Figure 5.1) also exist in an open and closed form. In their case, the spiro-C–O bond undergoes heterolytic cleavage upon UV irradiation which results in a zwitterionic conjugated system, called the merocyanine form (**5.6**).<sup>[118]</sup> This process is reversible both thermally and photochemically, by irradiation with visible light. But there are also cases where the isomerization behavior is reversed, that is, visible light shifts the equilibrium toward the open state and UV light leads to the closed form.<sup>[107e]</sup> The photoisomerization also results in a very large change in polarity (8–15 D) which has been found to be crucial for protein interactions.<sup>[119]</sup>

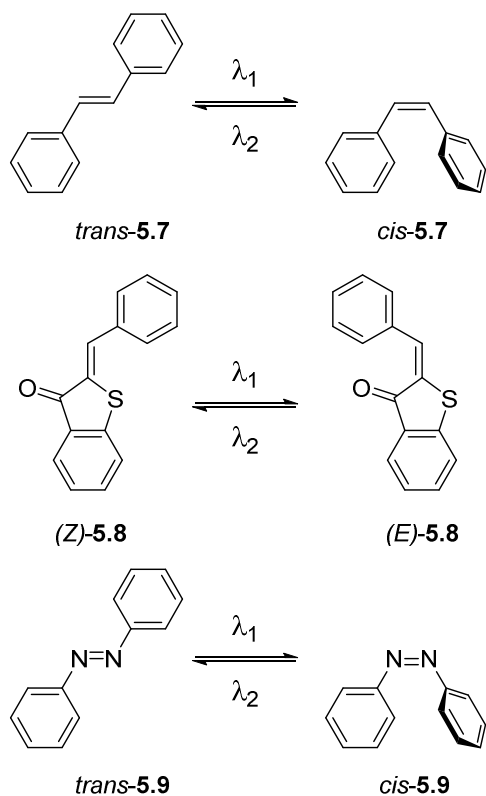


**Figure 5.2.** Photochromic switches that interconvert between *cis*- and *trans*-isomers.

Stilbenes can be considered a subclass of diarylethene chromophores but they isomerize between an *E* and *Z* form, instead of undergoing electrocyclization (Figure 5.2).<sup>[120]</sup> The irradiation of the parent compound **5.7** at 313 nm light leads to the *cis*-isomer, in which the angle between the planes of the phenyl rings is 43°. <sup>[121]</sup> They are stable switches since their barrier for thermal relaxation is too high for it to occur at room temperature. Stilbene switches have been used as phosphate backbone linkers in DNA oligomers and photoswitchable peptidomimetic inhibitors of *M. tuberculosis* ribonucleotide reductase.<sup>[122]</sup> A major disadvantage of stilbenes is their tendency to undergo irreversible cyclization and oxidation reactions in their *cis*-form.<sup>[123]</sup>

Photochromism based on *E* to *Z* isomerization can also be found in hemithioindigos (parent compound being **5.8**, Figure 5.2), unsymmetrical molecules consisting of a thioindigo fragment connected to a stilbene moiety. The *Z* form is thermodynamically more stable than the *E* form and the barrier for thermal relaxation is usually above 27 kcal/mol making hemithioindigos very bistable switches. Their main advantageous feature is that visible light suffices for isomerization and their switching behavior can be further tuned through the substituents on the aromatic rings. Drawbacks are possible side reactions that can occur upon irradiation such as intermolecular [2+2] cycloadditions.<sup>[124]</sup> Hemithioindigo-based amino acids incorporated into gramicidin ion channels were used to modulate the ion current by photoisomerization.<sup>[125]</sup>

The most widely employed photoresponsive moieties in photopharmacology are azobenzenes (simplest congener being **5.9**, Figure 5.2).<sup>[106, 126]</sup> They were discovered in the 1830's and due to their intense color were used as dyes in the beginning of the 20th century. Other applications include therapeutics (prontosil (**5.10**), sulfasalazine (**5.11**)) and food-colorants (sunset yellow FCF (**5.12**, E110), allura red AC (**5.13**, E129)) (Figure 5.3).<sup>[127]</sup>

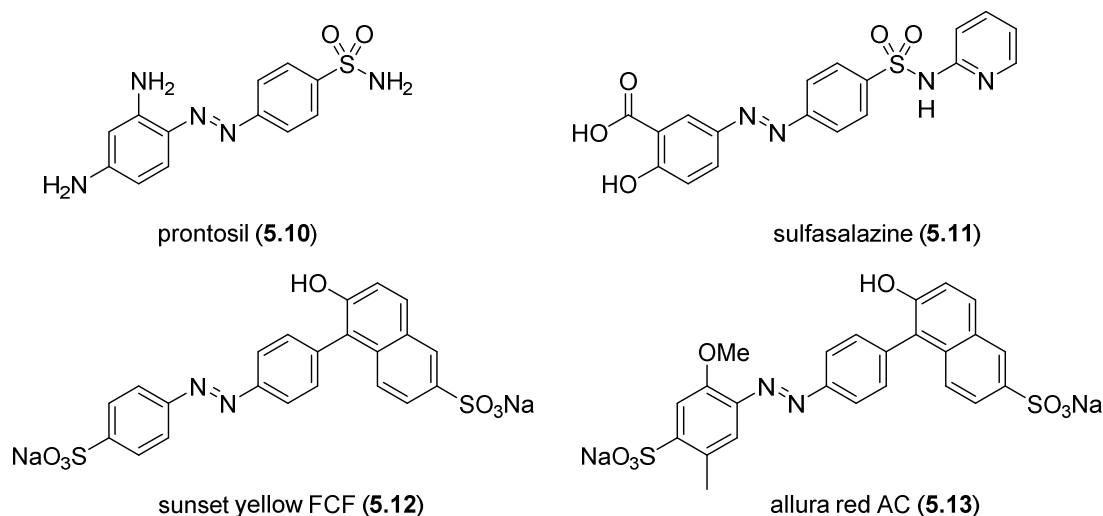


**Figure 5.3.** Structure of azobenzenes used as therapeutics and food-colorants.

Azobenzenes are diazene derivatives that switch between the *trans*- and *cis*-form which results in a big geometrical change (the end-to-end atom distance of *trans*-**5.9** is 1.6 times larger than the *cis* one) and a shift in polarity.<sup>[128]</sup> Relaxation to the thermodynamically more stable *trans*-form (the difference between *cis* and *trans* is about 10 kcal/mol) can be achieved either by irradiation with light or *via* thermal isomerization with the half-life of *cis*-**5.9** being about two days.<sup>[129]</sup> Azobenzenes exhibit many favorable features such as high extinction coefficients and quantum yields, which means that light of relatively low intensity can be used for photoisomerization. In addition, they switch at very fast rates, thus avoiding intersystem crossing and the formation of triplet diradicals that could lead to the generation of highly reactive and cytotoxic singlet oxygen. Therefore, azobenzenes are relatively photostable and can be switched over many cycles. Furthermore, they are easy to synthesize<sup>[130]</sup> and their spectral properties can be tuned by incorporations of different substituents on the aromatic rings. (see Chapter 5.3.). For these reasons, azobenzenes have become the most applied photoswitch in photopharmacology to date.<sup>[106, 109a, 127]</sup>

### 5.3. Design Principles

The following section will discuss various aspects that should be considered when designing a photoswitch.<sup>[106, 127]</sup> The focus will be on azobenzenes but many principles can also be applied to other switches.

#### Biological Activity

Two general design strategies for turning a drug photoresponsive have evolved so far (Figure 5.4.a). The first is based on coupling of a photoswitch with the pharmacophore, either through partial incorporation into the parent structure or by appendage to it. For this strategy to be successful, the photochromic derivative must show a high affinity to the receptor in only one of its photoisomeric states. The decrease in binding affinity upon switching can be caused by either unfavorable drug-receptor interactions or the inability of the isomer to enter the binding pocket due to its shape, size, or polarity.

The second strategy is only applicable to multivalent drugs, that is, drugs possessing two or more pharmacophores connected by a spacer unit (Figure 5.4.b).<sup>[131]</sup> This spacer unit can be replaced by a photoswitch which upon photoisomerization alters the rigidity of the spacer and the distance between pharmacophores consequently leading to a change in drug activity. This method has been exploited for the development of photoswitchable mast cell activation inhibitors<sup>[132]</sup> and photoswitchable peptidomimetics.<sup>[133]</sup>

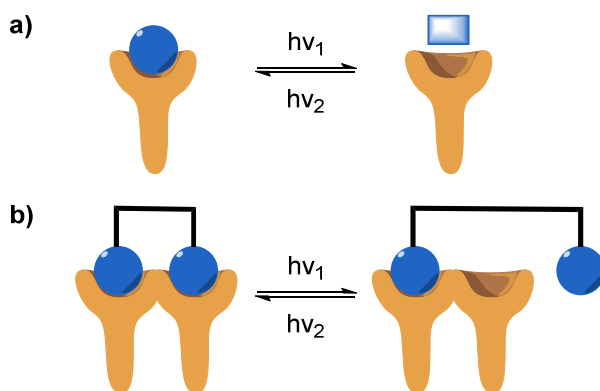


**Figure 5.4.** Schematic representation of the two major strategies employed for designing a photochromic ligand. a) The photochromic ligand is not able to bind to the receptor upon switching. b) A multivalent ligand that possesses a photoswitch in the spacer unit. The change in distance upon isomerization prevents interaction with the receptor.<sup>[106]</sup>

After incorporation of a photoswitchable moiety, the biological activity of the parent compound needs to be retained in at least one of the isomers. Most of the time, the structure of therapeutics is highly optimized in order to obtain maximal potency and efficacy.<sup>[134]</sup> Therefore, light-responsive derivatives of a drug will frequently exhibit decreased activity and further SAR (structure activity relationship) studies will be necessary. It is therefore advisable to look at SAR studies of the drug one aims to modify and at crystal structures of it bound to the receptor as indicators for the likelihood of activity loss. When looking for suitable targets for derivatization, one can search for isosteres that can be replaced by the photochromic switch to be employed. In the case of azobenzenes, a selection of structural motifs that can be mimicked by an azobenzene is depicted in Figure 5.5 They include styrenes (**5.7**), *N*-phenyl benzamides (**5.14**), other types of (hetero)aryl–(hetero)aryl amides (**5.15**, **5.16**), benzyl anilines (**5.17**), benzyl phenyl (thio)ethers (**5.18**, **5.19**), 1,2-diaryl ethanes (**5.20**), and related structures.<sup>[127]</sup> Several examples for this approach (“azologization”) are depicted in Figure 5.6. Azocholine (**5.22**) is a photoswitchable agonist selective for  $\alpha 7$  nAChRs based on the antagonist MG-624 (**5.21**).<sup>[135]</sup> With alloswitch-1 (**5.24**), a positive allosteric modulator of metabotropic glutamate receptors derived from VU-415374 (**5.23**), Gorostiza and co-workers were able to control the motility of living tadpoles with light.<sup>[136]</sup> In fotocain (**5.26**), the benzyl phenyl ether of the anesthetic fomocain (**5.25**) was successfully replaced by an azobenzene.<sup>[137]</sup>

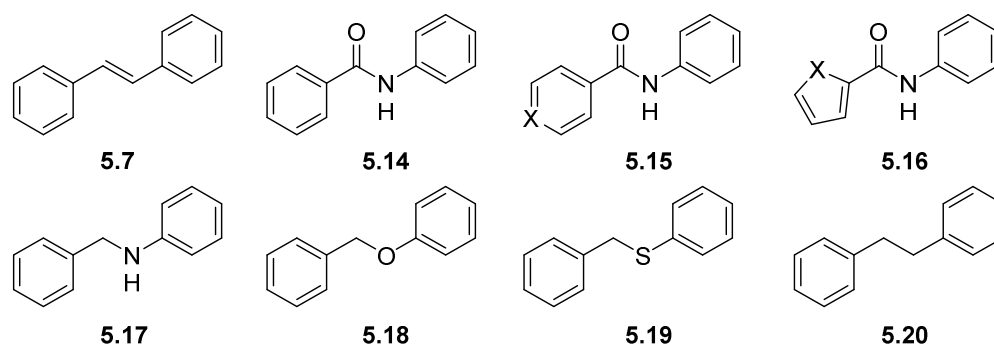


**Figure 5.5.** A selection of structural motifs that can be mimicked by azobenzenes.

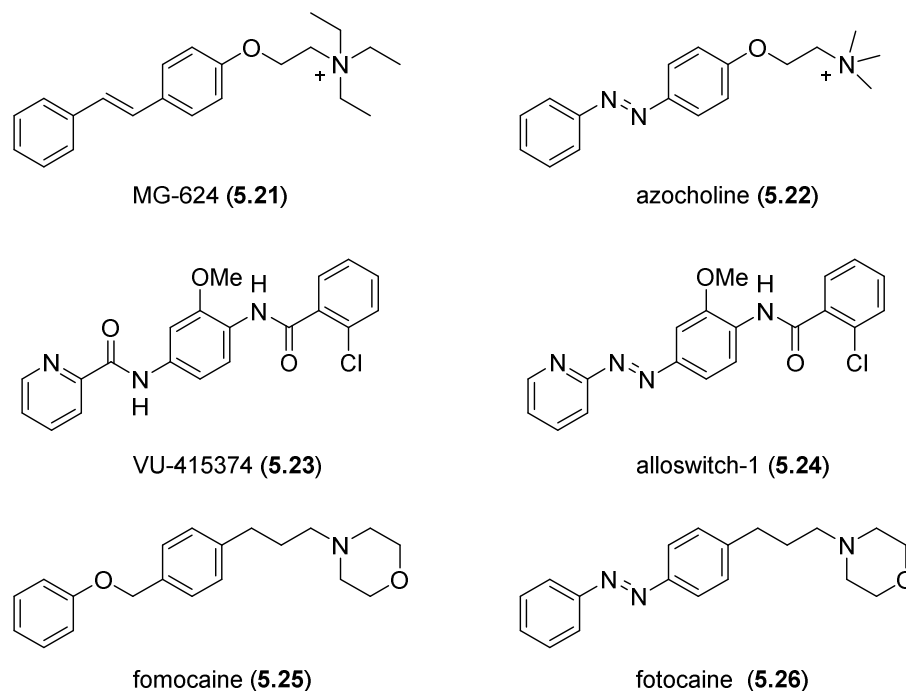


**Figure 5.6.** Examples of isosteres being replaced by azobenzenes.

Another strategy to guide the development of a light-responsive ligand is based on SAR studies. These data often reveal which substituents of the parent compound can be varied without completely losing biological activity, indicating a good position to incorporate a photoswitchable moiety. Some examples of successful appendage of an azobenzene to an existing bioactive scaffold are depicted in Figure 5.7. The Feringa group developed quinolone-2 (**5.28**) based on ciprofloxacin (**5.27**) and demonstrated optical control of antibacterial activity using it.<sup>[138]</sup> Propofol (**5.29**), a structurally simple GABA<sub>A</sub> receptor potentiator, could be extended in the 4-position, resulting in AP-2 (**5.30**) which was used as a light-dependent anesthetic in translucent tadpoles.<sup>[139]</sup> The third example is AC-4 (**5.32**) which is a photoswitchable antagonist of the TRPV1 ion channel derived by replacing the chlorine residue of capsazepine (**5.31**) with an azobenzene moiety.<sup>[140]</sup>

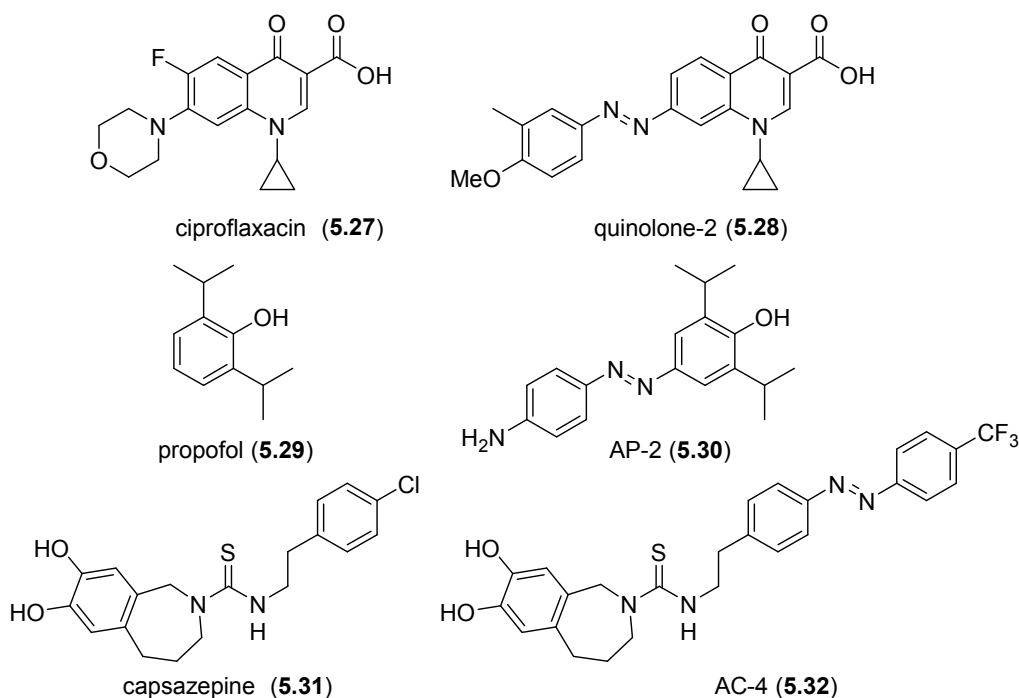


**Figure 5.7.** Examples of azobenzene appendage to a known ligand.

After having synthesized a suitable photoresponsive ligand, it is possible that the isomerization is inhibited after binding to the receptor. Usually, this does not pose a problem though, since receptor binding is a dynamic event and as soon as the compound leaves the binding pocket, it will switch.<sup>[106]</sup>

#### Photoisomer Ratio at Photostationary State

It is important to consider the difference in relative concentration of the two photoisomers since the extent of isomerization translates directly to the biological effect. For most of the photoswitches, it is impossible to push them completely into their thermodynamically less stable state through irradiation. Therefore, one needs to take into account the background activity of the remaining isomer. In the case of azobenzenes, they can exist 100% in the thermodynamically more stable *trans*-form (also called the dark-adapted form) and their photostationary *cis/trans*-ratios have been reported to exceed 9:1 using appropriate wavelengths.<sup>[141]</sup> But even if a ligand isomerizes only partially, the biological response can easily be optimized by changing the concentration of the drug. This independence of a direct attachment to the receptor is one of the advantages of photopharmacology in comparison to other methods such as optogenetics.

### Tuning of Wavelength and Thermal Relaxation

The wavelength needed for isomerization is a crucial characteristic of a photoswitch and should be amenable to tuning. For potential clinical application, UV light cannot be employed as it is carcinogenic and can cause mutations. Ideally, only light in the range of 600 to 1200 nm can be used, since hemoglobin absorbs shorter wavelengths and water longer ones. For non-invasive treatment, tissue penetration of light is an important factor. It is estimated that wavelengths of 800 nm reach about 2 cm deep and can therefore only interact with areas that are lying close to the skin surface.<sup>[142]</sup>

The absorption spectra of most chromophores can be modified by changing the substitution pattern. Azobenzenes offer the advantage that many methods are available for their synthesis<sup>[130]</sup> and it is possible to adorn the aromatic rings with a broad variety of substituents. In addition, the influence of different functional groups on their switching behavior is well studied.<sup>[143]</sup> Since unmodified azo compounds need UV-light for photoisomerization, shifting their absorption spectra to longer wavelengths (red-shifting) is important for biological research and future applications *in vivo*. It was found that red-shifting can be achieved by introducing an electron donating group (EDG) on one side of the azo unit and electron withdrawing group (EWG) on the other, creating a so called “push-pull system”<sup>[144]</sup> (Figure 5.8, compound **5.33**). It is also possible to put a single electron-donating group (EDG) at the *para*- or *ortho*-position to change the absorption maximum to higher wavelengths (Figure 5.8, compound **5.30**).<sup>[139]</sup> This shift is generally accompanied by a significant increase in the thermal relaxation rate, which makes an intense light source necessary to produce a large steady state fraction of the *cis*-isomer. Recently though, tetra-*ortho*-substituted azobenzenes such as compound **5.34** or **5.36** were developed that can be isomerized with visible light and are thermally stable, i.e. exhibit a half-life of several days.<sup>[141c]</sup> Using this strategy, Woolley and co-workers could photoisomerize tetrachloro-**5.35** cross-linked with fluorescent reporter peptide with red light ( $\lambda = 635$  nm) in zebrafish embryos.<sup>[145]</sup>

Another type of azobenzene that can be switched with visible light is characterized by a C2-linker between the two phenyl groups (Figure 5.8). This bridge generates a highly twisted *trans*-isomer that is less stable than the *cis*-isomer, conversely to standard azobenzenes. It was shown that the conformation of a helical peptide linked with cycloazobenzene **5.37** could be controlled with visible light.<sup>[141b]</sup>

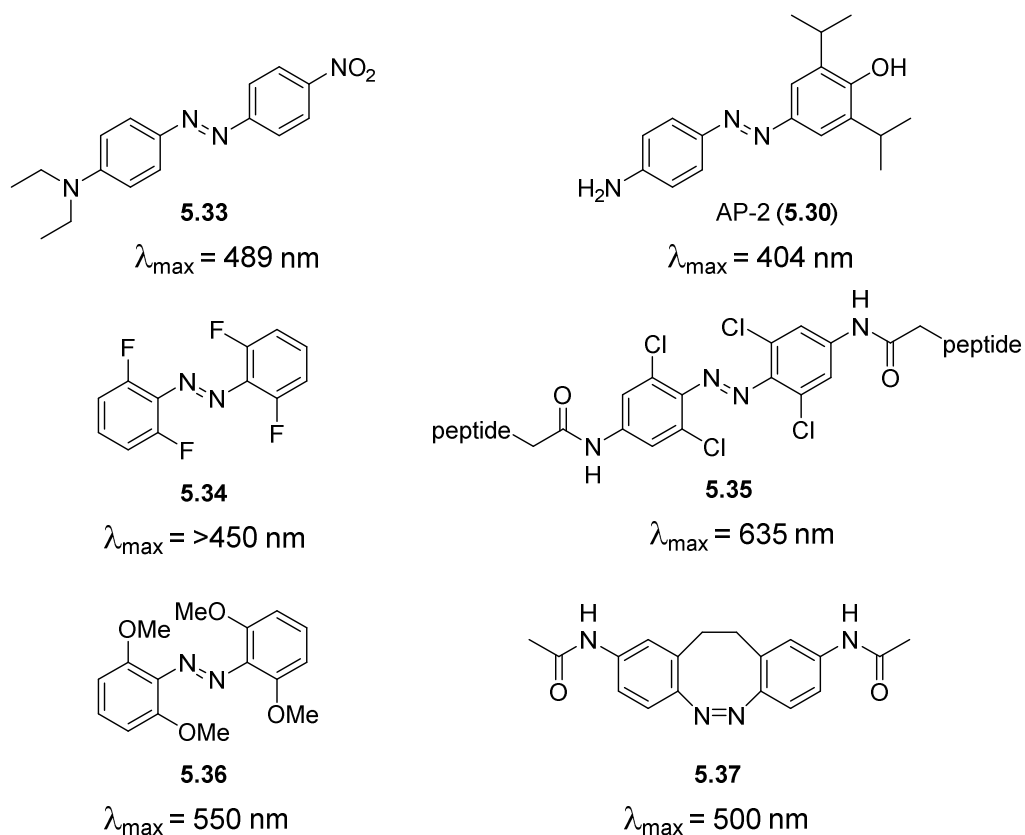


**Figure 5.8.** Examples of red-shifted azobenzenes.

#### Stability in the Cellular Environment and Toxicity

Two other issues that need to be addressed with regards to clinical applications is the possible degradation of photochromic ligands through enzymes<sup>[146]</sup> or glutathione, the predominant intracellular reductant. For azobenzenes, it was shown that reduction to the respective hydrazobenzenes by glutathione is possible but that this process is also dependent on the substitution pattern and can therefore be prevented.<sup>[147]</sup>

Also important is the toxicity of the modified drug and its metabolites. Since azobenzenes have been used as dyes for decades, their toxicity has been the subject of various studies. They showed that azobenzenes can be cleaved to carcinogenic aromatic amines or oxidized to strongly electrophilic diazonium salts.<sup>[148]</sup> But these findings should not preclude this class of compounds from future applications since metabolic stability depends on the exact structure of a molecule. In the case of azobenzenes, some congeners have already been used as therapeutics as well as food dyes (see Chapter 5.2., Figure 5.3).

Even though extensive research still needs to be done to fulfill all the prerequisites for pharmacotherapy with photoswitchable drugs, the field of photopharmacology is still in its infancy and offers great potential for development.

## 6. AMPA Receptors

### 6.1. Ionotropic Glutamate Receptors

Glutamate receptors (GluRs) are integral membrane proteins that are activated by L-Glutamate (6.1, Figure 6.2), the major excitatory neurotransmitter in the mammalian central nervous system (CNS). GluRs are responsible for excitatory synaptic transmission and influence synaptic plasticity, which is important for memory formation, learning, and regulation.<sup>[149]</sup> Glutamate receptors can be divided into two families: ionotropic (ligand-gated cation channels) and metabotropic (G-protein coupled) receptors, of which only the former will be discussed in this thesis.

Ionotropic GluRs (iGluRs) consist of four large subunits (>900 residues) that form a central ion channel pore (Figure 6.1). These receptor subunits are modular and contain four discrete domains: the extracellular amino-terminal domain (ATD), the extracellular ligand-binding domain (LBD), the transmembrane domain (TMD) that forms the cation-selective pore and an intracellular carboxyl-terminal domain (CTD). The form of both the ATD and LBD of iGluRs are often described as clamshells (or Venus fly-traps).<sup>[150]</sup>

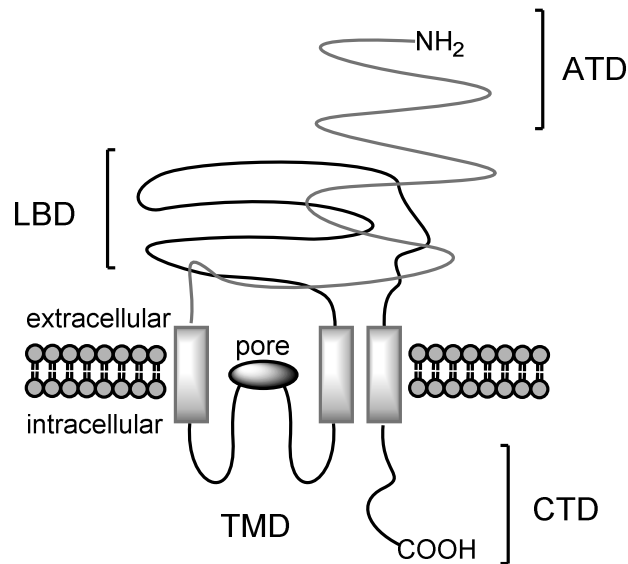


**Figure 6.1.** Schematic depiction of iGluRs.

iGluRs are grouped into four distinct classes based on pharmacology and structural homology: AMPA receptors (GluA1–GluA4), kainate receptors (GluK1–GluK5), NMDA receptors (GluN1,

GluN2A–GluN2D, GluN3A, and GluN3B), and the  $\delta$  receptors (GluD1 and GluD2). The first three subtypes are well studied and are named after their selective agonists: *N*-methyl-D-aspartate (**6.2**), kainic acid (**6.3**) and 2-amino-3-(5-methyl-3-hydroxyisoxazol-4-yl)propanoic acid (**6.4**) (Figure 6.2).<sup>[150-151]</sup> The last class,  $\delta$  receptors, is placed within the family of iGluRs only based on sequence homology.<sup>[152]</sup> So far, no ligand-mediated activation was observed and whether they serve as ion channels or have a metabotropic function is still a subject of ongoing research.<sup>[153]</sup>

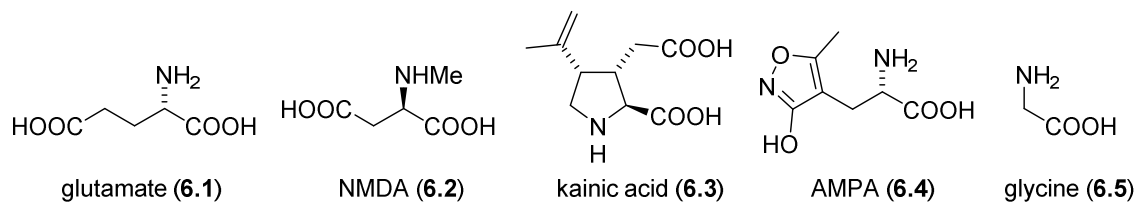


**Figure 6.2.** The universal and the three subtype-selective agonists, and co-agonist glycine (**6.5**).

NMDA receptors function as modulators of synaptic response as well as co-incidence detectors. They are heterotetramers and their activation requires the binding of both glutamate (**6.1**) and glycine (**6.5**). While this process is responsible for opening and closing of the ion channel, the current flow through the channel is voltage dependent. Extracellular  $Mg^{2+}$ - and  $Zn^{2+}$ -ions can block the channel pore, preventing the flow of ions. Depolarization of the cell is necessary to release this channel inhibition, allowing  $Na^+$ - and  $Ca^{2+}$ -ions into the cell and  $K^+$  out of the cell. The influx of  $Ca^{2+}$ -ions can then lead to the activation of a variety of signaling pathways.<sup>[154]</sup>

Kainate receptors are selectively activated by kainic acid (**6.3**) which was isolated from red algae *Digenea simplex* and is a powerful neurotoxin that when injected into the mammalian brain leads to neuropathological lesions and seizures. Kainate receptors are built from multimeric assemblies of GluK1-3 and GluK4,5 subunits. Their function is less understood compared to NMDA or AMPA receptors but recent studies have shown that they are not predominantly found in excitatory postsynaptic signaling complexes but act principally as modulators of synaptic transmission and neuronal excitability. One way to perform these functions is as presynaptic regulators of neurotransmitter release. In addition, findings indicate that some of their neuronal function is mediated through non-canonical metabotropic signaling pathways.<sup>[155]</sup>

AMPA receptors are responsible for fast synaptic transmission in the CNS and their expression, assembly, trafficking and turnover are crucial for synaptic plasticity, neuronal development and

neurological diseases.<sup>[156]</sup> They consist of tetramers composed of the subunits GluA1-4.<sup>[157]</sup> In addition, all AMPA subunits exist as two spliced forms, known as Flip and Flop. Although the change in the receptor subunits is small (they differ only in a few amino acids), the effect results in altered desensitization kinetics.

Each AMPA receptor exhibits four agonist-binding sites of which two need to be occupied by a ligand for activation of the ion channel to occur. Upon binding, a change in protein conformation opens the ion channel and cation influx leads to a local change in membrane potential known as an excitatory post-synaptic potential. Most AMPA receptors are permeable to only Na<sup>+</sup> and K<sup>+</sup> but not Ca<sup>2+</sup>.<sup>[158]</sup> It was found that this selectivity is regulated by the presence of the GluA2 subunit and receptors lacking GluA2 are Ca<sup>2+</sup> permeable.<sup>[159]</sup>

## 6.2. AMPA Agonists and Antagonists

Studies of crystal structures of agonists and antagonists bound to iGluR LBDs have shown that agonists bind in the cleft between each shell which leads to a partial closure of the LBD-clamshell.<sup>[160]</sup> Most agonists and partial agonists of AMPA receptors are derivatives of glutamate (**6.1**) as they invariably feature the  $\alpha$ -amino acid moiety of the neurotransmitter. In contrast, the carboxylic acid end of **6.1** can be replaced by a variety of structural motifs without losing agonist activity.<sup>[151a]</sup> Some selected examples of agonists are shown in Figure 6.3. Quisqualic acid (**6.6**) is one of the most potent AMPA agonists known and is used in neuroscience to induce excitotoxicity. Originally, AMPA receptors were named after quisqualic acid (**6.6**) but were renamed because **6.6** would also bind to other glutamate receptors.<sup>[161]</sup> Willardiine (**6.7**) is another natural occurring agonist and has been subject to SAR studies. It was found that halogenation at the C5-position has a huge influence on potency (decreases with increasing bulk of the residue) and selectivity.<sup>[162]</sup>

Many agonists bind to both AMPA and kainate receptors but despite the large number of ligand-bound X-ray structures, it is not possible to predict selectivity based on the molecular scaffold. AMPA (**6.4**) has been used as a template for many derivatives and the structure-activity relationships of this class of agonists are well defined. The isoxazole ring can be substituted with a variety of residues at position 5, which can lead to selectivity within receptor families. For instance, the bulky *tert*-butyl substituent on the heterocycle in ATPA (**6.8**) provides very high selectivity for GluK1<sup>[163]</sup> while Bn-Tet-AMPA (**6.9**) was found to be selective for GluA2-4.<sup>[164]</sup>

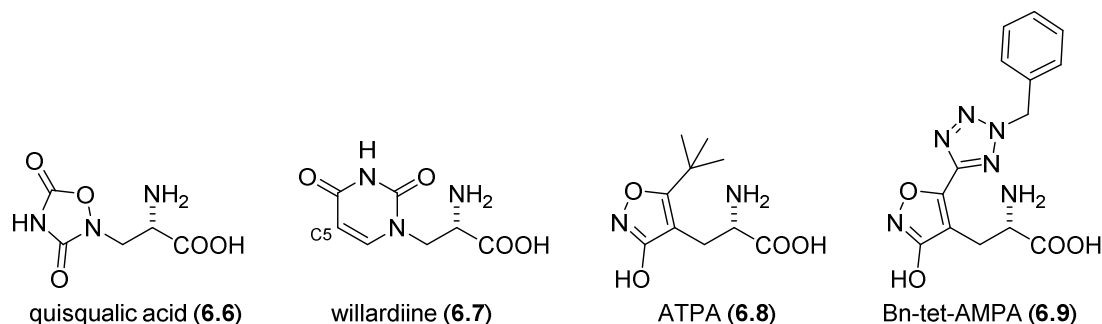


**Figure 6.3.** Examples of AMPA receptor agonists.

The two biggest classes of AMPA antagonists comprise amino acid derivatives and quinoxalines.<sup>[165]</sup> For the former, the structure of AMPA (6.4) has been used as a template, an interesting example being APPA (6.10) whose (*S*)-form is a full agonist whereas the (*R*)-form acts as an antagonist (Figure 6.4).<sup>[166]</sup> Other examples are AMOA (6.11), a selective but weak AMPA receptor antagonist,<sup>[167]</sup> ATOA (6.12) and ATPO (6.13) which are more potent and selective than AMOA (6.11). SAR studies showed that the distal acid moiety is important for the activity, with the phosphonic acid generally being more effective than the corresponding carboxylic acid.<sup>[168]</sup>

Another well studied amino-acid based family of antagonists is the decahydroisoquinolines. In this case, receptor activity was found to depend on the length of the polar side chain and the ring-junction (*trans*-derivatives are inactive).<sup>[169]</sup> Two examples are compounds LY293558 (6.14) and LY377770 (6.15) which both have shown *in vivo* efficacy as neuroprotectants.

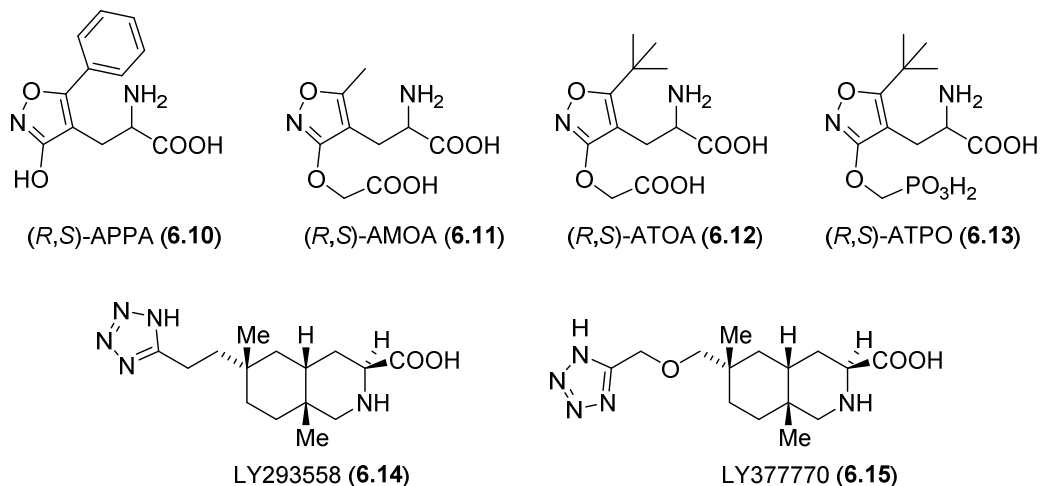


**Figure 6.4.** Examples of amino acid derived AMPA receptor antagonists.

The second big class of AMPA antagonists constitutes quinoxaline derivatives with CNQX (**6.16**), DNQX (**6.17**) and NBQX (**6.18**) being some of the first members of this family (Figure 6.5.a).<sup>[170]</sup> While **6.16** and **6.17** also bind to the Gly/NMDA binding site, NBQX (**6.18**) exhibits better selectivity and was therefore frequently used to study AMPA receptors in the past.<sup>[171]</sup> One of the biggest drawbacks of these first generation antagonists is their poor water solubility. To alleviate this issue, hydrophilic groups were introduced to the quinoxalinedione scaffold, resulting in compounds such as YM872 (**6.19**, Zonampanel)<sup>[172]</sup> or MPQX (**6.20**, fanampanel, ZK200775).<sup>[173]</sup> Both have entered clinical trials for treating cerebral ischemia, but these trials had to be halted due to severe side effects.<sup>[174]</sup>

Based on a broad body of SAR studies, a number of structural features could be revealed that are important for antagonist activity: (i) the amino group at position 1 that acts as a proton donor and binds to a proton acceptor site of the receptor; (ii) the 2,3-dione moiety, which serves as a potent hydrogen bond acceptor; (iii) a strong EWG, such as NO<sub>2</sub>, CN, CF<sub>3</sub> or halogen, as R<sub>4</sub>, which increases the acidity of the nitrogen at position 1 and can engage in a weak hydrogen bond interaction with a suitable receptor site. In addition, the introduction of a polar hydrophilic functionality as R<sub>1</sub> improves solubility (Figure 6.5.b).<sup>[165, 175]</sup>

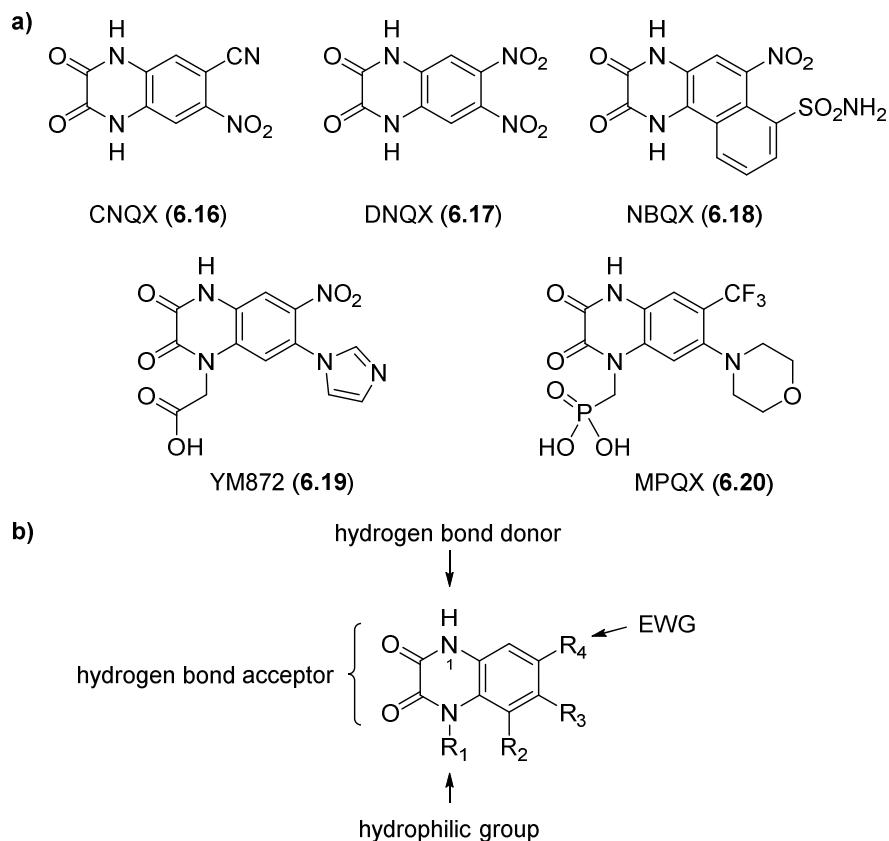


**Figure 6.5.** a) Examples of quinoxaline based AMPA receptor antagonists. b) Crucial structural features for quinoxaline-antagonists.

### 6.3. Photochromic AMPA Receptor Agonist

Due to the crucial role AMPA receptors play in the CNS, the ability to control their activity by light represents a useful tool for studying their function. Previous efforts in our group have resulted in the development of a photochromic AMPA receptor agonist.<sup>[176]</sup> The design of the photoswitch was based on the highly selective agonist Bn-Tet-AMPA (**6.9**), a derivative of AMPA (**6.4**). The X-ray structure of Bn-Tet-AMPA (**6.9**) bound to the GluA2 LBD, published in 2005, indicated that substitution of the benzene ring of **6.9** in *meta*-position would be tolerated without loss of activity.<sup>[177]</sup> Based on this hypothesis, azobenzenes **6.21–6.23** were synthesized and termed ATAs (azobenzene tetrazolyl AMPAs) (Figure 6.6). Their biological activity was assessed using whole-cell patch-clamp electrophysiology in mouse cortical slices and HEK293T cells, transiently expressing GluA2 receptors. Out of compounds **6.21–6.23**, **6.23** proved to be the most effective *trans*-agonist in HEK293T cells. ATA-3 (**6.23**) elicited the strongest inward current in its dark-adapted *trans*-state,

while irradiation with 480 nm light led to isomerization to its inactive *cis*-form (Figure 6.7). In addition, ATA-3 (**6.23**) was able to control the action potential firing of mouse cortical neurons and exhibited selectivity for AMPA over kainate and NMDA receptors.

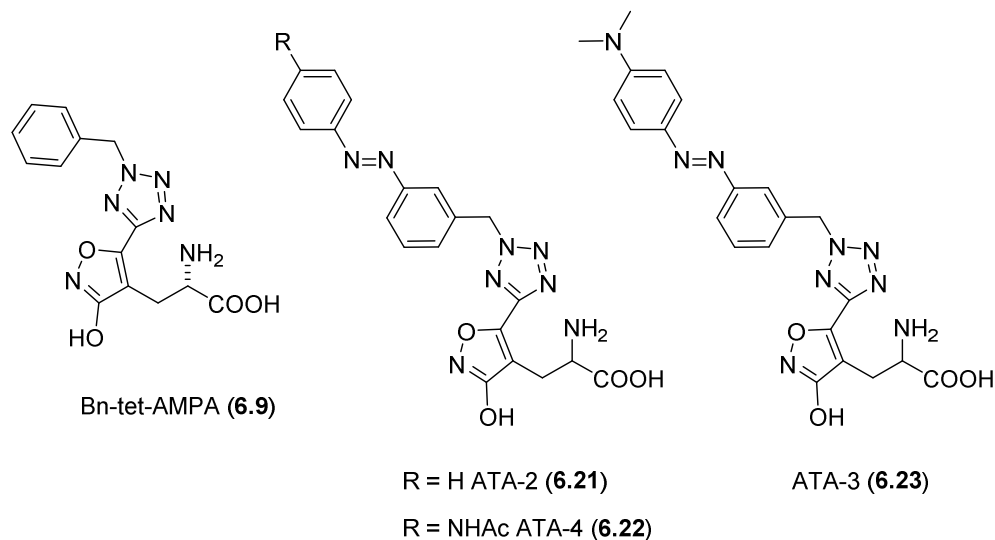


**Figure 6.6.** Structure of Bn-Tet-AMPA (**6.9**) and ATA-2-4 (**6.21–6.23**).

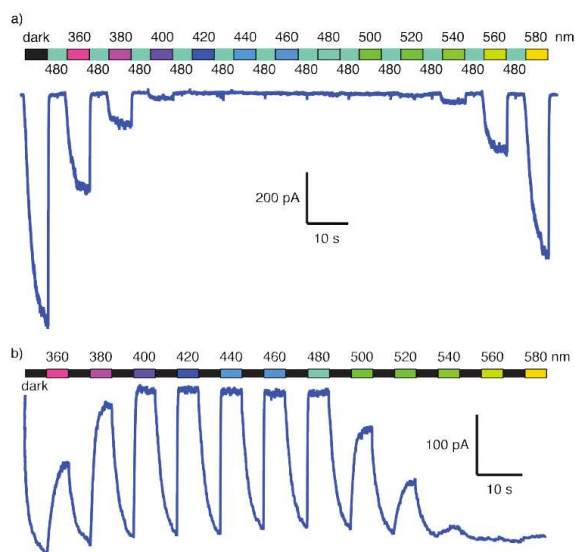


**Figure 6.7.** Light-induced current recorded from GluA2-expressing cells. a) Action spectrum of ATA-3 (**6.23**), b) Action spectrum recorded with intermittent darkness from a different cell ( $c = 50$  mM).

Subsequent studies in blind mice retinae revealed that ATA-3 (**6.23**) was able to confer light sensitivity on the retinal tissue by primarily acting on amacrine and retinal ganglion cells. This approach represented a conceptually novel way for the restoration of vision, as previously demonstrated using photochromic channel blockers.<sup>[178]</sup>

#### 6.4. Project Outline

AMPA receptors have been the focus of extensive research since they are responsible for the majority of the fast excitatory communication at synapses in the brain and influence synaptic plasticity, assumed to be crucial for memory and learning.<sup>[149, 151a, 179]</sup> In addition, they are involved in many neurological diseases such as amyotrophic lateral sclerosis, epilepsy and Alzheimer's disease which make them potential therapeutic targets.<sup>[180]</sup> Much effort has been put into the development of AMPA antagonists for clinical applications and in 2012 perampanel (**6.24**) was the first non-competitive antagonist to be approved (Figure 6.8). Sold under the name Fycompa, **6.24** is used for the treatment of partial-onset seizures in people with epilepsy.<sup>[181]</sup>

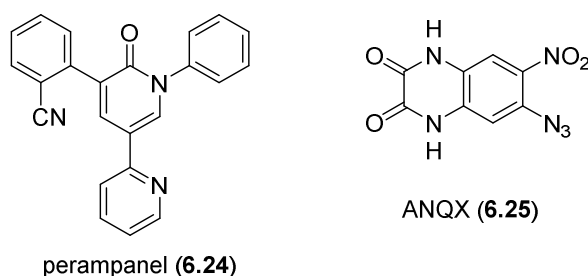
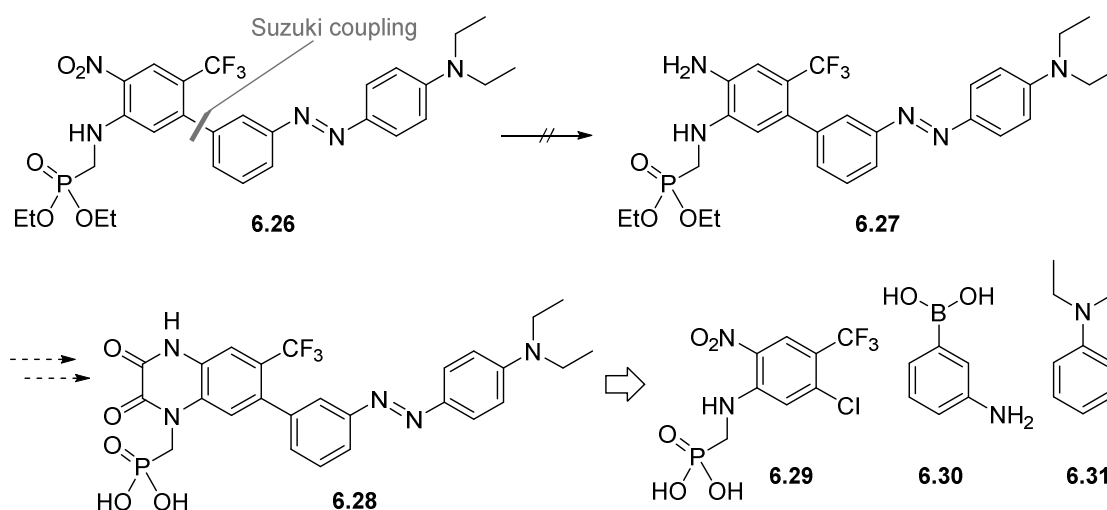


**Figure 6.8.** Structure of perampanel (**6.24**), the first non-competitive AMPA antagonist used as a therapeutic and and ANQX (**6.25**), a caged AMPA antagonist.

Even though AMPA receptors have been the focus of many studies, there is still a lot unknown about their function and regulation. Being able to reversibly activate an AMPA selective ligand with light would provide a useful tool for investigating these issues with unparalleled spatiotemporal control. At that point, only one light-responsive antagonist existed, the caged ligand ANQX (**6.25**) (Figure 6.8).<sup>[182]</sup> With **6.25** the England group showed the inhibition of AMPA receptors in *Xenopus* oocytes upon irradiation with UV light. The disadvantage of this approach is its irreversibility: uncaging of ANQX (**6.25**) leads to the formation of a nitrene species (structure

not shown) that inserts into either the peptide backbone or the amino acid side chains of the protein to which it is bound, permanently altering the receptor. We therefore aimed to develop a photoswitchable antagonist that can be reversibly turned on and off. To this end, we used the antagonist MPQX (**6.20**)<sup>[173]</sup> as a template and wanted to replace the morpholine group with an azobenzene. Previous work in our group focusing on the synthesis of azobenzene **6.27** (Scheme 6.1) showed that intermediate **6.26** could be accessed *via* Suzuki-coupling but reduction of the nitro group was problematic. In light of this issue, we wanted to synthesize **6.27** using a different route, including Suzuki coupling of **6.29** and **6.30** and late-stage formation of the azobenzene moiety through an azo-coupling with **6.31**. This strategy would also be amenable for the preparation of other derivatives with different substitution patterns.



**Scheme 6.1.** Past and future approach towards azobenzene **6.27**.

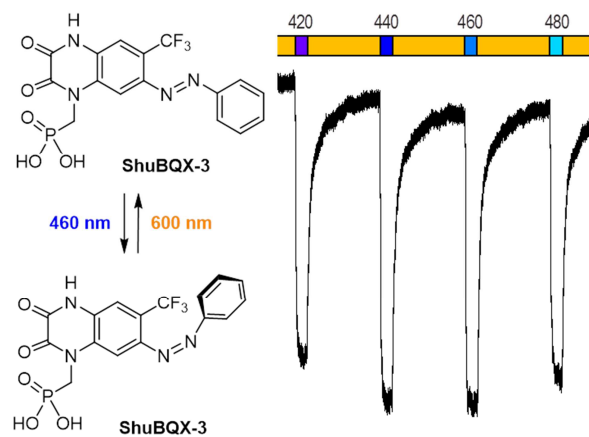
## 7. Results and Discussion

### 7.1. Optical control of AMPA receptors using a photoswitchable quinoxaline-2,3-dione antagonist

Reprinted with permission from:

D. M. Barber, S.-A. Liu, K. Gottschling, M. Sumser, M. Hollmann, D. Trauner,  
*Chem. Sci.* **2017**, *8*, 611-615.

Copyright © 2016 The Royal Society of Chemistry




 CrossMark  
 click for updates
Cite this: *Chem. Sci.*, 2017, 8, 611

## Optical control of AMPA receptors using a photoswitchable quinoxaline-2,3-dione antagonist†

David M. Barber,‡<sup>a</sup> Shu-An Liu,‡<sup>a</sup> Kevin Gottschling,<sup>b</sup> Martin Sumser,<sup>a</sup> Michael Hollmann<sup>b</sup> and Dirk Trauner\*<sup>a</sup>

AMPA receptors respond to the neurotransmitter glutamate and play a critical role in excitatory neurotransmission. They have been implicated in several psychiatric disorders and have rich pharmacology. Antagonists of AMPA receptors have been explored as drugs and one has even reached the clinic. We now introduce a freely diffusible photoswitchable antagonist that is selective for AMPA receptors and endows them with light-sensitivity. Our photoswitch, **ShuBQX-3**, is active in its dark-adapted *trans*-isoform but is significantly less active as its *cis*-isoform. **ShuBQX-3** exhibits a remarkable red-shifting of its photoswitching properties through interactions with the AMPA receptor ligand binding site. Since it can be used to control action potential firing with light, it could emerge as a powerful tool for studying synaptic transmission with high spatial and temporal precision.

Received 12th April 2016  
Accepted 1st August 2016

DOI: 10.1039/c6sc01621a

www.rsc.org/chemicalscience

### Introduction

Photopharmacology is the attempt to endow biological targets with light sensitivity using small photoswitchable molecules.<sup>1</sup> It has been applied to a wide variety of molecular targets, including ion channels,<sup>2</sup> G-protein coupled receptors (GPCRs)<sup>3</sup> and enzymes.<sup>4</sup> As such, it has enabled the light-dependent control of diverse cellular processes, such as proliferation<sup>5</sup> and neuronal excitability.<sup>6</sup>

The ionotropic glutamate receptors (iGluRs) are attractive targets for photopharmacology due to their fundamental roles in excitatory neurotransmission<sup>7</sup> and their involvement in neurodegenerative conditions and psychiatric disorders.<sup>8</sup> The iGluRs are natively gated by the neurotransmitter glutamate and are divided into three subclasses due to their individual responses to selective agonists: AMPA receptors (GluAs), kainate receptors (GluKs) and NMDA receptors (GluNs).<sup>9</sup>

To date, all three of the iGluR subtypes have been addressed with photopharmacology, using freely diffusible photoswitchable agonists.<sup>10</sup> Although synthetic agonists for neurotransmitter receptors are powerful tools, they do create a non-physiological situation that can complicate the analyses of

neural networks. This is perhaps the reason why antagonists of glutamatergic signaling are more widely used in neuroscience and why they have undergone extensive development as drugs to treat psychiatric diseases.<sup>11</sup> It would be advantageous to use light to precisely control glutamate receptor antagonists and target their actions to specific locations. To that end, a few caged antagonists of iGluRs have been disclosed<sup>12</sup> but their activation is irreversible. This prompted us to develop a photoswitchable antagonist that can be reversibly turned on and off. Our studies resulted in a quinoxaline-2,3-dione derivative, termed **ShuBQX-3**,<sup>§</sup> that enables the optical control of AMPA receptor-mediated action potential firing of hippocampal neurons.

### Results and discussion

Our design of **ShuBQX-3** was based on the vast array of antagonists for AMPA receptors that have been developed.<sup>13</sup> These encompass compounds that exhibit non-competitive antagonism, such as perampanel,<sup>14</sup> which is clinically used, as well as those that compete for the glutamate binding site. Competitive AMPA receptor antagonists that contain the quinoxaline-2,3-dione motif (Fig. 1a and b), are an extremely well developed family of antagonists and have undergone extensive structure-activity relationship (SAR) studies.<sup>15</sup>

Starting from the parent compound **DNQX**, a wide array of more selective and more soluble derivatives have been developed, including **CNQX** and **NBQX** (Fig. 1a). To increase solubility, carboxylate or phosphonate moieties were introduced on the nitrogen in position 4, which gave rise to **zonampanel**, **LU115455** and **MPQX** (fanampanel) (Fig. 1b).<sup>14</sup>

<sup>a</sup>Department of Chemistry and Center for Integrated Protein Science, Ludwig Maximilians University Munich, Butenandstraße 5-13, 81377 Munich, Germany. E-mail: dirk.trauner@lmu.de

<sup>b</sup>Department of Biochemistry I – Receptor Biochemistry, Ruhr-Universität-Bochum, Bochum 44780, Germany

† Electronic supplementary information (ESI) available: Experimental procedures and characterisation data. See DOI: 10.1039/c6sc01621a

‡ These authors contributed equally.

## Chemical Science

## Edge Article

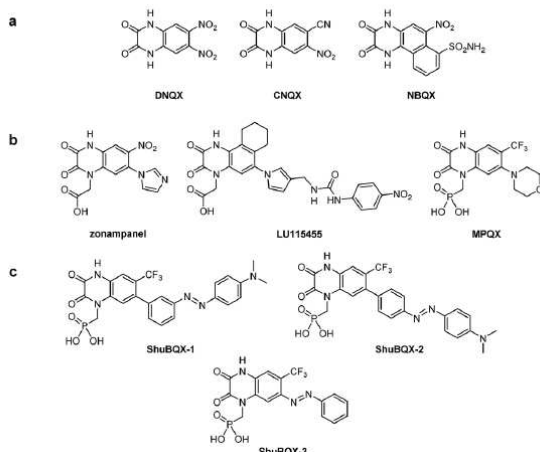
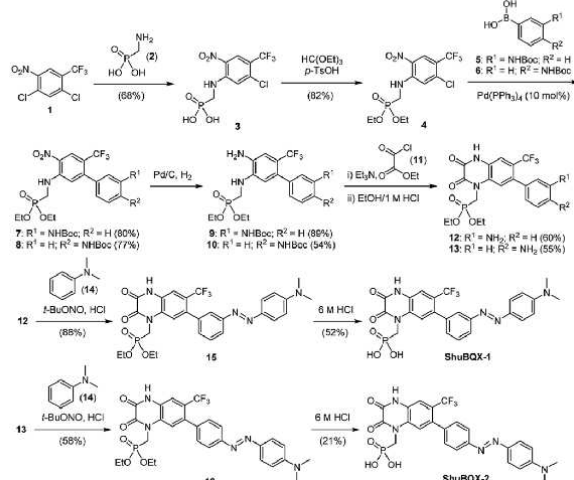


Fig. 1 (a) Molecular structures of quinoxaline-2,3-dione AMPA receptor antagonists. (b) Molecular structures of quinoxaline-2,3-dione AMPA receptor antagonists with increased solubility. (c) Molecular structures of the designed photochromic AMPA receptor antagonists ShuBQX-1, ShuBQX-2 and ShuBQX-3.

We postulated that an azobenzene moiety could be accommodated in the 6-position of the quinoxaline-2,3-dione core as sterically bulky substituents are tolerated in this position. Our design hypothesis was also supported by a X-ray crystal structure of the compound **MPQX** bound to a GluA2 receptor.<sup>16</sup> The crystal structure strongly suggested that a reasonable amount of steric bulk could be accommodated in the 6-position of the quinoxaline-2,3-dione without interfering with the binding of the antagonist. On the other hand, we concluded that photoisomerization of such a moiety would change the affinity of a ligand bound to the clamshell-like ligand binding domain. At the very least, this could be mediated by a reorganization of the solvation sphere upon photoisomerization. We also added the phosphonic acid side chain from the antagonist **MPQX** as it dramatically improves the solubility of the compound in aqueous solutions.<sup>17</sup> When considering all of our strategic aspects, the photoswitchable antagonists **ShuBQX-1**, **ShuBQX-2** and **ShuBQX-3** were designed (Fig. 1c).

We then set about preparing our target photoswitches, initially focusing on **ShuBQX-1** and **ShuBQX-2** (Scheme 1). Starting from dichloride **1** and aminomethylphosphonic acid (**2**) a  $S_NAr$  reaction furnished phosphonic acid **3**, which was protected to afford phosphonate ester **4**. Suzuki coupling reactions using boronic acids **5** and **6**, bearing Boc-protected anilines in the *meta*- and *para*-positions, respectively, were performed to provide biaryls **7** and **8**. Subsequent reduction of the nitro group followed by cyclization with ethyl chlorooxoacetate (**11**) afforded the desired *meta*- and *para*-amino substituted quinoxaline-2,3-diones **12** and **13**. Quinoxaline **12** was then converted to *meta*-azobenzene **15** in an azo-coupling reaction with *N,N*-dimethylaniline (**14**) and **ShuBQX-1** was furnished after deprotection of the phosphonate ester using 6 M HCl followed by reverse phase chromatography. The preparation of **ShuBQX-2** followed the same azo-coupling and deprotection procedures as **ShuBQX-1**,

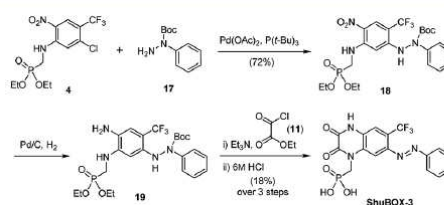


Scheme 1 Synthesis of the photochromic AMPA receptor antagonists **ShuBQX-1** and **ShuBQX-2**.

with moderate yields of the desired products being obtained in both reactions.

We next accomplished the synthesis of **ShuBQX-3** starting from phosphonate ester **4** (Scheme 2). A Buchwald–Hartwig cross-coupling of *N*-Boc protected hydrazine **17** with phosphonate ester **4** afforded protected hydrazine **18** in 72% yield. Reduction of the nitro group followed by cyclization to the quinoxaline-2,3-dione using ethyl chlorooxoacetate (**11**) and subsequent deprotection of the phosphonate ester gave **ShuBQX-3** in 18% yield (over three steps).

With our small family of soluble, photochromic ligands in hand, we first deduced the optimum photoswitching wavelengths using UV-Vis spectroscopy (Fig. S1†) and then determined their functional properties as light-controllable AMPA receptor antagonists. Whole-cell patch-clamp electrophysiology of HEK293T cells expressing GluA1-L497Y receptors (a non-desensitizing AMPA receptor mutant)<sup>18</sup> found that the photochromic ligands **ShuBQX-1** (5  $\mu$ M) and **ShuBQX-2** (5  $\mu$ M) are good antagonists of AMPA receptors in the presence of glutamate (300  $\mu$ M). However, upon photoisomerization using blue (460 nm) and green (560 nm) light only a small change in AMPA receptor antagonism was observed (Fig. 2a). We then evaluated **ShuBQX-3** (5  $\mu$ M) and discovered that it is an excellent photo-switchable antagonist of AMPA receptors.



Scheme 2 Synthesis of the photochromic AMPA receptor antagonist **ShuBQX-3**.

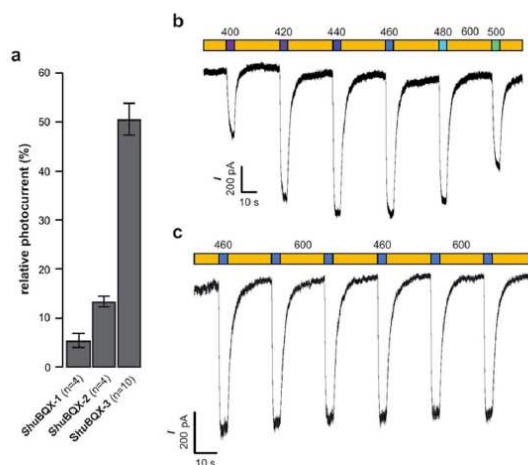


Fig. 2 Whole-cell patch-clamp characterization of ShuBQX-1, ShuBQX-2 and ShuBQX-3 in the presence of glutamate (300  $\mu\text{M}$ ) using HEK293T cells transfected with GluA1-L497Y receptors. (a) Comparison of relative photocurrent of ShuBQX-1, ShuBQX-2 and ShuBQX-3 (5  $\mu\text{M}$ ). Values represent mean  $\pm$  SEM. (b) Action spectrum of ShuBQX-3 (20  $\mu\text{M}$ ) under illumination with orange light (600 nm) and varying wavelengths (400–500 nm). (c) Photoswitching of ShuBQX-3 (10  $\mu\text{M}$ ) using 460 nm and 600 nm light over multiple switching cycles. Traces representative of  $n = 5$  cells.

First, we determined the  $\text{IC}_{50}$  value of ShuBQX-3 in the absence of light and in the presence of glutamate (300  $\mu\text{M}$ ). It was found to be 3.1  $\mu\text{M}$  (Fig. S3†). A very similar value ( $\text{IC}_{50} = 3.3 \mu\text{M}$ ) was obtained when illuminating ShuBQX-3 with orange light (600 nm). At this wavelength, the photoswitch largely resides in the *trans*-form. Under blue light illumination (460 nm), which favors the *cis*-state of ShuBQX-3, the antagonist was significantly less potent than in the dark-adapted state (Fig. 2). Finally, experiments conducted using ShuBQX-3 with differing concentrations of glutamate (100  $\mu\text{M}$  and 1 mM) confirmed that it is a competitive antagonist of GluA1 receptors (Fig. S4†). Further studies on the biological activity of ShuBQX-3 using patch-clamp electrophysiology showed that glutamate-induced currents are completely blocked in its *trans*-form. Upon illumination with 460 nm light, 50% of the glutamate-induced current (compared to the current induced in the absence of ShuBQX-3) could be released (Fig. 2a). We then determined the action spectrum of ShuBQX-3 in the presence of glutamate. When the wavelength was switched between orange light (600 nm) and different wavelengths of purple blue and green light (400–500 nm), we observed large differences in current (Fig. 2b). The maximum inward current was consistently observed when illuminating with 440 nm or 460 nm (Fig. S5†) whereas minimum inward currents were observed using long wavelength light or in the dark. Reversible photoactivation of AMPA receptors with ShuBQX-3 is robust and could be repeated over many times without any significant loss of receptor antagonism (Fig. 2c). Highly reproducible photoswitching of ShuBQX-3 was also obtained when operating in current-clamp mode (Fig. S6†).

To determine the selectivity profile of ShuBQX-3 (5  $\mu\text{M}$ ) in its dark state, we evaluated its effects on *Xenopus* oocytes expressing a variety of glutamate receptors (Fig. 3). ShuBQX-3 (5  $\mu\text{M}$ ) showed excellent antagonism of all GluA1-containing receptors that were tested (85–93%). By contrast, the amount of antagonism observed at this concentration on the GluK2 receptor was significantly reduced (25%) when inducing the current using glutamate (100  $\mu\text{M}$ ). Reducing the concentration of glutamate (30  $\mu\text{M}$ ) increased the amount of antagonism exhibited by ShuBQX-3 at the GluK2 receptor (49%). Thus, indicating that the dark state of ShuBQX-3 is a competitive antagonist of the GluK2 receptor. Additionally, ShuBQX-3 (5  $\mu\text{M}$ ) was evaluated against several GluN1-1a-containing receptors. ShuBQX-3 (5  $\mu\text{M}$ ) displayed minimal antagonism at the GluN1-1a-containing glutamate receptors, demonstrating that ShuBQX-3 is partially selective for AMPA receptors over kainate, whilst having significantly reduced levels of antagonism at NMDA receptors.

With the full evaluation of ShuBQX-3 in transfected HEK293T cells and *Xenopus* oocytes complete, we set out to demonstrate that ShuBQX-3 could control native AMPA receptors in excitable cells. For these experiments we used acute mouse brain slice preparations and whole cell patch-clamp electrophysiology of hippocampal CA1 neurons. Pleasingly, when ShuBQX-3 (10  $\mu\text{M}$ ) and glutamate (100  $\mu\text{M}$ ) were locally applied in a brain slice preparation, the induced action potential firing of a single neuron could be effectively controlled by switching between blue (460 nm) and orange (620 nm) light (Fig. 4). The NMDA-receptor antagonist AP-5 (50  $\mu\text{M}$ ) was locally added to ensure that the action potential firing was not caused by any interactions between the NMDA receptors and glutamate. Additionally, we were able to optically control hippocampal CA1 neurons when using AMPA as the agonist (Fig. S7†). Demonstrating that ShuBQX-3 is selective for AMPA receptors.

The action spectrum of ShuBQX-3 is noteworthy, as we observed a significant difference between the optimal

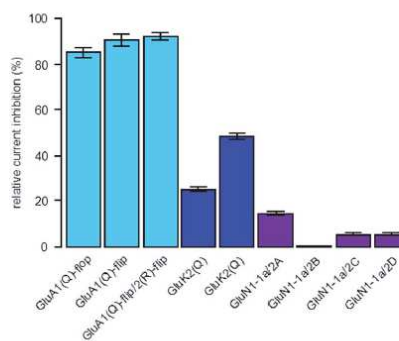


Fig. 3 Selectivity profile of ShuBQX-3 (5  $\mu\text{M}$ ) in the dark at various glutamate receptors expressed in *Xenopus* oocytes. Currents were induced using the following methods: GluA1-containing receptors = kainic acid (100  $\mu\text{M}$ ); GluK2 – containing receptors = glutamate (100  $\mu\text{M}$ , left column) and glutamate (30  $\mu\text{M}$ , right column); GluN1-1a-containing receptors = glutamate (100  $\mu\text{M}$ ) and glycine (10  $\mu\text{M}$ ). Values represent mean  $\pm$  SEM ( $n = 5$  oocytes).

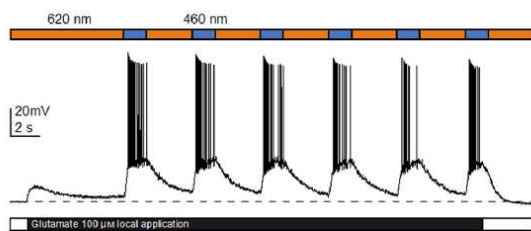


Fig. 4 Optical control of action potential firing in hippocampal CA1 neurons using ShuBQX-3 (10  $\mu$ M) in the presence of glutamate (100  $\mu$ M) and AP-5 (50  $\mu$ M).

photoswitching wavelengths established by the UV-Vis experiments and the physiological patch-clamp experiments. In our UV-Vis experiments, a solution of ShuBQX-3 (50  $\mu$ M in DMSO) displayed optimal photoswitching at 380 nm (*trans* to *cis*) and 460 nm (*cis* to *trans*), with a  $\lambda_{\text{max}} = 365$  nm for the *trans*-isomer (Fig. 5a, S1†). However, in the patch-clamp experiments in HEK293T cells expressing the GluA1 receptor, ShuBQX-3 exhibited a bathochromic shift in its action spectrum, with optimal photoswitching now taking place when illuminating with 460 nm and 600 nm light.<sup>19</sup> In an attempt to ascertain why this bathochromic shift was occurring, we consulted the X-ray crystal structure of the non-photoswitchable antagonist MPQX bound to a GluA2 receptor (Fig. 5c).<sup>16</sup> The structure features prominent interaction between the guanidinium moiety of arginine R-485, which is also involved in glutamate binding, and the quinoxaline-2,3-dione core of MPQX. We therefore postulated that this interaction could have an effect on the photoswitching properties of ShuBQX-3 when it is bound to the GluA1 receptor.

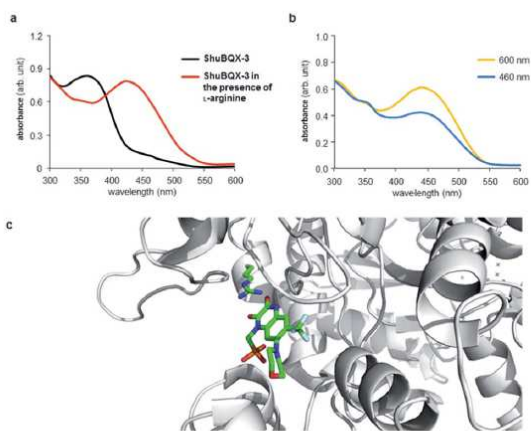


Fig. 5 UV-Vis analysis of the photoswitching properties of ShuBQX-3. (a) UV-Vis spectrum showing ShuBQX-3 (50  $\mu$ M in DMSO) and the bathochromic shift in the presence of 1 mM L-arginine. (b) UV-Vis spectrum ShuBQX-3 (50  $\mu$ M) in DMSO in the presence of 1 mM L-arginine when illuminated with 460 nm and 600 nm light. (c) X-ray structure of MPQX bound to a GluA2 receptor ligand binding domain, showing the interaction between a conserved arginine and the quinoxaline-2,3-dione.<sup>16</sup>

To probe this possible interaction, we took the UV-Vis solution of ShuBQX-3 (50  $\mu$ M in DMSO) and doped it with L-arginine. Indeed, a bathochromic shift of 75 nm ( $\lambda_{\text{max}} = 440$  nm) in the UV-Vis spectrum of ShuBQX-3 was observed (Fig. 5a) with a 20-fold excess of L-arginine. The optimum photoswitching wavelengths of ShuBQX-3 were now demonstrated to be 460 nm and 600 nm (Fig. 5b). When L-arginine was replaced by guanidine, a similar bathochromic shift was observed (Fig. S8†), substantiating our hypothesis. UV-Vis experiments conducted with the diethyl phosphonate of ShuBQX-3 showed that the phosphonic acid side chain is not crucial for the interaction (Fig. S9†). We also measured the thermal relaxation rate of ShuBQX-3 in the presence of L-arginine ( $\tau = 1.68$  min) and found it to be faster than the rate of ShuBQX-3 alone ( $\tau = 7.37$  min). This is in accordance to the rate acceleration of red-shifted azobenzenes in comparison to their non red-shifted analogues.<sup>20</sup> To the best of our knowledge, this is the first example of an azobenzene-based photoswitch to exhibit such red-shifting properties. Control experiments using ShuBQX-3 (50  $\mu$ M) dissolved in Ringer's solution showed almost no change in the absorption maximum (Fig. S1†). Our findings suggest that the interaction between R-485 and the quinoxaline-2,3-dione is responsible for the bathochromic shift in the action spectrum of ShuBQX-3.

## Conclusions

In summary, we have developed a photochromic antagonist that permits the precise optical control of AMPA receptors. Our photoswitch, ShuBQX-3, is active as its *trans*-isomer and is converted to its *cis*-isomer using blue light illumination enabled by red-shifting upon binding to AMPA receptors. ShuBQX-3 expands the photopharmacology of iGluRs and demonstrates that potent photoswitchable antagonists for these receptors can be developed. We envision that ShuBQX-3 will be an important tool for studying the function of AMPA receptors *in vivo*.

## Live subject statement

All animal procedures were performed in accordance with the guidelines of the Regierung Oberbayern/the Tierschutzgesetz (TierSchG) and the Tierschutzversuchsverordnung (TierSchVersV).

## Acknowledgements

D. M. B. gratefully acknowledges the European Commission for a Marie Skłodowska-Curie Intra-European Fellowship (PIEF-GA-2013-627990). S. L. thanks the Studienstiftung des deutschen Volkes for a PhD studentship. D. T. thanks the Munich Centre for Integrated Protein Science (CIPSM) and the European Research Council (Advanced Grant 268795). K. G. was funded by the International Graduate School of Neuroscience (IGSN) at the Ruhr University Bochum and the RUB Research School. We thank Dr Laura Salonen for initial studies toward the synthesis of ShuBQX-1 and Luis de la Osa de la Rosa for technical assistance. In addition, we are grateful to Dr Johannes Broichhagen

for helpful discussions and Philipp Leippe for assistance with the UV-Vis experiments.

## Notes and references

§ ShuBQX is a combination of the names of the authors D. M. B. and S. L. and the antagonist MPQX.

- (a) T. Fehrentz, M. Schönberger and D. Trauner, *Angew. Chem., Int. Ed.*, 2011, **50**, 12156–12182; (b) A. A. Beharry and G. A. Woolley, *Chem. Soc. Rev.*, 2011, **40**, 4422–4437; (c) C. Briek, F. Rohrbach, A. Gottschalk, G. Mayer and A. Heckel, *Angew. Chem., Int. Ed.*, 2012, **51**, 8446–8476; (d) W. Szymański, J. M. Beierle, H. A. V. Kistemaker, W. A. Velema and B. L. Feringa, *Chem. Rev.*, 2013, **113**, 6114–6178; (e) W. A. Velema, W. Szymanski and B. L. Feringa, *J. Am. Chem. Soc.*, 2014, **136**, 2178–2191.
- (a) M. Schönberger, M. Althaus, M. Fronius, W. Claus and D. Trauner, *Nat. Chem.*, 2014, **6**, 712–719; (b) J. Broichhagen, M. Schönberger, S. C. Cork, J. A. Frank, P. Marchetti, M. Bugliani, A. M. J. Shapiro, S. Trapp, G. A. Rutter, D. J. Hodson and D. Trauner, *Nat. Commun.*, 2014, **5**, 5116; (c) A. Damijonaitis, J. Broichhagen, T. Urushima, K. Hüll, J. Nagpal, L. Laprell, M. Schönberger, D. H. Woodmansee, A. Rafiq, M. P. Sumser, W. Kummer, A. Gottschalk and D. Trauner, *ACS Chem. Neurosci.*, 2015, **6**, 701–707.
- (a) M. Schönberger and D. Trauner, *Angew. Chem., Int. Ed.*, 2014, **53**, 3264–3267; (b) S. Pittolo, X. Gómez-Santacana, K. Eckelt, X. Rovira, J. Dalton, C. Goudet, J.-P. Pin, A. Llobet, J. Giraldo, A. Llebaria and P. Gorostiza, *Nat. Chem. Biol.*, 2014, **10**, 813–815.
- (a) C. Falenczyk, M. Schiedel, B. Karaman, T. Rumpf, N. Kuzmanovic, M. Grotli, W. Sippl, M. Jung and B. König, *Chem. Sci.*, 2014, **5**, 4794–4799; (b) B. Reisinger, N. Kuzmanovic, P. Löffler, R. Merkl, B. König and R. Sterner, *Angew. Chem., Int. Ed.*, 2014, **53**, 595–598; (c) X. Chen, S. Wehle, N. Kuzmanovic, B. Merget, U. Holzgrabe, B. König, C. A. Sotriuffer and M. Decker, *ACS Chem. Neurosci.*, 2014, **5**, 377–389; (d) J. Broichhagen, I. Jurastow, K. Iwan, W. Kummer and D. Trauner, *Angew. Chem., Int. Ed.*, 2014, **53**, 7657–7660.
- M. Borowiak, W. Nahaboo, M. Reynders, K. Nekolla, P. Jalinot, J. Hasserodt, M. Rehberg, M. Delattre, S. Zahler, A. Vollmar, D. Trauner and O. Thorn-Seshold, *Cell*, 2015, **162**, 403–411.
- (a) A. Polosukhina, J. Litt, I. Tochitsky, J. Nemargut, Y. Sychev, I. De Kouchkovsky, T. Huang, K. Borges, D. Trauner, R. N. Van Gelder and R. H. Kramer, *Neuron*, 2012, **75**, 271–282; (b) A. Mouro, T. Fehrentz, Y. Le Feuvre, C. M. Smith, C. Herold, D. Dalkara, F. Nagy, D. Trauner and R. H. Kramer, *Nat. Methods*, 2012, **9**, 396–402; (c) I. Tochitsky, A. Polosukhina, V. E. Degtyar, N. Gallerani, C. M. Smith, A. Friedman, R. N. Van Gelder, D. Trauner, D. Kaufer and R. H. Kramer, *Neuron*, 2014, **81**, 800–813.
- S. F. Traynelis, L. P. Wollmuth, C. J. McBain, F. S. Menniti, K. M. Vance, K. K. Ogden, K. B. Hansen, H. Yuan, S. J. Myers and R. Dingledine, *Pharmacol. Rev.*, 2010, **62**, 405–496.
- (a) S. A. Lipton, *Nat. Rev. Drug Discovery*, 2006, **5**, 160–170; (b) A. Alt, E. S. Nisenbaum, D. Bleakman and J. M. Witkin, *Biochem. Pharmacol.*, 2006, **71**, 1273–1288; (c) D. E. Jane, D. Lodge and G. L. Collingridge, *Neuropharmacology*, 2009, **56**, 90–113.
- R. W. Gereau and G. T. Swanson, *The Glutamate Receptors*, Humana Press, Totowa, 2008.
- (a) A. Reiner, J. Levitz and E. Y. Isacoff, *Curr. Opin. Pharmacol.*, 2015, **20**, 135–143; (b) M. Volgraf, P. Gorostiza, S. Szobota, M. R. Helix, E. Y. Isacoff and D. Trauner, *J. Am. Chem. Soc.*, 2007, **129**, 260–261; (c) P. Stawski, M. Sumser and D. Trauner, *Angew. Chem., Int. Ed.*, 2012, **51**, 5748–5751; (d) L. Laprell, E. Repak, V. Franckevicius, F. Hartrampf, J. Terhag, M. Hollmann, M. Sumser, N. Rebola, D. A. DiGregorio and D. Trauner, *Nat. Commun.*, 2015, **6**, 8076.
- P. K. Y. Chang, D. Verbich and R. A. McKinney, *Eur. J. Neurosci.*, 2012, **35**, 1908–1916.
- (a) K. P. S. J. Murphy, G. P. Reid, D. R. Trentham and T. V. P. Bliss, *J. Physiol.*, 1997, **504**, 379–385; (b) J. E. Reeve, M. M. Kohl, A. Rodríguez-Moreno, O. Paulsen and H. L. Anderson, *Commun. Integr. Biol.*, 2012, **5**, 240–242; (c) J. J. Chambers, H. Gouda, D. M. Young, I. D. Kuntz and P. M. England, *J. Am. Chem. Soc.*, 2004, **126**, 13886–13887.
- (a) S. S. Nikam and B. E. Kornberg, *Curr. Med. Chem.*, 2001, **8**, 155–170; (b) P. Stawski, H. Janovjak and D. Trauner, *Bioorg. Med. Chem.*, 2010, **18**, 7759–7772.
- S. Hibi, K. Ueno, S. Nagato, K. Kawano, K. Ito, Y. Norimine, O. Takenaka, T. Hanada and M. Yonaga, *J. Med. Chem.*, 2012, **55**, 10584–10600.
- D. Catarzi, V. Colotta and F. Varano, *Med. Res. Rev.*, 2007, **27**, 239–278.
- A. I. Sobolevsky, M. P. Rosconi and E. Gouaux, *Nature*, 2009, **462**, 745–756.
- L. Turski, A. Huth, M. Sheardown, F. McDonald, R. Neuhaus, H. H. Schneider, U. Dirnagl, F. Wiegand, P. Jacobsen and E. Ottow, *Proc. Natl. Acad. Sci. U. S. A.*, 1998, **95**, 10960–10965.
- Y. Stern-Bach, S. Russo, M. Neuman and C. Rosenmund, *Neuron*, 1998, **21**, 907–918.
- We also conducted patch-clamp experiments in which ShuBQX-1 and ShuBQX-2 were irradiated with varying wavelengths of light but no bathochromic shift was observed for either of these compounds (Fig. S2†).
- J. Garcia-Amorós and D. Velasco, *Beilstein J. Org. Chem.*, 2012, **8**, 1003–1017.

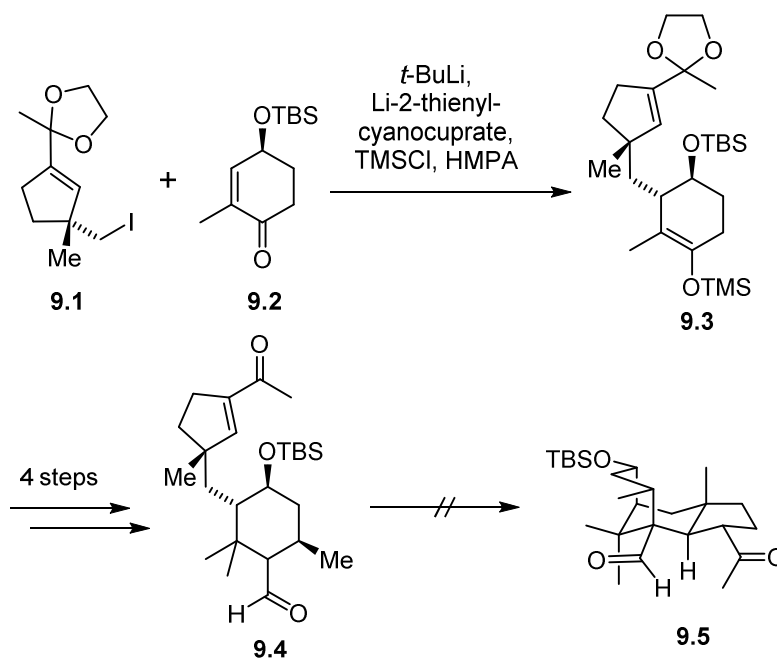
## 8. Conclusion and Outlook

In the second part of this thesis, the development of the first photoswitchable AMPA receptor antagonist, named ShuBQX-3, is described. The design is based on the known antagonist MPQX (6.20) in which the morpholine residue is replaced by a phenylazo group. ShuBQX-3 was synthesized in six steps from commercially available material including a Buchwald-Hartwig cross-coupling to connect the two aromatic rings. Using patch-clamp electrophysiology of HEK293T cells expressing GluA1 receptors ShuBQX-3 was identified as an excellent photoswitchable antagonist of AMPA receptors. ShuBQX-3 is active in its *trans*-form and switches to its less active *cis*-isomer upon illumination with 460 nm light. We could also show that ShuBQX-3 is able to control action potential firing in hippocampal CA1 neurons. In addition, a significant difference between the optimal photoswitching wavelengths established by the UV-Vis experiments and the physiological patch-clamp experiments was observed. Presumably, this interesting red-shift is caused by interactions with the AMPA receptor ligand binding site.

Efforts to make a tethered ligand out of ShuBQX-3 are under way in our laboratory.

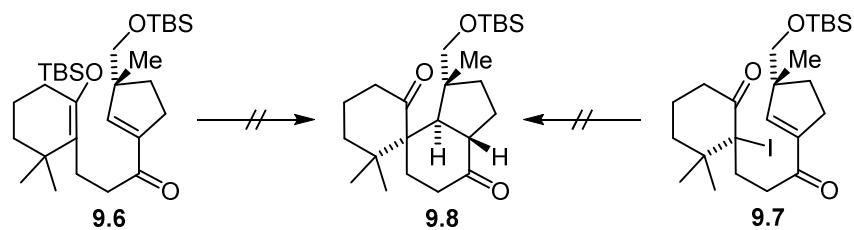
## 9. Summary

**Part I:** In the first part of this thesis, the total synthesis of wickerol A is described. Our initial approach was based on a Robinson annulation to construct the congested scaffold of the natural product. To this end, we prepared building block **9.1** and **9.2** which were combined through a conjugate addition. Silyl enol ether **9.3** was then methylated twice and elaborated to aldehyde **9.4** using a Peterson olefination, followed by hydrolysis. With key intermediate **9.4** in hand, we tested various amines and bases for the intramolecular conjugate addition, the initial step of the Robinson annulation but could not observe any product **9.5**, presumably due to the steric hindrance of the substrate. In light of these results, we began investigating a different approach towards the synthesis of wickerol A.



**Scheme 9.1.1<sup>st</sup>** generation route to wickerol A featuring a Robinson annulation as key the step.

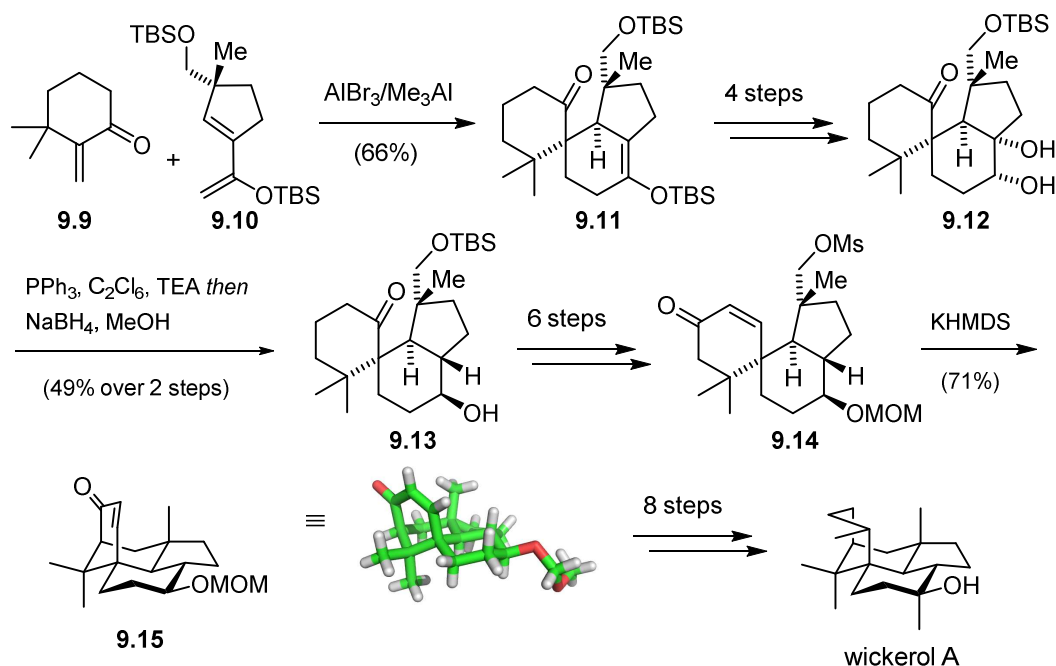
In our 2<sup>nd</sup> generation approach we planned to access wickerol A *via* spirocycle **9.8** which could arise from either an intramolecular Mukaiyama–Michael reaction of **9.6** or a radical cyclization of  $\alpha$ -iodoketone **9.7**. Unfortunately, all our attempts to close the 6-membered ring were met with failure, therefore we turned our attention to a Diels–Alder reaction to access **9.8**, which ultimately led to the successful synthesis of wickerol A.



**Scheme 9.2.** Attempts at formation of spirocycle **9.8**.

The envisioned intermolecular cycloaddition represented a major challenge since both partners (**9.9** and **9.10**), though electronically matched, were very sterically hindered. After extensive experimentation, we found that a mixture of  $\text{AlBr}_3/\text{AlMe}_3$  gave the desired product **9.11** as a single diastereomer. Through this single step, two crucial stereocenters of wickerol A, both of which are neopentyl and one a quaternary carbon, were set.

With three of the four rings of the natural product established, we installed the challenging *trans*-BA ring junction using a Pinacol-type rearrangement of diol **9.12**. Alcohol **9.13** was then elaborated to enone **9.14** which underwent the key intramolecular alkylation, completing the congested 6-5-6-6 scaffold of wickerol A. This ring closure is rather remarkable considering the *syn*-pentane strain built up in the C–C bond formation between the two neopentyl positions. Subsequent modifications of enone **9.15** include a stereoselective conjugate addition to introduce the C6-methyl group and a Barton–McCombie deoxygenation. The final challenge was the installation of the tertiary alcohol. Addition of a nucleophilic methyl group to the requisite ketone gave the undesired epimer of wickerol A. To overcome this strong, unfavorable substrate bias a sequence of olefination followed by Mukaiyama hydration was employed.



**Scheme 9.3.** Synthesis of wickerol A.

**Part II:** The second part of this thesis focuses on the development of a photoswitchable AMPA receptor antagonist. AMPA receptors represent one of four subclasses of ionotropic glutamate receptors and mediate most excitatory neurotransmission in the central nervous system. They are also implicated in processes such as memory and learning as well as various psychiatric disorders. Based on the antagonist MPQX (**6.20**), several derivatives incorporating an azobenzene moiety were synthesized and evaluated using patch-clamp electrophysiology of HEK293T cells expressing GluA1 receptors. Amongst them, ShuBQX-3 was identified as an excellent photoswitchable antagonist of AMPA receptors. Active in its *trans*-form, ShuBQX-3 can be switched to its less active *cis*-isomer upon illumination with 460 nm light. Using *Xenopus* oocytes expressing a variety of glutamate receptors, we found that ShuBQX-3 is partially selective for AMPA receptors over kainate, whilst having significantly reduced levels of antagonism at NMDA receptors. We could also show that ShuBQX-3 is able to control action potential firing of mouse cortical neurons. Furthermore, a remarkable difference between the optimal photoswitching wavelengths established by the UV-Vis experiments and the physiological patch-clamp experiments was observed. Presumably, this interesting red-shift is caused through interactions of ShuBQX-3 with the AMPA receptor ligand binding site.

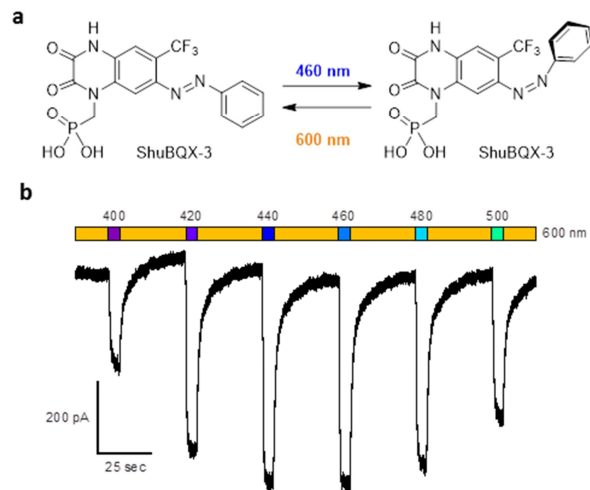


**Figure 9.1.** a) *trans*- and *cis*-form of ShuBQX-3. b) Action spectrum of ShuBQX-3 (20  $\mu$ m) under illumination with orange light (600 nm) and varying wavelengths (400 nm – 500 nm).

## **Experimental Section**

## 10. Experimental Section

### 10.1. General Experimental Details

All reactions were carried out with magnetic stirring, and if moisture or air sensitive, under nitrogen atmosphere using standard Schlenk techniques in oven-dried glassware (200 °C oven temperature), further dried under vacuum with a heat-gun at 450 °C. External bath temperatures were used to record all reaction temperatures. Low temperature reactions were carried out in a Dewar vessel filled with Et<sub>2</sub>O/liq. N<sub>2</sub> (−115 °C), acetone/dry ice (−78 °C) or distilled water/ice (0 °C). High temperature reactions were conducted using a heated silicon oil bath in reaction vessels equipped with a reflux condenser or in a pressure tube. Tetrahydrofuran (THF) and diethyl ether (Et<sub>2</sub>O) were distilled over sodium and benzophenone prior to use. Dichloromethane (DCM), triethylamine (Et<sub>3</sub>N), diisopropylethylamine (DIPEA) and diisopropylamine (DIPA) were distilled over calcium hydride under a nitrogen atmosphere. All other solvents were purchased from Acros Organics as 'extra dry' reagents. All other reagents with a purity > 95% were obtained from commercial sources (Sigma Aldrich, Acros, Alfa Aesar and others) and used without further purification.

**Flash column chromatography** was carried out with Merck silica gel 60 (0.040-0.063 mm).

**Analytical thin layer chromatography** (TLC) was carried out using Merck silica gel 60 F254 glass-backed plates and visualized under UV light at 254 nm. Staining was performed with ceric ammonium molybdate (CAM) or by oxidative staining with an aqueous basic potassium permanganate (KMnO<sub>4</sub>) solution and subsequent heating.

**NMR spectra** (<sup>1</sup>H NMR and <sup>13</sup>C NMR) were recorded in deuterated chloroform (CDCl<sub>3</sub>), benzene (C<sub>6</sub>D<sub>6</sub>) or dichloromethane (CD<sub>2</sub>Cl<sub>2</sub>) on a Bruker Avance III HD 400 MHz spectrometer equipped with a CryoProbe™, a Varian VXR400 S spectrometer, a Bruker AMX600 spectrometer or a Bruker Avance III HD 800 MHz spectrometer equipped with a CryoProbe™ and are reported as follows: chemical shift  $\delta$  in ppm (multiplicity, coupling constant  $J$  in Hz, number of protons) for <sup>1</sup>H NMR spectra and chemical shift  $\delta$  in ppm for <sup>13</sup>C NMR spectra. Multiplicities are abbreviated as follows: s = singlet, d = doublet, t = triplet, q = quartet, quint = quintet, br = broad, m = multiplet, or

combinations thereof. Residual solvent peaks of  $\text{CDCl}_3$  ( $\delta_{\text{H}} = 7.26$  ppm,  $\delta_{\text{C}} = 77.16$  ppm),  $\text{C}_6\text{D}_6$  ( $\delta_{\text{H}} = 7.16$  ppm,  $\delta_{\text{C}} = 128.06$  ppm),  $\text{CD}_2\text{Cl}_2$  ( $\delta_{\text{H}} = 5.32$  ppm,  $\delta_{\text{C}} = 54.00$  ppm),  $\text{CD}_3\text{OD}$  (3.31 ppm) and  $(\text{CD}_3)_2\text{SO}$  (2.50 ppm) were used as an internal reference. The  $^{19}\text{F}$  NMR shifts are reported in ppm related to the chemical shift of trichlorofluoromethane. The  $^{31}\text{P}$  NMR shifts are reported in ppm related to the chemical shift of 85% phosphoric acid. NMR spectra were assigned using information ascertained from COSY, HMBC, HSQC and NOESY experiments. All raw fid files were processed and the spectra analysed using the program MestReNova 9.0 from Mestrelab Research S. L.

**High resolution mass spectra** (HRMS) were recorded on a Varian MAT CH7A or a Varian MAT 711 MS instrument by electron impact (EI) or electrospray ionization (ESI) techniques at the Department of Chemistry, Ludwig-Maximilians-University Munich.

**Infrared spectra** (IR) were recorded from  $4000\text{ cm}^{-1}$  to  $600\text{ cm}^{-1}$  on a PERKIN ELMER Spectrum BX II, FT-IR instrument. For detection a SMITHS DETECTION DuraSamplIR II Diamond ATR sensor was used. Samples were prepared as a neat film or a thin powder layer. IR data in frequency of absorption ( $\text{cm}^{-1}$ ) is reported as follows: w = weak, m = medium, s = strong, br = broad or combinations thereof.

**Melting points** were measured with a BÜCHI Melting Point B-450 instrument in open glascapillaries and are uncorrected.

**Optical rotation** values were recorded on an Anton Paar MCP 200 polarimeter. The specific rotation is calculated as follows: 
$$[\alpha]_{\text{D}}^{25} = \frac{\alpha \times 100}{c \times d}$$

Thereby, the wavelength  $\lambda$  is reported in nm and the measuring temperature in °C.  $\alpha$  represents the recorded optical rotation,  $c$  the concentration of the analyte in 10 mg/mL and  $d$  the length of the cuvette in dm. Thus, the specific rotation is given in  $10^{-1} \cdot \text{deg} \cdot \text{cm}^2 \cdot \text{g}^{-1}$ . Use of the sodium  $D$  line ( $\lambda = 589$  nm) is indicated by  $D$  instead of the wavelength in nm. The sample concentration as well as the solvent is reported in the relevant section of the experimental part.

**X-ray diffraction analysis** was carried out by Dr. Peter Mayer (Ludwig-Maximilians-Universität München). The data collections were performed on a Bruker D8Venture using MoK $\alpha$ -radiation ( $\lambda = 0.71073 \text{ \AA}$ , graphite monochromator). The CrysAlisPro software (version 1.171.33.41) was applied for the integration, scaling and multi-scan absorption correction of the data. The structures were solved by direct methods with SIR9713 and refined by least-squares methods against F2 with SHELXL-97.14. All non-hydrogen atoms were refined anisotropically. The hydrogen atoms were placed in ideal geometry riding on their parent atoms. Further details are summarized in the tables at the different sections. Plotting of thermal ellipsoids in this document and in the main text was carried out using Ortep-3 for Windows.

**UV-Vis spectra** were recorded on a Varian Cary 50 Scan UV-Vis spectrometer using Helma SUPRASIL precision cuvettes (10 mm light path).

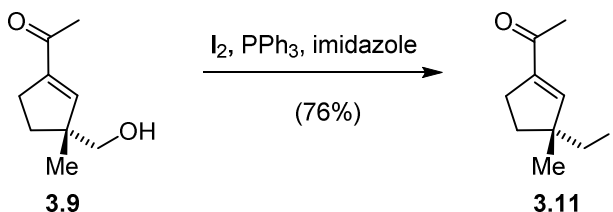
**LCMS** was performed on an Agilent 1260 Infinity HPLC System, MS-Agilent 1100 Series, Type: 1946D, Model: SL, equipped with a Agilent Zorbax Eclipse Plus C18 (100  $\times$  4.6 mm, particle size 3.5 micron) reverse phase column. Retention times ( $t_R$ ) are given in minutes (min).

**All yields** are isolated, unless otherwise specified.

## 10.2. Supporting Information for Chapter 3.1.

### 10.2.1. Experimental Procedures

#### Synthesis and characterization of compound 3.11



To a pale yellow solution of alcohol **3.9** (1.00 g, 6.48 mmol, 1.00 eq.) in THF (75 mL) was added PPh<sub>3</sub> (1.87 g, 7.13 mmol, 1.10 eq.) and imidazole (0.883 g, 13.0 mmol, 2.00 eq.). The solution was cooled to 0 °C and I<sub>2</sub> (2.14 g, 8.43 mmol, 1.30 eq.) was added. The mixture was stirred for 5 h at r.t. and then quenched with a sat. aq. solution of Na<sub>2</sub>S<sub>2</sub>O<sub>3</sub> (100 mL). The aqueous phase was extracted with Et<sub>2</sub>O (3 x 100 mL) and the combined organic layers were dried over MgSO<sub>4</sub>, filtrated, concentrated *in vacuo* to give a yellow-brown solid. Purification by flash column chromatography (hexanes/EtOAc = 1:0 to 9:1) afforded iodide **3.11** (1.30 g, 4.92 mmol, 76%) as a yellow oil.

R<sub>f</sub> = 0.30 (hexanes/EtOAc 9:1).

<sup>1</sup>H NMR (400 MHz, C<sub>6</sub>D<sub>6</sub>): δ = 5.80 (q, *J* = 1.6 Hz, 1H), 2.65 (d, *J* = 1.5 Hz, 2H), 2.53 – 2.36 (m, 2H), 1.89 (d, *J* = 1.0 Hz, 3H), 1.58 – 1.48 (m, 1H), 1.32 (ddd, *J* = 13.7, 8.7, 5.6 Hz, 1H), 0.86 (d, *J* = 1.0 Hz, 3H).

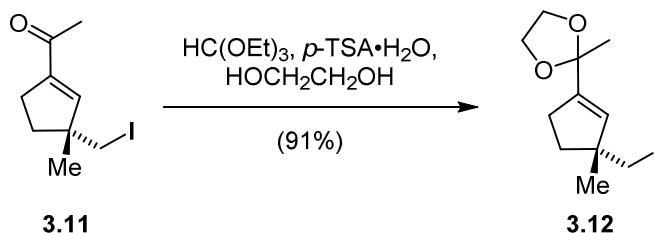
<sup>13</sup>C NMR (100 MHz, C<sub>6</sub>D<sub>6</sub>): δ = 195.2, 147.1, 144.9, 50.1, 36.1, 30.1, 26.4, 25.7, 19.2.

IR (ATR):  $\tilde{\nu}$  = 2957 (m), 2862 (w), 1667 (s), 1616 (m), 1452 (m), 1367 (m), 1306 (m), 1271 (m), 1199 (m), 1131 (w), 933 (w), 867 (m) cm<sup>-1</sup>.

HRMS (EI): calc. for C<sub>9</sub>H<sub>13</sub>OI [*M+H*]<sup>+</sup>: 265.0084, found: 265.0079.

[α]<sub>D</sub><sup>25</sup> = -8.1 (c = 1.0, CHCl<sub>3</sub>)

### Synthesis and characterization of compound **3.12**



To a solution of iodide **3.11** (0.553 g, 2.09 mmol, 1.00 eq.) in DCM (31 mL) was added *p*-TSA·H<sub>2</sub>O (39.8 mg, 0.209 mmol, 0.100 eq.), ethylene glycol (2.52 mL, 41.8 mmol, 20.0 eq.) and HC(OEt)<sub>3</sub> (3.48 mL, 20.9 mmol, 10.0 eq.). The solution was stirred for 1 h at r.t. before the reaction was quenched through addition of Et<sub>3</sub>N (1 mL) and a sat. aq. solution of NaHCO<sub>3</sub> (30 mL). The reaction mixture was extracted with DCM (4 x 30 mL), dried over MgSO<sub>4</sub>, filtered and concentrated *in vacuo*. Thus obtained crude material was purified by flash column chromatography (hexanes/EtOAc = 1:0 to 9:1) to give acetal **3.12** (0.586 g, 1.90 mmol, 91%) as a colorless oil.

$R_f = 0.42$  (hexanes/EtOAc 9:1).

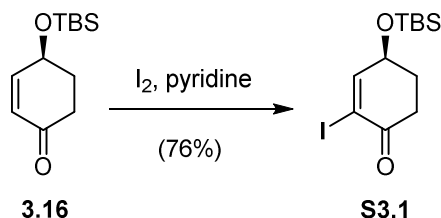
<sup>1</sup>H NMR (400 MHz, C<sub>6</sub>D<sub>6</sub>):  $\delta = 5.43$  (q,  $J = 1.7$  Hz, 1H), 3.59 – 3.52 (m, 4H), 2.83 (s, 1H), 2.39 – 2.19 (m, 3H), 1.78 (ddd,  $J = 13.9, 8.8, 5.4$  Hz, 1H), 1.52 (s, 3H), 1.51 – 1.45 (m, 1H), 0.99 (s, 3H).

<sup>13</sup>C NMR (100 MHz, C<sub>6</sub>D<sub>6</sub>):  $\delta = 146.0, 132.9, 107.3, 64.8, 64.6, 49.1, 37.2, 30.8, 26.3, 24.2, 21.8$ .

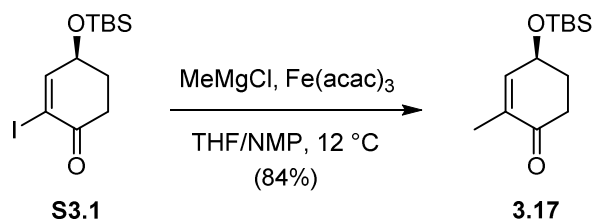
IR (ATR):  $\tilde{\nu} = (\text{cm}^{-1})$ : 2951 (m), 2882 (m), 1452 (w), 1371 (m), 1302 (w), 1254 (m), 1187 (s), 1131 (m), 1107 (m), 1039 (s), 946 (m), 858 (s) cm<sup>-1</sup>.

HRMS (EI): calc. for C<sub>11</sub>H<sub>17</sub>O<sub>2</sub>I [*M-H*]<sup>+</sup>: 307.0195, found: 307.0191.

$[\alpha]_D^{25} = -19.7$  (c = 1.00, CHCl<sub>3</sub>)

**Synthesis and characterization of compound S3.1**

A solution of enone **3.16** (1.72 g, 7.61 mmol, 1.00 eq.) and pyridine (1.66 mL, 20.5 mmol, 2.70 eq.) in DCM (39 mL) was cooled to 0 °C. I<sub>2</sub> (2.90 g, 11.4 mmol, 1.50 eq.) was added and the solution warmed to r.t.. After stirring for 3 h a sat. aq. solution of Na<sub>2</sub>S<sub>2</sub>O<sub>3</sub> (40 mL) was added and the aqueous phase was extracted with Et<sub>2</sub>O (3 x 40mL). The combined organic layers were dried over MgSO<sub>4</sub>, filtered and concentrated *in vacuo*. The crude material was purified by flash column chromatography (hexanes/EtOAc = 1:0 to 9:1) to give iodocyclohexenone **S3.1** (2.04 g, 5.78 mmol, 76%) as a dark yellow oil. The analytical data of **S3.1** was in accordance to the reported one.<sup>[183]</sup>

**Synthesis and characterization of compound 3.17**

To solution of cyclohexenone **S3.1** (1.93 g, 5.48 mmol, 1.00 eq.) in THF (67 mL) and NMP (4.8 mL) was added Fe(acac)<sub>3</sub> (0.194 g, 0.548 mmol, 0.100 eq.). The solution was cooled to 12 °C and a solution of MeMgCl in THF (3.0 M, 2.00 mL, 6.03 mmol, 1.10 eq.) was added slowly. After stirring at 12 °C for 40 min, the reaction was quenched through addition of aq. HCl (1M, 20 mL) and H<sub>2</sub>O (50 mL). The aqueous phase was extracted with Et<sub>2</sub>O (4 x 50 mL), the combined organic layers were washed with a sat. aq. solution of NaHCO<sub>3</sub> (200 mL), dried over MgSO<sub>4</sub>, filtered and concentrated *in vacuo*. Thus obtained crude product was subjected to flash column chromatography (hexanes/EtOAc = 1:0 → 98:2 → 97:3 → 95:5) to afford methylcyclohexenone **3.17** (1.11 g, 4.60 mmol, 84%) as a pale yellow liquid.

$R_f = 0.32$  (hexanes/EtOAc 9:1).

$^1\text{H NMR}$  (400 MHz,  $\text{CDCl}_3$ ):  $\delta = 6.59$  (q,  $J = 1.8$  Hz, 1H), 4.49 (ddd,  $J = 9.1, 4.7, 2.3$  Hz, 1H), 2.57 (dt,  $J = 16.7, 4.5$  Hz, 1H), 2.31 (ddd,  $J = 17.0, 12.9, 4.6$  Hz, 1H), 2.18 (dq,  $J = 11.0, 4.6$  Hz, 1H), 1.95 (tdd,  $J = 13.0, 9.1, 4.3$  Hz, 1H), 1.76 (s, 3H), 0.91 (s, 9H), 0.12 (s, 3H), 0.11 (s, 3H).

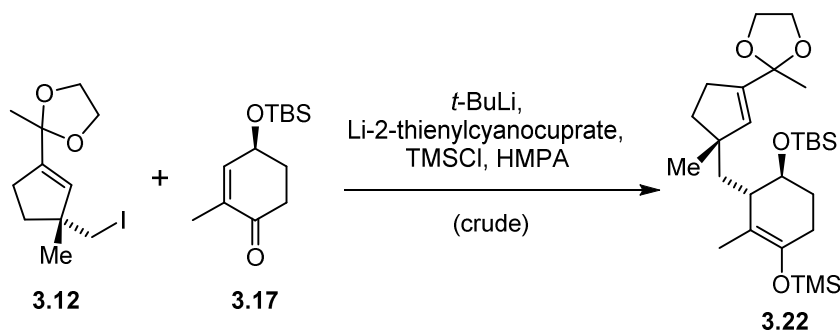
$^{13}\text{C NMR}$  (100 MHz,  $\text{CDCl}_3$ ):  $\delta = 199.3, 149.1, 135.1, 67.5, 35.7, 33.5, 25.9, 18.3, 15.9, -4.5, -4.6$ .

**IR (ATR):**  $\tilde{\nu} = 2953$  (m), 2929 (m), 2886 (w), 2857 (m), 1681 (s), 1471 (w), 1359 (m), 1252 (m), 1118 (m), 1103 (s), 1075 (s), 987 (w), 965 (w), 868 (s), 836 (s), 808 (m), 776 (s), 667 (w)  $\text{cm}^{-1}$ .

**HRMS (EI):** calc. for  $\text{C}_{13}\text{H}_{24}\text{O}_2\text{Si}$  [ $M$ ] $^+$ : 240.1540, found: 240.1543.

$[\alpha]_D^{25} = -54.2$  ( $c = 0.31$ , DCM)

### Synthesis of compound 3.22

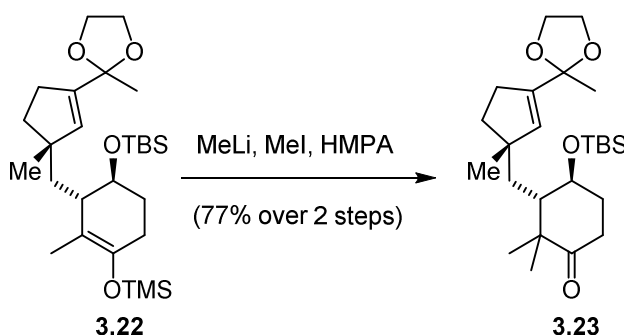


A solution of iodide **3.12** (1.33 g, 4.32 mmol, 2.00 eq.) in  $\text{Et}_2\text{O}$  (77 mL) was cooled to  $-78^\circ\text{C}$  and a solution of  $t\text{-BuLi}$  in pentane (1.44 M, 4.7 mL, 6.77 mmol 3.00 eq.) was added. The mixture was stirred for 1 h at  $-78^\circ\text{C}$  before a solution of Li-thienylcyanocuprate in THF (0.25 M, 17.3 mL, 4.32 mmol, 2.00 eq.) was added. After 30 min stirring at  $-78^\circ\text{C}$ , a solution of compound **3.17** (562 mg, 2.34 mmol, 1.00 eq.) with freshly distilled TMSCl (0.90 mL, 7.09 mmol, 3.03 eq.) and HMPA (1.00 mL, 5.75 mmol, 2.46 eq.) in THF (23 mL) was added. After stirring for 1 h at  $-78^\circ\text{C}$  the reaction was quenched through addition of a mixture of aq. sat.  $\text{NH}_4\text{Cl}$ -solution and aq.  $\text{NH}_3$ -solution (9:1, 200 mL). The aqueous layer was extracted with  $n$ -pentane (3 x 150 mL) and the combined organic layers were washed with brine. The organic phase was dried over  $\text{MgSO}_4$ ,

filtered and concentrated *in vacuo* to afford the crude product **3.22** (1.53 g, 3.10 mmol) as a blue-green oil which was used in the next step without further purification.

$R_f = 0.53$  (hexanes/EtOAc 9:1)

### Synthesis and characterization of compound **3.23**



A solution of silyl enol ether **3.22** (1.53 g, 3.10 mmol, 1.00 eq.) in THF (130 mL) was cooled to 0 °C and a solution of MeLi in Et<sub>2</sub>O (1.6 M, 2.35 mL, 3.76 mmol, 1.21 eq.) was added. The solution was stirred for 30 min at 0 °C before it was cooled to -78 °C and HMPA (8 mL) followed by MeI (2.30 mL, 37.0 mmol, 11.9 eq.) was added slowly. The reaction mixture was warmed to -30 °C over 2 h and then quenched through addition of an aq. sat. solution of NH<sub>4</sub>Cl (150 mL) and H<sub>2</sub>O (100 mL). The aqueous layer was extracted with EtOAc (3 x 200 mL), the combined organic layers were washed with brine (3 x 200 mL), dried over MgSO<sub>4</sub>, filtered and concentrated *in vacuo*. The crude material was purified by flash column chromatography (hexanes/Et<sub>2</sub>O = 1:0 to 85:15) to afford compound **3.23** (788 mg, 1.80 mmol, 77% over two steps) as a pale yellow oil.

$R_f = 0.43$  (hexanes/EtOAc 85:15)

<sup>1</sup>H NMR (600 MHz, C<sub>6</sub>D<sub>6</sub>):  $\delta$  = 5.60 (t,  $J$  = 1.9 Hz, 1H), 3.75 (td,  $J$  = 5.3, 3.3 Hz, 1H), 3.58 (dd,  $J$  = 3.1, 1.7 Hz, 4H), 2.67 (ddd,  $J$  = 14.0, 10.4, 6.0 Hz, 1H), 2.46 – 2.41 (m, 2H), 2.12 (dt,  $J$  = 14.1, 5.9 Hz, 1H), 1.93 (ddd,  $J$  = 12.8, 8.7, 6.5 Hz, 1H), 1.83 (dddd,  $J$  = 13.7, 10.3, 5.6, 3.3 Hz, 1H), 1.73 (ddt,  $J$  = 7.4, 4.3, 1.4 Hz, 1H), 1.56 (s, 3H), 1.55 – 1.51 (m, 2H), 1.47 (dd,  $J$  = 14.7, 2.6 Hz, 1H), 1.39 (s, 3H), 1.04 (s, 3H), 1.02 (dd,  $J$  = 8.7, 5.9 Hz, 1H), 1.00 (s, 3H), 0.96 (s, 9H), 0.11 (s, 3H), 0.04 (s, 3H).

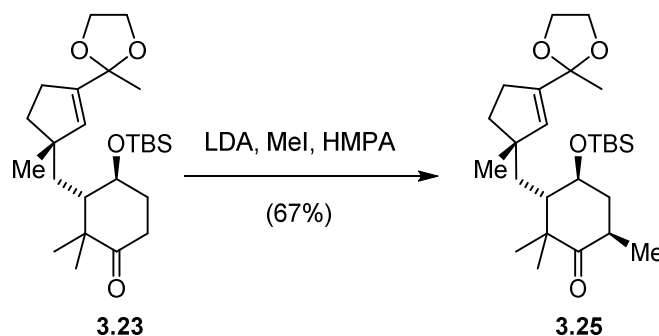
$^{13}\text{C}$  NMR (100 MHz,  $\text{C}_6\text{D}_6$ ):  $\delta$  = 213.2, 144.5, 135.3, 107.5, 72.9, 64.8, 64.8, 51.0, 49.0, 48.5, 39.6, 37.2, 34.0, 32.4, 30.9, 28.2, 28.1, 26.1, 24.4, 23.5, 18.2, -4.1, -4.7.

IR (ATR):  $\tilde{\nu}$  = 2951 (m), 2931 (m), 2886 (m), 2858 (m), 1707 (s), 1471 (w), 1463 (w), 1387 (w), 1371 (w), 1309 (w), 1254 (m), 1189 (m), 1087 (m), 1069 (m), 1041 (s), 1006 (w), 989 (w), 946 (w), 875 (m), 855 (s), 835 (s), 810 (m), 773 (s), 735 (m), 702 (w), 667 (w)  $\text{cm}^{-1}$ .

HRMS (EI): calc. for  $\text{C}_{25}\text{H}_{44}\text{O}_4\text{Si}$  [ $M$ ] $^+$ : 436.3003, found: 436.3011.

$[\alpha]_D^{25}$  = +4.95 ( $c$  = 1, DCM)

### Synthesis and characterization of compound 3.25



A solution of ketone **3.23** (300 mg, 0.687 mmol, 1.00 eq.) in THF (20 mL) was cooled to  $-78$  °C and a solution of LDA in THF (0.5 M, 1.50 mL, 0.75 mmol, 1.10 eq.) was added. The solution was stirred for 30 min at  $-78$  °C before HMPA (0.72 mL) followed by MeI (0.210 mL, 3.37 mmol, 4.90 eq.) was added. The reaction mixture was stirred for 1 h and then quenched through addition of an aq. sat. solution of  $\text{NaHCO}_3$  (50 mL) and  $\text{H}_2\text{O}$  (20 mL). The aqueous layer was extracted with EtOAc (3 x 100 mL), the combined organic layers were washed with brine (3 x 100 mL), dried over  $\text{MgSO}_4$ , filtered and concentrated *in vacuo*. The crude material was purified by flash column chromatography (hexanes/ $\text{Et}_2\text{O}$  = 1:0 to 85:15) to afford compound **3.25** (207 mg, 0.460 mmol, 67%) as a pale green oil. A small sample was repurified by flash column chromatography (hexanes/ $\text{Et}_2\text{O}$  = 1:0 to 85:15) to afford a pale yellow solid of which a X-ray crystal structure could be obtained.

$R_f = 0.56$  (hexanes/EtOAc 85:15).

**$^1\text{H}$  NMR (600 MHz,  $\text{C}_6\text{D}_6$ ):**  $\delta = 5.62 - 5.61$  (m, 1H), 3.77 (ddd,  $J = 10.6, 9.3, 4.3$  Hz, 1H), 3.61 – 3.55 (m, 4H), 2.52 – 2.46 (m, 3H), 2.39 – 2.32 (m, 1H), 1.98 (ddd,  $J = 12.8, 6.0, 4.3$  Hz, 1H), 1.59 – 1.58 (m, 1H), 1.56 (s, 3H), 1.52 (ddd,  $J = 12.9, 6.1, 3.3$  Hz, 2H), 1.48 (dd,  $J = 13.8, 3.0$  Hz, 1H), 1.26 – 1.23 (m, 1H), 1.19 (s, 3H), 1.13 (s, 3H), 1.00 (d,  $J = 6.4$  Hz, 3H), 0.97 (s, 9H), 0.79 (s, 3H), 0.11 (s, 3H), 0.06 (s, 3H).

**$^{13}\text{C}$  NMR (100 MHz,  $\text{C}_6\text{D}_6$ ):**  $\delta = 213.3, 144.3, 136.3, 107.6, 72.4, 64.9, 64.8, 49.7, 49.2, 48.3, 43.9, 38.9, 37.9, 36.0, 31.2, 29.7, 26.3, 25.2, 24.4, 21.1, 18.3, 15.4, -3.4, -4.8$ .

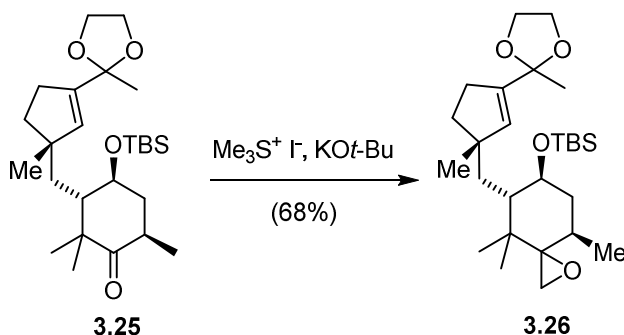
**IR (ATR):**  $\tilde{\nu} = 2931$  (m), 2884 (m), 2858 (m), 1709 (m), 1472 (w), 1371 (w), 1255 (m), 1189 (w), 1085 (s), 1041 (s), 1005 (w), 914 (w), 835 (s), 774 (s), 664 (w)  $\text{cm}^{-1}$ .

**HRMS (EI):** calc. for  $\text{C}_{26}\text{H}_{46}\text{O}_4\text{Si}$  [ $M$ ] $^+$ : 450.3160, found: 450.3151.

**Melting point** = 81.5–83.0 °C.

**$[\alpha]_D^{25}$**  = -32.8 (c = 0.97, DCM)

### Synthesis and characterization of compound 3.26



To a solution of trimethylsulfonium iodide (52.0 mg, 0.255 mmol, 1.50 eq.) in DMSO/THF (1:1, 2 mL), was added a solution of KOt-Bu in DMSO (1 M, 0.190 mL, 0.190 mmol, 1.11 eq.) at 0 °C. The reaction mixture was stirred for 5 min. and then a solution of ketone **3.25** (77.0 mg, 0.171 mmol, 1.00 eq.) in DMSO/THF (1:1, 2.8 mL) was added. After 2 h stirring at 0 °C the reaction was quenched through the addition of H<sub>2</sub>O (5 mL). The aqueous phase was extracted with EtOAc (3 x 10 mL) and the combined organic layers were washed with brine (5 x 20 mL), dried over MgSO<sub>4</sub>, filtered and concentrated *in vacuo*. Subsequent flash column chromatography (hexanes/Et<sub>2</sub>O = 1:0 to 85:15) gave product **3.26** (54.0 mg, 0.116 mmol, 68%) as a 1:1.3 mixture of diastereomers in form of a colorless oil.

$R_f = 0.43$  (hexanes/EtOAc 9:1).

#### Data for the minor diastereomer:

<sup>1</sup>H NMR (800 MHz, C<sub>6</sub>D<sub>6</sub>):  $\delta$  = 5.59 (t,  $J = 1.9$  Hz, 1H), 3.64 – 3.62 (m, 3H), 3.58 – 3.57 (m, 1H), 3.57 – 3.55 (m, 1H), 2.67 (ddd,  $J = 13.1, 9.6, 6.3$  Hz, 1H), 2.55 – 2.54 (m, 1H), 2.35 (d,  $J = 4.2$  Hz, 1H), 2.17 (ddq,  $J = 13.4, 6.8, 2.8$  Hz, 1H), 1.93 (dt,  $J = 12.6, 4.1$  Hz, 1H), 1.61 (d,  $J = 1.5$  Hz, 2H), 1.61 (d,  $J = 2.0$  Hz, 1H), 1.58 (s, 4H), 1.49 (dd,  $J = 14.6, 3.6$  Hz, 1H), 1.19 (d,  $J = 5.7$  Hz, 1H), 1.17 (s, 4H), 1.01 (s, 9H), 0.97 (s, 3H), 0.84 (s, 3H), 0.66 (d,  $J = 6.7$  Hz, 3H), 0.12 (s, 3H), 0.07 (s, 3H).

<sup>13</sup>C NMR (200 MHz, C<sub>6</sub>D<sub>6</sub>):  $\delta$  = 143.7, 137.3, 107.7, 73.5, 65.1, 64.9, 64.8, 49.3, 46.3, 44.9, 44.3, 39.0, 38.8, 35.7, 31.4, 30.2, 29.7, 26.4, 24.3, 23.9, 19.2, 18.4, 15.1, -3.3, -4.7.

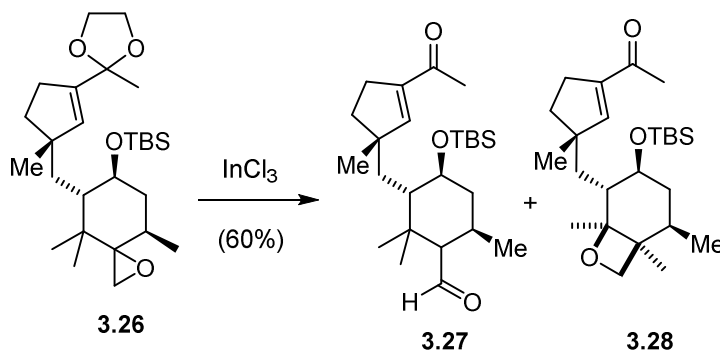
**Data for the major diastereomer:**

**$^1\text{H}$  NMR (800 MHz,  $\text{C}_6\text{D}_6$ ):**  $\delta$  = 5.67 (t,  $J$  = 1.9 Hz, 1H), 3.73 – 3.69 (m, 2H), 3.65 – 3.63 (m, 1H), 3.60 – 3.58 (m, 2H), 2.73 (ddd,  $J$  = 12.9, 9.3, 6.4 Hz, 1H), 2.58 – 2.55 (m, 1H), 2.52 (ddt,  $J$  = 7.3, 6.5, 1.8 Hz, 1H), 2.42 (d,  $J$  = 4.2 Hz, 1H), 2.30 (d,  $J$  = 4.2 Hz, 1H), 2.00 (ddt,  $J$  = 13.3, 6.6, 3.4 Hz, 1H), 1.80 (dt,  $J$  = 12.4, 4.1 Hz, 1H), 1.66 (s, 3H), 1.66 – 1.64 (m, 1H), 1.64 – 1.62 (m, 2H), 1.54 (dd,  $J$  = 4.7, 3.5 Hz, 1H), 1.38 (dt,  $J$  = 10.0, 3.5 Hz, 1H), 1.20 (s, 3H), 1.01 (s, 9H), 0.78 (s, 6H), 0.62 (d,  $J$  = 6.6 Hz, 3H), 0.14 (s, 3H), 0.10 (s, 3H).

**$^{13}\text{C}$  NMR (200 MHz,  $\text{C}_6\text{D}_6$ ):**  $\delta$  = 144.2, 136.3, 107.9, 73.6, 64.8, 64.7, 64.3, 49.4, 49.4, 46.8, 43.6, 39.2, 38.8, 36.3, 31.5, 30.3, 28.7, 26.4, 24.5, 23.3, 20.8, 15.1, -3.2, -4.6.

**IR (ATR):**  $\tilde{\nu}$  = 291 (s), 2931 (s), 2884 (m), 2858 (m), 1472 (w), 1371 (w), 1256 (m), 1191 (w), 1091 (s), 1046 (s), 1005 (w), 836 (s), 774 (m)  $\text{cm}^{-1}$ .

**HRMS (EI):** calc. for  $\text{C}_{26}\text{H}_{45}\text{O}_4\text{Si}$  [ $M$ ] $^+$ : 464.3316, found: 464.3305.

**Synthesis and characterization of compound 3.27 and 3.28**

To a solution of epoxide **3.26** (15 mg, 32.3  $\mu\text{mol}$ , 1.00 eq.) in toluene (1 mL) was added  $\text{InCl}_3$  (3.5 mg, 15.8  $\mu\text{mol}$ , 0.50 eq.) and the mixture was heated to 44  $^\circ\text{C}$  for 5 h after which it was filtered through a short plug of silica. Subsequent flash column chromatography (hexanes/EtOAc = 1:0 to 8:2) gave a 1:0.6 mixture of product **3.27** and side product **3.28** (8.08 mg, 19.2  $\mu\text{mol}$ , 60%) in form of a colorless oil. A small sample was repurified for analysis using prep-TLC.

**Data for aldehyde 3.27:**

$R_f = 0.36$  (hexanes/EtOAc 85:15).

**$^1\text{H NMR}$  (800 MHz,  $\text{C}_6\text{D}_6$ ):**  $\delta = 9.70$  (d,  $J = 5.0$  Hz, 1H), 6.17 (t,  $J = 1.8$  Hz, 1H), 3.49 (td,  $J = 10.8, 4.0$  Hz, 1H), 2.73 (dddd,  $J = 16.2, 9.5, 4.7, 1.7$  Hz, 1H), 2.66 (dddd,  $J = 16.6, 8.9, 6.6, 2.0$  Hz, 1H), 2.42 (ddd,  $J = 13.1, 9.5, 6.5$  Hz, 1H), 2.05 (s, 2H), 1.72 – 1.68 (m, 3H), 1.63 (dt,  $J = 10.4, 3.5$  Hz, 1H), 1.53 – 1.48 (m, 3H), 1.46 – 1.43 (m, 1H), 1.37 – 1.34 (m, 1H), 1.02 (s, 3H), 0.97 (s, 9H), 0.75 (s, 3H), 0.74 (d,  $J = 6.7$  Hz, 3H), 0.60 (s, 3H), 0.06 (s, 3H), 0.04 (s, 3H).

**$^{13}\text{C NMR}$  (200 MHz,  $\text{C}_6\text{D}_6$ ):**  $\delta = 204.8, 195.3, 151.5, 143.8, 74.0, 63.8, 50.7, 45.1, 42.2, 37.9, 35.7, 30.7, 28.9, 28.7, 28.6, 26.7, 26.4, 26.1, 22.7, 19.5, 18.4, -3.3, -4.7$ .

**IR (ATR):**  $\tilde{\nu} = 2954$  (s), 2929 (s), 2857 (m), 1718 (m), 1669 (s), 1616 (w), 1458 (w), 1369 (m), 1257 (m), 1097 (m), 1063 (m), 1005 (w), 836 (s), 774 (s), 667 (w)  $\text{cm}^{-1}$ .

**HRMS (EI):** calc. for  $\text{C}_{25}\text{H}_{44}\text{O}_3\text{Si}$  [ $M$ ] $^+$ : 420.3054, found: 420.3050.

$[\alpha]_D^{25} = +28.0$  ( $c = 0.1$ , DCM)

**Data for oxetane 3.28:**

$R_f = 0.39$  (hexanes/EtOAc 85:15).

**$^1\text{H NMR}$  (800 MHz,  $\text{C}_6\text{D}_6$ ):**  $\delta = 5.96$  (t,  $J = 1.8$  Hz, 1H), 4.29 (t,  $J = 5.4$  Hz, 1H), 4.10 (d,  $J = 9.8$  Hz, 1H), 4.01 (d,  $J = 9.8$  Hz, 1H), 2.59 (ddd,  $J = 8.7, 6.7, 1.8$  Hz, 2H), 1.97 (s, 3H), 1.79 (dd,  $J = 12.3, 8.4$  Hz, 1H), 1.66 (dddt,  $J = 9.7, 4.8, 2.9, 1.5$  Hz, 1H), 1.49 (dt,  $J = 12.8, 7.2$  Hz, 1H), 1.43 – 1.39 (m, 1H), 1.26 (dd,  $J = 14.3, 3.5$  Hz, 1H), 1.19 (s, 4H), 1.18 – 1.15 (m, 1H), 1.11 (d,  $J = 6.9$  Hz, 3H), 1.03 (s, 3H), 1.01 – 0.99 (m, 1H), 0.97 (s, 9H), 0.83 (s, 3H), 0.04 (s, 3H), 0.04 (s, 3H).

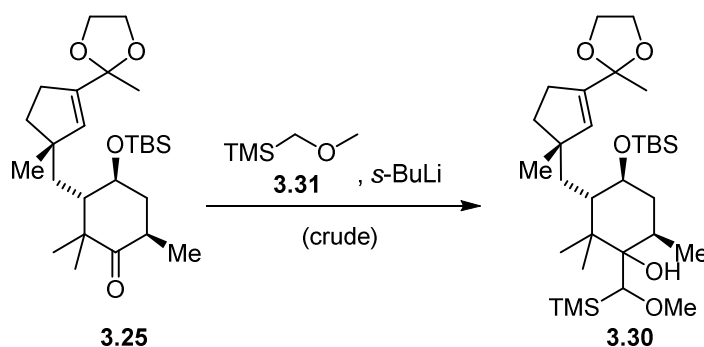
**$^{13}\text{C NMR}$  (200 MHz,  $\text{C}_6\text{D}_6$ ):**  $\delta = 195.3, 150.7, 143.9, 89.7, 80.9, 61.3, 50.8, 49.6, 43.0, 37.9, 37.2, 33.7, 33.1, 29.8, 29.0, 26.4, 26.0, 25.6, 21.7, 19.2, 18.3, -5.6, -5.8$ .

**IR (ATR):**  $\tilde{\nu}$  = 2954 (s), 2929 (s), 2858 (m), 1670 (s), 1616 (w), 1462 (w), 1367 (w), 1257 (m), 1095 (s), 978 (w), 935 (w), 838 (s), 775 (s)  $\text{cm}^{-1}$ .

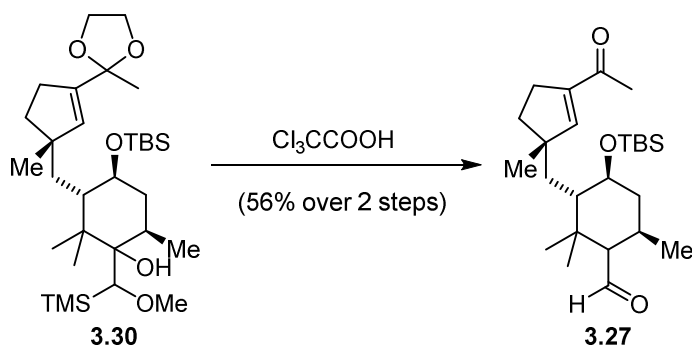
**HRMS (EI):** calc. for  $\text{C}_{25}\text{H}_{44}\text{O}_3\text{Si}$   $[M]^+$ : 420.3054, found: 420.3055.

$[\alpha]_D^{25} = +12.7$  ( $c = 0.49$ , DCM)

### Synthesis of compound **3.30**

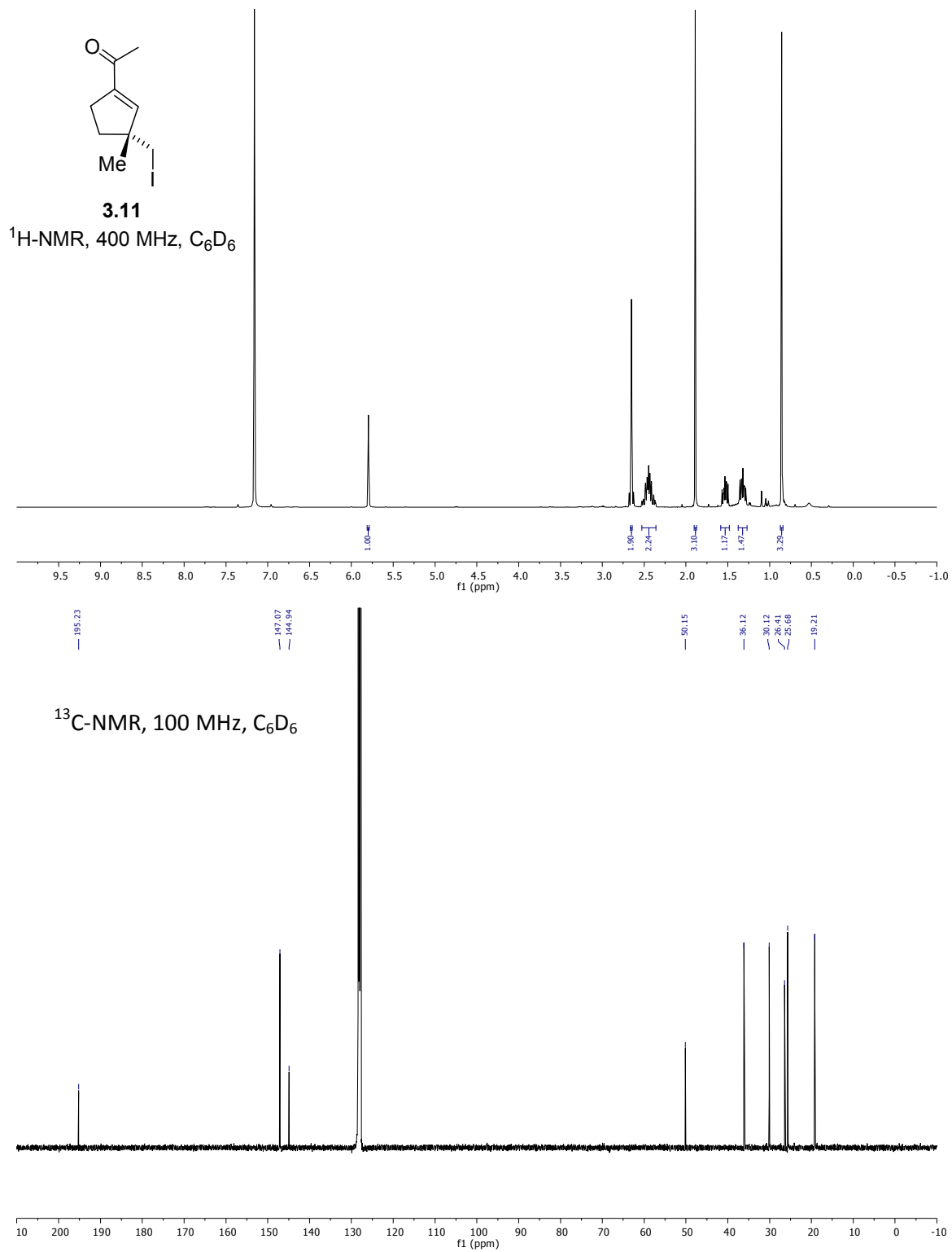


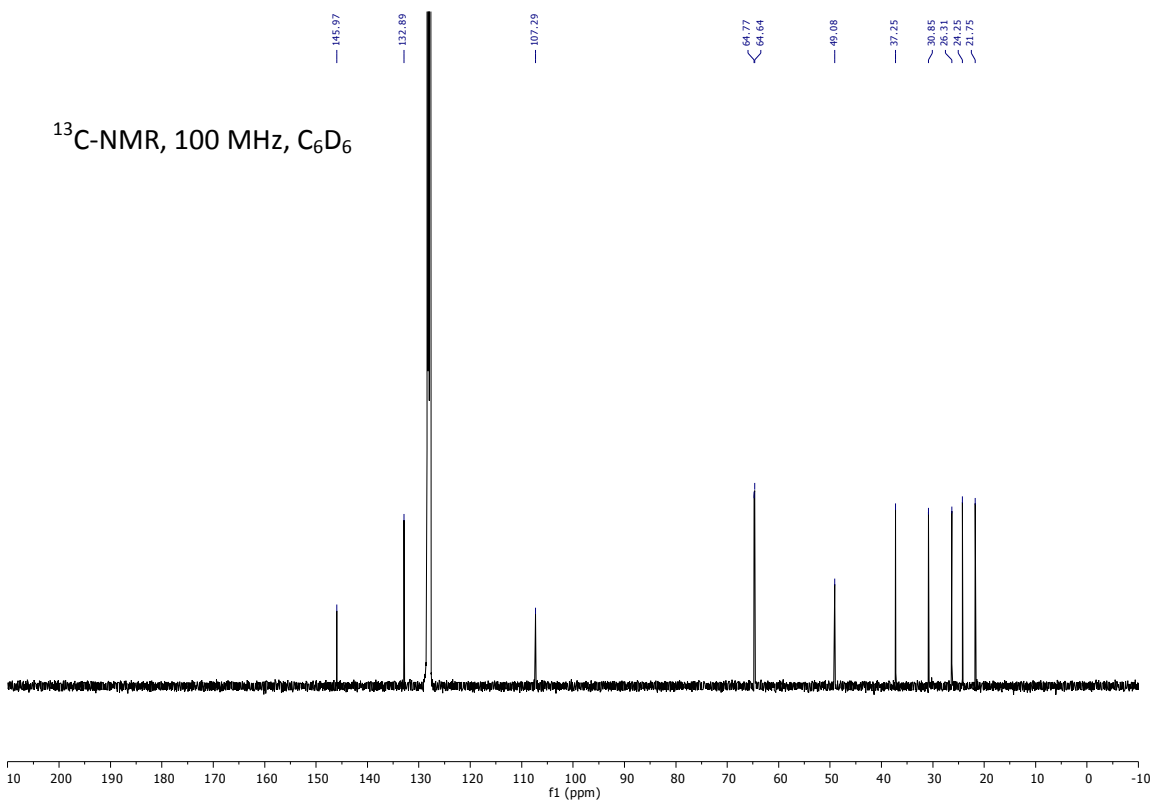
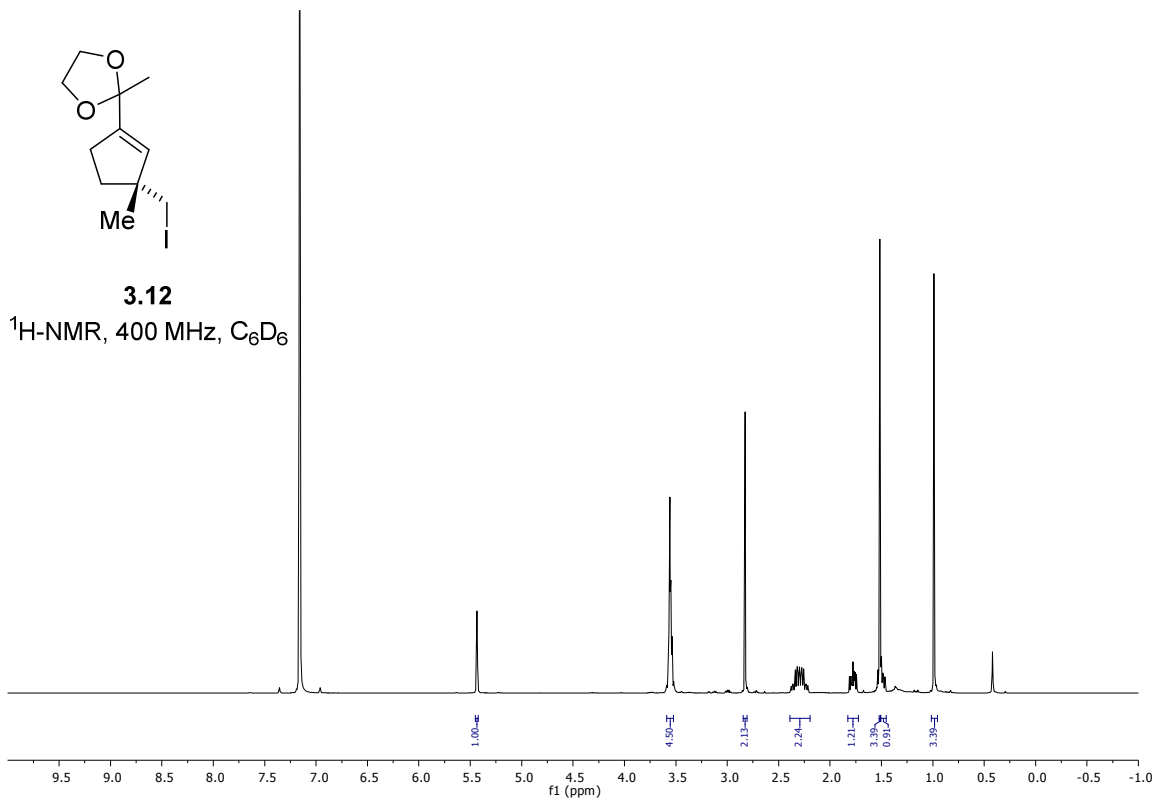
To a solution of **3.31** (0.38 mL, 2.44 mmol, 7.05 eq.) in THF (0.52 mL) at  $-78$  °C was added a solution of *s*-BuLi (1.2 M, 1.80 mL, 2.16 mmol, 6.24 eq.). The mixture was stirred at  $24$  °C for 35 min after which an aliquot of 1.80 mL (1.44 mmol, 4.16 eq.) was taken and added to ketone **3.25** (156 mg, 0.346 mmol, 1.00 eq.) dissolved in THF (4 mL) at  $-78$  °C. After 45 min, the reaction was quenched through addition of an aq. saturated solution of  $\text{NH}_4\text{Cl}$  (20 mL). The aqueous phase was extracted with  $\text{Et}_2\text{O}$  (3 x 10 mL) and the combined organic layers were washed with brine, dried over  $\text{Na}_2\text{SO}_4$ , filtered and concentrated *in vacuo*. The crude product (207 mg) was used in the next step without further purification.

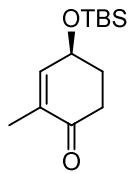
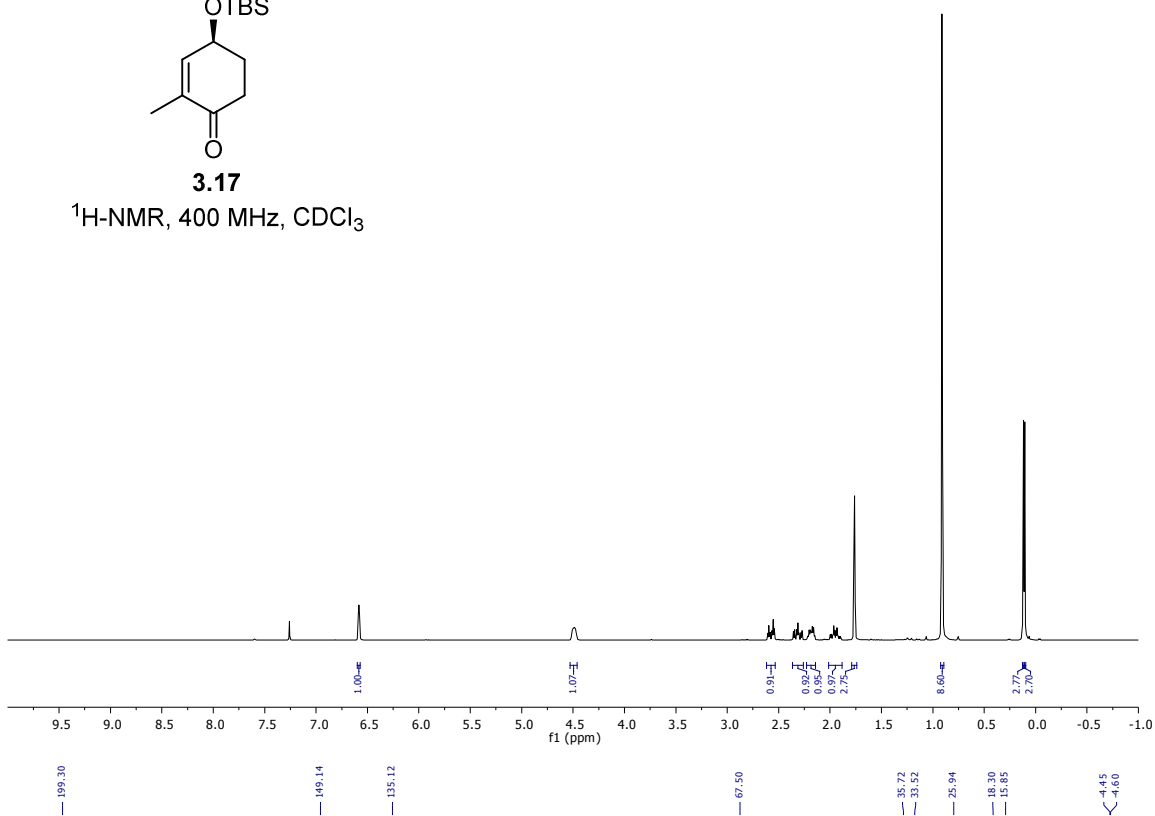
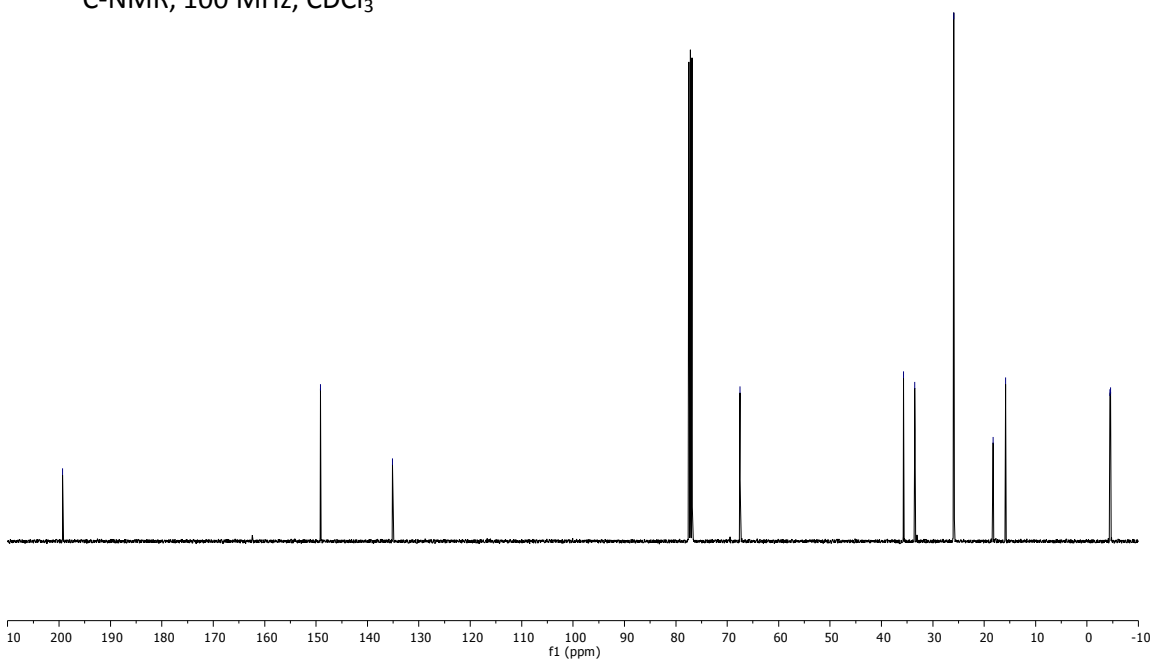
Synthesis of compound **3.27**

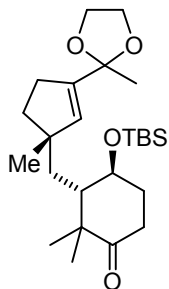
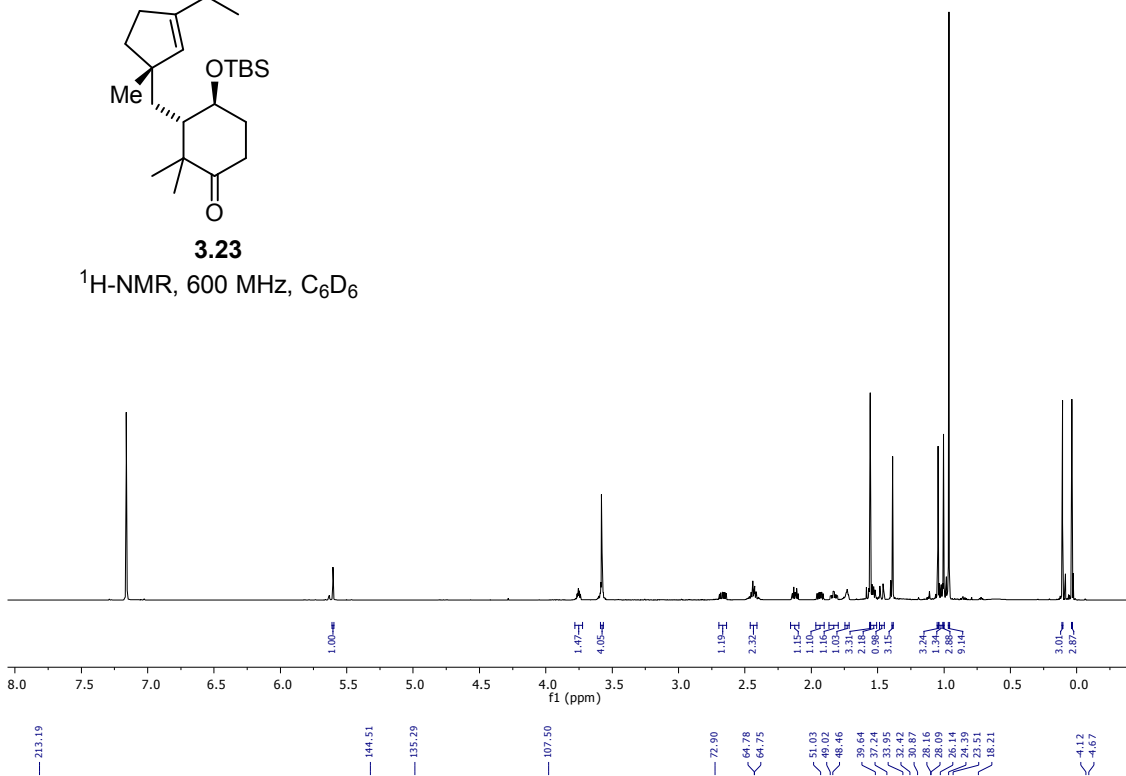
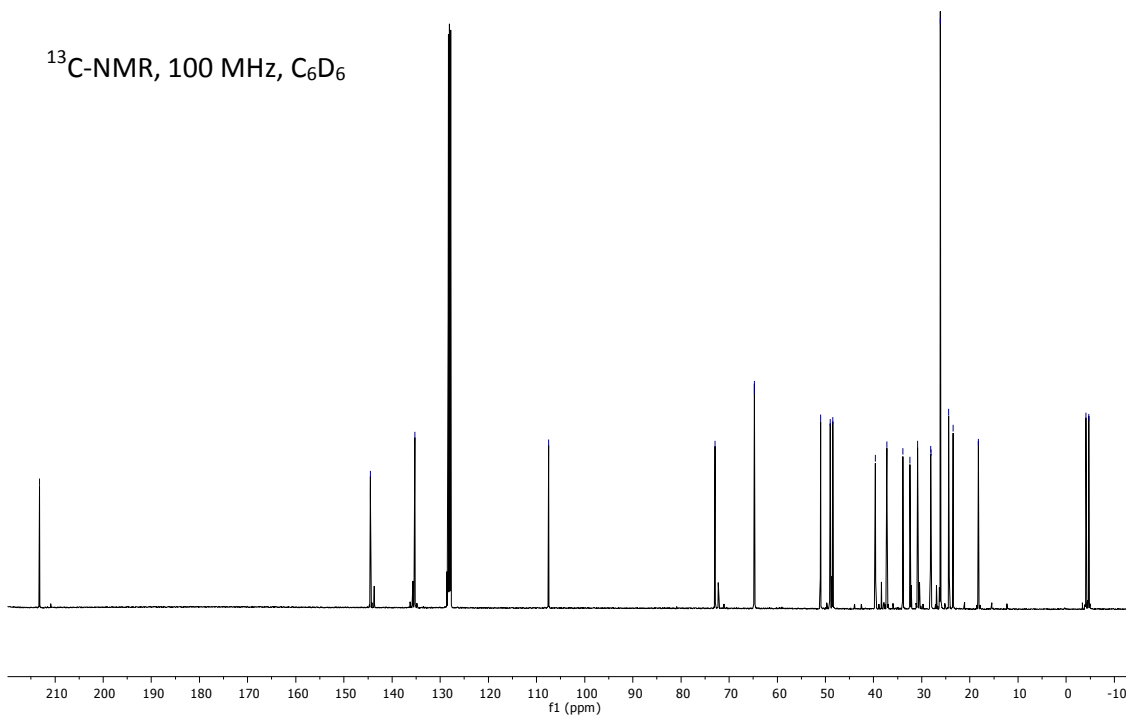
To a solution of crude **3.30** in DCM at 0 °C was added trichloroacetic acid (0.58 mL, 5.79 mmol, 16.7 eq.). The reaction mixture was stirred for 1 h at 0 °C and 30 min at r.t. after which it was quenched through the addition of an aq. NaOH-solution (10%) (5 mL). The aqueous phase was extracted with DCM (3 x 10 mL) and the combined organic layers were washed with brine, dried over  $\text{Na}_2\text{SO}_4$ , filtered and concentrated *in vacuo*. Subsequent flash column chromatography (hexanes/ $\text{Et}_2\text{O}$  = 1:0 to 85:15) gave product **3.27** (81.5 mg, 0.194 mmol, 56%) as a 1:1.8 mixture of diastereomers together with an inseparable side product in form of a colorless oil.

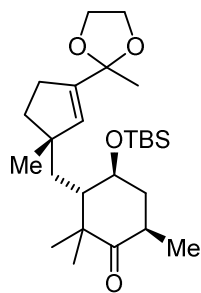
## 10.2.2. NMR Spectra for Chapter 3.1.





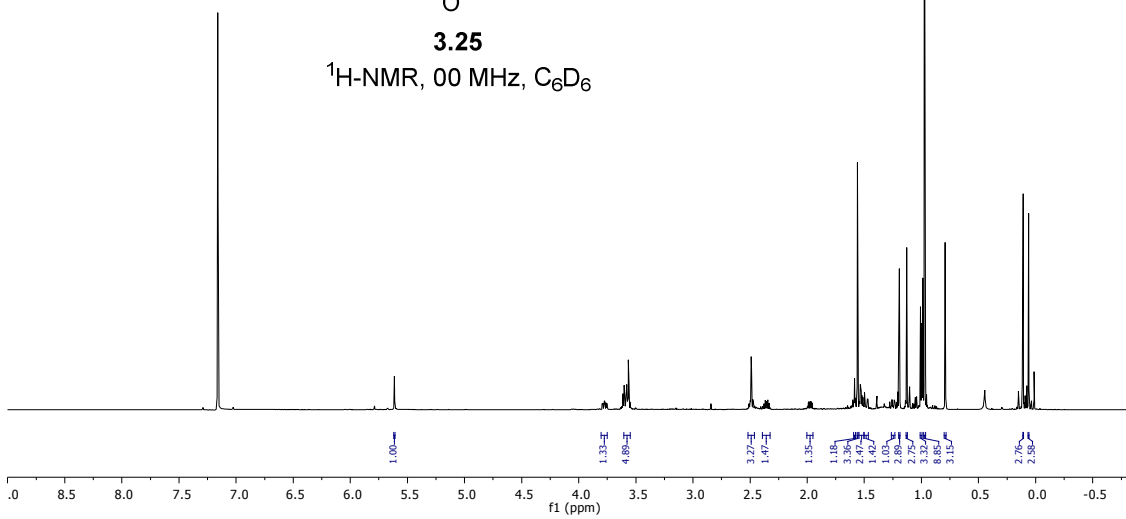
**3.17** $^1\text{H-NMR}$ , 400 MHz,  $\text{CDCl}_3$  $^{13}\text{C-NMR}$ , 100 MHz,  $\text{CDCl}_3$ 

**3.23** $^1\text{H-NMR}$ , 600 MHz,  $\text{C}_6\text{D}_6$  $^{13}\text{C-NMR}$ , 100 MHz,  $\text{C}_6\text{D}_6$ 

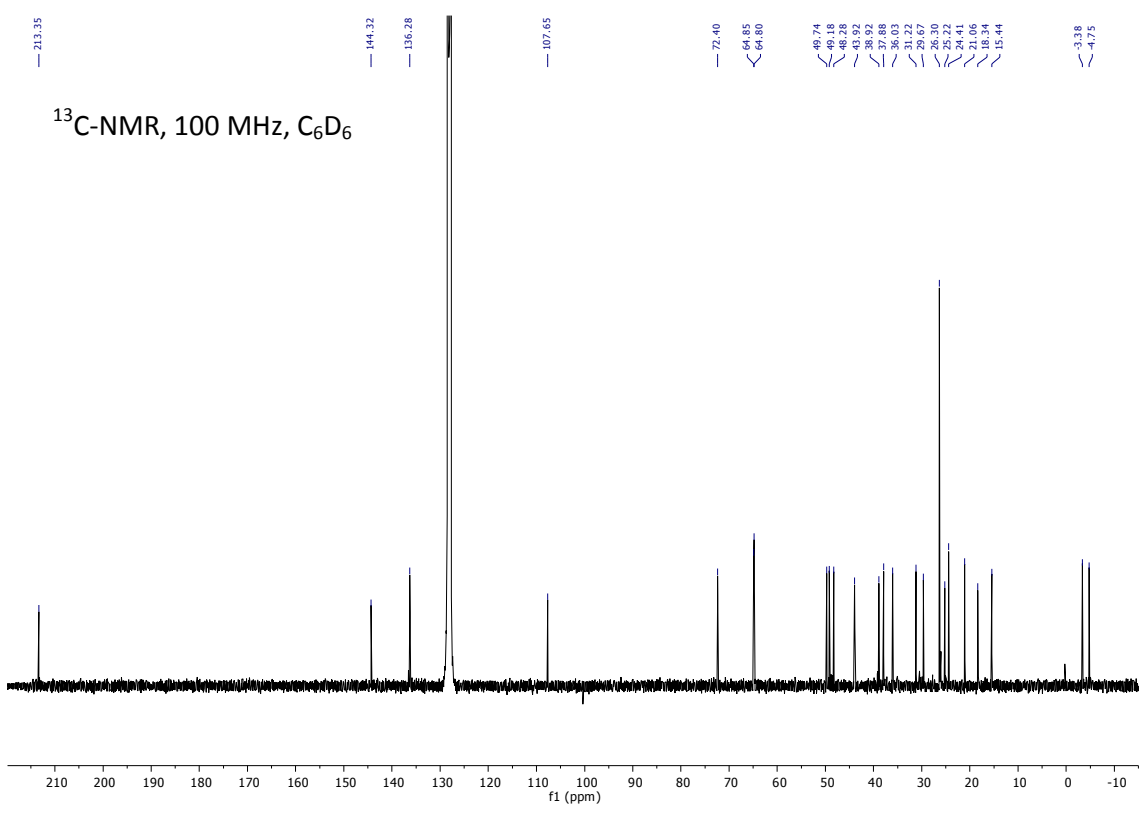


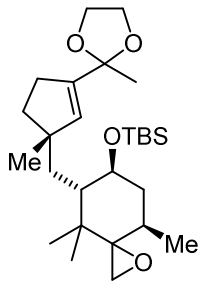
**3.25**

<sup>1</sup>H-NMR, 00 MHz, C<sub>6</sub>D<sub>6</sub>

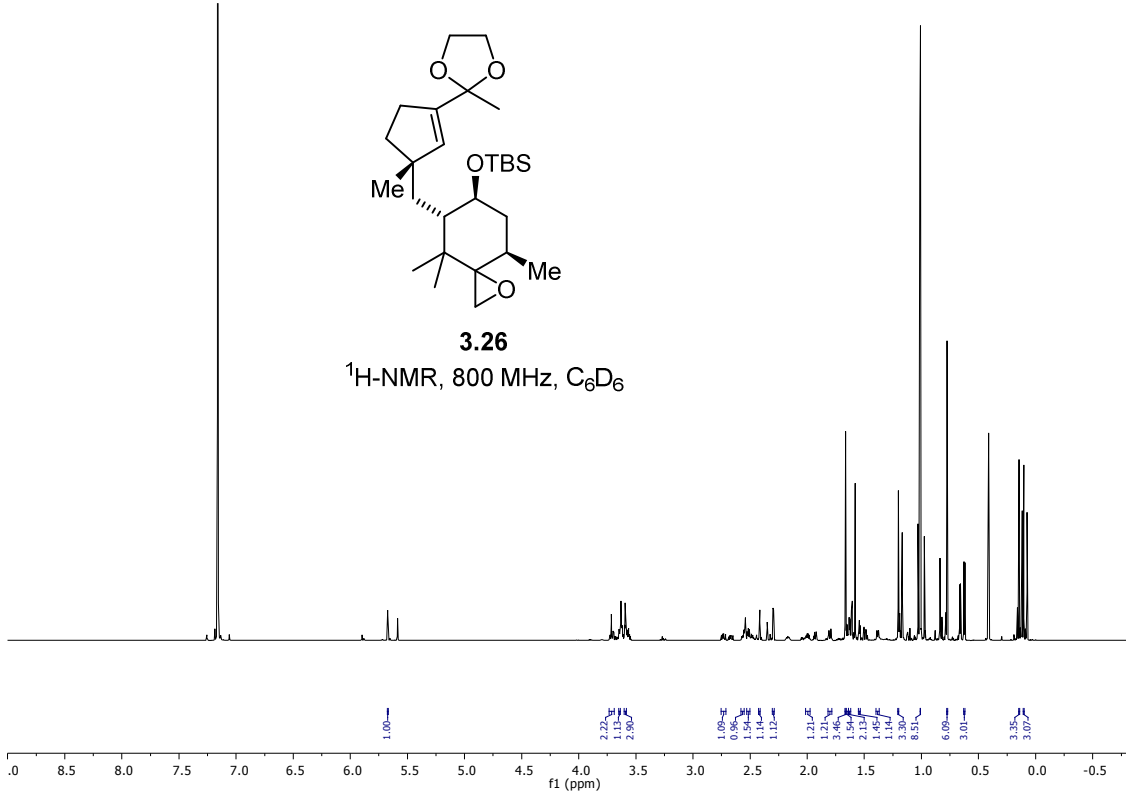


<sup>13</sup>C-NMR, 100 MHz, C<sub>6</sub>D<sub>6</sub>

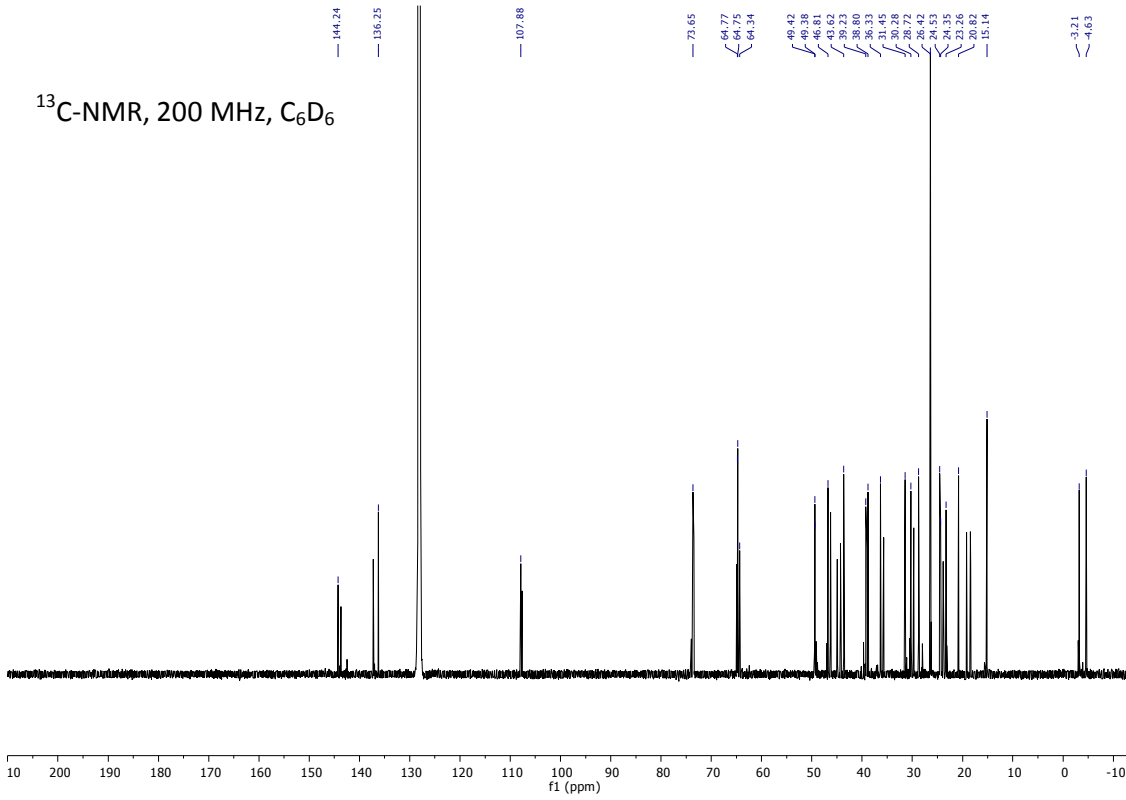


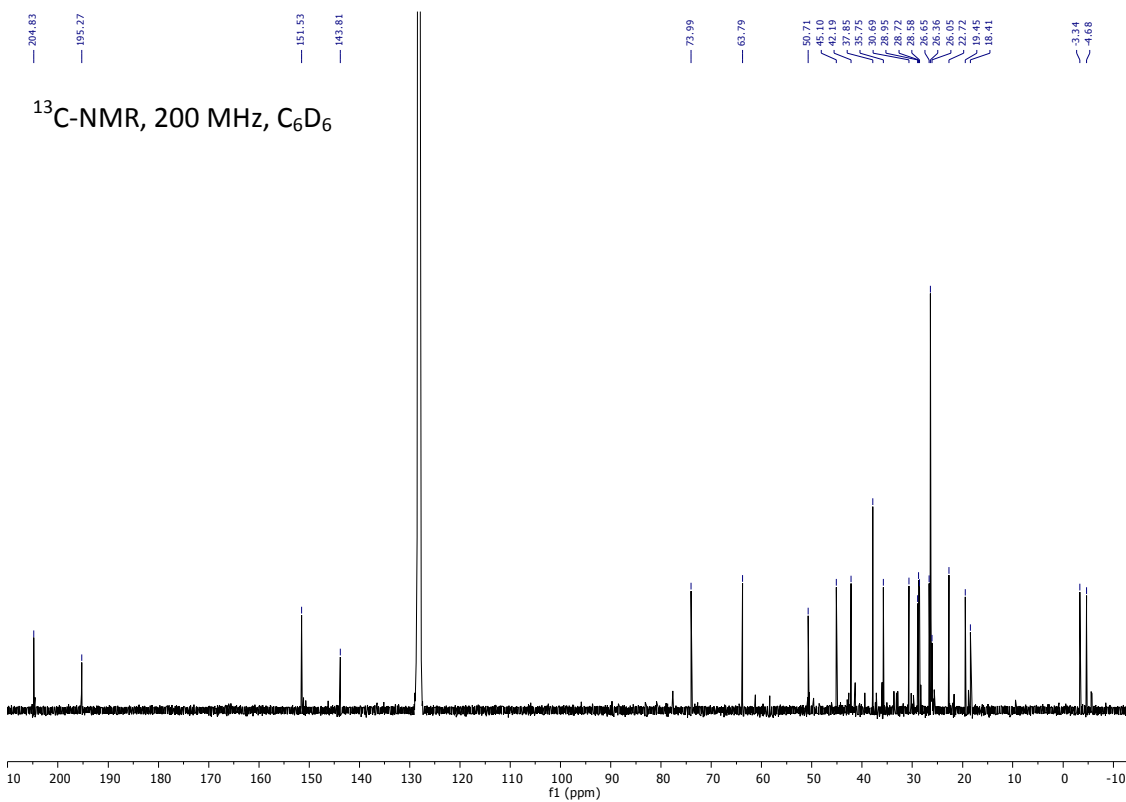
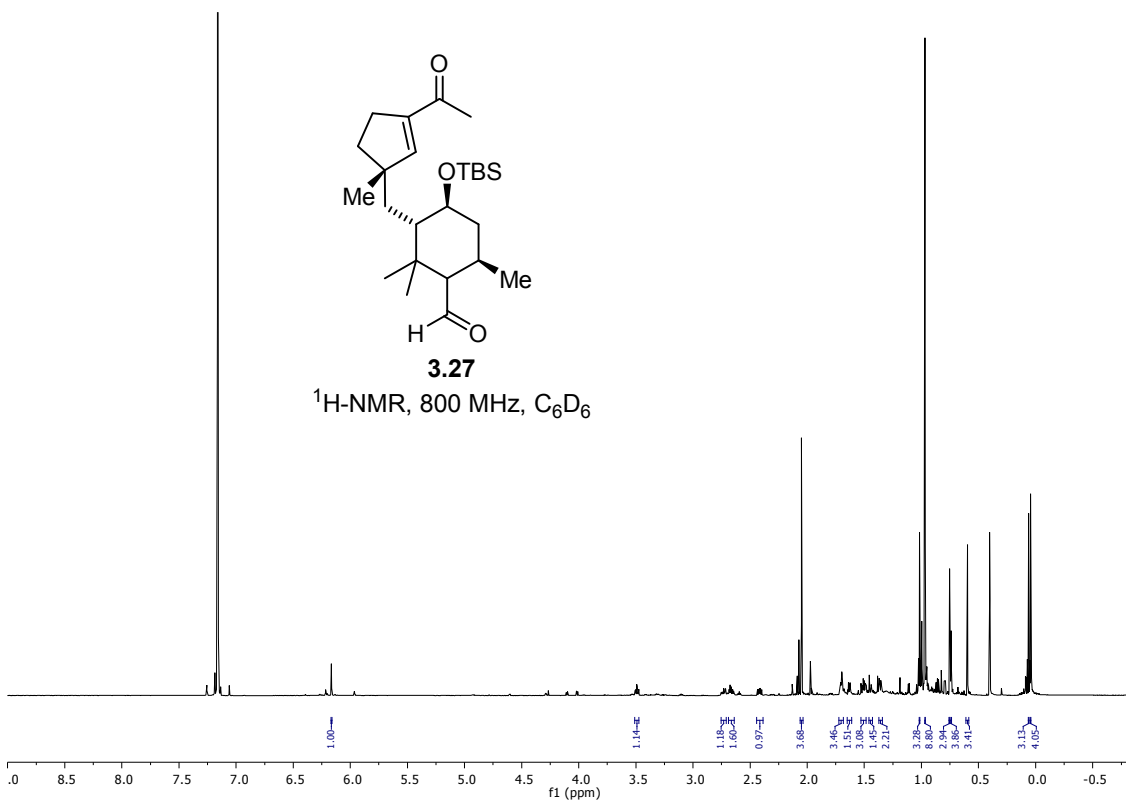


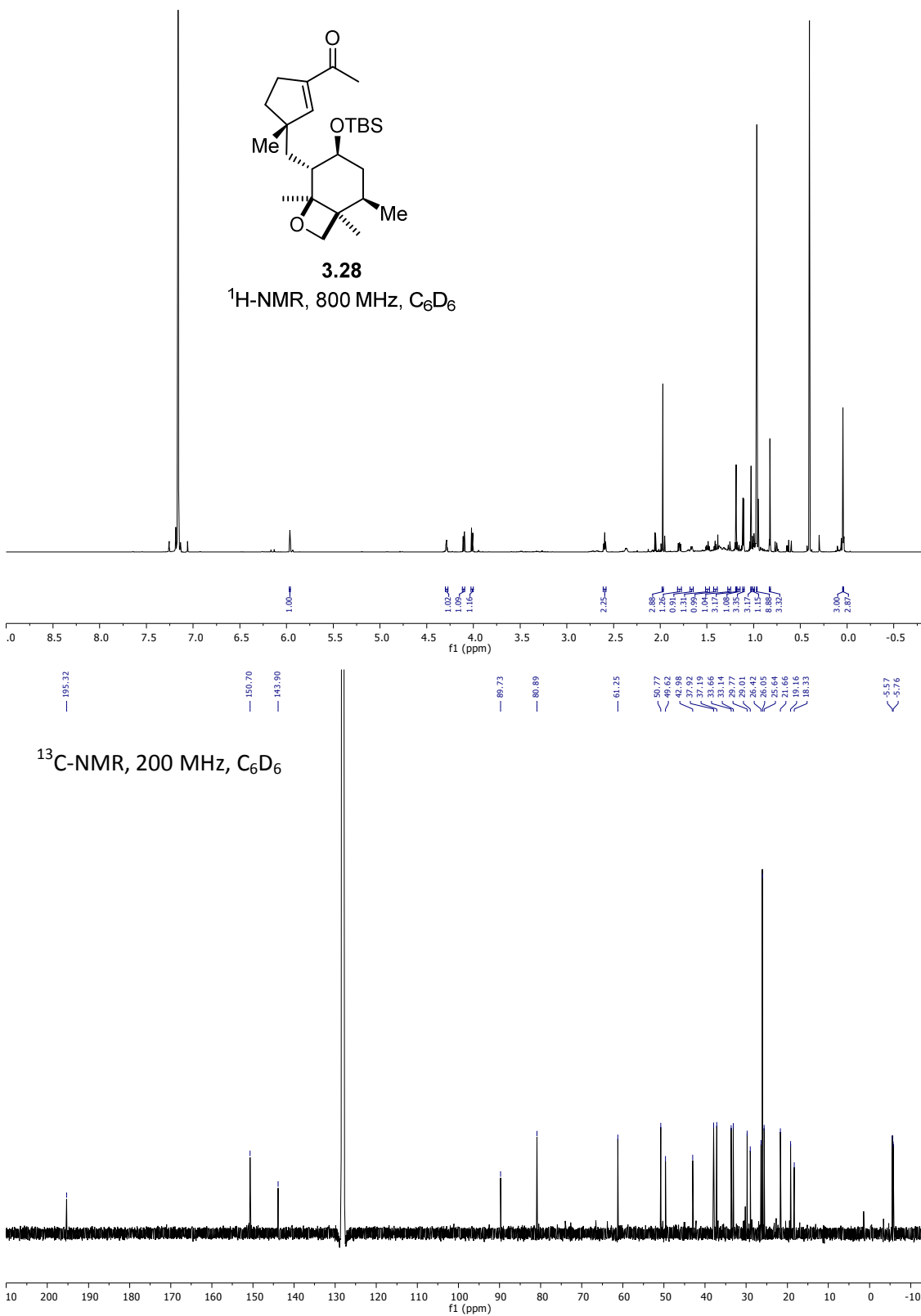
**3.26**  
<sup>1</sup>H-NMR, 800 MHz, C<sub>6</sub>D<sub>6</sub>



<sup>13</sup>C-NMR, 200 MHz, C<sub>6</sub>D<sub>6</sub>







## 10.2.3. X-ray Crystallographic Data for Chapter 3.1.

## Tetrahydropyran 3.24

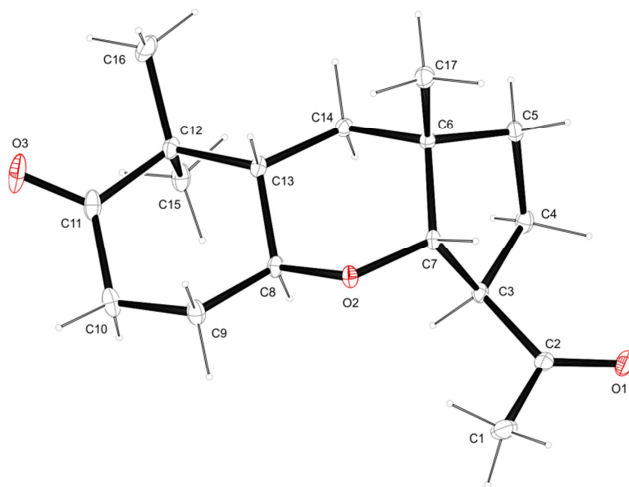


Figure 10.1. ORTEP depiction of 3.24.

Table 10.1. Crystallographic data for 3.24.

net formula	$C_{17}H_{26}O_3$
$M_r/g\ mol^{-1}$	278.38
crystal size/mm	$0.100 \times 0.090 \times 0.080$
$T/K$	100(2)
radiation	MoK $\alpha$
diffractometer	'Bruker D8Venture'
crystal system	orthorhombic
space group	'P 21 21 21'
$a/\text{\AA}$	9.3994(3)
$b/\text{\AA}$	10.0557(4)
$c/\text{\AA}$	16.2420(6)
$\alpha/^\circ$	90
$\beta/^\circ$	90
$\gamma/^\circ$	90
$V/\text{\AA}^3$	1535.15(10)

---

Z	4
calc. density/g cm <sup>-3</sup>	1.204
$\mu/\text{mm}^{-1}$	0.081
absorption correction	multi-scan
transmission factor range	0.9075–0.9585
refls. measured	28512
$R_{\text{int}}$	0.0472
mean $\sigma(I)/I$	0.0230
$\theta$ range	2.382–26.38
observed refls.	2980
x, y (weighting scheme)	0.0385, 0.4296
hydrogen refinement	constr
Flack parameter	0.4(3)
refls in refinement	3161
parameters	185
restraints	0
$R(F_{\text{obs}})$	0.0362
$R_w(F^2)$	0.0835
S	1.097
shift/error <sub>max</sub>	0.001
max electron density/e Å <sup>-3</sup>	0.209
min electron density/e Å <sup>-3</sup>	-0.234

## Ketone 3.25

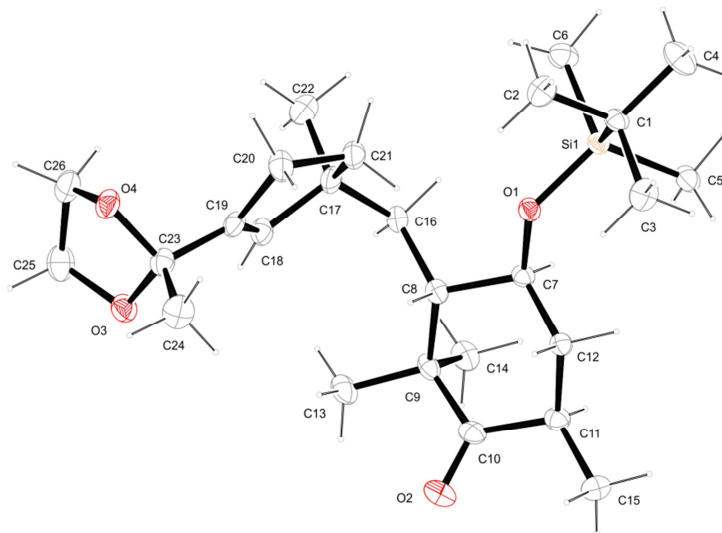


Figure 10.2. ORTEP depiction of 3.25.

Table 10.2. Crystallographic data for 3.25.

net formula	$C_{26}H_{46}O_4Si$
$M_r/g\ mol^{-1}$	450.72
crystal size/mm	$0.429 \times 0.195 \times 0.103$
$T/K$	123(2)
radiation	MoK $\alpha$
diffractometer	'Oxford XCalibur'
crystal system	orthorhombic
space group	'P 21 21 21'
$a/\text{\AA}$	7.5629(5)
$b/\text{\AA}$	17.4948(9)
$c/\text{\AA}$	20.6940(10)
$\alpha/^\circ$	90
$\beta/^\circ$	90
$\gamma/^\circ$	90
$V/\text{\AA}^3$	2738.1(3)

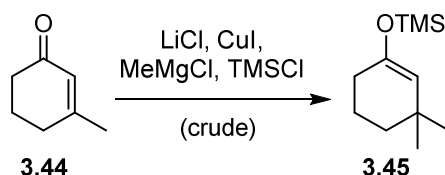
---

Z	4
calc. density/g cm <sup>-3</sup>	1.093
$\mu$ /mm <sup>-1</sup>	0.112
absorption correction	'multi-scan'
transmission factor range	0.99531–1.00000
refls. measured	14872
$R_{\text{int}}$	0.0625
mean $\sigma(I)/I$	0.0832
$\theta$ range	4.413–25.347
observed refls.	3725
x, y (weighting scheme)	0.0467, 0.0000
hydrogen refinement	constr
Flack parameter	–0.06(11)
refls in refinement	4966
parameters	290
restraints	0
$R(F_{\text{obs}})$	0.0538
$R_w(F^2)$	0.1131
S	1.023
shift/error <sub>max</sub>	0.001
max electron density/e Å <sup>-3</sup>	0.308
min electron density/e Å <sup>-3</sup>	–0.209

### 10.3. Supporting Information for Chapter 3.2.

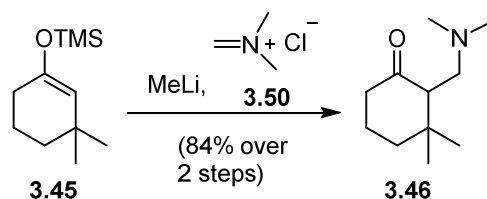
#### 10.3.1. Experimental Procedures

##### Synthesis of compound 3.45



A solution of LiCl (0.154 g, 3.63 mmol, 0.100 eq.) and CuI (0.346 g, 1.82 mmol, 0.050 eq.) in THF (200 mL) was stirred for 1 h at r.t.. The solution was cooled to  $-40\text{ }^{\circ}\text{C}$ , enone **3.44** (4.12 mL, 36.3 mmol, 1.00 eq.), TMSCl (5.21 mL, 41.0 mmol, 1.13 eq.) were added and the solution was stirred for additional 10 min at  $-40\text{ }^{\circ}\text{C}$ . A solution of MeMgCl (3.0 M, 18.2 mL, 54.5 mmol, 1.50 eq.) was added dropwise. After 1 h stirring at  $-40\text{ }^{\circ}\text{C}$  the starting material was not consumed yet (TLC analysis). Therefore, the solution was warmed up to  $-30\text{ }^{\circ}\text{C}$ . After 2.5h additional methylmagnesium chloride (5.00 mL, 15.0 mmol, 0.413 eq.) was added dropwise and the solution was stirred for overall 4 h until complete consumption of the starting material was observed. The reaction was quenched through addition of a sat. aq. solution of  $\text{NH}_4\text{Cl}$  (200 mL) and the aqueous phase was extracted with  $\text{Et}_2\text{O}$  (3 x 200 mL) to give silyl enol ether **3.45** (6.47 g, 32.6 mmol) as a yellowish oil which was used in the next step without further purification.

$R_f = 0.96$  (hexanes/EtOAc 9:1)

**Synthesis and characterization of compound 3.46**

A solution of silyl enol ether **3.45** (6.47 g, 32.6 mmol, 1.00 eq.) in THF (106 mL) was cooled to 0 °C. A solution of MeLi in Et<sub>2</sub>O (1.6 M, 22.4 mL, 35.8 mmol 1.10 eq.) was added slowly after which the solution was warmed up to r.t.. After 30 min stirring the reaction mixture was cooled to 0 °C and added to a suspension of *N,N*-dimethylmethyleniminium chloride (**3.50**) (5.50 g, 58.7 mmol, 1.80 eq.) in THF (68 mL) at -78 °C. The mixture was allowed to warm to r.t. and then stirred for 1 h and 45 min. The reaction was quenched through addition of brine (200mL) and H<sub>2</sub>O (50 mL). The pH of the aqueous phase was increased to 10 through addition of a sat. aq. solution of Na<sub>2</sub>CO<sub>3</sub>. The aqueous phase was extracted with EtOAc (3 x 200 mL), the combined organic layers were dried over MgSO<sub>4</sub>, filtered and concentrated *in vacuo*. The crude product was purified by flash column chromatography (hexanes/EtOAc = 3:7 to 0:1) to afford the amine **3.46** (5.59 g, 30.5 mmol, 84% over 2 steps) as a yellow oil.

R<sub>f</sub> = 0.31, hexanes/EtOAc 9:1.

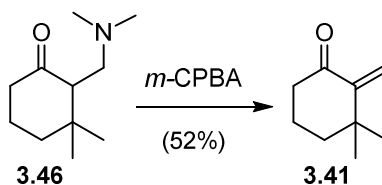
<sup>1</sup>H NMR (400 MHz, CDCl<sub>3</sub>): δ = 2.87 (dd, *J* = 12.3, 10.1 Hz, 1H), 2.42 – 2.33 (m, 1H), 2.30 – 2.25 (m, 1H), 2.25 – 2.20 (m, 1H), 2.15 (s, 6H), 2.04 (dd, *J* = 12.3, 3.3 Hz, 1H), 1.87 – 1.76 (m, 2H), 1.64 – 1.49 (m, 2H), 1.01 (s, 3H), 0.75 (s, 3H).

<sup>13</sup>C NMR (100 MHz, CDCl<sub>3</sub>): δ = 212.7, 59.2, 55.2, 45.8, 40.3, 38.8, 37.9, 28.9, 23.7, 23.2.

IR (ATR):  $\tilde{\nu}$  = 2941 (m), 2870 (m), 2819 (m), 2765 (m), 1710 (s), 1461 (m), 1367 (w), 1310 (w), 1260 (m), 1228 (m), 1184 (w), 1152 (w), 1079 (w), 1043 (m), 1030 (m), 935 (w), 843 (m) cm<sup>-1</sup>.

HRMS (ESI): calc. for C<sub>11</sub>H<sub>22</sub>ON [*M+H*]<sup>+</sup>: 184.1696, found: 184.1693.

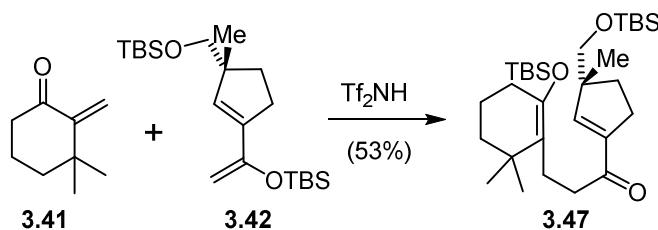
**Synthesis of compound 3.41**



A solution of amine **3.46** (7.58 g, 41.3 mmol, 1.00 eq.) in DCM (93 mL) was cooled to 0 °C and *m*-CPBA (18.5 g, 82.6 mmol, 2.00 eq.) was added. The mixture was stirred at 0 °C for 10 min and then for 6 h at r.t. before it was directly subjected to flash column chromatography (*n*-pentane/Et<sub>2</sub>O = 1:0 to 98:2). The solvent was removed *in vacuo* under ice bath cooling to afford the volatile enone **3.41** (2.97 g, 21.5 mmol, 52%) which was stored as a 1 M solution in toluene at -25 °C. The analytical data of **3.41** was in accordance to the reported one.<sup>[87]</sup>

R<sub>f</sub> = 0.53 (hexanes/EtOAc 9:1)

#### Synthesis and characterization of compound **3.47**



To a solution of silyl enol ether **3.42** (100 mg, 0.261 mmol, 1.00 eq.) and enone **3.41** (0.5 M in toluene, 0.58 mL, 0.290 mmol, 1.10 eq.) in DCM at -78 °C was added a solution of Tf<sub>2</sub>NH (0.1 M, 0.11 mL, 0.011 mmol, 0.04 eq.) dropwise. The reaction mixture was stirred for 80 min before it was quenched through the addition of Et<sub>3</sub>N (0.1 mL), filtered through a short plug of silica and concentrated *in vacuo*. Subsequent flash column chromatography (hexanes/Et<sub>2</sub>O = 1:0 to 95:5) gave product **3.47** (72.1 mg, 0.138 mmol, 53%) as a colorless oil.

R<sub>f</sub> = 0.67 (hexanes/EtOAc 9:1).

<sup>1</sup>H NMR (400 MHz, C<sub>6</sub>D<sub>6</sub>): δ = 6.39 (t, *J* = 1.8 Hz, 1H), 3.28 (d, *J* = 2.0 Hz, 2H), 3.13 – 2.94 (m, 2H), 2.75 (ddd, *J* = 9.1, 7.1, 1.7 Hz, 2H), 2.62 (td, *J* = 10.3, 9.6, 5.5 Hz, 2H), 1.99 (t, *J* = 6.4 Hz, 2H), 1.81 –

1.71 (m, 1H), 1.53 (ddt,  $J = 9.0, 6.4, 2.9$  Hz, 2H), 1.46 – 1.38 (m, 1H), 1.36 – 1.31 (m, 2H), 1.03 (s, 3H), 1.02 (s, 3H), 1.00 (s, 3H), 1.00 (s, 9H), 0.95 (s, 9H), 0.12 (s, 6H), 0.01 (d,  $J = 0.9$  Hz, 6H).

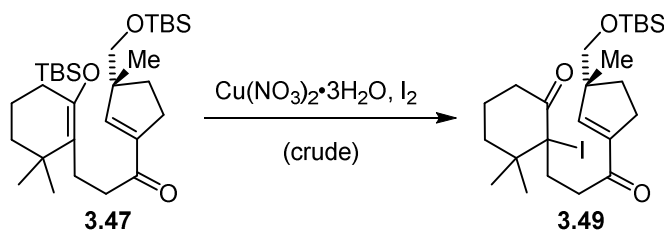
$^{13}\text{C}$  NMR (100 MHz,  $\text{C}_6\text{D}_6$ ):  $\delta = 198.6, 147.1, 145.1, 145.1, 122.6, 70.3, 52.6, 39.6, 39.3, 34.9, 33.5, 31.5, 30.6, 28.7, 28.7, 26.2, 26.1, 22.8, 21.4, 19.9, 18.5, 18.5, -3.4, -3.5, -5.3, -5.3$ .

IR (ATR):  $\tilde{\nu} = 2954$  (s), 2930 (s), 2857 (m), 1667 (m), 1471 (w), 1360 (w), 1257 (m), 1201 (w), 1148 (w), 1079 (m), 934 (w), 836 (s), 776 (s), 668 (w)  $\text{cm}^{-1}$ .

HRMS (EI): calc. for  $\text{C}_{30}\text{H}_{57}\text{O}_3\text{Si}_2$   $[M+H]^+$ : 521.3841, found: 521.3840.

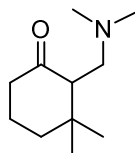
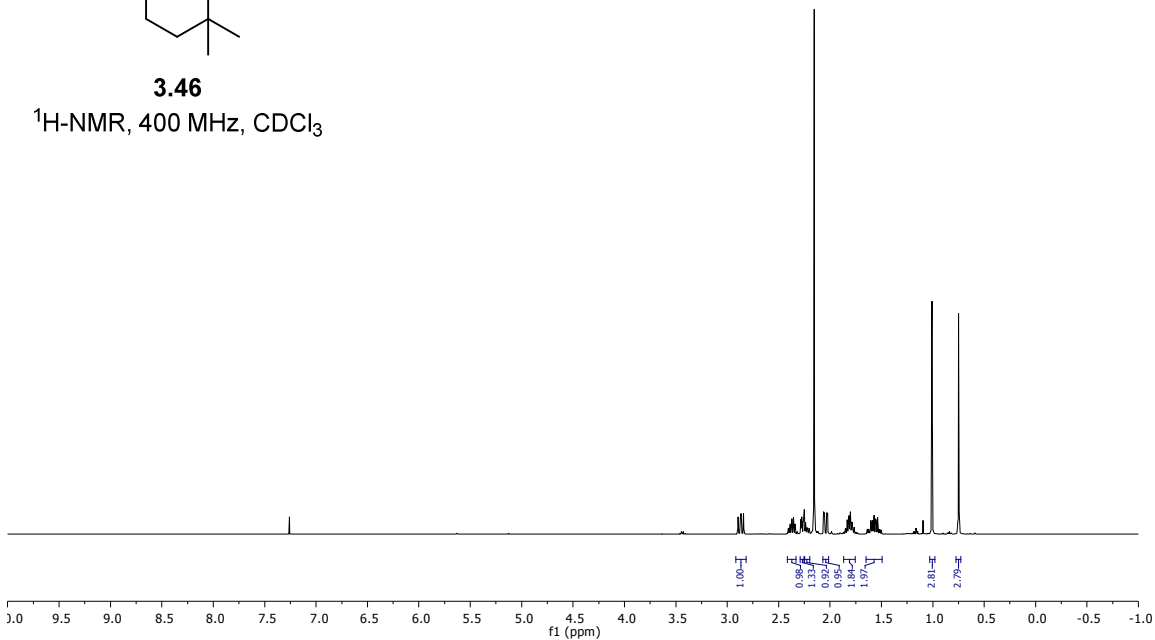
$[\alpha]_D^{25} = +15.2$  ( $c = 1.0$ , DCM)

### Synthesis of compound 3.49

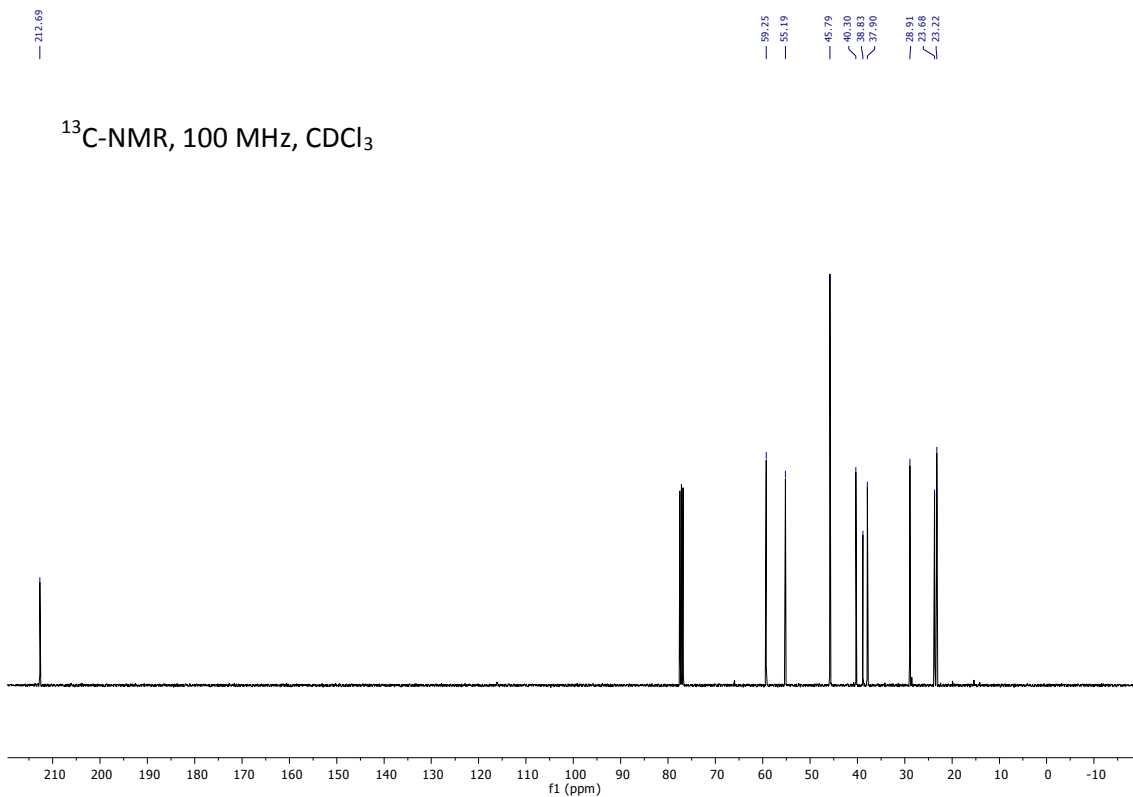


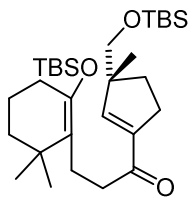
To a solution of  $\text{Cu}(\text{NO}_3)_2 \cdot \text{H}_2\text{O}$  in MeCN was added  $\text{I}_2$  and the resulting mixture was stirred for 5 min after which silyl enol ether **3.47** (69 mg, 0.133 mmol, 1.00 eq.) was added in THF/MeCN (1:1, 1.5 mL). The reaction mixture was stirred for 30 min and then quenched through addition of an aq. saturated solution of  $\text{Na}_4\text{S}_2\text{O}_3$  (5 mL). The aqueous phase was extracted with  $\text{Et}_2\text{O}$  (3 x 10 mL) and the combined organic layers were washed with brine, dried over  $\text{Na}_2\text{SO}_4$ , filtered and concentrated *in vacuo*. The crude product (72 mg) was used in the next step without further purification.

## 10.3.2. NMR Spectra for Chapter 3.3.

**3.46**<sup>1</sup>H-NMR, 400 MHz, CDCl<sub>3</sub>

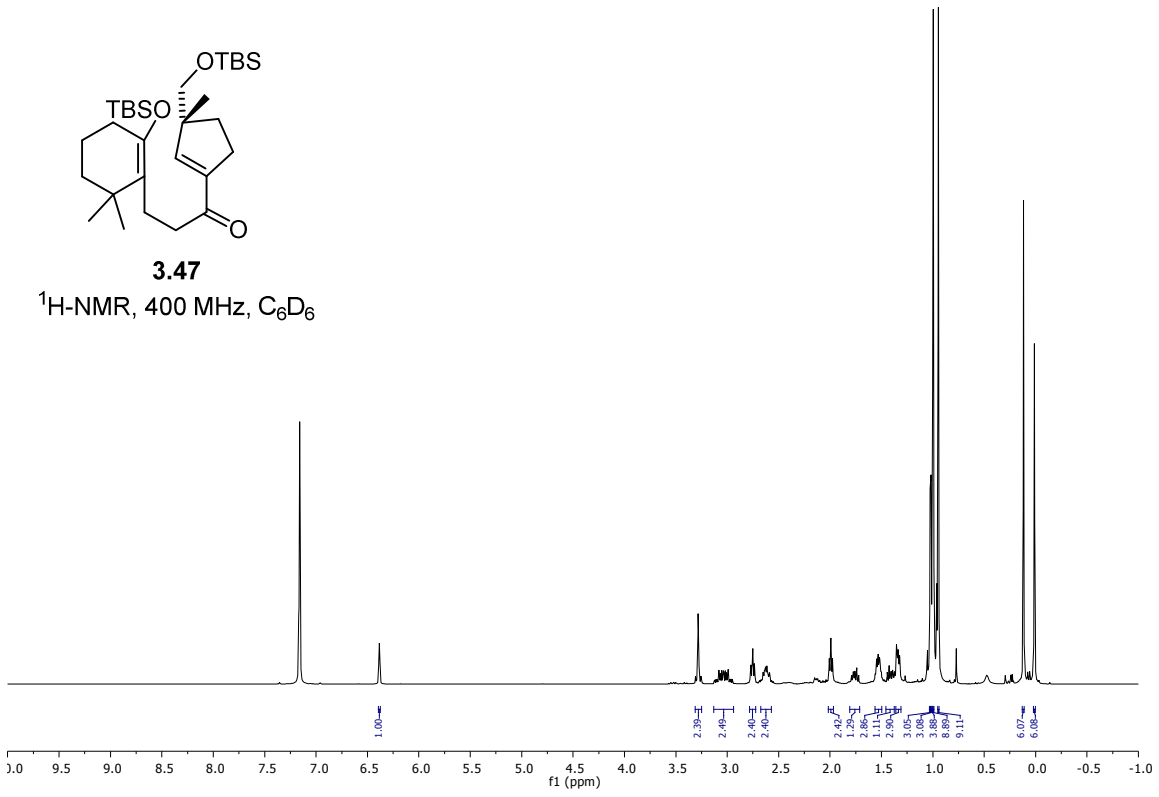
- 212.69

<sup>13</sup>C-NMR, 100 MHz, CDCl<sub>3</sub>

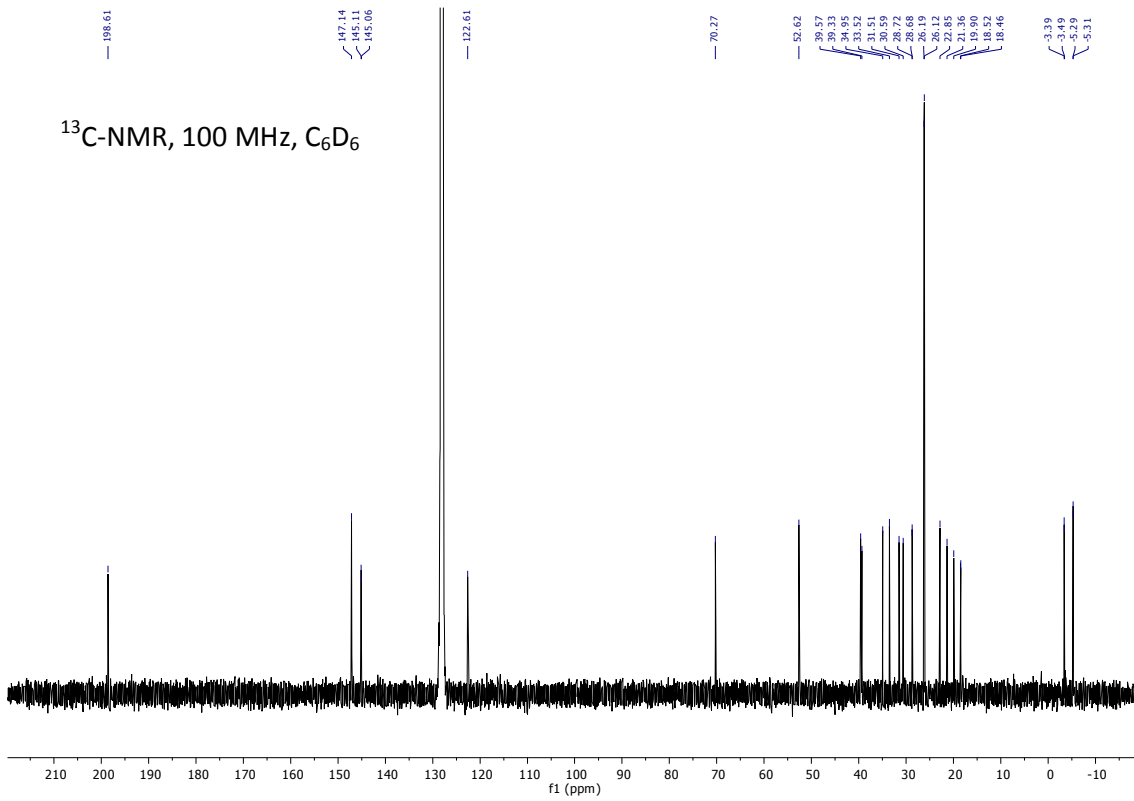


**3.47**

<sup>1</sup>H-NMR, 400 MHz, C<sub>6</sub>D<sub>6</sub>

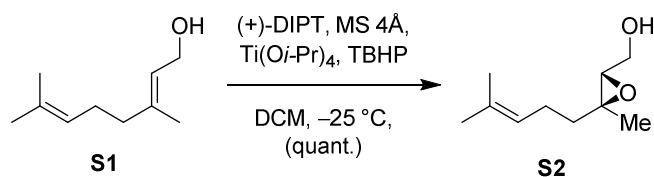


<sup>13</sup>C-NMR, 100 MHz, C<sub>6</sub>D<sub>6</sub>



## 10.4. Supporting Information for Chapter 3.3.

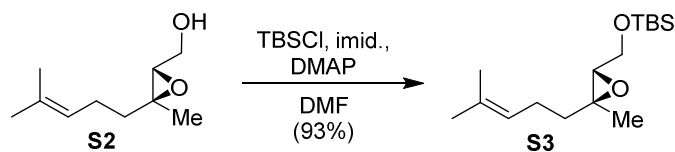
### 10.4.1. Experimental Procedures



A mixture of (+)-diisopropyl L-tartrate (0.831 mL, 3.94 mmol, 0.075 eq.) with activated 4 Å molecular sieves (5.60 g) in DCM (80 mL) was cooled to -10 °C. Freshly distilled titanium(IV)isopropoxide (0.933 mL, 3.15 mmol, 0.060 eq.) and TBHP in decane (5–6 M, 15.6 mL, 85.5 mmol, 1.63 eq.) were added. After stirring for additional 20 min at -10 °C, the mixture was cooled to -25 °C and geraniol (**S1**) (9.20 mL, 52.5 mmol, 1.00 eq.) was added. The mixture was stirred for 1 h at -25 °C before the reaction was quenched by adding H<sub>2</sub>O (16 mL). The suspension was stirred for 30 min at r.t. and aqueous NaOH solution (10%, 18 mL) was added. After additional stirring for 30 min the reaction mixture was filtered through a pad of celite. Then an aqueous solution of citric acid (10%, 18 mL) was added and the suspension was stirred for 1 h. The aqueous phase was extracted with DCM (6 x 50 mL) and the combined organic layers were washed with brine (300 mL), dried over MgSO<sub>4</sub>, filtered and concentrated *in vacuo*. The obtained crude material was purified by flash column chromatography (hexanes/EtOAc = 9:1 to 1:1) to afford epoxide **S2** as a colorless oil (9.06 g, 53.2 mmol, quant.). The analytical data of **S2** was in accordance to the reported one.<sup>[64]</sup> The *ee* was determined to be 80% by Mosher ester analysis.<sup>[63]</sup>

$R_f = 0.28$  (hexanes/EtOAc 7:3)

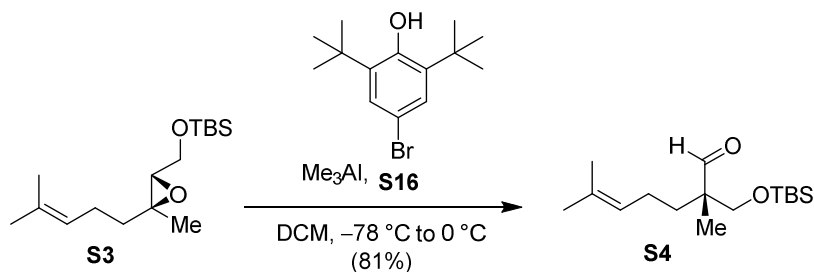
$[\alpha]_D^{25} = -4.3$  (c = 3.00, CHCl<sub>3</sub>)



A solution of epoxide **S2** (8.94 g, 52.5 mmol, 1.00 eq.) in DMF (74 mL) was cooled to 0 °C and imidazole (8.94 g, 131 mmol, 2.50 eq.), TBSCl (10.3 g, 68.3 mmol, 1.30 eq.) and 4-(dimethylamino)pyridine (3.85 g, 31.5 mmol, 0.600 eq.) were added. The mixture was warmed to r.t. and stirred for 1 h before the reaction was quenched by adding a solution of sat. aq.  $\text{NH}_4\text{Cl}$  (100 mL). The layers were separated and the aqueous layer was extracted with  $\text{Et}_2\text{O}$  (3 x 100 mL). The combined organic phases were washed with brine (300 mL), dried over  $\text{MgSO}_4$ , filtered and concentrated *in vacuo*. The obtained colorless oil was purified by flash column chromatography (hexanes/ $\text{EtOAc}$  = 1:0 to 95:5) to give compound **S3** (13.8 g, 48.5 mmol, 93% yield) as a colorless oil. The analytical data of **S3** was in accordance to the reported one.<sup>[64]</sup>

$R_f$  = 0.44 (hexanes/ $\text{EtOAc}$  95:5)

$[\alpha]_D^{25} = -3.07$  (c = 1.00,  $\text{CHCl}_3$ )

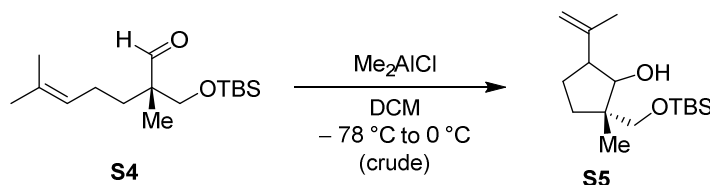


To a solution of 4-bromo-2,6-di-*tert*-butylphenol (**S16**) (12.5 g, 43.7 mmol, 2.30 eq.) in DCM (200 mL) was added a solution of  $\text{Me}_3\text{Al}$  in hexanes (2.0 M, 11.0 mL, 22.0 mmol, 1.15 eq.) (methane evolution!). After stirring for 1 h at r.t., the solution was cooled to -78 °C and a solution of epoxide **S3** (5.48 g, 19.3 mmol, 1.00 eq.) in DCM (20 mL) was added. Stirring at -78 °C was continued for 1.5 h before the reaction mixture was quenched through the addition of NaF (3.9 g) and  $\text{H}_2\text{O}$  (2 mL). The mixture was stirred for additional 25 min at -78 °C. The mixture was warmed up to 0 °C and was stirred for 30 min at r.t before the suspension was filtered over a pad of silica. The filtrate was then concentrated *in vacuo* to afford a slurry that was taken up in DCM and silica (30 g). Purification by flash column chromatography (hexanes/ $\text{Et}_2\text{O}$  = 99:1 to 9:1) afforded aldehyde **S4**

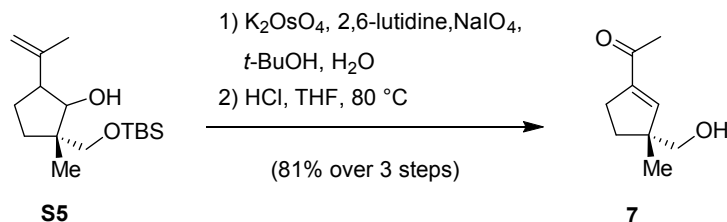
(4.42 g, 15.5 mmol, 81%) as a yellow oil. The analytical data of **S4** was in accordance to the reported one.<sup>[64]</sup>

$R_f = 0.62$ , hexanes/EtOAc 95:5

$[\alpha]_D^{25} = +5.24$  ( $c = 1.00$ ,  $\text{CHCl}_3$ )



The solution of aldehyde **S4** (8.28 g, 29.1 mmol, 1.00 eq.) in DCM (80 mL) was cooled to  $-78\text{ }^\circ\text{C}$  and a solution of  $\text{Me}_2\text{AlCl}$  in hexanes (1.0 M, 29.1 mL, 1.00 eq.) was added dropwise. The resulting solution was stirred for 1 h at  $-78\text{ }^\circ\text{C}$  before the reaction was warmed to  $0\text{ }^\circ\text{C}$ . After additional stirring for 1.5 h, the reaction was quenched by adding  $\text{H}_2\text{O}$  (20 mL) and aq. HCl solution (10%, 40 mL). The layers were separated and the aqueous layer was extracted with DCM (2 x 100 mL). The combined organic layers were washed with a sat. aq. solution of  $\text{NaHCO}_3$  (100 mL) and brine (100 mL), dried over  $\text{MgSO}_4$ , filtered and concentrated *in vacuo* to afford **S5** as a yellow oil (8.20 g, 28.8 mmol). The crude mixture of diastereomers was used in the next step without further purification.

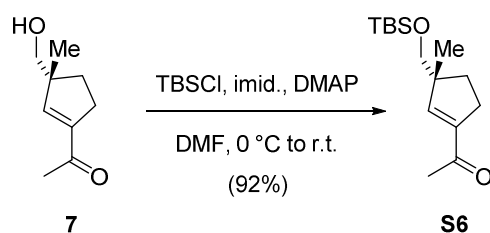


To a solution of cyclopentanol **S5** (8.20 g, 28.8 mmol, 1.00 eq.) in  $t\text{-BuOH}$  (134 mL) and  $\text{H}_2\text{O}$  (44 mL) was added potassium osmium(IV) oxide dihydrate (114 mg, 0.310 mmol, 0.011 eq.), 2,6-lutidine (6.67 mL, 57.6 mmol, 2.00 eq.) and sodium periodate (23.4 g, 109 mmol, 3.80 eq.). The suspension was stirred for 15 h at r.t. before the reaction was quenched by adding  $\text{Na}_2\text{SO}_3$  (30.8 g) at  $0\text{ }^\circ\text{C}$ . The mixture was allowed to warm to r.t., stirred an additional 1 h and was then diluted with  $\text{H}_2\text{O}$  (50 mL) and extracted with EtOAc (4 x 100 mL). The combined organic layers were washed with brine (400 mL), dried over  $\text{MgSO}_4$  and concentrated *in vacuo* to afford a dark yellow

oil. The crude product was dissolved in a 1:1 mixture of aq. HCl (6 M, 82 mL) and THF (82 mL) and the reaction mixture was refluxed at 80 °C for 4 h. The biphasic mixture was cooled to 0 °C and the pH was set to 7 by carefully adding aq. NaOH (10%, 200 mL). The organic layer was separated and the aqueous layer was extracted with EtOAc (3 x 400 mL). The organic layers were washed with brine (400 mL) and dried over MgSO<sub>4</sub>, filtered and concentrated *in vacuo*. The obtained dark brown oil was purified by flash column chromatography (hexanes/EtOAc = 7:3 to 4:6) to provide enone **7** (3.60 g, 23.3 mmol, 81% over three steps) as a red-brown oil. The analytical data of **7** was in accordance to the reported one.<sup>[61]</sup>

$R_f = 0.38$  (hexanes/EtOAc 7:3)

$[\alpha]_D^{25} = +38.5$  (c = 1.00, CHCl<sub>3</sub>)



A solution of **7** (6.54 g, 42.4 mmol, 1.00 eq.) in DMF (65 mL) was cooled to 0 °C. Imidazole (7.21 g, 106 mmol, 2.50 eq.), TBSCl (8.31 g, 55.1 mmol, 1.30 eq.), and DMAP (3.10 g, 25.4 mmol, 0.60 eq.) were added and the resulting suspension was stirred at r.t. for 1 h, after which the reaction mixture was quenched through the addition of a sat. aq. solution of NH<sub>4</sub>Cl (100 mL). The layers were separated and the aqueous layer was extracted with EtOAc (4 x 100 mL) and the combined organic phases were washed with brine (4 x 250 mL), dried over Na<sub>2</sub>SO<sub>4</sub>, and concentrated. The crude product was purified by column chromatography (SiO<sub>2</sub>, hexanes/EtOAc = 99:1 to 9:1). The product **S6** (10.5 g, 39.0 mmol, 92%) was obtained as an orange oil.

$R_f = 0.45$  (hexanes/EtOAc 9:1)

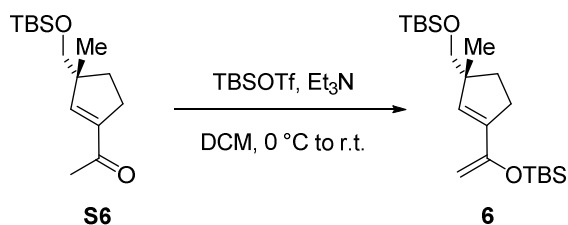
**$^1\text{H}$  NMR (400 MHz,  $\text{C}_6\text{D}_6$ ):**  $\delta$  = 6.15 (t,  $J$  = 1.8 Hz, 1H), 3.24 (d,  $J$  = 1.4 Hz, 2H), 2.63 (td,  $J$  = 7.5, 1.8 Hz, 2H), 1.99 (s, 3H), 1.70 (dt,  $J$  = 12.8, 7.0 Hz, 1H), 1.37 (dt,  $J$  = 12.9, 7.6 Hz, 1H), 0.96 (s, 3H), 0.93 (s, 9H), 0.00 (d,  $J$  = 1.2 Hz, 6H).

**$^{13}\text{C}$  NMR (100 MHz,  $\text{C}_6\text{D}_6$ ):**  $\delta$  = 195.3, 148.4, 145.2, 70.2, 52.6, 33.6, 30.3, 26.4, 26.1, 22.7, 18.5, -5.3, -5.3.

**IR (ATR):**  $\tilde{\nu}$  = 2954 (m), 2929 (m), 2887 (w), 2856 (m), 1670 (s), 1618 (w), 1471 (w), 1363 (m), 1312 (w), 1252 (m), 1087 (s), 1006 (w), 928 (w), 834 (s), 773 (s), 668 (m), 604 (m)  $\text{cm}^{-1}$ .

**HRMS (EI):** calc. for  $\text{C}_{15}\text{H}_{28}\text{O}_2\text{Si}$  [ $M$ ] $^+$ : 268.1853, found: 268.1855.

$[\alpha]_D^{25}$  = +79.4 ( $c$  = 1.0,  $\text{CHCl}_3$ )

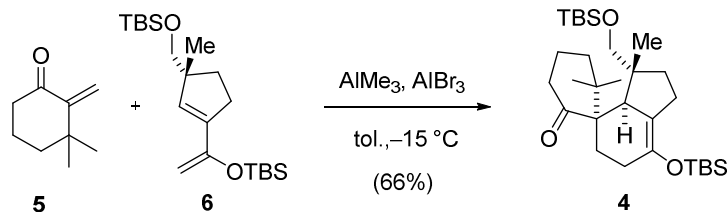


To a solution of enone **S6** (9.23 g, 34.4 mmol, 1.00 eq.) in DCM (160 mL) at 0 °C was added  $\text{Et}_3\text{N}$  (16.90 mL, 120.4 mmol, 3.50 eq.) and TBSOTf (11.9 mL, 51.6 mmol, 1.50 eq.). After stirring the resulting yellow solution at r.t. for 2 h, the reaction mixture was quenched through the addition of a sat. aq. solution of  $\text{NaHCO}_3$  (200 mL). The layers were separated and the aqueous layer was extracted with pentane (3  $\times$  300 mL). The combined organic phases were washed with brine, dried over  $\text{Na}_2\text{SO}_4$  and concentrated under reduced pressure to yield **6** (10.2 g, 26.6 mmol) as an orange oil. The crude product was used in the next step.

$R_f$  = 0.88 (hexanes/EtOAc 95:5)

**$^1\text{H}$  NMR (400 MHz,  $\text{C}_6\text{D}_6$ ):**  $\delta$  = 6.10 (d,  $J$  = 1.7 Hz, 1H), 4.39 (d,  $J$  = 1.7 Hz, 2H), 3.37 (s, 2H), 2.48 (td,  $J$  = 7.6, 1.5 Hz, 2H), 1.89 (ddd,  $J$  = 12.7, 7.9, 6.5 Hz, 1H), 1.55 (dt,  $J$  = 12.8, 7.8 Hz, 1H), 1.12 (s, 3H), 1.04 (s, 9H), 0.99 (s, 9H), 0.19 (s, 3H), 0.19 (s, 3H), 0.05 (s, 3H), 0.04 (s, 3H).

**$^{13}\text{C}$  NMR (100 MHz,  $\text{C}_6\text{D}_6$ ):**  $\delta$  = 154.6, 140.9, 135.5, 93.0, 70.9, 51.6, 34.5, 31.7, 26.2, 26.1, 23.6, 18.5, 18.5, -4.5, -5.3.



To a solution of enone **5** (3.00 mL, 3.00 mmol, 1.00 eq.) in toluene at  $-15$  °C was added sequentially a solution of  $\text{AlMe}_3$  in toluene (2 M, 0.60 mL, 1.20 mmol, 0.40 eq.), a solution of  $\text{AlBr}_3$  in toluene (1 M, 2.00 mL, 2.00 mmol, 0.67 eq.) and a solution of diene **6** (1.20 g, 3.10 mmol, 1.03 eq.) in toluene (1.6 mL). The resulting red-orange reaction mixture was stirred at  $-15$  °C for 20 min after which it was quenched with pyridine (3.2 mL), warmed to r.t. and filtered through a plug of silica. Concentration under reduced pressure and purification by flash chromatography ( $\text{SiO}_2$ , hexanes/ $\text{Et}_2\text{O}$  = 1:0 to 99:1 to 97:3) afforded the product **4** (1.03 g, 1.98 mmol, 66% yield) as a yellow oil.

$R_f$  = 0.68 (hexanes/ $\text{EtOAc}$  9:1)

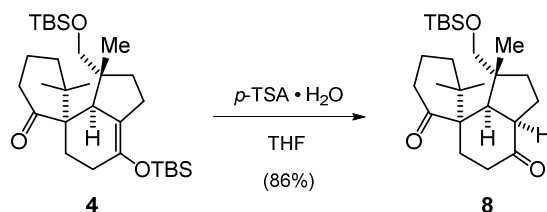
**$^1\text{H}$  NMR (400 MHz,  $\text{C}_6\text{D}_6$ ):**  $\delta$  = 3.42 (d,  $J$  = 11.0 Hz, 1H), 3.15 (d,  $J$  = 10.8 Hz, 1H), 3.20 – 3.10 (m, 1H), 2.75 (s, 1H), 2.55 (ddd,  $J$  = 15.7, 9.6, 6.6 Hz, 1H), 2.50 – 2.45 (m, 1H), 2.44 – 2.37 (m, 1H), 2.22 (td,  $J$  = 13.3, 4.8 Hz, 1H), 2.14 – 2.09 (m, 2H), 2.05 (dd,  $J$  = 12.1, 6.7 Hz, 1H), 1.99 – 1.91 (m, 1H), 1.84 – 1.76 (m, 1H), 1.70 – 1.59 (m, 2H), 1.05 (s, 3H), 1.03 (m, 1H), 1.02 (s, 9H), 0.99 – 0.97 (m, 1H), 0.96 (s, 9H), 0.78 (s, 3H), 0.74 (s, 3H), 0.12 (s, 3H), 0.10 (s, 3H), -0.00 (s, 3H), -0.03 (s, 3H).

**$^{13}\text{C}$  NMR (100 MHz,  $\text{C}_6\text{D}_6$ ):**  $\delta$  = 214.4, 143.2, 122.1, 67, 55.9, 45.7, 43.7, 41.5, 41.4, 39.6, 35.3, 29.6, 28.7, 27.2, 26.1, 26.1, 24.4, 22.2, 21.3, 19.1, 18.5, 18.4, -3.4, -3.6, -5.3, -5.5.

**IR (ATR):**  $\tilde{\nu}$  = 2954 (m), 2929 (m), 2897 (w), 2857 (m), 1692 (m), 1472 (w), 1463 (w), 1389 (w), 1361 (w), 1353 (w), 1251 (m), 1221 (w), 1206 (w), 1195 (w), 1181 (w), 1155 (w), 1098 (m), 1087 (m), 1070 (m), 1042 (w), 1006 (w), 975 (w), 953 (w), 938 (w), 921 (w), 835 (s), 775 (s), 729 (w), 668 (w)  $\text{cm}^{-1}$ .

**HRMS (EI):** calc. for  $C_{30}H_{56}O_3Si_2$   $[M]^+$ : 520.3763, found: 520.3768.

$[\alpha]_D^{25} = +51.8$  ( $c = 1.0$ , DCM)



To a solution of silyl enol ether **4** (6.40 g, 12.3 mmol, 1.00 eq.) in THF (550 mL) was added  $p\text{-TSA} \cdot \text{H}_2\text{O}$  (11.8 g, 62.0 mmol, 5.04 eq.) at r.t.. The reaction mixture was stirred for 11 h after which it was quenched with a sat. aq. solution of  $\text{NaHCO}_3$  (200 mL) and diluted with  $\text{Et}_2\text{O}$  (200 mL). The layers were separated and the aqueous layer was extracted with  $\text{Et}_2\text{O}$  (3 x 200 mL). The combined organic layers were washed with brine, dried over  $\text{Na}_2\text{SO}_4$ , filtered and concentrated under reduced pressure. The crude was purified by flash chromatography ( $\text{SiO}_2$ , hexanes/ $\text{EtOAc} = 99:1$  to 95:5) to afford the product **8** (4.31 g, 10.6 mmol, 86% yield) as a pale yellow oil.

$R_f = 0.41$  (hexanes/ $\text{EtOAc}$  9:1).

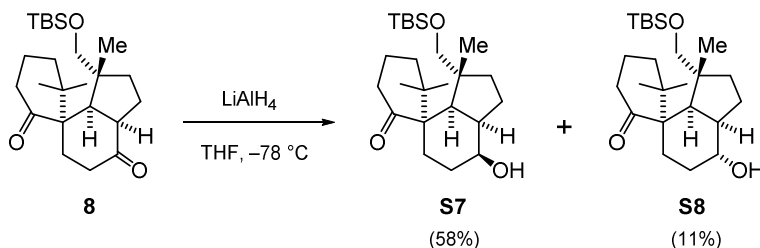
**$^1\text{H NMR}$  (400 MHz,  $\text{C}_6\text{D}_6$ ):**  $\delta = 3.27$  (d,  $J = 10.8$  Hz, 1H), 3.09 – 2.96 (m, 1H), 2.98 (d,  $J = 10.9$  Hz, 1H), 2.87 – 2.76 (m, 2H), 2.65 – 2.58 (m, 1H), 2.58 – 2.50 (m, 1H), 2.47 (ddd,  $J = 17.1, 5.9, 4.3$  Hz, 1H), 2.40 – 2.33 (m, 1H), 2.29 (ddd,  $J = 17.1, 12.8, 6.0$  Hz, 1H), 2.06 (ddd,  $J = 13.8, 11.6, 6.2$  Hz, 1H), 1.82 (ddd,  $J = 12.5, 10.2, 8.0$  Hz, 1H), 1.71 (dddd,  $J = 15.5, 6.1, 4.3, 1.6$  Hz, 1H), 1.60 – 1.46 (m, 3H), 1.07 (ddt,  $J = 13.2, 8.9, 4.7$  Hz, 1H), 0.97 – 0.94 (m, 1H), 0.92 (s, 9H), 0.87 (s, 3H), 0.64 (s, 3H), 0.62 (s, 3H), -0.06 (s, 3H), -0.08 (s, 3H).

**$^{13}\text{C NMR}$  (200 MHz,  $\text{C}_6\text{D}_6$ ):**  $\delta = 213.4, 211.4, 67.6, 56.5, 52.7, 47.0, 44.8, 42.2, 41.2, 38.2, 38.1, 38.0, 29.9, 26.7, 26.0, 24.8, 22.2, 21.3, 19.9, 18.3, -5.4, -5.6$ .

**IR (ATR):**  $\tilde{\nu} = 2954$  (s), 2929 (s), 2857 (m), 2362 (w), 2336 (w), 1695 (s), 1471 (m), 1389 (w), 1258 (w), 1093 (m), 838 (s), 777 (m), 668 (w)  $\text{cm}^{-1}$ .

**HRMS (EI):** calc. for  $C_{24}H_{42}O_3Si$  [ $M$ ] $^+$ : 406.2898, found: 406.2905.

$[\alpha]_D^{25} = -9.0$  ( $c = 1.0$ , DCM)



Diketone **8** (3.21 g, 7.90 mmol, 1.00 eq.) was dissolved in THF (290 mL) and cooled to  $-78\text{ }^\circ\text{C}$ .  $LiAlH_4$  (448 mg, 11.9 mmol, 1.51 eq.) was added and the reaction was stirred for 3.5 h after which Glauber's salt was added until effervescence stopped. The resulting slurry was then filtered and concentrated to give a solid that was purified by flash chromatography ( $SiO_2$ , pentanes/EtOAc = 95:5 to 8:2). The desired product **S7** (1.88 g, 4.60 mmol, 58% yield) was obtained as a white solid together with alcohol **S8** (355 mg, 0.869 mmol, 11% yield, viscous oil).

#### Data for **S7**:

$R_f = 0.61$  (hexanes/EtOAc 8:2).

$Mp = 110 - 111\text{ }^\circ\text{C}$ .

$^1\text{H NMR}$  (400 MHz,  $C_6D_6$ ):  $\delta = 3.56 - 3.51$  (m, 1H), 3.49 (d,  $J = 10.4$  Hz, 1H), 3.27 (d,  $J = 10.4$  Hz, 1H), 2.91 (td,  $J = 12.5, 7.7$  Hz, 1H), 2.73 (dd,  $J = 8.1, 1.5$  Hz, 1H), 2.48 – 2.36 (m, 3H), 2.19 – 2.09 (m, 1H), 1.88 – 1.82 (m, 1H), 1.79 – 1.73 (m, 2H), 1.73 – 1.67 (m, 1H), 1.66 – 1.55 (m, 3H), 1.39 – 1.30 (m, 1H), 1.20 (s, 3H), 1.04 (s, 3H), 1.01 – 0.99 (m, 1H), 0.98 (s, 9H), 0.74 (s, 3H), 0.02 (s, 3H), 0.00 (s, 3H).

$^{13}\text{C NMR}$  (100 MHz,  $C_6D_6$ ):  $\delta = 214.4, 71.3, 67.8, 57.3, 46.6, 45.2, 42.9, 42.1, 41.6, 41.1, 39.7, 31.4, 31.2, 26.1, 25.4, 24.8, 23.1, 22.8, 20.4, 18.4, -5.4, -5.4$ .

**IR (ATR):**  $\tilde{\nu}$  = 3493 (br), 2954 (s), 2930 (s), 2880 (m), 2858 (m), 1689 (m), 1472 (m), 1448 (w), 1389 (w), 1361 (w), 1256 (m), 1088 (s), 1006 (w), 984 (w), 941 (w), 851 (s), 837 (s), 815 (w), 775 (m), 668 (w)  $\text{cm}^{-1}$ .

**HRMS (EI):** calc. for  $\text{C}_{24}\text{H}_{44}\text{O}_3\text{Si}$   $[M]^+$ : 408.3054, found: 408.3050.

$[\alpha]_{\text{D}}^{25} = +29.6$  ( $c = 0.5$ ,  $\text{Et}_2\text{O}$ )

**Data for minor isomer S8:**

$R_f = 0.28$  (hexanes/EtOAc 8:2)

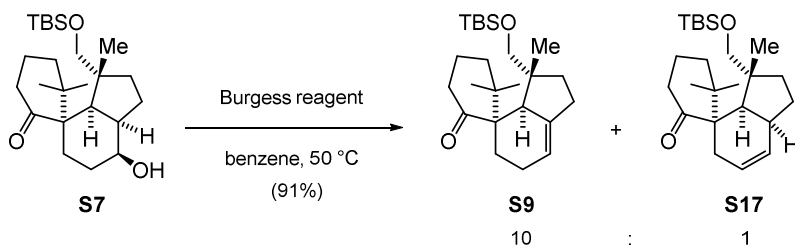
**$^1\text{H}$  NMR (400 MHz,  $\text{C}_6\text{D}_6$ ):**  $\delta$  = 3.44 (td,  $J = 10.7, 6.0$  Hz, 1H), 3.32 (d,  $J = 10.6$  Hz, 1H), 3.10 (d,  $J = 10.6$  Hz, 1H), 2.96 (td,  $J = 12.6, 7.8$  Hz, 1H), 2.74 (dd,  $J = 7.5, 1.8$  Hz, 1H), 2.42 (t,  $J = 3.3$  Hz, 1H), 2.39 (dd,  $J = 4.4, 2.2$  Hz, 1H), 2.29 (td,  $J = 15.5, 4.6$  Hz, 1H), 2.13 (td,  $J = 13.0, 5.4$  Hz, 1H), 1.85 (ddd,  $J = 15.4, 7.5, 4.8$  Hz, 2H), 1.79 – 1.73 (m, 1H), 1.72 – 1.63 (m, 2H), 1.62 – 1.50 (m, 3H), 1.25 (dt,  $J = 12.5, 7.9$  Hz, 1H), 1.15 (s, 3H), 0.98 (q,  $J = 2.5$  Hz, 1H), 0.95 (s, 9H), 0.85 (s, 3H), 0.73 (s, 3H), –0.01 (s, 3H), –0.04 (s, 3H).

**$^{13}\text{C}$  NMR (100 MHz,  $\text{C}_6\text{D}_6$ ):**  $\delta$  = 215.0, 72.1, 69.7, 57.3, 49.0, 46.5, 43.3, 42.9, 41.9, 39.7, 39.4, 32.5, 32.0, 27.2, 26.4, 26.1, 25.3, 23.0, 22.8, 18.4, –5.4, –5.5.

**IR (ATR):**  $\tilde{\nu}$  = 3364 (br), 2953 (s), 2932 (s), 2879 (m), 2858 (m), 1691 (m), 1506 (w), 1471 (m), 1449 (w), 1390 (w), 1361 (w), 1325 (w), 1252 (m), 1091 (s), 1044 (m), 1006 (w), 946 (w), 837 (s), 815 (w), 776 (m), 668 (w)  $\text{cm}^{-1}$ .

**HRMS (EI):** calc. for  $\text{C}_{24}\text{H}_{44}\text{O}_3\text{Si}$   $[M]^+$ : 408.3054, found: 408.3054.

$[\alpha]_{\text{D}}^{25} = -16.4$  ( $c = 1.0$ , THF)



Alcohol **S7** (1.88 g, 4.60 mmol, 1.00 eq.) in benzene (95 mL) was added to Burgess' reagent (2.52 g, 10.6 mmol, 2.30 eq.) and the resulting solution was heated to 50 °C for 3 h. The reaction mixture was concentrated, redissolved in Et<sub>2</sub>O (100 mL) and washed with a sat. aq. solution of NH<sub>4</sub>Cl (100 mL). The aqueous layer was extracted with Et<sub>2</sub>O (2 x 100 mL) and the combined organic layers were washed with brine, dried over Na<sub>2</sub>SO<sub>4</sub>, filtered and concentrated under reduced pressure. The residue was purified by column chromatography (SiO<sub>2</sub>, pentanes/EtOAc = 99:1 to 96:4) to give the product **S9** and **S17** (1.62 g, 4.15 mmol, 91% yield) as an inseparable 10:1 mixture of alkenes.

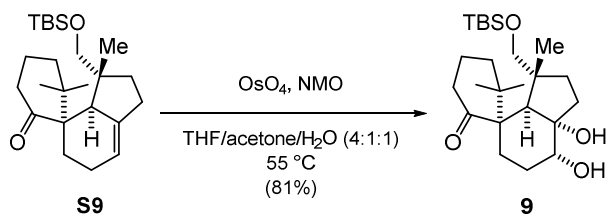
#### Data for **S9**:

$R_f$  = 0.61 (hexanes/EtOAc 9:1)

**<sup>1</sup>H NMR (400 MHz, C<sub>6</sub>D<sub>6</sub>):**  $\delta$  = 5.47 (dd,  $J$  = 5.3, 2.5 Hz, 1H), 3.42 (d,  $J$  = 11.0 Hz, 1H), 3.15 (d,  $J$  = 11.0 Hz, 1H), 3.14 – 3.06 (m, 1H), 2.66 (s, 1H), 2.47 (ddt,  $J$  = 13.8, 4.4, 2.4 Hz, 1H), 2.29 – 2.21 (m, 1H), 2.21 – 2.10 (m, 2H), 2.08 – 2.01 (m, 2H), 1.96 (dd,  $J$  = 13.6, 4.8 Hz, 1H), 1.85 – 1.78 (m, 1H), 1.70 – 1.59 (m, 2H), 1.06 (q,  $J$  = 3.0 Hz, 1H), 1.02 (s, 3H), 1.00 – 0.98 (m, 1H), 0.96 (s, 9H), 0.80 (s, 3H), 0.77 (s, 3H), -0.01 (s, 3H), -0.03 (s, 3H).

**<sup>13</sup>C NMR (100 MHz, C<sub>6</sub>D<sub>6</sub>):**  $\delta$  = 214.6, 144.4, 119.7, 67.5, 56.3, 45.2, 43.0, 41.6, 41.4, 39.6, 34.7, 28.3, 26.5, 26.1, 25.8, 24.4, 24.3, 22.3, 20.1, 18.4, -5.3, -5.5.

**HRMS (EI):** calc. for C<sub>24</sub>H<sub>42</sub>O<sub>2</sub>Si [ $M$ ]<sup>+</sup>: 390.2949, found: 390. 2947.



To a solution of mixture of alkenes **S9** and **S17** (10:1) (1.44 g, 3.69 mmol, 1.00 eq.) in THF/Acetone (8:2, 100 mL) was added NMO (870 mg, 7.40 mmol, 2.01 eq.) in water (20 mL) followed by OsO<sub>4</sub> (4 wt% in water, 3.10 mL, 0.488 mmol, 0.13 eq.). The reaction mixture was heated to 55 °C for 36 h after which it was quenched with a sat. aq. solution of Na<sub>2</sub>SO<sub>3</sub> (100 mL). The layers were separated and the aqueous layer was extracted with EtOAc (2 x 100 mL). The combined organic layers were washed with brine, dried over Na<sub>2</sub>SO<sub>4</sub>, filtered and concentrated under reduced pressure. The crude product was purified by column chromatography (SiO<sub>2</sub>, pentanes/EtOAc = 8:2), giving the diol **9** (1.27 g, 2.99 mmol, 81% yield) as a yellow oil.

$R_f = 0.31$  (hexanes/EtOAc 7:3)

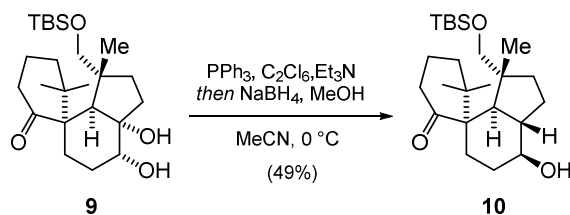
**<sup>1</sup>H NMR (400 MHz, C<sub>6</sub>D<sub>6</sub>):**  $\delta = 3.76$  (td,  $J = 7.1, 4.8$  Hz, 1H), 3.57 (d,  $J = 9.8$  Hz, 1H), 3.37 (d,  $J = 9.8$  Hz, 1H), 2.81 (s, 1H), 2.52 – 2.44 (m, 1H), 2.43 (s, 1H), 2.23 – 2.14 (m, 1H), 2.09 (dd,  $J = 15.4, 8.0$  Hz, 1H), 2.03 – 1.97 (m, 2H), 1.73 (dt,  $J = 13.9, 5.4$  Hz, 1H), 1.68 – 1.59 (m, 3H), 1.60 – 1.52 (m, 2H), 1.46 – 1.38 (m, 2H), 1.20 (s, 3H), 1.15 – 1.10 (m, 1H), 1.07 (s, 3H), 0.99 (s, 12H), 0.06 (s, 6H).

**<sup>13</sup>C NMR (200 MHz, C<sub>6</sub>D<sub>6</sub>):**  $\delta = 213.9, 84.5, 71.3, 69.2, 59.1, 50.5, 47.2, 41.4, 38.9, 37.2, 36.5, 36.2, 28.5, 27.6, 27.5, 27.2, 26.2, 23.2, 20.5, 18.6, -5.3, -5.3$ .

**IR (ATR):**  $\tilde{\nu} = 3426$  (br), 2956 (s), 2929 (s), 2858 (m), 2361 (w), 1698 (m), 1472 (w), 1391 (w), 1258 (m), 1092 (s), 1035 (m), 837(s), 800 (m), 775 (m), 668 (w) cm<sup>-1</sup>.

**HRMS (EI):** calc. for C<sub>24</sub>H<sub>44</sub>O<sub>4</sub>Si [ $M$ ]<sup>+</sup>: 424.3003, found: 424.3009.

$[\alpha]_D^{25} = -20.5$  (c = 0.4, THF)



To a solution of  $\text{PPh}_3$  (1.89 g, 7.20 mmol, 2.20 eq.) in MeCN (55 mL) was added  $\text{C}_2\text{Cl}_6$  (1.70 g, 7.20 mmol, 2.20 eq.). The resulting solution was stirred for 20 minutes at r.t., upon which  $\text{Et}_3\text{N}$  (1.96 mL, 14.7 mmol, 4.50 eq.) was added. Then the reaction mixture was cooled to  $0\text{ }^\circ\text{C}$  and diol **9** (1.39 g, 3.27 mmol, 1.00 eq.) in MeCN (33.5 mL) was added dropwise. After 30 min. the reaction was warmed to r.t. and stirred for 1 h. MeOH (17 mL) followed by  $\text{NaBH}_4$  (1.25 g, 33.0 mmol, 10.1 eq.) was then added at  $0\text{ }^\circ\text{C}$ . After 2 h, the reaction was quenched by the addition of water (50 mL). The layers were separated and the aqueous layer was extracted with EtOAc (3 x 80 mL). The combined organic layers were washed with brine, dried over  $\text{Na}_2\text{SO}_4$ , filtered and concentrated under reduced pressure. The residue was suspended in  $\text{Et}_2\text{O}$  and filtered through a short plug of silica to remove parts of triphenylphosphineoxide. The solution was concentrated under reduced pressure and the crude product was purified by column chromatography ( $\text{SiO}_2$ , pentanes/EtOAc = 8:2 to 7:3) giving the alcohol **10** (659 mg, 1.61 mmol, 49% yield) as a colorless oil.

$R_f = 0.27$  (hexanes/EtOAc 7:3)

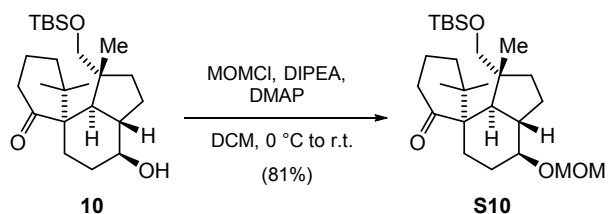
$^1\text{H NMR}$  (800 MHz,  $\text{C}_6\text{D}_6$ ):  $\delta = 3.72$  (d,  $J = 9.7$  Hz, 1H), 3.33 (d,  $J = 9.7$  Hz, 1H), 3.09 (td,  $J = 10.3, 4.4$  Hz, 1H), 2.60 (tdd,  $J = 11.4, 10.4, 6.1$  Hz, 1H), 2.09 – 2.04 (m, 2H), 2.01 (dddd,  $J = 13.9, 8.1, 5.6, 2.6$  Hz, 1H), 1.96 (ddd,  $J = 12.7, 8.7, 2.3$  Hz, 1H), 1.90 (ddd,  $J = 14.2, 4.2, 3.0$  Hz, 1H), 1.74 (td,  $J = 13.7, 5.5$  Hz, 1H), 1.67 (d,  $J = 11.9$  Hz, 1H), 1.64 – 1.58 (m, 2H), 1.52 (ddd,  $J = 12.7, 11.1, 7.9$  Hz, 1H), 1.40 – 1.35 (m, 1H), 1.34 (s, 3H), 1.20 – 1.16 (m, 1H), 1.16 – 1.11 (m, 1H), 1.00 – 0.99 (m, 3H), 0.99 (s, 9H), 0.97 – 0.94 (m, 1H), 0.89 (s, 3H), 0.81 – 0.78 (m, 1H), 0.05 (s, 3H), 0.04 (s, 3H).

$^{13}\text{C NMR}$  (100 MHz,  $\text{C}_6\text{D}_6$ ): 212.4, 76.9, 71.4, 62.0, 50.2, 49.1, 47.3, 42.0, 41.0, 38.5, 37.9, 34.0, 31.8, 29.8, 28.9, 26.2, 24.5, 24.1, 21.1, 18.5, -5.4, -5.4.

**IR (ATR):**  $\tilde{\nu}$  = 3397 (br), 2954 (s), 2930 (s), 2858 (m), 2284 (w), 1704 (m), 1602 (w), 1472 (m), 1387 (w), 1361 (w), 1313 (w), 1256 (m), 1216 (w), 1087 (s), 1006 (w), 935 (w), 853 (s), 814 (w), 774 (s), 670 (w)  $\text{cm}^{-1}$ .

**HRMS (EI):** calc. for  $\text{C}_{24}\text{H}_{44}\text{O}_3\text{Si}$  [ $M\text{-H}_2\text{O}$ ] $^+$ : 390.2954, found: 390.2969.

$[\alpha]_D^{25} = +34.0$  ( $c = 0.4$ , THF)



A solution of alcohol **10** (702 mg, 1.72 mmol, 1.00 eq.) in DCM (47 mL) and DIPEA (0.90 mL, 5.17 mmol, 3.00 eq.) was cooled to 0 °C and MOMCl (1.18 mL, 15.5 mmol, 9.05 eq.) and DMAP (210 mg, 1.72 mmol, 1.00 eq.) was added. The reaction mixture was stirred for 6 h and was quenched through the addition of a sat. aq. solution of  $\text{NH}_4\text{Cl}$  (50 mL). The aqueous phase was extracted with DCM (3 x 50 mL). The combined organic layers were washed with brine, dried over  $\text{Na}_2\text{SO}_4$ , filtered and concentrated. The resulting residue was purified by column chromatography ( $\text{SiO}_2$ , pentanes/EtOAc = 95:5 to 7:3) to afford the desired product **S10** (628 mg, 1.39 mmol, 81% yield) as a colorless oil.

$R_f = 0.52$  (hexanes/EtOAc 8:2)

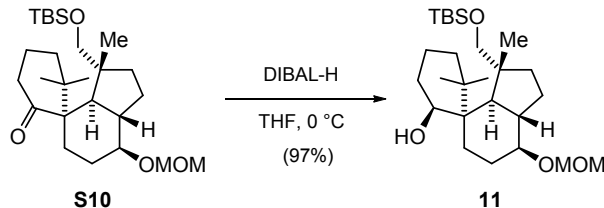
**$^1\text{H}$  NMR (800 MHz,  $\text{C}_6\text{D}_6$ ):**  $\delta$  = 4.73 (d,  $J = 6.8$  Hz, 1H), 4.60 (d,  $J = 6.8$  Hz, 1H), 3.73 (d,  $J = 9.7$  Hz, 1H), 3.37 (d,  $J = 9.7$  Hz, 1H), 3.26 (s, 3H), 3.23 – 3.18 (m, 1H), 2.94 (dddd,  $J = 12.1, 11.2, 10.0, 6.0$  Hz, 1H), 2.25 (dddd,  $J = 11.6, 8.0, 6.0, 2.1$  Hz, 1H), 2.09 – 2.06 (m, 2H), 1.99 (ddd,  $J = 12.7, 8.6, 2.1$  Hz, 1H), 1.94 (ddd,  $J = 13.9, 4.3, 2.7$  Hz, 1H), 1.82 (dtd,  $J = 12.0, 4.4, 2.6$  Hz, 1H), 1.76 (td,  $J = 13.7, 5.6$  Hz, 1H), 1.72 (d,  $J = 12.1$  Hz, 1H), 1.64 – 1.58 (m, 1H), 1.58 – 1.54 (m, 1H), 1.40 – 1.36 (m, 1H), 1.35 (s, 3H), 1.26 (qd,  $J = 11.3, 8.7$  Hz, 1H), 1.16 (td,  $J = 14.1, 2.6$  Hz, 1H), 1.11 – 1.06 (m, 1H), 1.02 – 1.01 (m, 3H), 0.99 (s, 9H), 0.92 (s, 3H), 0.83 – 0.79 (m, 1H), 0.06 (s, 3H), 0.05 (s, 3H).

**$^{13}\text{C}$  NMR (100 MHz,  $\text{C}_6\text{D}_6$ ):**  $\delta$  = 212.2, 95.1, 82.2, 71.5, 61.9, 55.0, 49.5, 48.1, 47.2, 41.9, 41.0, 38.5, 38.0, 33.8, 30.4, 28.9, 28.7, 26.2, 24.5, 24.2, 21.0, 18.5, -5.4, -5.4.

**IR (ATR):**  $\tilde{\nu}$  = 2954 (s), 2930 (s), 2882 (m), 2862 (m), 2162 (w), 2040 (w), 1706 (m), 1472 (w), 1387 (w), 1256 (w), 1147 (m), 1091 (s), 1043 (s), 918 (w), 852 (s), 837 (s), 775 (m), 670 (w).

**HRMS (EI):** calc. for  $\text{C}_{26}\text{H}_{48}\text{O}_4\text{Si}$  [ $M$ ] $^+$ : 452.3316, found: 452.3308.

**$[\alpha]_D^{25}$**  = +37.1 ( $c$  = 0.21, THF)



A solution of ketone **S10** (623 mg, 1.38 mmol, 1.00 eq.) in THF (58 mL) was cooled to 0 °C and DIBAL-H (1 M solution in toluene, 13.7 mL, 13.7 mmol, 9.93 eq.) was added dropwise. The reaction was stirred for 2 h and was quenched through the addition of Glauber's salt (portionwise addition until effervescence ceased). The mixture was then allowed to stir for 15 min at r.t., after which it was filtered and concentrated under reduced pressure. The crude product was purified by column chromatography ( $\text{SiO}_2$ , pentanes/EtOAc = 90:10 to 85:15). The desired product **11** (611 mg, 1.34 mmol, 97%) was obtained as a colorless oil.

**$R_f$**  = 0.42 (hexanes/EtOAc 8:2)

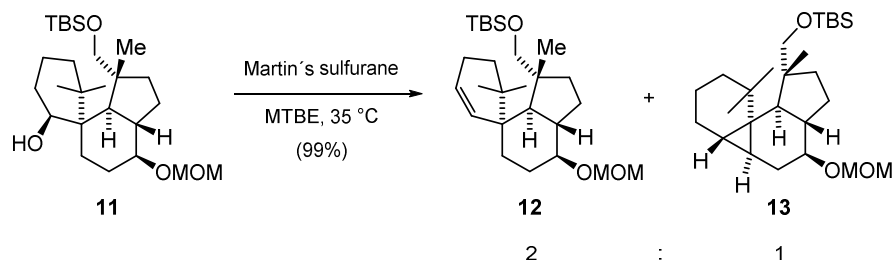
**$^1\text{H}$  NMR (400 MHz,  $\text{C}_6\text{D}_6$ ):**  $\delta$  = 4.76 (d,  $J$  = 6.7 Hz, 1H), 4.61 (d,  $J$  = 6.7 Hz, 1H), 3.97 (q,  $J$  = 3.5 Hz, 1H), 3.82 (d,  $J$  = 9.6 Hz, 1H), 3.65 (d,  $J$  = 9.6 Hz, 1H), 3.33 (dd,  $J$  = 10.2, 6.0 Hz, 1H), 3.30 (s, 3H), 2.33 (dt,  $J$  = 20.2, 8.3 Hz, 1H), 2.24 – 2.14 (m, 1H), 2.08 – 1.99 (m, 1H), 1.95 (ddd,  $J$  = 18.0, 9.1, 4.7 Hz, 1H), 1.82 (d,  $J$  = 12.3 Hz, 1H), 1.77 (dt,  $J$  = 5.8, 3.5 Hz, 1H), 1.71 – 1.57 (m, 2H), 1.51 (s, 3H), 1.50 – 1.41 (m, 3H), 1.35 – 1.29 (m, 1H), 1.28 (s, 3H), 1.19 (td,  $J$  = 13.9, 3.7 Hz, 2H), 1.12 – 1.05 (m, 1H), 1.03 (s, 9H), 0.95 (s, 3H), 0.11 (s, 6H).

$^{13}\text{C}$  NMR (100 MHz,  $\text{C}_6\text{D}_6$ ):  $\delta = 95.2, 82.9, 71.8, 68.6, 55.1, 52.6, 49.2, 47.8, 45.2, 41.5, 39.8, 36.8, 33.8, 30.4, 29.1, 28.5, 27.8, 27.3, 26.3, 23.6, 18.6, 17.0, -5.2, -5.3$ .

IR (ATR):  $\tilde{\nu} = 3473$  (br), 2951 (s), 2928 (s), 2858 (m), 1472 (w), 1388 (w), 1362 (w), 1256 (m), 1214 (w), 1137 (m), 1086 (s), 1038 (s), 918 (w), 853 (s), 836 (s), 814 (w), 774 (s), 669 (w)  $\text{cm}^{-1}$ .

HRMS (ESI): calc. for  $\text{C}_{26}\text{H}_{50}\text{O}_4\text{Si}$   $[M+H]^+$ : 455.3551, found: 455.3557.

$[\alpha]_D^{25} = +27.0$  ( $c = 0.63$ , THF)



Martin's sulfurane (1.98 g, 2.94 mmol, 2.19 eq.) was dissolved in MTBE (22 mL). To this was added a solution of spirocycle **11** (610 mg, 1.34 mmol, 1.00 eq.) in MTBE (25 mL) and the reaction was heated to 35 °C for 1.5 h. The reaction mixture was then concentrated under reduced pressure and the crude product was purified by column chromatography ( $\text{SiO}_2$ , pentanes/ $\text{Et}_2\text{O} = 1:0$  to 97:3) which gave a 2:1 mixture of product **12** and side product **13** (583 mg, 1.33 mmol, 99% combined yield). A small sample of pure product could be obtained for characterization.

#### Data for alkene **12**:

$R_f = 0.53$  (hexanes/ $\text{EtOAc}$  9:1)

$^1\text{H}$  NMR (400 MHz,  $\text{C}_6\text{D}_6$ ):  $\delta = 5.85$  (dt,  $J = 10.4, 2.0$  Hz, 1H), 5.53 (dq,  $J = 10.6, 2.0$  Hz, 1H), 4.76 (d,  $J = 6.7$  Hz, 1H), 4.60 (d,  $J = 6.8$  Hz, 1H), 3.82 (d,  $J = 9.7$  Hz, 1H), 3.44 (d,  $J = 9.7$  Hz, 1H), 3.28 (s, 3H), 3.23 (dt,  $J = 10.5, 5.2$  Hz, 1H), 2.22 (qd,  $J = 9.7, 5.1$  Hz, 1H), 2.18 – 2.10 (m, 1H), 2.06 – 1.93 (m, 3H), 1.88 – 1.77 (m, 2H), 1.74 (d,  $J = 12.1$  Hz, 1H), 1.62 – 1.50 (m, 1H), 1.39 (dt,  $J = 13.7, 3.8$  Hz, 1H),

1.34 – 1.30 (m, 1H), 1.29 (dd,  $J = 4.3, 2.8$  Hz, 1H), 1.24 – 1.16 (m, 1H), 1.15 (dq,  $J = 12.0, 6.2, 5.2$  Hz, 1H), 1.01 (d,  $J = 1.9$  Hz, 12H), 0.95 (s, 3H), 0.86 (s, 3H), 0.07 (s, 6H).

**$^{13}\text{C}$  NMR (100 MHz,  $\text{C}_6\text{D}_6$ ):**  $\delta = 130.8, 125.4, 94.7, 81.9, 70.5, 54.6, 49.8, 47.8, 46.6, 44.3, 39.9, 35.6, 35.0, 33.4, 28.9, 27.7, 27.3, 25.8, 24.4, 23.4, 22.9, 18.2, -5.7, -5.8$ .

**IR (ATR):**  $\tilde{\nu} = 2953$  (m), 2930 (m), 2858 (w), 1472 (w), 1448 (m), 1387 (w), 1310 (m), 1297 (w), 1256 (w), 1154 (s), 1106 (m), 1042 (m), 999 (w), 852 (w), 837 (m), 763 (m), 734 (w), 690 (m)  $\text{cm}^{-1}$ .

**HRMS (EI):** calc. for  $\text{C}_{26}\text{H}_{48}\text{O}_3\text{Si}$  [ $M$ ] $^+$ : 436.3367, found: 436.3367.

**$[\alpha]_D^{25} = +49.6$**  ( $c = 0.5, \text{CHCl}_3$ )

#### Data for cyclopropane 13:

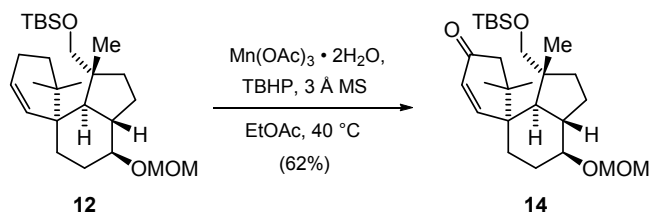
$R_f = 0.53$  (hexanes/EtOAc 9:1)

**$^1\text{H}$  NMR (400 MHz,  $\text{C}_6\text{D}_6$ ):**  $\delta = 4.68$  (d,  $J = 6.7$  Hz, 1H), 4.58 (d,  $J = 6.7$  Hz, 1H), 3.76 (d,  $J = 9.7$  Hz, 1H), 3.41 (td,  $J = 10.1, 5.9$  Hz, 1H), 3.33 (d,  $J = 9.7$  Hz, 1H), 3.24 (s, 3H), 2.52 (ddd,  $J = 13.0, 9.5, 6.0$  Hz, 1H), 2.31 (d,  $J = 11.3$  Hz, 1H), 2.07 (ddd,  $J = 9.6, 5.9, 3.5$  Hz, 1H), 1.99 (dd,  $J = 12.3, 7.4$  Hz, 1H), 1.95 – 1.87 (m, 1H), 1.63 – 1.50 (m, 1H), 1.46 (ddd,  $J = 12.8, 10.2, 2.2$  Hz, 1H), 1.35 (dd,  $J = 10.3, 5.0$  Hz, 2H), 1.32 – 1.23 (m, 3H), 1.17 (s, 3H), 1.08 – 1.03 (m, 2H), 1.03 (s, 9H), 1.01 (s, 3H), 0.96 (d,  $J = 4.0$  Hz, 1H), 0.86 (s, 3H), 0.46 (ddd,  $J = 9.0, 6.3, 2.1$  Hz, 1H), 0.08 (s, 6H).

**$^{13}\text{C}$  NMR (100 MHz,  $\text{C}_6\text{D}_6$ ):**  $\delta = 95.3, 79.0, 71.3, 54.9, 48.1, 46.1, 45.9, 41.5, 38.4, 33.4, 32.4, 31.5, 30.5, 28.9, 28.5, 27.3, 26.2, 23.0, 22.8, 21.8, 18.8, 18.5, -5.3, -5.4$ .

**IR (ATR):**  $\tilde{\nu} = 2950$  (s), 2928 (s), 2858 (m), 1471 (w), 1383 (w), 1361 (w), 1256 (w), 1148 (w), 1097 (s), 1040 (s), 918 (w), 853 (s), 836 (s), 774 (m), 668 (w)  $\text{cm}^{-1}$ .

**HRMS (EI):** calc. for  $\text{C}_{26}\text{H}_{48}\text{O}_3\text{Si}$  [ $M$ ] $^+$ : 436.3367, found: 436.3359.



To a 2:1 mixture of alkene **12** and side product **13** (combined 583 mg, 1.33 mmol, 1.00 eq.) in EtOAc (16.5 mL) and 3 Å molecular sieves (583 mg) was added TBHP (2.66 mL, 5-6 M in decane, ~13.3 mmol, ~10.0 eq.). The suspension was stirred at r.t. for 30 min. and  $\text{Mn(OAc)}_3 \cdot 2\text{H}_2\text{O}$  (340 mg, 1.27 mmol, 0.95 eq.) was added. The red-brown reaction mixture was heated to 40 °C for 21 h after which it was filtered over celite and concentrated under reduced pressure. Column chromatography ( $\text{SiO}_2$ , hexanes/EtOAc = 1:0 to 85:15) gave the desired product **14** (250 mg, 0.555 mmol, 62% yield) as a colorless oil.

$R_f = 0.38$  (hexanes/EtOAc 8:2)

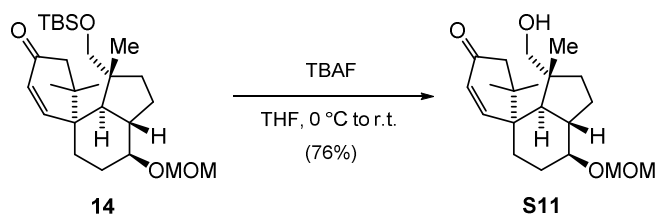
**$^1\text{H NMR}$  (400 MHz,  $\text{C}_6\text{D}_6$ , 60 °C):**  $\delta = 6.60$  (d,  $J = 10.5$  Hz, 1H), 5.95 (d,  $J = 10.5$  Hz, 1H), 4.68 (dd,  $J = 6.6, 0.7$  Hz, 1H), 4.56 (dd,  $J = 6.5, 0.7$  Hz, 1H), 3.65 (d,  $J = 10.0$  Hz, 1H), 3.29 (dd,  $J = 10.1, 1.0$  Hz, 1H), 3.26 (d,  $J = 0.8$  Hz, 3H), 3.15 (td,  $J = 10.3, 4.8$  Hz, 1H), 2.71 (d,  $J = 16.5$  Hz, 1H), 2.18 (d,  $J = 16.5$  Hz, 1H), 2.11 (ddd,  $J = 14.4, 7.4, 4.4$  Hz, 1H), 1.98 – 1.90 (m, 2H), 1.81 (d,  $J = 12.4$  Hz, 1H), 1.77 (dt,  $J = 8.0, 3.8$  Hz, 1H), 1.40 – 1.35 (m, 3H), 1.25 – 1.21 (m, 1H), 1.20 – 1.14 (m, 2H), 0.96 (s, 3H), 0.95 (s, 9H), 0.81 (s, 3H), 0.73 (d,  $J = 0.8$  Hz, 3H), 0.02 (dd,  $J = 2.6, 0.7$  Hz, 6H).

**$^{13}\text{C NMR}$  (100 MHz,  $\text{C}_6\text{D}_6$ , 60 °C):**  $\delta = 197.8, 151.6, 95.4, 81.8, 70.3, 55.1, 52.5, 50.6, 48.0, 47.3, 47.0, 40.3, 39.3, 34.0, 30.2, 29.0, 28.4, 27.6, 26.2, 24.7, 23.5, 18.5, -5.3, -5.4$ .

**IR (ATR):**  $\tilde{\nu} = 2954$  (m), 2929 (m), 2858 (m), 1675 (m), 1471 (w), 1389 (w), 1362 (w), 1258 (m), 1092 (s), 1041 (s), 917 (m), 837 (s), 815 (m), 776 (s), 668 (m)  $\text{cm}^{-1}$ .

**HRMS (EI):** calc. for  $\text{C}_{26}\text{H}_{46}\text{O}_4\text{Si}$  [ $M$ ] $^+$ : 450.3165, found: 450.3162.

**$[\alpha]_D^{25} = +35.4$**  (c = 0.39, THF)



To a solution of enone **14** (250 mg, 0.555 mmol, 1.00 eq. in THF (25 mL) was added TBAF (2.42 mL, 1 M in THF, 2.42 mmol, 4.40 eq.) at 0 °C. After 30 min, the reaction was allowed to warm to r.t. and stirred for 6 h. The reaction was quenched with a sat. aq. solution of NH<sub>4</sub>Cl (25 mL) and the aqueous phase was extracted with EtOAc (3 x 25 mL). The combined organic layers were washed with brine, dried over Na<sub>2</sub>SO<sub>4</sub>, filtered and concentrated. The resulting residue was purified by column chromatography (SiO<sub>2</sub>, hexanes/EtOAc = 9:1 to 1:1) to afford the desired product **S11** (141 mg, 0.419 mmol, 76% yield) as a pale brown oil.

$R_f = 0.32$  (hexanes/EtOAc 1:1)

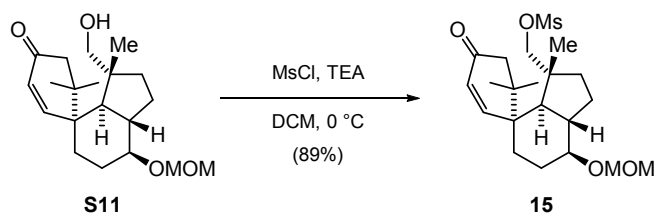
**<sup>1</sup>H NMR (400 MHz, C<sub>6</sub>D<sub>6</sub>, 60 °C):**  $\delta = 6.55$  (d,  $J = 10.5$  Hz, 1H), 5.93 (d,  $J = 10.5$  Hz, 1H), 4.67 (d,  $J = 6.7$  Hz, 1H), 4.54 (d,  $J = 6.7$  Hz, 1H), 3.40 (d,  $J = 10.6$  Hz, 1H), 3.26 (d,  $J = 0.5$  Hz, 3H), 3.09 (dq,  $J = 10.3, 5.2$  Hz, 3H), 2.66 (d,  $J = 16.6$  Hz, 1H), 2.16 (d,  $J = 16.5$  Hz, 1H), 2.08 – 2.00 (m, 1H), 1.95 – 1.86 (m, 1H), 1.80 – 1.70 (m, 2H), 1.64 (d,  $J = 12.3$  Hz, 1H), 1.34 – 1.27 (m, 2H), 1.16 – 1.07 (m, 3H), 0.89 (s, 3H), 0.78 (s, 3H), 0.66 (s, 3H).

**<sup>13</sup>C NMR (100 MHz, C<sub>6</sub>D<sub>6</sub>, 60 °C):**  $\delta = 197.9, 151.5, 129.0, 95.3, 81.5, 69.8, 55.1, 52.4, 50.9, 47.8, 47.1, 39.5, 39.3, 34.0, 28.5, 28.4, 27.7, 24.4, 23.2$ .

**IR (ATR):**  $\tilde{\nu} = 3460$  (br), 2956 (m), 2935 (m), 2880 (m), 1671 (s), 1441 (w), 1400 (w), 1266 (w), 1202 (m), 1146 (w), 1102 (m), 1039 (s), 915 (w) cm<sup>-1</sup>.

**HRMS (EI):** calc. for C<sub>20</sub>H<sub>32</sub>O<sub>4</sub> [ $M$ ]<sup>+</sup>: 336.2301, found: 336.2301.

**$[\alpha]_D^{25} = +74.5$**  (c = 0.22, THF)



Alcohol **S11** (140 mg, 0.416 mmol, 1.00 eq.) was dissolved in DCM (14 mL) and cooled to 0 °C. Triethylamine (141  $\mu\text{L}$ , 1.01 mmol, 2.43 eq.) and MsCl (91  $\mu\text{L}$ , 1.18 mmol, 2.83 eq.) were added and the reaction was stirred for 1.5 h, after which it was quenched with water (10 mL). The layers were separated and the aqueous phase was extracted with DCM (3 x 10 mL). The combined organic layers were washed with brine, dried over sodium sulfate, filtered and concentrated. The resulting residue was purified by column chromatography ( $\text{SiO}_2$ , hexanes/EtOAc = 8:2 to 1:1) to afford the desired product **15** (156 mg, 0.37 mmol, 89% yield) as a colorless oil.

$R_f = 0.28$  (hexanes/EtOAc 1:1)

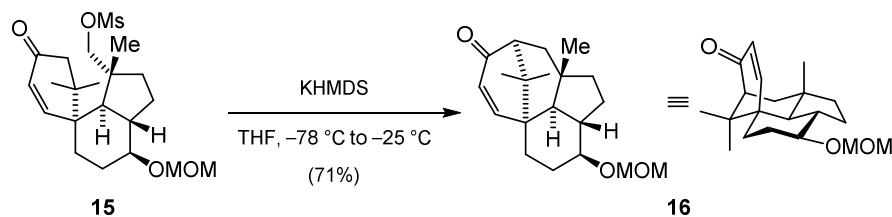
**$^1\text{H NMR}$  (400 MHz,  $\text{C}_6\text{D}_6$ , 60 °C):**  $\delta = 6.45$  (d,  $J = 10.5$  Hz, 1H), 5.89 (d,  $J = 10.5$  Hz, 1H), 4.65 (d,  $J = 6.7$  Hz, 1H), 4.52 (d,  $J = 6.7$  Hz, 1H), 4.04 – 3.97 (m, 2H), 3.25 (s, 3H), 3.02 (td,  $J = 10.4, 4.8$  Hz, 1H), 2.41 (d,  $J = 16.7$  Hz, 1H), 2.22 (s, 3H), 2.17 (d,  $J = 16.6$  Hz, 1H), 2.01 – 1.94 (m, 1H), 1.81 (ddt,  $J = 13.6, 10.2, 3.4$  Hz, 2H), 1.72 – 1.65 (m, 1H), 1.40 (d,  $J = 12.3$  Hz, 1H), 1.31 – 1.16 (m, 2H), 1.16 – 1.02 (m, 3H), 0.80 (s, 3H), 0.71 (s, 3H), 0.66 (s, 3H).

**$^{13}\text{C NMR}$  (100 MHz,  $\text{C}_6\text{D}_6$ , 60 °C):**  $\delta = 197.1, 150.9, 129.1, 95.3, 81.0, 76.2, 55.1, 52.2, 51.9, 47.1, 46.8, 46.1, 39.7, 39.3, 36.8, 34.3, 28.3, 28.1, 27.1, 24.7, 22.4$ .

**IR (ATR):**  $\tilde{\nu} = 3358$  (w), 2957 (s), 2925 (s), 2673 (s), 1633 (w), 1468 (w), 1400 (w), 1357 (s), 1261 (m), 1212 (w), 1176 (s), 1101 (m), 1039 (s), 957 (m), 800 (m)  $\text{cm}^{-1}$ .

**HRMS (ESI):** calc. for  $\text{C}_{21}\text{H}_{34}\text{O}_6\text{S}$  [ $M+\text{NH}_4$ ] $^+$ : 432.2414, found: 432.2416.

$[\alpha]_D^{25} = +31.8$  ( $c = 0.22$ , THF)



To a solution of KHMDS (0.5 M in toluene, 0.770 mL, 0.385 mmol, 4.00 eq.) in THF (7.6 mL) was added enone **15** (40 mg, 0.0965 mmol, 1.00 eq.) in THF (7.6 mL) dropwise at  $-78\text{ }^\circ\text{C}$ . After 1 h, the reaction mixture was allowed to warm up to  $-25\text{ }^\circ\text{C}$  over 1 h and kept at that temperature for 2 h, after which it was quenched through the addition of water (20 mL). The aqueous phase was extracted with  $\text{Et}_2\text{O}$  (3 x 25 mL), the combined organic layers were washed with brine, dried over sodium sulfate, filtered and concentrated. The resulting residue was purified by column chromatography ( $\text{SiO}_2$ , hexanes/ $\text{EtOAc}$  = 9:1 to 8:2) to afford the desired product **16** (44 mg, 0.138 mmol, 71% yield) as a white solid.

$R_f$  = 0.38 (hexanes/ $\text{EtOAc}$  8:2)

**Mp** = 77.6 – 79.0  $^\circ\text{C}$

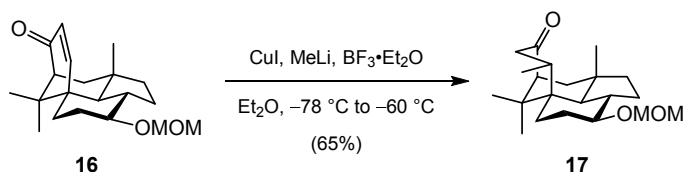
**$^1\text{H}$  NMR (400 MHz,  $\text{C}_6\text{D}_6$ ):**  $\delta$  = 6.05 (s, 2H), 4.69 (d,  $J$  = 6.8 Hz, 1H), 4.58 (d,  $J$  = 6.8 Hz, 1H), 3.26 (s, 3H), 3.11 (td,  $J$  = 10.2, 3.9 Hz, 1H), 2.13 (dd,  $J$  = 4.6, 3.1 Hz, 1H), 1.94 (dd,  $J$  = 13.7, 3.0 Hz, 1H), 1.90 – 1.82 (m, 1H), 1.82 – 1.76 (m, 1H), 1.68 (dd,  $J$  = 13.7, 4.7 Hz, 1H), 1.60 – 1.49 (m, 1H), 1.41 (dddd,  $J$  = 13.4, 11.1, 7.0, 1.8 Hz, 1H), 1.26 (dd,  $J$  = 10.6, 3.9 Hz, 1H), 1.22 – 1.18 (m, 1H), 1.16 (d,  $J$  = 13.5 Hz, 1H), 1.02 (dt,  $J$  = 13.9, 3.9 Hz, 1H), 0.98 – 0.90 (m, 2H), 0.82 (s, 3H), 0.77 (s, 3H), 0.67 (s, 3H).

**$^{13}\text{C}$  NMR (100 MHz,  $\text{C}_6\text{D}_6$ ):**  $\delta$  = 202.9, 149.5, 133.4, 94.9, 82.1, 57.9, 55.0, 48.6, 43.6, 42.2, 41.8, 40.4, 39.8, 39.0, 29.1, 28.1, 27.1, 23.6, 22.3, 22.2.

**IR (ATR):**  $\tilde{\nu}$  = 2930 (s), 1674 (s), 1466 (w), 1445 (w), 1386 (w), 1146 (m), 1103 (m), 1042 (s), 918 (w), 823 (w)  $\text{cm}^{-1}$ .

**HRMS (EI):** calc. for  $\text{C}_{20}\text{H}_{30}\text{O}_3$  [ $M$ ] $^+$ : 318.2189, found: 318.2193.

$[\alpha]_D^{25} = +155$  ( $c = 0.24$ , THF)



To a suspension of CuCN (11.7 mg, 0.131 mmol, 5.20 eq.) in Et<sub>2</sub>O at -40 °C was added a solution of MeLi (1.54 M in Et<sub>2</sub>O, 0.080 mL, 0.123 mmol, 4.90 eq.). The mixture was stirred for 15 min., then cooled to -78 °C and enone **16** (8.0 mg, 0.0251 mmol, 1.00 eq.) in Et<sub>2</sub>O (0.25 mL) was added dropwise, upon which the reaction turned bright orange. After 1 h, the reaction mixture was allowed to warm up to -60 °C and stirred for an additional 1 h, after which it was quenched with a 9:1 mixture of sat. aq. NH<sub>4</sub>Cl-solution and aq. NH<sub>3</sub>-solution (3 mL). The aqueous phase was extracted with Et<sub>2</sub>O (3 x 5 mL), the combined organic layers were washed with brine, dried over Na<sub>2</sub>SO<sub>4</sub>, filtered and concentrated. The resulting residue was purified by column chromatography (SiO<sub>2</sub>, hexanes/EtOAc = 95:5 to 8:2) to afford the desired product **17** (5.5 mg, 0.0164 mmol, 65% yield) as a colorless oil.

Note: The reaction was sensitive to scale up and gave varying yields on a larger scale.

$R_f = 0.32$  (hexanes/EtOAc 8:2)

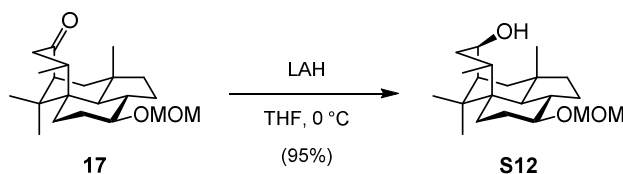
**<sup>1</sup>H NMR (400 MHz, C<sub>6</sub>D<sub>6</sub>):**  $\delta = 4.72$  (d,  $J = 6.8$  Hz, 1H), 4.59 (d,  $J = 6.8$  Hz, 1H), 3.28 (s, 3H), 3.13 (td,  $J = 10.1, 4.2$  Hz, 1H), 2.69 (dd,  $J = 20.3, 9.3$  Hz, 1H), 2.06 – 1.99 (m, 2H), 1.96 (dd,  $J = 8.6, 4.5$  Hz, 2H), 1.93 – 1.87 (m, 1H), 1.84 (dt,  $J = 7.6, 4.5$  Hz, 1H), 1.72 (dtd,  $J = 13.0, 9.3, 6.3$  Hz, 1H), 1.61 (dd,  $J = 13.3, 4.7$  Hz, 1H), 1.53 – 1.42 (m, 2H), 1.28 – 1.17 (m, 2H), 1.15 (d,  $J = 13.2$  Hz, 1H), 0.91 (qd,  $J = 14.2, 12.7, 9.4$  Hz, 2H), 0.77 (d,  $J = 7.0$  Hz, 3H), 0.74 (s, 3H), 0.68 (s, 3H), 0.65 (s, 3H).

**<sup>13</sup>C NMR (100 MHz, C<sub>6</sub>D<sub>6</sub>):**  $\delta = 214.7, 94.9, 82.7, 58.3, 55.0, 53.9, 48.7, 43.0, 41.0, 39.7, 39.5, 39.0, 38.2, 30.6, 27.5, 26.9, 26.3, 25.2, 24.4, 21.0, 20.9$ .

**IR (ATR):**  $\tilde{\nu} = 2937$  (m), 2877 (m), 1700 (m), 1446 (w), 1386 (w), 1247 (w), 1219 (w), 1188 (w), 1148 (m), 1101 (m), 1044 (s), 1033 (m), 926 (w), 915 (w), 799 (w) cm<sup>-1</sup>.

**HRMS (EI):** calc. for  $C_{21}H_{34}O_3$   $[M]^+$ : 334.2508, found: 334.2502.

$[\alpha]_D^{25} = +40.5$  ( $c = 0.16$ , THF)



A solution of ketone **17** (25.0 mg, 0.0747 mmol, 1.00 eq.) in THF (2.5 mL) was cooled to 0 °C and LAH (1 M solution in Et<sub>2</sub>O, 0.75 mL, 0.750 mmol, 10.0 eq.) was added dropwise. The reaction was stirred for 2.5 h and was quenched through the addition of water (0.03 mL), NaOH (0.04 mL of an aq. 10% solution) and water (0.08 mL). The mixture was then allowed to stir for 5 min at r.t., after which Na<sub>2</sub>SO<sub>4</sub> was added. The mixture was stirred for 10 min and then filtered through a plug of silica and concentrated under reduced pressure. The crude product was purified by column chromatography (SiO<sub>2</sub>, hexanes/EtOAc = 98:2 to 9:1). The desired product **S12** (23.9 mg, 0.0710 mmol, 95%) was obtained as a colorless oil.

$R_f = 0.32$  (hexanes/EtOAc 8:2)

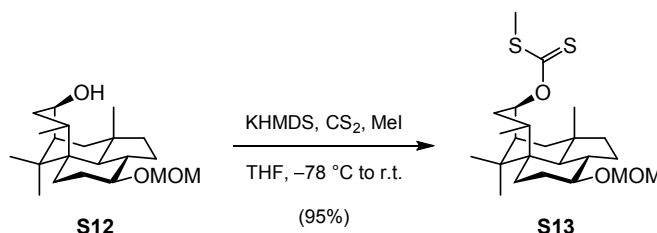
**<sup>1</sup>H NMR (400 MHz, C<sub>6</sub>D<sub>6</sub>):**  $\delta = 4.74$  (d,  $J = 6.8$  Hz, 1H), 4.62 (d,  $J = 6.8$  Hz, 1H), 4.05 (dd,  $J = 12.5, 6.8$  Hz, 1H), 3.29 (s, 3H), 3.21 (ddd,  $J = 14.4, 9.1, 4.2$  Hz, 1H), 2.15 – 2.07 (m, 2H), 1.99 – 1.93 (m, 2H), 1.92 – 1.86 (m, 1H), 1.86 – 1.77 (m, 1H), 1.70 – 1.61 (m, 1H), 1.58 – 1.50 (m, 2H), 1.46 – 1.38 (m, 3H), 1.31 – 1.20 (m, 2H), 1.16 (d,  $J = 13.2$  Hz, 1H), 1.11 (t,  $J = 7.0$  Hz, 1H), 1.06 (s, 3H), 0.99 (dd,  $J = 14.1, 3.6$  Hz, 1H), 0.88 (d,  $J = 6.6$  Hz, 3H), 0.85 (s, 3H), 0.81 (s, 3H).

**<sup>13</sup>C NMR (100 MHz, C<sub>6</sub>D<sub>6</sub>):**  $\delta = 94.9, 83.0, 66.9, 55.0, 53.5, 47.9, 44.5, 40.4, 40.2, 39.3, 38.1, 37.9, 33.3, 30.9, 27.8, 27.7, 27.5, 25.8, 24.6, 23.1, 20.9$ .

**IR (ATR):**  $\tilde{\nu} = 2476$  (br), 2930 (s), 2872 (m), 1465 (w), 1448 (w), 1384 (w), 1147 (w), 1101 (m), 1083 (w), 1050 (s), 919 (w)  $\text{cm}^{-1}$ .

**HRMS (EI):** calc. for  $C_{21}H_{36}O_3$   $[M]^+$ : 336.2659, found: 336.2661.

$[\alpha]_D^{25} = +29.2$  ( $c = 0.14$ , THF)



A solution of alcohol **S12** (13.0 mg, 0.0386 mmol, 1.00 eq.) in THF (1.0 mL) was cooled to  $-78\text{ }^\circ\text{C}$  and  $\text{CS}_2$  (0.055 mL, 0.915 mmol, 23.7 eq.) and KHMDs (1 M solution in toluene, 0.12 mL, 0.060 mmol, 1.55 eq.) were added. After 20 min., the orange reaction mixture was allowed to warm to r.t. and stirred for 55 min after which MeI (0.060 mL, 0.964 mmol, 24.9 eq.) was added. The yellow-white suspension was stirred for another 45 min and then quenched through the addition of water (5 mL). The aqueous phase was extracted with  $\text{Et}_2\text{O}$  (3 x 5 mL), the combined organic layers were washed with brine, dried over sodium sulfate, filtered and concentrated. The resulting residue was purified by column chromatography ( $\text{SiO}_2$ , hexanes/ $\text{Et}_2\text{O} = 95:5$  to  $9:1$ ) to afford the desired product **S13** (15.6 mg, 0.0367 mmol, 95% yield) as a yellow oil.

$R_f = 0.57$  (hexanes/ $\text{EtOAc}$  9:1)

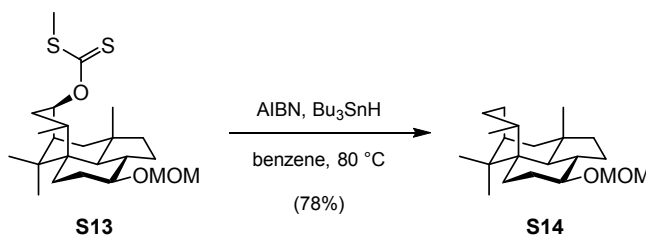
**$^1\text{H NMR}$  (400 MHz,  $\text{C}_6\text{D}_6$ ):**  $\delta = 6.21$  (ddd,  $J = 10.7, 8.9, 3.9$  Hz, 1H), 4.72 (d,  $J = 6.8$  Hz, 1H), 4.60 (d,  $J = 6.8$  Hz, 1H), 3.28 (s, 3H), 3.15 (td,  $J = 10.1, 4.1$  Hz, 1H), 2.19 (s, 3H), 2.12 – 2.02 (m, 3H), 2.01 – 1.96 (m, 1H), 1.92 (ddd,  $J = 14.1, 8.4, 2.7$  Hz, 2H), 1.88 – 1.82 (m, 1H), 1.81 – 1.74 (m, 1H), 1.58 – 1.51 (m, 1H), 1.49 – 1.39 (m, 3H), 1.23 – 1.17 (m, 1H), 1.12 (d,  $J = 13.2$  Hz, 1H), 1.09 – 1.04 (m, 1H), 1.04 (s, 3H), 0.91 (dd,  $J = 13.7, 3.3$  Hz, 1H), 0.82 (s, 3H), 0.79 (d,  $J = 6.7$  Hz, 3H), 0.77 (s, 3H).

**$^{13}\text{C NMR}$  (100 MHz,  $\text{C}_6\text{D}_6$ ):**  $\delta = 215.2, 94.9, 82.8, 81.9, 55.0, 53.4, 44.2, 43.9, 40.2, 39.3, 38.2, 38.0, 36.6, 34.7, 30.9, 27.7, 27.4, 25.4, 24.2, 22.6, 20.8, 18.8, 1.4$ .

**IR (ATR):**  $\tilde{\nu}$  = 2925 (m), 1464 (w), 1381 (w), 1258 (m), 1214 (m), 1145 (w), 1099 (m), 1044 (s), 797 (m)  $\text{cm}^{-1}$ .

**HRMS (EI):** calc. for  $\text{C}_{23}\text{H}_{38}\text{O}_3\text{S}_2$  [ $M-\text{C}_2\text{H}_3\text{S}_2$ ] $^+$ : 335.2581, found: 335.2586.

$[\alpha]_D^{25} = +32.0$  ( $c = 0.13$ , THF)



To a solution of xanthate **S13** (22.7 mg, 0.0532 mmol, 1.00 eq.) in degassed benzene (2.0 mL) were added AIBN (4.1 mg, 0.0250 mmol, 0.47 eq.) and  $\text{Bu}_3\text{SnH}$  (0.070 mL, 0.260 mmol, 4.89 eq.). The reaction mixture was heated to  $80\text{ }^\circ\text{C}$  for 40 min after which it was concentrated. The resulting residue was purified by column chromatography ( $\text{SiO}_2$ , hexanes/ $\text{Et}_2\text{O} = 1:0$  to  $95:5$ ) to afford the desired product **S14** (13.3 mg, 0.0415 mmol, 78% yield) as a colorless oil.

$R_f = 0.43$  (hexanes/ $\text{EtOAc} 9:1$ )

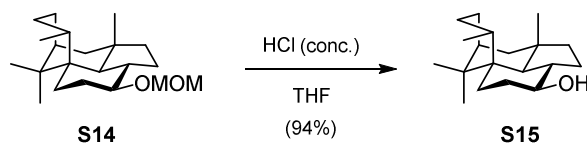
**$^1\text{H}$  NMR (600 MHz,  $\text{C}_6\text{D}_6$ ):**  $\delta$  = 4.76 (dd,  $J = 6.9, 1.1$  Hz, 1H), 4.63 (dd,  $J = 6.8, 1.1$  Hz, 1H), 3.30 (d,  $J = 1.0$  Hz, 3H), 3.21 (td,  $J = 10.1, 4.2$  Hz, 1H), 2.16 – 2.08 (m, 1H), 2.07 – 1.99 (m, 1H), 1.99 – 1.94 (m, 1H), 1.94 – 1.87 (m, 2H), 1.87 – 1.82 (m, 1H), 1.68 (dd,  $J = 13.4, 4.2$  Hz, 1H), 1.64 (dt,  $J = 13.9, 3.5$  Hz, 1H), 1.61 – 1.54 (m, 2H), 1.49 (dd,  $J = 13.4, 2.9$  Hz, 1H), 1.43 – 1.38 (m, 2H), 1.36 (td,  $J = 6.9, 6.1, 1.9$  Hz, 1H), 1.34 – 1.28 (m, 1H), 1.14 (d,  $J = 13.1$  Hz, 1H), 1.10 – 1.05 (m, 1H), 1.03 (dd,  $J = 14.0, 3.5$  Hz, 1H), 1.00 (s, 3H), 0.98 (d,  $J = 1.3$  Hz, 3H), 0.96 (dd,  $J = 6.9, 1.1$  Hz, 3H), 0.84 (s, 3H).

**$^{13}\text{C}$  NMR (100 MHz,  $\text{C}_6\text{D}_6$ ):**  $\delta$  = 94.9, 83.1, 55.0, 53.8, 43.9, 43.2, 41.5, 40.4, 39.3, 38.8, 38.4, 31.2, 29.0, 27.8, 27.3, 27.2, 26.0, 25.9, 25.0, 22.8, 20.6.

**IR (ATR):**  $\tilde{\nu}$  = 2931 (s), 2877 (m), 2360 (w), 1462 (w), 1380 (w), 1259 (w), 1146 (w), 1100 (m), 1045 (s), 1034 (s), 918 (w), 797 (w)  $\text{cm}^{-1}$ .

**HRMS (EI):** calc. for  $\text{C}_{21}\text{H}_{36}\text{O}_2$   $[M]^+$ : 320.2710, found: 320.2721.

$[\alpha]_D^{25} = +46.7$  ( $c = 0.12$ , THF)



To a solution of compound **S14** (12.0 mg, 0.0374 mmol, 1.00 eq.) in THF (1.4 mL) was added conc. HCl (0.090 mL, 1.08 mmol, 28.8 eq.). The reaction mixture was stirred for 4.5 h after which it was quenched through the addition of  $\text{Na}_2\text{CO}_3$  (3 mL). The aqueous phase was extracted with EtOAc (3 x 3 mL), the combined organic layers were washed with brine, dried over  $\text{Na}_2\text{SO}_4$ , filtered and concentrated. The resulting residue was purified by column chromatography ( $\text{SiO}_2$ , hexanes/ $\text{Et}_2\text{O} = 95:5$  to  $8:2$ ) to afford the desired alcohol **S15** (9.8 mg, 0.0354 mmol, 94% yield) as a milky oil.

$R_f = 0.41$  (hexanes/EtOAc 8:2)

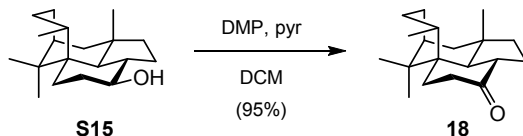
**$^1\text{H}$  NMR (400 MHz,  $\text{C}_6\text{D}_6$ ):**  $\delta$  = 3.02 (ddd,  $J = 10.4, 8.8, 4.3$  Hz, 1H), 2.09 – 1.96 (m, 2H), 1.96 – 1.84 (m, 2H), 1.73 – 1.64 (m, 2H), 1.59 (tt,  $J = 11.1, 3.5$  Hz, 2H), 1.53 – 1.43 (m, 3H), 1.43 – 1.32 (m, 3H), 1.18 (tdd,  $J = 13.2, 10.7, 2.9$  Hz, 1H), 1.10 – 1.01 (m, 3H), 1.00 (s, 3H), 0.98 – 0.94 (m, 6H), 0.83 (s, 3H).

**$^{13}\text{C}$  NMR (100 MHz,  $\text{C}_6\text{D}_6$ ):**  $\delta$  = 78.0, 53.6, 44.0, 43.2, 42.3, 41.5, 39.3, 38.8, 38.4, 34.7, 29.0, 28.0, 27.3, 26.7, 26.0, 25.9, 24.9, 22.8, 20.7.

**IR (ATR):**  $\tilde{\nu}$  = 3323 (br), 3011 (w), 2984 (w), 2931 (s), 2876 (s), 1461 (m), 1380 (m), 1364 (w), 1350 (w), 1286 (w), 1224 (w), 1186 (w), 1149 (w), 1119 (w), 1082 (w), 1049 (m), 1013 (w), 996(w), 962 (w), 941(w), 875 (w), 703 (w)  $\text{cm}^{-1}$ .

**HRMS (EI):** calc. for C<sub>19</sub>H<sub>32</sub>O [*M*]<sup>+</sup>: 276.2448, found: 276.2444.

[ $\alpha$ ]<sub>D</sub><sup>25</sup> = +33.3 (c = 0.24, THF)



To a solution of alcohol **15** (9.5 mg, 0.0344 mmol, 1.00 eq.) in DCM (0.75 mL) were added pyridine (0.015 mL, 0.185 mmol, 5.40 eq.) and DMP (81.0 mg, 0.191 mmol, 5.56 eq.). The reaction mixture was stirred for 4 h after which it was quenched through the addition of aq. Na<sub>2</sub>S<sub>2</sub>O<sub>3</sub>-solution (0.5 mL) and sat. aq. NaHCO<sub>3</sub>-solution (3 mL). The aqueous phase was extracted with DCM (3 x 3 mL), the combined organic layers were washed with brine, dried over sodium sulfate, filtered and concentrated. The resulting residue was purified by column chromatography (SiO<sub>2</sub>, hexanes/Et<sub>2</sub>O = 95:5 to 9:1) to afford the desired ketone **18** (8.9 mg, 0.0324 mmol, 95% yield) as a white solid.

R<sub>f</sub> = 0.38 (hexanes/EtOAc 9:1)

Mp = 95.5 – 97.8 °C

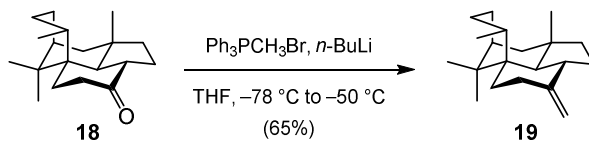
**<sup>1</sup>H NMR (400 MHz, C<sub>6</sub>D<sub>6</sub>):**  $\delta$  = 2.43 (dddd, *J* = 13.3, 11.0, 6.7, 1.6 Hz, 1H), 2.24 – 2.14 (m, 2H), 2.02 – 1.91 (m, 2H), 1.92 – 1.78 (m, 2H), 1.67 (ddd, *J* = 13.8, 5.2, 2.9 Hz, 1H), 1.64 – 1.56 (m, 1H), 1.55 – 1.45 (m, 2H), 1.43 (d, *J* = 14.4 Hz, 1H), 1.40 – 1.30 (m, 3H), 1.30 – 1.24 (m, 2H), 0.95 (d, *J* = 10.8 Hz, 1H), 0.91 (s, 3H), 0.87 (d, *J* = 6.6 Hz, 3H), 0.84 (s, 3H), 0.64 (s, 3H).

**<sup>13</sup>C NMR (100 MHz, C<sub>6</sub>D<sub>6</sub>):**  $\delta$  = 210.1, 57.9, 46.6, 42.9, 42.4, 41.3, 40.7, 40.4, 38.9, 38.8, 31.2, 28.9, 26.5, 25.7, 25.7, 24.9, 23.2, 20.2, 19.8.

**IR (ATR):**  $\tilde{\nu}$  = 2955 (m), 2924 (s), 2864 (m), 1720 (m), 1462 (w), 1380 (w), 1260 (m), 1083 (m), 1017 (m), 797 (m) cm<sup>-1</sup>.

**HRMS (EI):** calc. for C<sub>19</sub>H<sub>30</sub>O [*M*]<sup>+</sup>: 274.2291, found: 274.2286.

[ $\alpha$ ]<sub>D</sub><sup>25</sup> = +17.6 (c = 0.34, CHCl<sub>3</sub>)



To a suspension of Ph<sub>3</sub>CH<sub>2</sub>Br (82.2 mg, 0.230 mmol, 15.8 eq.) in THF at -78 °C was added *n*-BuLi (2.27 M in hexanes, 0.10 mL, 0.227 mmol, 15.6 eq.). The mixture was allowed to warm to 0 °C and stirred for 30 min., after which it was an orange solution. An aliquot (0.13 mL, 0.0260 mmol, 2.47 eq.) was taken, cooled to -78 °C and ketone **18** (4.0 mg, 0.0146 mmol, 1.00 eq.) in THF (0.48 mL) was added. The reaction mixture was stirred for 1 h and then allowed to warm to -50 °C over the course of 1 h. The reaction was quenched through the addition of water (3 mL). The aqueous phase was extracted with Et<sub>2</sub>O (3 x 3 mL), the combined organic layers were washed with brine, dried over sodium sulfate, filtered and concentrated. The resulting residue was purified by column chromatography (SiO<sub>2</sub>, pentane) to afford the desired alkene **19** (2.6 mg, 0.00954 mmol, 65% yield) as a colorless oil.

R<sub>f</sub> = 0.73 (hexanes)

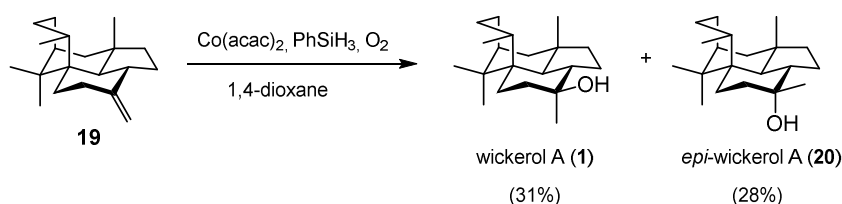
**<sup>1</sup>H NMR (400 MHz, C<sub>6</sub>D<sub>6</sub>):** δ = 4.83 (dd, *J* = 20.8, 2.1 Hz, 2H), 2.26 – 2.21 (m, 1H), 2.21 – 2.15 (m, 1H), 2.11 – 2.00 (m, 3H), 1.99 – 1.92 (m, 1H), 1.91 – 1.86 (m, 1H), 1.86 – 1.78 (m, 1H), 1.78 – 1.73 (m, 1H), 1.68 (dd, *J* = 13.4, 4.3 Hz, 1H), 1.59 (ddd, *J* = 14.3, 10.8, 6.1 Hz, 1H), 1.50 – 1.42 (m, 2H), 1.38 (dq, *J* = 10.5, 4.0, 3.1 Hz, 2H), 1.26 (d, *J* = 13.7 Hz, 1H), 1.24 – 1.16 (m, 1H), 1.09 (td, *J* = 10.6, 10.0, 7.7 Hz, 1H), 0.99 (d, *J* = 6.7 Hz, 9H), 0.84 (s, 3H).

**<sup>13</sup>C NMR (100 MHz, C<sub>6</sub>D<sub>6</sub>):** δ = 153.3, 103.2, 56.7, 43.6, 43.3, 41.4, 39.4, 39.3, 39.2, 38.9, 34.8, 30.8, 29.2, 27.0, 26.0, 25.9, 24.9, 23.5, 23.2, 20.4.

**IR (ATR):**  $\tilde{\nu}$  = 3074 (w), 2985 (m), 2877 (s), 2929 (s), 1650 (m), 1461 (m), 1448 (m), 1378 (m), 1364 (w), 1349 (w), 1259 (w), 1223 (w), 1192 (w), 1148 (w), 1084 (w), 1056 (w), 1035 (w), 942 (w), 883 (s), 798 (w), 704 (w)  $\text{cm}^{-1}$ .

**HRMS (EI):** calc. for  $\text{C}_{20}\text{H}_{32}$   $[M]^+$ : 272.2499, found: 272.2507.

$[\alpha]_{\text{D}}^{25} = +13.7$  ( $c = 0.19$ ,  $\text{CHCl}_3$ )



To a solution of alkene **19** (3.0 mg, 0.011 mmol, 1.00 eq.) in 1,4-dioxane (0.46 mL, purged with  $\text{O}_2$  for 20 min.) was added  $\text{Co}(\text{acac})_2$  (0.6 mg, 0.00233 mmol, 0.21 eq.).  $\text{O}_2$  was bubbled through for 30 sec and then  $\text{PhSiH}_3$  was added (1 M in 1,4-dioxane, 55  $\mu\text{L}$ , 5.0 eq.). The pink-purple reaction mixture was stirred for 3 h, after which it has turned green and was quenched through the addition of aq.  $\text{Na}_2\text{S}_2\text{O}_3$ -solution (0.5 mL). The aqueous phase was extracted with  $\text{Et}_2\text{O}$  (3 x 0.5 mL), the combined organic layers, dried over sodium sulfate, filtered and concentrated. The resulting residue was purified by column chromatography ( $\text{SiO}_2$ , hexanes/ $\text{Et}_2\text{O}$  = 95:5 to 8:2) to afford *epi*-wickerol A (**20**) (0.90 mg, 30.8  $\mu\text{mol}$ , 28% yield) and wickerol A (**1**) (1.0 mg, 3.44  $\mu\text{mol}$ , 31% yield) as a colorless oil.

**Data for *epi*-wickerol A (**20**):**

$R_f = 0.41$  (hexanes/ $\text{EtOAc}$  9:1)

**$^1\text{H}$  NMR (600 MHz,  $\text{C}_6\text{D}_6$ ):**  $\delta$  = 2.12 – 2.03 (m, 1H), 1.99 – 1.91 (m, 2H), 1.78 (dd,  $J = 13.3, 4.2$  Hz, 1H), 1.71 (d,  $J = 13.2$  Hz, 1H), 1.67 – 1.60 (m, 3H), 1.59 – 1.54 (m, 1H), 1.53 (ddd,  $J = 13.3, 3.0, 1.1$  Hz, 1H), 1.50 – 1.42 (m, 4H), 1.42 – 1.37 (m, 2H), 1.23 (tdd,  $J = 13.8, 3.4, 1.0$  Hz, 1H), 1.12 (dtt,  $J = 11.1, 9.8, 1.3$  Hz, 1H), 1.04 (s, 3H), 1.03 (d,  $J = 1.0$  Hz, 3H), 1.02 (s, 3H), 0.99 (d,  $J = 6.0$  Hz, 6H).

**$^{13}\text{C}$  NMR (100 MHz,  $\text{C}_6\text{D}_6$ ):**  $\delta$  = 69.7, 48.3, 44.0, 43.4, 43.0, 41.5, 39.2, 39.1, 38.9, 38.8, 29.8, 29.2, 26.6, 26.2, 26.1, 24.9, 23.8, 23.6, 21.5, 20.4.

**IR (ATR):**  $\tilde{\nu}$  = 3474 (br), 3177(w), 2956 (s), 2929 (s), 2878 (s), 2525 (w), 1583 (m), 1506 (m), 1380 (s), 1330 (s), 1114 (m), 1039 (m), 911 (m), 891 (s), 695 (m)  $\text{cm}^{-1}$ .

**HRMS (EI):** calc. for  $\text{C}_{20}\text{H}_{34}\text{O}$   $[M]^+$ : 290.2604, found: 290.2603.

**$[\alpha]_D^{25}$**  = +15.3 (c = 0.17,  $\text{CHCl}_3$ )

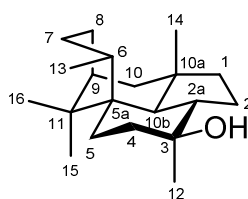
**Data for wickerol A (1):**

**$R_f$**  = 0.33 (hexanes/EtOAc 8:2)

**IR (ATR):**  $\tilde{\nu}$  = 3372 (br), 2954 (s), 2927 (s), 2877 (m), 1584 (w), 1464 (w), 1382 (m), 1329 (w), 1133 (w), 1099 (w), 907 (w), 891 (w), 698 (w)  $\text{cm}^{-1}$ .

**HRMS (EI):** calc. for  $\text{C}_{20}\text{H}_{34}\text{O}$   $[M]^+$ : 290.2604, found: 290.2596.

**$[\alpha]_D^{25}$**  = +21.7 (c = 0.23,  $\text{CHCl}_3$ )

**Table 1.** Comparison of  $^1\text{H}$  NMR data of synthetic and isolated wickerol A (**1**).wickerol A (**1**)

No.	$^1\text{H}$ NMR Isolation 600 MHz, $\text{CDCl}_3$ [ppm]	$^1\text{H}$ NMR Synthetic 600 MHz, $\text{CDCl}_3$ [ppm]
1	1.01 (d, $J = 11.2$ Hz, 1H) 1.41 (d, $J = 11.2$ Hz, 1H)	1.00 (dd, $J = 10.3, 1.3$ Hz, 1H) 1.42 – 1.40 (m, 1H)
2	1.56 (m, 1H) 1.78 (m, 1H)	1.58 – 1.54 (m, 1H) 1.82 – 1.75 (m, 1H)
2a	1.87 (ddd, $J = 13.4, 10.0, 6.1$ Hz, 1H)	1.87 (ddd, $J = 13.2, 10.0, 6.1$ Hz, 1H)
3	-	-
4	1.44 (m, 1H) 1.57 (ddd, $J = 12.8, 3.6, 3.5$ Hz, 1H)	1.45 – 1.42 (m, 1H) 1.58 (dt, $J = 12.7, 3.5$ Hz, 1H)
5	1.2 (ddd, $J = 14.2, 14.2, 3.5$ Hz, 1H) 1.68 (m, 1H)	1.21 (td, $J = 14.2, 3.5$ Hz, 1H) 1.71 – 1.68 (m, 1H)
5a	-	-
6	2.11 (m, 1H)	2.14 – 2.10 (m, 1H),
7	1.46 (m, 1H) 2.00 (dddd, $J = 15.5, 11.2, 11.2, 2.6$ Hz, 1H)	1.48 – 1.45 (m, 1H) 2.00 (dtd, $J = 15.6, 11.0, 2.7$ Hz, 1H)
8	1.61 (m, 1H) 2.09 (m, 1H)	1.64 – 1.60 (m, 1H) 2.10 (s, 1H)
9	1.48 (m, 1H)	1.51 – 1.48 (m, 2H)
10	1.49 (m, 1H) 1.67 (dd, $J = 12.3, 4.2$ Hz, 1H)	1.51 – 1.48 (m, 2H) 1.69 – 1.66 (m, 1H)
10a	-	-
10b	1.27 (d, $J = 13.4$ Hz, 1H)	1.27 (d, $J = 13.5$ Hz, 1H)
11	-	-
12	1.17 (s, 3H)	1.18 (s, 3H)
13	1.02 (d, $J = 7.0$ Hz, 3H)	1.02 (d, $J = 7.0$ Hz, 3H)
14	1.046 (s, 3H)	1.05 (s, 3H)
15	0.94 (s, 3H)	0.94 (s, 3H)
16	1.051 (s, 3H)	1.05 (s, 3H)

**Table 2.** Comparison of  $^{13}\text{C}$  NMR data of synthetic and isolated wickerol A (1).

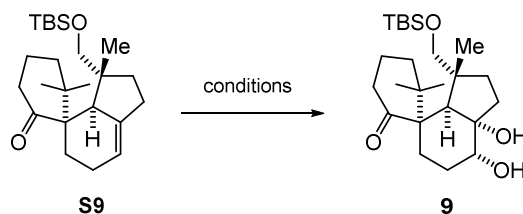
No.	$^{13}\text{C}$ NMR Isolation 125 MHz, $\text{CDCl}_3$ [ppm]	$^{13}\text{C}$ NMR Synthetic 100 MHz, $\text{CDCl}_3$ [ppm]
1	43.9	43.0
2	21.6	21.7
2a	44.4	44.5
3	73.9	74.1
4	40.8	40.9
5	26.4	26.5
5a	38.8	38.9
6	26.6	26.8
7	28.8	29.0
8	25.7	25.8
9	41.1	41.1
10	43.0	43.1
10a	39.2	39.4
10b	52.0	52.1
11	38.7	38.8
12	20.5	20.6
13	22.9	23.1
14	19.9	20.0
15	25.6	25.8
16	24.6	24.8

## 10.4.2. Screening Tables

Table 3. Hydrolysis of **4**.<sup>a</sup>

Entry	Reagent	Solvent	Observation
1	HCl (6 M)	THF	<b>8</b> + TBS-deprotection
2	AcOH	THF	starting material <b>4</b>
3	<i>p</i> -TSA	THF	<b>8</b>
4	<i>p</i> -TSA	MeOH	starting material <b>4</b>
5	Sc(OTf) <sub>3</sub>	DCM	<b>8</b>
6	Yb(OTf) <sub>3</sub>	DCM	<b>8</b>
7	TiCl <sub>4</sub>	DCM	<b>8</b>

a) Reactions were carried out on a 0.010 mmol scale.

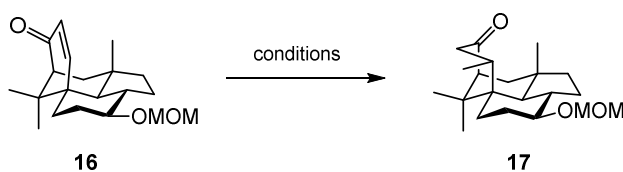
Table 4. Dihydroxylation of **S9**.<sup>a</sup>

Entry	Reagents	Solvent	Additive	T	Outcome/Yield <sup>b</sup>
1	AD mix $\beta$	<i>t</i> -BuOH/H <sub>2</sub> O	-	RT	starting material <b>S9</b>
2	RuCl <sub>3</sub> , NaIO <sub>4</sub> , H <sub>2</sub> SO <sub>4</sub>	MeCN/EtOAc/H <sub>2</sub> O	-	RT	starting material <b>S9</b>
3	OsO <sub>4</sub> (1.0 eq.)	pyridine	-	RT	30%
4	OsO <sub>4</sub> (0.7 eq.)	THF/ acetone/ <i>t</i> -BuOH/H <sub>2</sub> O	-	RT	28%
5	OsO <sub>4</sub> (0.3 eq.)	<i>t</i> -BuOH/H <sub>2</sub> O	-	RT	starting material <b>S9</b>
6	OsO <sub>4</sub> (0.1 eq.)	THF/ acetone/ <i>t</i> -BuOH/H <sub>2</sub> O	-	55 °C	50%

7	OsO <sub>4</sub> (0.1 eq.)	THF/ acetone/ <i>t</i> -BuOH/H <sub>2</sub> O	methansulfonamide	40 °C	45%
8	OsO <sub>4</sub> (0.1 eq.)	THF/ acetone/ <i>t</i> -BuOH/H <sub>2</sub> O	pyridine	55 °C	23%
9	OsO <sub>4</sub> (0.1 eq.)	THF/ acetone/ <i>t</i> -BuOH/H <sub>2</sub> O	DABCO	55 °C	35%
10	OsO <sub>4</sub> (0.1 eq.)	THF/ acetone/ <i>t</i> -BuOH/H <sub>2</sub> O	quinuclidine	55 °C	20%
11	OsO <sub>4</sub> (0.1 eq.)	THF/ acetone/H <sub>2</sub> O	-	55 °C	81%

a) Reactions were carried out on a 0.010 mmol scale. b) Yields are determined by <sup>1</sup>H-NMR analysis with tetrachloroethane as external standard.

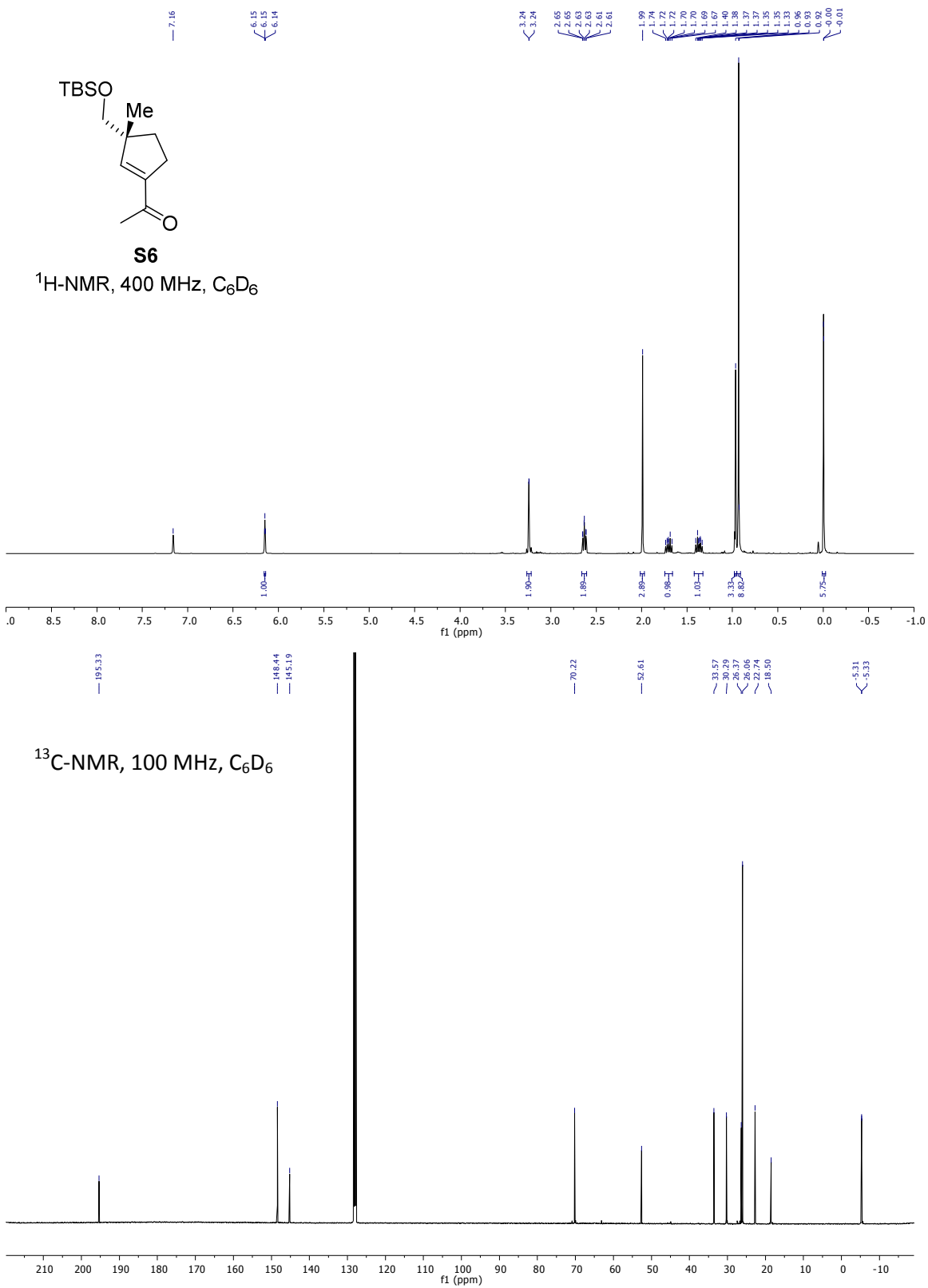
**Table 5.** Methyl cuprate addition to enone **16**.<sup>a</sup>

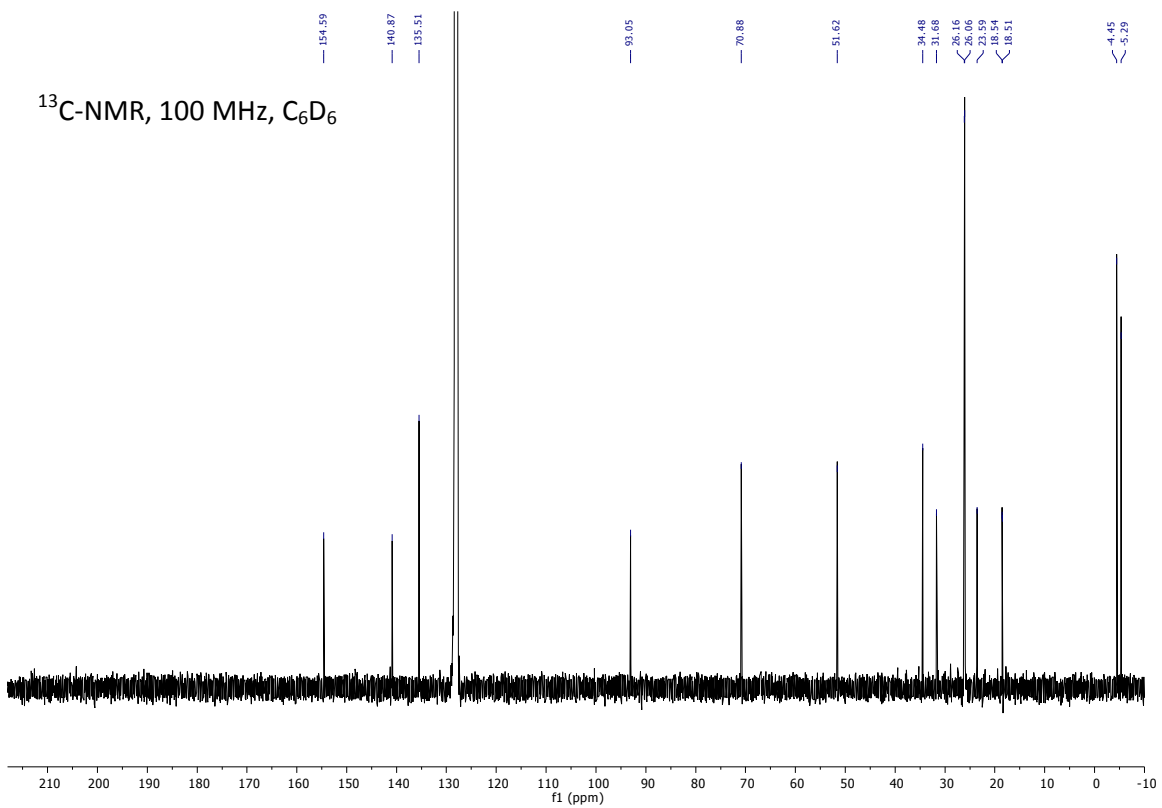
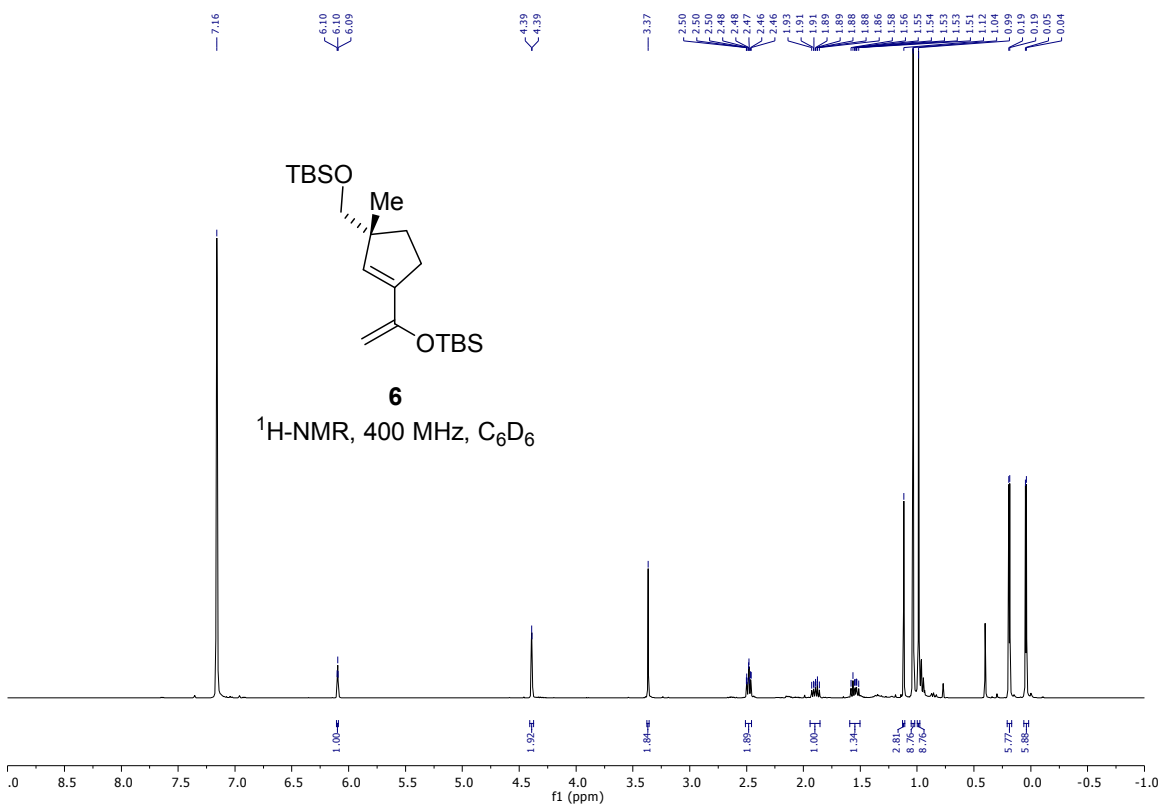


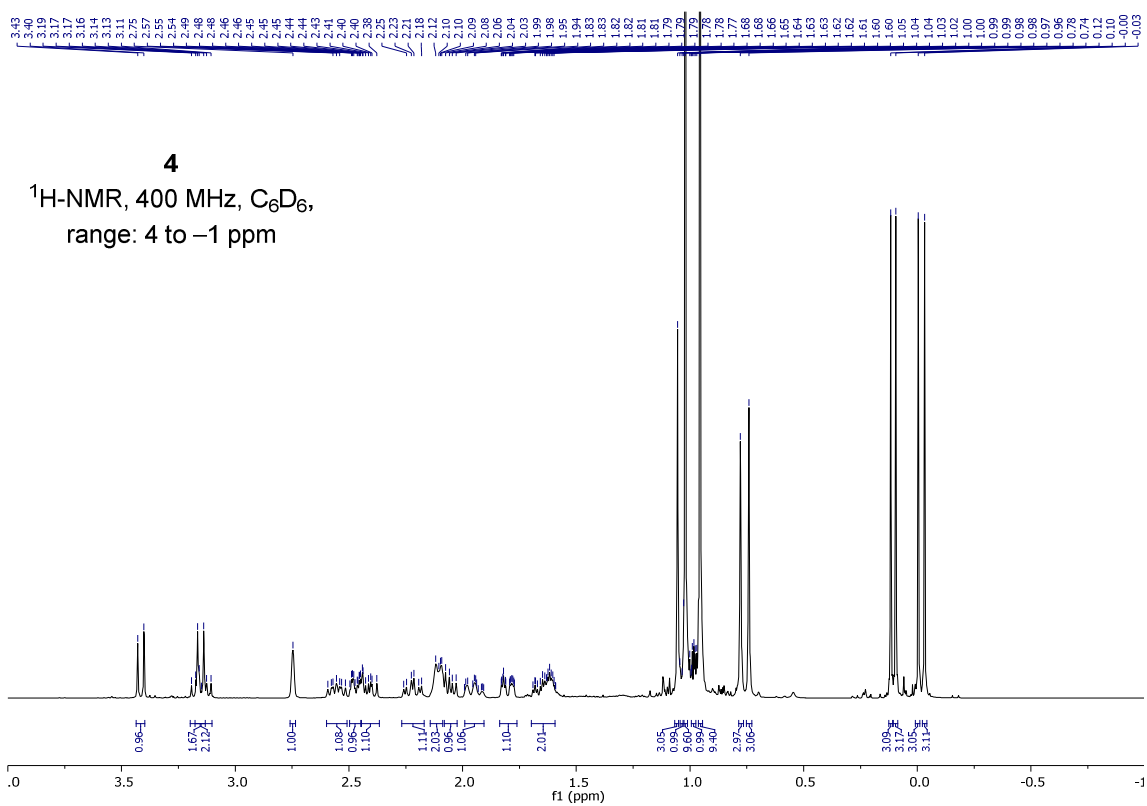
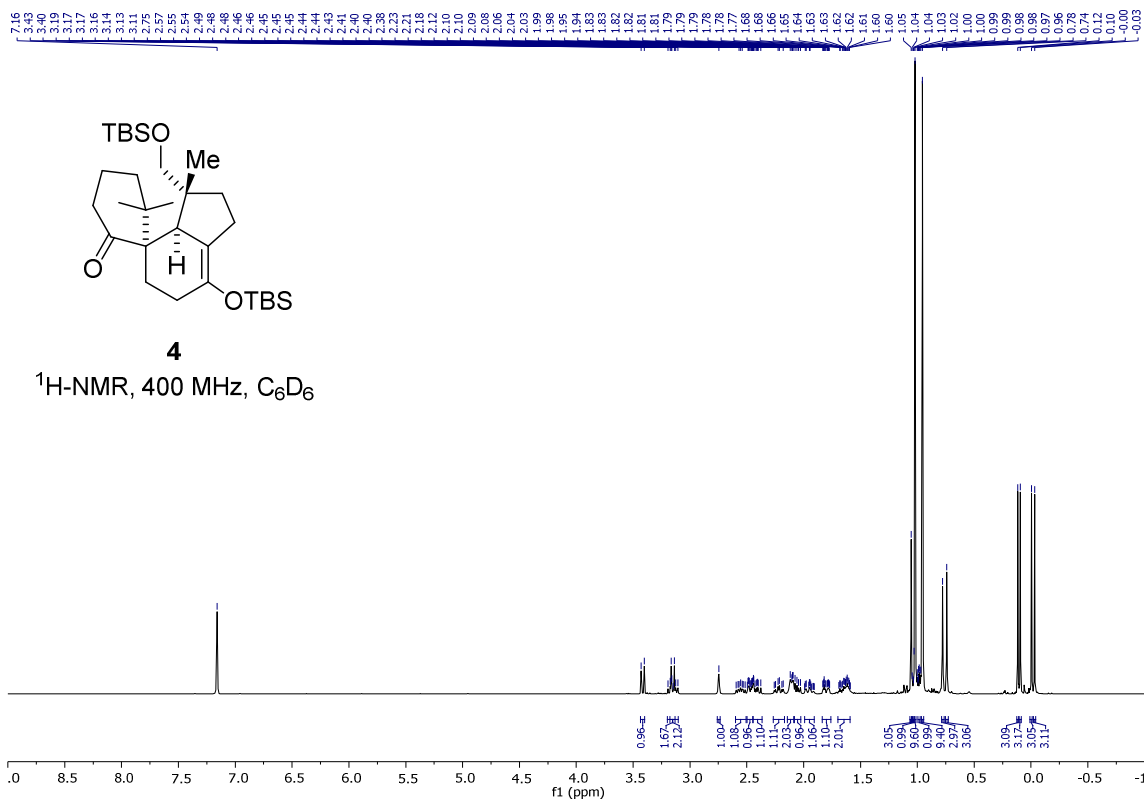
Entry	Cu-source	Lewis Acid	T	Outcome/Yield
1 <sup>b</sup>	Li-thienylcyanocuprate (2.3 eq.)	BF <sub>3</sub> ·Et <sub>2</sub> O	-78 °C	<b>16 + 17</b>
2 <sup>b</sup>	Li-thienylcyanocuprate (5.0 eq.)	BF <sub>3</sub> ·Et <sub>2</sub> O	-78 °C	<b>16 + 17</b>
3 <sup>b</sup>	Li-thienylcyanocuprate (10.0 eq.)	TMSCl/HMPA	-78 to -20 °C	starting material <b>16</b>
4	CuI (10.0 eq.)	BF <sub>3</sub> ·Et <sub>2</sub> O	-78 to -10 °C	side product
5	CuBr·DMS (5.0 eq.)	BF <sub>3</sub> ·Et <sub>2</sub> O	-78 to -20 °C	<b>16 + 17</b>
6	CuCN (10.0 eq.)	BF <sub>3</sub> ·Et <sub>2</sub> O	-78 to -50 °C	50%
7 <sup>c</sup>	CuCN (10.0 eq.)	BF <sub>3</sub> ·Et <sub>2</sub> O	-78 to -50 °C	starting material <b>16</b>

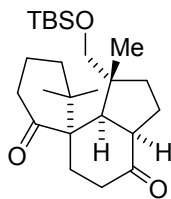
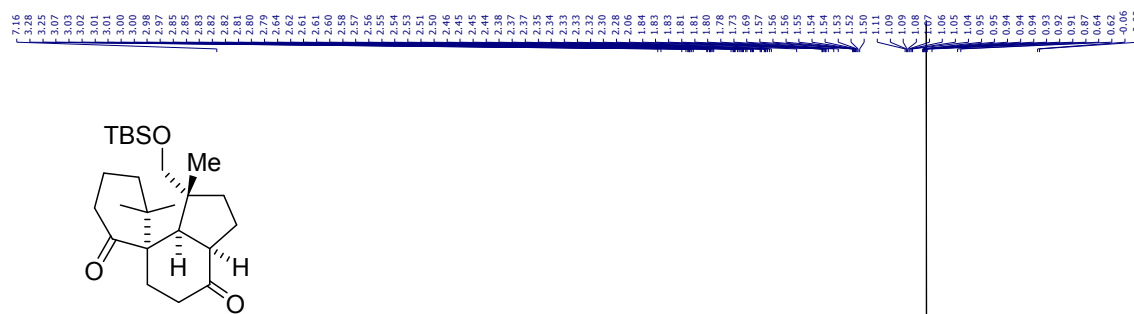
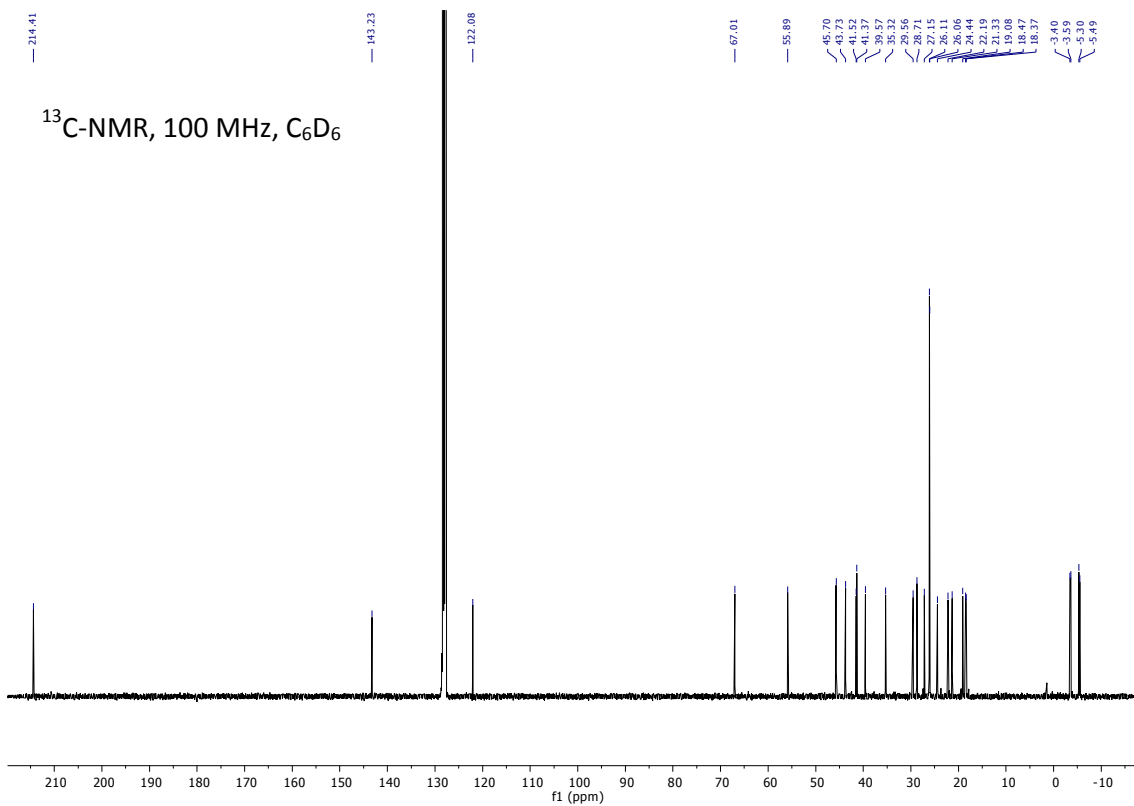
a) Reactions were carried out in Et<sub>2</sub>O with MeLi unless otherwise stated. b) Reactions were carried out in a mixture of THF and Et<sub>2</sub>O. c) MeMgBr was used.

## 10.4.3. NMR Spectra for Chapter 3.3.



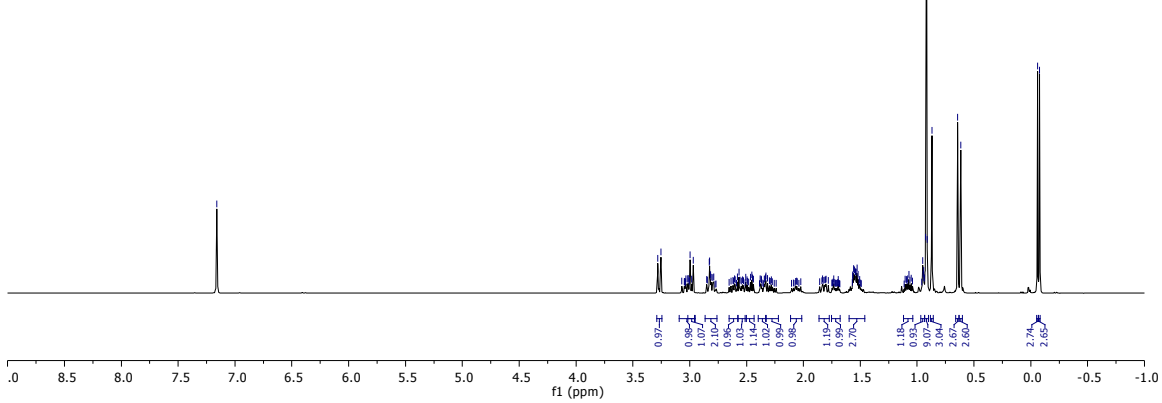


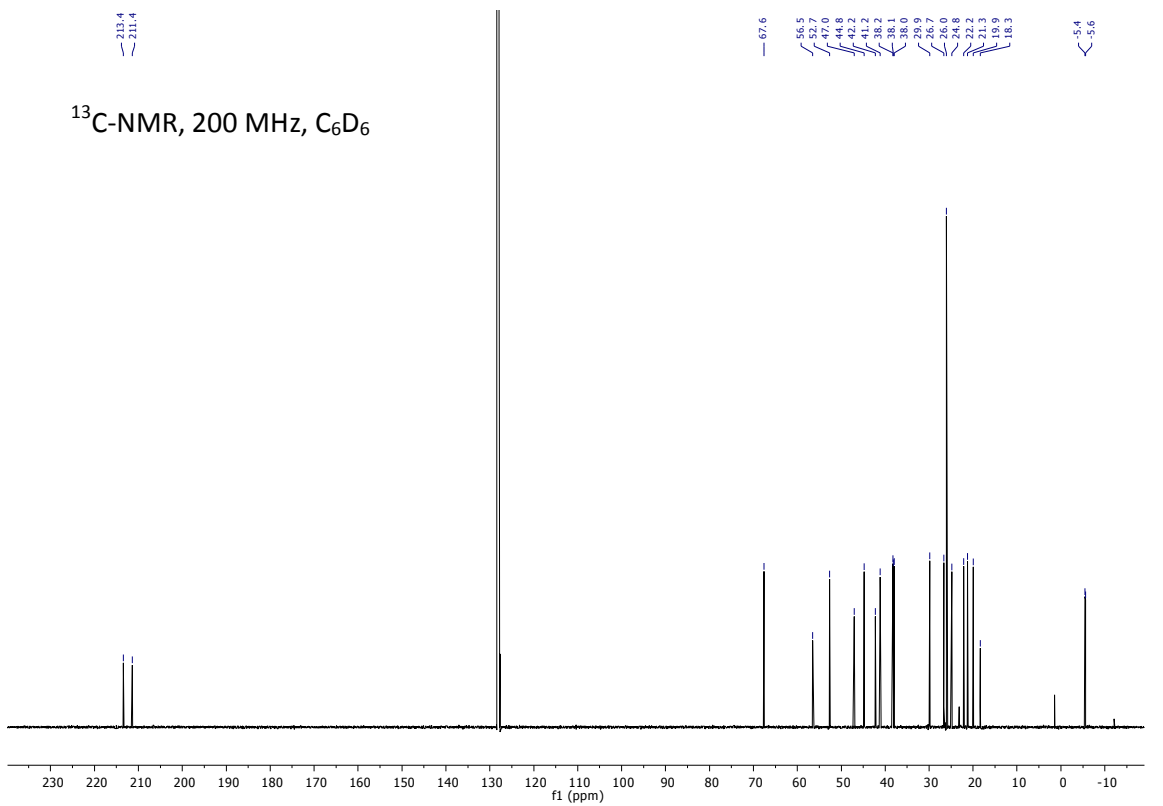
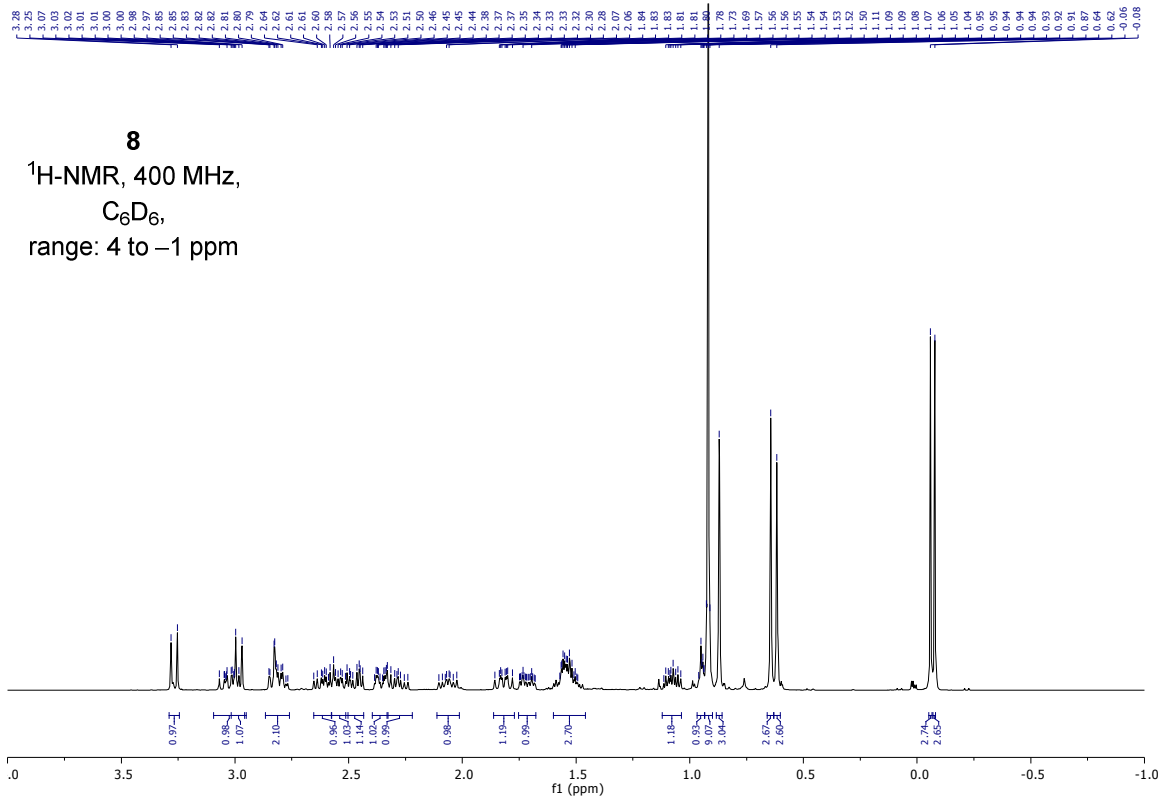


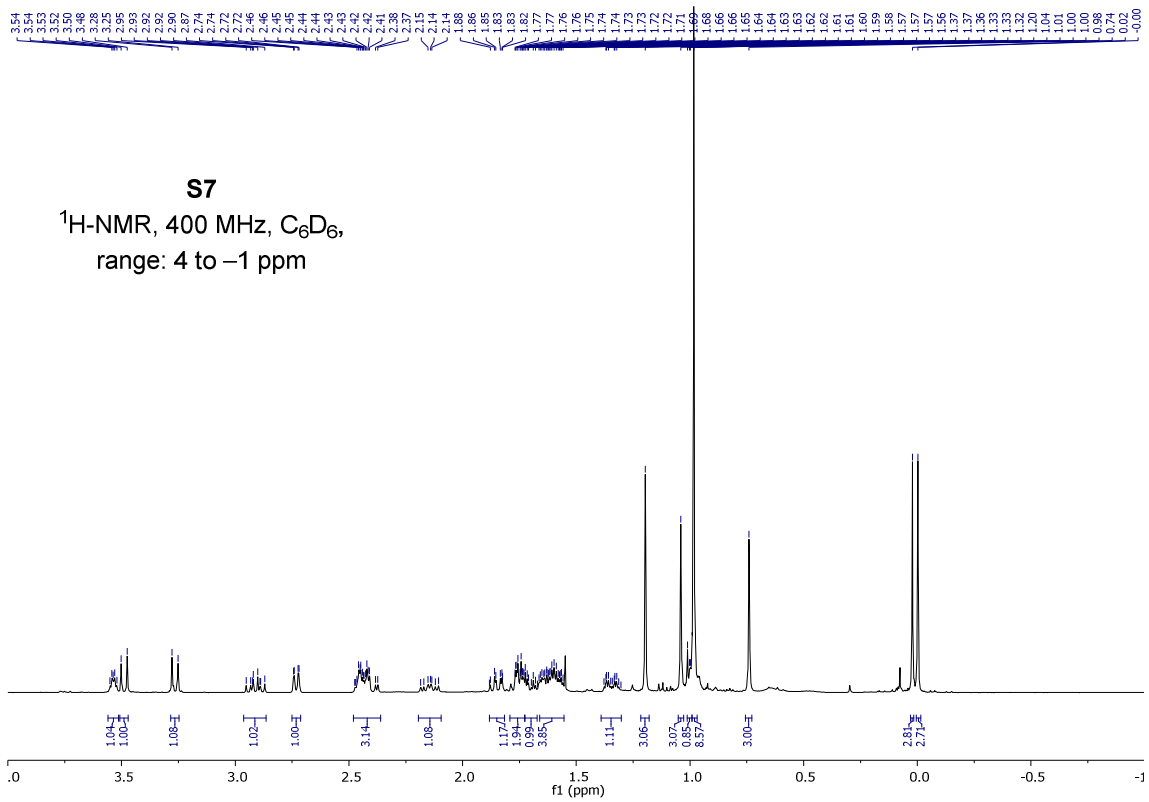
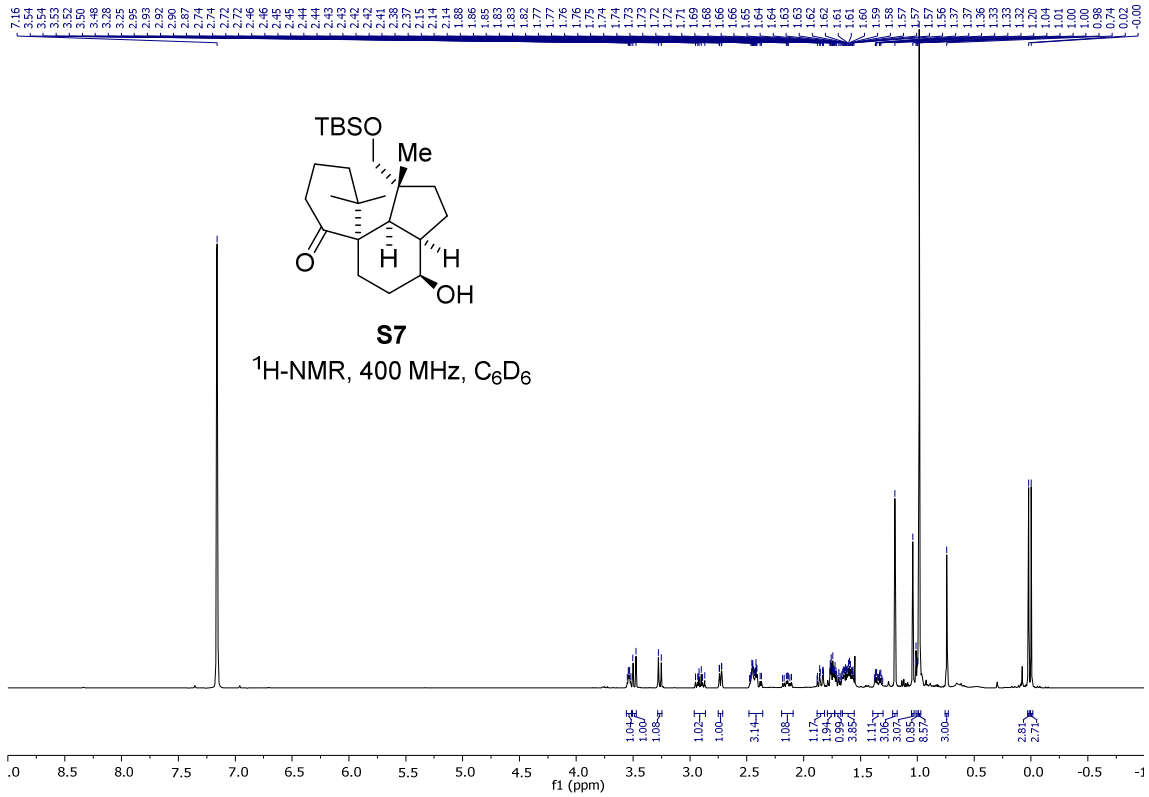


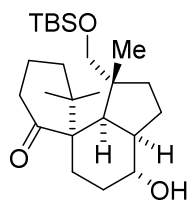
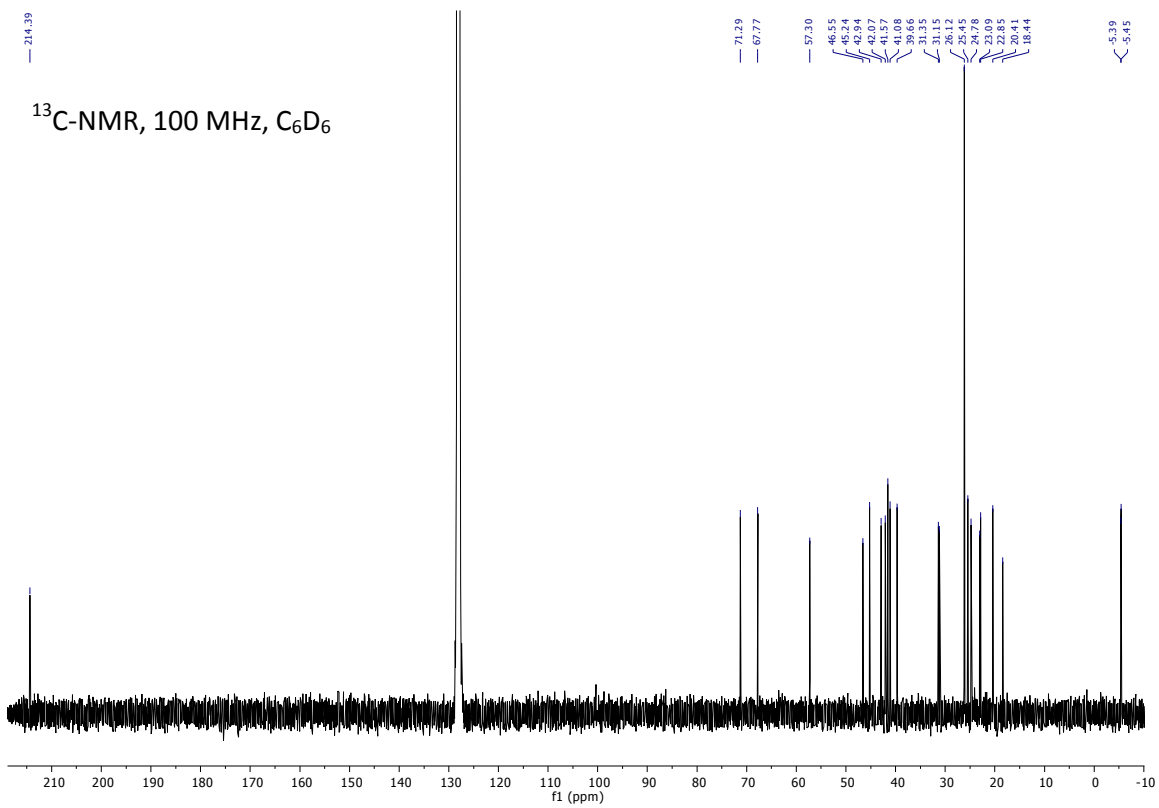
**8**

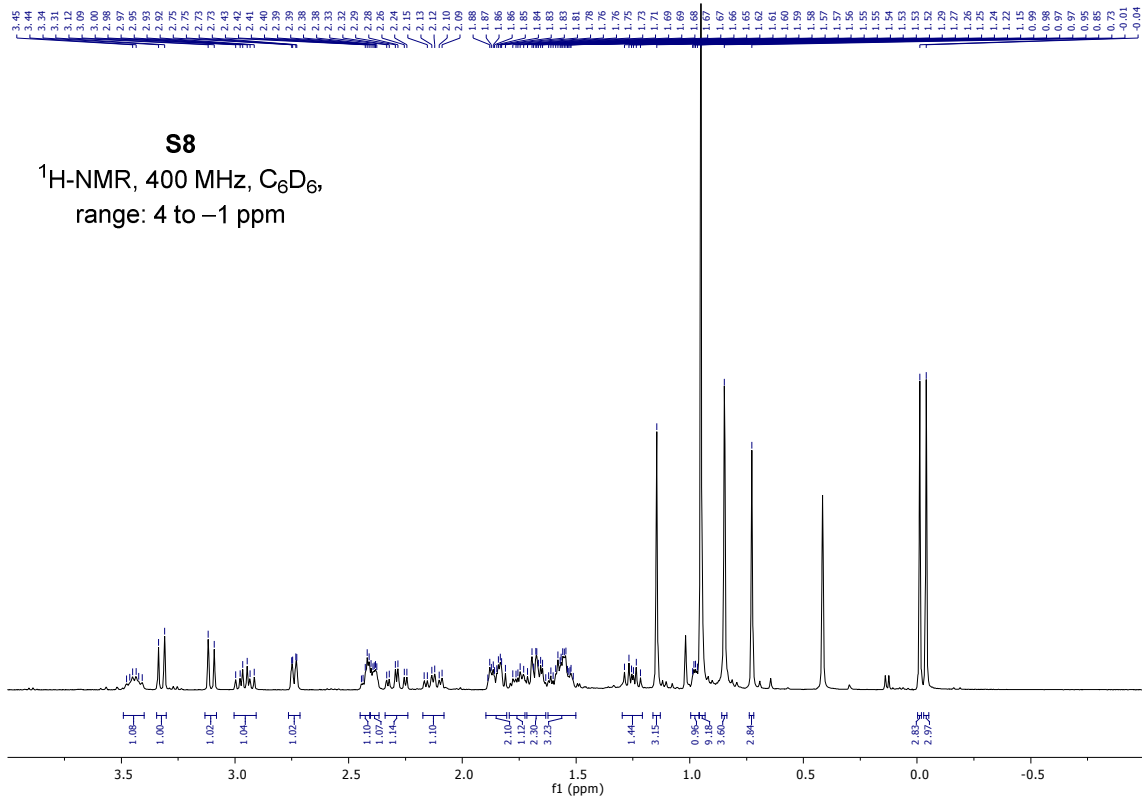
$^1\text{H-NMR}$ , 400 MHz,  $\text{C}_6\text{D}_6$



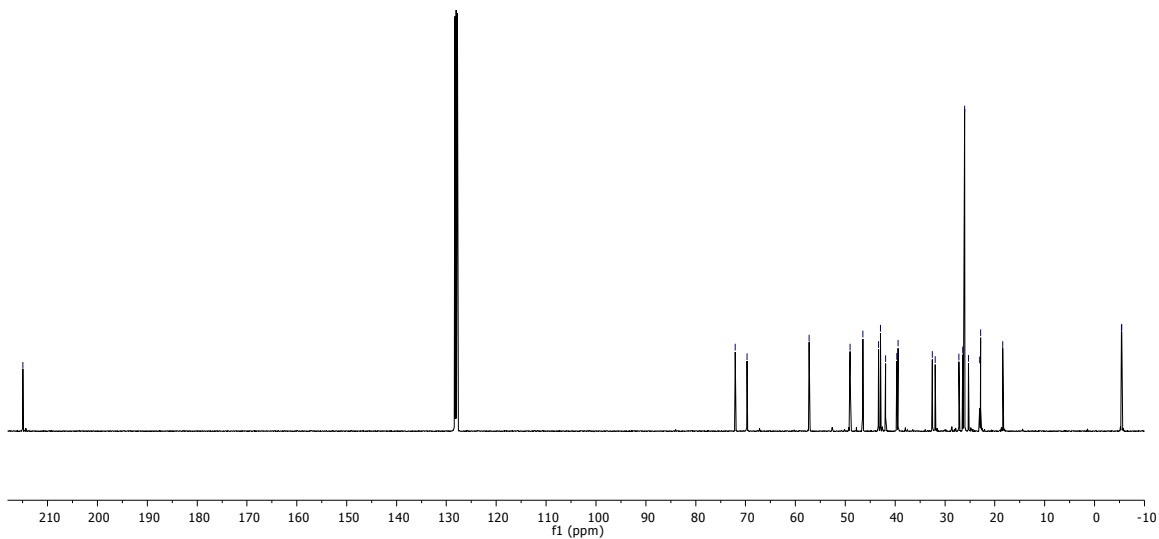


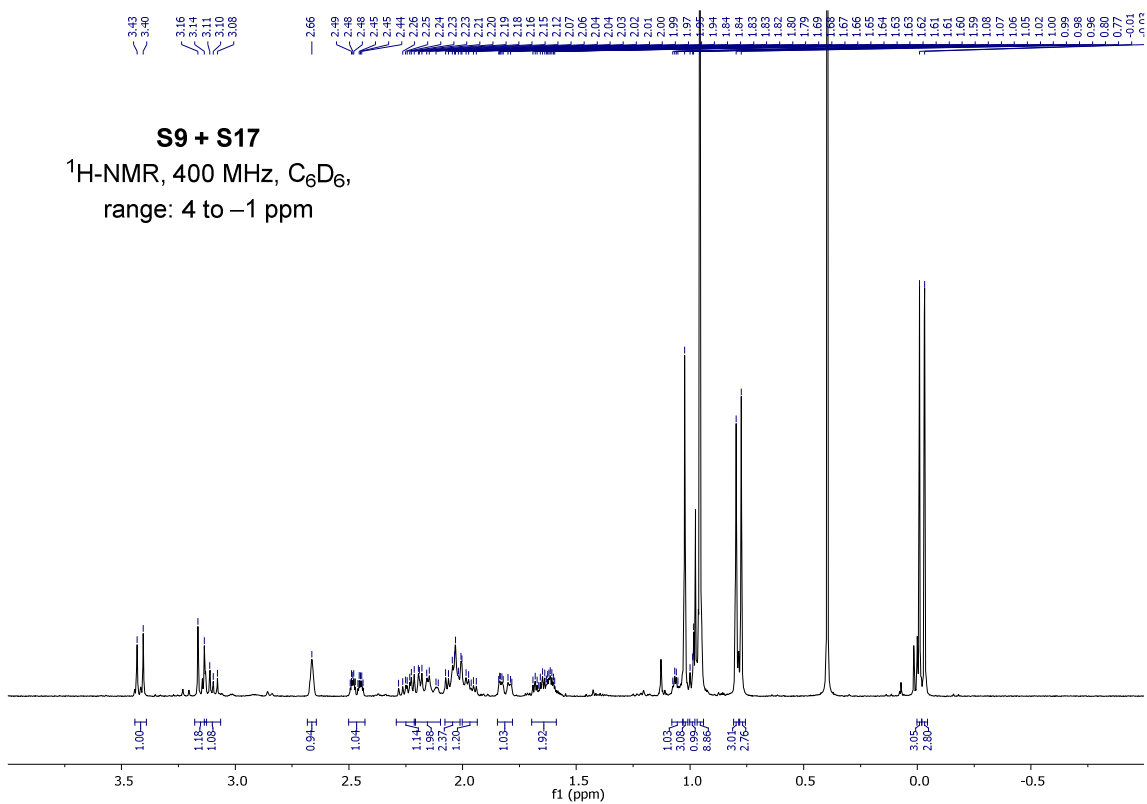
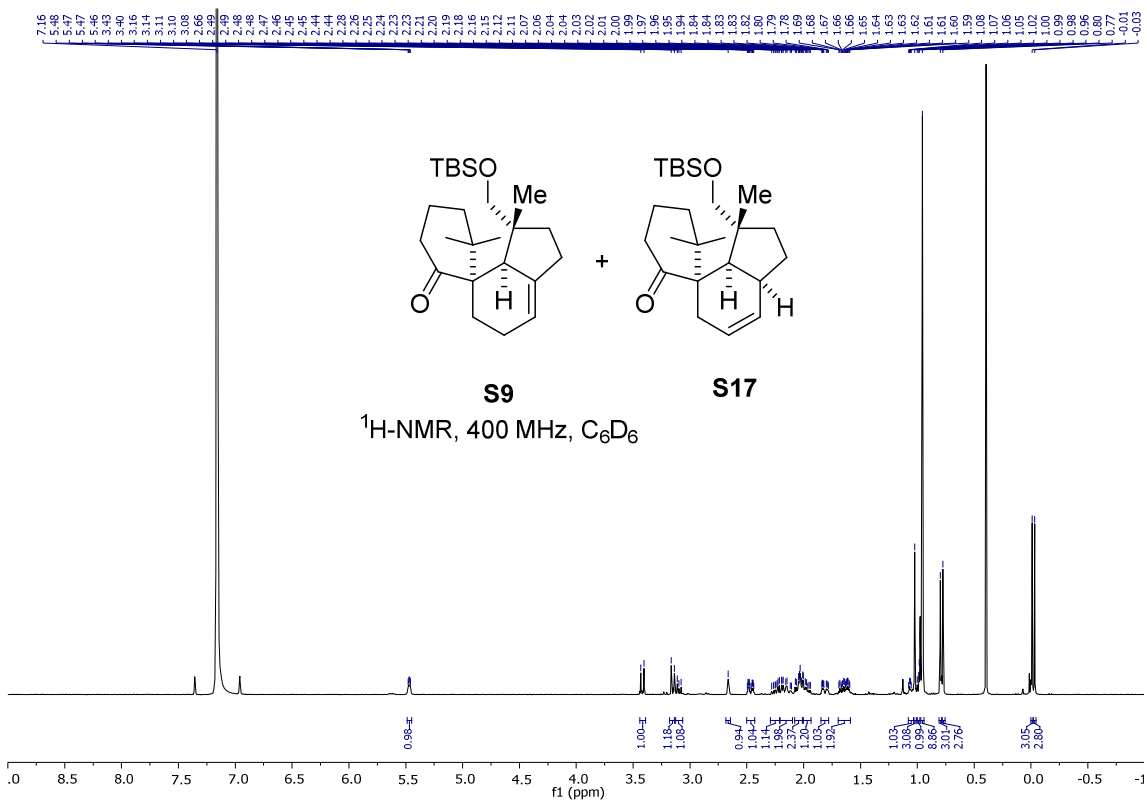


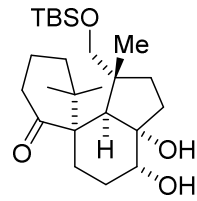
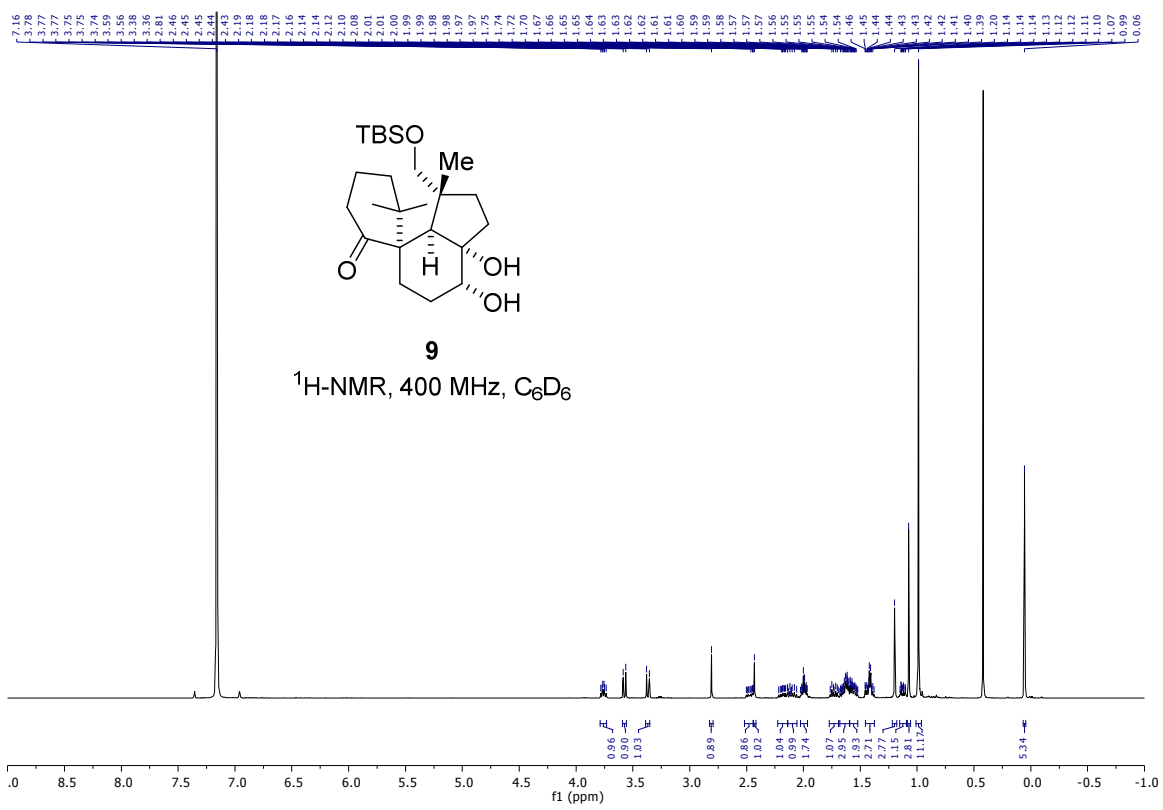
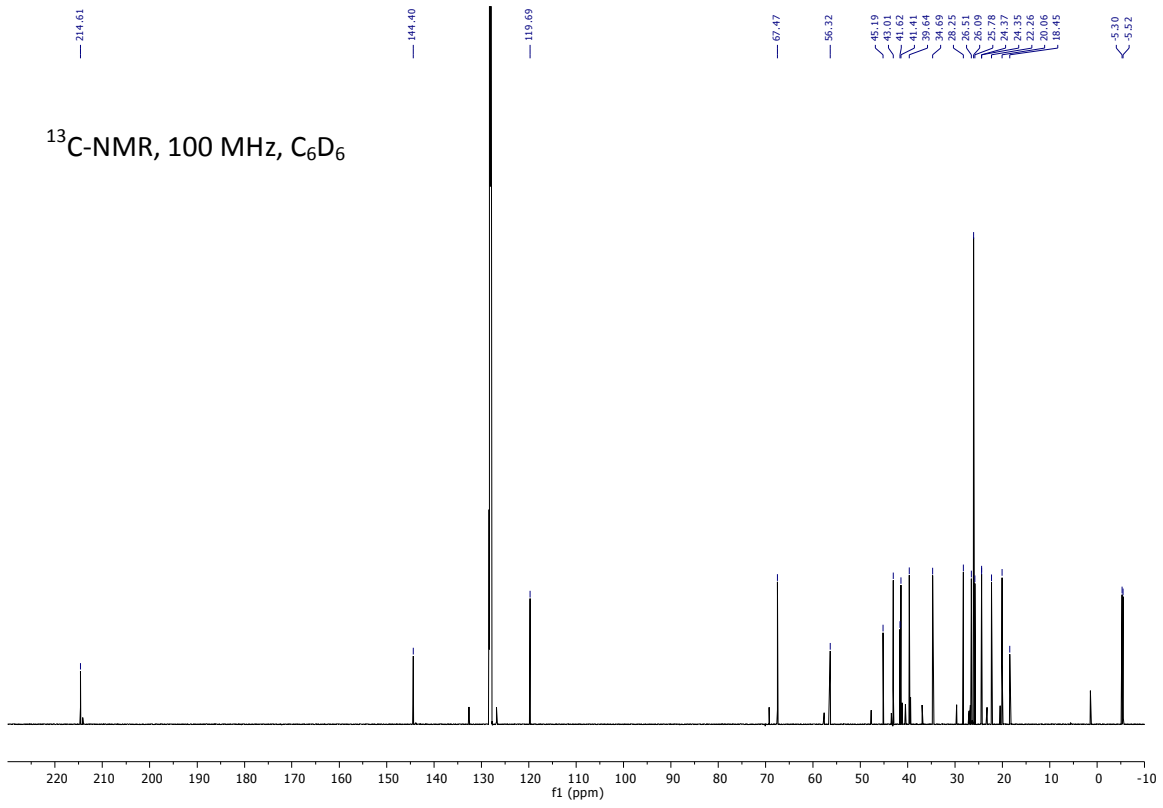
**S8** $^1\text{H}$ -NMR, 400 MHz,  $\text{C}_6\text{D}_6$



<sup>13</sup>C-NMR, 100 MHz, C<sub>6</sub>D<sub>6</sub>



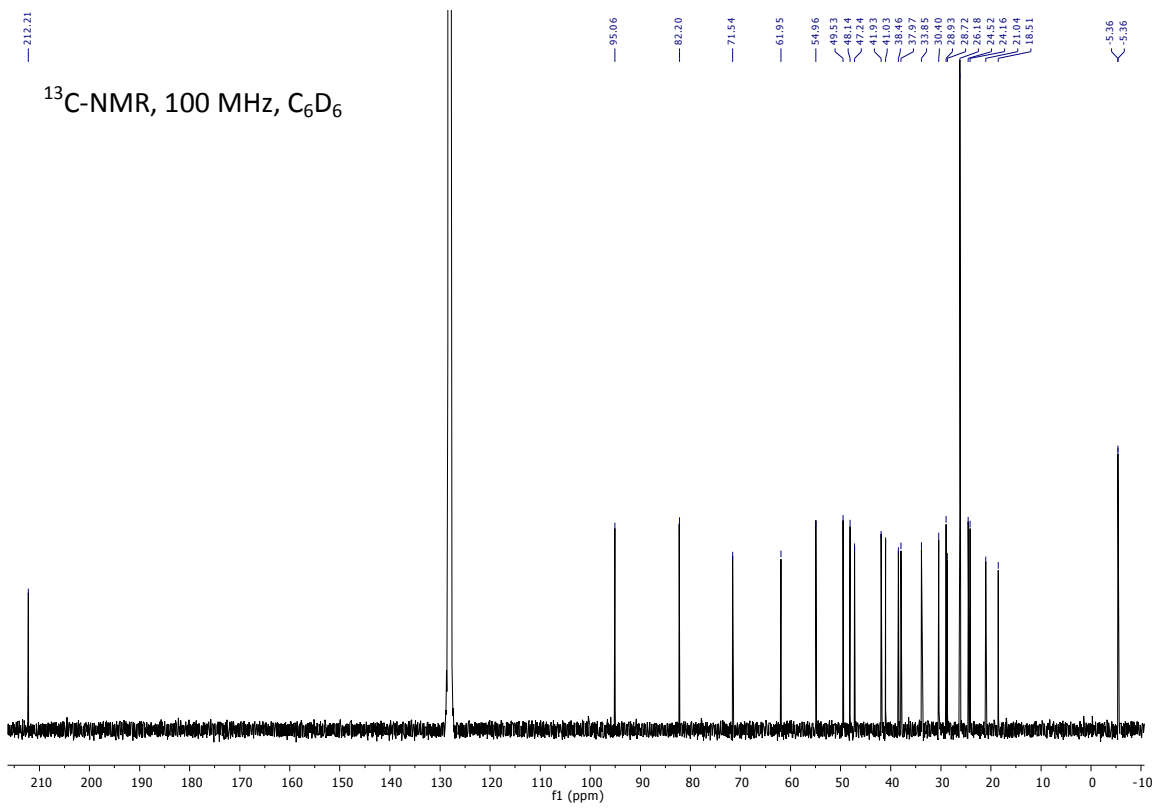
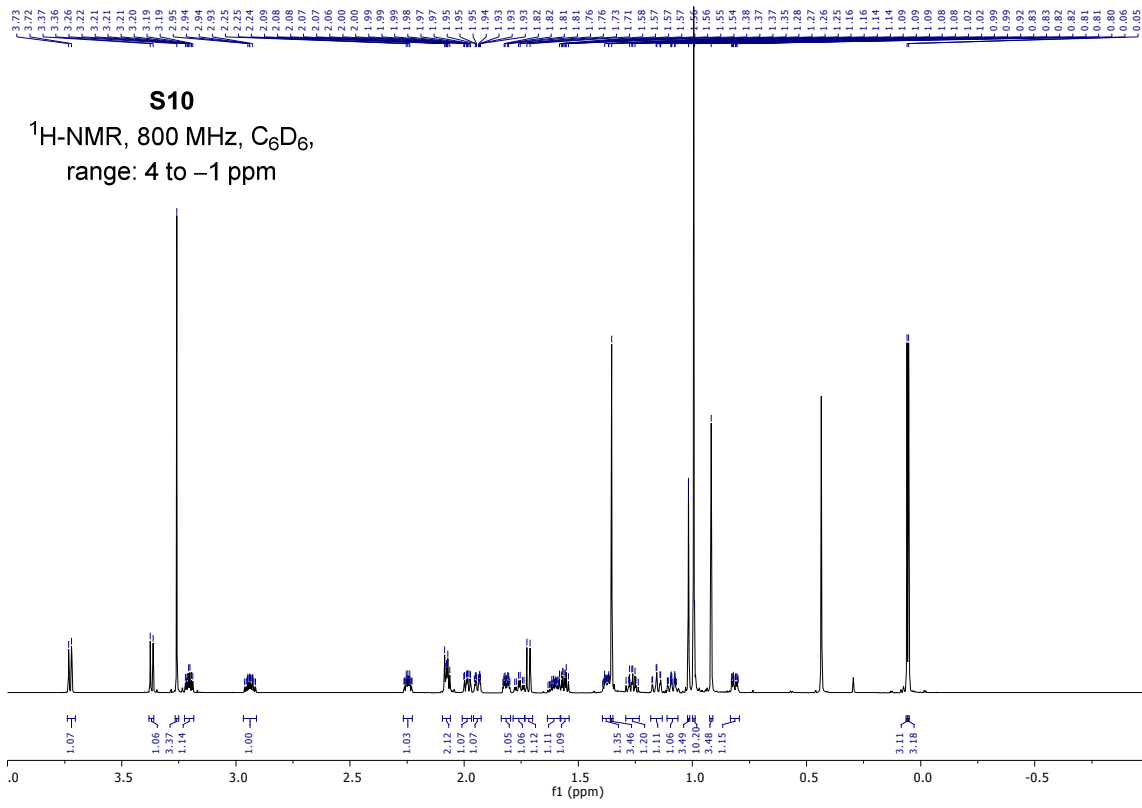




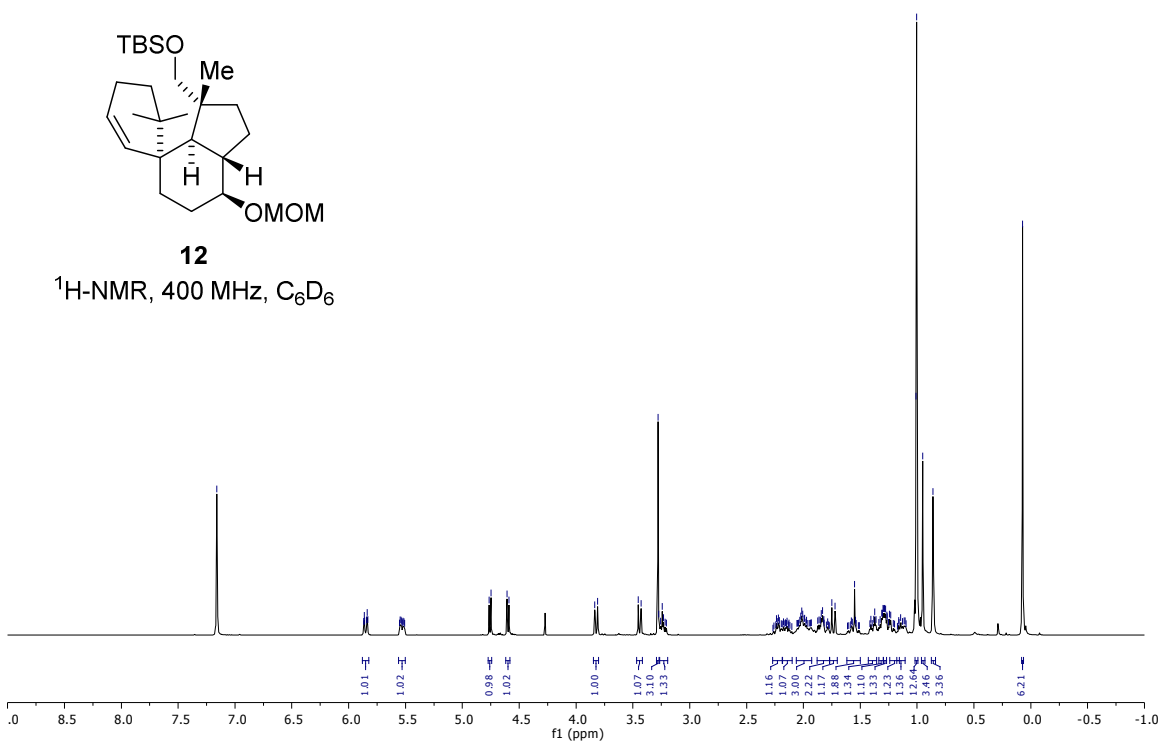
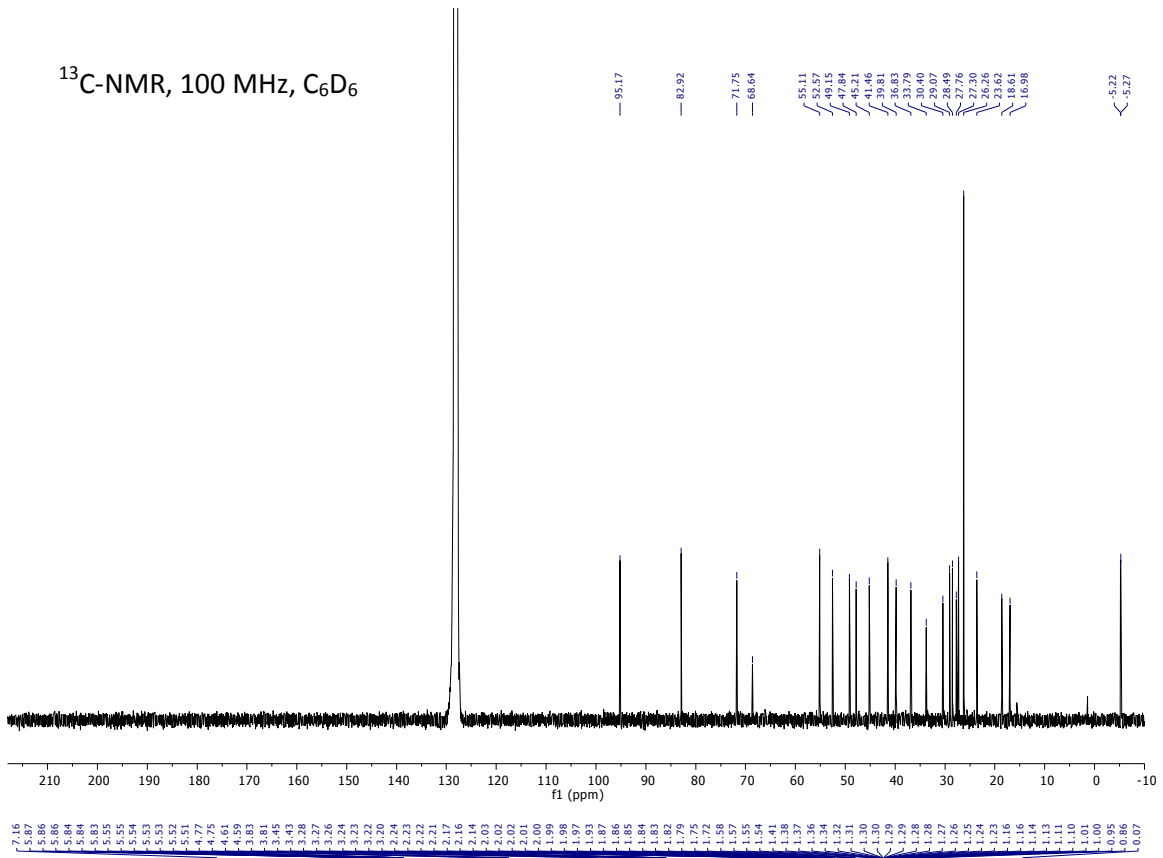


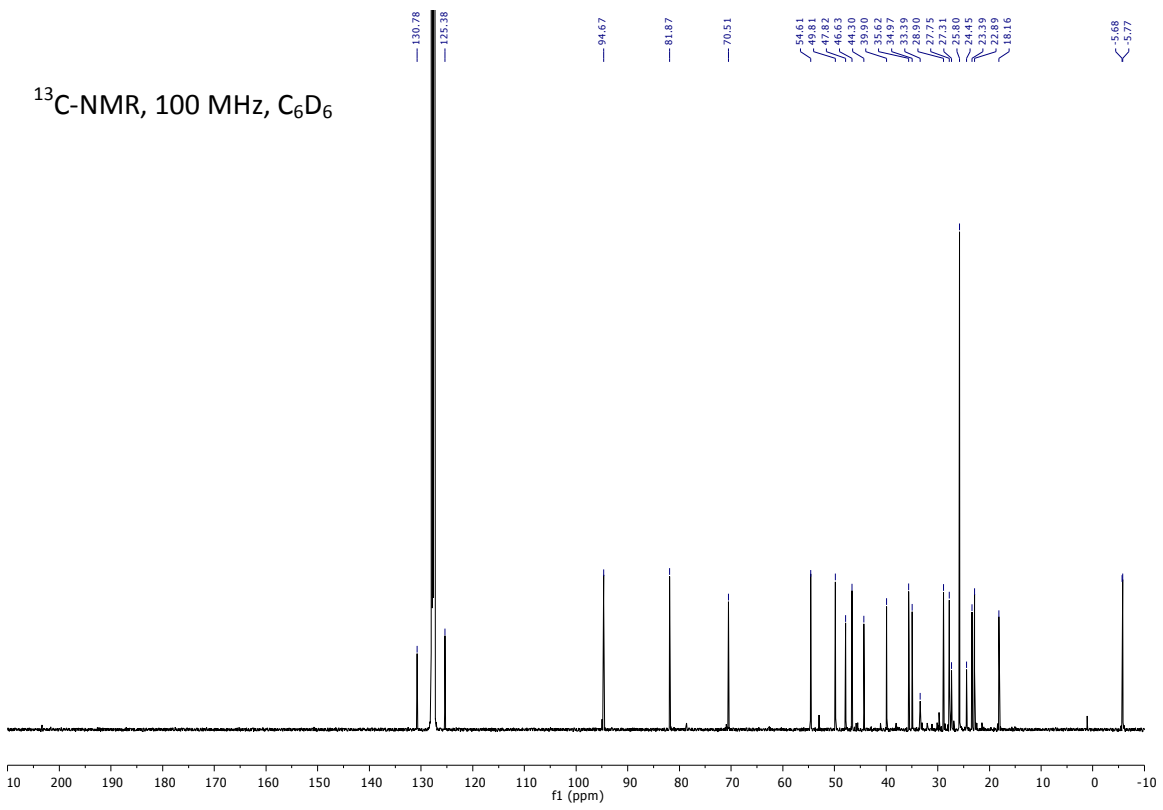
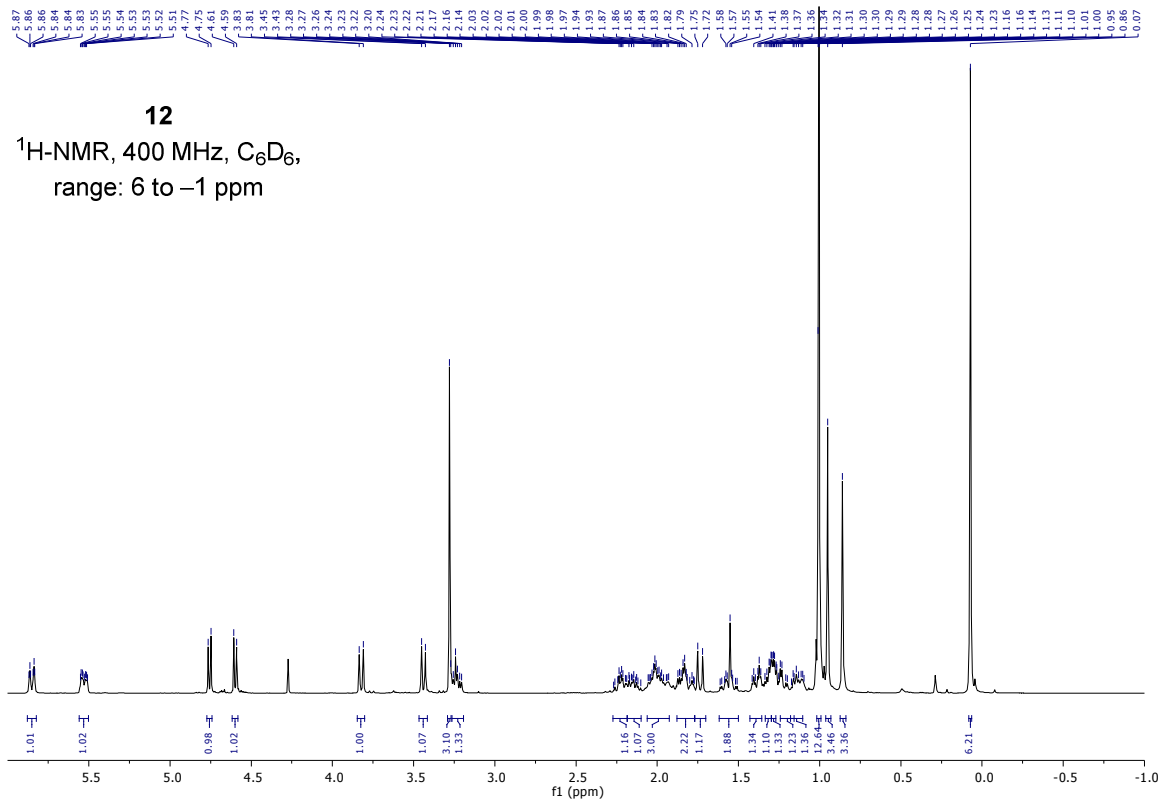


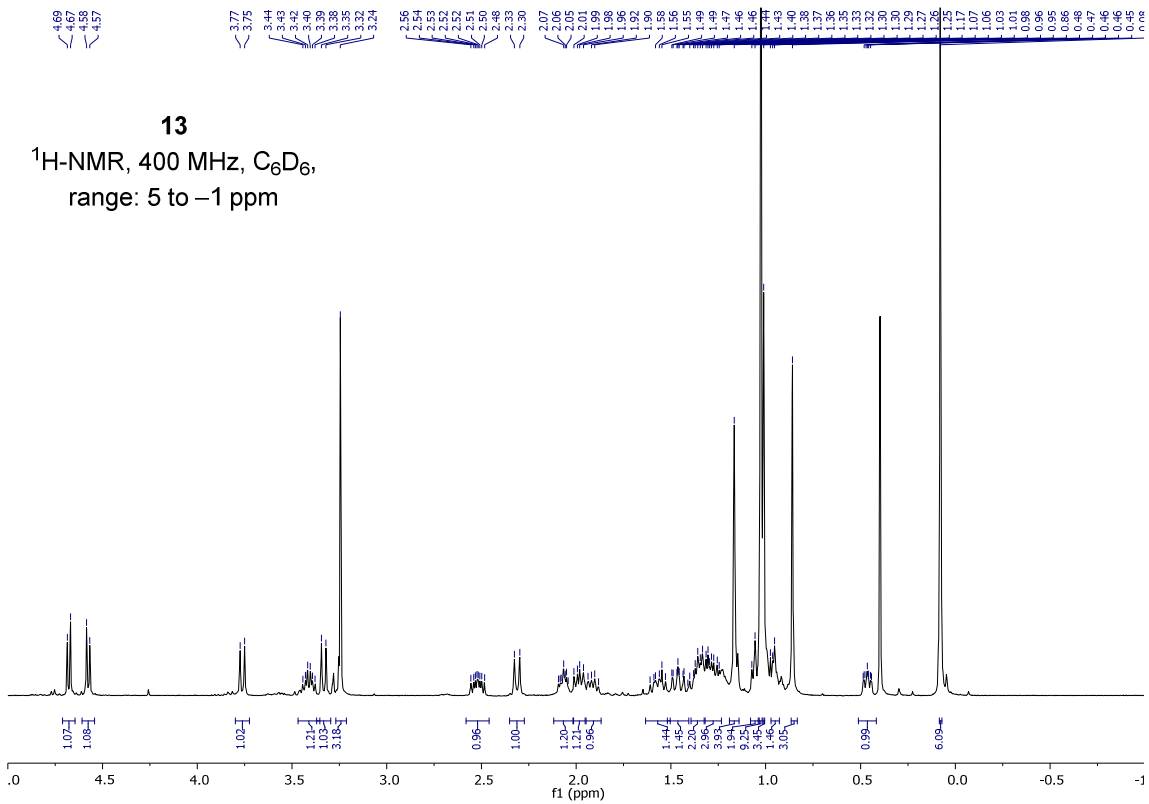
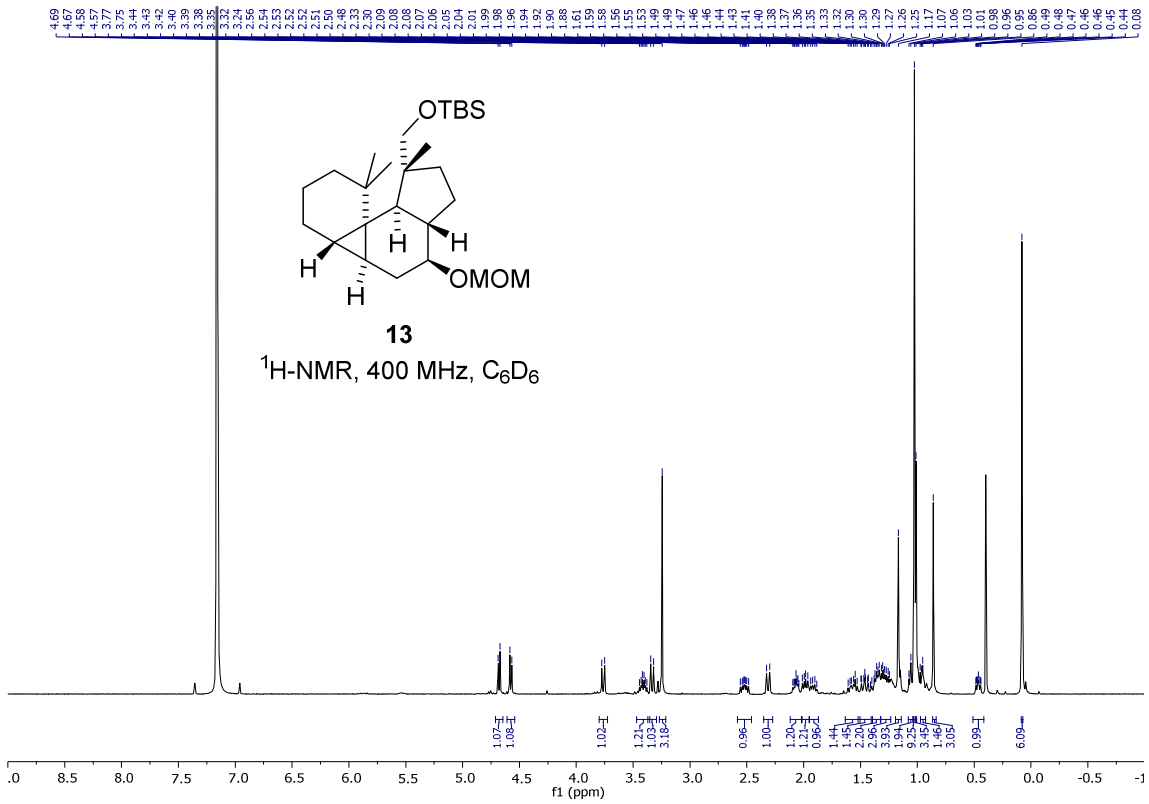


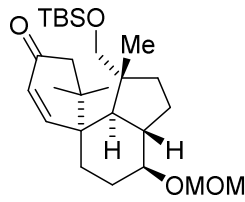
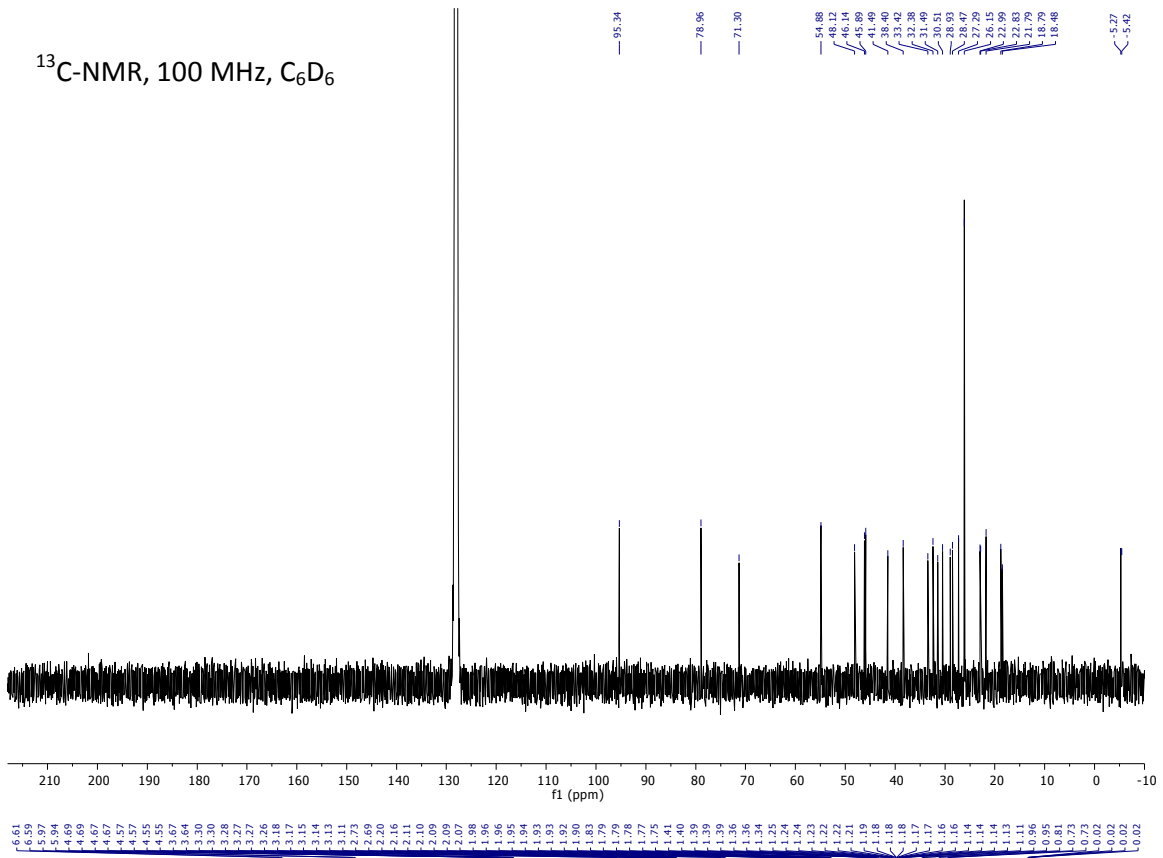




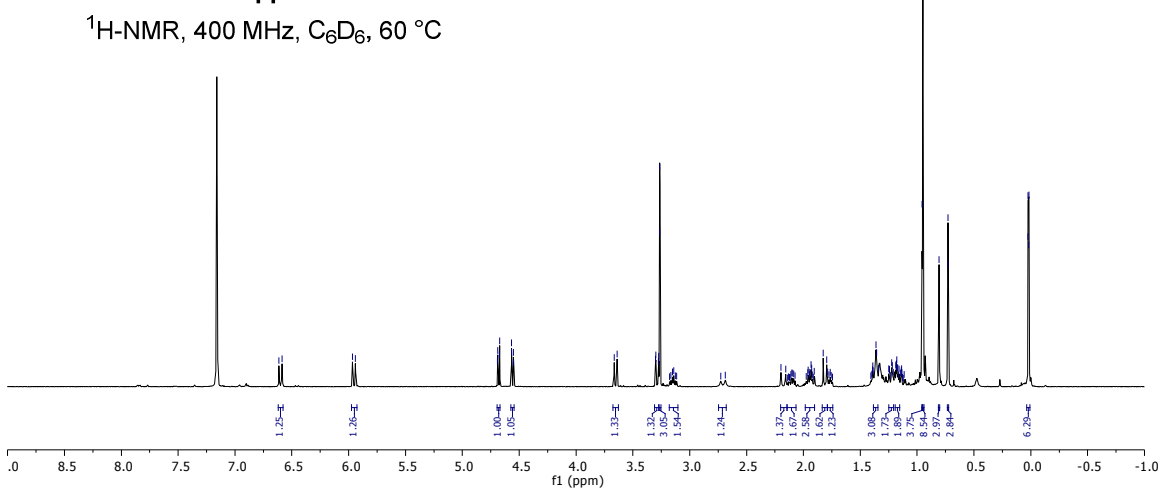


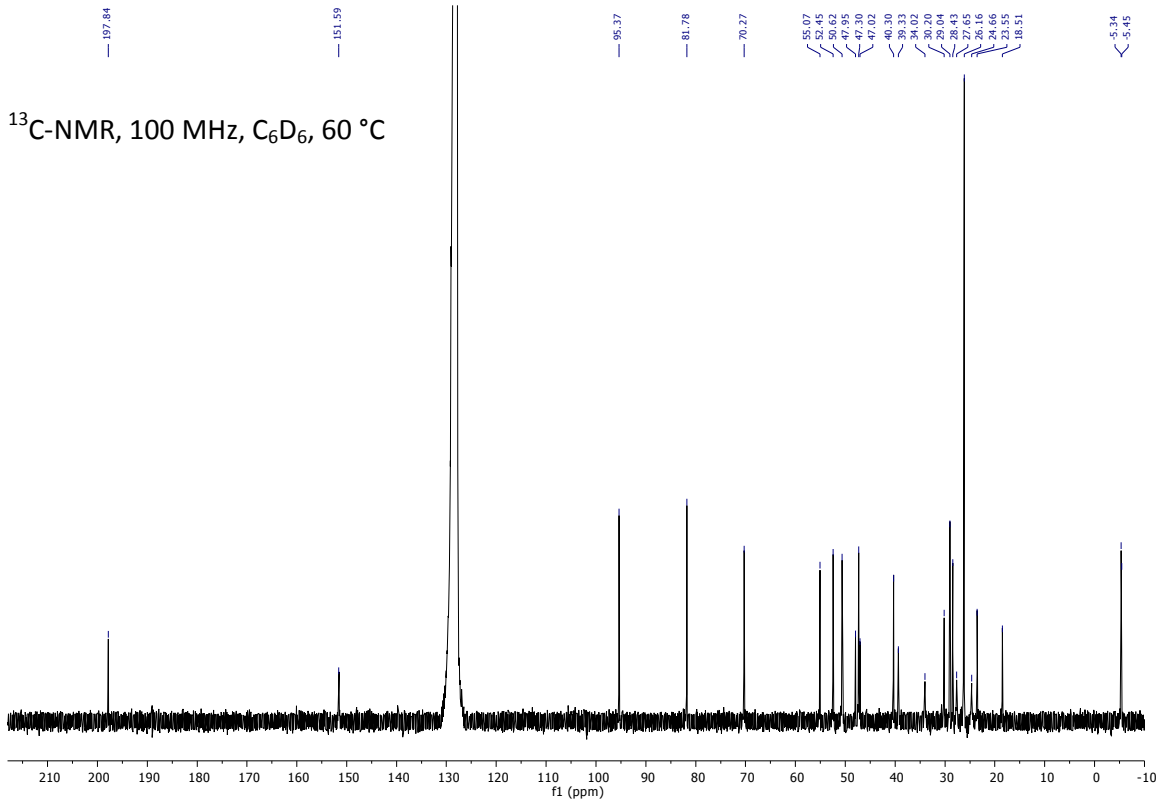
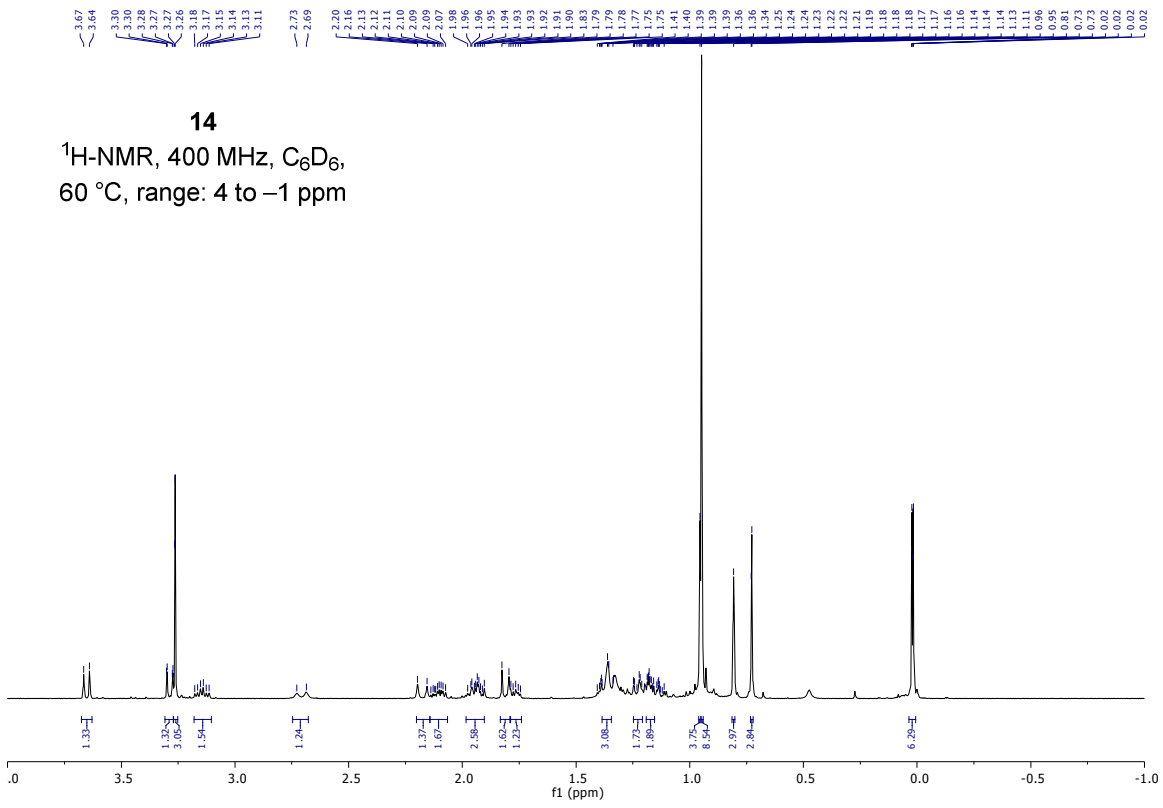


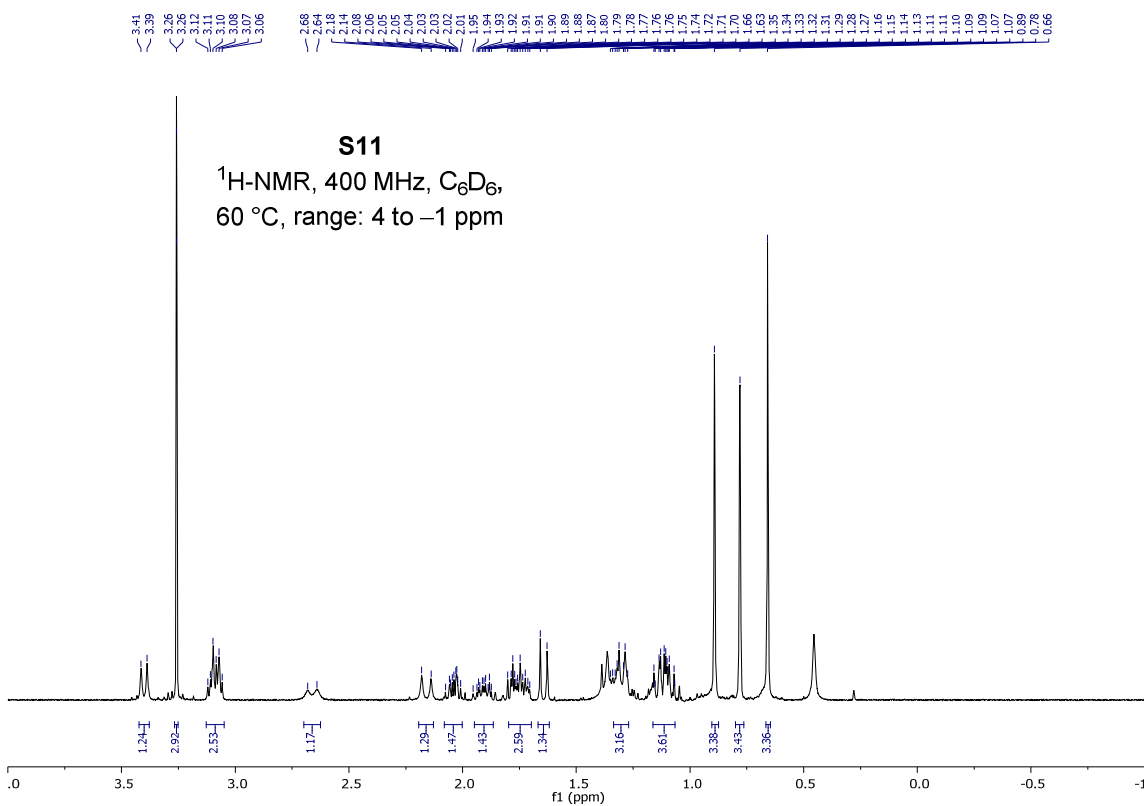
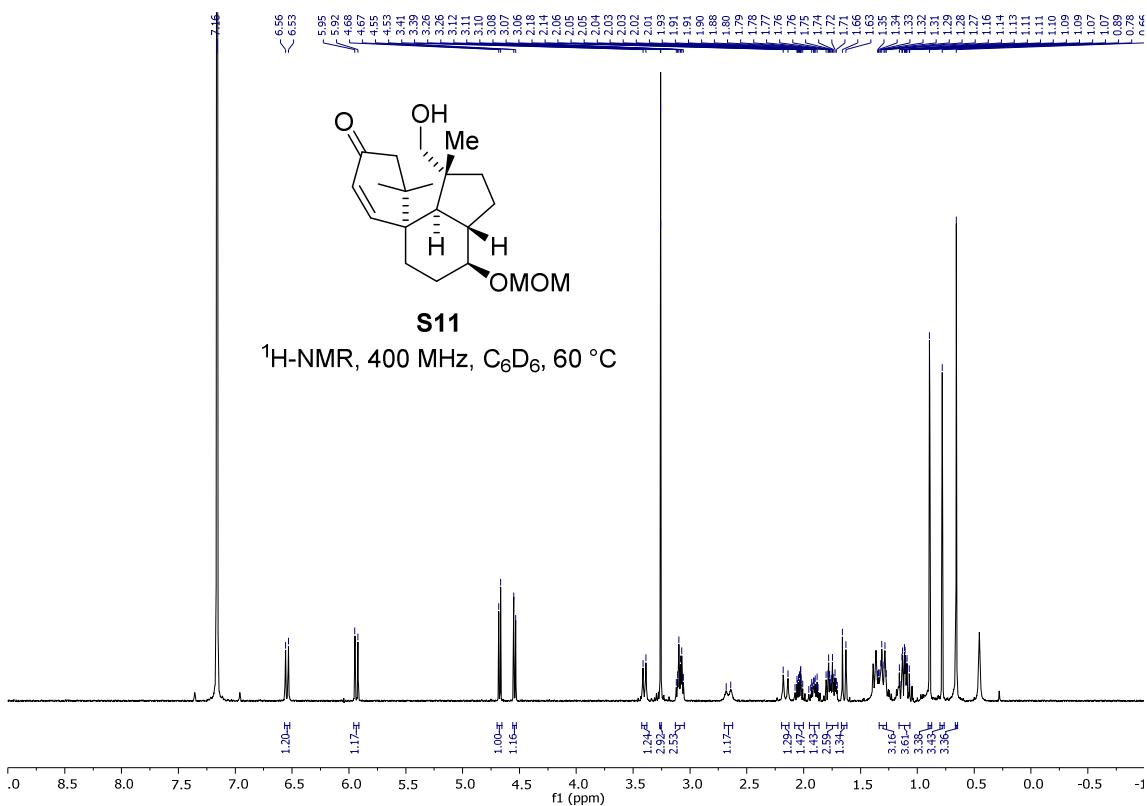


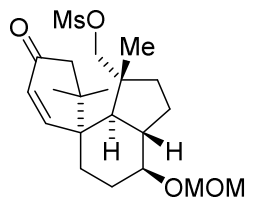
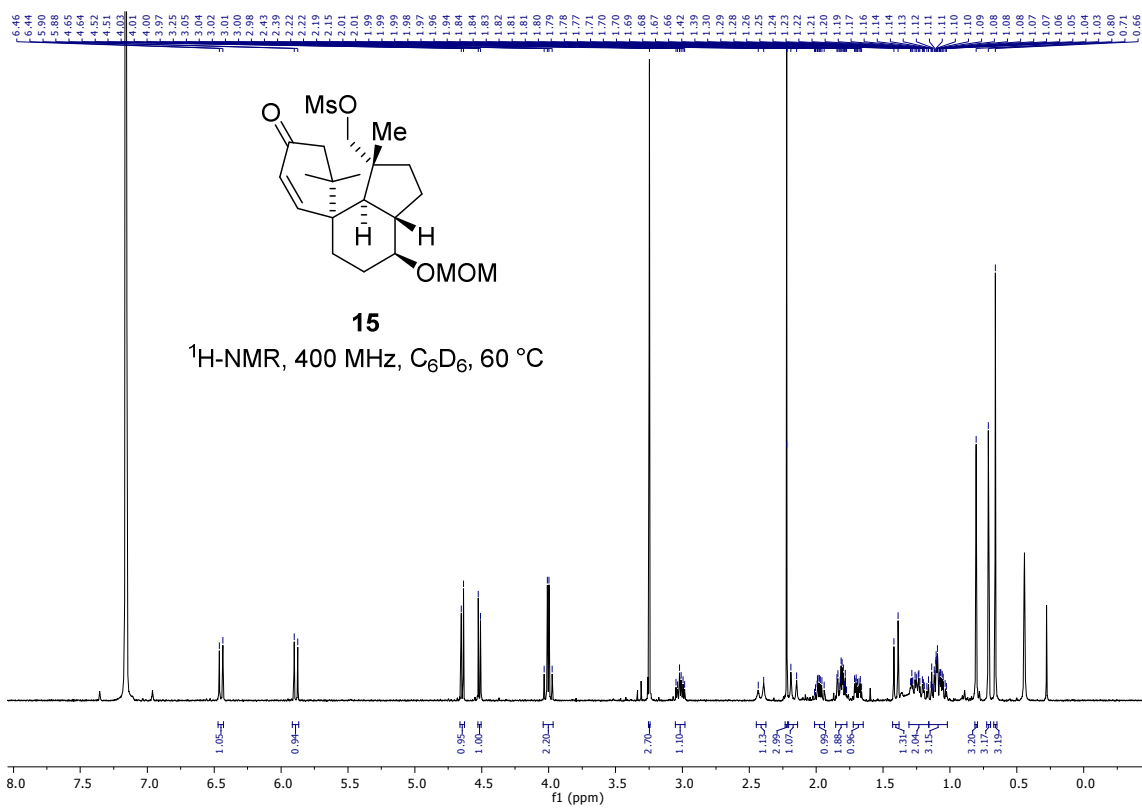
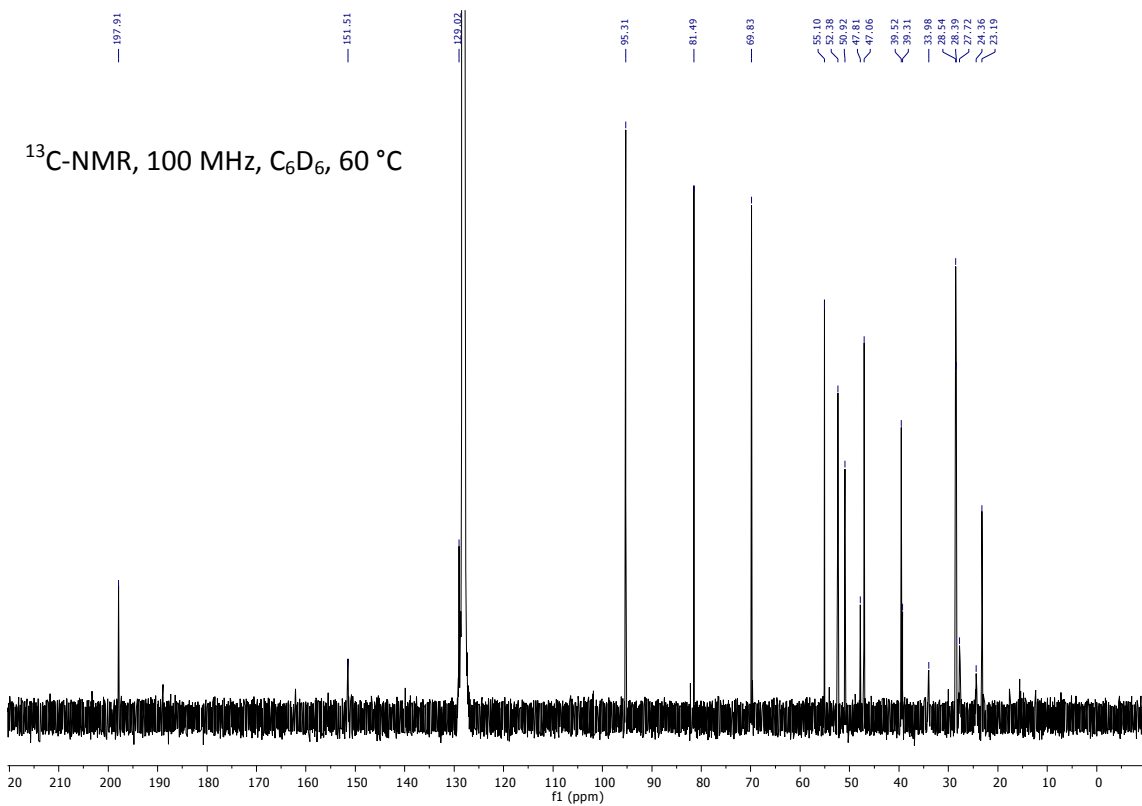


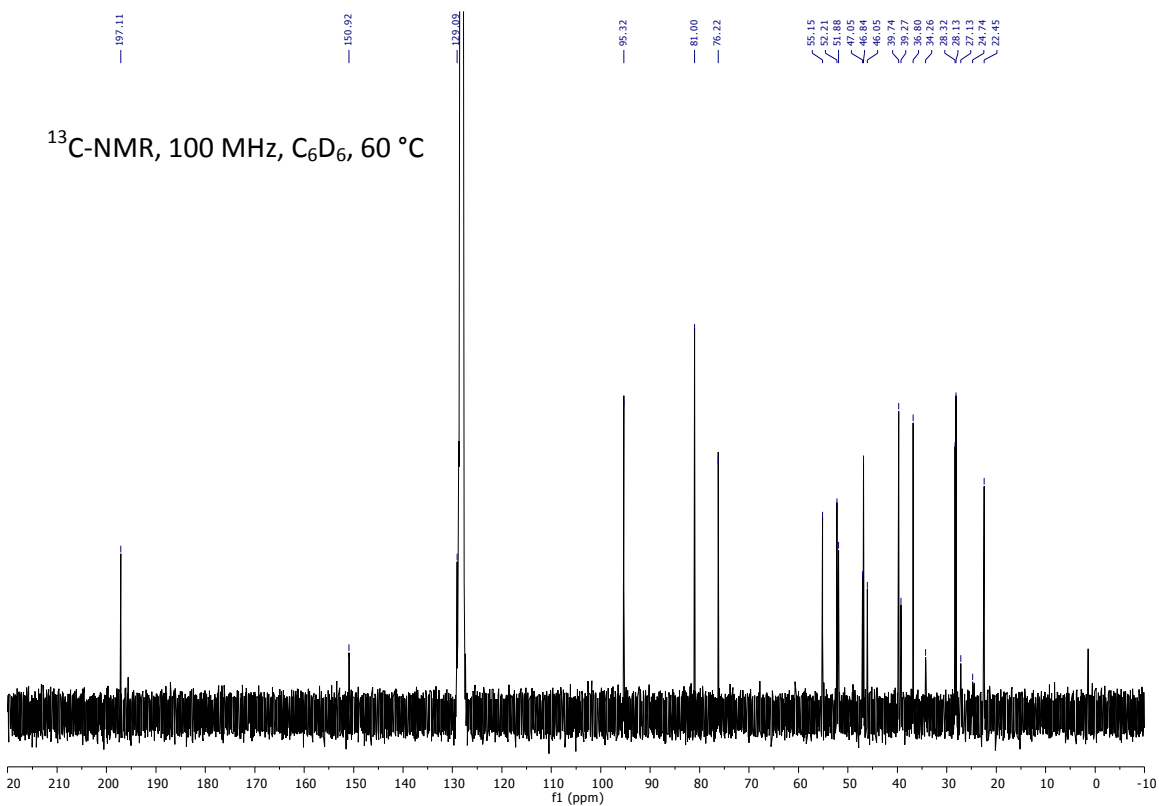
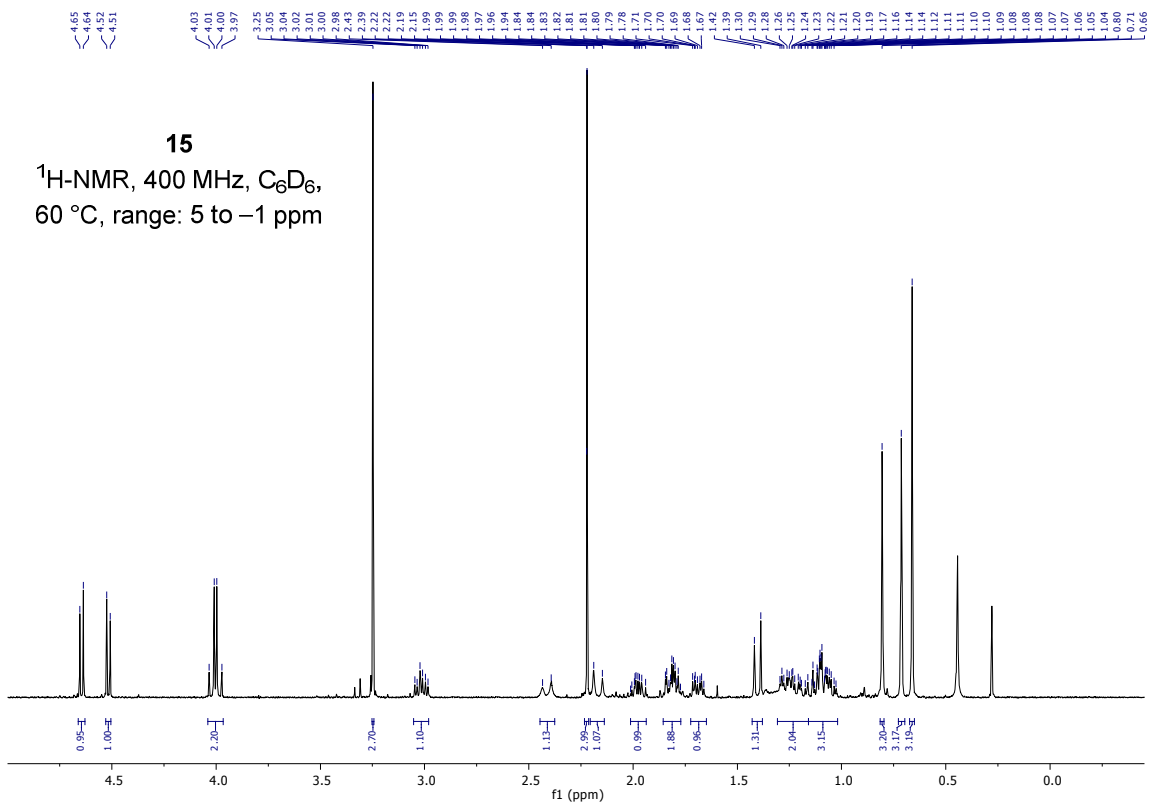
**14**

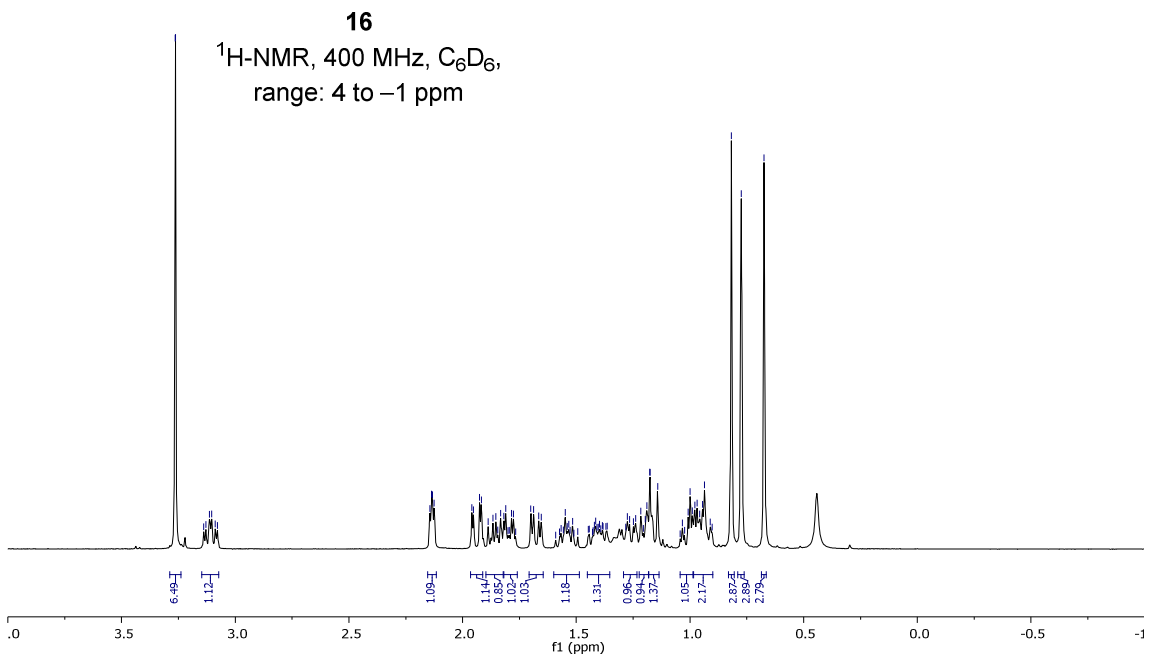
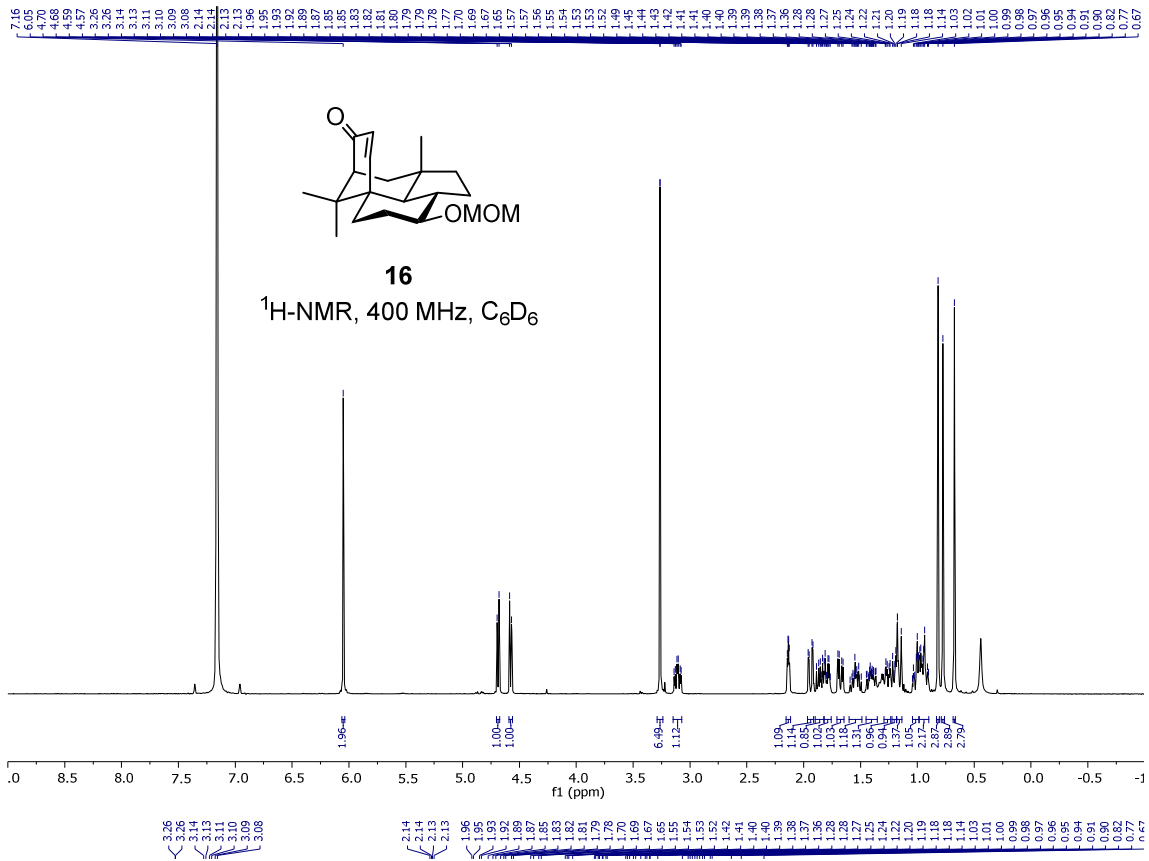


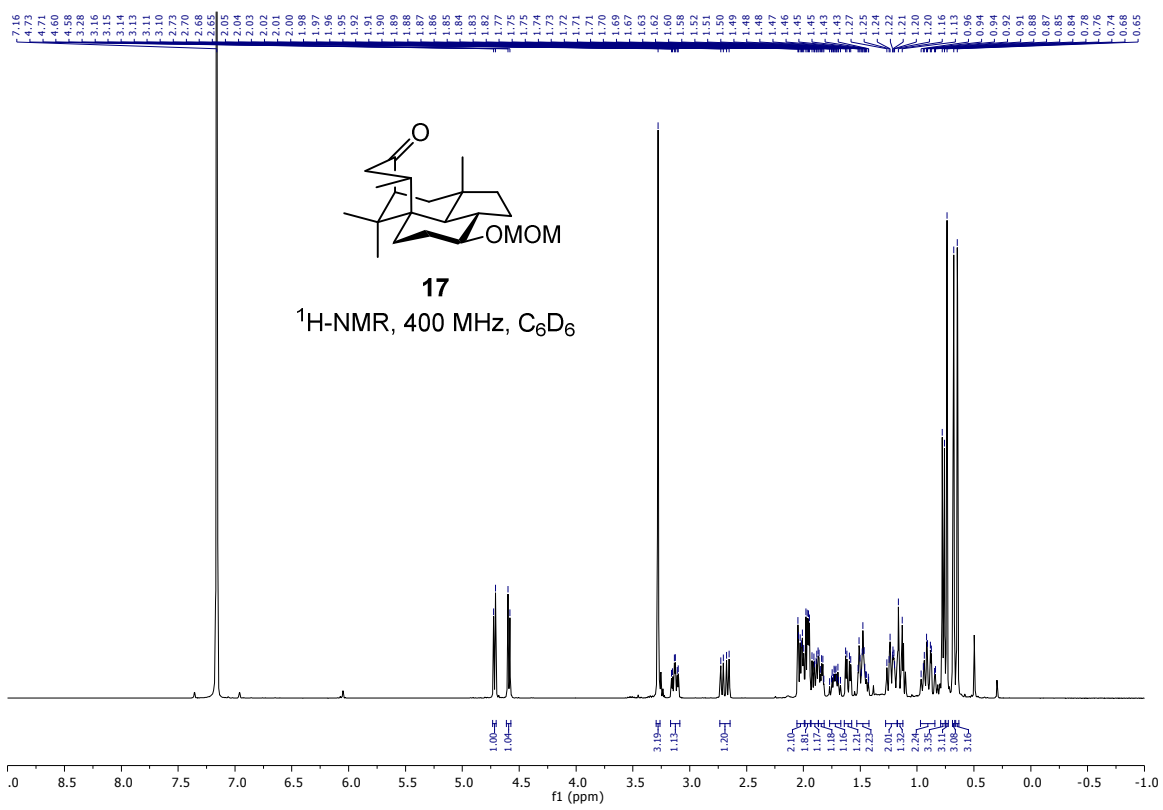
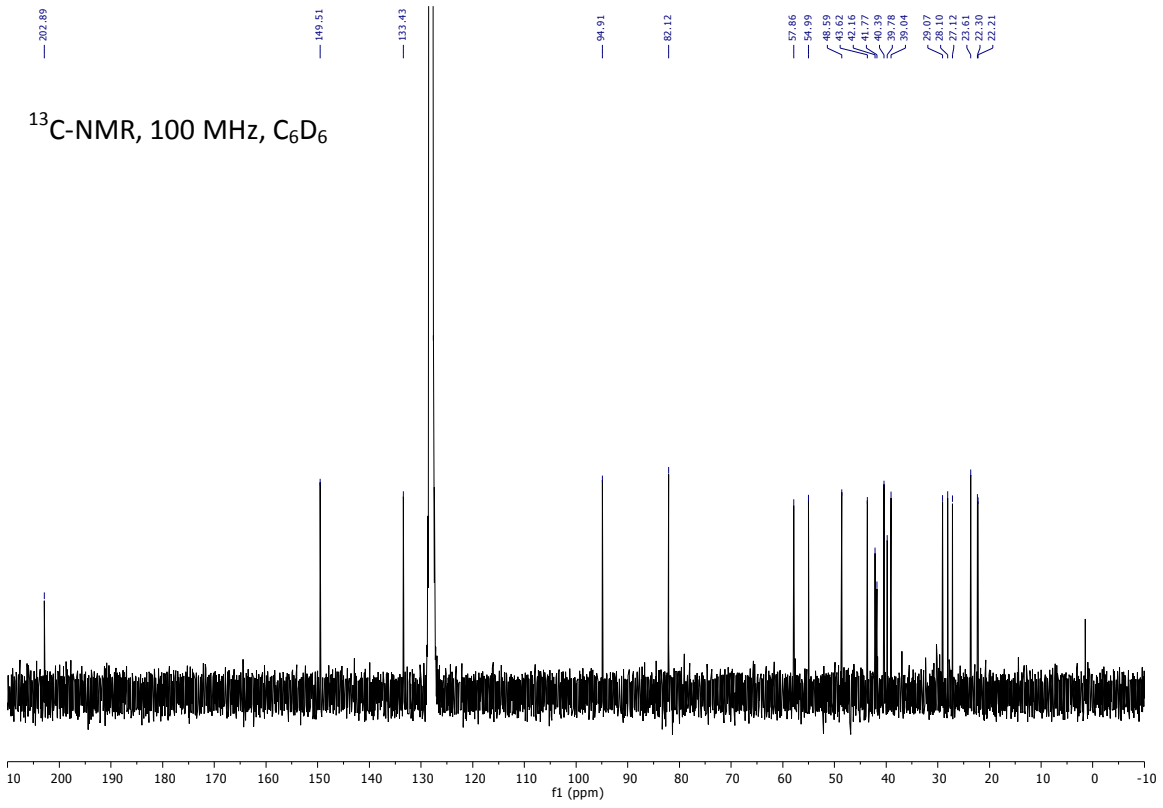


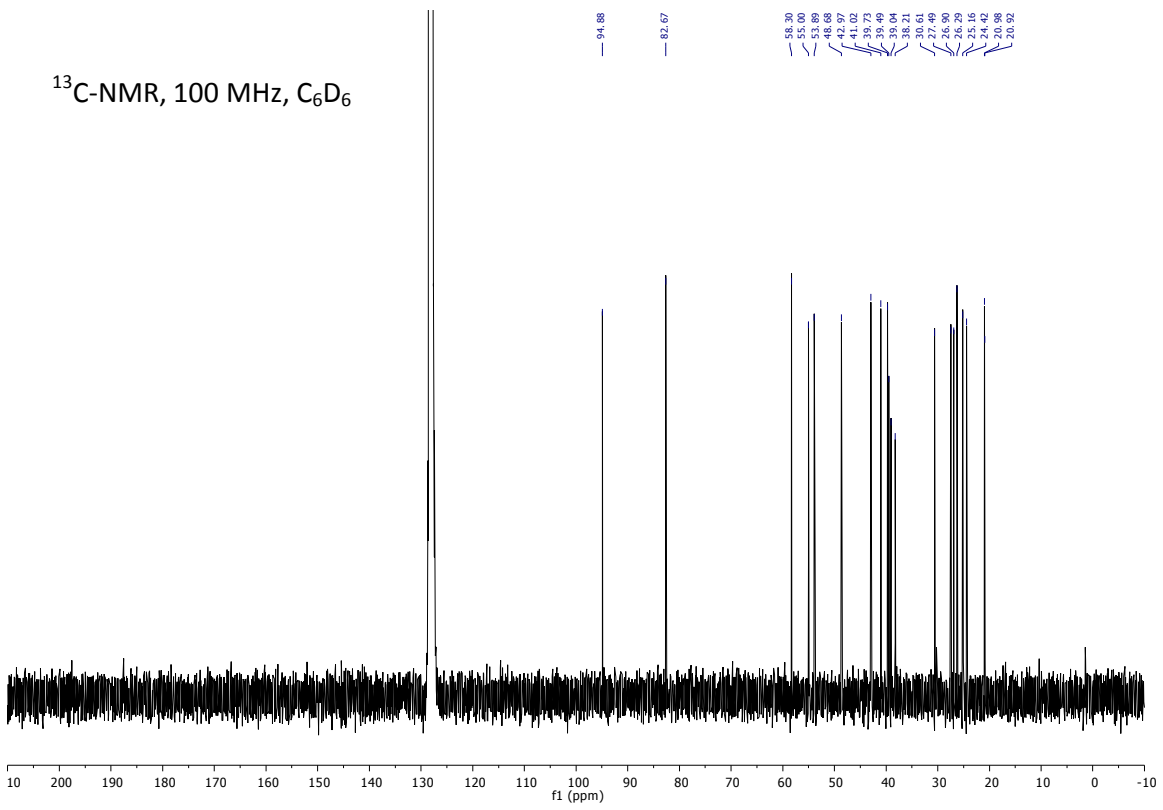
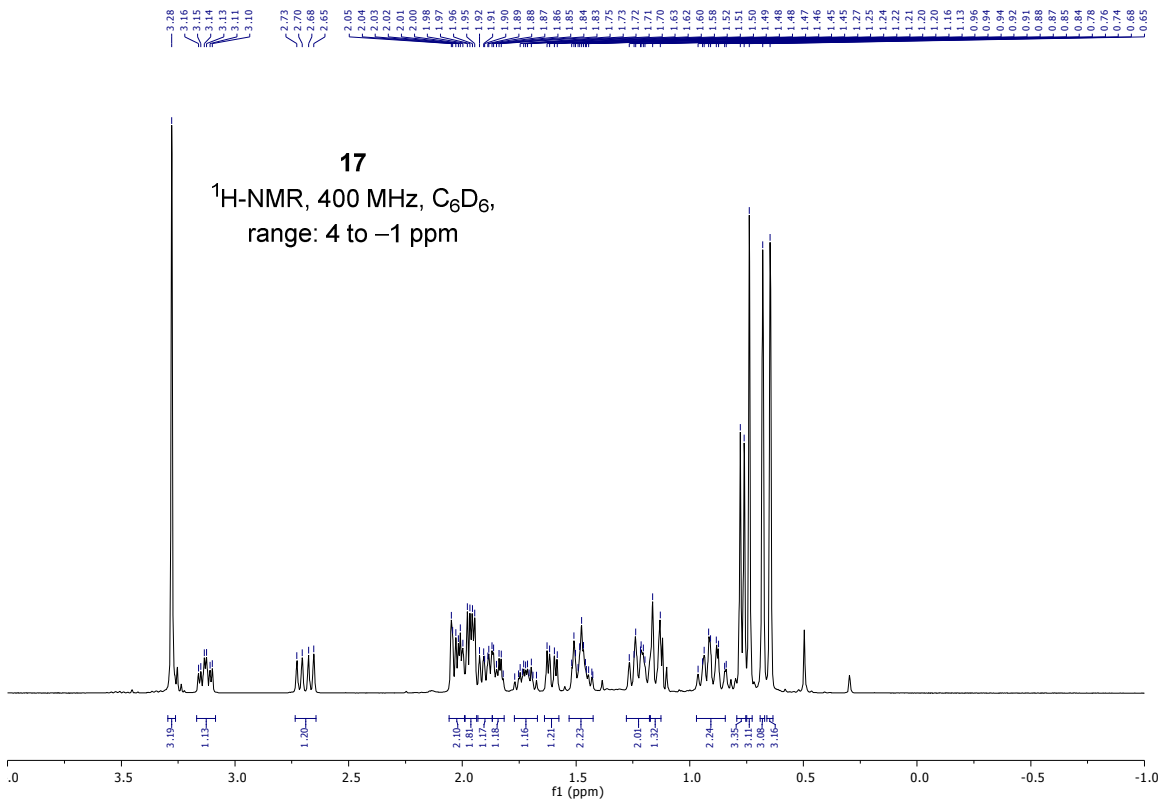


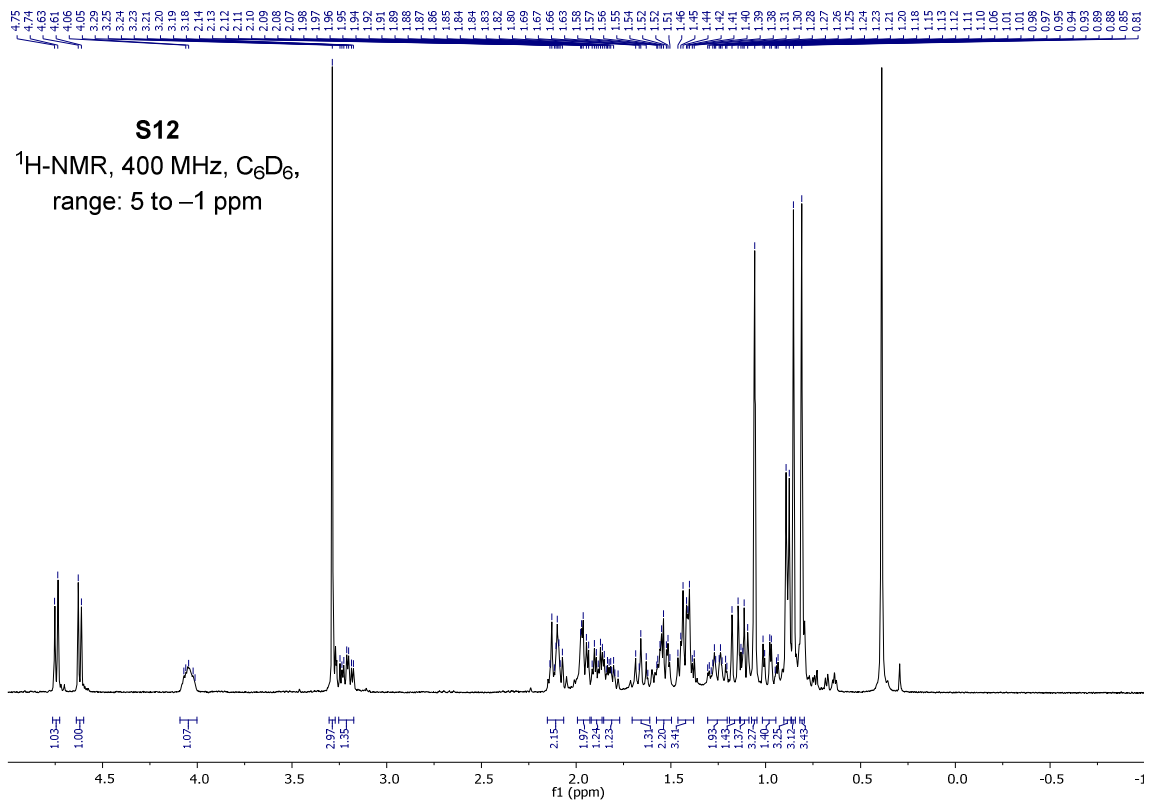
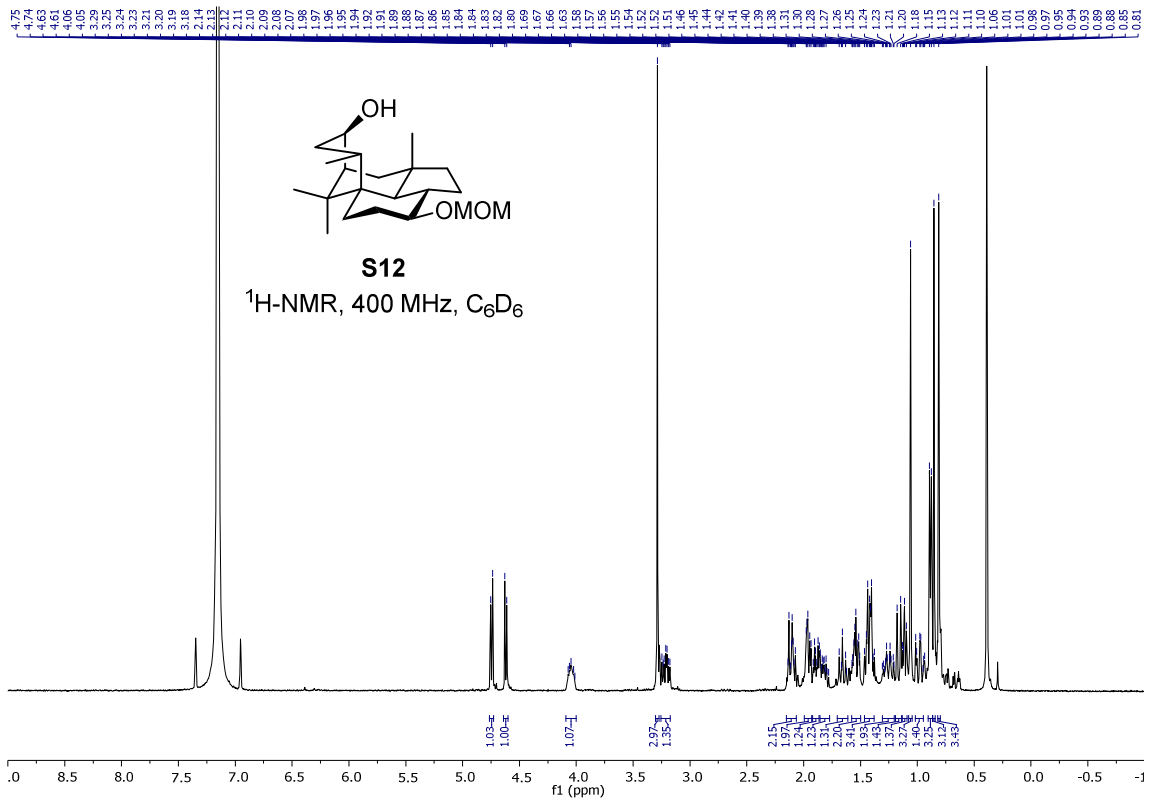


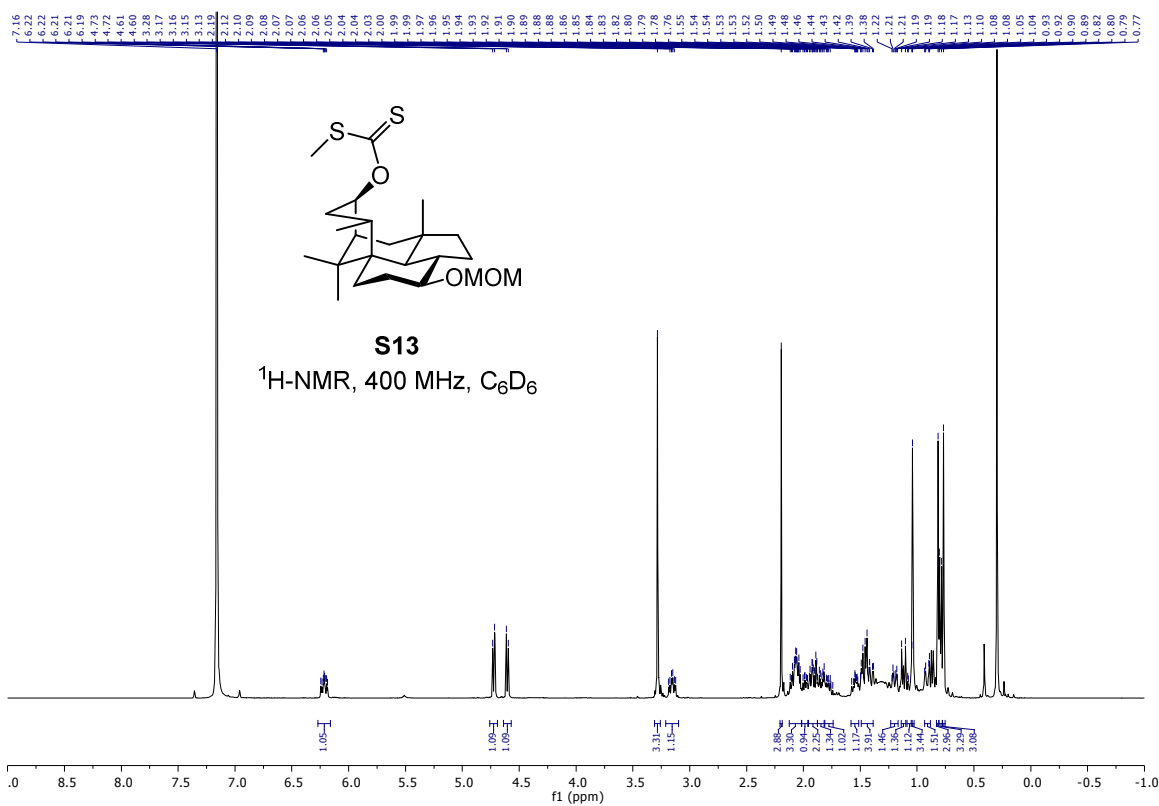
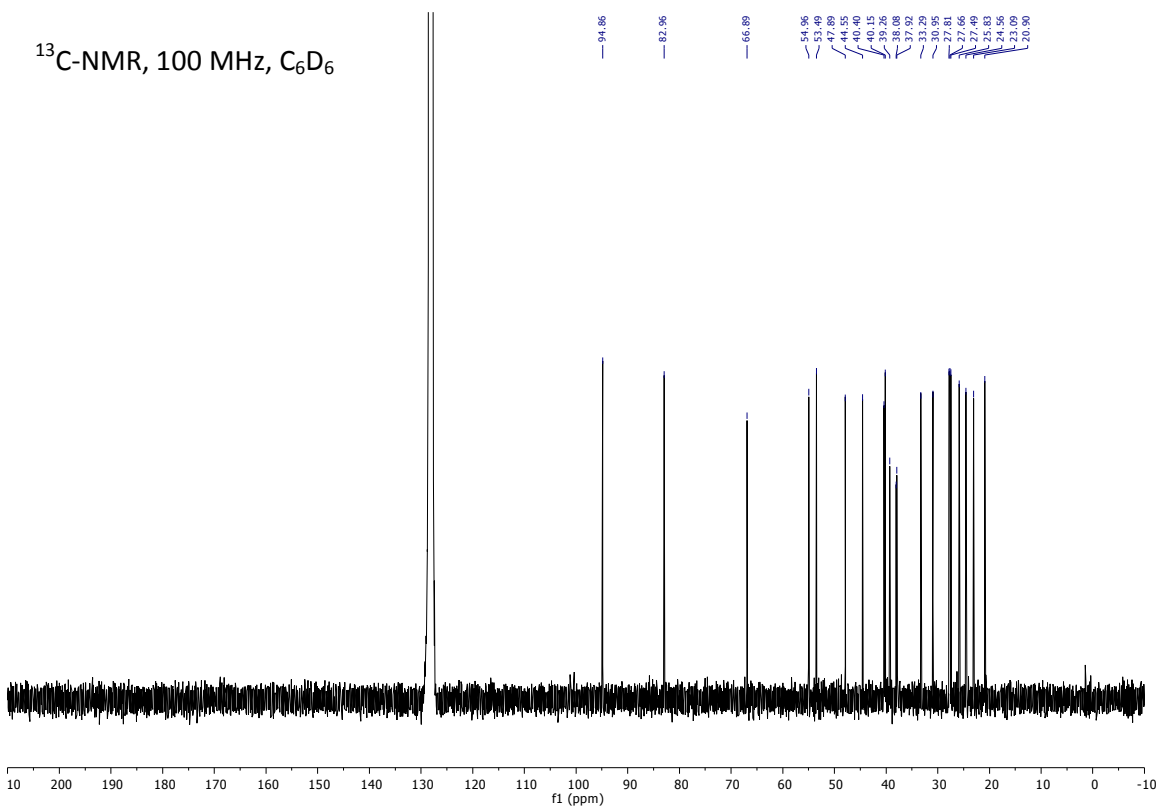


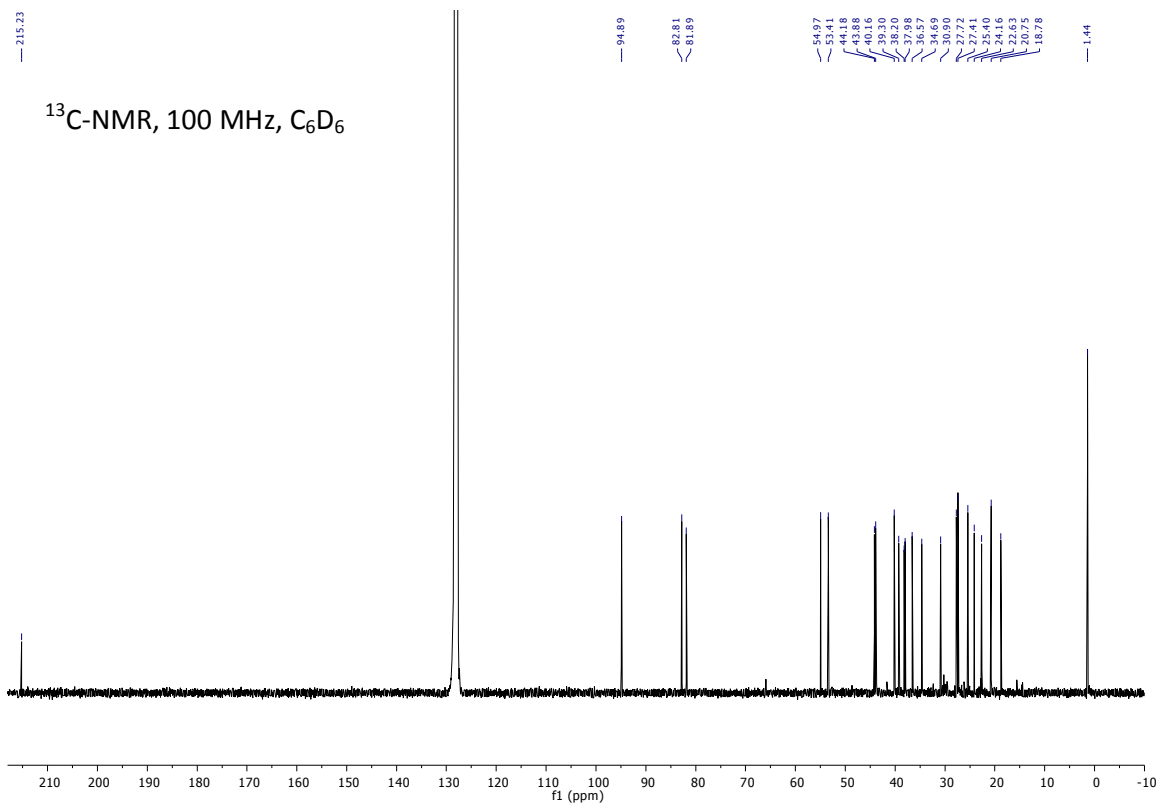
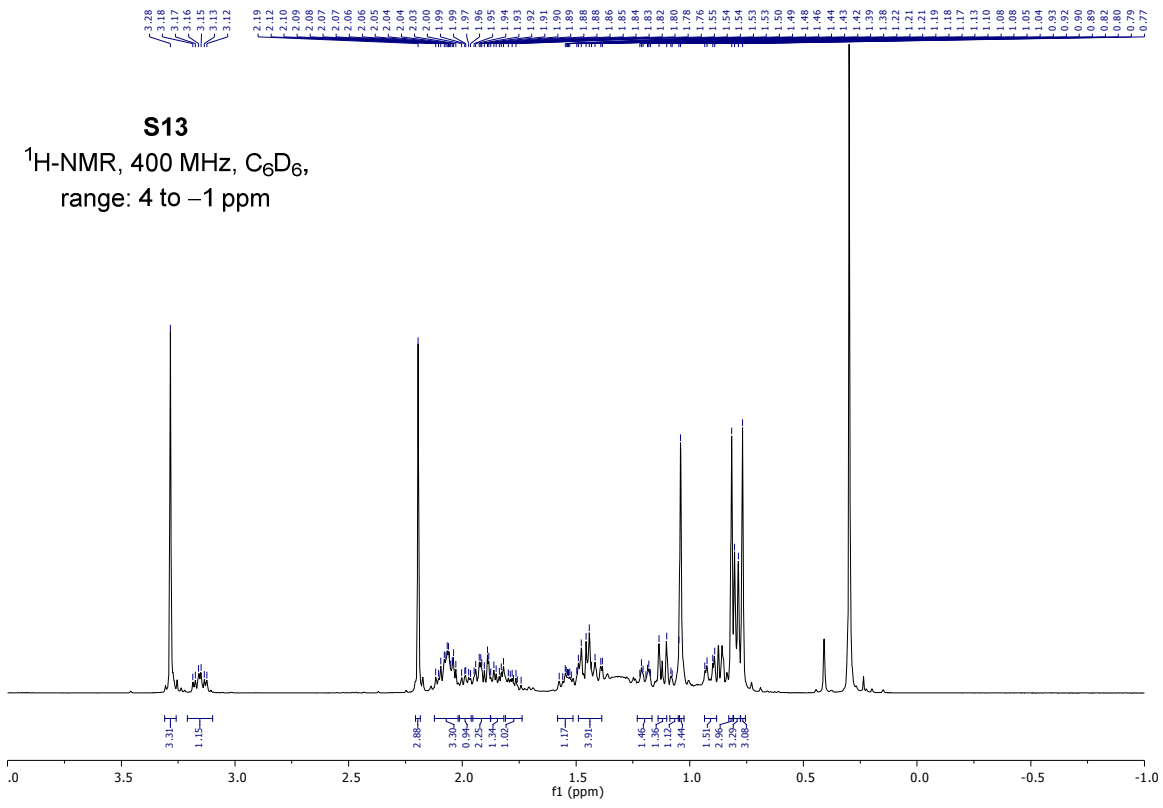


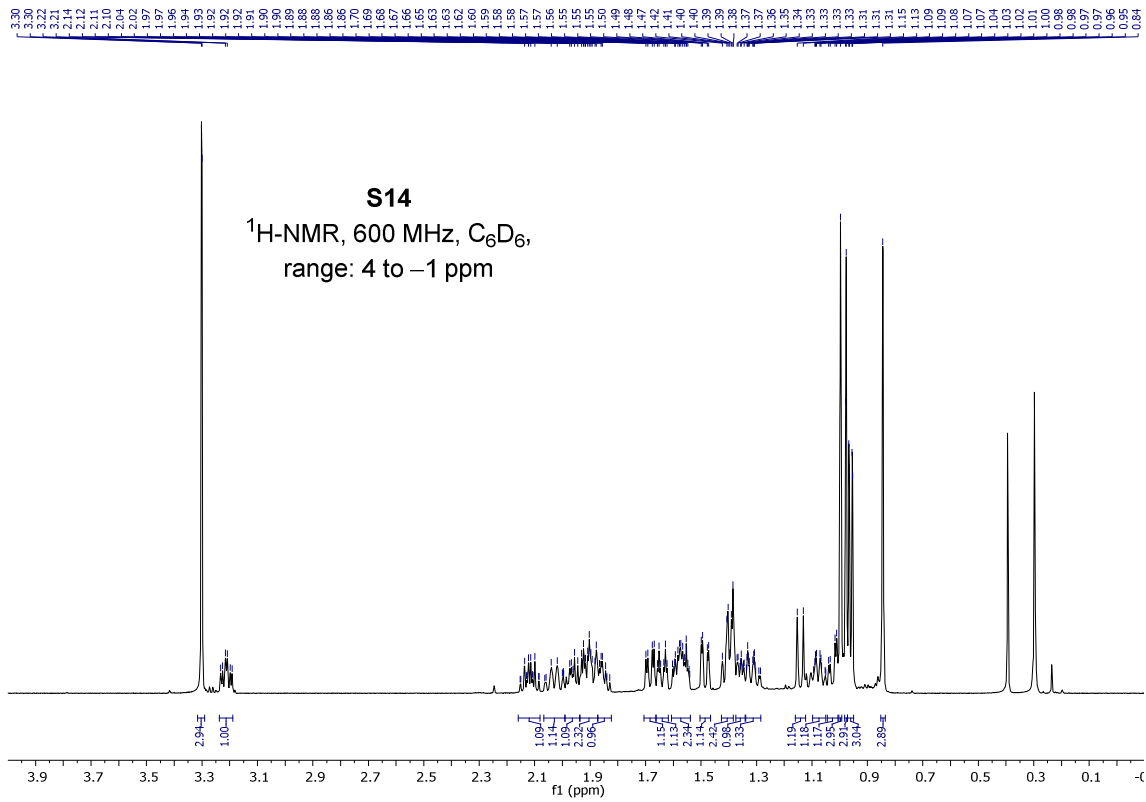
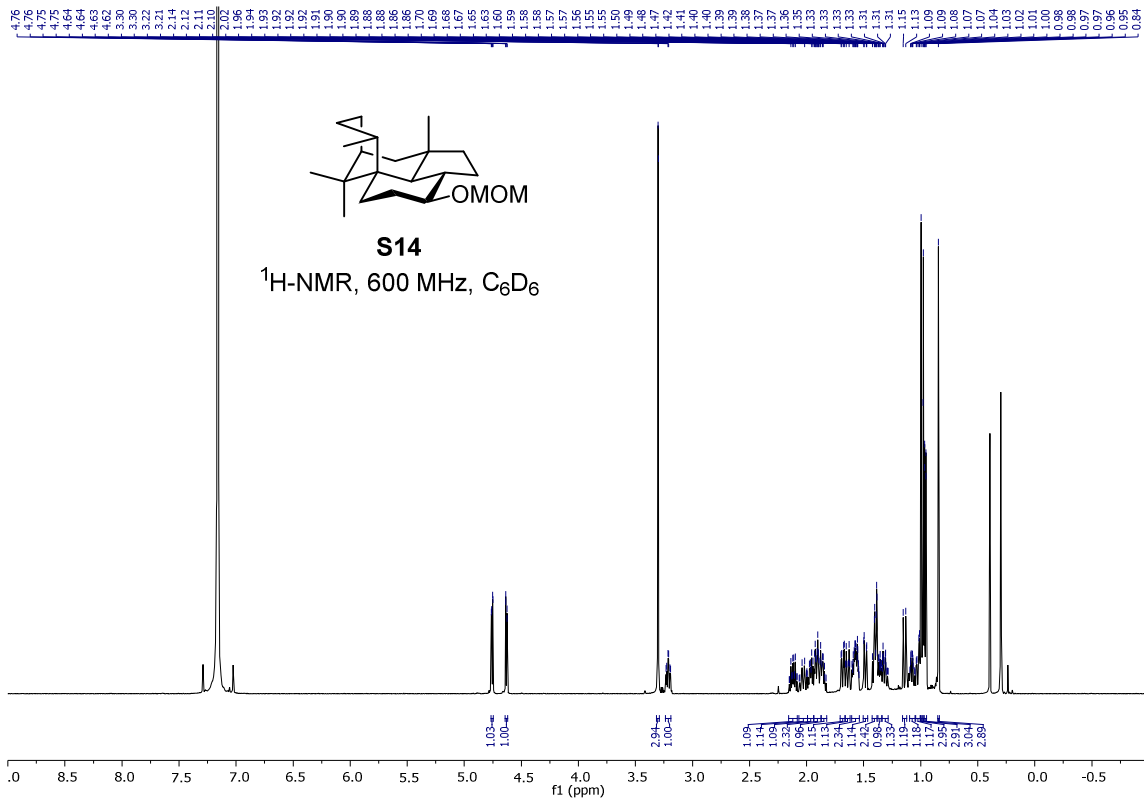


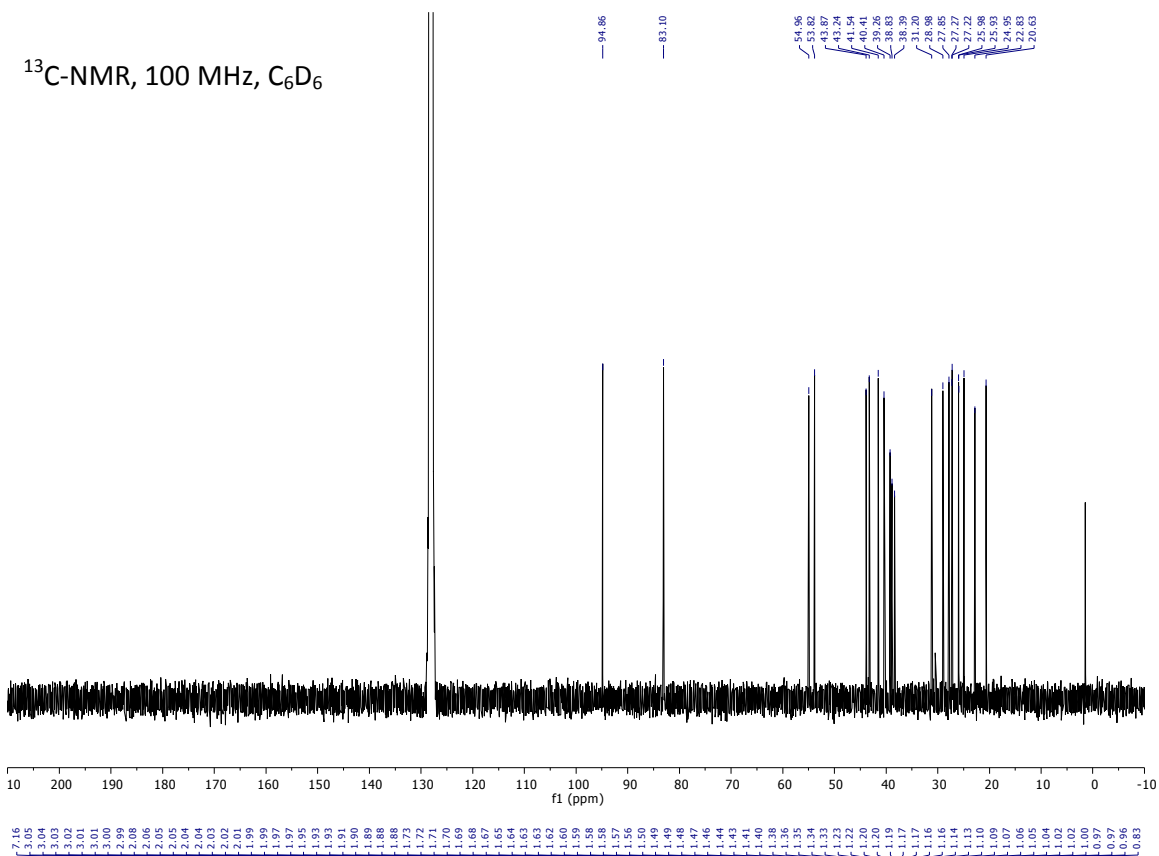






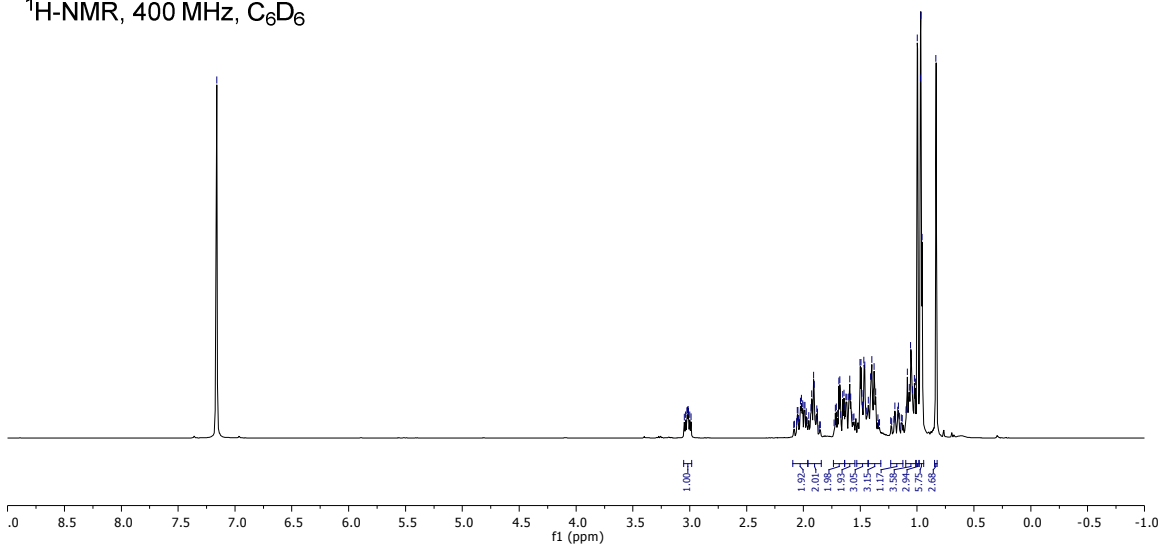






S15

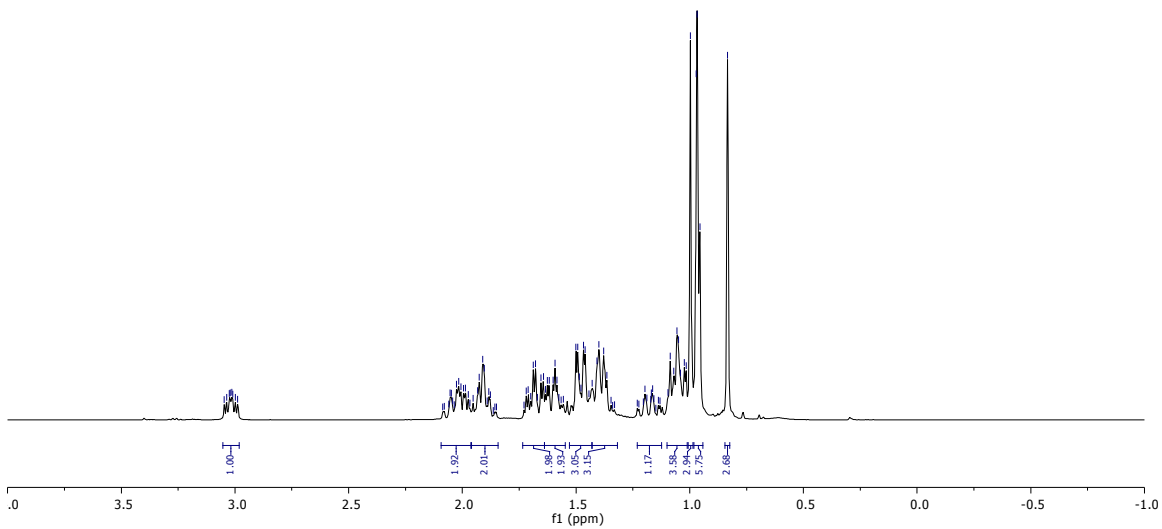
<sup>1</sup>H-NMR, 400 MHz, C<sub>6</sub>D<sub>6</sub>



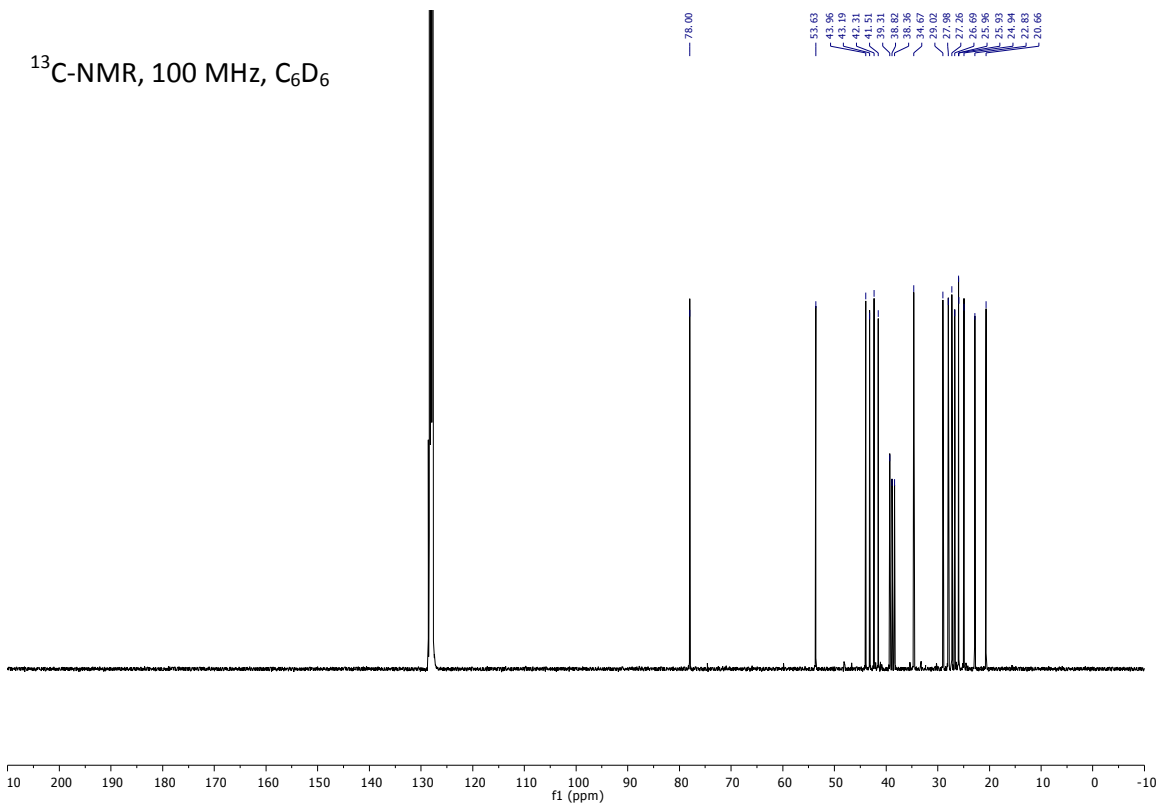


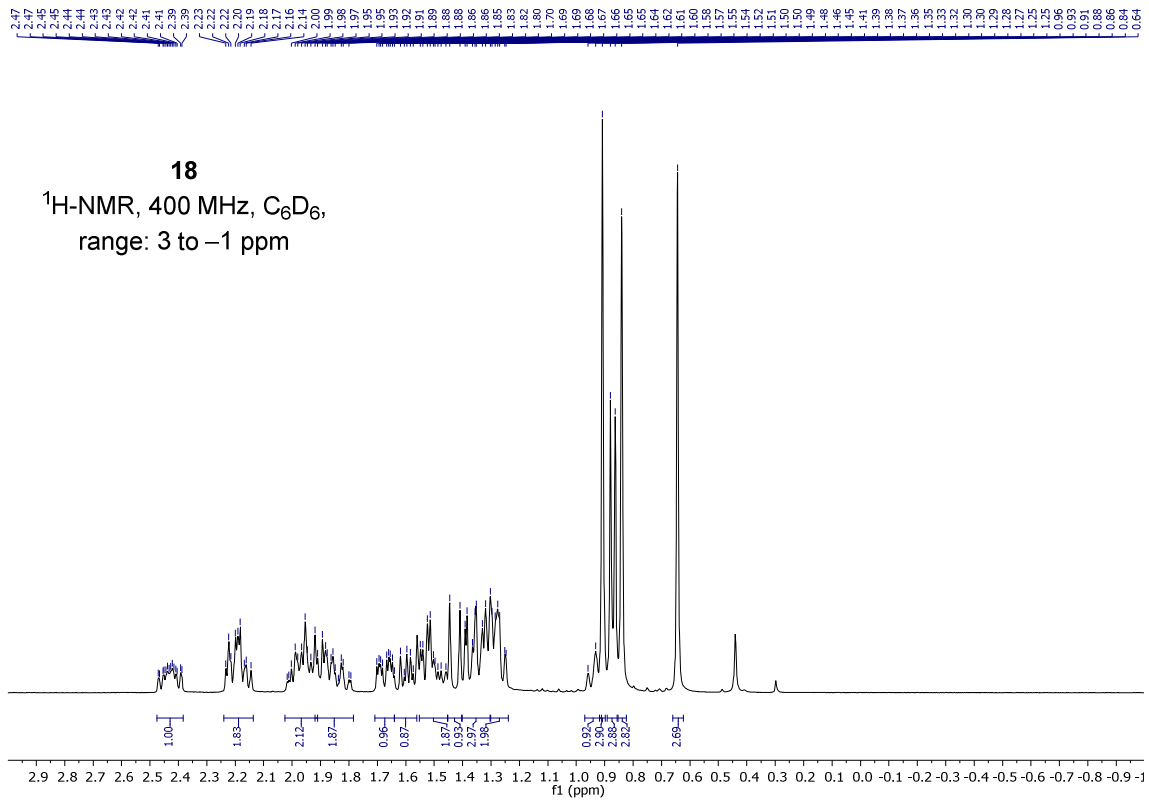
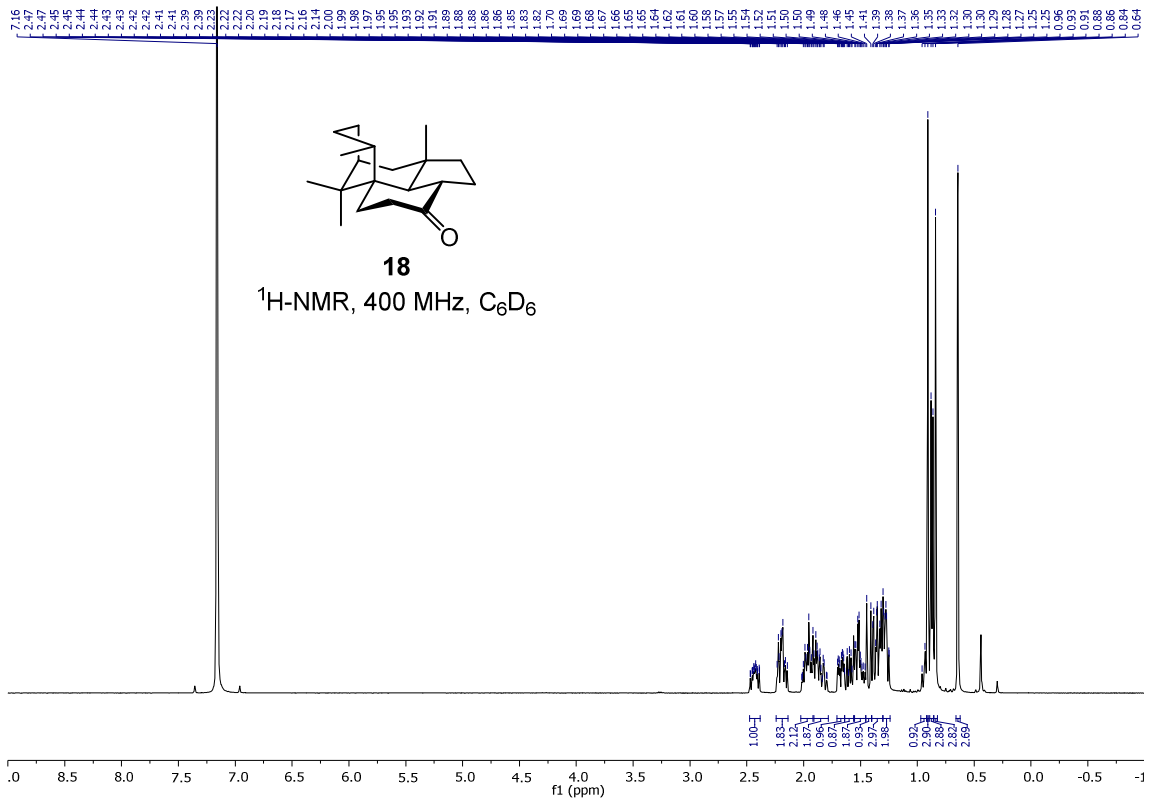
**S15**

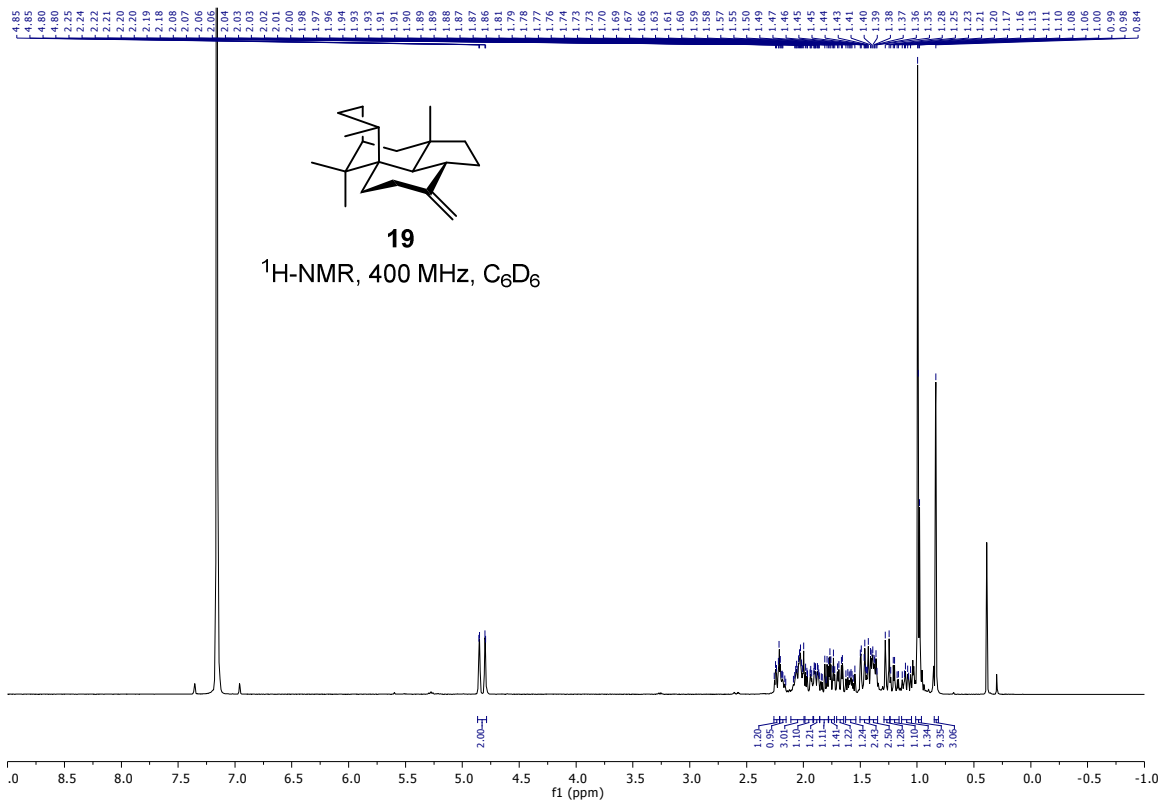
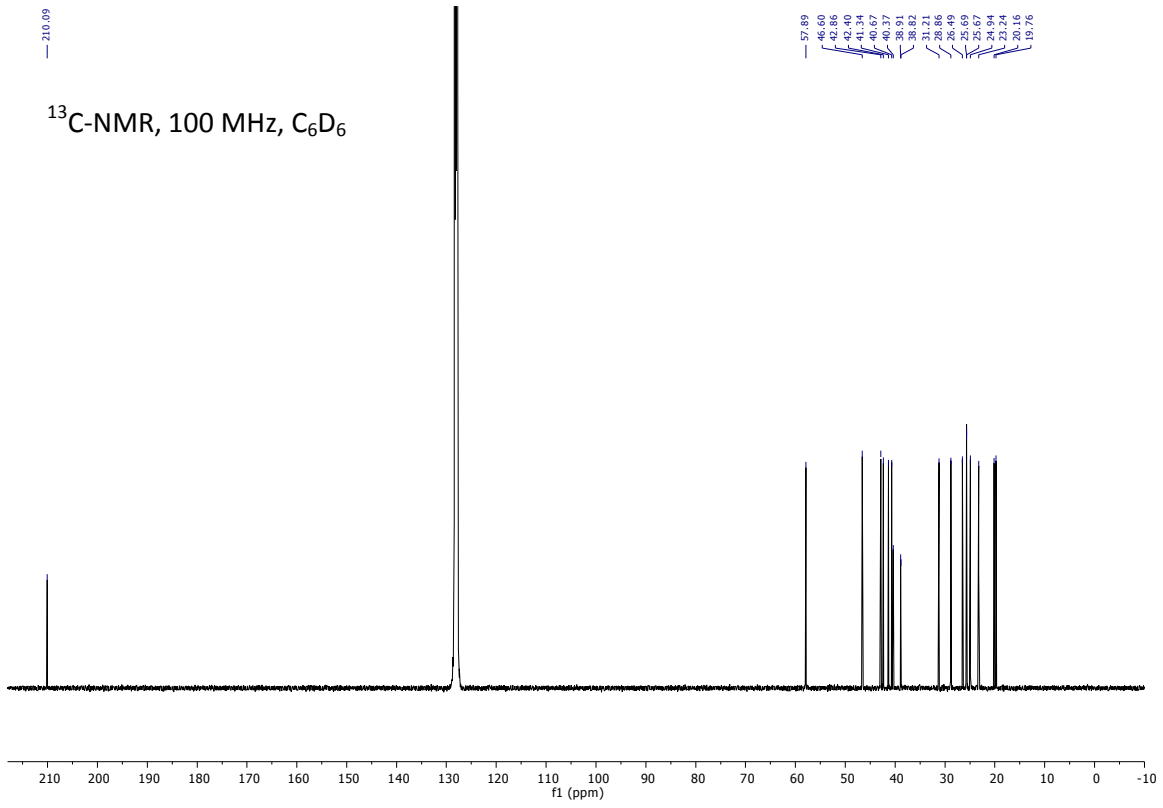
$^1\text{H-NMR}$ , 400 MHz,  $\text{C}_6\text{D}_6$ ,  
range: 4 to  $-1$  ppm

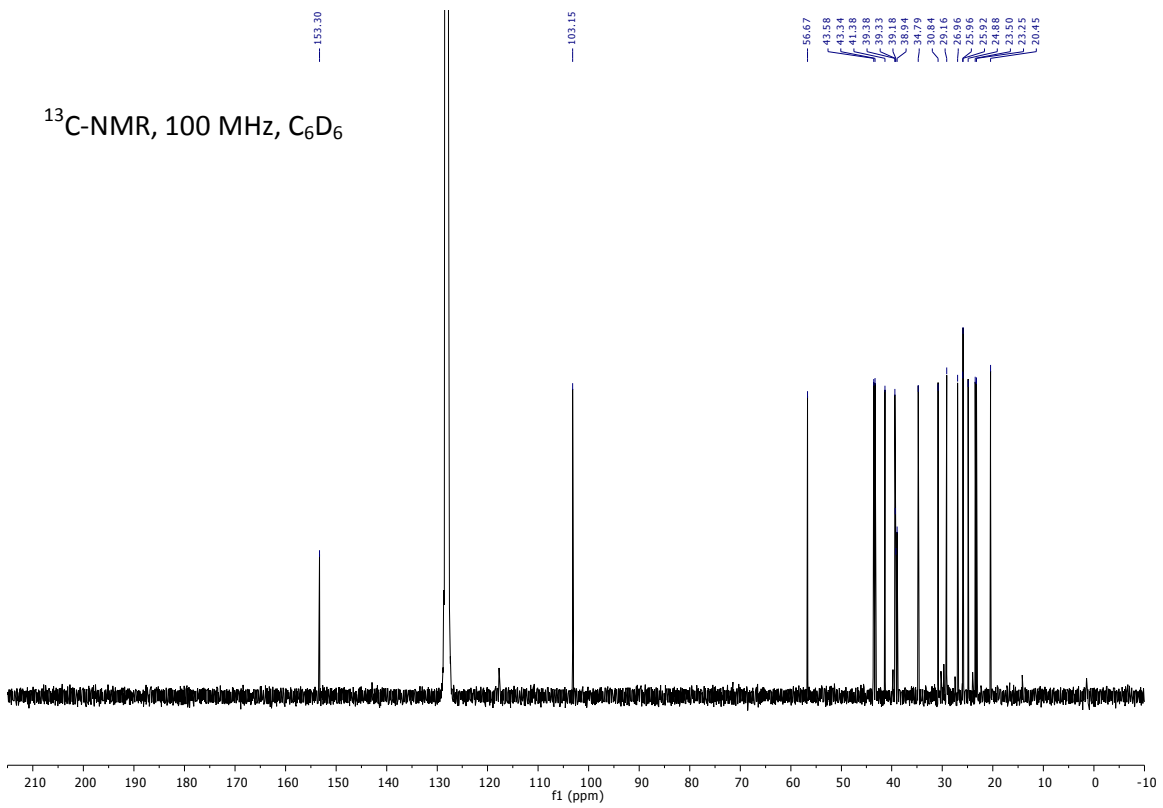
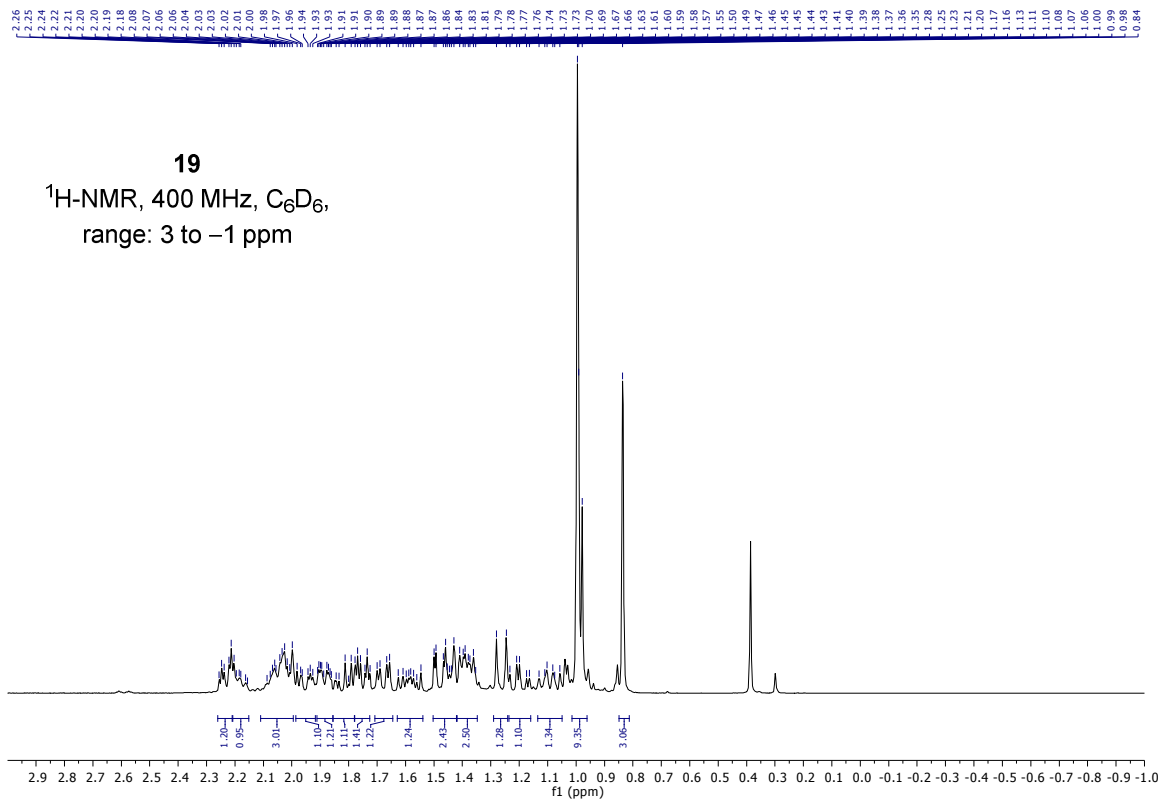


$^{13}\text{C-NMR}$ , 100 MHz,  $\text{C}_6\text{D}_6$



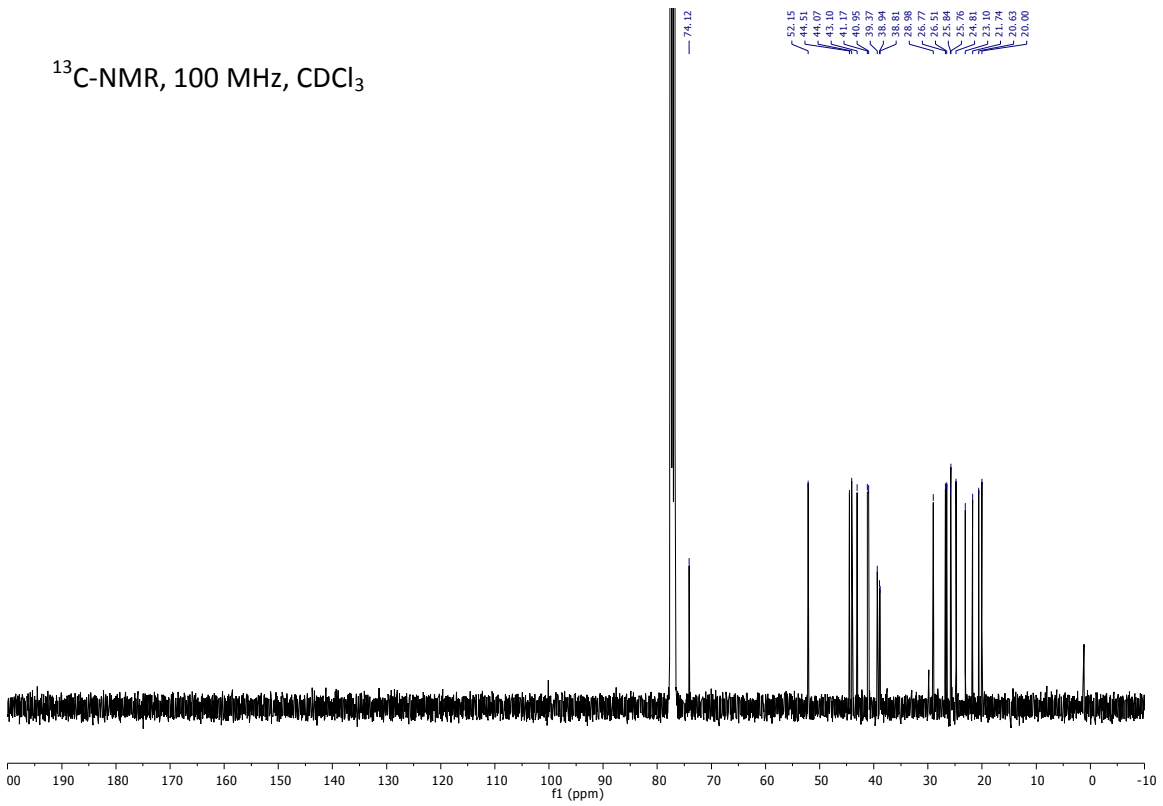
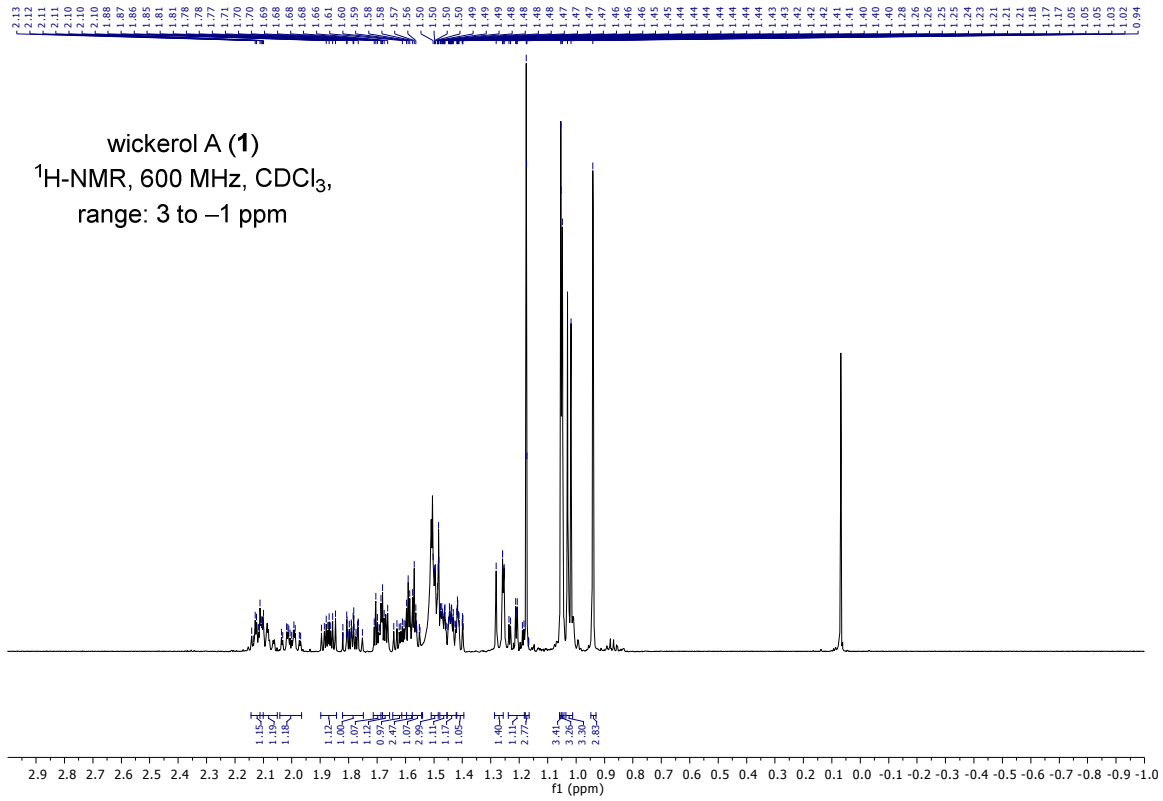


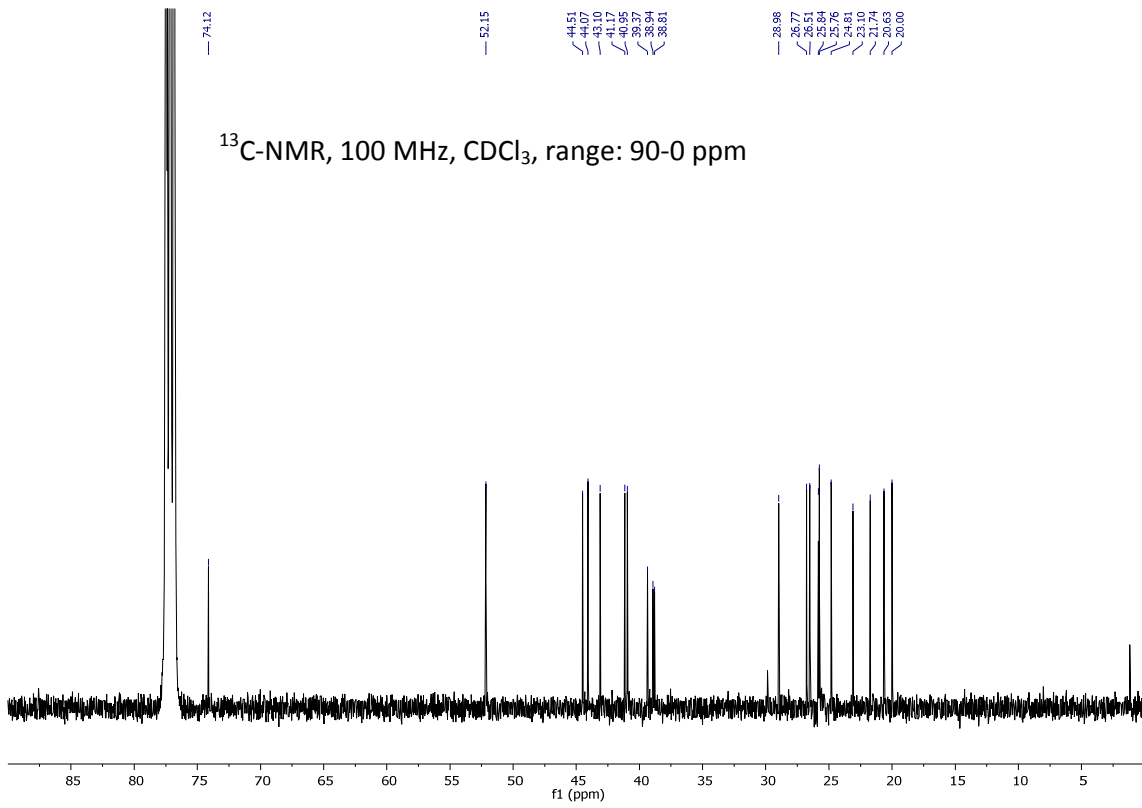












#### 10.4.4. X-ray Crystallographic Data for Chapter 3.3.

##### Diol **21**

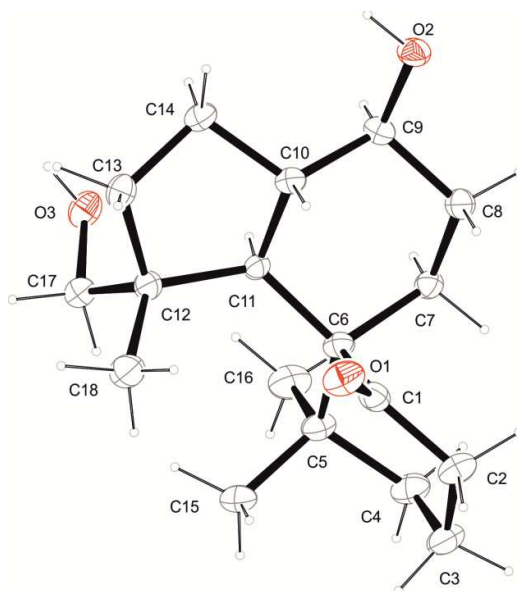


**Figure 10.3.** ORTEP projection of the molecular structure of diol **21**.

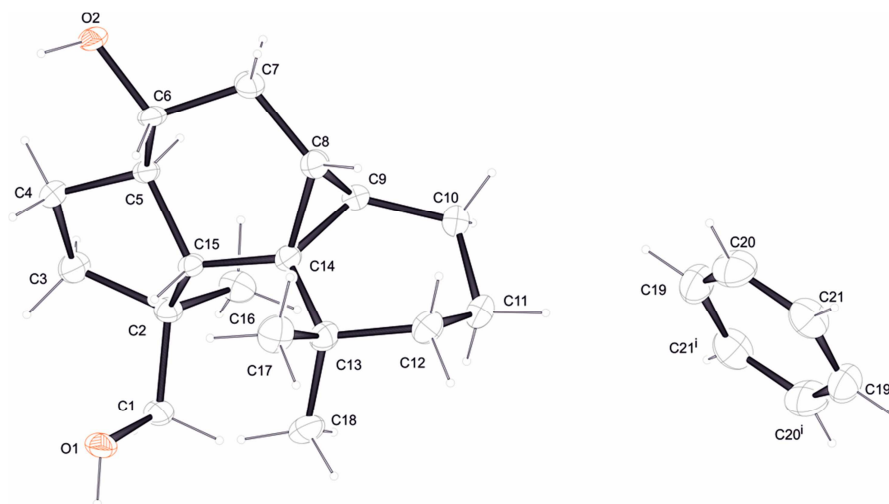
CCDC 1550221 contains the supplementary crystallographic data for diol **21**. These data can be obtained free of charge from The Cambridge Crystallographic Data Centre via [www.ccdc.cam.ac.uk/data\\_request/cif](http://www.ccdc.cam.ac.uk/data_request/cif).

**Table 10.3.** Crystallographic data. for diol **21**.

net formula	$C_{18}H_{30}O_3$
$M_r/g\ mol^{-1}$	294.42
crystal size/mm	$0.100 \times 0.090 \times 0.020$
$T/K$	100.(2)
radiation	MoK $\alpha$
diffractometer	'Bruker D8 Venture TXS'
crystal system	monoclinic
space group	'P 1 21/c 1'
$a/\text{\AA}$	8.5414(4)

$b/\text{\AA}$	27.3619(14)
$c/\text{\AA}$	13.5613(7)
$\alpha/^\circ$	90
$\beta/^\circ$	90.133(2)
$\gamma/^\circ$	90
$V/\text{\AA}^3$	3169.4(3)
$Z$	8
calc. density/ $\text{g cm}^{-3}$	1.234
$\mu/\text{mm}^{-1}$	0.082
absorption correction	Multi-Scan
transmission factor range	0.8773–0.9705
refls. measured	37294
$R_{\text{int}}$	0.0701
mean $\sigma(I)/I$	0.0672
$\theta$ range	3.185–28.283
observed refls.	5887
$x, y$ (weighting scheme)	0.0299, 3.1756
hydrogen refinement	C-H: constr, O-H: refall
refls in refinement	7852
parameters	402
restraints	15
$R(F_{\text{obs}})$	0.0689
$R_w(F^2)$	0.1419
$S$	1.083
shift/error $_{\text{max}}$	0.001
max electron density/ $\text{e \AA}^{-3}$	0.386
min electron density/ $\text{e \AA}^{-3}$	-0.249

Refined as two-component twin (pseudo-merohedral with TWIN -1 0 0 0 -1 0 0 0 1, BASF 0.17209(176)).

Cyclopropane **22**

**Figure 10.4.** ORTEP projection of the molecular structure of cyclopropane **22**.

CCDC 1550223 contains the supplementary crystallographic data for cyclopropane **22**. These data can be obtained free of charge from The Cambridge Crystallographic Data Centre via [www.ccdc.cam.ac.uk/data\\_request/cif](http://www.ccdc.cam.ac.uk/data_request/cif).

**Table 10.4.** Crystallographic data. for cyclopropane **22**.

net formula	$C_{21}H_{33}O_2$
$M_r/g\ mol^{-1}$	317.47
crystal size/mm	$0.090 \times 0.070 \times 0.040$
$T/K$	100.(2)
radiation	MoK $\alpha$
diffractometer	'Bruker D8 Venture TXS'
crystal system	triclinic
space group	'P -1'
$a/\text{\AA}$	8.8933(3)
$b/\text{\AA}$	9.3676(4)
$c/\text{\AA}$	11.1619(5)
$\alpha/^\circ$	95.392(2)

---

$\beta/^\circ$	104.2140(10)
$\gamma/^\circ$	90.3290(10)
$V/\text{\AA}^3$	897.03(6)
$Z$	2
calc. density/ $\text{g cm}^{-3}$	1.175
$\mu/\text{mm}^{-1}$	0.073
absorption correction	Multi-Scan
transmission factor range	0.9347–0.9705
refls. measured	9511
$R_{\text{int}}$	0.0313
mean $\sigma(I)/I$	0.0421
$\theta$ range	3.171–26.368
observed refls.	2842
$x, y$ (weighting scheme)	0.0389, 0.4511
hydrogen refinement	H(C) constr, H(O) refall
refls in refinement	3620
parameters	219
restraints	0
$R(F_{\text{obs}})$	0.0446
$R_w(F^2)$	0.1102
$S$	1.026
shift/error <sub>max</sub>	0.001
max electron density/ $\text{e \AA}^{-3}$	0.244
min electron density/ $\text{e \AA}^{-3}$	-0.206

## 3. Enone 16

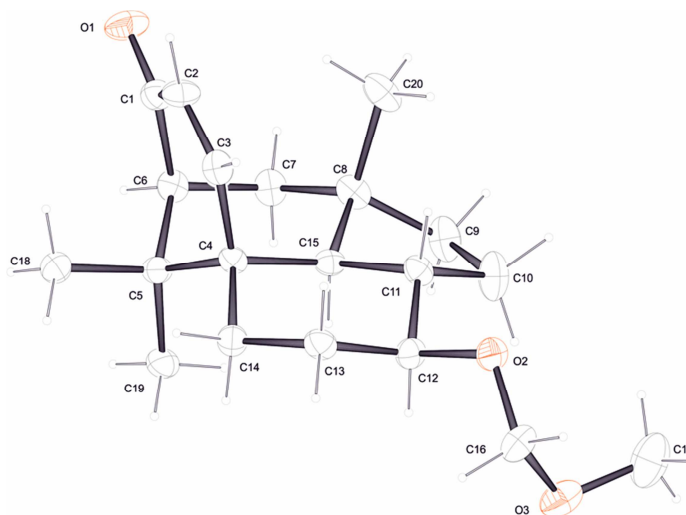


**Figure 10.5.** ORTEP projection of the molecular structure of enone **16**.

CCDC 1550222 contains the supplementary crystallographic data for enone **16**. These data can be obtained free of charge from The Cambridge Crystallographic Data Centre via [www.ccdc.cam.ac.uk/data\\_request/cif](http://www.ccdc.cam.ac.uk/data_request/cif).

**Table 10.5.** Crystallographic data for enone **16**.

net formula	$C_{20}H_{30}O_3$
$M_r/g\ mol^{-1}$	318.44
crystal size/mm	$0.090 \times 0.070 \times 0.010$
$T/K$	100.(2)
radiation	MoK $\alpha$
diffractometer	'Bruker D8 Venture TXS'
crystal system	tetragonal
space group	'P 43 21 2'
$a/\text{\AA}$	10.7220(4)
$b/\text{\AA}$	10.7220(4)
$c/\text{\AA}$	60.769(2)
$\alpha/^\circ$	90
$\beta/^\circ$	90
$\gamma/^\circ$	90

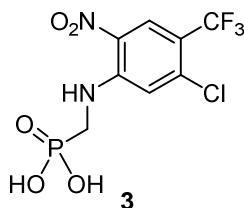
$V/\text{\AA}^3$	6986.1(6)
$Z$	16
calc. density/g cm <sup>-3</sup>	1.211
$\mu/\text{mm}^{-1}$	0.079
absorption correction	Multi-Scan
transmission factor range	0.8421–0.9705
refls. measured	18900
$R_{\text{int}}$	0.0433
mean $\sigma(I)/I$	0.0471
$\theta$ range	3.167–25.350
observed refls.	5876
$x, y$ (weighting scheme)	0.0484, 5.5202
hydrogen refinement	constr
Flack parameter	0.5
refls in refinement	6376
parameters	423
restraints	10
$R(F_{\text{obs}})$	0.0606
$R_w(F^2)$	0.1443
$S$	1.198
shift/error <sub>max</sub>	0.002
max electron density/e $\text{\AA}^{-3}$	0.246
min electron density/e $\text{\AA}^{-3}$	-0.292

There are two disordered atoms in a side chain. They have been isotropically refined in a split model. Fig. 3 shows only the ordered molecule.

## 10.5. Supporting Information for Chapter 7.1.

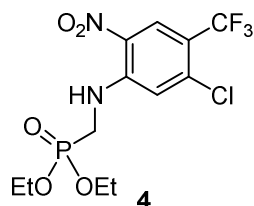
### 10.5.1. Experimental Procedures 7.1.

#### Synthesis and characterization of compound **3**



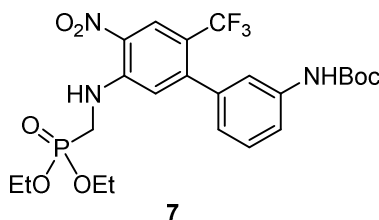
To a suspension of compound **2** (3.12 g, 12.0 mmol) in EtOH/H<sub>2</sub>O (100 mL, 1:1) at r.t. was added compound **1** (1.29 g, 11.6 mmol) and Na<sub>2</sub>CO<sub>3</sub> (1.32 g, 12.5 mmol). The resulting mixture was heated to 105 °C for 6 h. The reaction mixture was cooled to r.t. and the EtOH was removed under reduced pressure. The resulting mixture was diluted with H<sub>2</sub>O (100 mL) and washed with EtOAc (100 mL). The aqueous phase was acidified with 1 M HCl (40 mL) and extracted with EtOAc (3 × 100 mL). The combined organic extracts were washed with H<sub>2</sub>O (40 mL), dried over Na<sub>2</sub>SO<sub>4</sub>, filtered and concentrated under reduced pressure to afford compound **3** (1.37 g, 68%) as a yellow solid.

**mp:** 207 – 209 °C decomp; **<sup>1</sup>H NMR** (400 MHz, CD<sub>3</sub>OD): δ 8.47 (s, 1H), 7.39 (s, 1H), 3.82 (d, *J* = 13.0 Hz, 2H); **<sup>13</sup>C NMR** (100 MHz, CD<sub>3</sub>OD): δ 148.1 (d, *J* = 6.0 Hz), 139.9, 131.2, 127.7 (q, *J* = 6.0 Hz), 124.0 (q, *J* = 270.5 Hz), 118.5, 116.0 (q, *J* = 33.0 Hz), 41.2 (d, *J* = 152.5 Hz); **<sup>19</sup>F NMR** (376 MHz, CD<sub>3</sub>OD): δ -62.7; **<sup>31</sup>P NMR** (162 MHz, CD<sub>3</sub>OD): δ 18.6; **IR** (neat): 3350, 2767, 1621, 1575, 1525, 1511, 1426, 1413, 1353, 1301, 1272, 1234, 1209, 1176, 1131, 1114, 1073, 1014, 946, 917, 877, 846, 742, 702 cm<sup>-1</sup>; **HRMS** (ESI, *m/z*): [(M-H)<sup>-</sup>] calcd. for C<sub>8</sub>H<sub>6</sub>ClF<sub>3</sub>N<sub>2</sub>O<sub>5</sub>P<sup>-</sup>, 332.9660; found 332.9665.

**Synthesis and characterization of compound 4**

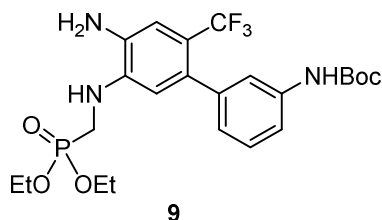
To a solution of compound **3** (1.67 g, 5.00 mmol) in triethyl orthoformate (22.3 g, 150 mmol, 25 mL) at r.t. was added *p*-TsOH (190 mg, 1.00 mmol). The resulting mixture was heated to 150 °C and stirred for 3.5 h. The reaction mixture was cooled to r.t. and concentrated under reduced pressure. The residue was diluted with H<sub>2</sub>O (40 mL) and extracted with EtOAc (2 × 40 mL). The combined organic extracts were dried over Na<sub>2</sub>SO<sub>4</sub>, filtered and concentrated under reduced pressure. Purification by flash column chromatography on silica gel eluting with *i*-Hex/EtOAc (1:1) afforded compound **4** (1.61 g, 82%) as a yellow solid.

**mp:** 87 – 89 °C; **TLC** (*i*-Hex/EtOAc, 1:1): R<sub>f</sub> = 0.20 (UV/KMnO<sub>4</sub>); **<sup>1</sup>H NMR** (400 MHz, CDCl<sub>3</sub>): δ 8.51 (s, 1H), 8.50 – 8.41 (m, 1H), 7.09 (s, 1H), 4.27 – 4.12 (m, 4H), 3.71 (dd, *J* = 13.5, 6.0 Hz, 2H), 1.35 (t, *J* = 7.0 Hz, 6H); **<sup>13</sup>C NMR** (100 MHz, CDCl<sub>3</sub>): δ 146.4 (d, *J* = 6.5 Hz), 139.9, 130.2, 127.2 (q, *J* = 5.5 Hz), 122.3 (q, *J* = 271.5 Hz), 116.6, 116.5 (q, *J* = 33.5 Hz), 63.23 (d, *J* = 7.0 Hz), 39.6 (d, *J* = 157.8 Hz), 16.6 (d, *J* = 6.0 Hz); **<sup>19</sup>F NMR** (376 MHz, CDCl<sub>3</sub>): δ –61.6; **<sup>31</sup>P NMR** (162 MHz, CDCl<sub>3</sub>): δ 20.0; **IR** (thin film): 3361, 2985, 1621, 1579, 1530, 1435, 1354, 1317, 1302, 1243, 1205, 1157, 1126, 1049, 1024, 969, 945, 917, 897, 838, 781, 764, 702 cm<sup>-1</sup>; **HRMS** (ESI, *m/z*): [(*M*-H)<sup>-</sup>] calcd. for C<sub>12</sub>H<sub>14</sub>ClF<sub>3</sub>N<sub>2</sub>O<sub>5</sub>P<sup>-</sup>, 389.0286; found 389.0296.

**Synthesis and characterization of compound 7**

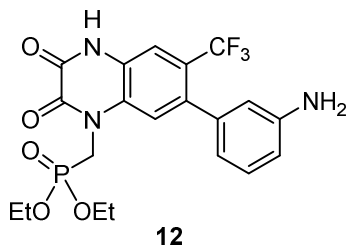
To a mixture of compound **4** (781 mg, 2.00 mmol) and 3-(*N*-boc-amino)phenylboronic acid (**5**) (522 mg, 2.20 mmol) in PhMe/EtOH (3.5:1, 45 mL) at r.t. under argon was added a solution of Na<sub>2</sub>CO<sub>3</sub> (4 mL, 2.0 m in H<sub>2</sub>O) and Pd(PPh<sub>3</sub>)<sub>4</sub> (116 mg, 0.100 mmol). The resulting mixture was degassed and flushed with argon (× 3) and then heated to 95 °C for 17 h. The reaction mixture was cooled to r.t., concentrated under reduced pressure and the resulting residue was directly purified by flash column chromatography eluting with CH<sub>2</sub>Cl<sub>2</sub>/EtOAc (4:1) to afford compound **7** (873 mg, 80%) as a yellow oil.

**TLC** (CH<sub>2</sub>Cl<sub>2</sub>/EtOAc, 4:1): R<sub>f</sub> = 0.41 (UV/ninhydrin); **<sup>1</sup>H NMR** (400 MHz, CDCl<sub>3</sub>): δ 8.57 (s, 1H), 8.45 (q, *J* = 6.0 Hz, 1H), 7.44 – 7.36 (m, 2H), 7.35 – 7.28 (m, 1H), 6.97 (d, *J* = 7.5 Hz, 1H), 6.83 (s, 1H), 6.64 (s, 1H), 4.18 (dq, *J* = 8.5, 7.0 Hz, 4H), 3.69 (dd, *J* = 13.5, 6.0 Hz, 2H), 1.51 (s, 9H), 1.33 (t, *J* = 7.0 Hz, 6H); **<sup>13</sup>C NMR** (100 MHz, CDCl<sub>3</sub>): δ 152.7, 148.6 (q, *J* = 1.5 Hz), 145.5 (d, *J* = 7.5 Hz), 139.0, 138.3, 130.8, 128.8, 126.1 (q, *J* = 6.0 Hz), 123.4 (q, *J* = 272.5 Hz), 123.0 (q, *J* = 1.5 Hz), 118.6, 118.4, 117.6, 117.4 (q, *J* = 32.0 Hz), 80.8, 63.1 (d, *J* = 7.0 Hz), 39.4 (d, *J* = 157.0 Hz), 28.4, 16.6 (d, *J* = 5.5 Hz); **<sup>19</sup>F NMR** (376 MHz, CDCl<sub>3</sub>): δ -56.6; **<sup>31</sup>P NMR** (162 MHz, CDCl<sub>3</sub>): δ 20.5; **IR** (thin film): 3355, 2981, 2931, 1720, 1625, 1609, 1575, 1532, 1486, 1427, 1346, 1305, 1268, 1235, 1153, 1122, 1048, 1019, 971, 794, 764, 735 cm<sup>-1</sup>; **HRMS** (ESI, *m/z*): [(*M*+Na)<sup>+</sup>] calcd. for C<sub>23</sub>H<sub>29</sub>F<sub>3</sub>N<sub>3</sub>NaO<sub>7</sub>P<sup>+</sup>, 570.1587; found 570.1590.

**Synthesis and characterization of compound 9**

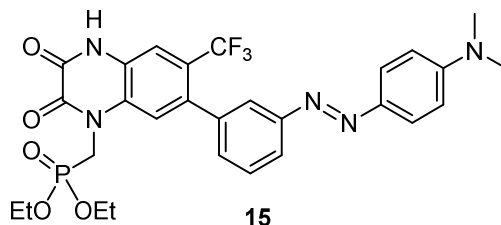
To a solution of compound **7** (1.04 g, 1.90 mmol) in MeOH (30 mL) at r.t. was added Pd/C (104 mg, 10 wt. % Pd labelling). The reaction vessel was flushed with hydrogen ( $\times 3$ ) and the resulting mixture was stirred at r.t. for 8 h. The reaction mixture was filtered through a pad of Celite® washing with MeOH (30 mL). The filtrate was concentrated under reduced pressure to afford compound **9** (876 mg, 89%) as a pale brown oil, which was used in the next step without further purification.

**TLC** (CH<sub>2</sub>Cl<sub>2</sub>/MeOH, 19:1): R<sub>f</sub> = 0.27 (UV/ninhydrin); **<sup>1</sup>H NMR** (400 MHz, CD<sub>3</sub>OD):  $\delta$  7.42 – 7.31 (m, 2H), 7.25 – 7.18 (m, 1H), 7.05 (s, 1H), 6.93 (d,  $J$  = 7.5 Hz, 1H), 6.60 (s, 1H), 4.11 (dq,  $J$  = 8.0, 7.0 Hz, 4H), 3.69 (d,  $J$  = 10.5 Hz, 2H), 1.51 (s, 9H), 1.27 (dt,  $J$  = 7.0, 0.5 Hz, 6H); **<sup>13</sup>C NMR** (100 MHz, CD<sub>3</sub>OD):  $\delta$  155.3, 143.1, 139.9, 139.4 – 139.3 (m), 135.0, 133.9 (q,  $J$  = 2.0 Hz), 128.8, 126.4 (q,  $J$  = 271.5 Hz), 124.9 (q,  $J$  = 2.0 Hz), 121.1 – 120.8 (m), 118.7 (q,  $J$  = 30.0 Hz), 118.5 – 118.3 (m), 115.4 – 115.2 (m), 114.2 (q,  $J$  = 5.5 Hz), 80.8, 64.0 (d,  $J$  = 7.0 Hz), 40.3 (d,  $J$  = 158.5 Hz), 28.7, 16.7 (d,  $J$  = 5.5 Hz); **<sup>19</sup>F NMR** (376 MHz, CD<sub>3</sub>OD):  $\delta$  -56.2; **<sup>31</sup>P NMR** (162 MHz, CD<sub>3</sub>OD):  $\delta$  25.0; **IR** (thin film): 3362, 2979, 2936, 1703, 1607, 1583, 1530, 1488, 1367, 1302, 1233, 1197, 1152, 1106, 1049, 1019, 973, 789 cm<sup>-1</sup>; **HRMS** (ESI,  $m/z$ ): [(M-H)<sup>-</sup>] calcd. for C<sub>23</sub>H<sub>30</sub>F<sub>3</sub>N<sub>3</sub>O<sub>5</sub>P<sup>-</sup>, 516.1881; found 516.1881.

**Synthesis and characterization of compound 12**

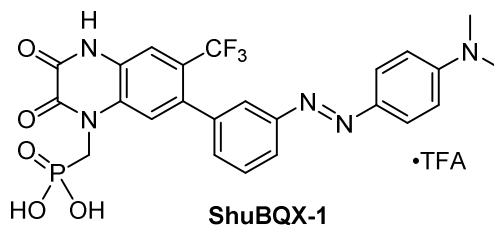
To a solution of compound **9** (932 mg, 1.80 mmol) in THF (90 mL) and Et<sub>3</sub>N (1.28 g, 12.6 mmol, 1.76 mL) at r.t. was added ethyl chlorooxoacetate (**11**) (639 mg, 4.68 mmol, 0.52 mL) dropwise. The resulting mixture was stirred at r.t. for 20 h. After this time the reaction mixture was filtered and the filtrate was concentrated under reduced pressure. The resulting residue was dissolved in EtOH (60 mL) and a solution of HCl (60 mL, 1.0 m in H<sub>2</sub>O) was added. The mixture was heated to 120 °C for 2.5 h, cooled to r.t. and the ethanol was removed under reduced pressure. The resulting aqueous layer was washed with CH<sub>2</sub>Cl<sub>2</sub> (2 × 50 mL) and its pH was adjusted to 10-11 using a solution of Na<sub>2</sub>CO<sub>3</sub> (2.0 m in H<sub>2</sub>O). The aqueous layer was then back extracted with CH<sub>2</sub>Cl<sub>2</sub> (2 × 50 mL). The combined organic extracts were dried over Na<sub>2</sub>SO<sub>4</sub>, filtered and concentrated under reduced pressure. Purification by flash column chromatography on silica gel eluting with CH<sub>2</sub>Cl<sub>2</sub>/MeOH (19:1) afforded compound **12** (505 mg, 60%) as an off-white solid.

**mp:** 305 – 308 °C, decomp; **TLC** (CH<sub>2</sub>Cl<sub>2</sub>/MeOH, 19:1): R<sub>f</sub> = 0.29 (UV/ninhydrin); **<sup>1</sup>H NMR** (400 MHz, CD<sub>3</sub>OD): δ 7.57 (s, 1H), 7.44 (s, 1H), 7.13 (t, *J* = 8.0 Hz, 1H), 6.80 – 6.69 (m, 2H), 6.65 (d, *J* = 7.5 Hz, 1H), 4.80 (d, *J* = 12.5 Hz, 2H), 4.14 (dq, *J* = 7.0, 1.0 Hz, 4H), 1.23 (t, *J* = 7.0, 6H); **<sup>13</sup>C NMR** (100 MHz, CD<sub>3</sub>OD): δ 157.4 (d, *J* = 1.5 Hz), 155.2, 148.6, 141.0, 138.7 (q, *J* = 1.5 Hz), 129.6, 126.0, 125.3 (q, *J* = 31.0 Hz), 125.1 (q, *J* = 273.0 Hz), 120.8, 120.0 (q, *J* = 1.5 Hz), 117.2 (q, *J* = 1.5 Hz), 116.0, 115.1 (q, *J* = 5.5 Hz), 64.6 (d, *J* = 6.5 Hz), 39.9 (d, *J* = 157.0 Hz), 16.5 (d, *J* = 6.0 Hz); **<sup>19</sup>F NMR** (376 MHz, CD<sub>3</sub>OD): δ -57.9; **<sup>31</sup>P NMR** (162 MHz, CD<sub>3</sub>OD): δ 20.1; **IR** (neat): 3851, 3744, 3648, 3334, 2980, 1699, 1652, 1558, 1489, 1373, 1231, 1163, 1122, 1080, 1019, 787 cm<sup>-1</sup>; **HRMS** (ESI, *m/z*): [(M+H)<sup>+</sup>] calcd. for C<sub>20</sub>H<sub>22</sub>F<sub>3</sub>N<sub>3</sub>O<sub>5</sub>P<sup>+</sup>, 472.1244; found 472.1242.

**Synthesis and characterization of compound 15**

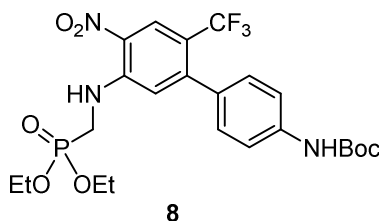
To a solution of compound **12** (95.0 mg, 0.200 mmol) in MeOH (4 mL) at 0 °C was added conc. HCl (0.1 mL) dropwise. *t*-Butyl nitrite (45.0 mg, 0.440 mmol, 52  $\mu$ L, 90% purity) was added dropwise and the resulting solution was stirred at 0 °C for 1 h. The diazonium salt was then added dropwise to a flask containing *N,N*-dimethylaniline (**14**) (27.0 mg, 0.220 mmol, 28  $\mu$ L) in MeOH (4 mL) and conc. HCl (0.1 mL) at 0 °C. The resulting solution was stirred at 0 °C for 1.5 h and then at r.t. for 2 h. The reaction was quenched with sat. aq. NaHCO<sub>3</sub> (20 mL) and extracted with EtOAc (2  $\times$  20 mL). The combined organic extracts were dried over Na<sub>2</sub>SO<sub>4</sub>, filtered and concentrated under reduced pressure. Purification by flash column chromatography on silica gel eluting with CH<sub>2</sub>Cl<sub>2</sub>/MeOH (94:6) afforded compound **15** (106 mg, 88%) as an orange oil.

**TLC** (CH<sub>2</sub>Cl<sub>2</sub>/MeOH, 94:6): R<sub>f</sub> = 0.31 (UV/ninhydrin); **<sup>1</sup>H NMR** (400 MHz, CDCl<sub>3</sub>):  $\delta$  7.88 – 7.77 (m, 3H), 7.70 – 7.61 (m, 1H), 7.47 (t, *J* = 7.5 Hz, 1H), 7.41 – 7.29 (m, 3H), 6.76 – 6.69 (m, 2H), 4.70 – 4.57 (m, 2H), 4.24 – 4.10 (m, 4H), 3.07 (s, 6H), 1.27 – 1.18 (m, 6H); **<sup>13</sup>C NMR** (200 MHz, CDCl<sub>3</sub>):  $\delta$  155.6 – 155.1 (m), 153.8 – 153.3 (m), 152.8, 152.7, 143.6, 139.5, 136.9, 130.1, 129.4 – 129.0 (m), 128.6, 128.1, 128.0, 125.2, 123.5 (q, *J* = 274.0 Hz), 123.0, 122.0, 119.3, 115.3 – 114.7 (m), 111.6, 63.6 (d, *J* = 6.0 Hz), 40.4, 39.4 (d, *J* = 156.5 Hz), 16.4 (d, *J* = 7.0 Hz); **<sup>19</sup>F NMR** (282 MHz, CDCl<sub>3</sub>):  $\delta$  –56.6; **<sup>31</sup>P NMR** (162 MHz, CDCl<sub>3</sub>):  $\delta$  19.2; **IR** (thin film): 3058, 2983, 2905, 1698, 1622, 1598, 1518, 1364, 1264, 1235, 1153, 1120, 1047, 1017, 945, 822, 733, 700 cm<sup>-1</sup>; **HRMS** (ESI, *m/z*): [(M+H)<sup>+</sup>] calcd. for C<sub>28</sub>H<sub>30</sub>F<sub>3</sub>N<sub>5</sub>O<sub>5</sub>P<sup>+</sup>, 604.1931; found 604.1930.

**Synthesis and characterization of ShuBQX-1**

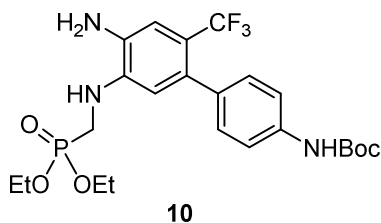
To a suspension of compound **15** (36.0 mg, 0.0600 mmol) in H<sub>2</sub>O (1.5 mL) at r.t. was added conc. HCl (1.5 mL) dropwise. The resulting mixture was heated to 120 °C for 1.5 h and then cooled to r.t.. The reaction mixture was directly purified by reverse phase column chromatography eluting with H<sub>2</sub>O [0.1% TFA]/MeCN [0.1% TFA] (9:1 → 7:3). The H<sub>2</sub>O was removed by lyophilisation to afford compound **ShuBQX-1** (21 mg, 52%) as a dark red powder.

**mp:** >350 °C; **<sup>1</sup>H NMR** (800 MHz, (CD<sub>3</sub>)<sub>2</sub>SO): δ 12.35 (s, 1H), 7.83 (ddd, *J* = 8.0, 2.0, 1.0 Hz, 1H), 7.81 – 7.78 (m, 2H), 7.76 (t, *J* = 2.0 Hz, 1H), 7.64 (s, 1H), 7.61 (s, 1H), 7.60 (t, *J* = 8.0 Hz, 1H), 7.41 – 7.39 (m, 1H), 6.86 – 6.81 (m, 2H), 4.56 (d, *J* = 12.0 Hz, 2H), 3.06 (s, 6H); **<sup>13</sup>C NMR** (200 MHz, (CD<sub>3</sub>)<sub>2</sub>SO): δ 171.5, 158.1 (q, *J* = 35.0 Hz), 155.0, 153.2, 152.7, 152.0, 142.5, 139.7, 134.1, 130.1, 129.0 – 128.8 (m), 125.1, 124.9, 123.9 (q, *J* = 273.5 Hz), 122.7, 121.6 (q, *J* = 31.5 Hz), 121.0, 120.5, 113.1 (q, *J* = 6.0 Hz), 111.6, 40.0 (d, *J* = 156.0 Hz, estimated from HSQC), 39.6 (estimated from HSQC); note that only one CF<sub>3</sub> peak was observed in this spectrum; **<sup>19</sup>F NMR** (376 MHz, (CD<sub>3</sub>)<sub>2</sub>SO): δ -54.8, -74.5; **<sup>31</sup>P NMR** (162 MHz, CD<sub>3</sub>OD): δ 14.0; **IR** (neat): 3070, 2892, 1697, 1608, 1559, 1374, 1276, 1241, 1159, 1132, 1079, 932, 850, 828, 799, 714 cm<sup>-1</sup>; **HRMS** (ESI, *m/z*): [(M+H)<sup>+</sup>] calcd. for C<sub>24</sub>H<sub>22</sub>F<sub>3</sub>N<sub>5</sub>O<sub>5</sub>P<sup>+</sup>, 548.1305; found 548.1311; **LCMS**: H<sub>2</sub>O [0.1% FA]/MeCN [0.1% FA] (90:10 → 5:95), flow rate 1.0 mL/min over 8 min; **t<sub>R</sub>** = 6.062 min, **MS** (ESI, *m/z*): [(M+H)<sup>+</sup>] = 548.0, **UV-Vis**: λ<sub>max</sub> = 430 nm.

**Synthesis and characterization of compound 8**

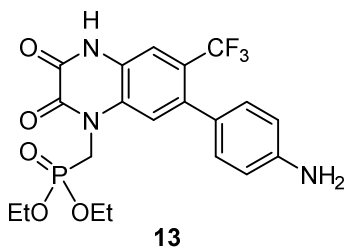
To a mixture of compound **4** (254 mg, 0.650 mmol) and 4-(*N*-*boc*-amino)phenylboronic acid (**6**) (170 mg, 0.715 mmol) in PhMe/EtOH (3.5:1, 15.5 mL) at r.t. under argon was added a solution of Na<sub>2</sub>CO<sub>3</sub> (1.5 mL, 2.0 M in H<sub>2</sub>O) and Pd(PPh<sub>3</sub>)<sub>4</sub> (38.0 mg, 0.0330 mmol). The resulting mixture was degassed and flushed with argon (× 3) and then heated to 95 °C for 16 h. The reaction mixture was cooled to r.t., concentrated under reduced pressure and the resulting residue was directly purified by flash column chromatography eluting with CH<sub>2</sub>Cl<sub>2</sub>/EtOAc (4:1) to afford compound **8** (273 mg, 77%) as a yellow oil.

**TLC** (CH<sub>2</sub>Cl<sub>2</sub>/EtOAc, 4:1): R<sub>f</sub> = 0.22 (UV/ninhydrin); **<sup>1</sup>H NMR** (400 MHz, CDCl<sub>3</sub>): δ 8.57 (s, 1H), 8.44 (q, *J* = 6.0 Hz, 1H), 7.47 – 7.40 (m, 2H), 7.29 – 7.22 (m, 2H), 6.82 (s, 1H), 6.71 (s, 1H), 4.17 (dq, *J* = 8.5, 7.0 Hz, 4H), 3.70 (dd, *J* = 13.5, 6.0 Hz, 2H), 1.52 (s, 9H), 1.32 (t, *J* = 7.0 Hz, 6H); **<sup>13</sup>C NMR** (100 MHz, CDCl<sub>3</sub>): δ 152.7, 148.6 (q, *J* = 1.0 Hz), 145.6 – 145.4 (m), 139.1, 132.7, 130.7, 129.2 (q, *J* = 2.0 Hz), 126.2 (q, *J* = 6.0 Hz), 123.5 (q, *J* = 272.5 Hz), 118.0, 117.7, 117.5 (q, *J* = 32.0 Hz), 81.0, 63.1 (d, *J* = 7.0 Hz), 39.4 (d, *J* = 157.5 Hz), 28.4, 16.6 (d, *J* = 5.5 Hz); **<sup>19</sup>F NMR** (282 MHz, CDCl<sub>3</sub>): δ -56.5; **<sup>31</sup>P NMR** (162 MHz, CD<sub>3</sub>OD): δ 20.6; **IR** (thin film): 3355, 3100, 2980, 2930, 1721, 1624, 1574, 1521, 1405, 1366, 1346, 1314, 1287, 1264, 1232, 1151, 1115, 1047, 1016, 971, 836, 764, 735 cm<sup>-1</sup>; **HRMS** (ESI, *m/z*): [(M+Na)<sup>+</sup>] calcd. for C<sub>23</sub>H<sub>29</sub>F<sub>3</sub>N<sub>3</sub>NaO<sub>7</sub>P<sup>+</sup>, 570.1587; found 570.1587.

**Synthesis and characterization of compound 10**

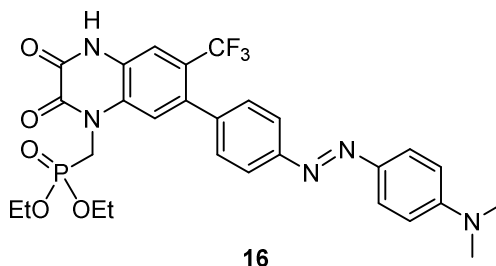
To a solution of compound **8** (328 mg, 0.600 mmol) in MeOH (12 mL) at r.t. was added Pd/C (33.0 mg, 10 wt. % Pd labelling). The reaction vessel was flushed with hydrogen ( $\times 3$ ) and the resulting mixture was stirred at r.t. for 16 h. The reaction mixture was filtered through a pad of Celite® washing with MeOH (20 mL) and the filtrate was concentrated under reduced pressure. Purification by flash column chromatography on silica gel eluting with EtOAc/MeOH (19:1  $\rightarrow$  9:1) to afford compound **10** (168 mg, 54%) as a colourless oil.

**TLC** (EtOAc/MeOH, 19:1):  $R_f = 0.55$  (UV/ninhydrin);  **$^1\text{H NMR}$**  (400 MHz,  $\text{CD}_3\text{OD}$ ):  $\delta$  7.38 (d,  $J = 8.0$  Hz, 2H), 7.18 (d,  $J = 8.0$  Hz, 2H), 7.06 (s, 1H), 6.58 (s, 1H), 4.10 (q,  $J = 7.0$  Hz, 4H), 3.67 (d,  $J = 10.5$  Hz, 2H), 1.52 (s, 9H), 1.25 (t,  $J = 7.0$  Hz, 6H);  **$^{13}\text{C NMR}$**  (100 MHz,  $\text{CD}_3\text{OD}$ ):  $\delta$  155.3, 139.4, 139.4, 136.8, 134.7, 133.8 (q,  $J = 2.0$  Hz), 130.7 (q,  $J = 1.0$  Hz), 126.4 (q,  $J = 271.5$  Hz), 118.9, 118.8 (q,  $J = 30.0$  Hz), 115.5, 114.3 (q,  $J = 5.5$  Hz), 80.8, 64.1 (d,  $J = 7.0$  Hz), 40.4 (d,  $J = 159.0$  Hz), 28.7, 16.7 (d,  $J = 6.0$  Hz);  **$^{19}\text{F NMR}$**  (376 MHz,  $\text{CD}_3\text{OD}$ ):  $\delta$  -56.2;  **$^{31}\text{P NMR}$**  (162 MHz,  $\text{CD}_3\text{OD}$ ):  $\delta$  24.8; **IR** (neat): 3364, 2978, 2930, 1703, 1584, 1511, 1431, 1403, 1391, 1366, 1312, 1232, 1150, 1103, 1048, 1017, 971, 897, 838, 805, 773  $\text{cm}^{-1}$ ; **HRMS** (ESI,  $m/z$ ):  $[(\text{M}+\text{Na})^+]$  calcd. for  $\text{C}_{23}\text{H}_{31}\text{F}_3\text{N}_3\text{NaO}_5\text{P}^+$ , 540.1846; found 540.1844.

**Synthesis and characterization of compound 13**

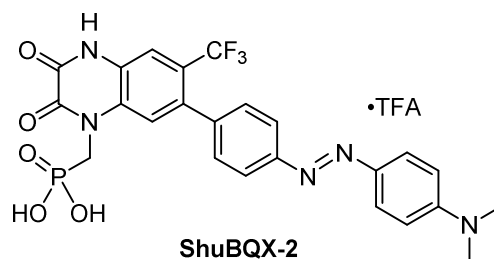
To a solution of compound **10** (124 mg, 0.240 mmol) in THF (12 mL) and Et<sub>3</sub>N (170 mg, 1.68 mmol, 234 μL) at r.t. was added ethyl chlorooxoacetate (**11**) (85.0 mg, 0.624 mmol, 69 μL) dropwise. The resulting mixture was stirred at r.t. for 20 h. After this time the reaction mixture was filtered and the filtrate was concentrated under reduced pressure. The resulting residue was dissolved in EtOH (8 mL) and a solution of HCl (8 mL, 1.0 M in H<sub>2</sub>O) was added. The mixture was heated to 120 °C for 2.5 h, cooled to r.t. and the ethanol was removed under reduced pressure. The resulting aqueous layer was washed with CH<sub>2</sub>Cl<sub>2</sub> (2 × 20 mL) and its pH was adjusted to 10-11 using a solution of Na<sub>2</sub>CO<sub>3</sub> (2.0 M in H<sub>2</sub>O). The aqueous layer was then back extracted with CH<sub>2</sub>Cl<sub>2</sub> (2 × 20 mL). The combined organic extracts were dried over Na<sub>2</sub>SO<sub>4</sub>, filtered and concentrated under reduced pressure. Purification by flash column chromatography on silica gel eluting with CH<sub>2</sub>Cl<sub>2</sub>/MeOH (19:1) afforded compound **13** (62 mg, 55%) as an off-white solid.

**mp**: 315 – 318 °C, decomp; **TLC** (CH<sub>2</sub>Cl<sub>2</sub>/MeOH, 19:1): R<sub>f</sub> = 0.27 (UV/ninhydrin); **<sup>1</sup>H NMR** (400 MHz, CD<sub>3</sub>OD): δ 7.57 (s, 1H), 7.42 (s, 1H), 7.15 – 7.08 (m, 2H), 6.79 – 6.73 (m, 2H), 4.82 (d, *J* = 12.0 Hz, 2H), 4.19 – 4.08 (m, 4H), 1.23 (t, *J* = 7.0 Hz, 6H); **<sup>13</sup>C NMR** (100 MHz, CD<sub>3</sub>OD): δ 157.8, 156.0 – 155.7 (m), 149.1, 138.8 (q, *J* = 2.0 Hz), 131.0 (q, *J* = 2.0 Hz), 129.7, 129.5, 126.5 – 126.3 (m), 125.6 (q, *J* = 30.5 Hz), 125.3 (q, *J* = 273.0 Hz), 121.1, 116.1 – 115.8 (m), 115.7, 64.6 (d, *J* = 6.5 Hz), 39.9 (d, *J* = 156.5 Hz), 16.6 (d, *J* = 6.0 Hz); **<sup>19</sup>F NMR** (376 MHz, CD<sub>3</sub>OD): δ -57.9; **<sup>31</sup>P NMR** (162 MHz, CD<sub>3</sub>OD): δ 20.2; **IR** (neat): 3360, 2984, 1698, 1620, 1505, 1381, 1350, 1238, 1182, 1158, 1119, 1080, 1019, 835 cm<sup>-1</sup>; **HRMS** (ESI, *m/z*): [(M+H)<sup>+</sup>] calcd. for C<sub>20</sub>H<sub>22</sub>F<sub>3</sub>N<sub>3</sub>O<sub>5</sub>P<sup>+</sup>, 472.1244; found 472.1240.

**Synthesis and characterization of compound 16**

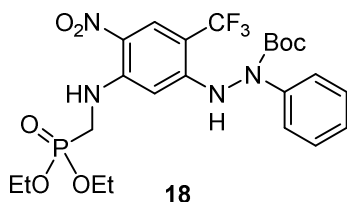
To a solution of compound **13** (38.0 mg, 0.0800 mmol) in MeOH (1.6 mL) at 0 °C was added conc. HCl (0.04 mL) dropwise. *t*-Butyl nitrite (17.0 mg, 0.160 mmol, 21  $\mu$ L, 90% purity) was added dropwise and the resulting solution was stirred at 0 °C for 30 min. The diazonium salt was then added dropwise to a flask containing *N,N*-dimethylaniline (**14**) (11.0 mg, 0.0880 mmol, 11  $\mu$ L) in MeOH (1.6 mL) and conc. HCl (0.04 mL) at 0 °C. The resulting solution was stirred at 0 °C for 2 h and then at r.t. for 2 h. The reaction was quenched with sat. aq. NaHCO<sub>3</sub> (10 mL) and extracted with EtOAc (2  $\times$  10 mL). The combined organic extracts were dried over Na<sub>2</sub>SO<sub>4</sub>, filtered and concentrated under reduced pressure. Purification by flash column chromatography on silica gel eluting with CH<sub>2</sub>Cl<sub>2</sub>/MeOH (98:2  $\rightarrow$  95:5) afforded compound **16** (28 mg, 58%) as an orange solid.

**mp:** 215 – 218 °C; **TLC** (CH<sub>2</sub>Cl<sub>2</sub>/MeOH, 19:1): R<sub>f</sub> = 0.36 (UV/CAM); **<sup>1</sup>H NMR** (400 MHz, CDCl<sub>3</sub>):  $\delta$  7.91 – 7.84 (m, 2H), 7.83 – 7.75 (m, 2H), 7.61 (s, 1H), 7.47 – 7.40 (m, 2H), 7.36 (s, 1H), 6.79 – 6.70 (m, 2H), 4.69 (d, *J* = 12.0 Hz, 2H), 4.30 – 4.13 (m, 4H), 3.09 (s, 6H), 1.26 (t, *J* = 7.0 Hz, 6H); **<sup>13</sup>C NMR** (100 MHz, CDCl<sub>3</sub>):  $\delta$  155.2, 153.5, 152.8, 152.7, 143.7, 139.7, 136.8 (q, *J* = 1.5 Hz), 130.0, 128.1, 125.3, 125.0 (q, *J* = 31.5 Hz), 124.3, 123.5 (q, *J* = 273.5 Hz), 121.8, 119.3, 114.9 (q, *J* = 5.0 Hz), 111.7, 63.7 (d, *J* = 6.5 Hz), 40.4, 39.4 (d, *J* = 156.0 Hz), 16.4 (d, *J* = 6.0 Hz); **<sup>19</sup>F NMR** (376 MHz, CDCl<sub>3</sub>):  $\delta$  -56.5; **<sup>31</sup>P NMR** (162 MHz, CDCl<sub>3</sub>):  $\delta$  19.2; **IR** (thin film): 3153, 3075, 2984, 2909, 1704, 1622, 1600, 1519, 1421, 1366, 1312, 1237, 1157, 1139, 1082, 1047, 1020, 846, 822 cm<sup>-1</sup>; **HRMS** (ESI, *m/z*): [(M+H)<sup>+</sup>] calcd. for C<sub>28</sub>H<sub>30</sub>F<sub>3</sub>N<sub>5</sub>O<sub>5</sub>P<sup>+</sup>, 604.1931; found 604.1941.

**Synthesis and characterization of ShuBQX-2**

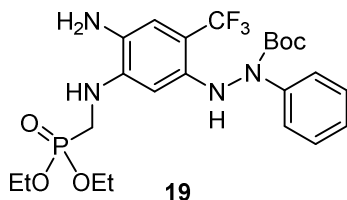
To a suspension of compound **16** (24.0 mg, 0.0400 mmol) in H<sub>2</sub>O (1 mL) at r.t. was added conc. HCl (1 mL) dropwise. The resulting mixture was heated to 120 °C for 12 h and then cooled to r.t.. The reaction mixture was directly purified by reverse phase column chromatography eluting with H<sub>2</sub>O [0.1% TFA]/MeCN [0.1% TFA] (9:1 → 7:3). The H<sub>2</sub>O was removed by lyophilisation to afford compound **ShuBQX-2** (5.6 mg, 21%) as a dark brown solid.

**mp:** >350 °C; **<sup>1</sup>H NMR** (800 MHz, (CD<sub>3</sub>)<sub>2</sub>SO): δ 12.33 (s, 1H), 7.86 – 7.77 (m, 4H), 7.65 (s, 1H), 7.59 (s, 1H), 7.52 – 7.46 (m, 2H), 6.89 – 6.81 (m, 2H), 4.49 (br s, 2H), 3.07 (s, 6H); **<sup>13</sup>C NMR** (200 MHz, (CD<sub>3</sub>)<sub>2</sub>SO): δ 157.7, 157.6, 154.9, 153.2, 152.7, 151.9, 142.6, 139.8, 134.0, 130.1, 128.9, 125.0, 124.9, 123.9 (q, *J* = 274.0 Hz), 121.3, 120.6, 113.1 (q, *J* = 5.0 Hz), 111.6, 40.0 (d, *J* = 155.5 Hz, estimated by HSQC), 39.6 (estimated by HSQC); note that only one CF<sub>3</sub> peak was observed in this spectrum; **<sup>19</sup>F NMR** (376 MHz, (CD<sub>3</sub>)<sub>2</sub>SO): δ -54.7, -73.4; **<sup>31</sup>P NMR** (162 MHz, (CD<sub>3</sub>)<sub>2</sub>SO): δ 13.4; **IR** (neat): 3063, 2950, 1682, 1671, 1620, 1594, 1543, 1367, 1350, 1274, 1241, 1207, 1169, 1137, 1123, 1108, 1074, 955, 937, 909, 894, 838, 824, 726 cm<sup>-1</sup>; **HRMS** (ESI, *m/z*): [(M+H)<sup>+</sup>] calcd. for C<sub>24</sub>H<sub>22</sub>F<sub>3</sub>N<sub>5</sub>O<sub>5</sub>P<sup>+</sup>, 548.1305; found 548.1212; **LCMS**: H<sub>2</sub>O [0.1% FA]/MeCN [0.1% FA] (90:10 → 5:95), flow rate 1.0 mL/min over 8 min; **t<sub>R</sub>** = 6.095 min, **MS** (ESI, *m/z*): [(M+H)<sup>+</sup>] = 548.0, **UV-Vis**: λ<sub>max</sub> = 435 nm.

**Synthesis and characterisation of compound 18**

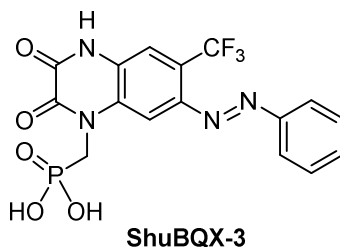
To a mixture of compound **4** (200 mg, 0.512 mmol) and hydrazide **17** (120 mg, 0.576 mmol) in PhMe (6 mL) at r.t. was added  $\text{Cs}_2\text{CO}_3$  (280 mg, 0.726 mmol),  $\text{Pd}(\text{OAc})_2$  (44.0 mg, 0.196 mmol) and a solution of  $\text{P}(t\text{-Bu})_3$  (0.510 mL, 0.510 mmol, 1.0 M in PhMe). The resulting mixture was stirred for 30 min. at r.t. and then heated to 120 °C for 2 h. The reaction mixture was cooled to r.t., concentrated under reduced pressure and the resulting residue was directly purified by flash column chromatography eluting with *i*-Hex/EtOAc (8:2 → 1:1) to afford compound **18** (163 mg, 57%) as an orange solid.

**mp:** 230 °C, decomp; **TLC** (*i*-Hex/EtOAc, 1:1):  $R_f = 0.37$  (UV/ninhydrin);  **$^1\text{H NMR}$**  (400 MHz,  $\text{CD}_3\text{OD}$ ):  $\delta$  8.40 (s, 1H), 7.64 – 7.55 (m, 2H), 7.42 – 7.33 (m, 2H), 7.24 – 7.14 (m, 1H), 6.30 (s, 1H), 4.12 – 3.97 (m, 4H), 3.71 (d,  $J = 12.0$  Hz, 2H), 1.47 (s, 9H), 1.23 (t,  $J = 7.0$  Hz, 6H);  **$^{13}\text{C NMR}$**  (100 MHz,  $\text{CD}_3\text{OD}$ ):  $\delta$  154.9, 151.7, 149.4 (d,  $J = 5.0$  Hz), 143.0, 129.8, 128.6 (q,  $J = 6.0$  Hz), 126.6, 125.9, 123.7, 104.6 (q,  $J = 32.5$  Hz), 94.4, 83.8, 64.4 (d,  $J = 7.0$  Hz), 39.7 (d,  $J = 158.0$  Hz), 28.4, 16.7 (d,  $J = 5.5$  Hz); note that the  $\text{CF}_3$  peak was not observed in this spectrum;  **$^{19}\text{F NMR}$**  (376 MHz,  $\text{CD}_3\text{OD}$ ):  $\delta$  -62.8;  **$^{31}\text{P NMR}$**  (162 MHz,  $\text{CD}_3\text{OD}$ ):  $\delta$  22.3; **IR** (neat): 3346, 2981, 2931, 1723, 1633, 1577, 1541, 1425, 1355, 1339, 1301, 1251, 1213, 1153, 1112, 1048, 1022, 972, 761  $\text{cm}^{-1}$ ; **HRMS** (ESI,  $m/z$ ):  $[(\text{M}-\text{H})^-]$  calcd. for  $\text{C}_{23}\text{H}_{30}\text{F}_3\text{N}_4\text{NaO}_7\text{P}^-$ , 561.1731; found 561.1739.

**Synthesis and characterisation of compound 19**

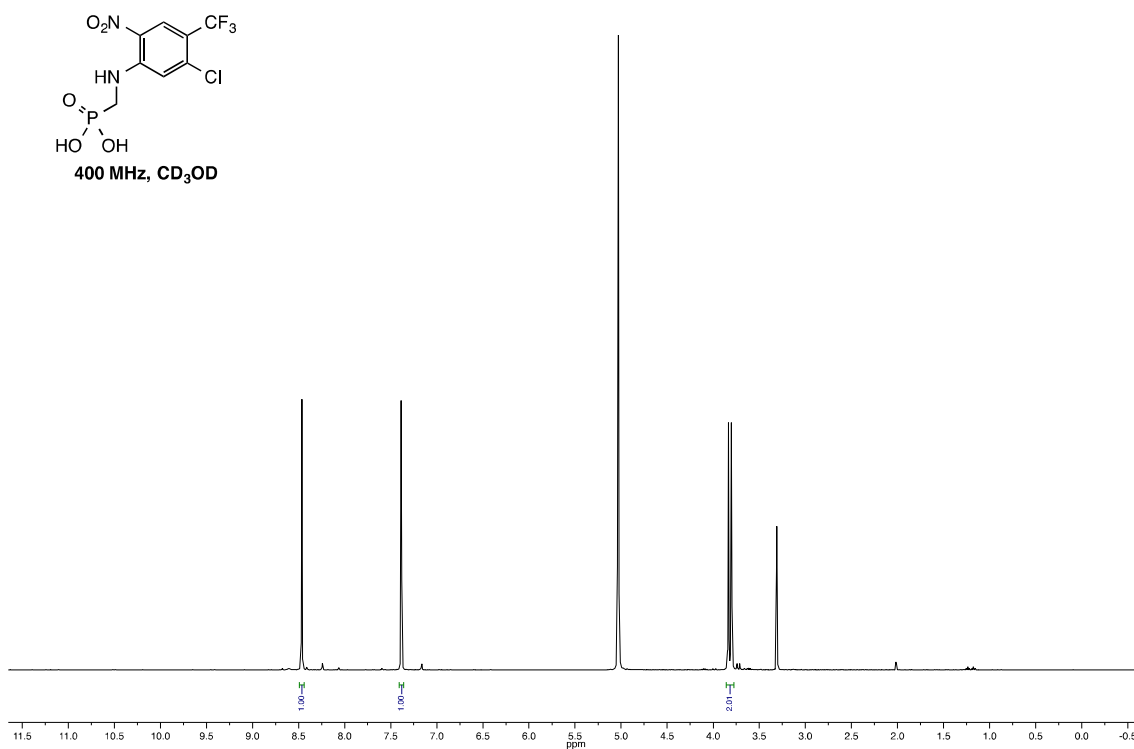
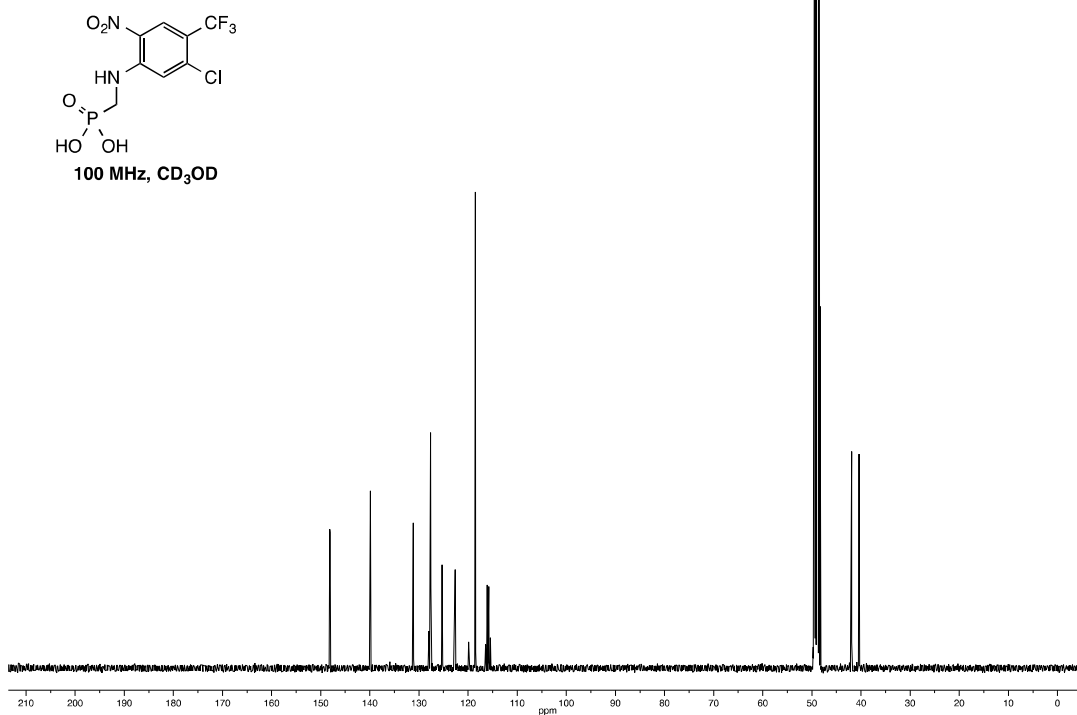
To a solution of compound **18** (163 mg, 0.290 mmol) in MeOH (5 mL) at r.t. was added Pd/C (34.0 mg, 20 wt. % Pd labelling). The reaction vessel was flushed with hydrogen ( $\times 3$ ) and the resulting mixture was stirred at r.t. for 5.5 h after which more Pd/C (16.0 mg, 10 wt. % Pd labelling) was added. The reaction mixture was stirred for 2.5 h at r.t. and then filtered through a pad of Celite® washing with EtOAc (20 mL). The filtrate was concentrated under reduced pressure to give a brown solid (132 mg, 86%), which was used in the next step without further purification. An analytical sample was obtained by purification using preparative TLC eluting with CH<sub>2</sub>Cl<sub>2</sub>/MeOH (19:1).

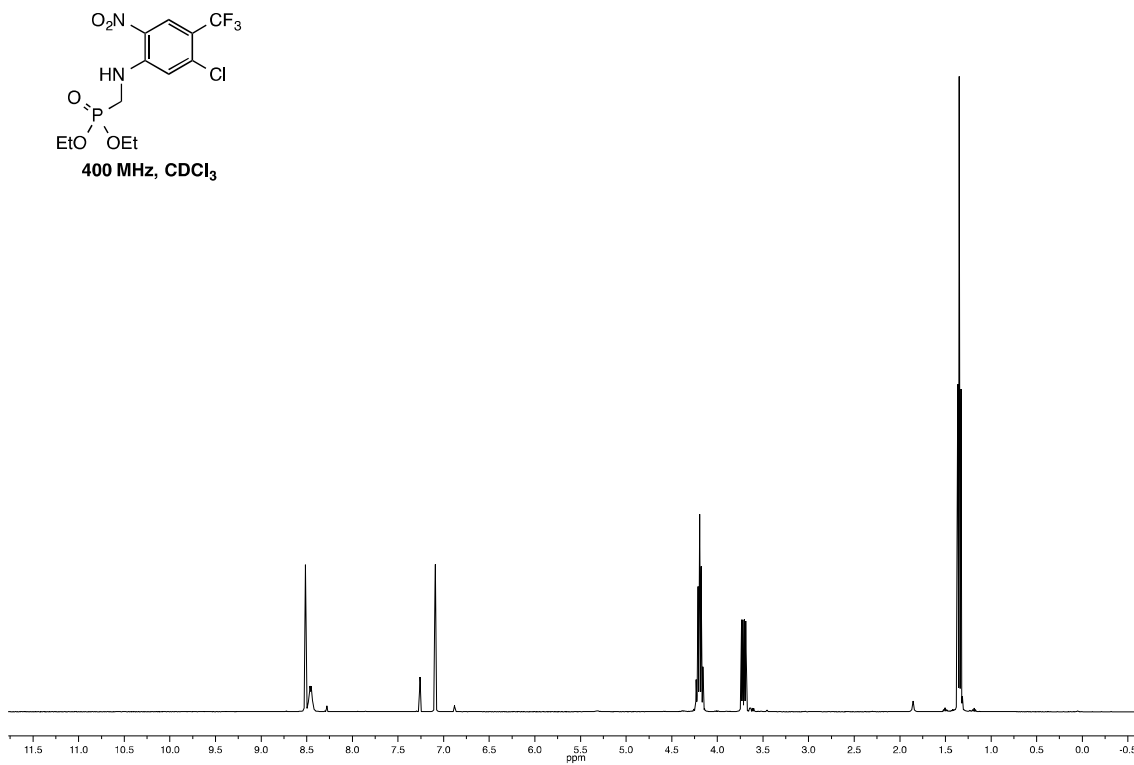
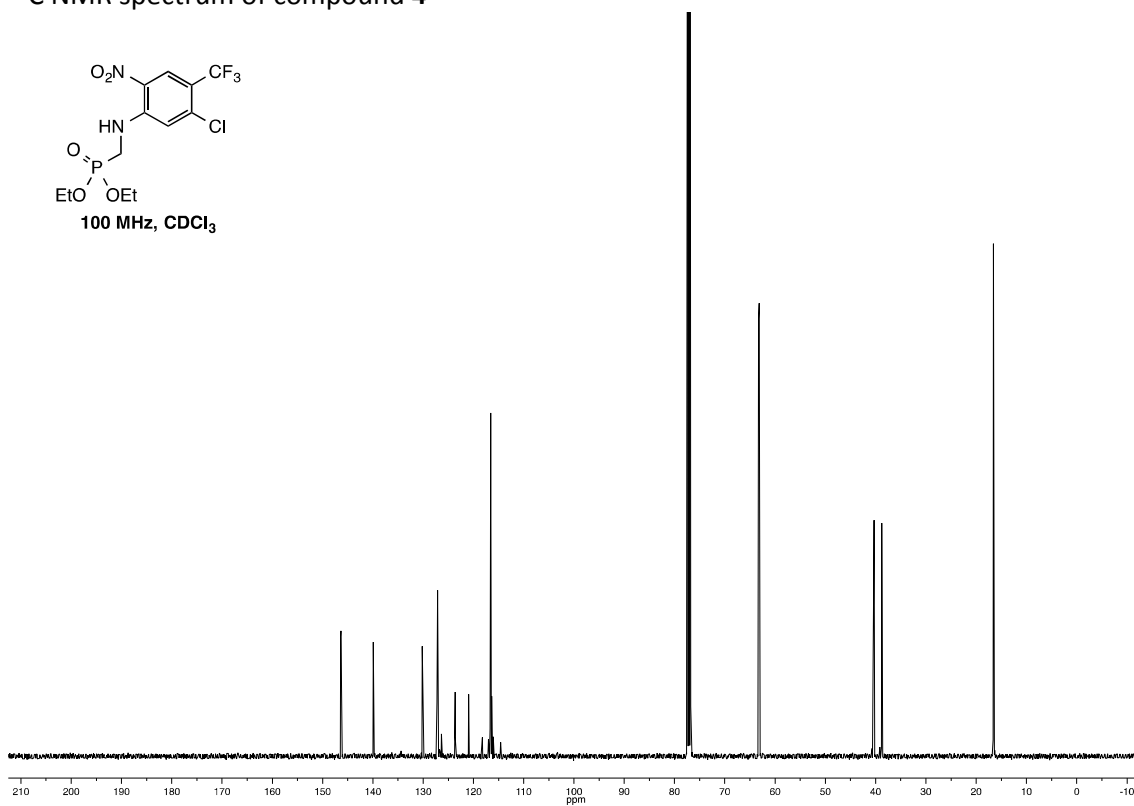
**mp:** 155 – 156 °C; **TLC** (CH<sub>2</sub>Cl<sub>2</sub>/MeOH, 19:1):  $R_f = 0.29$  (UV/ninhydrin); **<sup>1</sup>H NMR** (400 MHz, CD<sub>3</sub>OD):  $\delta$  7.67 – 7.59 (m, 2H), 7.39 – 7.28 (m, 2H), 7.13 (t,  $J = 7.5$  Hz, 1H), 6.94 (s, 1H), 6.25 (s, 1H), 4.08 – 3.92 (m, 4H), 3.51 (d,  $J = 10.5$  Hz, 2H), 1.40 (s, 9H), 1.20 (t,  $J = 7.1$  Hz, 6H); **<sup>13</sup>C NMR** (100 MHz, CD<sub>3</sub>OD):  $\delta$  155.9, 142.9 (d,  $J = 4.6$  Hz), 142.1 – 141.9 (m), 129.4, 127.6, 126.8 (q,  $J = 270.0$  Hz), 125.8, 123.5, 116.2 – 115.8 (m), 104.0 (q,  $J = 31.0$  Hz), 97.1 (q,  $J = 2.0$  Hz), 83.2, 64.4 – 63.7 (m), 41.5 – 41.3 (m, part of NCH<sub>2</sub>PO multiplet), 39.9 – 39.7 (m, part of NCH<sub>2</sub>PO multiplet), 28.7 – 28.0 (m), 17.0 – 16.3 (m); **<sup>19</sup>F NMR** (376 MHz, CD<sub>3</sub>OD):  $\delta$  -60.4; **<sup>31</sup>P NMR** (162 MHz, CD<sub>3</sub>OD):  $\delta$  24.4; **IR** (neat): 3370, 2981, 2931, 1713, 1622, 1597, 1537, 1489, 1453, 1392, 1369, 1335, 1300, 1245, 1198, 1150, 1094, 1048, 1023, 970, 867, 824, 757 cm<sup>-1</sup>; **HRMS** (ESI,  $m/z$ ): [(M+Na)<sup>+</sup>] calcd. for C<sub>23</sub>H<sub>32</sub>F<sub>3</sub>N<sub>4</sub>NaO<sub>5</sub>P<sup>+</sup>, 555.1955; found 555.1959.

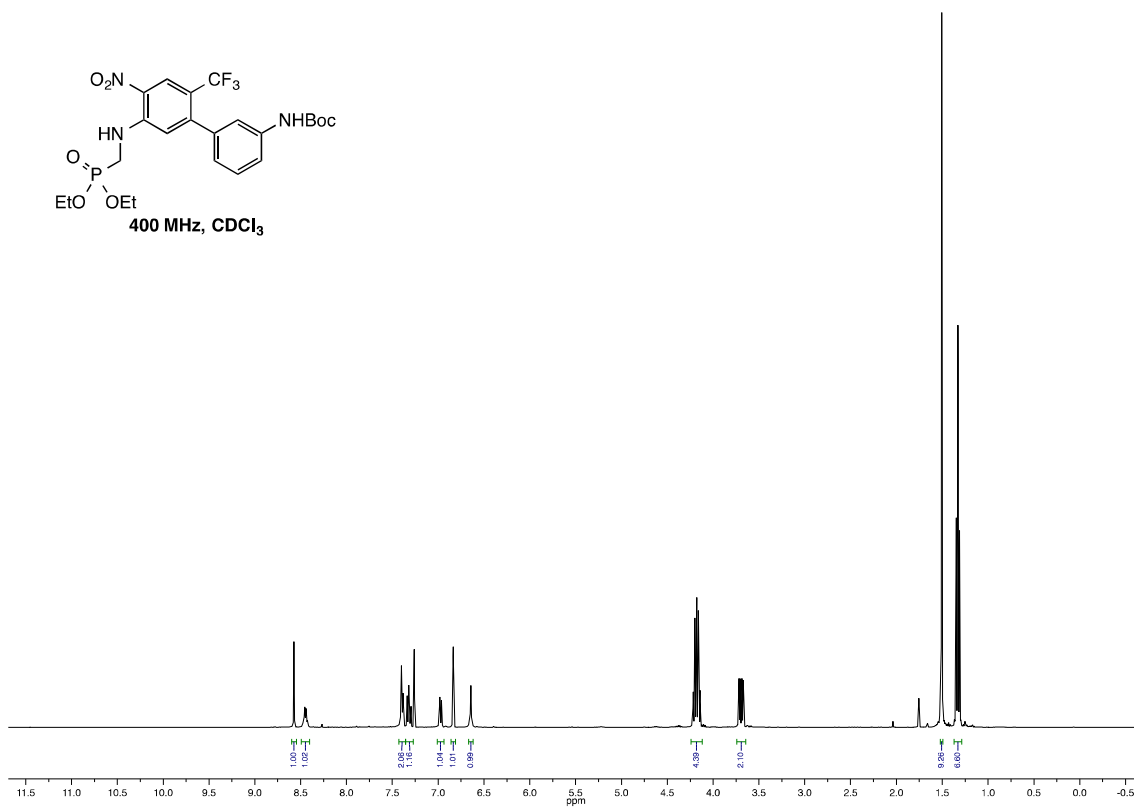
**Synthesis and characterisation of ShuBQX-3**

To a solution of compound **19** (132 mg, 0.248 mmol) in THF (11 mL) and Et<sub>3</sub>N (174 mg, 1.72 mmol, 0.240 mL) at r.t. was added ethyl chlorooxoacetate (**11**) (88 mg, 0.644 mmol, 72  $\mu$ L) dropwise. The resulting mixture was stirred at r.t. for 19 h. After this time the reaction mixture was filtered and the filtrate was concentrated under reduced pressure. The resulting residue was dissolved in EtOH (2 mL) and a solution of HCl (9 mL, 6.0 M in H<sub>2</sub>O) was added. The resulting mixture was heated to 90 °C for 3 h and then cooled to r.t.. The reaction mixture was directly purified by reverse phase column chromatography eluting with H<sub>2</sub>O [0.1% TFA]/MeCN [0.1% TFA] (9:1  $\rightarrow$  6:4). The H<sub>2</sub>O was removed by lyophilisation to afford compound **ShuBQX-3** (14.0 mg, 18% over three steps) as a dark brown solid.

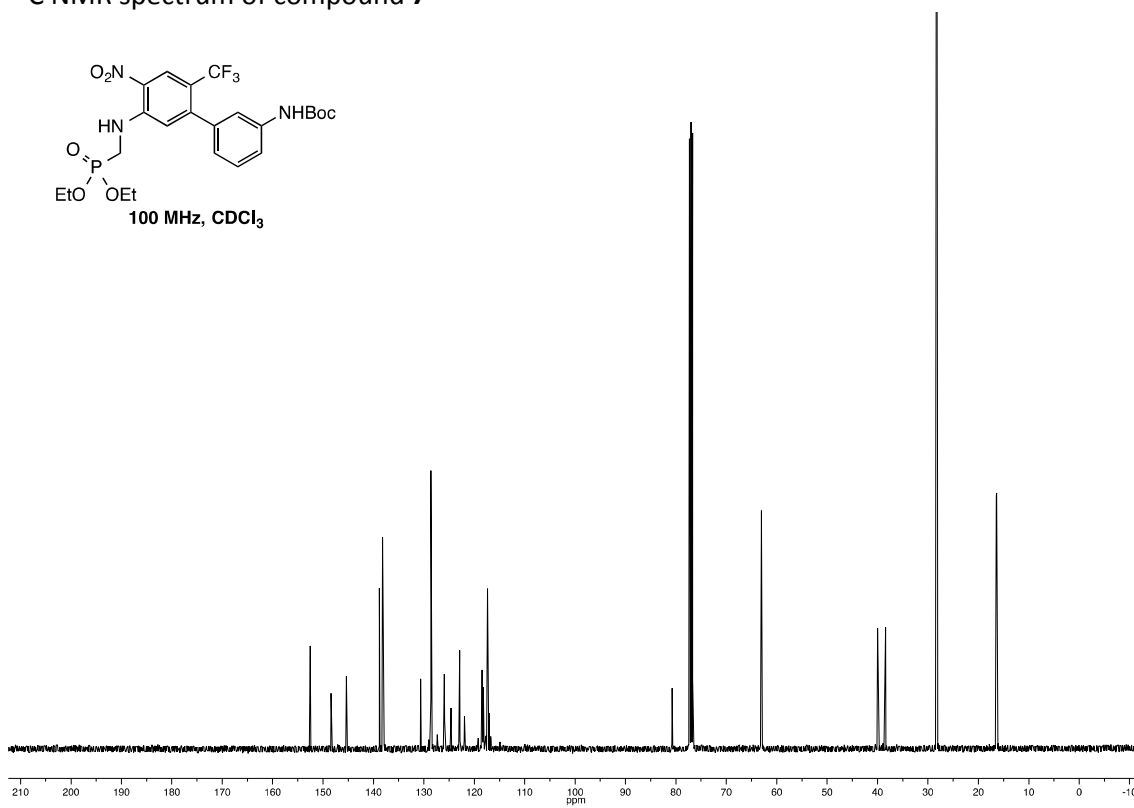
**mp:** 275 – 280 °C, decomp; **<sup>1</sup>H NMR** (400 MHz, CD<sub>3</sub>OD):  $\delta$  8.12 (s, 1H), 7.99 – 7.89 (m, 2H), 7.63 (s, 1H), 7.58 – 7.49 (m, 3H), 4.72 (d,  $J$  = 12.0 Hz, 2H); **<sup>13</sup>C NMR** (100 MHz, CD<sub>3</sub>OD):  $\delta$  157.0, 155.3, 153.8, 145.8, 133.2, 131.1, 130.4, 129.0, 125.9 (q,  $J$  = 32.0 Hz), 124.8, q,  $J$  = 272.5 Hz), 124.4, 115.2, (q,  $J$  = 6.0 Hz), 105.5, 41.7 (d,  $J$  = 152.0 Hz); **<sup>19</sup>F NMR** (376 MHz, CD<sub>3</sub>OD):  $\delta$  -58.5; **<sup>31</sup>P NMR** (162 MHz, CD<sub>3</sub>OD):  $\delta$  15.3; **IR** (neat): 3415, 3073, 2961, 1694, 1619, 1393, 1358, 1298, 1269, 1241, 1136, 1062, 1019, 933, 771, 732, 687 cm<sup>-1</sup>; **HRMS** (ESI,  $m/z$ ): [(M+H)<sup>+</sup>] calcd. for C<sub>16</sub>H<sub>13</sub>F<sub>3</sub>N<sub>4</sub>O<sub>5</sub>P<sup>+</sup>, 429.0570; found 429.0580; **LCMS**: H<sub>2</sub>O [0.1% FA]/MeCN [0.1% FA] (90:10  $\rightarrow$  10:90), flow rate 2.0 mL/min over 5 min; **t<sub>R</sub>** = 2.858 min, **MS** (ESI,  $m/z$ ): [(M+H)<sup>+</sup>] = 429.0, **UV-Vis**:  $\lambda_{\text{max}}$  = 360 nm.

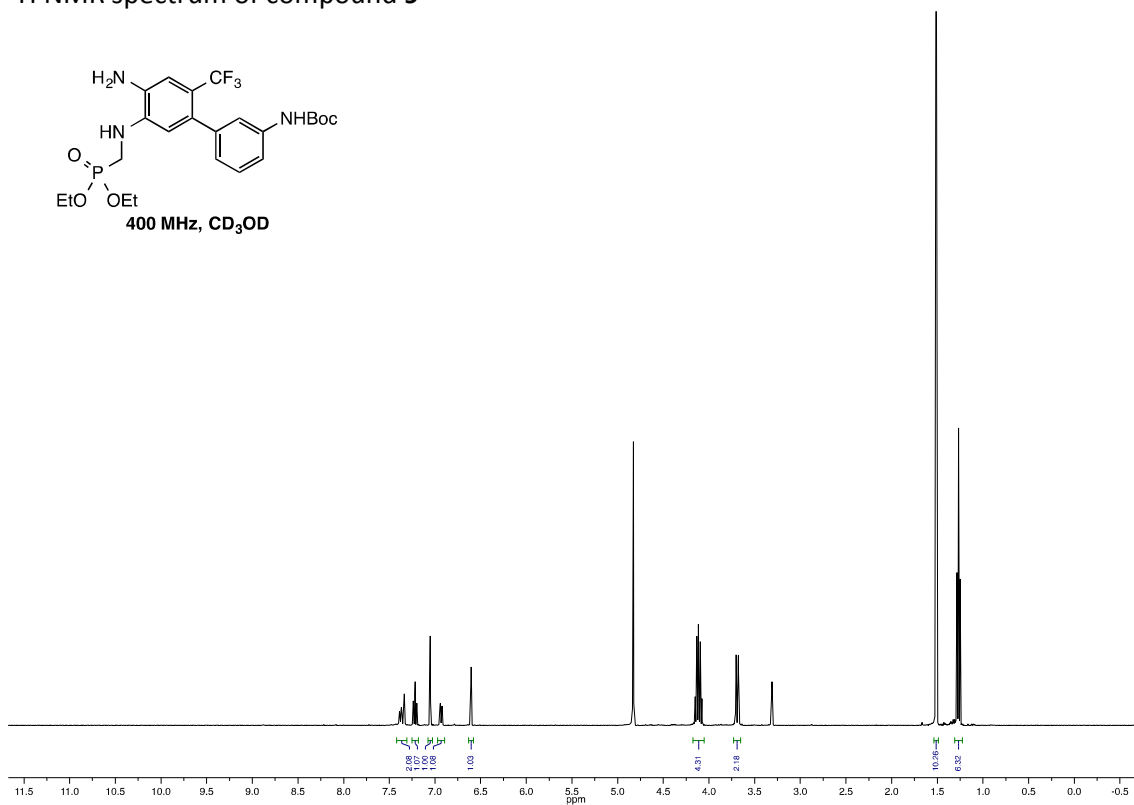
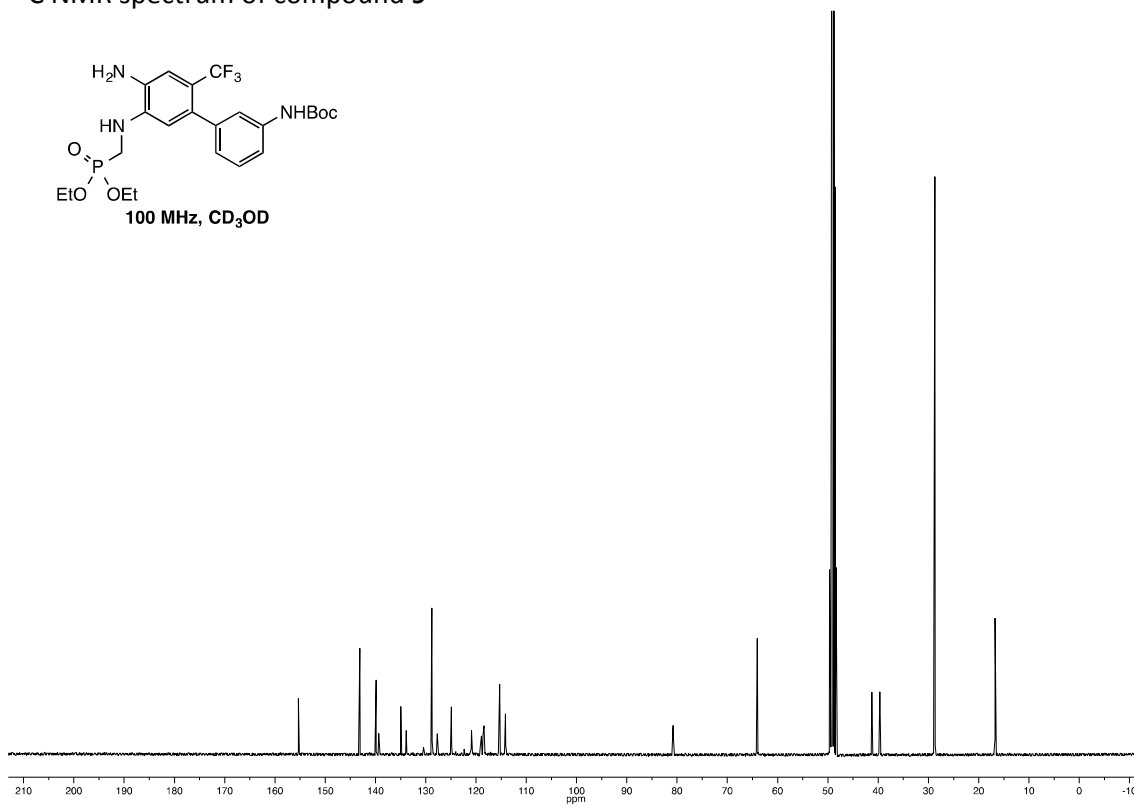
**10.5.2. NMR Spectra for Chapter 7.1.**<sup>1</sup>H NMR spectrum of compound **3**<sup>13</sup>C NMR spectrum of compound **3**<sup>1</sup>H NMR spectrum of compound **4**

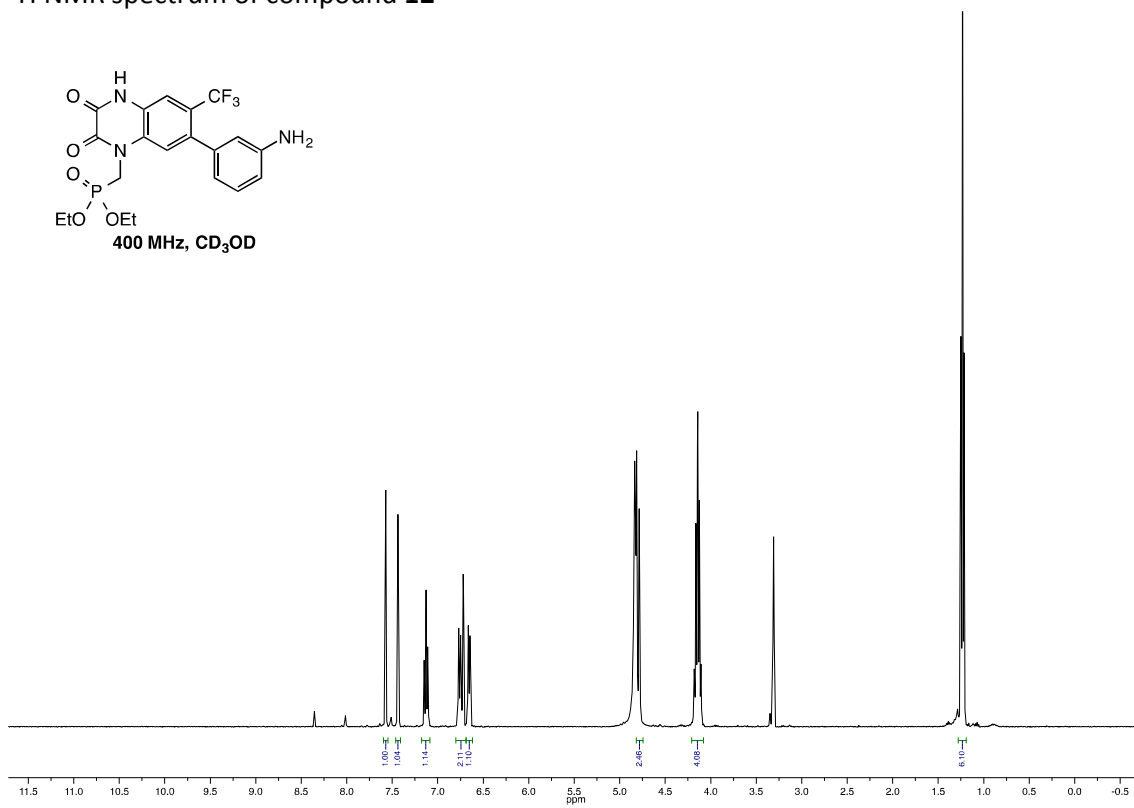
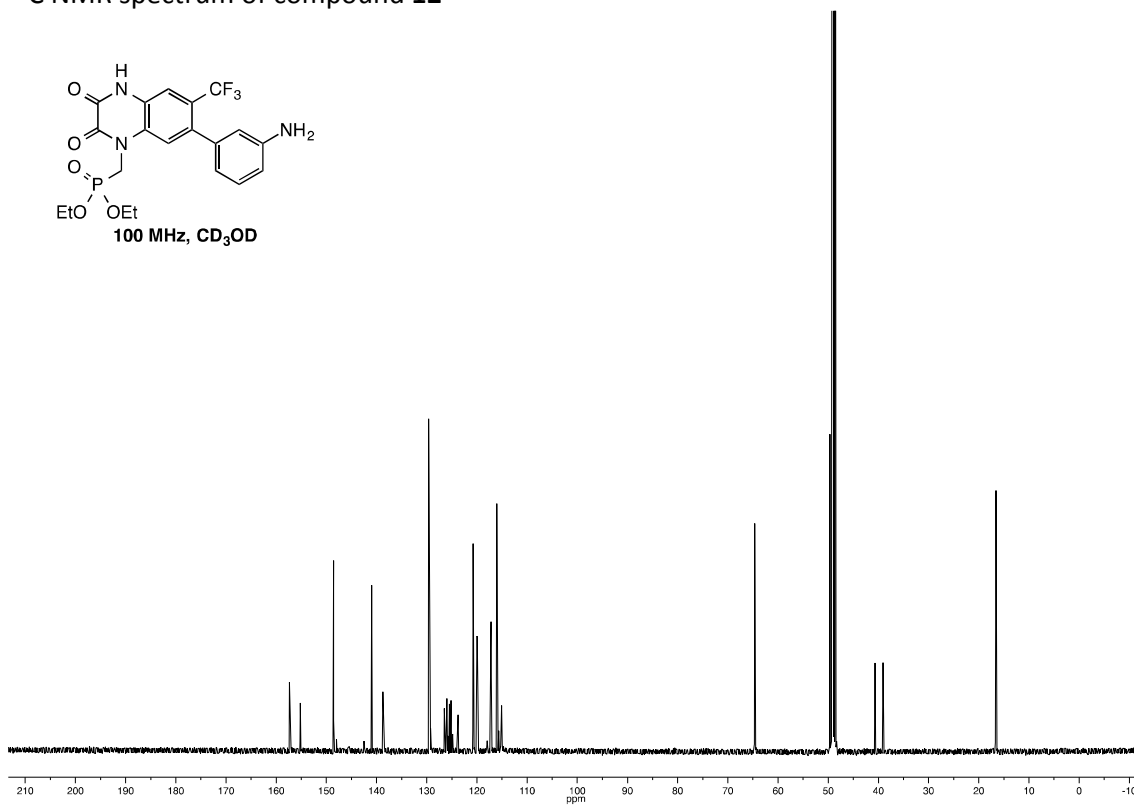
<sup>13</sup>C NMR spectrum of compound 4<sup>1</sup>H NMR spectrum of compound 7

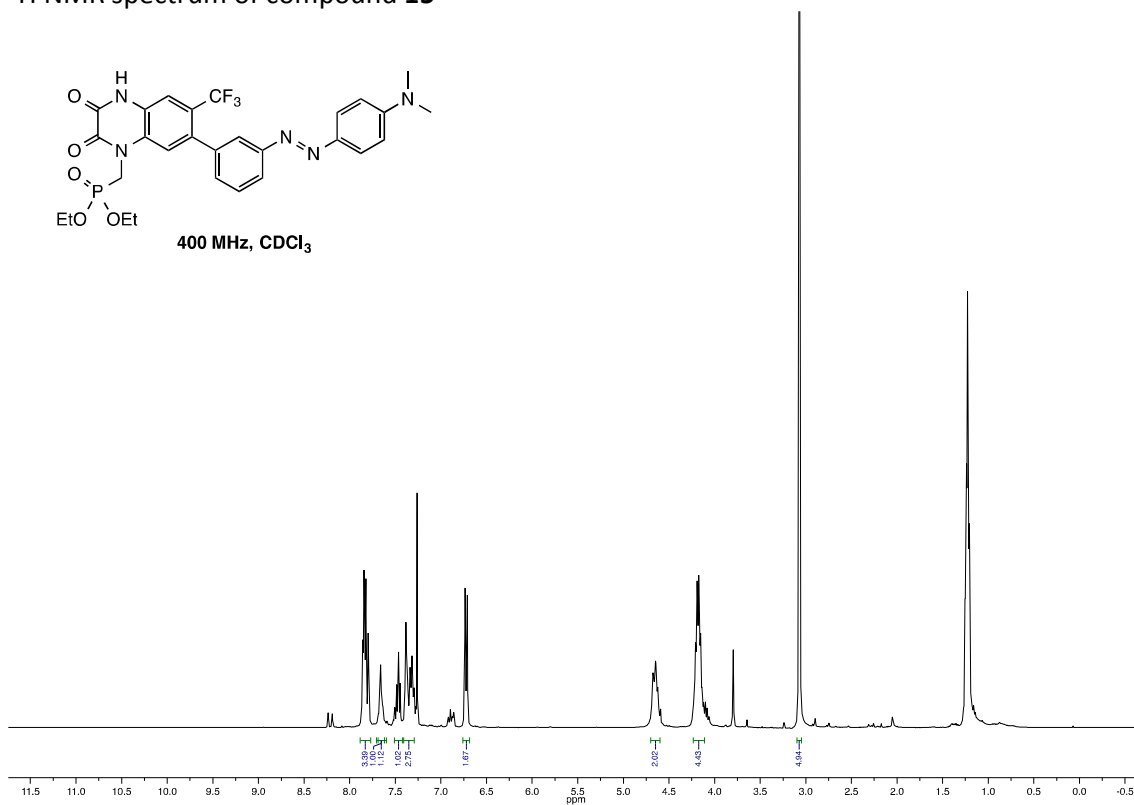
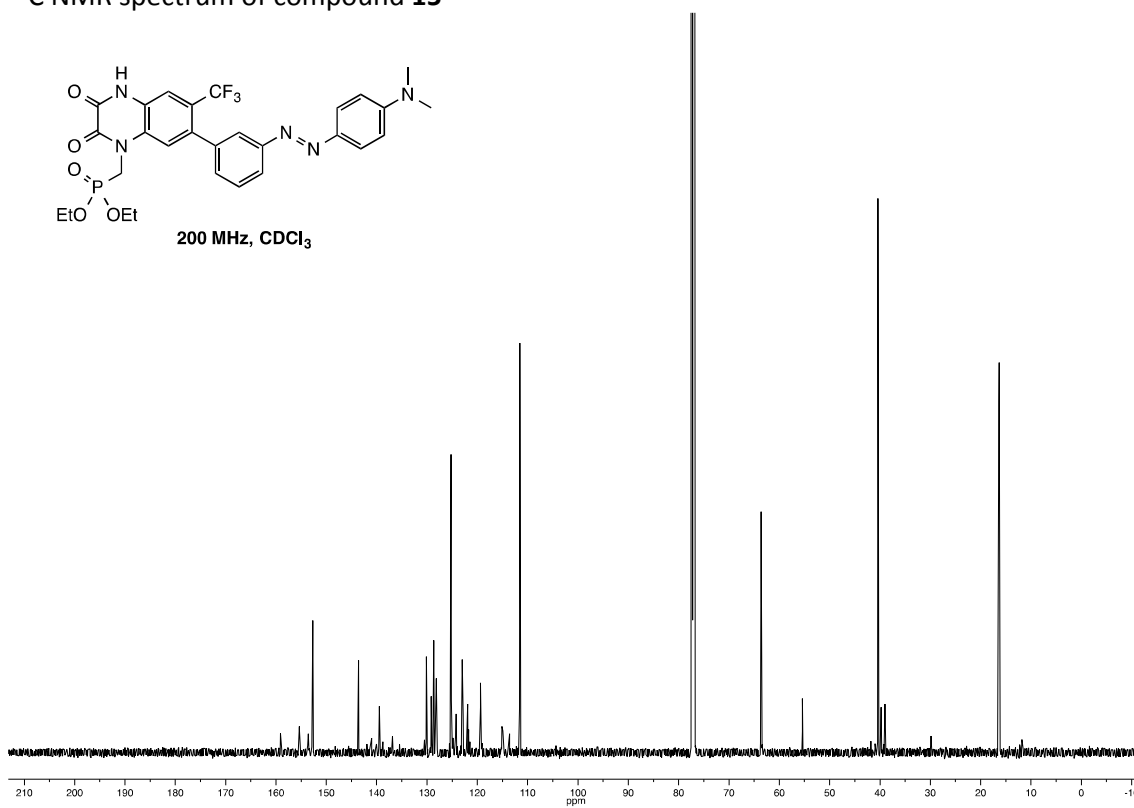


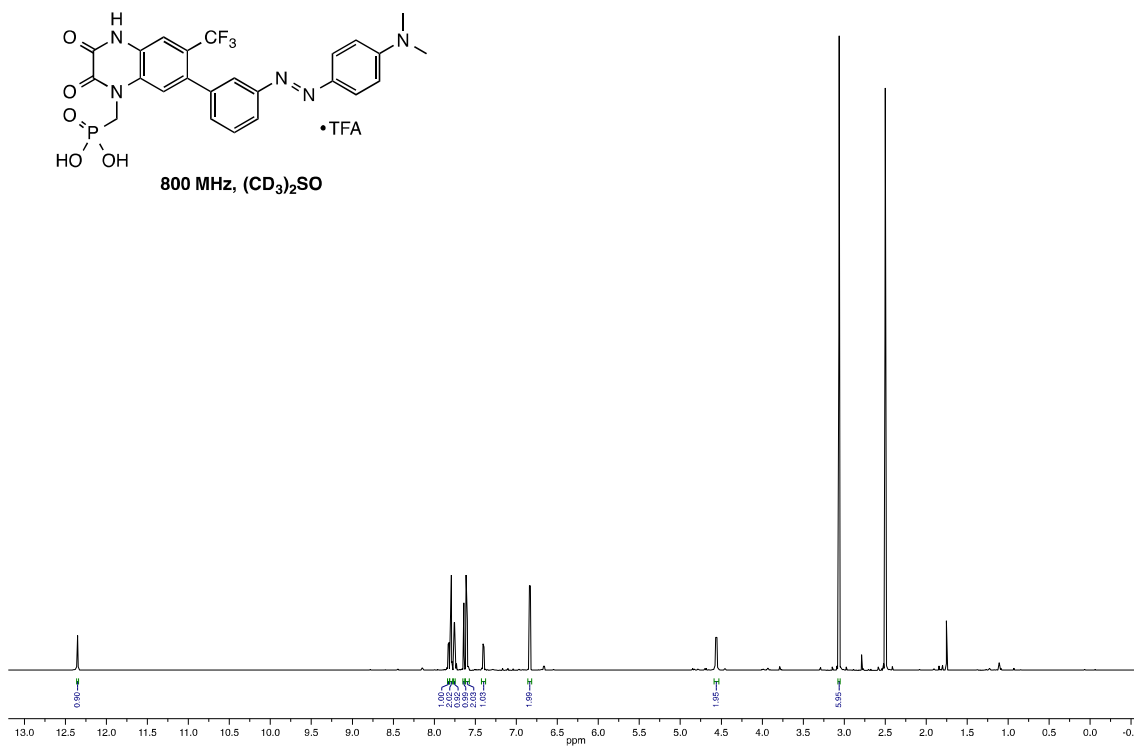
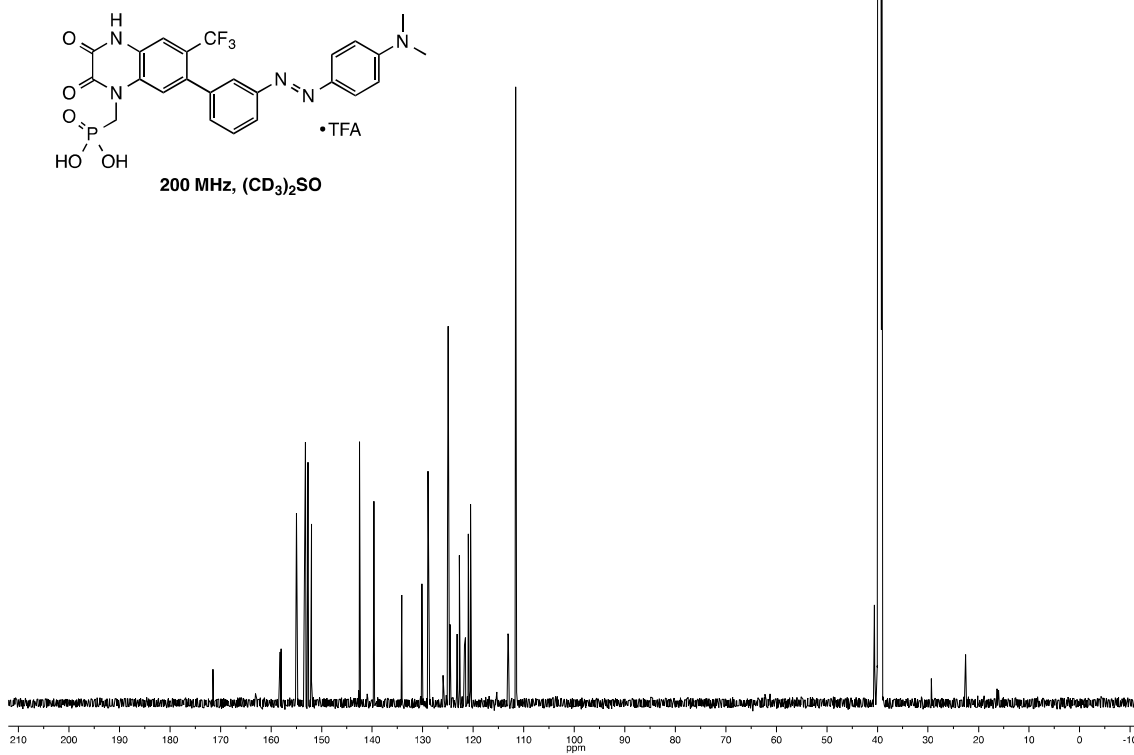
<sup>13</sup>C NMR spectrum of compound **7**

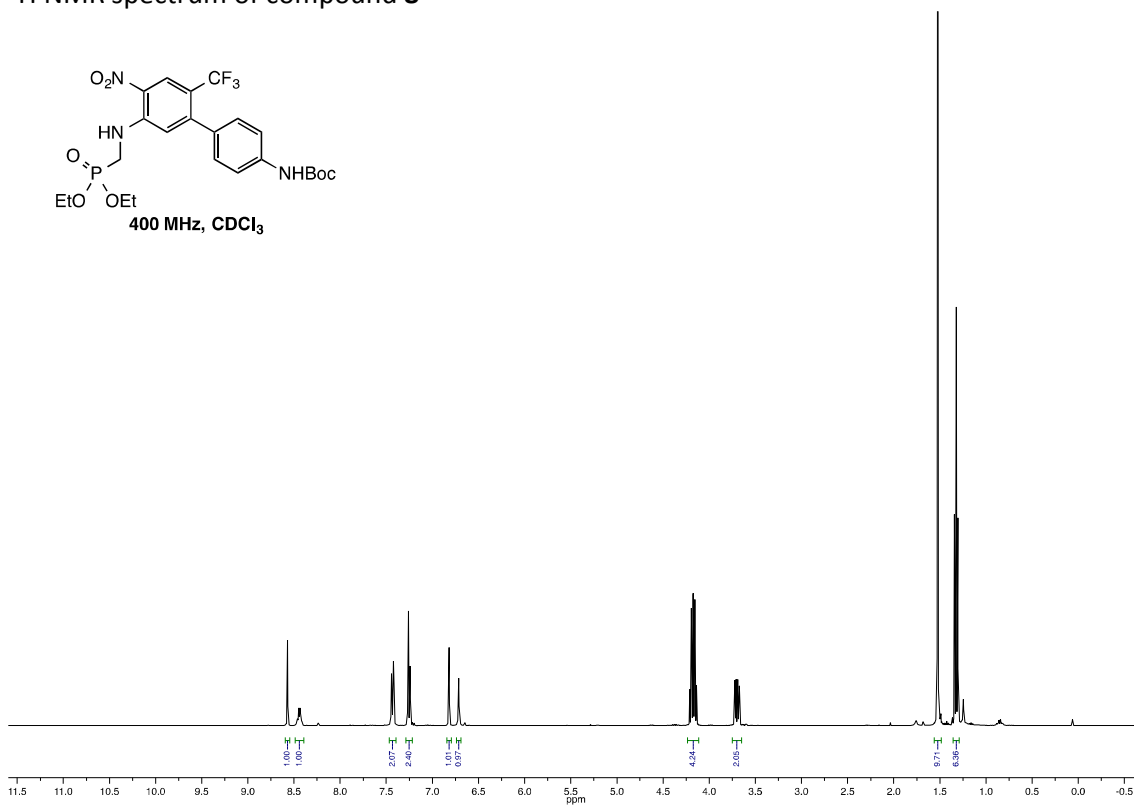
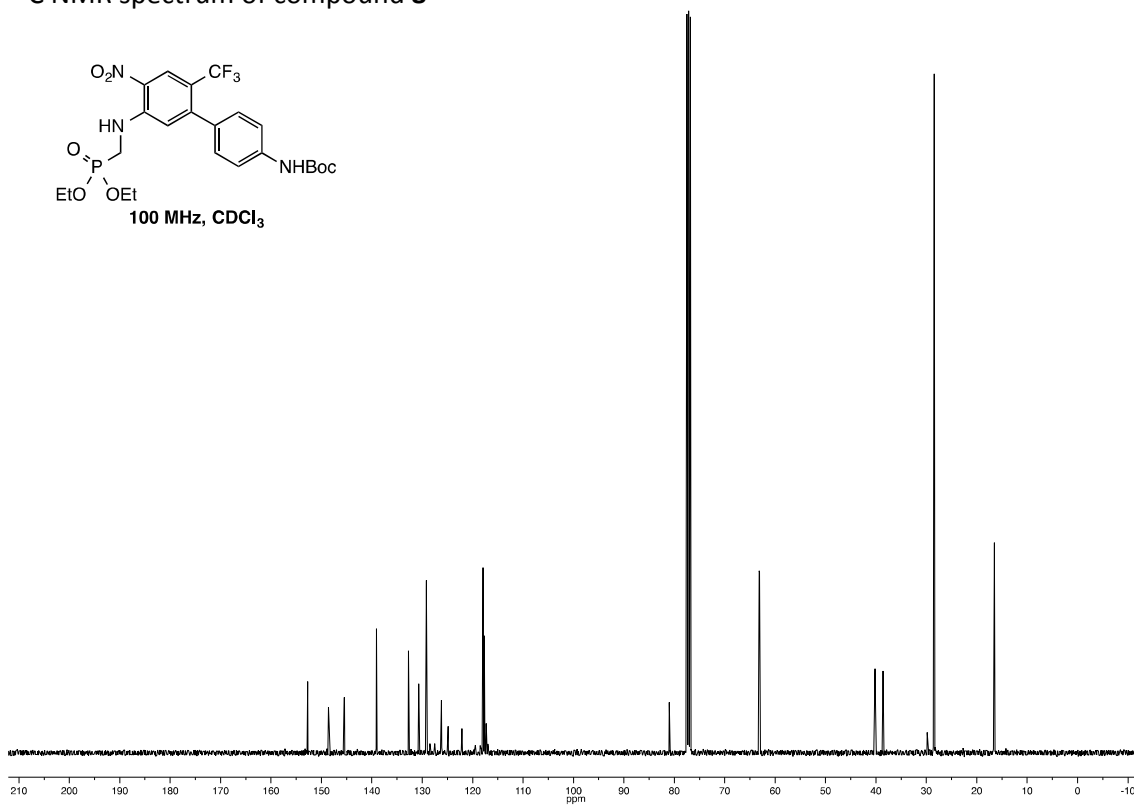


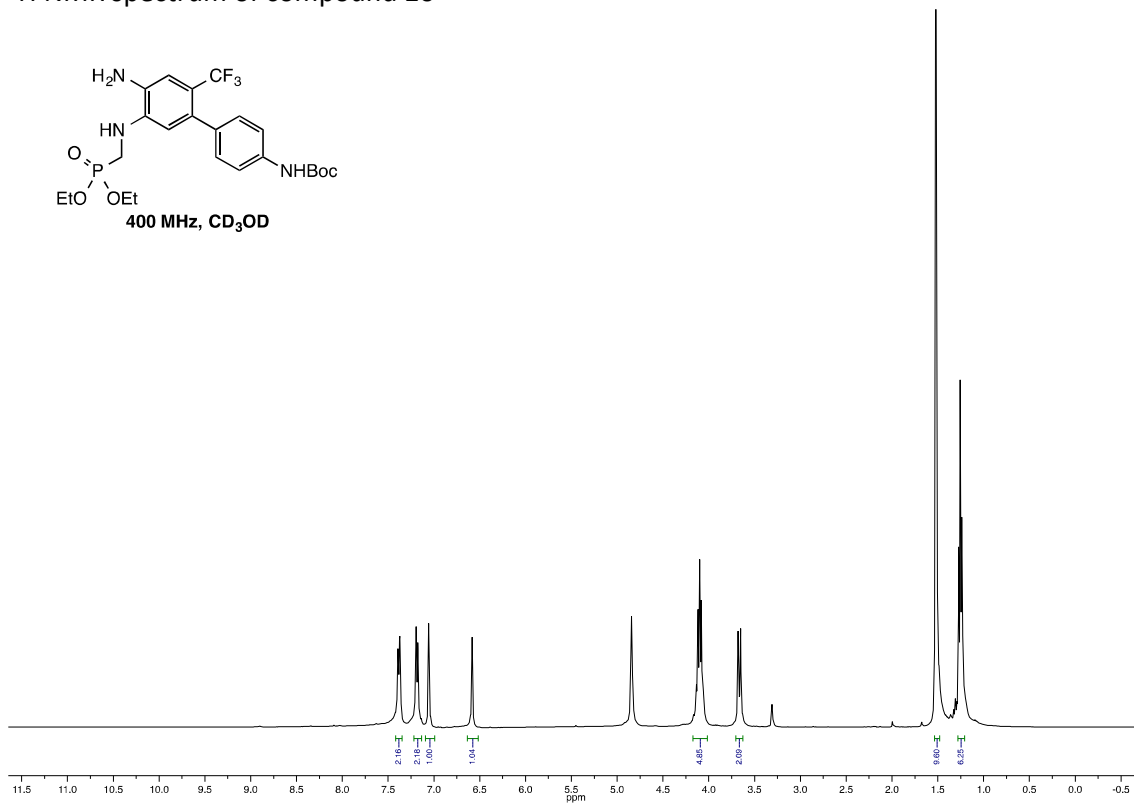
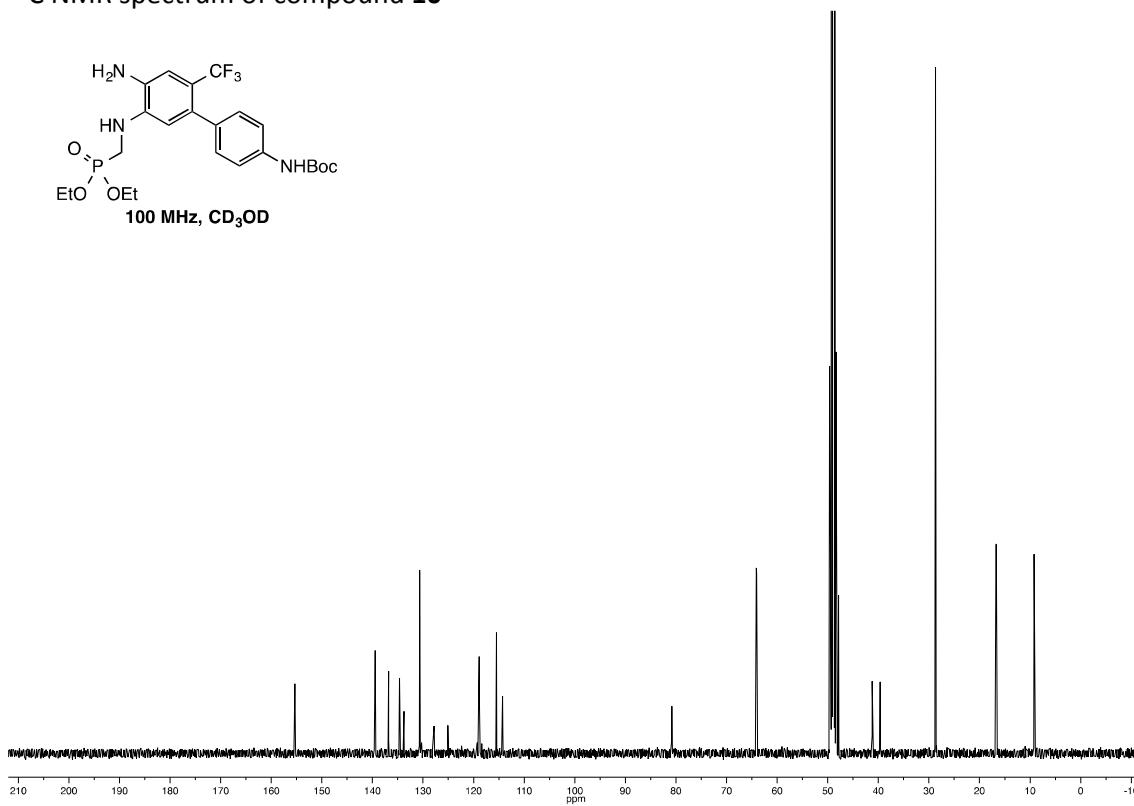
<sup>1</sup>H NMR spectrum of compound **9**<sup>13</sup>C NMR spectrum of compound **9**

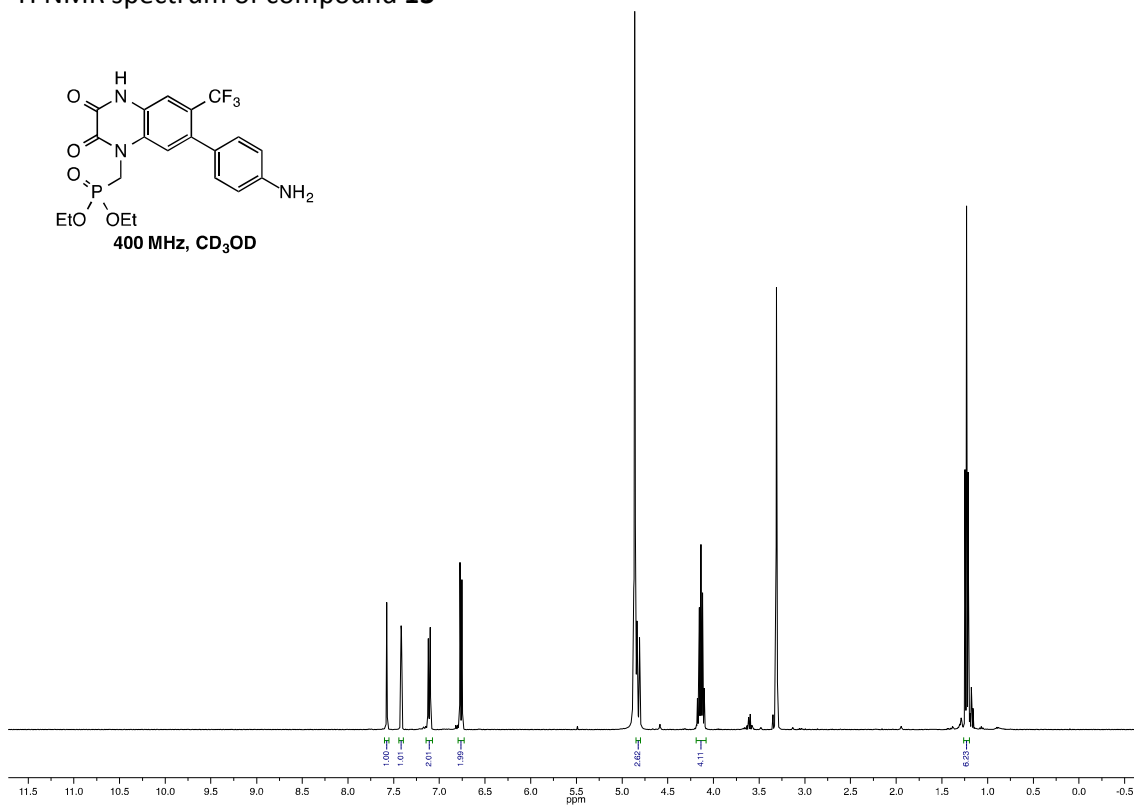
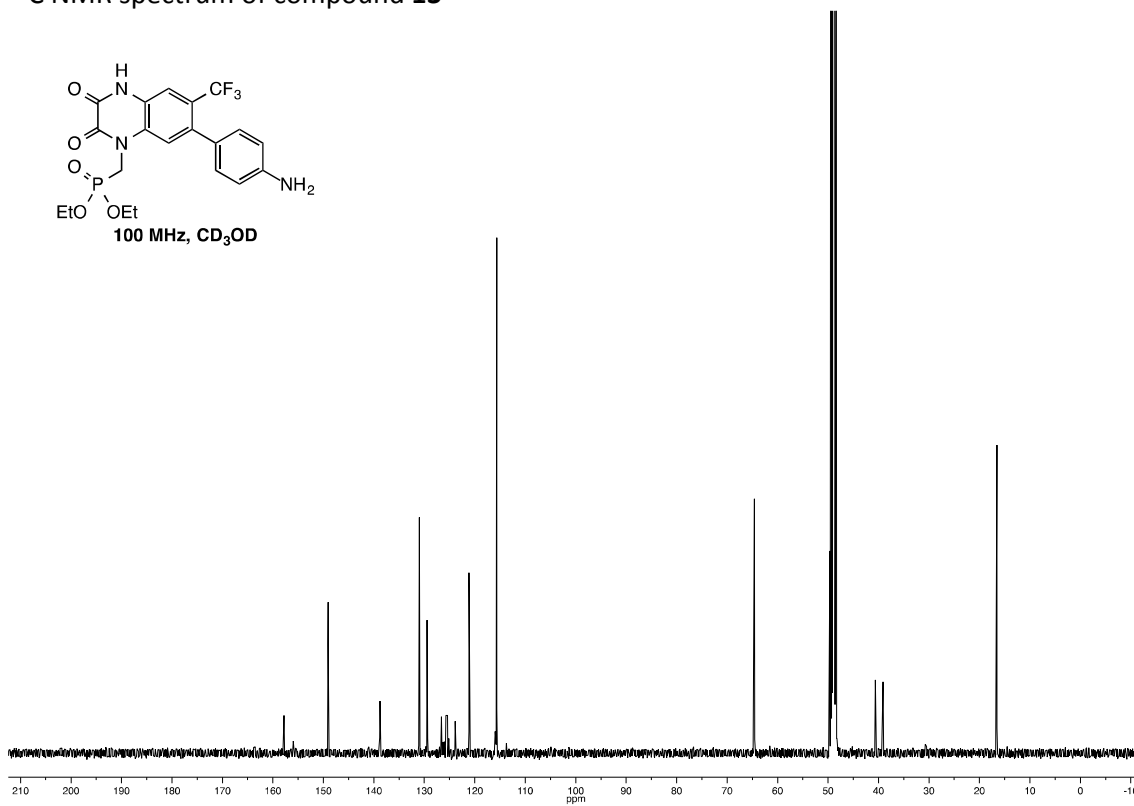
<sup>1</sup>H NMR spectrum of compound **12**<sup>13</sup>C NMR spectrum of compound **12**

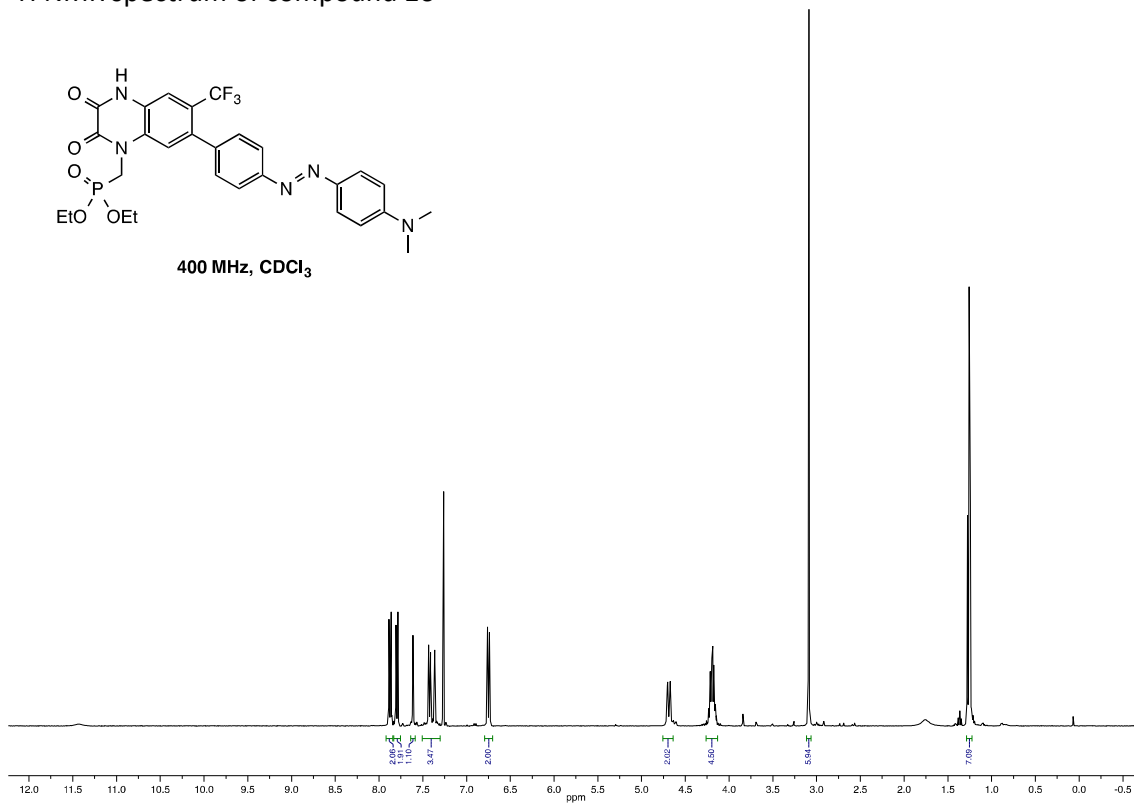
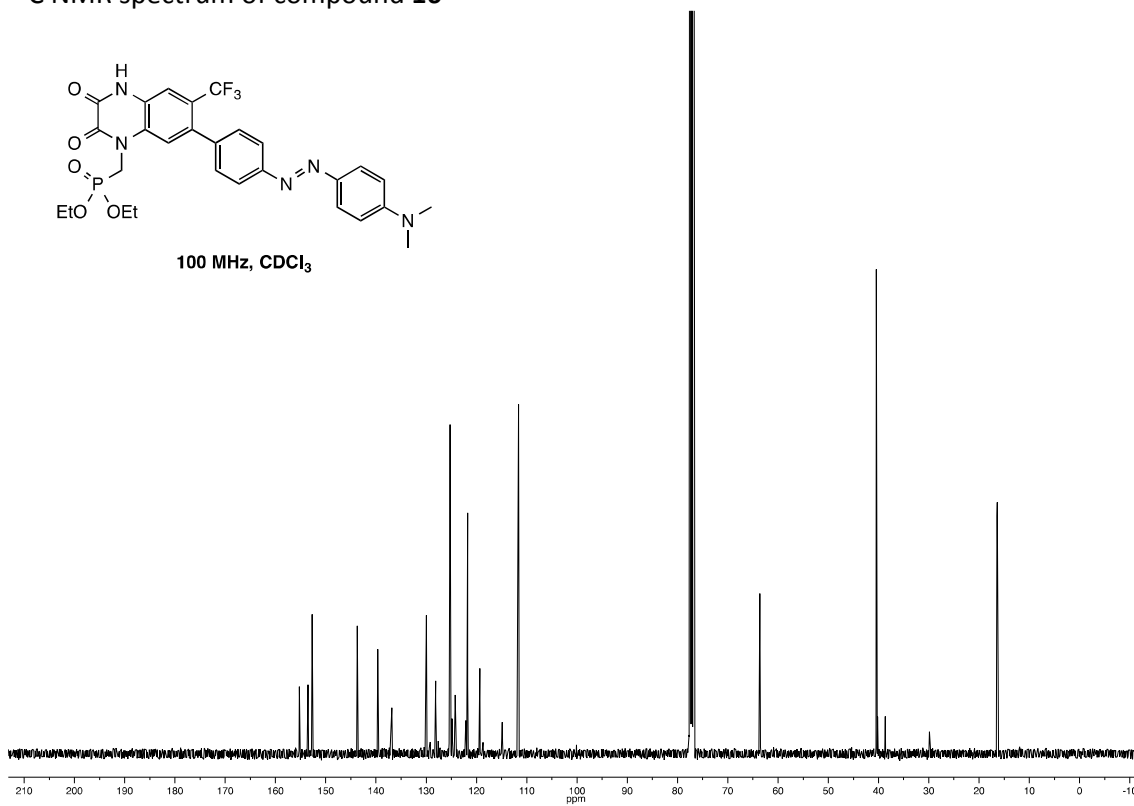
<sup>1</sup>H NMR spectrum of compound **15**<sup>13</sup>C NMR spectrum of compound **15**

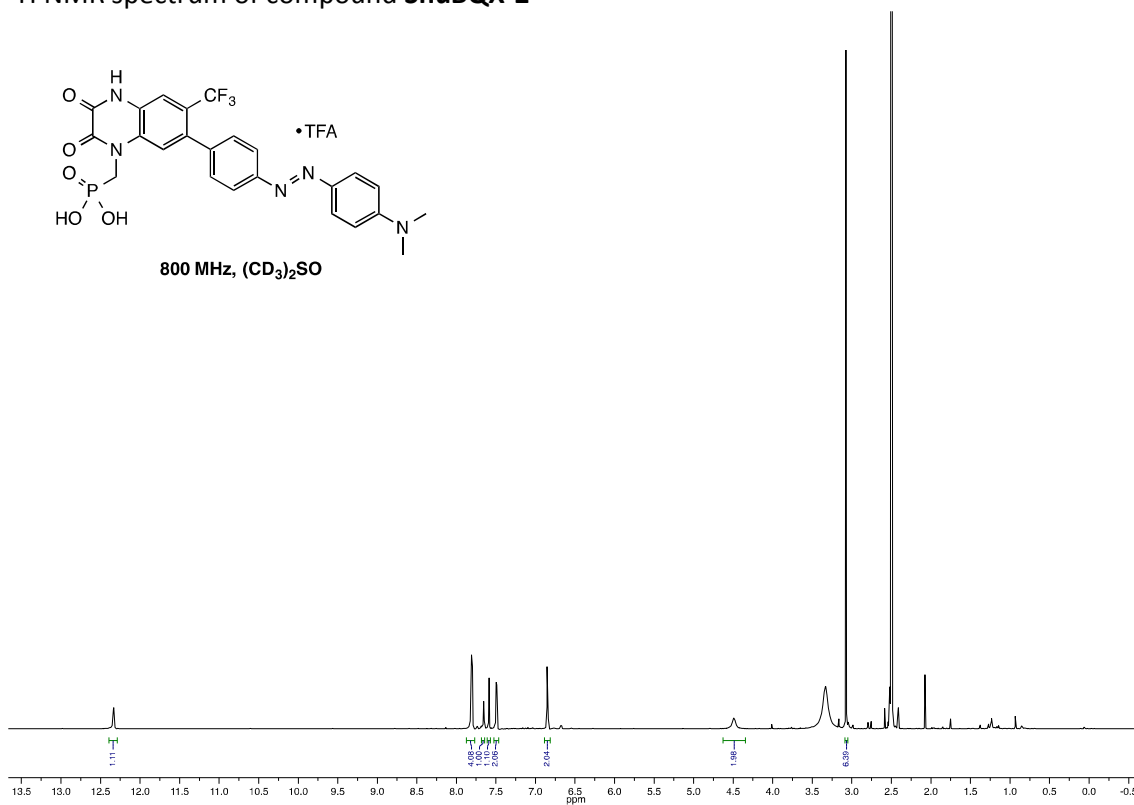
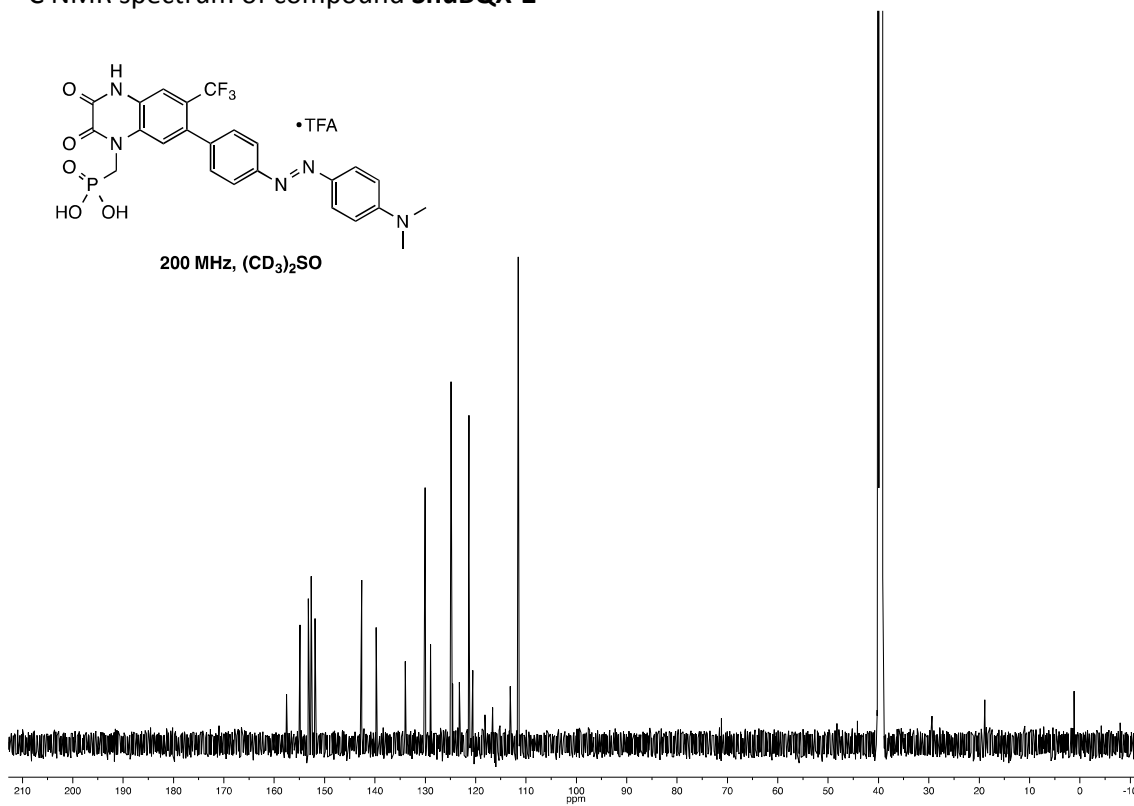
<sup>1</sup>H NMR spectrum of compound **ShuBQX-1**<sup>13</sup>C NMR spectrum of compound **ShuBQX-1**

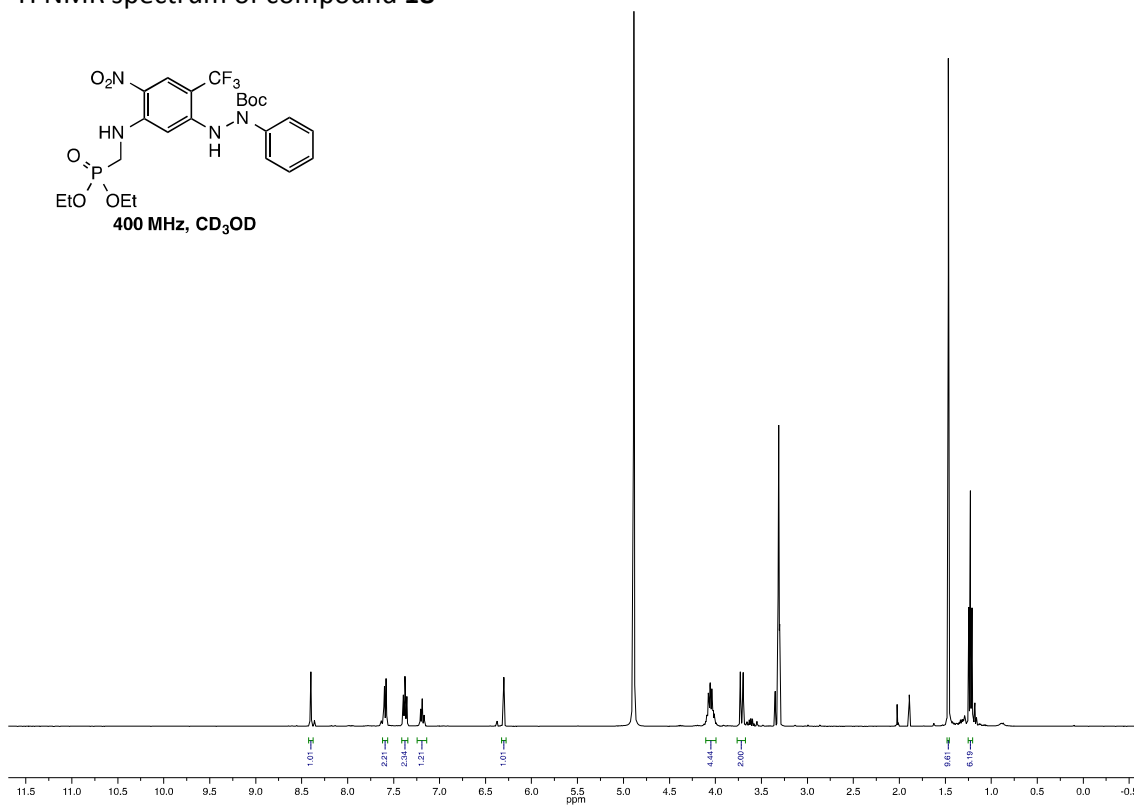
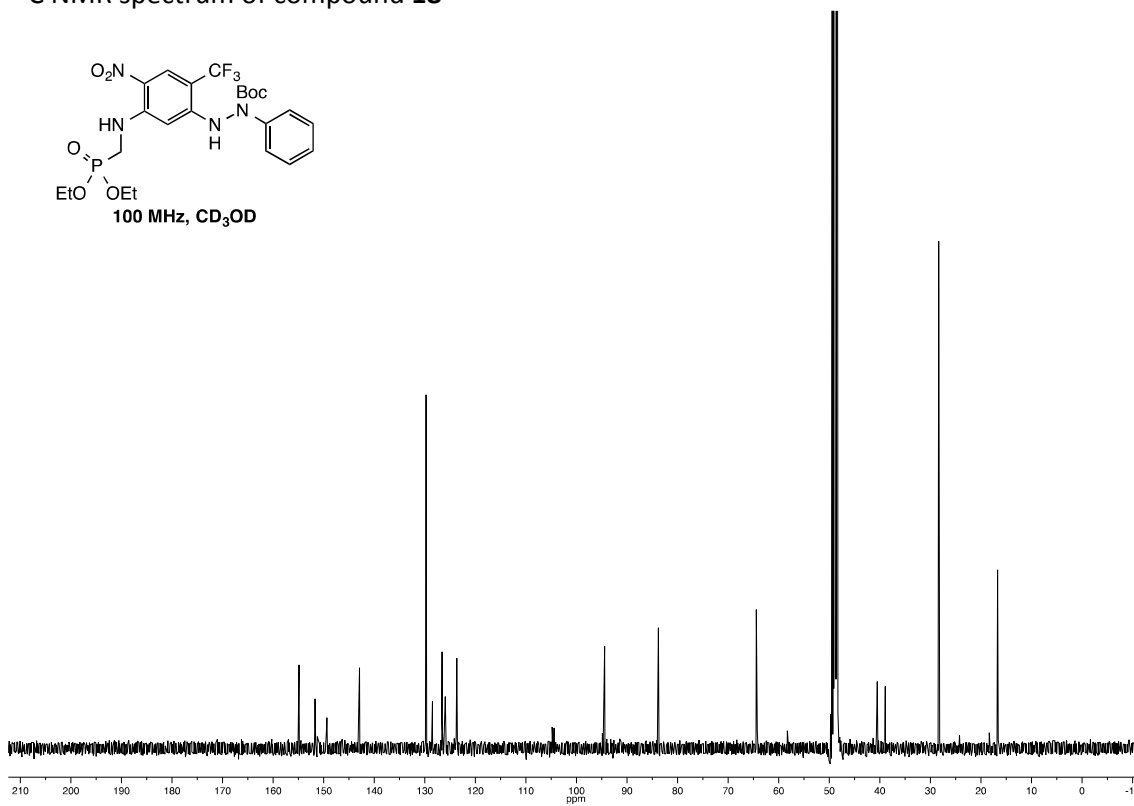
<sup>1</sup>H NMR spectrum of compound **8**<sup>13</sup>C NMR spectrum of compound **8**

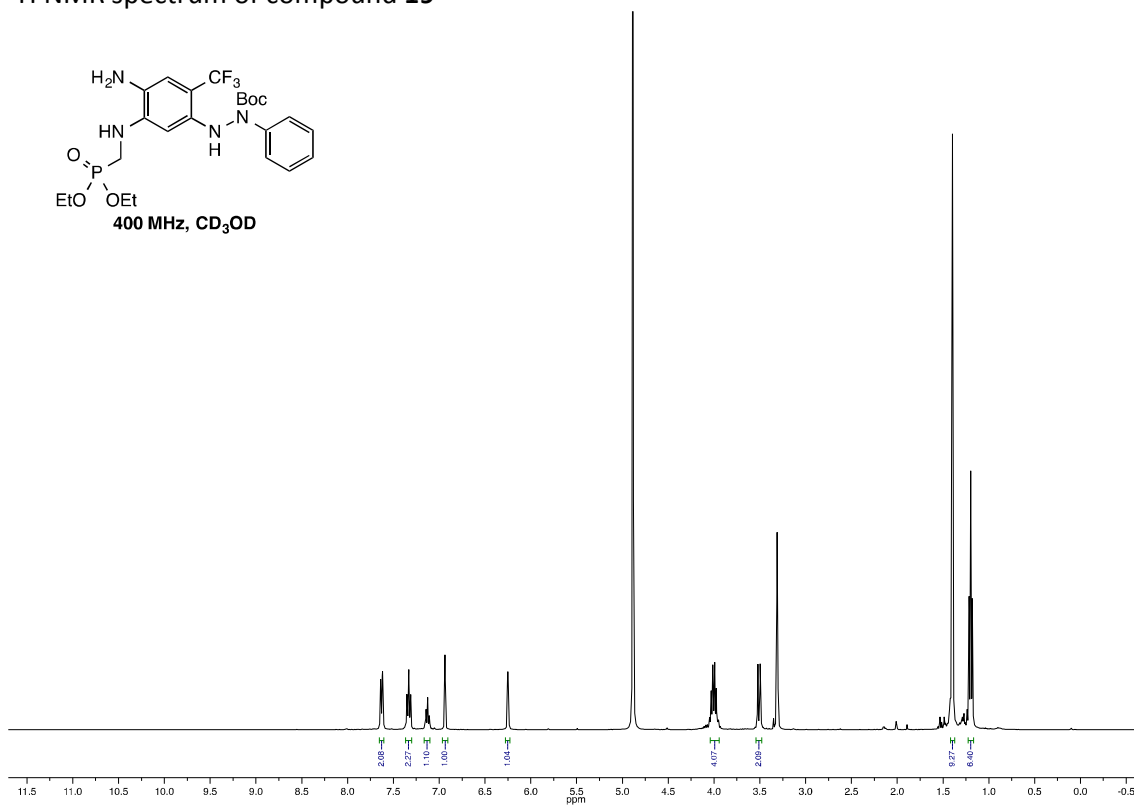
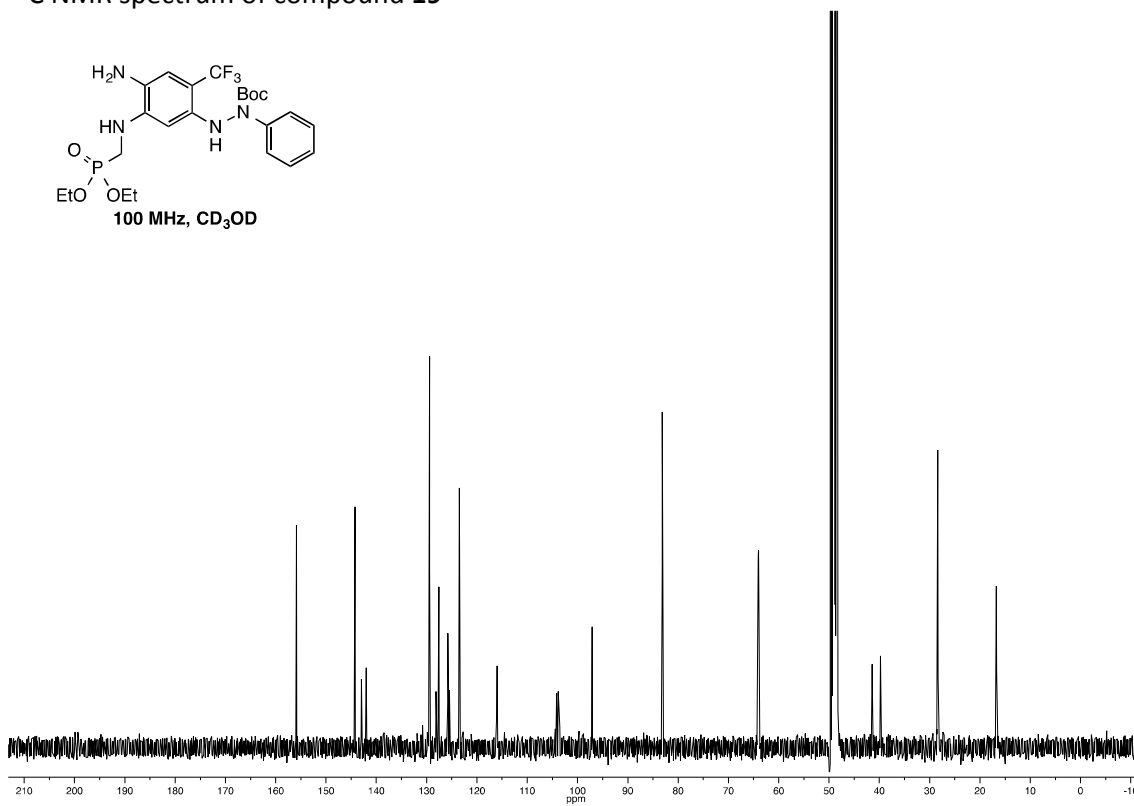
<sup>1</sup>H NMR spectrum of compound **10**<sup>13</sup>C NMR spectrum of compound **10**

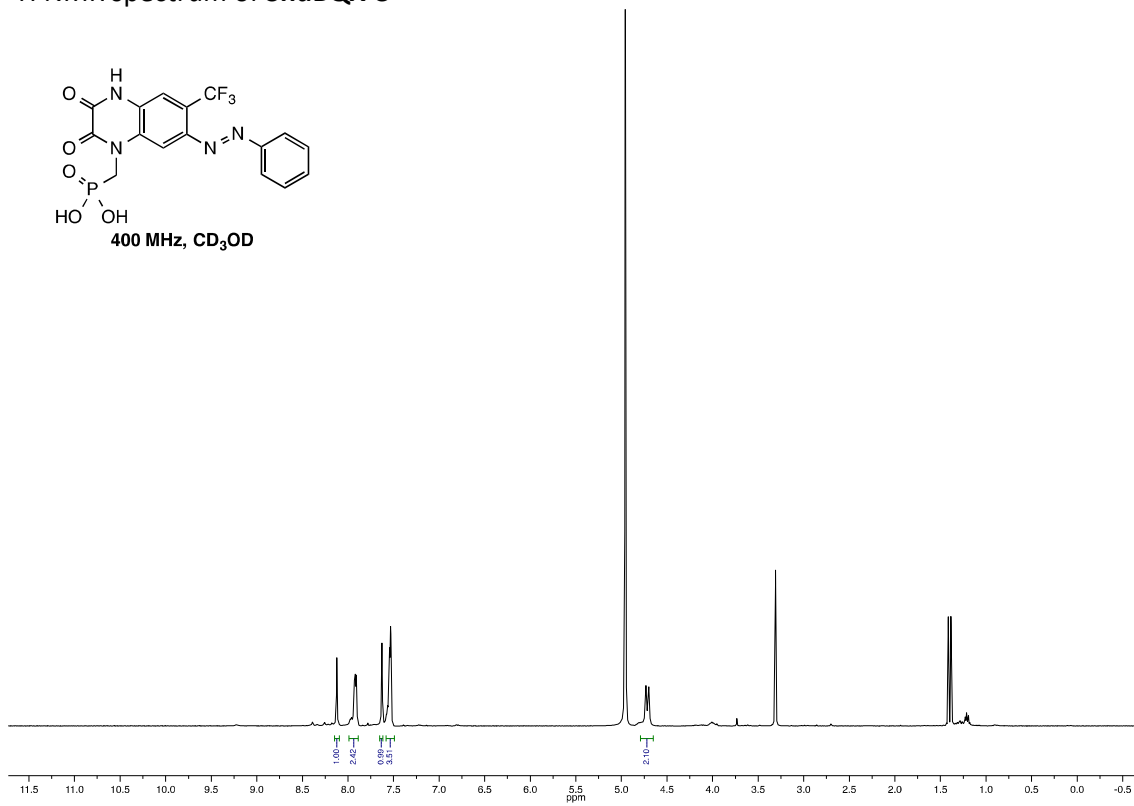
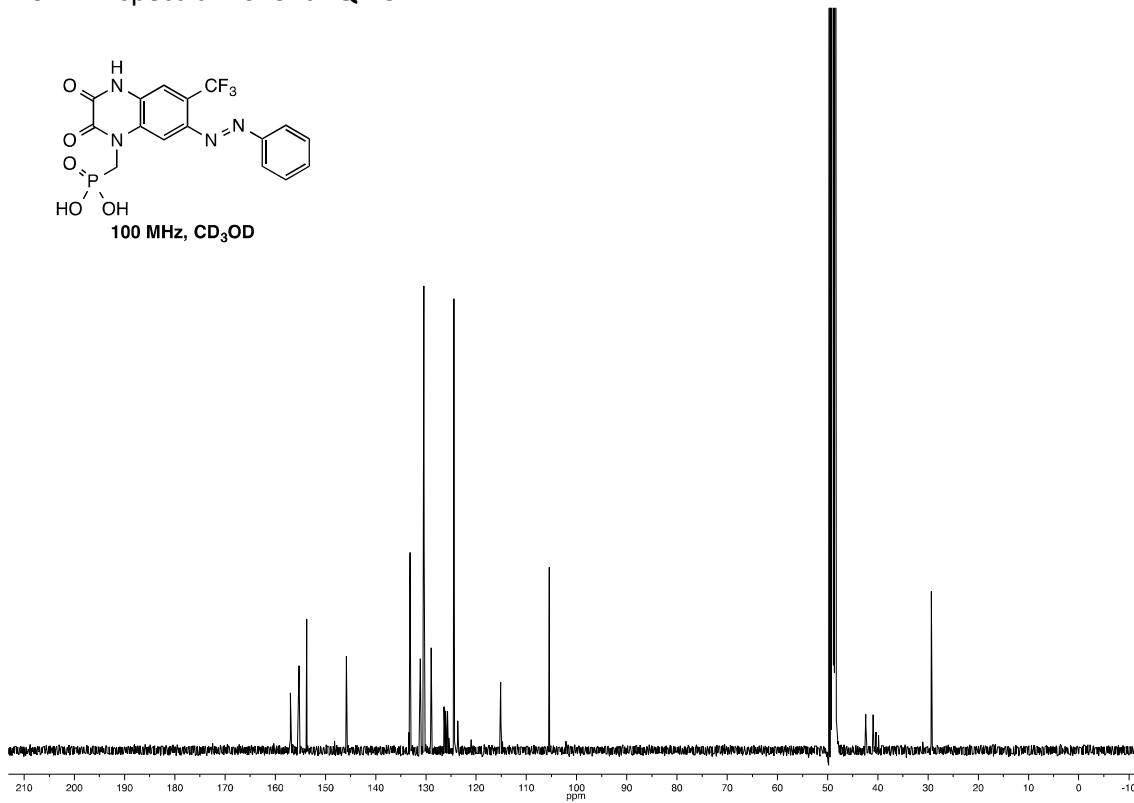
<sup>1</sup>H NMR spectrum of compound **13**<sup>13</sup>C NMR spectrum of compound **13**

<sup>1</sup>H NMR spectrum of compound **16**<sup>13</sup>C NMR spectrum of compound **16**

<sup>1</sup>H NMR spectrum of compound **ShuBQX-2**<sup>13</sup>C NMR spectrum of compound **ShuBQX-2**

<sup>1</sup>H NMR spectrum of compound **18**<sup>13</sup>C NMR spectrum of compound **18**

<sup>1</sup>H NMR spectrum of compound **19**<sup>13</sup>C NMR spectrum of compound **19**

<sup>1</sup>H NMR spectrum of **ShuBQX-3**<sup>13</sup>C NMR spectrum of **ShuBQX-3**

## 10.5.3. Supplementary Figures

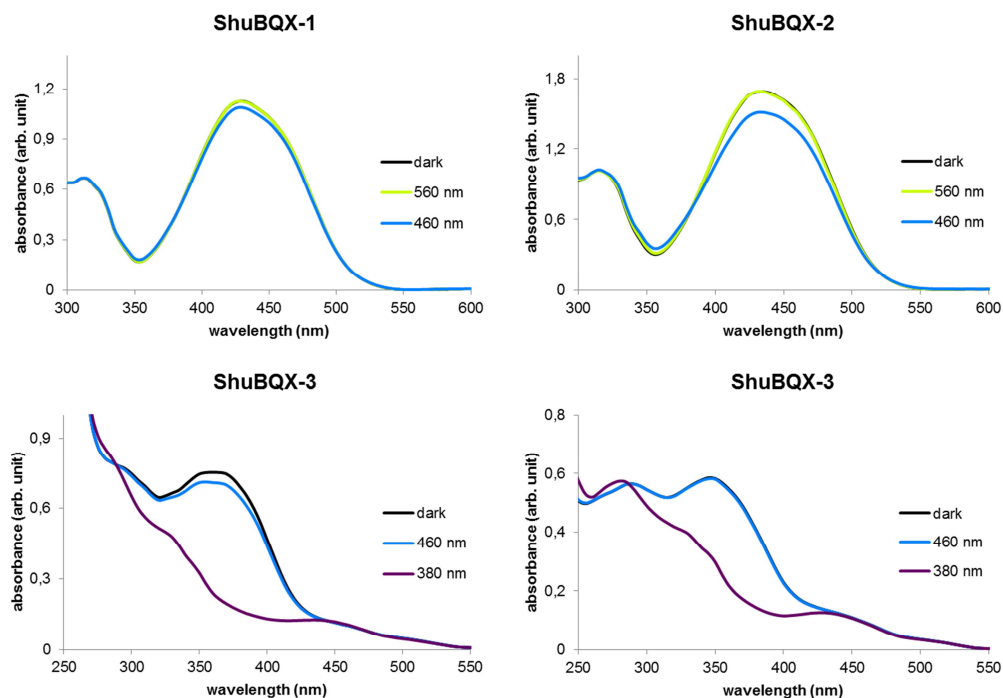


**Figure S1. UV-Vis absorption spectra of ShuBQX-1, ShuBQX-2 and ShuBQX-3.** Solutions of **ShuBQX-1** (50  $\mu\text{M}$  in DMSO), **ShuBQX-2** (50  $\mu\text{M}$  in DMSO), **ShuBQX-3** (50  $\mu\text{M}$  in DMSO, left and 50  $\mu\text{M}$  in Ringer buffer, right) were placed in a 1 mL quartz cuvette (10 mm diameter). A light-fibre cable connected to a Till Photonics Polychrome 5000 monochromator was placed in the cuvette until it penetrated the surface of the solution. Illumination was screened from wavelengths 380-600 nm in 20 nm steps (**ShuBQX-1** and **ShuBQX-2**) and 340-500 nm in 20 nm steps (**ShuBQX-3**) going from higher to lower wavelengths. Every wavelength was applied for 5 min before a UV-Vis spectrum was recorded. Illumination conditions that afforded the highest *trans*-isomer and *cis*-isomer enrichment are shown in Figure S1.

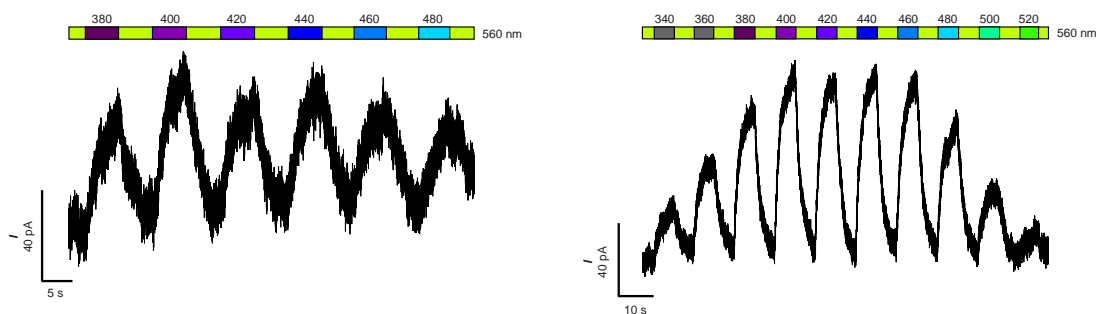


**Figure S2. Action spectra of ShuBQX-1 and ShuBQX-2.** Action spectra of **ShuBQX-1** (5  $\mu\text{M}$ , left) and **ShuBQX-2** (5  $\mu\text{M}$ , right) in the presence of glutamate (300  $\mu\text{M}$ ) under illumination with green light (580 nm) and varying wavelengths.

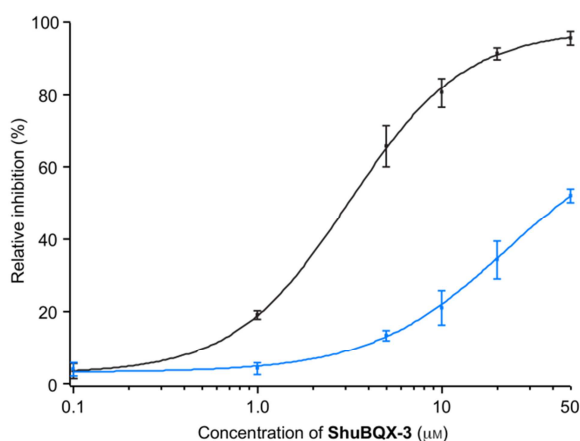


**Figure S3. ShuBQX-3 dose-response studies.** Normalized dose-response curve of **ShuBQX-3** in the presence of glutamate (300  $\mu\text{M}$ ). The *trans*-isomer of **ShuBQX-3** (black,  $\text{IC}_{50} = 3.1 \mu\text{M}$ ) displayed almost full antagonism ( $95.8\% \pm 1.8\%$ ) of HEK293T cells expressing GluA1-L497Y receptors at 50  $\mu\text{M}$ . The *cis*-isomer of **ShuBQX-3** (blue) was significantly less potent, exhibiting nearly half the antagonism ( $52.0\% \pm 1.9\%$ ) of the *trans*-isomer. The dose-response curve of **ShuBQX-3** ( $\text{IC}_{50} = 3.3 \mu\text{M}$ ) illuminated with orange light (600 nm) is not shown for clarity. Data points were fitted using the Hill equation from  $n=5$  independent cells. Values represent mean  $\pm$  SEM.

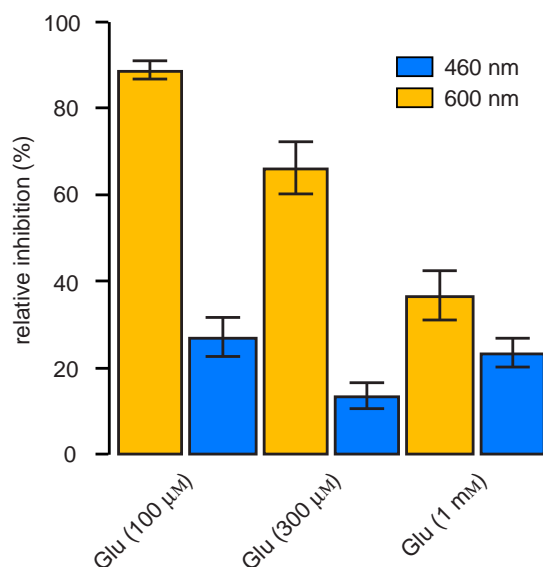


**Figure S4. ShuBQX-3 is a competitive antagonist of AMPA receptors.** ShuBQX-3 (5 μM) exhibits differing amounts of AMPA receptor antagonism when varying the concentration of glutamate (n=5 cells). Large light-dependent currents were observed when using 100 μM and 300 μM glutamate. Increasing the concentration of glutamate to 1 mM resulted in a significant reduction of light-dependent currents. Values represent mean ± SEM.

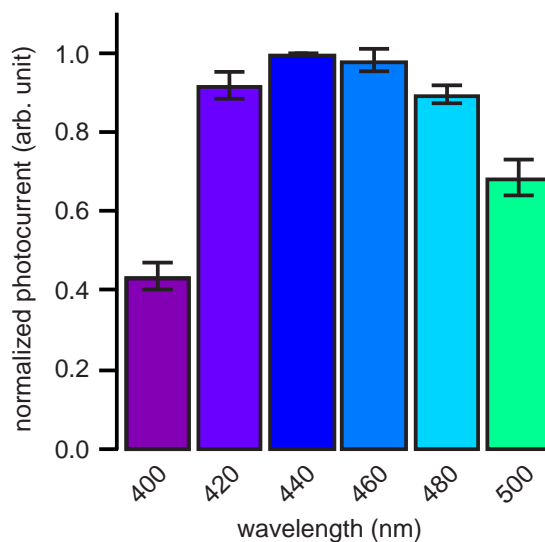


**Figure S5. Action spectrum of ShuBQX-3.** The current magnitude can be controlled by varying the wavelength of light (400-500 nm) used for photoswitching (ShuBQX-3, 20 μM). It was consistently shown that illuminating with blue light (440 nm and 460 nm) provided the maximum inward current (n=5 cells). Values represent mean ± SEM.

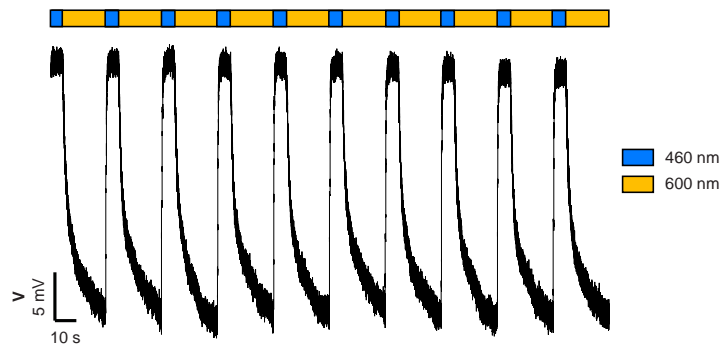


**Figure S6.** Current-clamp photoswitching of ShuBQX-3. The photoswitching of ShuBQX-3 (10  $\mu\text{M}$ ) was also highly reproducible when in current-clamp mode.

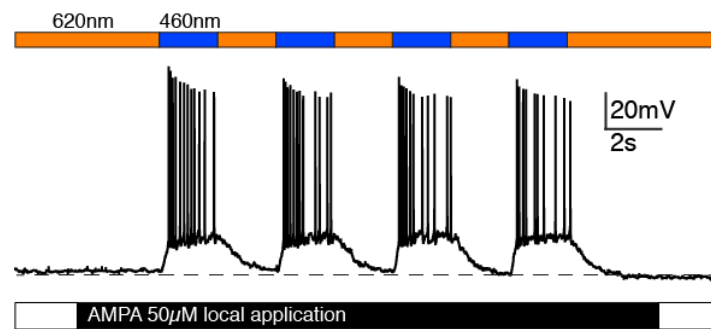


**Figure S7.** Optical control of action potential firing in hippocampal CA1 neurons using ShuBQX-3 (10  $\mu\text{M}$ ) in the presence of AMPA (50  $\mu\text{M}$ ).

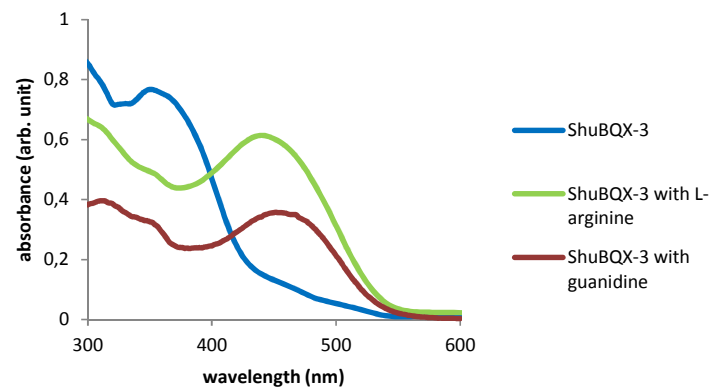


**Figure S8. UV-Vis absorption spectrum of ShuBQX-3.** Comparison of **ShuBQX-3** (50  $\mu\text{M}$ ) alone (blue) and in the presence of 1mM L-arginine (green) and 1 mM guanidine (red) in DMSO. Illumination conditions that afforded the highest *trans*-isomer enrichment are shown.

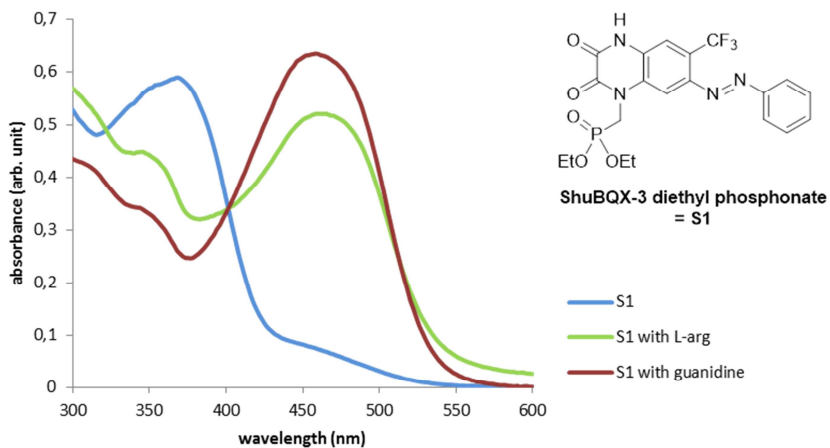


**Figure S9. UV-Vis absorption spectrum of ShuBQX-3 diethyl phosphonate (S1).** Comparison of **S1** (50  $\mu\text{M}$ ) alone (blue) and in the presence of 1mM L-arginine (green) and 1 mM guanidine (red) in DMSO. Illumination conditions that afforded the highest *trans*-isomer enrichment are shown.

### 10.5.4. Electrophysiology

#### HEK293T Cell Electrophysiology

HEK293T cells were incubated in dulbecco's minimal essential medium + 10% FBS and split at 80 to 90% confluency. For detachment, growth medium was removed, cells were washed with calcium free PBS buffer and cells were treated with trypsin solution at 37 °C for 2 min. Detached cells were diluted with growth medium and singularised by pipetting. For transfection, acid-etched coverslips were coated with poly-L-lysine and placed in a 24-well plate. 40 000 cells were added to each well in 500 µL standard growth medium. DNA (per coverslip: 350 ng GluA1-L497Y and 50 ng YFP) was mixed with 1 µL polyplus jetprime in 50 µL jetprime buffer. After standing at room temperature for 10-15 min, the DNA-mix was added to the cells shortly after seeding them into the abovementioned 24-well plate. After 3-5 hours the medium was exchanged for standard growth medium. Cells were used for electrophysiological recordings 24 hours post transfection.

Whole-cell patch clamp experiments were performed using a standard electrophysiology setup equipped with a HEKA Patch Clamp EPC10 USB amplifier and PatchMaster software (HEKA Elektronik). Micropipettes were generated from a Science Products GB200-F-8P with filament pipettes using a vertical puller. Resistance varied between 3-7 MΩ. The extracellular solution contained in mM: 138 NaCl, 1.5 KCl, 2.5 CaCl<sub>2</sub>, 1.2 MgCl<sub>2</sub>, 10 glucose and 5 HEPES (NaOH to pH 7.4). The intracellular solution contained in mM: 140 K-gluconate, 5 NaCl, 15 KCl, 5.0 MgATP, 0.5 Na<sub>2</sub>ATP and 12.5 HEPES (pH 7.3). The holding potential for voltage clamp experiments was -60 mV. The antagonists **ShuBQX-1**, **ShuBQX-2** and **ShuBQX-3** were diluted into the extracellular solution from 100 mM DMSO stock solutions. Glutamate was diluted into the extracellular solution from a 100 mM H<sub>2</sub>O stock solution. Illumination during electrophysiology experiments was provided by a Poly V, FEI monochromator.

#### Brain Slice Electrophysiology

All animal procedures were performed in accordance with the guidelines of the Regierung Oberbayern. Horizontal slices were prepared from C57Bl6Jrj mice (postnatal day 12-14). Following decapitation, the brain was rapidly removed and transferred to an ice-cold saline solution composed of (in mM) 87 NaCl, 75 sucrose, 25 NaHCO<sub>3</sub>, 2.5 KCl, 1.25 NaH<sub>2</sub>PO<sub>4</sub>, 0.5 CaCl<sub>2</sub>, 7 MgCl<sub>2</sub>, 25 glucose saturated with carbogen (95% O<sub>2</sub>/5% CO<sub>2</sub>). Slices (300 µm thick) were cut with a

vibratome (NPI Electronic), incubated at 34 °C for 1 h in saline solution and then kept at room temperature for up to 6 h before being used in patch-clamp recordings. Experiments were carried out in ACSF composed of (in mM) 125 NaCl, 26 NaHCO<sub>3</sub>, 2.5 KCl, 1.25 NaH<sub>2</sub>PO<sub>4</sub>, 2 CaCl<sub>2</sub>, 1 MgCl<sub>2</sub>, 20 glucose and AP-5 (50 μM) saturated with carbogen at room temperature.

Pyramidal CA1 neurons of the hippocampus were patched using glass electrodes (Science Products) with a resistance of 6–9 MΩ. Current-clamp recordings were carried out using the following intracellular solution (in mM): 140 K-gluconate, 10 HEPES, 12 KCl, 4 NaCl, 4 MgATP, 0.4 Na<sub>2</sub>GTP. Recordings were made with an EPC 10 USB amplifier, controlled by the Patchmaster software (HEKA). Data was filtered at 2.9 and 10 kHz. Data was analyzed using the Patcher's Power Tools (MPI Göttingen) and IgorPro (Wavemetrics). **ShuBQX-3** (10 μM) together with either (RS)-AMPA (50 μM) or glutamate (100 μM) dissolved in ACSF were locally applied through a glass pipette using a pressure application system at 2 psi (NPI Electronic). Photoswitching was achieved through a microscope coupled monochromator (Poly V, FEI).

### ***Xenopus* Oocytes Electrophysiology**

cRNA was synthesized from cDNA clones of GluN1-1a (GenBank accession number U08261), GluN2A (NM\_012573), NR2B (U11419), NR2C (NM\_012575), NR2D (NM\_022797), GluA1(Q)flip (P19490.2), GluA1(Q)flop (P19490.1), GluA2(R)flip (P19491.2), and GluK2(P42260) subcloned in the *X. laevis* oocyte expression vector pSGEM using the T7 mMESSAGE mMACHINE Kit (Ambion). Synthesized cRNA was isolated via the Clean & Concentrator 25 kit (Zymo), the quality of the cRNA controlled via denaturing agarose gel electrophoresis and the concentration, after photometrical determination, adjusted to 400 ng·μL<sup>-1</sup> with nuclease-free water.

All animal procedures were performed in accordance with the Tierschutzgesetz (TierSchG) and the TierschutzVersuchstierverordnung (TierSchVersV). Frog oocytes of stages V or VI were obtained by surgical removal of the ovaries of a *X. laevis* frog previously anesthetized with ethyl 3-aminobenzoate methanesulfonate (2.3 g·L<sup>-1</sup>; Sigma). The ovaries were cut and under constant shaking incubated with 300 U·mL<sup>-1</sup> (10 mg mL<sup>-1</sup>) collagenase type I (Worthington Biochemicals) for 3 h at 21 °C in Ca<sup>2+</sup>-free Barth's solution (in mM: 88 NaCl, 1.1 KCl, 2.4 NaHCO<sub>3</sub>, 0.8 MgSO<sub>4</sub>, 15 HEPES, pH adjusted to 7.6 with NaOH). The Ca<sup>2+</sup>-sensitive collagenase reaction was stopped by rinsing with Barth's solution with (in mM: 88 NaCl, 1.1 KCl, 2.4 NaHCO<sub>3</sub>, 0.8 MgSO<sub>4</sub>, 0.4 CaCl<sub>2</sub>, 0.3 Ca(NO<sub>3</sub>)<sub>2</sub>, 15 HEPES, pH adjusted to 7.6 with NaOH). Oocytes were kept in Barth's medium supplemented with 100 μg·mL<sup>-1</sup> gentamycin, 40 μg·mL<sup>-1</sup> streptomycin, and 63 mg/mL penicillin.

Oocytes of stages V or VI were selected and injected with cRNA within 8 h after surgery using a Nanoliter 2010 injector (WPI).

For expression of GluA1(Q)flip and GluA1(Q)flop homomeric and GluA1(Q)flip / GluA2(R)flip heteromeric receptors, 4 ng (25 nL) cRNA per subunit were injected. To express the GluK2(Q) homomeric receptor, 4 ng (20 nL) cRNA was injected. For the expression of the heteromeric NMDA receptors, 4 ng (10 nL) GluN1-1a cRNA were coinjected with one of the following: 7 ng (17 nL) GluN2A, or 6 ng (15 nL) GluN2B, or 5 ng (13 nL) GluN2C, or 5 ng (13 nL) GluN2D.

Electrophysiological recordings were performed on days 4-7. Two-electrode voltage clamping was performed using a TurboTec-10CX amplifier (npi electronic) controlled by Pulse software (HEKA). Borosilicate glass capillaries (Harvard Instruments) were pulled to resistances of 0.1-1.0 M $\Omega$  and filled with 3m KCl. Oocytes were clamped at 70 mV. All recordings were performed in barium ringer (BaR, in mM: 115 NaCl, 2.5 KCl, 1.8 BaCl<sub>2</sub>, 10 HEPES-NaOH, pH 7.2) supplemented with 250 mM niflumic acid (NFA) to prevent the opening of endogenous calcium-induced chloride channels. For the recording of kainate receptor currents either 100  $\mu$ M or 30  $\mu$ M glutamate were used, for the recording of AMPA receptor currents 100  $\mu$ M kainic acid, and for the recording of the NMDA receptor currents 100  $\mu$ M glutamate / 10  $\mu$ M glycine. Also, agonist solutions additionally containing 5  $\mu$ M **ShuBQX-3** were prepared. For the recording of the **ShuBQX-3**-mediated block of current responses, agonist solution without **ShuBQX-3** was perfused at least for 10 s until a steady state was reached, followed by a 10 s application of agonist solution containing 5  $\mu$ M **ShuBQX-3**. After a subsequent second application of agonist solution without **ShuBQX-3** a washout with BaR without agonist followed. The **ShuBQX-3**-mediated block was then calculated as the **ShuBQX-3**-induced percent inhibition of the total agonist-induced current response.

## 11. References

- [1] J. L. Bicas, A. P. Dionísio, G. M. Pastore, *Chem. Rev.* **2009**, *109*, 4518-4531.
- [2] E. Breitmaier, *Terpene – Aromen, Düfte, Pharmaka, Pheromone*, 2nd ed., Wiley-VCH, Weinheim, **2005**.
- [3] G. Wang, W. Tang, R. R. Bidigar, *Terpenoids as Therapeutic Drugs and Pharmaceutical Agents*, Humana Press Inc., Totowa, **2005**.
- [4] P. M. Dewick, *Medicinal Natural Products: A Biosynthetic Approach, 3rd Edition*, John Wiley & Sons, Ltd, Chichester, **2009**.
- [5] M. Christmann, *Angew. Chem. Int. Ed.* **2010**, *49*, 9580-9586.
- [6] L. Ruzicka, *Experientia* **1953**, *9*, 357-367.
- [7] a) F. Lynen, *Pure. Appl. Chem.* **1967**, *14*, 137-167; b) F. H. Westheimer, W. Lipscomb, *Biographical Memoirs of Fellows of the Royal Society* **2002**, *48*, 43-49.
- [8] a) L. Zhao, W.-c. Chang, Y. Xiao, H.-w. Liu, P. Liu, *Annu. Rev. Biochem.* **2013**, *82*, 497-530; b) A. Banerjee, T. D. Sharkey, *Nat. Prod. Rep.* **2014**, *31*, 1043-1055.
- [9] D. W. Christianson, *Chem. Rev.* **2006**, *106*, 3412-3442.
- [10] R. Meganathan, *FEMS Microbiol. Lett.* **2001**, *203*, 131-139.
- [11] J. Żwawiak, L. Zaprutko, *J. Med. Sci.* **2016**, *83*, 6.
- [12] S. A. Wilson, S. C. Roberts, *Plant Biotechnol. J.* **2012**, *10*, 249-268.
- [13] a) K. C. Nicolaou, D. Vourloumis, N. Winssinger, P. S. Baran, *Angew. Chem. Int. Ed.* **2000**, *39*, 44-122; b) K. C. Nicolaou, *J. Org. Chem.* **2009**, *74*, 951-972.
- [14] G. Komppa, *Chem. Ber.* **1903**, *36*, 4332-4335.
- [15] a) R. B. Woodward, F. Sondheimer, D. Taub, K. Heusler, W. M. McLamore, *J. Am. Chem. Soc.* **1951**, *73*, 2403-2404; b) R. B. Woodward, F. Sondheimer, D. Taub, K. Heusler, W. M. McLamore, *J. Am. Chem. Soc.* **1952**, *74*, 4223-4251.
- [16] E. J. Corey, J. E. Munroe, *J. Am. Chem. Soc.* **1982**, *104*, 6129-6130.
- [17] E. J. Corey, M. C. Kang, M. C. Desai, A. K. Ghosh, I. N. Houpis, *J. Am. Chem. Soc.* **1988**, *110*, 649-651.
- [18] a) E. J. Corey, M. C. Desai, T. A. Engler, *J. Am. Chem. Soc.* **1985**, *107*, 4339-4341; b) L. A. Paquette, J. Wright, G. J. Drtina, R. A. Roberts, *J. Org. Chem.* **1987**, *52*, 2960-2962; c) T. Hudlicky, L. Radesca-Kwart, L.-q. Li, T. Bryant, *Tetrahedron Lett.* **1988**, *29*, 3283-3286.
- [19] Z. G. Brill, M. L. Condakes, C. P. Ting, T. J. Maimone, *Chem. Rev.* **2017**, ASAP.
- [20] H.-H. Lu, M. D. Martinez, R. A. Shenvi, *Nature Chem.* **2015**, *7*, 604-607.
- [21] K. V. Chuang, C. Xu, S. E. Reisman, *Science* **2016**, *353*, 912-915.
- [22] a) T. J. Maimone, P. S. Baran, *Nat. Chem. Biol.* **2007**, *3*, 396-407; b) T. Busch, A. Kirschning, *Nat. Prod. Rep.* **2008**, *25*, 318-341.

- [23] I. Uchida, T. Ando, N. Fukami, K. Yoshida, M. Hashimoto, T. Tada, S. Koda, Y. Morimoto, *J. Org. Chem.* **1987**, *52*, 5292-5293.
- [24] a) J.-Y. Lu, D. G. Hall, *Angew. Chem. Int. Ed.* **2010**, *49*, 2286-2288; b) A. D. Hutters, N. K. Garg, *Chem. Eur. J.* **2010**, *16*, 8586-8595.
- [25] T. J. Maimone, J. Shi, S. Ashida, P. S. Baran, *J. Am. Chem. Soc.* **2009**, *131*, 17066-17067.
- [26] Q. Yang, J. T. Njardarson, C. Draghici, F. Li, *Angew. Chem. Int. Ed.* **2013**, *52*, 8648-8651.
- [27] A. Mendoza, Y. Ishihara, P. S. Baran, *Nat. Chem.* **2012**, *4*, 21-25.
- [28] N. C. Wilde, M. Isomura, A. Mendoza, P. S. Baran, *J. Am. Chem. Soc.* **2014**, *136*, 4909-4912.
- [29] C. Yuan, Y. Jin, N. C. Wilde, P. S. Baran, *Angew. Chem. Int. Ed.* **2016**, *55*, 8280-8284.
- [30] E. Hecker, *Cancer Res.* **1968**, *28*, 2338-2349.
- [31] M. Blanco-Molina, G. C. Tron, A. Macho, C. Lucena, M. A. Calzado, E. Muñoz, G. Appendino, *Chem. Biol.* **2001**, *8*, 767-778.
- [32] L. Jørgensen, S. J. McKerrall, C. A. Kuttruff, F. Ungeheuer, J. Felding, P. S. Baran, *Science* **2013**, *341*, 878-882.
- [33] I. Kuwajima, K. Tanino, *Chem. Rev.* **2005**, *105*, 4661-4670.
- [34] J. D. Winkler, M. B. Rouse, M. F. Greaney, S. J. Harrison, Y. T. Jeon, *J. Am. Chem. Soc.* **2002**, *124*, 9726-9728.
- [35] K. Tanino, K. Onuki, K. Asano, M. Miyashita, T. Nakamura, Y. Takahashi, I. Kuwajima, *J. Am. Chem. Soc.* **2003**, *125*, 1498-1500.
- [36] A. Nickel, T. Maruyama, H. Tang, P. D. Murphy, B. Greene, N. Yusuff, J. L. Wood, *J. Am. Chem. Soc.* **2004**, *126*, 16300-16301.
- [37] O. L. Rakotonandrasana, F. H. Raharinjato, M. Rajaonarivelo, V. Dumontet, M.-T. Martin, J. Bignon, P. Rasoanaivo, *J. Nat. Prod.* **2010**, *73*, 1730-1733.
- [38] S. Breitler, E. M. Carreira, *Angew. Chem. Int. Ed.* **2013**, *52*, 11168-11171.
- [39] J. Y. Cha, J. T. S. Yeoman, S. E. Reisman, *J. Am. Chem. Soc.* **2011**, *133*, 14964-14967.
- [40] J. T. S. Yeoman, V. W. Mak, S. E. Reisman, *J. Am. Chem. Soc.* **2013**, *135*, 11764-11767.
- [41] E. Piers, J. Renaud, *J. Org. Chem.* **1993**, *58*, 11-13.
- [42] T. Kang, S. B. Song, W.-Y. Kim, B. G. Kim, H.-Y. Lee, *J. Am. Chem. Soc.* **2014**, *136*, 10274-10276.
- [43] P. Tang, Q.-H. Chen, F.-P. Wang, *Tetrahedron Lett.* **2009**, *50*, 460-462.
- [44] J. Gong, H. Chen, X.-Y. Liu, Z.-X. Wang, W. Nie, Y. Qin, *Nat. Commun.* **2016**, *7*.
- [45] S.-H. Li, J. Wang, X.-M. Niu, Y.-H. Shen, H.-J. Zhang, H.-D. Sun, M.-L. Li, Q.-E. Tian, Y. Lu, P. Cao, Q.-T. Zheng, *Org. Lett.* **2004**, *6*, 4327-4330.
- [46] a) P. J. Krawczuk, N. Schöne, P. S. Baran, *Org. Lett.* **2009**, *11*, 4774-4776; b) J. Gong, G. Lin, C.-c. Li, Z. Yang, *Org. Lett.* **2009**, *11*, 4770-4773; c) F. Peng, M. Yu, S. J. Danishefsky, *Tetrahedron Lett.* **2009**, *50*, 6586-6587; d) K. C. Nicolaou, L. Dong, L. Deng, A. C. Talbot,

- D. Y. K. Chen, *Chem. Commun.* **2010**, 46, 70-72; e) L. Dong, L. Deng, Y. H. Lim, G. Y. C. Leung, D. Y. K. Chen, *Chem. Eur. J.* **2011**, 17, 5778-5781; f) Z. Gu, A. Zakarian, *Org. Lett.* **2011**, 13, 1080-1082; g) I. Baitinger, P. Mayer, D. Trauner, *Org. Lett.* **2010**, 12, 5656-5659; h) K. E. Lazarski, D. X. Hu, C. L. Stern, R. J. Thomson, *Org. Lett.* **2010**, 12, 3010-3013.
- [47] K. E. Lazarski, B. J. Moritz, R. J. Thomson, *Angew. Chem. Int. Ed.* **2014**, 53, 10588-10599.
- [48] J. Gong, G. Lin, W. Sun, C.-C. Li, Z. Yang, *J. Am. Chem. Soc.* **2010**, 132, 16745-16746.
- [49] W.-b. Zhang, W.-b. Shao, F.-z. Li, J.-x. Gong, Z. Yang, *Chem. Asian J.* **2015**, 10, 1874-1880.
- [50] F. Peng, S. J. Danishefsky, *J. Am. Chem. Soc.* **2012**, 134, 18860-18867.
- [51] P. Lu, A. Mailyan, Z. Gu, D. M. Guptill, H. Wang, H. M. L. Davies, A. Zakarian, *J. Am. Chem. Soc.* **2014**, 136, 17738-17749.
- [52] C. Zheng, I. Dubovyk, K. E. Lazarski, R. J. Thomson, *J. Am. Chem. Soc.* **2014**, 136, 17750-17756.
- [53] A. Cernijenko, R. Risgaard, P. S. Baran, *J. Am. Chem. Soc.* **2016**, 138, 9425-9428.
- [54] T. Yamamoto, N. Izumi, H. Ui, A. Sueki, R. Masuma, K. Nonaka, T. Hirose, T. Sunazuka, T. Nagai, H. Yamada, S. Ōmura, K. Shiomi, *Tetrahedron* **2012**, 68, 9267-9271.
- [55] P.-X. Sun, C.-J. Zheng, W.-C. Li, G.-L. Jin, F. Huang, L.-P. Qin, *J. Nat. Med.* **2011**, 65, 381-384.
- [56] G. Li, F. Liu, L. Shen, H. Zhu, K. Zhang, *J. Nat. Prod.* **2011**, 74, 296-299.
- [57] D. Kwong Jia Ye, J.-A. Richard, *Tetrahedron Lett.* **2014**, 55, 2183-2186.
- [58] WHO, *Pandemic (H1N1) 2009 - update 100*, **2010**.
- [59] E. D. Kilbourne, *Emerg. Infect. Dis.* **2006**, 12, 9-14.
- [60] M. Enserink, *WHO Declares Official End to H1N1 'Swine Flu' Pandemic*, **2010**.
- [61] Z.-Y. Yang, H.-Z. Liao, K. Sheng, Y.-F. Chen, Z.-J. Yao, *Angew. Chem. Int. Ed.* **2012**, 51, 6484-6487.
- [62] Y. Gao, J. M. Klunder, R. M. Hanson, H. Masamune, S. Y. Ko, K. B. Sharpless, *J. Am. Chem. Soc.* **1987**, 109, 5765-5780.
- [63] a) J. A. Dale, H. S. Mosher, *J. Am. Chem. Soc.* **1973**, 95, 512-519; b) G. R. Sullivan, J. A. Dale, H. S. Mosher, *J. Org. Chem.* **1973**, 38, 2143-2147.
- [64] K. Maruoka, T. Ooi, S. Nagahara, H. Yamamoto, *Tetrahedron* **1991**, 47, 6983-6998.
- [65] B. B. Snider, *Acc. Chem. Res.* **1980**, 13, 426-432.
- [66] R. Pappo, J. D. S. Allen, R. U. Lemieux, W. S. Johnson, *J. Org. Chem.* **1956**, 21, 478-479.
- [67] P. J. Garegg, R. Johansson, C. Ortega, B. Samuelsson, *J. Chem. Soc., Perkin Trans. 1* **1982**, 681-683.
- [68] L. Kurti, B. Czako, *Strategic Applications of Named Reactions in Organic Synthesis* 1st Edition ed., Elsevier Ltd, Oxford, **2004**.

- [69] a) Y. Hayashi, J. Yamaguchi, T. Sumiya, M. Shoji, *Angew. Chem.* **2004**, *116*, 1132-1135; b) Y. Hayashi, J. Yamaguchi, T. Sumiya, K. Hibino, M. Shoji, *J. Org. Chem.* **2004**, *69*, 5966-5973.
- [70] M. Matsuzawa, H. Kakeya, J. Yamaguchi, M. Shoji, R. Onose, H. Osada, Y. Hayashi, *Chem. Asian J.* **2006**, *1*, 845-851.
- [71] a) G. Cahiez, H. Avedissian, *Synthesis* **1998**, *1998*, 1199-1205; b) A. Fürstner, A. Leitner, M. Méndez, H. Krause, *J. Am. Chem. Soc.* **2002**, *124*, 13856-13863; c) A. Fürstner, R. Martin, *Chem. Lett.* **2005**, *34*, 624-629.
- [72] E. Negishi, D. R. Swanson, C. J. Rousset, *J. Org. Chem.* **1990**, *55*, 5406-5409.
- [73] Y. Yamamoto, S. Yamamoto, H. Yatagai, Y. Ishihara, K. Maruyama, *J. Org. Chem.* **1982**, *47*, 119-126.
- [74] B. H. Lipshutz, M. Koerner, D. A. Parker, *Tetrahedron Lett.* **1987**, *28*, 945-948.
- [75] E. J. Corey, M. Chaykovsky, *J. Am. Chem. Soc.* **1965**, *87*, 1353-1364.
- [76] J. Totobenazara, H. Haroun, J. Remond, K. Adil, F. Denes, J. Lebreton, C. Gaulon-Nourry, P. Gosselin, *Org. Biomol. Chem.* **2012**, *10*, 502-505.
- [77] B. C. Ranu, U. Jana, *J. Org. Chem.* **1998**, *63*, 8212-8216.
- [78] S. G. Levine, *J. Am. Chem. Soc.* **1958**, *80*, 6150-6151.
- [79] C. Earnshaw, C. J. Wallis, S. Warren, *J. Chem. Soc., Perkin Trans. 1* **1979**, 3099-3106.
- [80] N. Karousis, J. Liebscher, G. Varvounis, *Synthesis* **2006**, *2006*, 1494-1498.
- [81] a) P. Magnus, G. Roy, *J. Chem. Soc., Chem. Commun.* **1979**, 822-823; b) P. Magnus, G. Roy, *Organometallics* **1982**, *1*, 553-559.
- [82] P. Li, J. N. Payette, H. Yamamoto, *J. Am. Chem. Soc.* **2007**, *129*, 9534-9535.
- [83] H. Yang, R. G. Carter, *Org. Lett.* **2010**, *12*, 3108-3111.
- [84] a) M. T. Hechavarria Fonseca, B. List, *Angew. Chem. Int. Ed.* **2004**, *43*, 3958-3960; b) K. L. Jensen, G. Dickmeiss, H. Jiang, Ł. Albrecht, K. A. Jørgensen, *Acc. Chem. Res.* **2011**, *45*, 248-264.
- [85] W. G. Dauben, D. M. Michno, *J. Org. Chem.* **1977**, *42*, 682-685.
- [86] M. Ihara, K. Fukumoto, *Angew. Chem. Int. Ed.* **1993**, *32*, 1010-1022.
- [87] a) M. Inoue, M. W. Carson, A. J. Frontier, S. J. Danishefsky, *J. Am. Chem. Soc.* **2001**, *123*, 1878-1889; b) J. Adams, C. Lepine-Frenette, D. M. Spero, *J. Org. Chem.* **1991**, *56*, 4494-4498.
- [88] D. Martinez-Solorio, M. P. Jennings, *Org. Lett.* **2009**, *11*, 189-192.
- [89] B. S. Matsuura, P. Kölle, D. Trauner, R. de Vivie-Riedle, R. Meier, *ACS Cent Sci* **2017**, *3*, 39-46.
- [90] M. E. Jung, D. G. Ho, *Org. Lett.* **2006**, *9*, 375-378.
- [91] a) C. P. Jasperse, D. P. Curran, T. L. Fevig, *Chem. Rev.* **1991**, *91*, 1237-1286; b) L. Yet, *Tetrahedron* **1999**, *55*, 9349-9403; c) M. Albert, L. Fensterbank, E. Lacôte, M. Malacria, in

- Radicals in Synthesis II, Vol. 264* (Ed.: A. Gansäuer), Springer Berlin Heidelberg, **2006**, pp. 1-62; d) W. Zhang, *Tetrahedron* **2001**, *57*, 7237-7262.
- [92] D. C. Antonella, *J. Org. Chem.* **1991**, *56*, 6708-6709.
- [93] a) C.-K. Sha, R.-T. Chiu, C.-F. Yang, N.-T. Yao, W.-H. Tseng, F.-L. Liao, S.-L. Wang, *J. Am. Chem. Soc.* **1997**, *119*, 4130-4135; b) C.-K. Sha, F.-K. Lee, C.-J. Chang, *J. Am. Chem. Soc.* **1999**, *121*, 9875-9876.
- [94] C. Chatgililoglu, D. Griller, M. Lesage, *J. Org. Chem.* **1988**, *53*, 3641-3642.
- [95] J. L. Fry, R. J. Rahaim, R. E. Maleczka, in *Encyclopedia of Reagents for Organic Synthesis*, John Wiley & Sons, Ltd, **2001**.
- [96] a) E. J. Corey, J. W. Suggs, *J. Org. Chem.* **1975**, *40*, 2554-2555; b) G. Stork, P. M. Sher, *J. Am. Chem. Soc.* **1986**, *108*, 303-304.
- [97] D. J. Edmonds, D. Johnston, D. J. Procter, *Chem. Rev.* **2004**, *104*, 3371-3404.
- [98] M. A. Chisholm-Burns, T. L. Schwinghammer, B. G. Wells, P. M. Malone, J. M. Kolesar, J. T. DiPiro, *Pharmacotherapy Principles & Practice*, McGraw-Hill Education, **2016**.
- [99] H. Selin, *Medicine Across Cultures*, Springer Netherlands, **2003**.
- [100] P. Vallance, T. G. Smart, *Br. J. Pharmacol.* **2006**, *147*, S304-S307.
- [101] a) I. R. Edwards, J. K. Aronson, *The Lancet* **2000**, *356*, 1255-1259; b) D. B. Longley, P. G. Johnston, *J. Pathol.* **2005**, *205*, 275-292.
- [102] a) J. P. Overington, B. Al-Lazikani, A. L. Hopkins, *Nat. Rev. Drug Discov.* **2006**, *5*, 993-996; b) A. L. Hopkins, *Nat. Chem. Biol.* **2008**, *4*, 682-690.
- [103] N. C. Nicolaides, P. M. Sass, L. Grasso, *Exp. Op. Drug Disc.* **2010**, *5*, 1123-1140.
- [104] a) C. L. Sawyers, *Nature* **2008**, *452*, 548-552; b) E. Raschi, V. Vasina, M. G. Ursino, G. Boriani, A. Martoni, F. De Ponti, *Pharmacol. Ther.* **2010**, *125*, 196-218.
- [105] J. A. DiMasi, L. Feldman, A. Seckler, A. Wilson, *Clin. Pharmacol. Ther.* **2010**, *87*, 272-277.
- [106] W. A. Velema, W. Szymanski, B. L. Feringa, *J. Am. Chem. Soc.* **2014**, *136*, 2178-2191.
- [107] a) G. Mayer, A. Heckel, *Angew. Chem. Int. Ed.* **2006**, *45*, 4900-4921; b) D. D. Young, A. Deiters, *Org. Biomol. Chem.* **2007**, *5*, 999-1005; c) A. Deiters, *ChemBioChem* **2010**, *11*, 47-53; d) C. Brieke, F. Rohrbach, A. Gottschalk, G. Mayer, A. Heckel, *Angew. Chem. Int. Ed.* **2012**, *51*, 8446-8476; e) W. Szymański, J. M. Beierle, H. A. V. Kistemaker, W. A. Velema, B. L. Feringa, *Chem. Rev.* **2013**, *113*, 6114-6178.
- [108] a) G. C. R. Ellis-Davies, *Nat. Meth.* **2007**, *4*, 619-628; b) P. Klán, T. Šolomek, C. G. Bochet, A. Blanc, R. Givens, M. Rubina, V. Popik, A. Kostikov, J. Wirz, *Chem. Rev.* **2013**, *113*, 119-191.
- [109] a) T. Fehrentz, M. Schönberger, D. Trauner, *Angew. Chem. Int. Ed.* **2011**, *50*, 12156-12182; b) K. Deisseroth, *Nat. Meth.* **2011**, *8*, 26-29; c) S. C. P. Williams, K. Deisseroth, *Proc. Natl. Acad. Sci.* **2013**, *110*, 16287.
- [110] C. Dugave, L. Demange, *Chem. Rev.* **2003**, *103*, 2475-2532.

- [111] M. Irie, *Chem. Rev.* **2000**, *100*, 1685-1716.
- [112] a) R. M. Kellogg, M. B. Groen, H. Wynberg, *J. Org. Chem.* **1967**, *32*, 3093-3100; b) K. A. Muszkat, E. Fischer, *J. Chem. Soc. B* **1967**, 662-678; c) K. A. Muszkat, D. Gegiou, E. Fischer, *Chem. Comm.* **1965**, 447-448; d) F. B. Mallory, C. S. Wood, J. T. Gordon, *J. Am. Chem. Soc.* **1964**, *86*, 3094-3102.
- [113] a) M. Irie, M. Mohri, *J. Org. Chem.* **1988**, *53*, 803-808; b) S. Nakamura, M. Irie, *J. Org. Chem.* **1988**, *53*, 6136-6138.
- [114] D. Vomasta, C. Högner, N. R. Branda, B. König, *Angew. Chem. Int. Ed.* **2008**, *47*, 7644-7647.
- [115] K. Fujimoto, M. Kajino, I. Sakaguchi, M. Inouye, *Chem. Eur. J.* **2012**, *18*, 9834-9840.
- [116] Y. Yokoyama, *Chem. Rev.* **2000**, *100*, 1717-1740.
- [117] I. Willner, M. Lion-Dagan, S. Rubin, J. Wonner, F. Effenberger, P. Bäuerle, *Photochem. Photobiol.* **1994**, *59*, 491-496.
- [118] G. Berkovic, V. Krongauz, V. Weiss, *Chem. Rev.* **2000**, *100*, 1741-1754.
- [119] T. Sakata, Y. Yan, G. Marriott, *Proc. Natl. Acad. Sci. U. S. A.* **2005**, *102*, 4759-4764.
- [120] D. H. Waldeck, *Chem. Rev.* **1991**, *91*, 415-436.
- [121] W.-G. Han, T. Lovell, T. Liu, L. Noodleman, *ChemPhysChem* **2002**, *3*, 167-178.
- [122] C. Karlsson, M. Blom, M. Johansson, A. M. Jansson, E. Scifo, A. Karlen, T. Govender, A. Gogoll, *Org. Biomol. Chem.* **2015**, *13*, 2612-2621.
- [123] H. K. Cammenga, V. N. Emel'yanenko, S. P. Verevkin, *Ind. Eng. Chem. Res.* **2009**, *48*, 10120-10128.
- [124] S. Wiedbrauk, H. Dube, *Tetrahedron Lett.* **2015**, *56*, 4266-4274.
- [125] T. Loughheed, V. Borisenko, T. Hennig, K. Ruck-Braun, G. A. Woolley, *Org. Biomol. Chem.* **2004**, *2*, 2798-2801.
- [126] A. A. Beharry, G. A. Woolley, *Chem. Soc. Rev.* **2011**, *40*, 4422-4437.
- [127] J. Broichhagen, J. A. Frank, D. Trauner, *Acc. Chem. Res.* **2015**, *48*, 1947-1960.
- [128] H. M. D. Bandara, S. C. Burdette, *Chem. Soc. Rev.* **2012**, *41*, 1809-1825.
- [129] E. Merino, M. Ribagorda, *Beilstein J. Org. Chem.* **2012**, *8*, 1071-1090.
- [130] E. Merino, *Chem. Soc. Rev.* **2011**, *40*, 3835-3853.
- [131] D. D. Long, J. B. Aggen, B. G. Christensen, J. K. Judice, S. S. Hegde, K. Kaniga, K. M. Krause, M. S. Linsell, E. J. Moran, J. L. Pace, *J. Antibiot.* **2008**, *61*, 595-602.
- [132] W. A. Velema, M. van der Toorn, W. Szymanski, B. L. Feringa, *J. Med. Chem.* **2013**, *56*, 4456-4464.
- [133] J. Kuil, L. T. M. van Wandelen, N. J. de Mol, R. M. J. Liskamp, *Bioorg. Med. Chem.* **2008**, *16*, 1393-1399.
- [134] W. L. Jorgensen, *Acc. Chem. Res.* **2009**, *42*, 724-733.

- [135] A. Damijonaitis, J. Broichhagen, T. Urushima, K. Hüll, J. Nagpal, L. Laprell, M. Schönberger, D. H. Woodmansee, A. Rafiq, M. P. Sumser, W. Kummer, A. Gottschalk, D. Trauner, *ACS Chem. Neurosci.* **2015**, *6*, 701-707.
- [136] S. Pittolo, X. Gómez-Santacana, K. Eckelt, X. Rovira, J. Dalton, C. Goudet, J.-P. Pin, A. Llobet, J. Giraldo, A. Llebaria, P. Gorostiza, *Nat. Chem. Biol.* **2014**, *10*, 813-815.
- [137] M. Schoenberger, A. Damijonaitis, Z. Zhang, D. Nagel, D. Trauner, *ACS Chem. Neurosci.* **2014**, *5*, 514-518.
- [138] W. A. Velema, J. P. van der Berg, M. J. Hansen, W. Szymanski, A. J. M. Driessen, B. L. Feringa, *Nat. Chem.* **2013**, *5*, 924-928.
- [139] M. Stein, S. J. Middendorp, V. Carta, E. Pejo, D. E. Raines, S. A. Forman, E. Sigel, D. Trauner, *Angew. Chem. Int. Ed.* **2012**, *51*, 10500-10504.
- [140] M. Stein, A. Breit, T. Fehrentz, T. Gudermann, D. Trauner, *Angew. Chem. Int. Ed.* **2013**, *52*, 9845-9848.
- [141] a) W. Szymański, B. Wu, C. Poloni, D. B. Janssen, B. L. Feringa, *Angew. Chem. Int. Ed.* **2013**, *52*, 2068-2072; b) S. Samanta, C. Qin, A. J. Lough, G. A. Woolley, *Angew. Chem. Int. Ed.* **2012**, *51*, 6452-6455; c) D. Bléger, J. Schwarz, A. M. Brouwer, S. Hecht, *J. Am. Chem. Soc.* **2012**, *134*, 20597-20600.
- [142] M. M. Lerch, M. J. Hansen, G. M. van Dam, W. Szymanski, B. L. Feringa, *Angew. Chem. Int. Ed.* **2016**, *55*, 10978-10999.
- [143] M. Dong, A. Babalhavaeji, S. Samanta, A. A. Beharry, G. A. Woolley, *Acc. Chem. Res.* **2015**, *48*, 2662-2670.
- [144] A. Goulet-Hanssens, T. C. Corkery, A. Priimagi, C. J. Barrett, *J. Mater. Chem.* **2014**, *2*, 7505-7512.
- [145] S. Samanta, A. A. Beharry, O. Sadovski, T. M. McCormick, A. Babalhavaeji, V. Tropepe, G. A. Woolley, *J. Am. Chem. Soc.* **2013**, *135*, 9777-9784.
- [146] a) S. Zbaida, *Drug Metab. Rev.* **1995**, *27*, 497-516; b) W. G. Levine, *Drug Metab. Rev.* **1991**, *23*, 253-309.
- [147] C. Boulègue, M. Löweneck, C. Renner, L. Moroder, *ChemBioChem* **2007**, *8*, 591-594.
- [148] M. A. Brown, S. C. DeVito, *Crit. Rev. Environ. Sci. Technol.* **1993**, *23*, 249-324.
- [149] D. Debanne, G. Daoudal, V. Sourdet, M. Russier, *J. Physiol.* **2003**, *97*, 403-414.
- [150] S. F. Traynelis, L. P. Wollmuth, C. J. McBain, F. S. Menniti, K. M. Vance, K. K. Ogden, K. B. Hansen, H. Yuan, S. J. Myers, R. Dingledine, *Pharmacol. Rev.* **2010**, *62*, 405-496.
- [151] a) J. N. C. Kew, J. A. Kemp, *Psychopharmacol.* **2005**, *179*, 4-29; b) R. W. Gereau, G. T. Swanson, *The Glutamate Receptors*, Humana Press, Totowa, **2008**.
- [152] A. Orth, D. Tapken, M. Hollmann, *Eur. J. Neurosci.* **2013**, *37*, 1620-1630.
- [153] S. M. Schmid, M. Hollmann, *Mol. Neurobiol.* **2008**, *37*, 126-141.

- [154] a) K. P. S. J. Murphy, G. P. Reid, D. R. Trentham, T. V. P. Bliss, *J. Physiol.* **1997**, *504*, 379-385; b) S. A. Lipton, *Nat. Rev. Drug Discov.* **2006**, *5*, 160-170.
- [155] A. Contractor, C. Mulle, G. T. Swanson, *Trends Neurosci.* **2011**, *34*, 154-163.
- [156] T. E. Chater, Y. Goda, *Front. Cell. Neurosci.* **2014**, *8*.
- [157] C. Rosenmund, Y. Stern-Bach, C. F. Stevens, *Science* **1998**, *280*, 1596-1599.
- [158] S. R. Platt, *Vet. J.* **2007**, *173*, 278-286.
- [159] S. Cull-Candy, L. Kelly, M. Farrant, *Curr. Opin. Neurobiol.* **2006**, *16*, 288-297.
- [160] E. Gouaux, *J. Physiol.* **2004**, *554*, 249-253.
- [161] W. Schmidt, M. Reith, *Dopamine and Glutamate in Psychiatric Disorders*, Humana Press, **2010**.
- [162] R. Jin, T. G. Banke, M. L. Mayer, S. F. Traynelis, E. Gouaux, *Nat. Neurosci.* **2003**, *6*, 803-810.
- [163] T. B. Stensbøl, L. Borre, T. N. Johansen, J. Egebjerg, U. Madsen, B. Ebert, P. Krogsgaard-Larsen, *Eur. J. Pharmacol.* **1999**, *380*, 153-162.
- [164] S. B. Vogensen, K. Frydenvang, J. R. Greenwood, G. Postorino, B. Nielsen, D. S. Pickering, B. Ebert, U. Bølcho, J. Egebjerg, M. Gajhede, J. S. Kastrop, T. N. Johansen, R. P. Clausen, P. Krogsgaard-Larsen, *J. Med. Chem.* **2007**, *50*, 2408-2414.
- [165] D. Catarzi, V. Colotta, F. Varano, *Med. Res. Rev.* **2007**, *27*, 239-278.
- [166] B. Ebert, U. L. F. Madsen, K. K. Soby, P. Krogsgaard-Larsen, *Neurochem. Int.* **1996**, *29*, 309-316.
- [167] P. Krogsgaard-Larsen, J. W. Ferkany, E. O. Nielsen, U. Madsen, B. Ebert, J. S. Johansen, N. H. Diemer, T. Bruhn, D. T. Beattie, D. R. Curtis, *J. Med. Chem.* **1991**, *34*, 123-130.
- [168] U. Madsen, B. Bang-Andersen, L. Brehm, I. T. Christensen, B. Ebert, I. T. S. Kristoffersen, Y. Lang, P. Krogsgaard-Larsen, *J. Med. Chem.* **1996**, *39*, 1682-1691.
- [169] a) P. L. Ornstein, M. B. Arnold, N. K. Allen, T. Bleisch, P. S. Borromeo, C. W. Lugar, J. D. Leander, D. Lodge, D. D. Schoepp, *J. Med. Chem.* **1996**, *39*, 2219-2231; b) P. L. Ornstein, M. B. Arnold, N. K. Allen, T. Bleisch, P. S. Borromeo, C. W. Lugar, J. D. Leander, D. Lodge, D. D. Schoepp, *J. Med. Chem.* **1996**, *39*, 2232-2244.
- [170] T. Honore, S. Davies, J. Drejer, E. Fletcher, P. Jacobsen, D. Lodge, F. Nielsen, *Science* **1988**, *241*, 701-703.
- [171] M. Sheardown, E. Nielsen, A. Hansen, P. Jacobsen, T. Honore, *Science* **1990**, *247*, 571-574.
- [172] A. Kohara, M. Okada, R. I. E. Tsutsumi, K. Ohno, M. Takahashi, M. Shimizu-Sasamata, J.-I. Shishikura, H. Inami, S. Sakamoto, T. Yamaguchi, *J. Pharm. Pharmacol.* **1998**, *50*, 795-801.
- [173] L. Turski, A. Huth, M. Sheardown, F. McDonald, R. Neuhaus, H. H. Schneider, U. Dirnagl, F. Wiegand, P. Jacobsen, E. Ottow, *Proc. Natl. Acad. Sci.* **1998**, *95*, 10960-10965.

- [174] M. R. Walters, M. Kaste, K. R. Lees, H. C. Diener, M. Hommel, J. De Keyser, H. Steiner, M. Versavel, *Cerebrovascs. Diss.* **2005**, *20*, 304-309.
- [175] J. Ohmori, M. Shimizu-Sasamata, M. Okada, S. Sakamoto, *J. Med. Chem.* **1997**, *40*, 2053-2063.
- [176] P. Stawski, M. Sumser, D. Trauner, *Angew. Chem. Int. Ed.* **2012**, *51*, 5748-5751.
- [177] S. B. Vogensen, R. P. Clausen, J. R. Greenwood, T. N. Johansen, D. S. Pickering, B. Nielsen, B. Ebert, P. Krogsgaard-Larsen, *J. Med. Chem.* **2005**, *48*, 3438-3442.
- [178] L. Laprell, K. Hüll, P. Stawski, C. Schön, S. Michalakis, M. Biel, M. P. Sumser, D. Trauner, *ACS Chem. Neurosci.* **2016**, *7*, 15-20.
- [179] R. Sprengel, *Cell Tissue Res.* **2006**, *326*, 447-455.
- [180] a) A. Alt, E. S. Nisenbaum, D. Bleakman, J. M. Witkin, *Biochem. Pharmacol.* **2006**, *71*, 1273-1288; b) P. K. Y. Chang, D. Verbich, R. A. McKinney, *Eur. J. Neurosci.* **2012**, *35*, 1908-1916.
- [181] a) S. Hibi, K. Ueno, S. Nagato, K. Kawano, K. Ito, Y. Norimine, O. Takenaka, T. Hanada, M. Yonaga, *J. Med. Chem.* **2012**, *55*, 10584-10600; b) D. J. Chong, A. M. Lerman, *Curr. Neurol. Neurosci. Rep.* **2016**, *16*, 39.
- [182] J. J. Chambers, H. Gouda, D. M. Young, I. D. Kuntz, P. M. England, *J. Am. Chem. Soc.* **2004**, *126*, 13886-13887.
- [183] M. T. Barros, C. D. Maycock, M. R. Ventura, *J. Chem. Soc., Perkin Trans. 1* **2001**, 166-173.